

Six Podocarpane-Type Trinorditerpenes from the Bark of *Taiwania cryptomerioides*

Yueh-Hsiung KUO,^{*,a} Chi-I CHANG,^a and Ching-Kuo LEE^b

Department of Chemistry, National Taiwan University,^a Taipei, Taiwan, R.O.C. and China Junior College of Medical Technology,^b Tainan, Taiwan, R.O.C. Received July 22, 1999; accepted December 18, 1999

Six podocarpane-type trinorditerpenes were isolated from the bark of *Taiwania cryptomerioides*. Their structures, 14-hydroxy-13-methoxy-8,11,13-podocarpatrien-7-one (1), 13-hydroxy-12-methoxy-8,11,13-podocarpatriene (2), 12-hydroxy-13-methoxy-8,11,13-podocarpatriene (3), 14-hydroxy-13-methoxy-8,11,13-podocarpatriene (4), 13-hydroxy-8,11,13-podocarpatriene (5), and 13,14-dihydroxy-8,11,13-podocarpatrien-7-one (6), were determined principally from spectral evidence.

Key words *Taiwania cryptomerioides*; Taxodiaceae; Trinorditerpene; podocarpane

Taiwania cryptomerioides HAYATA (Taxodiaceae) is an economically important tree species indigenous to Taiwan and *Taiwania* is one of the most decay-resistant species in the country. We have previously investigated the chemical components of its heartwood^{1–4} and bark,^{5–7} and found various sesquiterpenes, lignans, and abietane-type diterpenes. Kamil⁸) has described the bisflavones found in its leaves. Recently, many other compounds have been obtained from its leaves, including several with novel structural skeletons as described by Lin.^{9–12} A podocarpane-type trinorditerpene 1 β ,13,14-trihydroxy-8,11,13-podocarpatriene-7-one¹²) was isolated for the first time from this plant. Because many interesting novel skeletal components have been reported, we were encouraged to study the chemical constituents of its bark again. We report here six new podocarpane-type trinorditerpenes, 1–6, 14-hydroxy-13-methoxy-8,11,13-podocarpatrien-7-one (1), 13-hydroxy-12-methoxy-8,11,13-podocarpatriene (2), 12-hydroxy-13-methoxy-8,11,13-podocarpatriene (3), 14-hydroxy-13-methoxy-8,11,13-podocarpatriene (4), 13-hydroxy-8,11,13-podocarpatriene (5), and 13,14-dihydroxy-8,11,13-podocarpatrien-7-one (6).

The molecular formula of compound 1 was established as C₁₈H₂₄O₃ by high resolution mass spectroscopy (HR-MS). IR absorptions were attributable to a hydroxyl group (3473 cm⁻¹), an aromatic group (3041, 1580, 1481 cm⁻¹), and a conjugated carbonyl (1635 cm⁻¹). The UV absorption at λ_{\max} 221.5 and 269.5 nm was attributable to the phenone moiety. The ¹H-NMR spectrum showed three singlets of methyl groups at δ 0.92, 0.97 and 1.18 (H-18, H-19, H-20) (Table 1) and two aromatic *ortho* protons occurred at δ 6.71 (d, *J*=8.4 Hz, H-11) and 6.98 (d, *J*=8.4 Hz, H-12). No isopropyl group was observed by NMR. Compound 1 is a C₁₇ podocarpane diterpene with a methoxy group [δ_{H} 3.86 (3H, s), δ_{C} 56.2]. Comparison of the ¹³C-NMR (Table 2) data of 1 with that of the known 1 β ,13,14-trihydroxy-8,11,13-podocarpatrien-7-one (7),¹²) suggests that 1 possesses the same skeletal structure. Three of six aromatic carbon signals appear at lower field, δ 148.5, 146.5 and 153.1, and those signals were assigned to C-9,¹²) C-13, and C-14, respectively. The singlet at δ_{C} 12.98 indicates a hydrogen bond between a hydroxyl (C-14) and a carbonyl (C-7) group.^{12, 13}) A typical H β -1 signal at δ 2.32 (br d, *J*=12.3 Hz) for dehydroabietane and dehydropodocarpane type derivatives^{12, 14–16}) is present. An ABX system at δ 1.82 (1H, dd, *J*=4.5, 13.0 Hz), 2.59

(1H, dd, *J*=13.0, 18.9 Hz) and 2.69 (1H, dd, *J*=4.5, 18.9 Hz) was observed and was assigned to H-5 and H-6, respectively. Meanwhile, H-11 (δ 6.71) and H β -1 (δ 2.32), and MeO-13 (δ 3.86) and H-12 (δ 6.98) show correlations in nuclear Overhauser enhancement and exchange spectroscopy (NOESY), establishing the structure of the aromatic ring. This assignment is also supported by proton-detected heteronuclear multiple-quantum coherence (HMQC) and proton detected heteronuclear multiple bond correlation (HMBC) experiments. Accordingly, 1 is 14-hydroxy-13-methoxy-8,11,13-podocarpatrien-7-one.

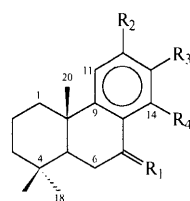
Compound 2 has the molecular formula C₁₈H₂₆O₂ on the basis of exact mass spectral data. Only two functional groups (aromatic, hydroxyl) were present in its IR spectrum. Four singlet methyl groups at δ 0.90, 0.92, 1.16, and 3.83 (–OCH₃) and two singlet phenyl protons at δ 6.56 and 6.72 (Table 1) in its ¹H-NMR spectrum indicated that 2 is also a tricyclic dehydropodocarpane skeleton diterpenoid with substitution at both C-12 and C-13. An H β -1 signal, indicating a dehydropodocarpane molecule, was also observed at δ 2.18 (br d, *J*=13.6 Hz). Three downfield ¹³C-NMR signals at δ 141.9, 143.1 and 144.6 (Table 2) were assigned as C-9, C-13 and C-12, respectively. C-12 and C-13 are phenyl carbons bond to oxygen; the connected groups are a hydroxyl (an exchangeable br s at δ 5.40) and a methoxyl (δ_{H} 3.83; δ_{C} 55.8). The phenyl proton at δ 6.72 exhibited an NOE correlation with H β -1 and with the methoxyl group. This evidence confirms the methoxyl group connecting at C-12. The ¹³C-NMR and HMBC data, in addition to the above evidence, show that 2 is 13-hydroxy-12-methoxy-8,11,13-podocarpatriene. Our identification of compound 2 is the first time it has been isolated from a natural source, although it has been synthesized from abietic acid (8).¹⁷)

Compound 3 has a tricyclic diterpenoid skeleton similar to that of 2, as indicated by the presence in the ¹H-NMR spectrum of four singlet methyl groups at δ 0.89, 0.92, 1.14 and 3.81 and the appearance of two singlet phenyl protons at δ 6.48 and 6.81. The molecular formula C₁₈H₂₆O₂, based on HR-MS, indicated that 3 is an isomer of 2. Comparison of the ¹H- and ¹³C-NMR data (Tables 1, 2) of 3 with those of 2 indicated that the difference between 2 and 3 is in the position of the hydroxyl and methoxyl groups. The expected signal for an H β -1 of dehydropodocarpane at δ 2.17 (1H, br d, *J*=13.2 Hz) is also present. NOESY data (H β -1 correlated

* To whom correspondence should be addressed. e-mail: yhkuo@ccms.ntu.edu.tw

with δ 6.81, and the methoxyl group correlated with δ 6.48) indicates that the structure of **3** is 12-hydroxy-13-methoxy-8,11,13-podocarpatriene. HMBC data also supported the assigned structure.

Compound **4**, an isomer of **3**, had HR-MS and ^{13}C -NMR data (Table 2) consistent with the molecular formula $\text{C}_{18}\text{H}_{26}\text{O}_2$. Analysis of the IR spectrum of **4** suggested it contained a hydroxyl group (3430 cm^{-1}) and a phenyl group ($1610, 1586, 1500\text{ cm}^{-1}$). It has a tricyclic diterpenoid skeleton similar to that of **3** as indicated by the presence in the ^1H -NMR spectrum (Table 1) of four singlet methyl groups at δ 0.92, 0.95, 1.17, and 3.81, and two aromatic *ortho* protons at δ 6.76 (d, $J=8.7\text{ Hz}$, H-11) and 6.69 (d, $J=8.7\text{ Hz}$, H-12).



- 1 $\text{R}_1 = \text{O}, \text{R}_2 = \text{H}, \text{R}_3 = \text{OMe}, \text{R}_4 = \text{OH}$
 2 $\text{R}_1 = \text{H}_2, \text{R}_2 = \text{OMe}, \text{R}_3 = \text{OH}, \text{R}_4 = \text{H}$
 3 $\text{R}_1 = \text{H}_2, \text{R}_2 = \text{OH}, \text{R}_3 = \text{OMe}, \text{R}_4 = \text{H}$
 4 $\text{R}_1 = \text{H}_2, \text{R}_2 = \text{H}, \text{R}_3 = \text{OMe}, \text{R}_4 = \text{OH}$
 5 $\text{R}_1 = \text{H}_2, \text{R}_2 = \text{R}_4 = \text{H}, \text{R}_3 = \text{OH}$
 6 $\text{R}_1 = \text{O}, \text{R}_2 = \text{H}, \text{R}_3 = \text{R}_4 = \text{OH}$

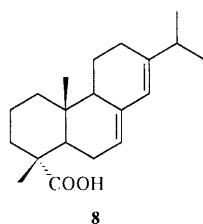
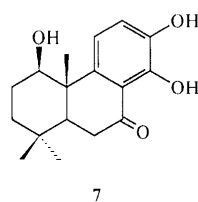


Chart 1

Comparison of the ^1H - and ^{13}C -NMR data of **4** with that of **3** indicated that the difference between **4** and **3** is the position of the hydroxyl (δ 5.64, br s, exchangeable with D_2O) and methoxyl groups. The expected signal for an $\text{H}_{\beta-1}$ of dehydropodocarpene at δ 2.40 (1H, br d, $J=12.8\text{ Hz}$) has a NOESY correlation with δ 6.76 (H-11), and the methoxyl group correlates with δ 6.69 (H-12). This evidence agrees with the structure of **4** being 14-hydroxy-13-methoxy-8,11,13-podocarpatriene. HMBC data also confirm the assigned structure.

Three singlet methyl groups and a 1,2,4-trisubstituted phenyl moiety in compound **5** are indicated by signals at δ 0.90, 0.92, 1.14 (3H each, s), 6.48 (1H, d, $J=2.8\text{ Hz}$), 6.57 (1H, dd, $J=2.8, 8.6\text{ Hz}$) and 7.08 (1H, d, $J=8.6\text{ Hz}$) (Table 1). One hydroxyl group attached to a phenyl group was revealed by the signals at δ 4.60 (exchangeable with D_2O) and δ_{C} 152.8 (Table 2). Analysis of the ^1H -, ^{13}C -, HMQC and HMBC NMR data indicated that the structure of **5** ($\text{C}_{17}\text{H}_{24}\text{O}$) is 12- or 13-hydroxy-8,11,13-podocarpatriene. The phenyl proton (δ 7.08) shows an NOE correlation with $\text{H}_{\beta-1}$ [δ 2.20 (1H, br d, $J=13.1\text{ Hz}$)], showing that the hydroxyl group is located at C-13. Akita¹⁷⁾ has synthesized this compound from abietic acid (**8**).

Compound **6** has the formula $\text{C}_{17}\text{H}_{22}\text{O}_3$, based on HR-MS and ^{13}C -NMR data (Table 2), indicating an index of hydrogen deficiency (IHD) of seven. Analysis of the IR spectrum suggested that the molecule contains a hydroxyl group (3363 cm^{-1}), a phenyl group ($1580, 1480\text{ cm}^{-1}$), and a conjugated ketone, together with a strong hydrogen bond ($1626, 3100\text{--}2600\text{ cm}^{-1}$). The UV absorption at λ_{max} 273 nm was consistent with this. Two exchangeable phenolic protons at δ 5.53 and 12.80 (Table 1) indicate that one of the hydroxyl groups is attached at C-14 with a strong hydrogen bond to the C-7 carbonyl group. Three singlet methyl groups are

Table 1. ^1H -NMR Spectral Data of Compounds **1**—**6** (300 MHz in CDCl_3)

H	1	2	3	4	5	6
1	1.47 m 2.24 br d (12.3)	1.36 m 2.18 br d (13.6)	1.32 m 2.17 br d (13.2)	1.36m 2.40 br d (12.8)	1.30 m 2.20 br d (13.1)	1.48 m 2.24 br d (13.6)
2	1.52 m 1.70 m	1.60 m 1.80 m	1.58 m 1.82m	1.60m 1.82m	1.62 m 1.81 m	1.64 m 1.74 m
3	1.22 m 1.55 m	1.22 m 1.44 m	1.18 m 1.44m	1.22 m 1.46 m	1.17 m 1.45 m	1.24 m 1.52 m
5	1.82 dd (4.5, 13.0)	1.27 ^{a)}	1.28 ^{a)}	1.28 ^{a)}	1.22 ^{a)}	1.82 dd (6.4, 11.2)
6	2.59 dd (13.0, 18.9) 2.69 dd (4.5, 18.9)	1.60 m 1.80 m	1.68 m 1.72 m	1.68m 1.90m	1.64 m 1.82 m	2.64 dd (11.2, 18.8) 2.70 dd (6.4, 18.8)
7		2.80 m	2.79 m	2.64m 2.92m	2.80 m	
11	6.71d (8.4)	6.72 s	6.81 s	6.76 (8.7)	7.08 d (8.6)	6.67 d (7.8)
12	6.98d (8.4)			6.69 (8.7)	6.57 dd (2.8, 8.6) 6.48 d (2.8)	7.01 d (7.8)
14		6.56 s	6.48 s			
18	0.92 s	0.92 s	0.92 s	0.95 s	0.92 s	0.92 s
19	0.97 s	0.90 s	0.89 s	0.92 s	0.90 s	0.97 s
20	1.18 s	1.16 s	1.14 s	1.17 s	1.14 s	1.18 s
—OH	12.98 s	5.40 br s	5.36 br s	5.64 br s	4.60 br s	5.53 s, 12.80 s
—OMe	3.86 s	3.83 s	3.81 s	3.81		

a) Overlapping with other signals.

Table 2. ^{13}C -NMR Spectral Data of Compounds 1–6 (75 MHz in CDCl_3)

C	1	2	3	4	5	6
1	38.0	39.2	39.0	39.1	39.0	37.9
2	18.8	19.2	19.2	19.3	19.0	18.8
3	41.3	41.7	41.7	41.7	41.7	41.2
4	33.2	33.4	33.4	33.3	33.4	33.2
5	49.2	50.6	50.6	50.0	50.5	49.5
6	36.3	19.3	19.3	19.3	19.3	36.1
7	206.5	29.9	30.2	24.1	30.4	206.7
8	115.4	128.2	126.6	122.3	136.9	115.1
9	148.5	141.9	143.1	144.3	143.0	148.2
10	37.7	37.6	37.4	37.3	37.3	37.7
11	112.8	106.9	110.5	114.8	125.6	113.6
12	117.9	144.6	144.6	108.8	112.8	120.8
13	146.1	143.1	143.3	143.2	152.8	142.7
14	153.1	114.2	110.6	142.4	114.8	149.4
18	32.5	33.3	33.3	33.3	33.3	32.5
19	21.4	21.6	21.6	21.6	21.6	21.4
20	23.6	24.7	24.7	25.0	24.9	23.6
–OCH ₃	56.2	55.8	55.8	55.9		

found at δ 0.92, 0.97 and 1.18. Three signals at δ 1.82 (1H, dd, $J=6.4$, 11.2 Hz), 2.64 (1H, dd, $J=11.2$, 18.8 Hz) and 2.70 (1H, dd, $J=6.4$, 18.8 Hz) were assigned as H-5 and H-6, respectively. Comparison of the spectral data of **6** with that of compound **1** suggested that a hydroxyl group in **6** replaces the methoxyl group in **1**. A pair of aromatic protons with *ortho* coupling at δ 6.67 (d, $J=7.8$ Hz) and δ 7.01 (d, $J=7.8$ Hz), as well as an NOE correlation between δ 6.67 and δ 2.24 (1H, br d, $J=13.6$ Hz, $H_{\beta-1}$), indicate that the hydroxyl groups are located at C-13 and C-14. Therefore, the structure of **6** is 13,14-dihydroxy-8,11,13-podocarpatrien-7-one. The results of HMBC and NOESY experiments confirmed the assigned structure.

Experimental

General Experimental Procedures Melting points were determined with a Yanagimoto micromelting point apparatus and are uncorrected. IR spectra were recorded on a Perkin-Elmer 781 spectrophotometer. ^1H - and ^{13}C -NMR spectra were obtained on a Bruker AM-300 at 300 and 75 MHz in CDCl_3 with tetramethylsilane (TMS) as an internal standard. EI-MS, FAB-MS, UV, and specific rotations were recorded on a JEOL JMS-HX 300, a JOEL JMS-HX 110, a Hitachi S-3200 spectrometer, and a JASCO DIP-180 digital polarimeter, respectively. Extracts were chromatographed on silica gel (Merck 3374, 70–230 mesh).

Plant Material The bark of *T. cryptomerioides* was collected in Tai-Chun, Taiwan, in 1996. The plant material was identified by Mr. Muh-Tsuen Gun, formerly a technician of the Department of Botany, National Taiwan University. A voucher specimen has been deposited at the Herbarium of the Department of Botany of the National Taiwan University, Taipei, Taiwan.

Extraction and Isolation Air-dried bark of *T. cryptomerioides* (12 kg) was extracted three times with acetone (60 l) at room temperature (7 d per extraction). The acetone extract was evaporated *in vacuo* to leave a black residue which was suspended in H_2O (8 l), and then partitioned (3 \times) with 1 l of ethyl acetate. The EtOAc fraction (360 g) was chromatographed on silica gel using a mixture of *n*-hexane and EtOAc of increasing polarity as eluent and further purified by HPLC, eluting with CH_2Cl_2 :EtOAc (50:1). Six components, 14-hydroxy-13-methoxy-8,11,13-podocarpatrien-7-one (**1**) (2.4 mg), 13-hydroxy-12-methoxy-8,11,13-podocarpatriene (**2**) (4.2 mg), 12-hydroxy-13-methoxy-8,11,13-podocarpatriene (**3**) (2.6 mg), 14-hydroxy-13-methoxy-8,11,13-podocarpatriene (**4**) (5 mg), 13-hydroxy-8,11,13-podocarpatriene (**5**) (5.3 mg), and 13,14-dihydroxy-8,11,13-podocarpatrien-7-one (**6**) (3.5 mg) were obtained in pure form.

14-Hydroxy-13-methoxy-8,11,13-podocarpatrien-7-one (**1**): Amorphous

solid; $[\alpha]_D^{22} = -7.7^\circ$ ($c=0.23$, CHCl_3); UV $\lambda_{\text{max}}^{\text{MeOH}}$ nm (log ϵ): 221 (4.04), 269 (3.84), 356 (3.39) nm; IR (film) ν_{max} 3473, 3041, 1635, 1580, 1481, 1351, 1250, 1050, 806 cm^{-1} ; ^1H -NMR, see Table 1, and ^{13}C -NMR, see Table 2; EI-MS (70 eV) (rel. int. %) m/z 288 [M^+] (100), 273 (46), 255 (47), 205 (38); HR-EI-MS m/z 288.1726 (M^+ Calcd for $\text{C}_{18}\text{H}_{24}\text{O}_3$, 288.1726).

13-Hydroxy-12-methoxy-8,11,13-podocarpatriene (**2**): Yellowish oil; $[\alpha]_D^{18} = +17.8^\circ$ ($c=0.40$, CHCl_3); IR (film) ν_{max} 3456, 3035, 1619, 1507, 1255, 1195, 1049, 870 cm^{-1} ; ^1H -NMR, see Table 1, and ^{13}C -NMR, see Table 2; EI-MS (70 eV) (rel. int. %) m/z 274 [M^+] (63), 259 (100), 201 (26), 189 (27); HR-EI-MS m/z 274.1934 (M^+ Calcd for $\text{C}_{18}\text{H}_{26}\text{O}_2$, 274.1929).

12-Hydroxy-13-methoxy-8,11,13-podocarpatriene (**3**): Yellowish oil; $[\alpha]_D^{15} = +19.2^\circ$ ($c=0.22$, CHCl_3); IR (dry film) ν_{max} 3395, 3039, 1621, 1593, 1503, 1275, 1175, 1029, 870 cm^{-1} ; ^1H -NMR, see Table 1, and ^{13}C -NMR, see Table 2; EI-MS (70 eV) (rel. int. %) m/z 274 [M^+] (58), 259 (100), 189 (42), 177 (40), 163 (47); HR-EI-MS m/z 274.1936 (M^+ Calcd for $\text{C}_{18}\text{H}_{26}\text{O}_2$, 274.1929).

14-Hydroxy-13-methoxy-8,11,13-podocarpatriene (**4**): Amorphous solid; $[\alpha]_D^{15} = +20.1^\circ$ ($c=0.40$, CHCl_3); UV $\lambda_{\text{max}}^{\text{MeOH}}$ nm (log ϵ): 278 (3.2); IR (film) ν_{max} 3430, 1610, 1586, 1500, 1202, 1062, 976, 804 cm^{-1} ; ^1H -NMR, see Table 1, and ^{13}C -NMR, see Table 2; EI-MS (70 eV) (rel. int. %) m/z 274 [M^+] (60), 259 (100), 203 (16), 189 (27); HR-EI-MS m/z 274.1941 (M^+ Calcd for $\text{C}_{18}\text{H}_{26}\text{O}_2$, 274.1929).

13-Hydroxy-8,11,13-podocarpatriene (**5**): Colorless needle; mp: 125–127 $^\circ\text{C}$; $[\alpha]_D^{21} = +16.7^\circ$ ($c=0.43$, CHCl_3); IR (film) ν_{max} 3390, 3041, 1501, 1222, 1155, 970 cm^{-1} ; ^1H -NMR, see Table 1, and ^{13}C -NMR, see Table 2; EI-MS (70 eV) (rel. int. %) m/z 244 [M^+] (26), 229 (86), 205 (46), 159 (30), 146 (100), 133 (60); HR-EI-MS m/z 244.1820 (M^+ Calcd for $\text{C}_{17}\text{H}_{24}\text{O}$, 244.1828).

13,14-Dihydroxy-8,11,13-podocarpatrien-7-one (**6**): Amorphous solid; $[\alpha]_D^{17} = -13.9^\circ$ ($c=0.21$, CHCl_3); UV $\lambda_{\text{max}}^{\text{MeOH}}$ nm (log ϵ): 211 (4.15), 227 (4.11), 273 (4.07), 360 (3.54) nm; IR (film) ν_{max} 3363, 3100–2600, 1626, 1580, 1480, 1250, 1116, 970, 830 cm^{-1} ; ^1H -NMR, see Table 1, and ^{13}C -NMR, see Table 2; EI-MS (70 eV) (rel. int. %) m/z 274 [M^+] (100), 259 (66), 191 (44), 189 (39), 177 (23), 91 (22); HR-EI-MS m/z 274.1559 (M^+ Calcd for $\text{C}_{17}\text{H}_{22}\text{O}_3$, 274.1567).

Acknowledgments This research was supported by the National Science Council of the Republic of China.

References

- Cheng Y. S., Kuo Y. H., Lin Y. T., *J. Chem. Soc., Chem. Commun.*, **1967**, 565–566.
- Lin Y. T., Cheng Y. S., Kuo Y. H., *Tetrahedron Lett.*, **1968**, 3881–3882.
- Kuo Y. H., Cheng Y. S., Lin Y. T., *Tetrahedron Lett.*, **1969**, 2375–2377.
- Lin Y. T., Cheng Y. S., Kuo Y. H., *J. Chin. Chem. Soc.*, **17**, 111–113 (1970).
- Kuo Y. H., Shih J. S., Lin Y. T., Lin Y. T., *J. Chin. Chem. Soc.*, **26**, 71–73 (1979).
- Kuo Y. H., Lin Y. T., Lin Y. T., *J. Chin. Chem. Soc.*, **32**, 381–383 (1985).
- Kuo Y. H., Lin Y. T., Lin Y. T., *Chem. Express*, **2**, 217–220 (1987).
- Kamil M., Ilyas M., Rahman W., Hasaka N., Okigawa M., Kawano N., *J. Chem. Soc., Perkin Trans. 1*, **1981**, 553–559.
- Lin W. H., Fang J. M., Cheng Y. S., *Phytochemistry*, **40**, 871–873 (1995).
- Lin W. H., Fang J. M., Cheng Y. S., *Phytochemistry*, **42**, 1657–1663 (1996).
- Lin W. H., Fang J. M., Cheng Y. S., *Phytochemistry*, **46**, 169–173 (1997).
- Lin W. H., Fang J. M., Cheng Y. S., *Phytochemistry*, **48**, 1391–1397 (1998).
- Kuo Y. H., Chen C. H., Huang S. L., *J. Nat. Prod.*, **61**, 829–831 (1998).
- Kuo Y. H., Yeh M. H., *Phytochemistry*, **49**, 2453–2455 (1998).
- Kuo Y. H., Yu M. T., *J. Nat. Prod.*, **60**, 648–650 (1997).
- Kuo Y. H., Yu M. T., *Chem. Pharm. Bull.*, **44**, 1431–1435 (1996).
- Akita H., Oishi T., *Chem. Pharm. Bull.*, **29**, 1567–1579 (1981).

Determination of Secnidazole in Urine by Adsorptive Stripping Voltammetry

Abd-Elgawad RAD^a and Amira HASSANEIN^{*b}

Department of Chemistry, Faculty of Science, Mansoura University,^a 34517 Demiatta, Egypt and Department of Chemistry, Faculty of Science,^b Tanta University, Tanta, Egypt. Received August 30, 1999; accepted January 11, 2000

Cyclic voltammetry was used to explore the adsorption behavior of secnidazole on a hanging mercury drop electrode (HMDE). The effects of various operational parameters on the accumulation behavior of the adsorbed species were tested. Thus, a sensitive stripping voltammetry procedure for the determination of secnidazole with an adsorptive accumulation on the surface of HMDE has been developed. Measurements were taken by differential-pulse voltammetry after determination of the optimum conditions. The linear concentration range was 1×10^{-8} – 1×10^{-7} M when using a 120 s preconcentration at -0.1 V vs. Ag/AgCl in acetate buffer of pH 4.0. The detection limit of secnidazole was 5×10^{-9} M. The precision, expressed by the coefficient of variation, was 2.5% ($n=10$) at a concentration of 1×10^{-7} M. The method was successfully applied to the analysis of secnidazole in urine.

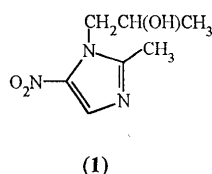
Key words secnidazole; adsorptive stripping voltammetry

Secnidazole (1), 1-(2-hydroxypropyl)-2-methyl-5-nitroimidazole, like many nitroheterocycles has proved to be an active drug against trichomoniasis, amebiasis and infection with anaerobic bacteria.^{1–3} In the treatment of infections, an oral medication is used in doses ranging from 500 mg to 2 g daily. After oral administration this compound is biotransformed in liver and excreted in urine and faeces.⁴ The electrochemical reduction of secnidazole, involving the nitro group, has been exploited for the polarographic determination of the drug.^{5,6} With direct-current polarography, millimolar and submillimolar concentration of secnidazole can be quantified,⁵ while differential-pulse polarography permits detection of micromolar level.⁶

The main challenge in developing a procedure for the measurement of any drug substance is high sensitivity coupled with applications to real samples. Adsorptive stripping voltammetry has been effectively used for the determination of nanomolar or subnanomolar level of several drugs.^{7–9} The present work is concerned with the trace quantification of secnidazole using differential-pulse cathodic stripping voltammetry. The adsorption of secnidazole onto a hanging-mercury drop electrode (HMDE) can be used as an effective preconcentration step before a voltammetric measurement. In this way, a highly sensitive measurement of this drug at the low level found in urine after therapeutic administration of secnidazole can be achieved. Such techniques for measuring concentrations of nitro compounds in urine are necessary in order to avoid toxic concentrations of such drugs.

Experimental

Reagents A stock solution (1×10^{-4} M) of secnidazole was freshly prepared in pure methanol and stored at 4 °C in the dark. A series of standard solutions was then prepared daily by dilution with methanol of the stock solution. Britton–Robinson or acetate or phosphate buffers were used as supporting electrolytes. All of the reagents used were of analytical-reagent



grade. Deionized double-distilled water was used throughout the work.

Apparatus Stripping and cyclic voltammograms were obtained with a PAR polarographic analyzer (Model 264A) coupled to an EG&G Princeton Applied Research (Model RE0091) X-Y recorder. The working electrode was a PAR 303 A static mercury drop electrode. A medium sized drop (surface area 0.014 cm^2) was employed. All of the potentials were referred to a Ag/AgCl reference electrode and a platinum wire was used as a counter electrode. Stirring was performed using a PAR (Model 305) magnetic stirrer.

Procedure A 10 ml volume of the supporting electrolyte solution containing a known amount of secnidazole was added to the cell and purged with purified nitrogen for 8 min. Preconcentration was then achieved at a new drop at potential of -0.1 V, while the solution was stirred at 400 rpm. The stirring was stopped, and the solution was allowed to equilibrate for 15 s. A negative-going scan was then applied at a rate of 100 mV s^{-1} for cyclic voltammetry and at 5 mV s^{-1} for differential-pulse voltammetry.

Analysis of Secnidazole in Urine A mixture of 0.5 ml of urine and 0.5 ml methanol was adjusted to pH 11.0 by addition of 0.1 ml NaOH (1 M). After having added 0.5 ml of 5% ZnSO_4 the solution was centrifuged for 15 min in a high-speed centrifuge. An aliquot (1 ml) of the clear supernatant was added to a mixture of 8 ml 0.02 M acetate buffer at pH 4.0 and 1 ml methanol. The solution was de-aerated for 8 min and after a preconcentration period of 120 s at an accumulation potential of -0.1 V the adsorptive stripping voltammogram was recorded after a rest period of 15 s. Determination of the secnidazole concentration was accomplished by the standard addition method.

Results and Discussion

Figure 1 shows repetitive cyclic voltammograms recorded after dipping the HMDE in stirred 5×10^{-7} M secnidazole in 0.02 M acetate buffer at pH 4.0, for an accumulation period of 60 s. Two well-defined reductive peaks were observed at -0.32 and -0.86 V. Subsequent scans exhibit a drastic decrease of the peak current of the first step to a stable value representing the response of solution species, indicating rapid desorption from the surface. The effects of the potential scan rate (v) on the peak current (i_p) and potential for the accumulated secnidazole is shown in Fig. 2. A $\log i_p$ versus $\log v$ graph was linear over the 5 – 500 mV s^{-1} range with a slope of 0.85. A slope of 1.0 is expected for an ideal reaction of surface species.¹⁰ For the second step i_p was a linear function of ($v^{1/2}$), as expected for a diffusion-controlled process.

The interfacial accumulation and redox behavior of secnidazole at the mercury electrode can be utilized for effective adsorptive stripping determinations of this drug. Figure 3A shows linear sweep voltammograms for 5.0×10^{-7} M of sec-

* To whom correspondence should be addressed. e-mail: mghoneim@cic.com.eg

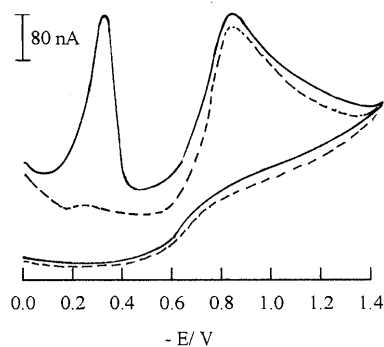


Fig. 1. Repetitive Cyclic Voltammograms for 5.0×10^{-7} M Secnidazole in 0.02 M Acetate Buffer at pH 4.0 after an Accumulation Period of 60 s in a Solution Stirred at 400 rpm

Scan rate; 100 mV s^{-1} . Solid line, first scan; broken line, fifth cycle at the same drop.

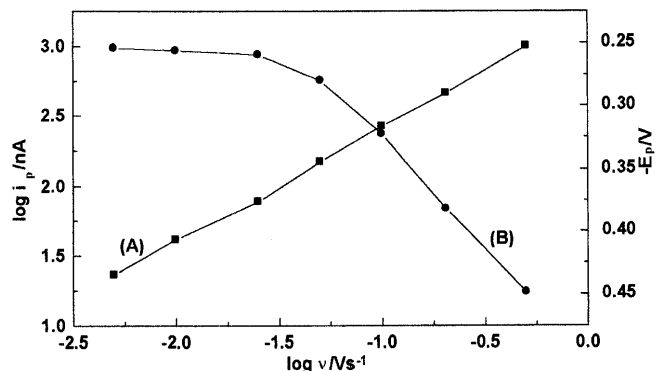


Fig. 2. Dependence of the Logarithm of the Peak Current (A) and of Peak Potential (B) on the Logarithm of Potential Scan Rate

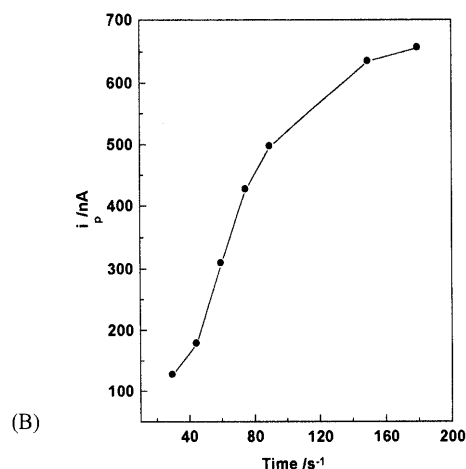
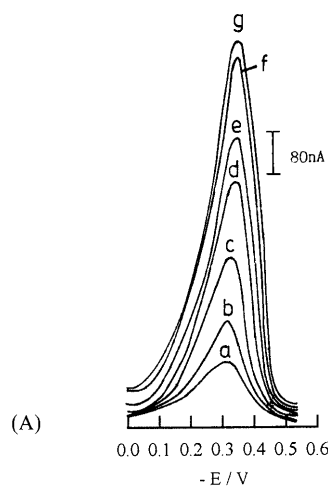


Fig. 3. (A) Voltammograms for 5×10^{-7} M Secnidazole in 0.02 M Acetate Buffer at pH 4.0 Recorded at the HMDE Following Different Preconcentration Periods

(a) 30, (b) 45, (c) 60, (d) 75, (e) 90, (f) 150, and (g) 180 s.

(B) Current-Time Graph at 5×10^{-7} M Level

Scan rate; 100 mV s^{-1} .

nidazole after different preconcentration times. The longer the preconcentration time, the more secnidazole is adsorbed and the larger the peak current. Figure 3B illustrates the dependence of the stripping peak on the preconcentration time for 5×10^{-7} M secnidazole. As the accumulation time increases, the peak current tends to level off, showing that the adsorptive equilibrium is established. For 5×10^{-7} M secnidazole, full surface coverage was achieved after a period of 180 s in stirred solution. Under these conditions, the charge transferred Q_a for the reduction step of secnidazole adsorbed at the electrode was $2.1 \mu\text{C}$ as calculated by the integration of the area under the peak, corrected for residual current.¹¹⁾

According to the equation

$$\Gamma = Q_a / (nFA)$$

The surface coverage Γ (mol cm^{-2}) can then be calculated. Where $n=4$, corresponds to the reduction of the nitro group to hydroxylamine, F is the Faraday constant and A is the surface area (0.014 cm^2). The surface coverage Γ was $4 \times 10^{-10} \text{ mol cm}^{-2}$. Therefore, each adsorbed molecule occupies an area of 0.43 nm^2 , if the adsorption of secnidazole was monolayer adsorption.

The nature, pH and concentration of the supporting elec-

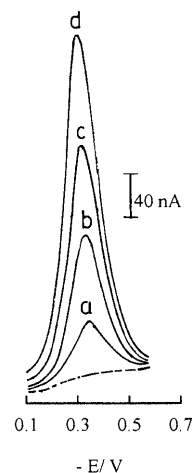


Fig. 4. Recovery Experiment of Secnidazole in Urine Sample

Differential-pulse adsorptive stripping voltammograms ($E_{\text{acc}} = -0.1 \text{ V}$, $t_{\text{acc}} = 120 \text{ s}$) for successive standard addition of secnidazole. (a) 50 ng ml^{-1} ; (b) 100 ng ml^{-1} ; (c) 150 ng ml^{-1} and (d) 200 ng ml^{-1} in 0.02 M acetate buffer of pH 4.0 according to the described procedure. The broken line represents the urine sample without secnidazole. Scan rate; 5 mV s^{-1} and pulse amplitude; 25 mV .

trolyte all influence the voltammetric response. Various supporting electrolytes such as Britton–Robinson, acetate or phosphate buffers were tested. It was found that acetate buffer at pH 4.0 resulted in the highest signal. The stripping peak current for 5×10^{-7} M of secnidazole was measured in acetate buffer at pH 4.0 of different ionic strengths, 0.01, 0.05 and 0.1 M. The enhancement of peak current is decreased on increasing ionic strength. The acetate buffer (0.02 M) at pH 4.0 was selected for analytical purposes.

Analytical Application When using optimal conditions (120 s preconcentration period; -0.1 V deposition potential; 0.02 M HOAc–NaOAc (pH 4.0) buffer and 400 rpm stirring rate), the response was linear over the concentration range 1×10^{-8} – 1×10^{-7} M following the equation i_p (nA) = $3.17 + 0.27C$ (nM) with correlation coefficient of 0.9993. A detection limit (3 s) of 5×10^{-9} M was determined. The precision, expressed by the relative standard deviation, was 2.5% ($n=10$) at 1×10^{-7} M.

Analysis of Secnidazole in Urine Secnidazole can be determined directly in urine, by reductive voltammetry at the HMDE without pretreatment. The measurements were performed in 8.5 ml of 0.02 M acetate buffer (pH 4.0), 1 ml methanol and 0.5 ml urine. When adsorptive stripping voltammetry was performed directly in urine without sample pretreatment, a significant depression of the stripping peak was observed. This was attributed to the adsorbing substances, such as protein competing with secnidazole for the adsorption site at the electrode surface. Then a sample preparation with ZnSO_4 was proposed. Figure 4 shows a recovery experiment for the determination of secnidazole within concentration range of 50–200 ng/ml of urine. The stripping peak current depends linearly on the secnidazole concentration according to the equation i_p (nA) = $2.50 + 1.27C$ (ng ml^{-1}) ($r=0.9998$). Recovery experiment was performed by repeated measurements ($n=6$) of urine samples containing different amounts of secnidazole (in the range 50 and 200 ng

per ml of urine). The mean recovery in the range mentioned above was 98.5% with a mean relative error of 3.2%. The precision of the measurement was calculated from the regression lines of the recovery experiments according to Miller and Miller.¹²⁾ The relative standard deviation was 3.6%. The detection limit (estimated as concentration corresponding to the signal to noise ratio of 3) was 5 ng per ml of urine.

In conclusion, this work demonstrates that highly sensitive voltammetric measurements of secnidazole are feasible utilizing the effective interfacial accumulation of the drug at the HMDE. Short pre-concentration periods permit convenient determination of secnidazole at nanomolar concentrations. Because of its inherent sensitivity, the method may be an effective alternative to the HPLC procedure.¹³⁾

References

- 1) Edwards D. I., "Antimicrobial Drug Action," Macmillan Press Ltd., 1980, p. 235.
- 2) Edwards D. I., "Comprehensive Medical Chemistry," ed. by Hansch C., Sammes P. G., Taylor J. B., Vol. 2, Pergamon Press, London, 1990, p. 725.
- 3) Edwards D. I., *Biochem. Pharmacol.*, **35**, 53–58 (1986).
- 4) Andrejus Korolkovas, "Essentials of Medicinal Chemistry," 2nd Ed., Wiley-Interscience, 1988.
- 5) Radi A., El-Laban S., El-Kourashy A., *Electroanalysis*, **9**, 625–629 (1997).
- 6) Lichtig J., Andrade R. F., Vaz J. M., *Anal. Chim. Acta*, **332**, 161–164 (1996).
- 7) Wang J., "Stripping Analysis and Instrumentation and Application," VCH, Deer-field Beach, FL, 1985.
- 8) Wang J., "Electroanalytical Chemistry," ed. by Bard A. J., Vol. 16, Dekker, New York, 1989, pp. 1–89.
- 9) Kalvoda R., Kapanica M., *Pure Appl. Chem.*, **61**, 97–101 (1989).
- 10) Laviron E., *J. Electroanal. Chem.*, **112**, 1–4 (1980).
- 11) Webber A., Shah M., Osteryoung J., *Anal. Chim. Acta*, **157**, 17–22 (1984).
- 12) Miller J. C., Miller J. N., "Statistics for Analytical Chemistry," Ellis Horwood Series, Prentice Hall, New York, London, 1993, p. 119.
- 13) Ray S., *East. Pharm.*, **33**, 139–142 (1990).

Effect of Polymethylene and Phenylene Linking Groups on the DNA Cleavage Specificity of Distamycin-Linked Hydroxamic Acid–Vanadyl Complexes

Shigeki HASHIMOTO, Takahiro INUI, and Yushin NAKAMURA*

Department of Biological Science and Technology, Science University of Tokyo, Yamazaki, Noda 278–8510, Japan.

Received September 14, 1999; accepted December 13, 1999

Two types of distamycin-linked hydroxamic acids (DHA), which contain various lengths of polymethylene chains (PM-DHA) and relatively rigid phenylene ones (Ph-DHA), have been synthesized for the first time. Their DNA cleavage specificities were investigated by an end-labeled fragment cleavage experiment in the presence of vanadyl ion and hydrogen peroxide. The DNA cleavage by the PM-DHA·VO(II) complexes was shown to be very dependent on the length of the chain and the AT sequences. The tetramethylene DHA (**1b**) complex exhibited highly specific cleavage patterns flanking the 8 and 10 AT sites. Interestingly, the Ph-DHA complexes selectively cleaved the 5' end-labeled strand at the AT sites, but did not cleave the 3' end-labeled strand. The vanadyl complexing moieties and the local sequence conformation of the AT tract are suggested to contribute significantly to the DNA recognition of the PM-DHA·VO(II) complexes.

Key words DNA cleavage; sequence-specific cleavage; distamycin; hydroxamic acid; vanadyl ion; pyrrolepeptide

The antitumor antibiotic, bleomycin, efficiently degrades DNA strands in 5'-GC-3' and 5'-GT-3' sequences.¹⁾ For the specific cleavage to occur, the metal binding domain of the antibiotic should be positioned near the C4'-H of the pyrimidine residue, which leads to the C4'-H abstraction responsible for DNA cleavage.²⁾ On the other hand, most of the conventional artificial DNA-cleaving metal complexes fail to successfully direct the complexing moiety to the reaction site of DNA. These complexes usually afford multiple cleavage patterns flanking the DNA recognition site.^{3,4)} One strategy for controlling the DNA cleavage is to choose the proper linkage group.⁵⁾

Hydroxamic acids have been used in calorimetric analyses of vanadium⁶⁾ and the complex formed has been characterized.⁷⁾ In the course of our continuing research into the DNA cleavage properties of the hydroxamic acid–metal system, we have recently found that hydroxamic acid conjugated to the tripyrrolepeptide, distamycin, induced highly specific DNA cleavage in the presence of vanadyl ion.⁸⁾ This highly specific DNA cleavage was not observed for other metal complexes of the ligand. To explore the optimum distance and relative orientation between the distamycin and hydroxamic acid complexing moieties, we have evaluated the effect of the group linking them on the DNA cleavage specificity. We have recently designed two types of distamycin-linked hydroxamic acid (DHA) which contain various lengths of polymethylene chains (PM-DHA) (**1a–d**) and relatively rigid phenylene ones (Ph-DHA) (**2a–c**) (Fig. 1).⁹⁾ The distances between the carbonyl carbons of the chain of these hydroxamic acids increase in the order **2a**<**1a**<**2b**<**1b**<**2c**<**1c**<**1d**. In the present study, the effect of the linker length of the PM-DHA·VO(II) complexes on DNA cleavage specificity was investigated using two restriction DNA fragments. The DNA cleavage specificities of conformationally restricted Ph-DHA complexes were also compared with that of the **1b** complex.

Results

Synthesis of Hydroxamic Acids

The syntheses of PM-DHA (**1a–d**) and Ph-DHA (**2a–c**) are outlined in Chart 1. The tripyrrole compound **4** was synthesized from *N*-methylpyrrole following a previously described procedure.^{8a,10)} The nitro compound **4** was catalytically hydrogenated to afford the unstable aromatic amines, which immediately reacted with the *p*-nitrophenol-activated alkyl esters to give the ester compounds **5a–d** in 31–37% yield. Similarly, the ester compounds **6a–c** were prepared in 40–53% yield from compound **4** by condensation with the phenylene monoesters *via* dicyclohexylcarbodiimide (DCC). The transformation of the ester groups of compounds **5a–d** and **6a–c** into the corresponding hydroxamic acids afforded **1a–d**

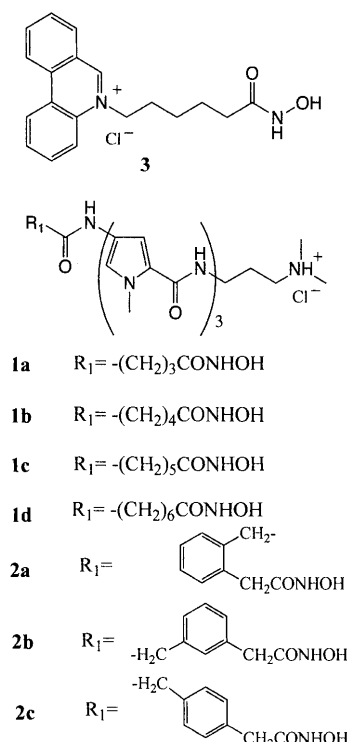


Fig. 1. DNA Cleaving Hydroxamic Acids

* To whom correspondence should be addressed. e-mail: ynakamu@rs.noda.sut.ac.jp

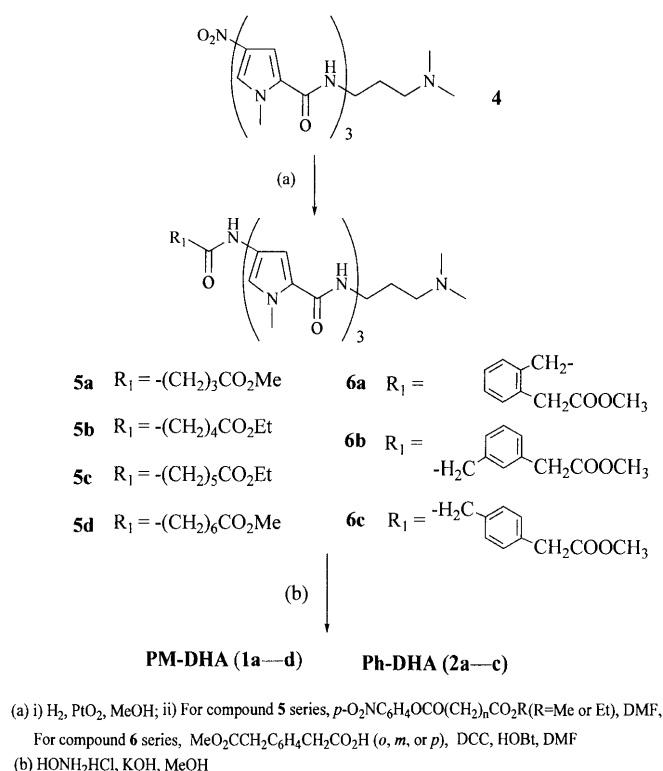


Chart 1

(54—70% yield) and **2a—c** (66—75% yield), respectively. All the hydroxamic acids were characterized by spectroscopic examination and gave a positive Fe(III) test which is characteristic of the hydroxamic acid group.

DNA Cleavage Patterns Produced by PM-DHA·VO(II) Complexes The DNA cleaving ability of PM-DHA·VO(II) complexes in the presence of hydrogen peroxide was initially examined using supercoiled Col E1 plasmid DNA. At a $10\ \mu\text{M}$ concentration of the complexes, maintained at 37°C for 30 min, all PM-DHA·VO(II) complexes showed almost the same DNA cleavage activity (data not shown). A comparative study of the DNA cleavage patterns produced by the PM-DHA·VO(II) complexes was carried out on the end-labeled 167 and 517 bp fragments of pBR 322 plasmid DNA. The 5' end-labeled DNA fragments were prepared by digesting pBR 322 DNA with *Eco*RI and successive treatment with calf intestine alkaline phosphatase, ($\gamma\text{-}^{32}\text{P}$)ATP and T4 polynucleotide kinase.¹¹⁾ A second enzymatic digestion with *Rsa*I yielded the 167 and 517 bp fragments labeled at the 5' end. The 3' end-labeled DNA fragments were prepared by digesting pBR 322 DNA with *Eco*RI and labeled with ($\alpha\text{-}^{32}\text{P}$)dATP using the Klenow fragment of DNA polymerase I.¹¹⁾ A second enzymatic digestion with *Rsa*I yielded two 3' end-labeled fragments, 167 and 517 bp. Figure 2a shows the 517 bp fragment cleavage patterns produced by the PM-DHA·VO(II) complexes. The sequenced portion of this DNA fragment contains 8 or 10 base pair AT contiguous sites (sites 1 and 2, respectively).¹²⁾ The DNA cleavage specificity of the PM-DHA complexes was compared with that of the phenanthridine-linked hydroxamic acid (**3**) complex. This hydroxamic acid ligand affords a sequence-neutral cleavage pattern in the presence of metal ions due to the intercalative binding of the phenanthridine ring.¹²⁾ Distinct cleavage patterns were observed for cleavage by the **1b** and **1d** com-

plexes. Noticeably, the **1b** complex produced doublet bands both at the labeled and non-labeled sides of site 2. In contrast to the DNA cleavage produced by this complex, no DNA cleavage patterns were observed for cleavage by the **1a** and **1c** complexes. These results indicate that the linker length is an important factor which strictly controls the DNA cleavage by the vanadyl complexes of PM-DHA at the 8 and 10 AT contiguous sites. We then examined the 167 bp fragment cleavage patterns produced by the PM-DHA·VO(II) complexes (Fig. 2b). The sequenced portion of this DNA fragment contains 7, 5, and 6 base pair AT contiguous sites (sites 3, 4, and 5, respectively). As can be seen from Fig. 2b, the complexes of **1b—d** with chains longer than **1a** produced almost similar cleavage patterns on both the 5' and 3' end-labeled strands. Doublet and triplet bands produced by these complexes were observed only for the 5' end-labeled strand at sites 3 and 4. No complexes produced a DNA cleavage at site 5. These results indicate that the DNA cleavage by the vanadyl complexes of PM-DHA at 5 and 7 AT contiguous sites is not significantly influenced by the linker length. Figure 3 shows a histogram of the 517 bp fragment cleavage pattern produced by the **1b**·VO(II) complex. Although the cleavage patterns at sites 1 and 2 are asymmetric and shifted to the 3' side of each strand, cleavage occurs almost exclusively at two nucleotide residues on both strands of site 2. This highly specific cleavage contrasts with the behavior of the affinity cleaving agent, distamycin-EDTA·Fe(II), which produces asymmetric multiple cleavage patterns.³⁾ We chose to use **1b** for comparison with the phenylene hydroxamic acids in the following experiments because of its high activity and specificity.

DNA Cleavage Patterns Produced by Ph-DHA·VO(II) Complexes We investigated the effect of the rigid linking group of DHA on the DNA cleavage specificity.¹³⁾ It has been proposed that the diffusible hydroxyl radical is involved in the DNA cleavage by vanadyl and hydrogen peroxide via a Fenton-like mechanism.¹⁴⁾ If the phenylene linkage can restrict the position and orientation of the vanadyl complexing moieties directing them toward the affected nucleotide and increase the local concentration of the cleaving species, single-site DNA cleavage might be induced by the phenylene complexes. Figure 4 shows the 517 bp fragment cleavage patterns produced by Ph-DHA·VO(II) complexes. As shown in Fig. 4a, the **2a** complex produced the same doublet band as that seen for cleavage by the **1b** complex at the 3' side of site 2. The **2b** and **2c** complexes, which have a linker length close to the optimum **1b** complex, produced the expected singlet band at site 1. This single-site cleavage may be the effect of the restrained orientation of the vanadyl complexing moiety of these complexes. No single-site cleavage, however, was observed in the opposite strand analysis (Fig. 4b). All the phenylene hydroxamic acid complexes produced no significant DNA cleavage on the 3' end-labeled 517 bp fragment. The DNA cleavage specificities of Ph-DHA·VO(II) complexes were also examined using the 167 bp fragment (Fig. 5). Although the **2a** complex produced no cleavage at sites 3, 4 and 5, much less specific cleavage patterns were observed for cleavage by the **2b** and **2c** complexes at these sites (Fig. 5a). To our surprise, the 3' end-labeled fragment was not cleaved by all the phenylene hydroxamic acid complexes (Fig. 5b). This result is consistent with the cleavage of the 3'

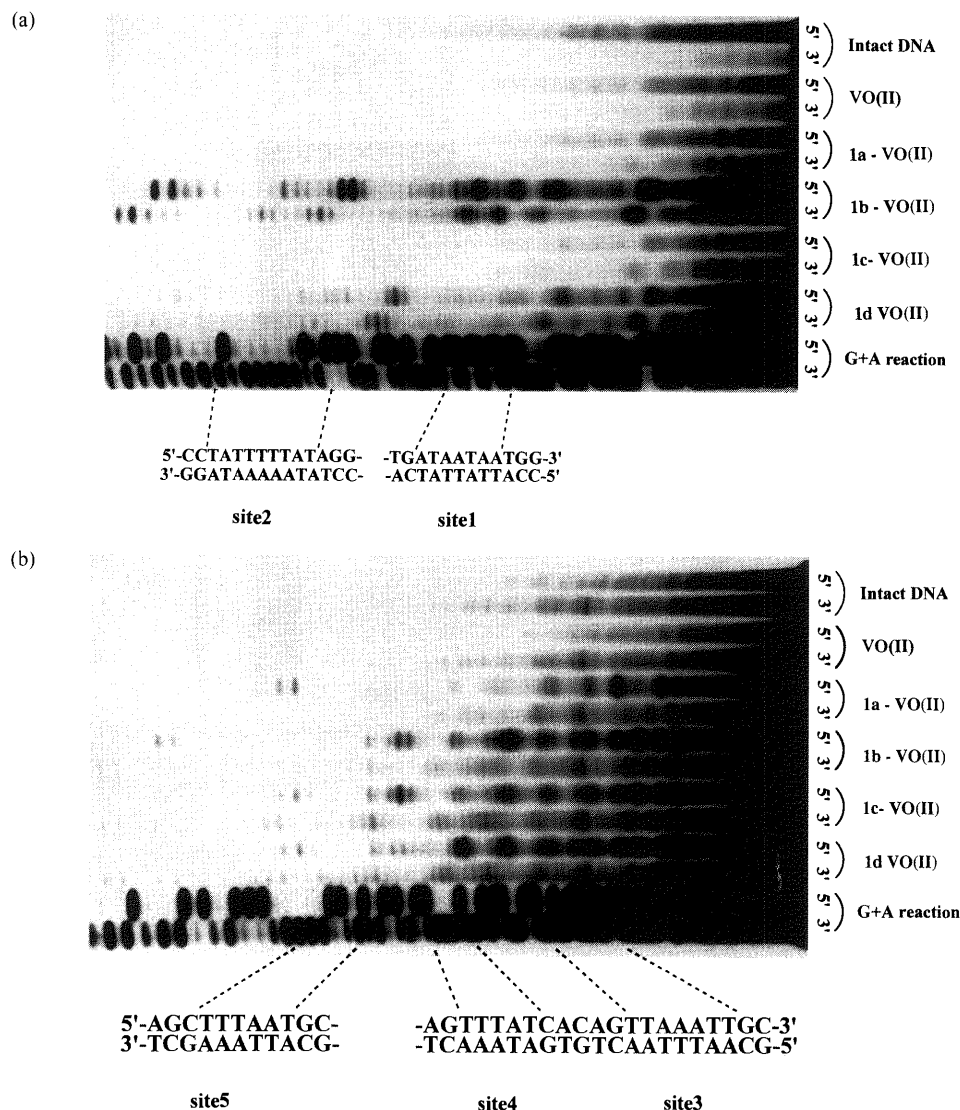


Fig. 2. Autoradiograms of a 10% Polyacrylamide Gel Showing Cleavage of End-Labeled 517 and 167 bp DNA Fragments by PM-DHA·VO(II) Complexes

In autoradiogram (a), the cleavage of the 5' end- and 3' end-labeled 517 bp fragments is alternatively sequenced. In autoradiogram (b), the cleavage of the 5' end- and 3' end-labeled 167 bp fragments is alternatively sequenced. End-labeled fragments were incubated with each hydroxamic acid (10 μ M) in the presence of vanadyl ion (10 μ M) and hydrogen peroxide (500 μ M) in 40 mM Tris-HCl (pH 8.0) at 37 °C for 3.0 h. In each reaction, sonicated calf thymus DNA was added to give a final concentration of 10 μ M (nucleotide concentration).

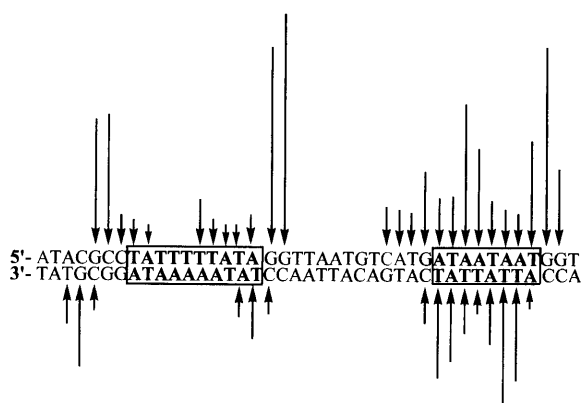


Fig. 3. Histograms of the Vanadyl Complex of the **1b** Cleavage Pattern Flanking Both Sites 1 (Right) and 2 (Left)

Bars indicate sites and extent of DNA cleavage.

end-labeled 517 bp fragment in Fig. 4b. It seems that the phenylene hydroxamic acid complexes bind tightly to one of the strands of pBR 322 DNA and not to the opposite strand.

Discussion

It was found that DNA cleavage by the vanadyl complexes of PM-DHA at the 8 and 10 AT sites was significantly influenced by the length of the polymethylene chain (Fig. 2a). At these AT contiguous sites, the vanadyl complex of tetramethylene compound **1b** afforded asymmetric and highly specific DNA cleavage patterns (Fig. 3). Asymmetric multiple cleavage patterns produced by the affinity cleaving agent show no association of the negatively charged Fe(II)·EDTA moiety with DNA and the generation of freely diffusible hydroxyl radical.³⁾ To attain highly specific DNA cleavage, the monohydroxamic acid vanadyl complex should associate with the DNA nucleotide. Vanadyl ion is known to strongly coordinate to the triphosphate group of ATP at neutral pH.¹⁵⁾ So, it is feasible to envisage the formation of a transient vanadyl

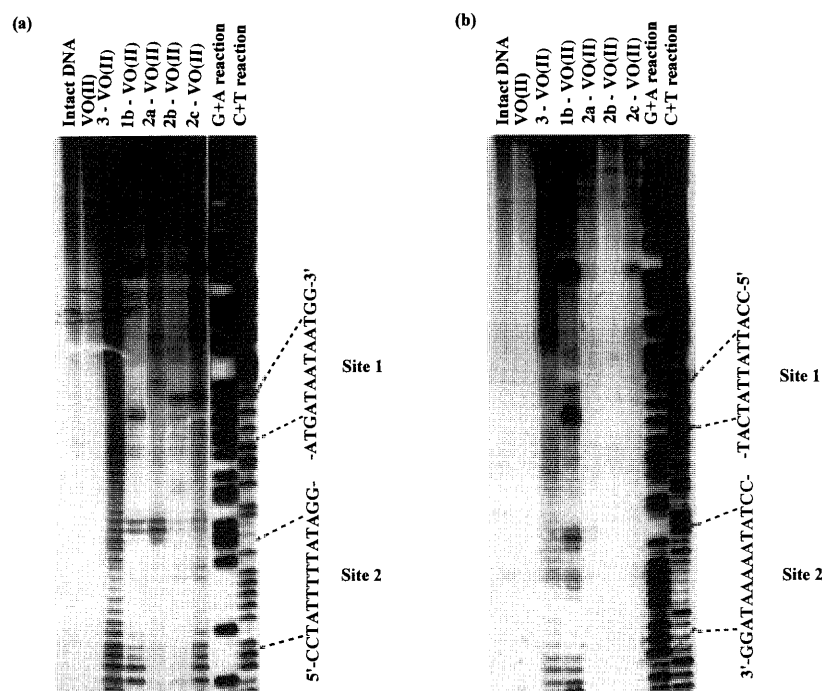


Fig. 4. Autoradiograms of a 10% Polyacrylamide Gel Showing Cleavage of the End-Labeled 517 bp DNA Fragment by Ph-DHA · VO(II) Complexes

Autoradiograms (a) and (b) show DNA fragments labeled at the (a) 5' end or (b) 3' end, respectively. End-labeled fragments were incubated with each hydroxamic acid (20 μ M) in the presence of vanadyl ion (20 μ M) and hydrogen peroxide (500 μ M) in 40 mM Tris-HCl (pH 8.0) at 37 °C for 5.0 h. In each reaction, sonicated calf thymus DNA was added to give a final concentration of 10 μ M (nucleotide concentration).

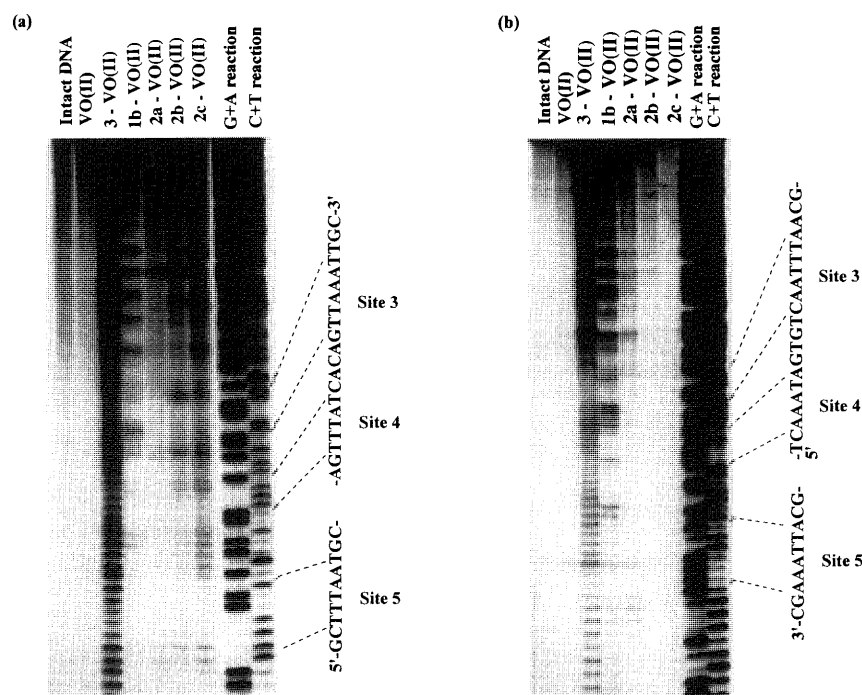


Fig. 5. Autoradiograms of a 10% Polyacrylamide Gel Showing Cleavage of the End-Labeled 167 bp DNA Fragment by Ph-DHA · VO(II) Complexes

Autoradiograms (a) and (b) show DNA fragments labeled at the (a) 5' end or (b) 3' end, respectively. The reaction conditions were the same as in Fig. 4.

complex with monohydroxamic acid and the phosphodiester of DNA.¹⁶⁾ The tetramethylene chain of **1b** may allow the transient complex to maintain a suitable position for the abstraction of the deoxyribose proton of DNA nucleotide. DNA cleavage by the vanadyl complex of **1b**—**d** at the 5 and 7 AT sites was almost independent of the length of the polymethylene chain (Fig. 2b). The vanadyl complex of **1b**, which showed highly specific DNA cleavage at the 8 and 10 AT

sites, afforded moderately specific cleavage patterns at these sites. The narrowness of the minor groove in B-DNA is known to depend on the local DNA sequence.^{3b,d,17)} This variation in local DNA structure will affect the groove binding mode of the distamycin moiety of the vanadyl complex of **1b**. We conclude that the DNA cleavage specificity of the vanadyl complex of distamycin-linked hydroxamic acid is a function of the binding affinity, which is based on a combina-

tion of tripyrrolepeptides and the monohydroxamic acid complex, and a sequence-dependent DNA structure.

It was expected that the vanadyl complexes of conformationally rigid Ph-DHA would exhibit more specific cleavage than the flexible PM-DHA complexes. Although the **2b** and **2c** complexes, which have a linker length close to the optimum **1b** complex, produced a single-site DNA cleavage at the 8 AT site (Fig. 4a), these complexes produced much less specific cleavage patterns at other AT sites (Fig. 5a). In addition, these complexes failed to cleave the 3' end-labeled sequences of AT-rich DNA (Fig. 4b, 5b). These complexes seem to selectively recognize one of the strands of AT-rich DNA and we believe that the van der Waals interaction between the benzene rings of phenylene hydroxamic acids and the Waals of the minor groove allows the monohydroxamic acid complex to direct itself away from the opposite strand of DNA. This unfavorable interaction may prevent the distamycin and vanadyl complexing moieties from synergistically binding to the AT sequence, which would lead to a reduction in the binding selectivity of the vanadyl complex of phenylene hydroxamic acid for the AT sequence.

In conclusion, we have synthesized DHAs and evaluated the effect of the length and rigidity of their chains on the DNA cleavage specificity in the presence of vanadyl ion. The tetramethylene chain was found to be the optimal linking group for connecting the distamycin and hydroxamic acid moieties. A suitably designed linking moiety would allow the creation of a more potent and sequence-specific DHA system.

Experimental

General Methods The evaporation of solvents was carried out in a rotary evaporator under reduced pressure. Dimethylformamide (DMF) was dried over anhydrous magnesium sulfate overnight and distilled under reduced pressure. Melting points were determined using a Yanagimoto micro-melting point apparatus and are uncorrected. The IR spectra were obtained using KBr discs on a Shimadzu IR-470 and only the principal peaks are reported. The UV spectra were recorded on a Shimadzu UV-2100 instrument. The ¹H-NMR spectra were recorded on a JEOL JNM-EX 400 (400 MHz) spectrometer using tetramethylsilane (TMS) as the internal reference. The low-resolution (LR) and high-resolution (HR) FAB-MS spectra were recorded on a JEOL JMS-SX102A instrument. TLC was performed on precoated aluminum sheets of Silica gel 60F₂₅₄ (Merck, No. 5554). The TLC systems were as follows: system A, 0.49% concentrated aqueous ammonia in 15% MeOH-CHCl₃; system B, 0.49% concentrated aqueous ammonia in 20% MeOH-CHCl₃; system C, *n*-BuOH-AcOH-H₂O in a 4 : 1 : 2 ratio. Silica gel column chromatography was carried out using a Fuji Silysia Chemical BW-127ZH. Polystyrene resin DIAION HP 20 was purchased from the Mitsubishi Chemical Co. Yields refer to chromatographically and spectroscopically (¹H-NMR) homogeneous materials.

Plasmid pBR 322 DNA was isolated from *Escherichia coli* strain JM109 by alkali lysis and was purified by precipitation with polyethylene glycol.¹⁸⁾ [γ -³²P]ATP (3000 Ci/mmol) and [α -³²P]dATP (3000 Ci/mmol) were obtained from NEN-Dupont. The microfine glass beads and chaotropic salt buffer were from Bio 101. Chemical DNA sequencing was carried out according to the method of Maxam and Gilbert.¹⁹⁾ All enzymes used were from commercial sources. Vanadyl sulfate trihydrate was purchased from Aldrich Chem. Co. and used without further purification.

4-[[[4-[[[4-[[4-(Methoxycarbonyl)butyryl]amino]-1-methyl-2-pyrrolyl]-carbonyl]amino]-1-methyl-2-pyrrolyl]carbonyl]amino]-1-methyl-N-[3-(*N,N*-dimethylamino)propyl]-2-pyrrolocarboxamide (5a**)]** A solution of compound **4** (1.0 g, 2.0 mmol) in MeOH (5.0 ml) was hydrogenated over PtO₂ (0.015 g) at room temperature and atmospheric pressure. After the calculated amount of hydrogen was taken up, the mixture was filtered through Celite. The filtrate was concentrated *in vacuo*, and the evaporation was repeated with some DMF. After the residue was cooled to 0 °C, methyl 5-[(*p*-nitrophenoxy)carbonyl]butyrate (0.53 g, 2.0 mmol) in dry DMF (3.0 ml) was added. The reaction mixture was stirred at 0 °C for 1 h and then at room tem-

perature overnight. The DMF was evaporated *in vacuo*, and the resulting residue was dissolved in CHCl₃. The organic phase was washed with two portions of 5% aqueous K₂CO₃ and dried over anhydrous Na₂SO₄. After removal of the solvent, the residue was purified by silica gel chromatography. Elution with a stepwise gradient of 5% and 10% MeOH in 0.49% concentrated aqueous ammonia-CHCl₃ provided pure **5a** as a yellow crystalline solid (0.44 g, 37%), *R*_f=0.34 (system A), mp 115–118 °C. IR (KBr) cm⁻¹: 3290, 2950, 1730 (C=O ester), 1640, 1580, 1530. ¹H-NMR (DMSO-*d*₆) δ : 1.62 (2H, t, *J*=7.2 Hz), 1.83 (2H, t, *J*=7.2 Hz), 2.14 (6H, s), 2.23–2.30 (4H, m), 2.35 (2H, t, *J*=7.6 Hz), 3.20 (2H, t, *J*=6.4 Hz), 3.60 (3H, s), 3.80, 3.84, 3.85 (3H \times 3, s), 6.83 (1H, s), 6.88 (1H, s), 7.04 (1H, s), 7.16 (1H, s), 7.19 (1H, s), 7.24 (1H, s), 8.07 (1H, s), 9.82 (1H, s), 9.89 (1H, s), 9.90 (1H, s). FAB-LR-MS *m/z*: 597 (MH⁺, 84%), 251 ((CONHpyrroleCONH(CH₂)₃-N(CH₃)₂)⁺, 36), 73 ((H₃COCOCH₂)⁺, 99).

4-[[[4-[[[4-[[5-(Ethoxycarbonyl)valery]amino]-1-methyl-2-pyrrolyl]-carbonyl]amino]-1-methyl-2-pyrrolyl]carbonyl]amino]-1-methyl-N-[3-(*N,N*-dimethylamino)propyl]-2-pyrrolocarboxamide (5b**)]** A synthetic procedure similar to that for compound **5a** was followed for the preparation of **5b**: yellow crystalline solid (yield: 35%), *R*_f=0.37 (system A), mp 100–105 °C. IR (KBr) cm⁻¹: 3290, 2940, 1730 (C=O ester), 1640, 1580, 1530. ¹H-NMR (DMSO-*d*₆) δ : 1.18 (3H, t, *J*=7.2 Hz), 1.54–1.64 (6H, m), 2.15 (6H, s), 2.24–2.27 (4H, m), 2.31 (2H, t, *J*=6.8 Hz), 3.20 (2H, t, *J*=6.8 Hz), 3.81, 3.84, 3.86 (3H \times 3, s), 4.05 (2H, q, *J*=7.2 Hz), 6.83 (1H, d, *J*=1.6 Hz), 6.89 (1H, d, *J*=1.6 Hz), 7.04 (1H, d, *J*=2.0 Hz), 7.16 (1H, d, *J*=1.2 Hz), 7.19 (1H, d, *J*=1.2 Hz), 7.24 (1H, d, *J*=1.2 Hz), 8.07 (1H, s), 9.78 (1H, s), 9.88 (1H, s), 9.90 (1H, s). FAB-LR-MS *m/z*: 625 (MH⁺, 26%), 279 ((H₃C₂OCO(CH₂)₄CONHpyrroleCO)⁺, 60).

4-[[[4-[[[4-[[6-(Ethoxycarbonyl)hexanoyl]amino]-1-methyl-2-pyrrolyl]carbonyl]amino]-1-methyl-2-pyrrolyl]carbonyl]amino]-1-methyl-N-[3-(*N,N*-dimethylamino)propyl]-2-pyrrolocarboxamide (5c**)]** A synthetic procedure similar to that for compound **5a** was followed for the preparation of **5c**: yellow crystalline solid (yield: 32%), *R*_f=0.40 (system A), mp 110.5–112.5 °C. IR (KBr) cm⁻¹: 3290, 2930, 1730 (C=O ester), 1650, 1580, 1530. ¹H-NMR (DMSO-*d*₆) δ : 1.17 (3H, t, *J*=7.2 Hz), 1.23–1.32 (2H, m), 1.51–1.63 (6H, m), 2.14 (3H, s), 2.21–2.30 (6H, m), 3.20 (2H, t, *J*=6.6 Hz), 3.80, 3.81, 3.83 (3H \times 3, s), 4.04 (2H, q, *J*=7.2 Hz), 6.84 (1H, s), 6.88 (1H, s), 7.04 (1H, s), 7.16 (1H, s), 7.19 (1H, s), 7.23 (1H, s), 8.08 (1H, s), 9.79 (1H, s), 9.89 (1H, s), 9.90 (1H, s). FAB-LR-MS *m/z*: 639 (MH⁺, 100%), 293 ((H₃C₂OCO(CH₂)₅CONHpyrroleCO)⁺, 45).

4-[[[4-[[[4-[[7-(Methoxycarbonyl)heptanoyl]amino]-1-methyl-2-pyrrolyl]carbonyl]amino]-1-methyl-2-pyrrolyl]carbonyl]amino]-1-methyl-N-[3-(*N,N*-dimethylamino)propyl]-2-pyrrolocarboxamide (5d**)]** A synthetic procedure similar to that for compound **5a** was followed for the preparation of **5d**: yellow solid (yield: 31%), *R*_f=0.41 (system A), mp 91–93.5 °C. IR (KBr) cm⁻¹: 3290, 2950, 1730 (C=O ester), 1640, 1575, 1525. ¹H-NMR (DMSO-*d*₆) δ : 1.28 (4H, m), 1.51–1.63 (6H, m), 2.10, 2.14 (3H \times 2, s), 2.21–2.31 (6H, m), 3.19 (2H, t, *J*=6.4 Hz), 3.58 (3H, s), 3.82, 3.83, 3.85 (3H \times 3, s), 6.83 (1H, d, *J*=1.6 Hz), 6.88 (1H, d, *J*=1.2 Hz), 7.03 (1H, d, *J*=2.0 Hz), 7.16 (1H, d, *J*=1.2 Hz), 7.19 (1H, s), 7.24 (1H, s), 8.07 (1H, s), 9.77 (1H, s), 9.88 (1H, s), 9.90 (1H, s). FAB-LR-MS *m/z*: 639 (MH⁺, 92%), 293 ((H₃COCO(CH₂)₆CONHpyrroleCO)⁺, 23).

4-[[[4-[[[4-[[*o*-(Methoxycarbonyl)phenylenecarbonyl]amino]-1-methyl-2-pyrrolyl]carbonyl]amino]-1-methyl-2-pyrrolyl]carbonyl]amino]-1-methyl-N-[3-(*N,N*-dimethylamino)propyl]-2-pyrrolocarboxamide (6a**)]** To a solution of [*o*-(methoxycarbonylmethyl)phenyl]acetic acid (0.083 g, 0.40 mmol) in dry DMF (3 ml) was added 1-hydroxybenzotriazole (HOBt) (0.070 g, 0.52 mmol). The mixture was cooled to 0 °C, and DCC (0.090 g, 0.44 mmol) was added dropwise. The reaction mixture was stirred at room temperature for 4 h. Separately, a solution of compound **4** (0.20 g, 0.40 mmol) in MeOH (5 ml) was hydrogenated over PtO₂ (0.010 g) at room temperature and atmospheric pressure. After the calculated amount of hydrogen was taken up, the mixture was filtered through Celite. The filtrate was concentrated *in vacuo*, and the concentration was repeated with some DMF. Immediately, the solution of DCC-activated phenylene monoester was cooled to 0 °C and the aromatic amine was added dropwise. The reaction mixture was stirred at 0 °C for 30 min and then at room temperature overnight. The DMF was evaporated *in vacuo*, and the resulting residue was dissolved in AcOEt. The organic phase was washed with two portions of 5% aqueous K₂CO₃ and dried over anhydrous Na₂SO₄. After removal of the solvent, the residue was purified by flash chromatography. Elution with 0.49% concentrated aqueous ammonia in 5% MeOH-CHCl₃ provided pure **6a** as pale-yellow microcrystals (0.14 g, 53%), *R*_f=0.55 (system B), mp 122–127 °C. IR (KBr) cm⁻¹: 3290, 2940, 1730 (C=O ester), 1650, 1580, 1530. ¹H-NMR (DMSO-*d*₆) δ : 1.64 (2H, m), 2.21 (6H, s), 2.33 (2H, t, *J*=6.8 Hz),

3.19 (2H, t, $J=6.8$ Hz), 3.61 (5H, s), 3.81 (2H, s), 3.83, 3.84, 3.85 (3H \times 3, s), 6.84 (1H, d, $J=2.0$ Hz), 6.90 (1H, d, $J=1.6$ Hz), 7.03 (1H, d, $J=2.0$ Hz), 7.14 (1H, d, $J=2.0$ Hz), 7.18 (1H, d, $J=1.6$ Hz), 7.21—7.30 (5H, m), 8.07 (1H, s), 9.87 (1H, s), 9.89 (1H, s), 10.04 (1H, s).

4-[[[4-[[[4-[[*m*-(Methoxycarbonyl)phenyl]enecarbonyl]amino]-1-methyl-2-pyrrolyl]carbonyl]amino]-1-methyl-2-pyrrolyl]carbonyl]amino]-1-methyl-*N*-[3-(*N,N*-dimethylamino)propyl]-2-pyrrolicarboxamide (6b) A synthetic procedure similar to that for compound **6a** was followed for the preparation of **6b**: Pale-yellow microcrystals (yield: 40%), $R_f=0.55$ (system B), mp 115—119 °C. IR (KBr) cm^{-1} : 3290, 2920, 2850, 1730 (C=O ester), 1640, 1580, 1530. $^1\text{H-NMR}$ (DMSO- d_6) δ : 1.61 (2H, m), 2.14 (6H, s), 2.25 (2H, t, $J=7.2$ Hz), 3.18 (2H, t, $J=6.4$ Hz), 3.55 (2H, s), 3.61 (3H, s), 3.66 (2H, s), 3.80, 3.83, 3.84 (3H \times 3, s), 6.82 (1H, d, $J=1.6$ Hz), 6.90 (1H, d, $J=1.6$ Hz), 7.02 (1H, d, $J=1.6$ Hz), 7.13—7.27 (7H, m), 8.07 (1H, s), 9.89 (1H, s), 9.90 (1H, s), 10.08 (1H, s).

4-[[[4-[[[4-[[*p*-(Methoxycarbonyl)phenyl]enecarbonyl]amino]-1-methyl-2-pyrrolyl]carbonyl]amino]-1-methyl-2-pyrrolyl]carbonyl]amino]-1-methyl-*N*-[3-(*N,N*-dimethylamino)propyl]-2-pyrrolicarboxamide (6c) A synthetic procedure similar to that for compound **6a** was followed for the preparation of **6c**: Pale-yellow microcrystals (yield: 41%), $R_f=0.55$ (system B), mp 117—121 °C. IR (KBr) cm^{-1} : 3290, 2950, 1730 (C=O ester), 1640, 1580, 1530. $^1\text{H-NMR}$ (DMSO- d_6) δ : 1.62 (2H, m), 2.17 (6H, s), 2.29 (2H, t, $J=6.8$ Hz), 3.18 (2H, t, $J=6.8$ Hz), 3.54 (2H, s), 3.60 (3H, s), 3.65 (2H, s), 3.80, 3.82, 3.84 (3H \times 3, s), 6.83 (1H, d, $J=1.6$ Hz), 6.89 (1H, d, $J=2.0$ Hz), 7.02 (1H, d, $J=1.6$ Hz), 7.15—7.28 (7H, m), 8.08 (1H, s), 9.89 (1H, s), 9.90 (1H, s), 10.06 (1H, s).

4-[[[4-[[[4-[[4-(Hydroxyaminocarbonyl)butyl]amino]-1-methyl-2-pyrrolyl]carbonyl]amino]-1-methyl-2-pyrrolyl]carbonyl]amino]-1-methyl-*N*-[3-(*N,N*-dimethylamino)propyl]-2-pyrrolicarboxamide (1a) Separate solutions of hydroxylamine hydrochloride (0.20 g, 2.9 mmol) in MeOH (2.5 ml), KOH (0.35 g, 6.2 mmol) in MeOH (3.0 ml) and compound **5a** (0.30 g, 0.48 mmol) in MeOH (3.0 ml) were prepared. The solution containing alkali was added *via* a syringe to the stirred hydroxylamine solution, and the mixture was allowed to stand in ice-water for 3 min under an argon atmosphere. To the alkaline mixture was added the solution of compound **5a** *via* a syringe, and the reaction mixture was then stirred overnight at room temperature under an argon atmosphere. The reaction was terminated by the addition of 2.0 M aqueous HCl (1.7 ml, 3.4 mmol) to the mixture which was then filtered to remove the salt. The filtrate was evaporated and the residue was taken up in 50% MeOH-EtOH and filtered. This procedure was repeated once more and then the filtrate was evaporated. The residue dissolved in H_2O was applied to an HP 20 column, which was successively washed with deionized H_2O . Elution with 50% MeOH- H_2O followed by evaporation of the appropriate fractions provided pure **1a** as a light-brown glassy solid (0.22 g, 70%), $R_f=0.47$ (system C), mp 151.5—154 °C. IR (KBr) cm^{-1} : 3250, 1650, 1635. $\lambda_{\text{max}}(\text{H}_2\text{O})/\text{nm}$ 300 (log $\epsilon=4.32$). $^1\text{H-NMR}$ (DMSO- d_6) δ : 1.80 (4H, m), 1.99 (2H, t, $J=7.2$ Hz), 2.24 (2H, t, $J=6.8$ Hz), 2.70 (3H, s), 2.72 (3H, s), 3.01 (2H, t, $J=6.0$ Hz), 3.24 (2H, m), 3.80, 3.83, 3.84 (3H \times 3, s), 6.89 (1H, s), 6.92 (1H, d, $J=2.0$ Hz), 7.05 (1H, s), 7.16 (1H, d, $J=1.2$ Hz), 7.19 (1H, s), 7.23 (1H, s), 8.18 (1H, s), 8.70 (1H, brs), 9.87 (1H, s), 9.92 (2H, s), 10.41 (1H, s). FAB-LR-MS m/z : 598 (M^+-Cl , 82%). FAB-HR-MS m/z : 598.3111 (Calcd for $\text{C}_{28}\text{H}_{40}\text{N}_9\text{O}_6$ M^+-Cl : 598.3101).

4-[[[4-[[[4-[[5-(Hydroxyaminocarbonyl)valeryl]amino]-1-methyl-2-pyrrolyl]carbonyl]amino]-1-methyl-2-pyrrolyl]carbonyl]amino]-1-methyl-*N*-[3-(*N,N*-dimethylamino)propyl]-2-pyrrolicarboxamide (1b) A synthetic procedure similar to that for **1a** was followed for the preparation of **1b**: Light-brown glassy solid (yield: 53%), $R_f=0.44$ (system C), mp 144—147.5 °C. IR (KBr) cm^{-1} : 3250, 1650, 1635. $\lambda_{\text{max}}(\text{H}_2\text{O})/\text{nm}$ 300 (log $\epsilon=4.27$). $^1\text{H-NMR}$ (DMSO- d_6) δ : 1.53 (4H, m), 1.84 (2H, m), 1.98 (2H, t, $J=6.6$ Hz), 2.22 (2H, t, $J=6.4$ Hz), 2.69 (6H, s), 2.98 (2H, t, $J=7.6$ Hz), 3.24 (2H, t, $J=5.6$ Hz), 3.82, 3.84, 3.85 (3H \times 3, s), 6.89 (1H, d, $J=2.0$ Hz), 6.93 (1H, d, $J=1.6$ Hz), 7.06 (1H, d, $J=1.6$ Hz), 7.16 (1H, d, $J=1.6$ Hz), 7.19 (1H, s), 7.24 (1H, s), 8.18 (1H, t, $J=5.3$ Hz), 8.70 (1H, brs), 9.84 (1H, s), 9.92 (2H, s), 10.41 (1H, s). FAB-LR-MS m/z : 612 (M^+-Cl , 68%). FAB-HR-MS m/z : 612.3258 (Calcd for $\text{C}_{29}\text{H}_{42}\text{N}_9\text{O}_6$ M^+-Cl : 612.3244).

4-[[[4-[[[4-[[6-(Hydroxyaminocarbonyl)hexanoyl]amino]-1-methyl-2-pyrrolyl]carbonyl]amino]-1-methyl-2-pyrrolyl]carbonyl]amino]-1-methyl-*N*-[3-(*N,N*-dimethylamino)propyl]-2-pyrrolicarboxamide (1c) A synthetic procedure similar to that for **1a** was followed for the preparation of **1c**: Yellow crystalline solid (yield: 57%), $R_f=0.45$ (system C), mp 151—154 °C. IR (KBr) cm^{-1} : 3250, 1640. $\lambda_{\text{max}}(\text{H}_2\text{O})/\text{nm}$ 299 (log $\epsilon=4.34$). $^1\text{H-NMR}$ (DMSO- d_6) δ : 1.27 (2H, m), 1.50—1.58 (4H, m), 1.88 (2H, m), 1.95 (2H, t, $J=7.2$ Hz), 2.23 (2H, t, $J=7.0$ Hz), 2.74, 2.77 (3H \times 2, s), 3.04 (2H, t,

$J=7.8$ Hz), 3.27 (2H, m), 3.82, 3.84, 3.85 (3H \times 3, s), 6.90 (1H, d, $J=1.2$ Hz), 6.94 (1H, d, $J=1.6$ Hz), 7.06 (1H, d, $J=1.6$ Hz), 7.16 (1H, s), 7.19 (1H, s), 7.24 (1H, s), 8.18 (1H, brs), 8.68 (1H, brs), 9.82 (1H, s), 9.92 (2H, s), 10.38 (1H, s). FAB-LR-MS m/z : 626 (M^+-Cl , 73%). FAB-HR-MS m/z : 626.3411 (Calcd for $\text{C}_{30}\text{H}_{44}\text{N}_9\text{O}_6$ M^+-Cl : 626.3414).

4-[[[4-[[[4-[[7-(Hydroxyaminocarbonyl)heptanoyl]amino]-1-methyl-2-pyrrolyl]carbonyl]amino]-1-methyl-2-pyrrolyl]carbonyl]amino]-1-methyl-*N*-[3-(*N,N*-dimethylamino)propyl]-2-pyrrolicarboxamide (1d) A synthetic procedure similar to that for **1a** was followed for the preparation of **1d**: Light-yellow crystalline solid (yield: 63%), $R_f=0.46$ (system C), mp 149.5—152.5 °C. IR (KBr) cm^{-1} : 3250, 1645, 1635. $\lambda_{\text{max}}(\text{H}_2\text{O})/\text{nm}$ 300 (log $\epsilon=4.32$). $^1\text{H-NMR}$ (DMSO- d_6) δ : 1.26 (4H, m), 1.48 (2H, m), 1.55 (2H, m), 1.86 (2H, t, $J=7.6$ Hz), 1.94 (2H, t, $J=7.2$ Hz), 2.22 (2H, t, $J=7.2$ Hz), 2.72 (6H, s), 3.02 (2H, t, $J=7.6$ Hz), 3.24 (2H, m), 3.81, 3.83, 3.84 (3H \times 3, s), 6.89 (1H, d, $J=2.0$ Hz), 6.92 (1H, d, $J=1.6$ Hz), 7.05 (1H, d, $J=2.0$ Hz), 7.16 (1H, s), 7.19 (1H, s), 7.24 (1H, s), 8.18 (1H, s), 8.68 (1H, brs), 9.83 (1H, s), 9.93 (2H, s), 10.37 (1H, s). FAB-LR-MS m/z : 640 (M^+-Cl , 27%). FAB-HR-MS m/z : 640.3582 (Calcd for $\text{C}_{31}\text{H}_{46}\text{N}_9\text{O}_6$ M^+-Cl : 640.3571).

4-[[[4-[[[4-[[*o*-(Hydroxyaminocarbonyl)phenyl]enecarbonyl]amino]-1-methyl-2-pyrrolyl]carbonyl]amino]-1-methyl-2-pyrrolyl]carbonyl]amino]-1-methyl-*N*-[3-(*N,N*-dimethylamino)propyl]-2-pyrrolicarboxamide (2a) Separate solutions of hydroxylamine hydrochloride (0.062 g, 0.89 mmol) in MeOH (2.0 ml), NaOH (0.071 g, 1.8 mmol) in MeOH (2.0 ml) and compound **6a** (0.10 g, 0.15 mmol) in MeOH (2.0 ml) were prepared and reacted as described in the procedure for **1a**. Purification using a Serva XAD-II polystyrene resin column and elution with 50% MeOH- H_2O provided pure **2a** as light-brown microcrystals (0.074 g, 75%), $R_f=0.50$ (system C), mp 138—144 °C. $\lambda_{\text{max}}(\text{H}_2\text{O})/\text{nm}$ 303 (log $\epsilon=4.51$). $^1\text{H-NMR}$ (DMSO- d_6) δ : 1.87 (2H, m), 2.75 (6H, s), 3.05 (2H, t, $J=6.4$ Hz), 3.25 (2H, t, $J=5.6$ Hz), 3.27 (2H, s), 3.74 (2H, s), 3.81, 3.82, 3.84 (3H \times 3, s), 6.91 (1H, s), 6.93 (1H, s), 7.04 (1H, s), 7.16 (1H, s), 7.17 (1H, s), 7.18 (1H, s), 7.23—7.29 (4H, m), 8.17 (1H, t, $J=5.6$ Hz), 9.91 (2H, s), 10.05 (1H, s), 10.80 (1H, s). FAB-LR-MS m/z : 660 (M^+-Cl , 33%), 245 ((pyrroleCONH $_2$ +H) $^+$, 12). FAB-HR-MS m/z : 660.3262 (Calcd for $\text{C}_{33}\text{H}_{42}\text{N}_9\text{O}_6$ M^+-Cl : 660.3258).

4-[[[4-[[[4-[[*m*-(Hydroxyaminocarbonyl)phenyl]enecarbonyl]amino]-1-methyl-2-pyrrolyl]carbonyl]amino]-1-methyl-2-pyrrolyl]carbonyl]amino]-1-methyl-*N*-[3-(*N,N*-dimethylamino)propyl]-2-pyrrolicarboxamide (2b) A synthetic procedure similar to that for **2a** was followed for the preparation of **2b**: yellow microcrystals (yield: 66%), $R_f=0.50$ (system C), mp 135—143 °C. $\lambda_{\text{max}}(\text{H}_2\text{O})/\text{nm}$ 302 (log $\epsilon=4.43$). $^1\text{H-NMR}$ (DMSO- d_6) δ : 1.86 (2H, m), 2.74 (6H, s), 3.03 (2H, t, $J=7.6$ Hz), 3.24 (2H, t, $J=5.6$ Hz), 3.27 (2H, s), 3.55 (2H, s), 3.82, 3.83, 3.84 (3H \times 3, s), 6.92 (1H, d, $J=2.0$ Hz), 6.93 (1H, d, $J=1.6$ Hz), 7.04 (1H, d, $J=2.0$ Hz), 7.12—7.26 (7H, m), 8.17 (1H, s), 8.83 (1H, s), 9.92 (2H, s), 10.13 (1H, s), 10.69 (1H, s). FAB-LR-MS m/z : 660 (M^+-Cl , 31%). FAB-HR-MS m/z : 660.3260 (Calcd for $\text{C}_{33}\text{H}_{42}\text{N}_9\text{O}_6$ M^+-Cl : 660.3258).

4-[[[4-[[[4-[[*p*-(Hydroxyaminocarbonyl)phenyl]enecarbonyl]amino]-1-methyl-2-pyrrolyl]carbonyl]amino]-1-methyl-2-pyrrolyl]carbonyl]amino]-1-methyl-*N*-[3-(*N,N*-dimethylamino)propyl]-2-pyrrolicarboxamide (2c) A synthetic procedure similar to that for **2a** was followed for the preparation of **2c**: yellow microcrystals (yield: 69%), $R_f=0.50$ (system C), mp 139—146 °C. $\lambda_{\text{max}}(\text{H}_2\text{O})/\text{nm}$ 301 (log $\epsilon=4.28$). $^1\text{H-NMR}$ (DMSO- d_6) δ : 1.84 (2H, m), 2.73 (6H, s), 3.02 (2H, t, $J=7.2$ Hz), 3.25 (4H, s), 3.53 (2H, s), 3.81, 3.82, 3.84 (3H \times 3, s), 6.90 (1H, d, $J=1.6$ Hz), 6.93 (1H, d, $J=2.0$ Hz), 7.04 (1H, d, $J=1.6$ Hz), 7.14 (1H, d, $J=1.6$ Hz), 7.18—7.25 (6H, m), 8.17 (1H, s), 9.90 (1H, s), 9.91 (1H, s), 10.06 (1H, s), 10.65 (1H, s). FAB-LR-MS m/z : 660 (M^+-Cl , 10%). FAB-HR-MS m/z : 660.3267 (Calcd for $\text{C}_{33}\text{H}_{42}\text{N}_9\text{O}_6$ M^+-Cl : 660.3258).

Preparation of 5'- ^{32}P End-Labeled Restriction Fragments Plasmid pBR 322 DNA was linearized with restriction endonuclease *Eco*RI, dephosphorylated with calf intestine alkaline phosphatase, then 5'- ^{32}P end-labeled with T4 polynucleotide kinase and [γ - ^{32}P]ATP.¹¹⁾ Digestion with *Rsa*I afforded the 167 and 517 bp fragments, which were purified on 4% sieve agarose gel. The gel was visualized by autoradiography, the bands of interest were excised from the gel, and the DNAs were isolated by the glass matrix method.²⁰⁾

Preparation of 3'- ^{32}P End Labeled Restriction Fragments Plasmid pBR 322 was digested with *Eco*RI and the linearized DNA was recovered by ethanol precipitation. The DNA was 3'- ^{32}P end-labeled with the Klenow fragment of DNA polymerase I and [α - ^{32}P]dATP.¹¹⁾ Digestion with the second enzyme *Rsa*I afforded the singly end-labeled 167 and 517 bp fragments, which were isolated as described in the preparation of the 5'- ^{32}P labeled

fragments.

Cleavage Reactions of Labeled DNA Fragments by the Vanadyl Complexes of Hydroxamic Acids The reaction mixtures contained 10 μ M (nucleotide concentration) sonicated calf thymus DNA and 10000–50000 cpm of the 5'- or 3'-³²P labeled DNA fragment in 40 mM Tris-Cl (pH 8.0). The reactions were initiated by the addition of the appropriate concentration of hydroxamic acid, vanadyl sulfate and hydrogen peroxide. The reaction mixtures were maintained at 37 °C for 3 or 5 h and stopped by the addition of stopping buffer (0.3 M AcONa, pH 7.0, 0.1 mM EDTA, 25 μ g/ml tRNA) followed by ethanol precipitation. The precipitated DNA was washed with 70% cold ethanol and dried *in vacuo*. The recovered DNA was dissolved in 5 μ l of loading buffer (80% v/v formamide, 10 mM NaOH, 1 mM EDTA, 0.1% bromophenol blue, 0.1% xylene cyanol). All DNA samples were heated at 90 °C for 3 min and loaded on a 10% polyacrylamide, 8 M urea sequencing gel. Electrophoresis was performed at 1500 V for approximately 2.5 h. Autoradiography of the gel was carried out at -80 °C with an intensifying screen on Fuji medical X-ray film. Densitometry of the gel was performed with a computer program, NIH image.

References and Notes

- 1) a) Kane S. A., Hecht S. M., *Prog. Nucleic Acid Res. Mol. Biol.*, **49**, 313–352 (1994); b) Quada, J. C., Jr., Zuber G. F., Hecht S. M., *Pure and Appl. Chem.*, **70**, 307–311 (1998).
- 2) a) Manderville R. A., Ellena J. F., Hecht S. M., *J. Am. Chem. Soc.*, **117**, 7891–7903 (1995); b) Sucheck S. J., Ellena J. F., Hecht S. M., *ibid.*, **120**, 7450–7460 (1998).
- 3) a) Schultz P. G., Dervan P. B., *J. Am. Chem. Soc.*, **105**, 7748–7750 (1983); b) Youngquist R. S., Dervan P. B., *Proc. Natl. Acad. Sci. U.S.A.*, **82**, 2565–2569 (1985); c) Youngquist R. S., Dervan P. B., *J. Am. Chem. Soc.*, **107**, 5528–5529 (1985); d) Dervan P. B., *Science*, **232**, 464–471 (1986).
- 4) a) Otsuka M., Masuda T., Haupt A., Ohno M., Shiraki T., Sugiura Y., Maeda K., *J. Am. Chem. Soc.*, **112**, 838–845 (1990); b) Bailly C., Sun J. S., Colson P., Houssier C., Helene C., Waring M. J., Henichart J. P., *Bioconjugate Chem.*, **3**, 100–103 (1992); c) Routier S., Bernier J. L., Catteau J. P., Bailly C., *Bioorg. Med. Chem. Lett.*, **7**, 1729–1732 (1997).
- 5) a) Oakley M. G., Turnbull K. D., Dervan P. B., *Bioconjugate Chem.*, **5**, 242–247 (1994); b) Semmelhack M. F., Gallagher J. J., *J. Org. Chem.*, **59**, 4357–4359 (1994).
- 6) Chatterjee B., *Coord. Chem. Rev.*, **26**, 281–303 (1978).
- 7) a) Fisher D. C., Barclay-Peet S. J., Balfe C. A., Raymond K. N., *Inorg. Chem.*, **28**, 4399–4406 (1989); b) Shechter Y., Shisheva A., Lazar R., Libman J., Shanzer A., *Biochemistry*, **31**, 2063–2068 (1992).
- 8) a) Hashimoto S., Yamamoto K., Yamada T., Nakamura Y., *Heterocycles*, **48**, 939–947 (1998); b) Hashimoto S., Itai K., Takeuchi Y., Nakamura Y., *Nucleic Acids Symp. Ser.*, **39**, 37–38 (1998).
- 9) Distamycin analogues having *n* amides characteristically bind to *n*+1 successive base pairs of AT DNA. According to this rule, the binding site size of PM-DHA and Ph-DHA is five base pairs.
- 10) Hashimoto S., Itai K., Takeuchi Y., Nakamura Y., *Heterocycl. Commun.*, **3**, 307–315 (1997).
- 11) Sambrook J., Fritsch E. F., Maniatis T., "Molecular Cloning, A Laboratory Manual," 2nd ed., Cold Spring Harbor Laboratory Press, New York, 1989, pp. 10.51–10.66.
- 12) a) Hashimoto S., Yamamoto K., Nakamura Y., *Nucleic Acids Symp. Ser.*, **37**, 7–8 (1997); b) Hashimoto S., Nakamura Y., *Chem. Pharm. Bull.*, **46**, 1941–1943 (1998).
- 13) The DNA cleavage abilities of Ph-DHA·VO(II) complexes were also examined by plasmid conversion assay. At 10 μ M concentration of the ligand, 37 °C for 30 min, **2b** showed almost the same DNA cleavage activity as **1b**, but **2a** and **2c** showed less cleavage activity in the presence of vanadyl ion (20 μ M) and hydrogen peroxide (500 μ M).
- 14) a) Kuwahara J., Suzuki T., Sugiura Y., *Biochem. Biophys. Res. Commun.*, **129**, 368–374 (1985); b) Sakurai H., Nakai M., Miki T., Tsuchiya K., Takada J., Matsushita R., *ibid.*, **189**, 1090–1095 (1992).
- 15) a) Imamura T., Hinton D. M., Belford R. L., Gumpert R. I., Haight G. P., Jr., *J. Inorg. Biochem.*, **11**, 241–259 (1979); b) Sakurai H., Goda T., Shimomura S., Yoshimura T., *Biochem. Biophys. Res. Commun.*, **104**, 1421–1426 (1982); c) Sakurai H., Goda T., Shimomura S., *ibid.*, **108**, 474–478 (1982).
- 16) Chiu F. C. K., Brownlee R. T. C., Mitchell K., Phillips D. R., *Bioorg. Med. Chem. Lett.*, **4**, 2721–2726 (1994).
- 17) Drew H. R., Travers A. A., *Cell*, **37**, 491–502 (1984).
- 18) Sambrook J., Fritsch E. F., Maniatis T., "Molecular Cloning, A Laboratory Manual," 2nd ed., Cold Spring Harbor Laboratory Press, New York, 1989, pp. 1.21–1.41.
- 19) a) Maxam A. M., Gilbert W., *Proc. Natl. Acad. Sci. U.S.A.*, **74**, 560–564 (1977); b) Maxam A. M., Gilbert W., *Methods Enzymol.*, **65**, 499–559 (1980).
- 20) Ausubel F. M., Brent R., Kingston R. E., Moore D. D., Seidman J. G., Smith J. A., Struhl K., "Current Protocols in Molecular Biology," Vol. 1, John Wiley and Sons, 1995, p. 2.1.5.

Electron Spin Resonance Studies of Dipalmitoylphosphatidylcholine Liposomes Containing Soybean-Derived Sterylglucoside

Kazunori MURAMATSU,^a Toshiki MASUMIZU,^b Yoshie MAITANI,^{*,a} Sung Hee HWANG,^a Masahiro KOHNO,^b Kozo TAKAYAMA,^a and Tsuneji NAGAI^a

Department of Pharmaceutics, Hoshi University,^a 2–4–41 Ebara, Shinagawa-ku, Tokyo 142–8501, Japan, and ESR Application Laboratory, Application and Research Center, Analytical Instruments Division, JEOL, Ltd.,^b 1–2 Musashino 3 Chome, Akishima, Tokyo 196–8558, Japan. Received October 4, 1999; accepted February 1, 2000

The effects of soybean-derived sterylglucoside (SG) on the fluidity of liposomal membrane composed of dipalmitoylphosphatidylcholine (DPPC) were investigated compared with those of soybean-derived sterol (SS) and cholesterol (Ch) using an electron spin resonance spectrometer. Three kinds of liposomes were prepared in the molar ratio of DPPC/X=7/4, where X is SS, Ch or SG. The fluidity close to the polar head groups increased with an increase of temperature in the DPPC membrane containing SS, Ch and SG in the range 35 to 45 °C. Those near the hydrophobic end changed with an increase in temperature in liposomes containing SS, Ch and SG, which had a fluidizing effect on the DPPC membrane below the transition temperature (*T_m*, 41.9 °C) and a condensing effect over the *T_m*. The fluidizing effects of these compounds around 37 °C near the polar head group and the hydrophobic end increased in the following order: Ch<SG≤SS and SS<Ch<SG, respectively. SG increased the fluidity of liposomal membrane dramatically above the *T_m* (35.4 °C). These results suggest that the high fluidity close to the hydrophobic end of the liposomal membranes around 37 °C, the decrease of *T_m*, and the sigmoidal nature of fluidity vs. temperature are important factors in the effectiveness of liposomes containing SG as a carrier of drugs.

Key words liposome; dipalmitoylphosphatidylcholine; soybean-derived sterylglucoside; ESR spectrum; spin label

Liposomes have been extensively explored as carriers for improving the delivery of various therapeutic drugs.^{1–4} When a liposomal drug is administered, it could have different pharmacokinetics than that of the free form.^{5,6} In many cases, the toxicity of a free drug can be decreased by the liposomal entrapment. However, the stability of liposomes remains a problem to be solved. Many researchers have investigated the stability of liposomes using cholesterol (Ch), which is mainly contained in animal cells. Plants contain sterols and their glycosides. Sterols have a similar function to Ch in biological membranes.^{7,8} Sterols in plants are present as complex mixtures. Soybeans contain sterol (SS) in its oil and sterylglucoside (SG), which remains in the residue after the oil has been extracted.

We previously demonstrated that the effectiveness of dipalmitoylphosphatidylcholine liposomes (DPPC-liposome) containing SG (DPPC/SG-liposomes) is significantly different from that containing SS or Ch in terms of accumulation in the liver,^{9,10} and a carrier of drugs administered nasally.¹¹ The administration of insulin containing in DPPC/SG (7/4, mol)-liposomes showing high fluidity caused a high glucose reduction and long duration of reduction effect, for 8 h. DPPC/SS and DPPC/Ch (7/4)-liposomes showing low fluidity caused low glucose reduction.

We have also reported the relationship between the rigidity of the liposomal membrane and the stability of DPPC/SG-liposomes as measured by differential scanning calorimetry (DSC)¹² and fluorescence anisotropy.^{12,13}

In this study, we examined the influence of added SG and temperature on the liposome bilayer fluidity of DPPC using ESR spectroscopy to elucidate its mechanism as a carrier of insulin administered nasally.

Ch was purchased from Sigma Chemical Co. (St. Louis, MO, U.S.A.). Ryukakusan Co. (Tokyo, Japan) kindly supplied SS and SG. The SG is a mixture of the monoglucosides of β -sitosterol (49.9%), campesterol (29.1%), stigmasterol (13.8%), and brassicasterol (7.2%), as shown in Fig. 1. SS is the aglycon of SG and contains each sterol in the same ratio as in SG. 5- and 16-doxylstearic acids (DSA) were purchased from Aldrich Chemical Co. (Milwaukee, WI, U.S.A.). All other chemicals used were of reagent grade.

Preparation of Liposomes Multilamellar liposomes were prepared according to a standard method¹⁴ as described in a previous study¹². Briefly, a mixed solution of DPPC (70 μ mol), Ch, SS or SG (20 or 40 μ mol) and an ESR spin probe were dissolved in chloroform and dried under reduced pressure. The obtained lipid film was then hydrated in 3 ml of pH 7.4 phosphate buffered saline (PBS) (1:10 dilution of PBS in distilled water; 137 mM NaCl/2.6 mM KCl/6.4 mM Na₂HPO₄/1.4 mM KH₂PO₄; pH 7.4). It was then mixed by vortexing, followed by sonication in a bath-type sonicator (Honda Electronics, W220R, Tokyo, Japan) and centrifugation at 9500 $\times g$ for 5 min to remove large particles and form a homogeneous size. The obtained liposomes contained a spin probe at a concentration of 0.6 mol/mol% of total lipids.¹⁵ DPPC-liposomes with SS, Ch or SG were composed of DPPC/SS, DPPC/Ch or DPPC/SG-liposomes at the molar ratio of 7/2 or 7/4, respectively.

ESR Measurements A JEOL JES-TE-200 spectrometer was used to determine ESR spectra at ambient temperature (30–44 °C). The effect of temperature on ESR spectra from the liposomes was measured using a variable temperature controller (JEOL ES-DVT3) at a heating value of 2 °C over the range 30–34 °C and 0.5 °C over the range 35–44 °C, respectively. The

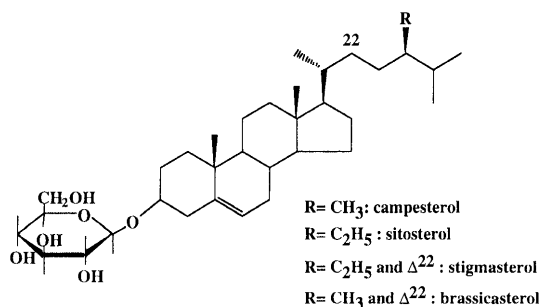


Fig. 1. Chemical Structures of Soybean-Derived Sterylglucoside (SG)

Experimental

Materials DPPC was purchased from NOF Co., Ltd. (Tokyo, Japan).

* To whom correspondence should be addressed. e-mail: yoshie@hoshi.ac.jp

liposomes were transferred to a glass capillary (20 μ l of sample volume). This spectrometer has the function of normalizing all spectra for accurate calculation using manganese dioxide as an internal standard. The conditions for measurement were as follows: microwave power, 4 mW for 5-DSA or 1 mW for 16-DSA; microwave frequency, 9.200–9.255 GHz; field modulation, 100 kHz/0.1 mT; scan time, 4 or 8 min; magnetic field, 328 ± 5 mT; gain, 1×100 ; response time, 0.3 s. Order parameters, S , with the expression given by Gaffney and McConnell:¹⁶⁾

$$S = (T_{\parallel} - T_{\perp} - c) / (T_{\parallel} + 2T_{\perp} + 2c) \times 1.723$$

where T_{\parallel} and T_{\perp} are the apparent parallel and perpendicular hyperfine splitting parameters of the spectra of 5-DSA, the constant $C = 1.4 - 0.053 \times (T_{\parallel} - T_{\perp})$ is an empirical correction for the difference between the true and apparent values of T_{\perp} , and the factor 1.723 is a solvent polarity correction factor.¹⁶⁾ These spectra of 16-DSA, the ratio of the low-field peak height to the central one ($h(+1)/h(0)$), can be used as empirical parameters for membrane fluidity.^{17,18)}

DSC Measurements DSC experiments were performed using a Thermoflex DSC 8230 (Rigaku Denki Co., Tokyo, Japan). The liposome suspension was concentrated by an ultrafilter (USY-5, Toyo Roshi Kaisha, Ltd., Tokyo, Japan). The liposome samples were transferred to an aluminum pan. The sample was analyzed by heating at a rate of 4 °C/min over the temperature range of 25–100 °C, using aluminum oxide as a reference. Each transition temperature value from gel to liquid crystalline of the DPPC, DPPC/SS (7/4), DPPC/Ch (7/4) and DPPC/SG (7/4)-liposomes was in the range of 40.0–43.9 °C, 37.9–45.7 °C, 36.8–44.3 °C and 31.4–41.4 °C, respectively. The transition temperature (T_m) was determined from the temperature at a peak.

Results and Discussion

The mean size of the liposomes was 106–111 nm. Ch can be contained up to 50% mol in DPPC-liposomes.¹⁹⁾ SG and SS can be contained up to almost 36%²⁰⁾ and 50%,¹³⁾ respectively.

Steady-state parameters for the membrane fluidity studies were obtained using two different types of ESR probes, 5-DSA and 16-DSA, which have been used as convenient parameters to monitor the rotational freedom of the nitroxide radical group. The nitroxide radical of 5-DSA is located close to the polar head groups of phospholipids in the liposomal membranes, and that of 16-DSA near the hydrophobic end. To determine the effects of SS, Ch and SG on the fluidity of liposomes, ESR spectra in the DPPC/X=7/4-liposomes (X=SS, Ch or SG) were determined.

ESR spectra of 5-DSA and 16-DSA in the DPPC/SG (7/4)-liposomes at various temperatures are shown in Figs. 2 and 3, respectively. As can be seen from Fig. 2, the order parameter decreased with increasing temperature, indicating a decrease in alkyl chain order near the phospholipid head groups, *i.e.*, an increase of fluidity in the liposomal membrane. The order parameter S indicates the molar motion of *gauche-trans* isomerization in the lipid bilayer.

The fluidity of the liposomal bilayer near the hydrophobic end was examined using a spin probe of 16-DSA. Three peaks, as shown in Fig. 3, characterized the ESR spectra of 16-DSA in the DPPC/SG (7/4)-liposomes. In these spectra, an increase in the values of ($h(+1)/h(0)$) reflects an increase in the mobility of the nitroxide radical near the hydrophobic end of the acyl chains.

Figure 4 shows that the order parameter S of the DPPC/SS (7/4), DPPC/Ch (7/4) and DPPC/SG (7/4)-liposomes at 30 °C and 44 °C was 0.661 and 0.595 (the difference of S values at 30 °C and 44 °C; $\Delta 0.066$), 0.689 and 0.626 ($\Delta 0.062$), 0.695 and 0.577 ($\Delta 0.118$), respectively. These results correspond with the transition temperature range of DPPC/SG (7/4)-liposomes being wide, 31.4–41.1 °C com-

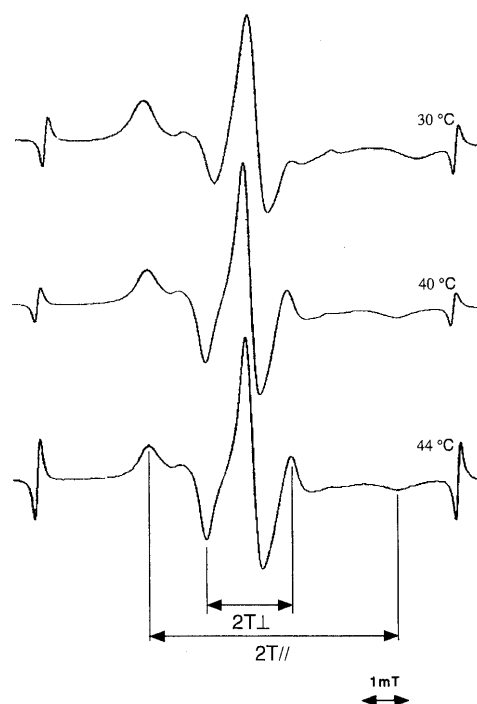


Fig. 2. ESR Spectra at Ambient Temperature (30–44 °C) of 5-DSA in DPPC/SG (7/4)-Liposomes

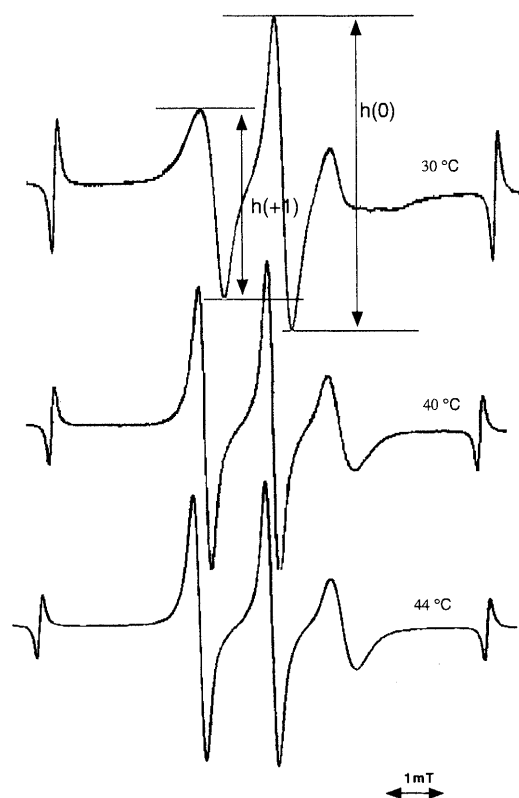


Fig. 3. ESR Spectra at Ambient Temperature (30–44 °C) of 16-DSA in DPPC/SG (7/4)-Liposomes

pared with DPPC/SS (7/4) and DPPC/Ch (7/4)-liposomes. The T_m of the DPPC, DPPC/SS (7/4), DPPC/Ch (7/4) and DPPC/SG (7/4)-liposomes were 41.9, 40.0, 41.5 and 35.4 °C, respectively. The DPPC/SS (7/4) and DPPC/Ch (7/4)-liposomes produced small changes in the order parameter at the T_m : 40.0 and 41.5 °C, respectively. The incorporation of SS

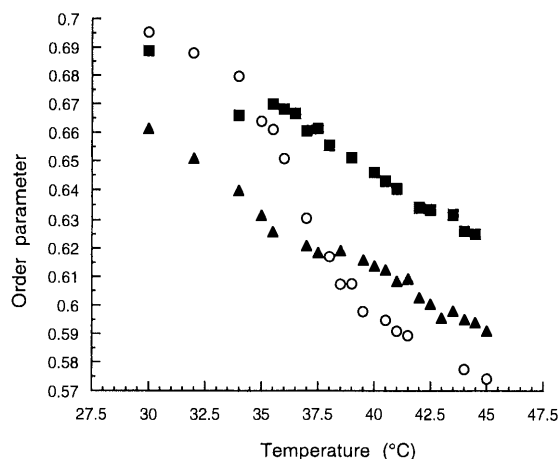


Fig. 4. Temperature Dependence of the Order Parameter S for 5-DSA (▲), DPPC/SS (7/4)-liposomes; (■), DPPC/Ch (7/4)-liposomes; (○), DPPC/SG (7/4)-liposomes.

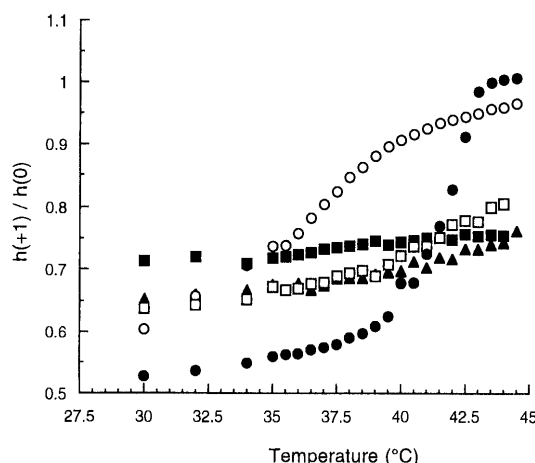


Fig. 5. Temperature Dependence of the Ratio of Peak Height of 16-DSA (●), DPPC-liposomes (control); (▲), DPPC/SS (7/4)-liposomes; (□), DPPC/Ch (7/2)-liposomes; (■), DPPC/Ch (7/4)-liposomes; (○), DPPC/SG (7/4)-liposomes.

into the DPPC-liposomes resulted in a greater increase of membrane fluidity than with Ch. The incorporation of SG into each sharply increased the membrane fluidity, indicating a decrease in alkyl chain order near the phospholipid head groups above the T_m (35.4 °C). Below the T_m (35.4 °C), SG decreased the membrane fluidity compared with SS and Ch. Around 37 °C, the DPPC/SG (7/4)-liposomes showed a slightly rigid membrane compared with that of DPPC/SS (7/4)-liposomes (Fig. 4). This result corresponded well with the data observed using dansylhexadecylamine (DSHA),¹¹⁾ although 5-DSA is located close to the polar head groups of the lipid bilayer, and DSHA was located to the polar head regions of the lipid bilayer. The fluidizing effect of these compounds around 37 °C is greater near the polar head group in liposomes in the following order: Ch < SG ≤ SS.

Figure 5 shows the change in the ratio of the low-field peak height ($h(+1)/h(0)$) value as a function of temperature in the presence of the DPPC/SS (7/4), DPPC/Ch (7/4) and (7/2), DPPC/SG (7/4)-liposomes and DPPC-liposomes as a control. A larger ($h(+1)/h(0)$) value means a more fluid membrane. In the case of the DPPC-liposomes, the ($h(+1)/h(0)$) value undergoes a gradual increase with increasing temperature and the abrupt large increase corresponds to the phase transition of gel to liquid-crystalline (40–43.9 °C). The main transition temperature of the control is around 41.9 °C (T_m), corresponding to the melting temperature of the lipid hydrocarbon chains. At the temperature below the T_m (41.9 °C), the fluidity near the hydrophobic end of the liposomal membrane increased on the addition of SS, Ch and SG (fluidizing effect) compared with the control. At temperatures above the T_m (41.9 °C), the fluidity of the membrane of the DPPC/SS (7/4), DPPC/Ch (7/4) and DPPC/SG (7/4)-liposomes, was lower than that of the control (condensing effect). The DPPC/Ch (7/2)-liposomes showed a lower fluidizing effect than the DPPC/Ch (7/4)-liposomes. Many researchers have reported such a contradictory effect of Ch.^{21,22)} It seems to be due to the formation of an intermediate gel state brought about by the hydrophobic interaction of Ch with the fatty acyl chains of the saturated phosphatidylcholine, and the formation of a hydrogen bond between Ch and phospholipid molecules.⁷⁾

We reported that based on the fluorescence anisotropy data of 1,6-diphenyl-1,3,5-hexatriene (DPH), which was partitioned deep in the hydrophobic interior in liposomes, the DPPC/SG (7/4)-liposomes decreased the anisotropy of DPH in liposomes more so than did the DPPC/SS (7/4) and DPPC/Ch (7/4)-liposomes in the range 25 to 48 °C.¹¹⁾ These findings from the fluorescence anisotropy data of DPH and the ESR spectra data of 16-DSA correspond well with the fact that their fluidizing effect around 37 °C is greater near the hydrophobic part in liposomes in the following order: SS < Ch < SG. However, at the temperature below the T_m (35.4 °C) (Fig. 5), SG slightly decreased the membrane fluidity near the hydrophobic group compared with SS and Ch. This finding from the ESR spin probe was different from that of the fluorescence anisotropy.¹¹⁾

The phase transition of pure DPPC-liposomes seems to be more or less retained in the presence of SG (Fig. 5). The phase transition of lipids in the presence of Ch and SS shows a different curve from the sigmoidal nature found in the case of pure DPPC (Fig. 5). SS as well as Ch may be ordered in the DPPC-liposomes by van der Waals force.²³⁾ SS appears to be more efficient than Ch in ordering the acyl chains near the hydrophobic end of the DPPC bilayer above 41.5 °C because the DPPC/SS (7/4)-liposomes showed lower ($h(+1)/h(0)$) values compared with the DPPC/Ch (7/4)-liposomes (Fig. 5). The ESR data showed clearly that SS decreased the fluidity of liposomes more than Ch compared with the result from fluorescence anisotropy above 41.5 °C.¹¹⁾

The acyl chain in the lower portion (16-DSA, Fig. 5) of DPPC/SS (7/4) and that in the upper portion (5-DSA, Fig. 4) of DPPC/Ch (7/4)-liposomes were highly ordered at the temperature above the T_m (40.0, 41.5 °C, respectively) compared with the DPPC liposomes. On the other hand, the acyl chain of the lower portion (Fig. 5) and the upper portion (Fig. 4) in the DPPC/SG (7/4)-liposomes was highly disordered at the temperature above the T_m (35.4 °C). In general, a polar head group of DPPC has 10 water molecules (binding water),²⁴⁾ whereas a glucose residue of SG may have only a few binding waters. The glucose residue of SG projected out of liposomes may change the packing state of the sterol group of SG in the liposomes.

We previously reported that DPPC/SG (7/4)-liposomes are effective carriers for the nasal absorption of insulin compared with DPPC/SS (7/4) and DPPC/Ch (7/4)-liposomes.¹¹⁾ SG greatly enhanced the permeation of insulin through the nasal mucosa with some effects on lipids in the nasal mucosa.²⁵⁾ Therefore, the high fluidity close to the hydrophobic end of the liposomal membranes around 37 °C, the decrease in transition temperature and the sigmoidal nature of fluidity vs. temperature may be important factors in the release of drug from liposomes containing SG, and/or to stimulate uptake of liposomes, perhaps as a result of the interaction of SG in liposomes on the nasal mucosa.

Acknowledgements The authors are grateful to Dr. Keizo Takeshita, National Institute of Radiological Sciences, for useful discussions regarding ESR spectroscopic measurements.

References

- 1) Papahadjopoulos D., Poste G., Vail W. J., Biedler J. L., *Cancer Res.*, **36**, 2988—2994 (1976).
- 2) Gregoriadis G., Leathwood P. D., Ryman B. E., *FEBS Lett.*, **14**, 95—99 (1971).
- 3) Weissmann G., Bloomgarden D., Kaplan R., Cohen C., Hoffstein S., Collins T., Gottlieb A., Nagel D. A., *Proc. Natl. Acad. Sci. U.S.A.*, **72**, 88—92 (1974).
- 4) Patel H. M., Ryman B. E., *FEBS Lett.*, **62**, 60—63 (1976).
- 5) Juliano R. L., Stamp D., *Biochem. Pharmacol.*, **27**, 21—27 (1978).
- 6) Muramatsu K., Maitani Y., Nagai T., *Biol. Pharm. Bull.*, **19**, 1055—1058 (1996).
- 7) Demel R. A., De Kruijff B., *Biochim. Biophys. Acta*, **457**, 109—132 (1976).
- 8) Schuler I., Duportail G., Glasser N., Benveniste P., Hartmann M. A., *Biochim. Biophys. Acta.*, **1028**, 82—88 (1990).
- 9) Muramatsu K., Maitani Y., Machida, Y., Nagai T., *Int. J. Pharm.*, **124**, 19—26 (1995).
- 10) Shimizu K., Maitani Y., Takayama K., Nagai T., *J. Drug Targeting*, **4**, 245—253 (1996).
- 11) Muramatsu K., Maitani Y., Takayama K., Nagai T., *Drug Dev. Ind. Pharm.*, **25**, 1099—1105 (1999).
- 12) Muramatsu K., Maitani Y., Machida Y., Nagai T., *Int. J. Pharm.*, **107**, 1—8 (1994).
- 13) Qi X. R., Maitani Y., Nagai T., *Chem. Pharm. Bull.*, **44**, 237—240 (1996).
- 14) Bangham A. D., Miller N. G. A., *J. Methods Membr. Biol.*, **1**, 1—68 (1974).
- 15) Morimoto Y., Hosokawa M., Sato H., Takeuchi Y., *Chem. Pharm. Bull.*, **42**, 123—129 (1994).
- 16) Gaffney B. J., McConnell M., *J. Magn. Reson.*, **16**, 1—28 (1974).
- 17) Mehlhorn R. J., Keith A. D., "Membrane Molecular Biology," ed. by Fox C. F., Keith A. D., Sinauer Associates, Inc., Stamford, 1972.
- 18) Glasgigij U., Sato Y., Suzuki Y., *Chem. Pharm. Bull.*, **36**, 1589—1592 (1988).
- 19) Barry R. L., David A. B., Mathias H., *Biochemistry*, **19**, 1943—1954 (1980).
- 20) Shimizu K., Maitani Y., Takayama K., Nagai T., *J. Pharm. Sci.*, **85**, 741—744 (1996).
- 21) Marsh D., *Biol. Magn. Reson.*, **8**, 255—303 (1989).
- 22) Nagumo A., Sato Y., Suzuki Y., *Chem. Pharm. Bull.*, **39**, 3071—3074 (1991).
- 23) Cevc G., "Liposome Technology," Vol. I, ed. by Gregory G., CRC Press, New York, 1993, pp. 1—36.
- 24) Chapman D., "Form and Function of Phospholipids," ed. by Ansell G. B., Hawthorne J. N., Dawson R. H. C., Elsevier Scientific, 1973, pp. 117—142.
- 25) Ando T., Maitani Y., Yamamoto T., Takayama K., Nagai T., *Biol. Pharm. Bull.*, **21**, 862—865 (1998).

New Cytotoxic Butanolides from *Lindera obtusiloba* BLUME

Hak Cheol KWON,^a Nam In BAEK,^b Sang Un CHOI,^c and Kang Ro LEE^{*,a}

Natural Products Laboratory, College of Pharmacy, Sungkyunkwan University,^a Suwon 440–746, Korea, Lab. of Natural Products Chemistry, College of Industry, Kyung Hee University,^b Yongin 449–701, Korea, and Korea Research Institute of Chemical Technology,^c Daejeon 136–702, Korea. Received October 12, 1999; accepted December 22, 1999

Three new butanolides, 2-(1-methoxy-11-dodecenyl)-penta-2,4-dien-4-olide (1), (2*Z*,3*S*,4*S*)-2-(11-dodecenylidene)-3-hydroxy-4-methylbutanolide (2) and (2*E*,3*R*,4*R*)-2-(11-dodecenylidene)-3-hydroxy-4-methoxy-4-methylbutanolide (3), were isolated from the stems of *Lindera obtusiloba* BLUME. Their chemical structures were assigned by spectroscopic evidence. They exhibited cytotoxicity against cultured human tumor cell lines with their ED₅₀ values ranging from 3.19 to 14.63 µg/ml.

Key words *Lindera obtusiloba* BLUME; Lauraceae; cytotoxicity; 2-(1-methoxyl-11-dodecenyl)-penta-2,4-dien-4-olide; (2*Z*,3*S*,4*S*)-2-(11-dodecenylidene)-3-hydroxy-4-methylbutanolide; (2*E*,3*R*,4*R*)-2-(11-dodecenylidene)-3-hydroxy-4-methoxy-4-methylbutanolide

Lindera obtusiloba BLUME (Lauraceae), a ubiquitous tree distributed mainly in Southeast Asia, has been used in traditional Chinese medicine for the treatment of bruise and extravasation.¹⁾ Several phytosterols²⁾ and obtusilactones^{3,4)} have been identified from this plant. In the course of searching for bioactive compounds from Korean natural sources, a methanolic extract of *Lindera obtusiloba* was investigated. We previously reported five moderate cytotoxic lignans from the methylene chloride soluble fraction of this plant.⁵⁾ In continuation of our search for cytotoxic compounds, three new butanolides were isolated from the hexane soluble fraction of this plant. The present paper describes the isolation, structural characterization and cytotoxic activity of these butanolide compounds.

Compound **1** was obtained as colorless oil and its molecular formula was determined to be C₁₈H₂₈O₃ by HR-EI-MS (*m/z* 292.203812, M⁺). The presence of one carbonyl carbon (δ 169.76) and four olefinic signals (δ 154.49, 137.76, 137.67, 97.82) in ¹³C-NMR, UV λ_{\max} of 264 nm, and the lactonic absorption band at 1775 cm⁻¹ in IR spectrum suggested that compound **1** contained a penta-2,4-dien-4-olide moiety.⁶⁾ ¹H-NMR spectrum showed the presence of an exomethylene group at δ 4.88 (1H, d, *J*=2.6 Hz) and 5.20 (1H, d, *J*=2.6 Hz), and an olefinic proton at δ 7.22 (1H, t, *J*=0.5 Hz), respectively. Also, it showed the signals corresponding to a methoxy functionality at δ 3.34 (3H, s), a terminal double bond at δ 5.81 (1H, ddt, *J*=17.0, 10.5, 6.5 Hz), 4.93 (1H,

dm, *J*=10.5 Hz) and 4.99 (1H, dtd, *J*=17.0, 2.3, 1.7 Hz), and long chain aliphatic hydrocarbons at δ 1.26 (10H, br s), 1.35 (4H, m), 1.64–1.74 (2H, m), and 2.03 (2H, m). Available chemical structures of the butanolides derived from the *Lindera* species^{3,7)} and our ¹H-NMR spectral data revealed that **1** also has a long aliphatic 11-dodecenyl chain. Based on the analysis of the ¹H–¹H correlated spectroscopy (COSY) and heteronuclear multiple bond correlation (HMBC) spectral data (Fig. 2), the structure of **1** was determined as 2-(1-methoxyl-11-dodecenyl)-penta-2,4-dien-4-olide. It is optically active ($[\alpha]_D +36.15^\circ$), but the configuration at C-6 remains uncertain.

Compound **2** was obtained as colorless oil, $[\alpha]_D -48.70^\circ$ (*c*=0.046, CHCl₃). Its molecular formula was determined as C₁₇H₂₈O₃ by HR-EI-MS (*m/z* 280.203734, M⁺). IR and NMR spectral data and the UV absorption band at 220 nm (log ϵ =3.98) suggested that **2** was a 2-alkylidene-3-hydroxy-4-methylbutanolide derivative.^{8–10)} The ¹H-NMR spectrum was very similar to that of litsenolide A₁,¹¹⁾ except for the $[\alpha]_D$ value, chemical shifts and coupling constants of H-3 and H-4 [δ 4.66 (1H, dd, *J*=5.1, 1.1 Hz, H-3), 4.56 (1H, qd, *J*=6.5, 5.1 Hz, H-4)] (Table 1). These data suggested that **2** was a C-4 epimer of litsenolide A₁ [as (2*Z*,3*S*,4*R*)-2-(11-dodecenylidene)-3-hydroxy-4-methylbutanolide]. The geometry of alkylidene side chain was *cis* to the carbonyl group based on the upfield shift of H-6 (δ 6.57) and the downfield shift of H-7 (δ 2.76) protons, compared with the chemical shifts of H-6 (δ 7.16) and H-7 (δ 2.40) in *E*-form.^{4,7)} This was also confirmed in nuclear overhauser enhancement spectroscopy (NOESY) spectrum which showed the cross peaks between H-3/H-6 (Fig. 3). Based on the analysis of $[\alpha]_D$ value and ¹H-NMR data, the configuration at C-3 was deter-

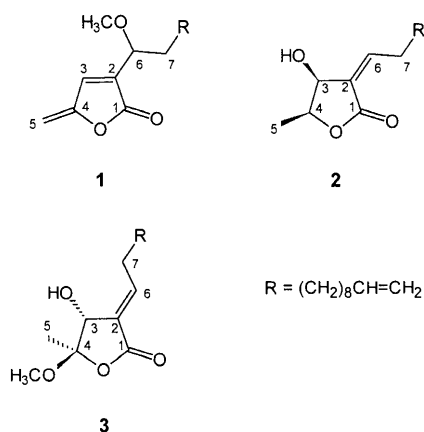


Fig. 1. Structures of Compounds **1**–**3**

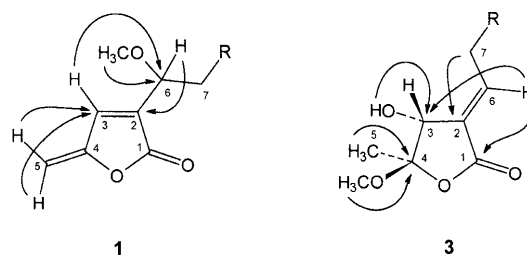


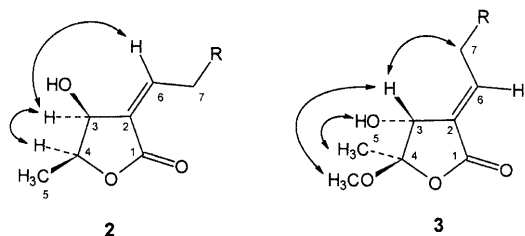
Fig. 2. HMBC Correlations of Compounds **1** and **3**

* To whom correspondence should be addressed. e-mail: krlee@yurim.skku.ac.kr

Table 1. ^1H -NMR Data for Compounds **1**–**3** (500 MHz, CDCl_3)^{a)}

Position	1	2	Litsenolide A_1 ¹¹⁾	3
3	7.22 t (0.5)	4.66 dd (5.1, 1.1)	4.37 m	4.52 dd (7.1, 1.1)
4		4.56 qd (6.5, 5.1)	4.33 qd (6.5, 4.0)	
5	4.88 d (2.6) 5.20 d (2.6)	1.40 d (6.5)	1.37 d (6.5)	1.61 s
6	4.11 ddd (7.4, 4.8, 1.1)	6.57 td (8.0, 1.1)	6.53 td (7.8, 1.5)	6.97 td (8.0, 1.5)
7	1.64–1.74 m	2.76 m	2.73 dr q	2.38 m
8	1.35 m	1.47 m	} 1.30 br s	1.51 br hep (7.5)
9–13	1.26 br s	1.28 br s		1.28 br s
14	1.35 m	1.34 m		1.36 m
15	2.03 m	2.04 m	2.05 br q	2.04 m
16	5.81 ddt (17.0, 10.5, 6.5)	5.82 ddt (17.0, 10.2, 7.0)	4.8–6.2 m	5.81 ddt (17.0, 10.5, 6.5)
17	4.93 dm (10.5)	4.93 dm (10.2)	4.8–6.2 m	4.93 dm (10.5)
	4.99 dtd (17.0, 2.3, 1.7)	4.99 dtd (17.0, 2.2, 1.7)		4.99 dtd (17.0, 2.0, 1.5)
OCH_3	3.34 s			3.78 s
OH				2.22 d (7.1)

a) Values in parentheses are coupling constants in Hz.

Fig. 3. NOESY Correlations of Compounds **2** and **3**

mined to be *S* as in the case of litsenolide A_1 .¹¹⁾ Martinez *et al.* studied the correlations between $[\alpha]_D$ value and the configuration at C-3 for 2-alkylidene-3-hydroxy-4-methylbutanolide derivatives; the *3S* form has a negative $[\alpha]_D$ value, while the *3R* form has a positive value.¹⁰⁾ The stereochemistry at C-4 was determined as *4S* by the coupling constants ($J_{3,4} = 5.1$ Hz) of H-3 and H-4.^{10,12,13)} The *cis* position of 3-OH and 4- CH_3 was also confirmed in NOESY spectrum (Fig. 3). The structure of **2** was, therefore, assigned as (2*Z*,3*S*,4*S*)-2-(11-dodecenylidene)-3-hydroxy-4-methylbutanolide.

Compound **3** was obtained as colorless oil and its molecular formula was determined to be $\text{C}_{18}\text{H}_{30}\text{O}_4$ by HR-EI-MS (m/z 310.214485, M^+). IR, UV and NMR spectrum data were similar to those of compound **2**. The major difference was in the presence of a methoxy group in **3**, which was shown at δ 3.78 (3H, s) in ^1H -NMR spectrum. Analysis of the HMBC spectrum (Fig. 2) allowed for the position of the methoxy group. The gross structure of **3** was speculated to be 2-(11-dodecenylidene)-3-hydroxy-4-methoxy-4-methylbutanolide. The geometry of alkylidene side chain of **3** was *trans* to the carbonyl group based on the chemical shifts of H-6 (δ 6.97) and H-7 (δ 2.38) in ^1H -NMR spectrum.⁴⁾ The downfield shift of H-6 (δ 6.97), compared with that of H-6 (δ 6.57) in compound **2**, can be ascribed to the effect of a carbonyl group of the lactone ring. Its *trans* geometry was confirmed in NOESY spectrum which showed the cross peaks between H-3/H-7 (Fig. 3). The stereochemistry of C-3 was determined to be *3R* based on the correlations between $[\alpha]_D$ value [$+29.33$ ($c=0.06$, CHCl_3)] and the configuration at C-3 for 2-alkylidene-3-hydroxy-4-methylbutanolide derivatives.^{7,10)} The stereochemistry of C-4 was determined to be *4R* by NOESY spectrum (Fig. 3) which showed correlations

Table 2. ^{13}C -NMR Data for Compounds **1**–**3** (125 MHz, CDCl_3)

Position	1	2	3
1	169.76	169.28	169.71
2	137.76	129.98	130.72
3	137.67	72.13	73.20
4	154.49	78.48	110.26
5	97.82	14.81	16.75
6	76.63	150.63	149.17
7	35.10	28.61	30.54
8	25.64	29.51	29.07
9–14 ^{a)}	29.63, 29.80, 30.08, 30.12, 30.16	29.62, 29.82, 29.96, 30.08, 30.14, 30.17	29.60, 29.79, 30.03 ($\times 2$), 30.12, 30.13
15	34.49	34.51	34.49
16	139.93	139.94	139.90
17	114.75	114.81	114.84
OCH_3	58.27		50.99

a) Values are interchangeable.

Table 3. Cytotoxicity of Compounds **1**–**3** against Five Cultured Human Tumor Cell Lines

Cancer Cell Lines	ED_{50} values ^{a)}				
	A549	SK-OV-3	SK-MEL-2	XF498	HCT15
1	9.65	4.73	3.19	3.88	3.57
2	9.43	6.71	4.06	7.14	5.21
3	14.63	12.92	10.07	12.80	10.14
Doxorubicin	0.12	0.13	0.11	0.23	2.40

a) ED_{50} was defined as the concentration ($\mu\text{g/ml}$) that caused a 50% inhibition of cell growth *in vitro*.

between 3-OH and 4- CH_3 signals and between 4- OCH_3 and H-3 signals, indicating that 3-OH and 4- CH_3 are in the *cis* position (Fig. 3). The structure of **3** was, therefore, assigned as (2*E*,3*R*,4*R*)-2-(11-dodecenylidene)-3-hydroxy-4-methoxy-4-methylbutanolide.

Compounds **1** and **2** showed good cytotoxicity against five human tumor cells, A549 (non small cell lung cancer), SK-OV-3 (ovarian cancer), SK-MEL-2 (skin cancer), XF498 (CNS cancer) and HCT15 (colon cancer), whereas **3** showed moderate activity against these cell lines (Table 3).

Experimental

General NMR: in CDCl_3 , Bruker AMX 500 and Varian UNITY INOVA 500. IR: in CCl_4 , Nicolet model 205 FT-IR spectrophotometer. EI-MS: VG70-VSEQ mass spectrometer. Column chromatography: silica gel (Merck, 230–400 mesh) and Sephadex LH-20 (Pharmacia). TLC: Merck precoated Si gel F_{254} plates and RP-18 F_{254} plates. Low pressure liquid chromatography: Merck Lichroprep Lobar®-A Si 60 ($240 \times 10 \text{ mm}$)

Plant Materials *Lindera obtusiloba* was collected in Suwon, Kyungido, Korea in September 1997. A voucher specimen (SKK-97-001) is deposited in the College of Pharmacy at Sungkyunkwan University.

Extraction and Isolation The dried and chopped stems of *Lindera obtusiloba* (5.8 kg) were extracted with MeOH three times at room temperature. The resultant MeOH extract (200 g) followed by successive solvent partition gave hexane (20 g), CH_2Cl_2 (10 g), EtOAc (20 g) and *n*-BuOH (40 g) soluble fractions. The hexane fraction was the most active in the sulforhodamine B (SRB) assay.¹⁴ Thus, the hexane soluble fraction (20 g) was chromatographed through a silica gel column using the gradient solvent system of hexane–EtOAc (15:1)→hexane–EtOAc (1:2) to give seven subfractions (A–G). The subfraction B (1.8 g) was chromatographed with silica gel eluting with hexane:EtOAc (4:1), followed by CH_2Cl_2 to give three subfractions. The second subfraction was rechromatographed over silica gel eluted with CH_2Cl_2 and further purified with silica gel Lobar®-A column (hexane:EtOAc=15:1) to yield **1** (5 mg). The subfraction E (1.7 g) was chromatographed with a silica gel column (CH_2Cl_2 :acetone=15:1→10:1 step gradient) to give four subfractions. The second subfraction (220 mg) was rechromatographed with silica gel (hexane:EtOAc=3:1) to yield two fractions. Each subfraction was further purified with Sephadex LH-20 column chromatography (CH_2Cl_2 :MeOH=1:1) to afford **2** (5 mg) and **3** (13 mg).

2-(1-Methoxyl-11-dodecenyloxy)-penta-2,4-dien-4-olide (**1**): Colorless oil. $[\alpha]_D^{25} + 36.15^\circ$ ($c=0.052$, CHCl_3). UV λ_{max} (EtOH) nm (log ϵ): 264 (4.08). IR (neat) cm^{-1} : 2927, 2855, 1775, 1652, 1291. EI-MS m/z (rel. int.): 292 (M^+ , 0.9), 140 (21.6), 139 (100), 111 (10.8). HR-EI-MS m/z : 292.203812 (Calcd for $\text{C}_{18}\text{H}_{28}\text{O}_3$: 292.203845). ^1H -NMR: Table 1; ^{13}C -NMR: Table 2

(2*Z*,3*S*,4*S*)-2-(11-Dodecenylidene)-3-hydroxy-4-methylbutanolide (**2**): Colorless oil. $[\alpha]_D^{25} - 48.70^\circ$ ($c=0.046$, CHCl_3). UV λ_{max} (EtOH) nm (log ϵ): 221 (3.98). IR (neat) cm^{-1} : 3427, 2926, 2855, 1739, 1675, 1183. EI-MS m/z (rel. int.): 280 (M^+ , 3.5), 262 (0.9), 198 (20.2), 164 (24.0), 155 (43.5), 142 (33.0), 137 (58.6), 123 (20.7), 109 (31.2), 81 (72.5), 70 (100). HR-EI-MS m/z : 280.203734 (Calcd for $\text{C}_{17}\text{H}_{28}\text{O}_3$: 280.203845). ^1H -NMR: Table 1; ^{13}C -NMR: Table 2.

(2*E*,3*R*,4*R*)-2-(11-Dodecenylidene)-3-hydroxy-4-methoxy-4-methylbutanolide (**3**): Colorless oil. $[\alpha]_D^{25} + 29.33^\circ$ ($c=0.06$, CHCl_3). UV λ_{max} (EtOH) nm (log ϵ): 221 (4.08). IR (neat) cm^{-1} : 3423, 2927, 2855, 1746, 1680, 1286. EI-MS m/z (rel. int.): 310 (M^+ , 1.0), 292 (2.2), 153 (11.8), 140 (58.1), 123 (16.2), 109 (15.4), 70 (100). HR-EI-MS m/z : 310.214485 (Calcd for $\text{C}_{18}\text{H}_{30}\text{O}_4$: 310.214410). ^1H -NMR: Table 1; ^{13}C -NMR: Table 2.

Test for Cytotoxicity in Vitro Sulforhodamine B (SRB) bioassay was used as a cytotoxicity screening method. Activities of each compound were monitored at several concentration levels against five cultured human tumor cells; A549 (non small cell lung adenocarcinoma), SK-OV-3 (ovarian), SK-MEL-2 (skin melanoma), XF498 (CNS) and HCT15 (colon) *in vitro*.¹⁴

References

- 1) Yook C. S., "Medicinal Plants of Korea," Academy Publishing Co., Seoul, 1989, p. 184.
- 2) Komae H., Hayashi H., *Phytochemistry*, **11**, 1182 (1972).
- 3) Niwa M., Iguchi M., Yamamura S., *Tetrahedron Lett.*, **1975**, 4395–4398.
- 4) Niwa M., Iguchi M., Yamamura S., *Chem. Lett.*, **1975**, 655–658.
- 5) Kwon H. C., Choi S. U., Lee J. O., Bae K. H., Zee O. P., Lee K. R., *Arch. Pharm. Res.*, **22**, 417–422 (1999).
- 6) Toyota M., Konoshima M., Nagashima F., Hirata S., Asakawa Y., *Phytochemistry*, **46**, 293–296 (1997).
- 7) Seki K., Sasaki T., Haga K., Kaneko R., *Phytochemistry*, **36**, 949–951 (1994).
- 8) Chen I. S., Lai-Yaun I.-L., Duh C. Y., Tsai I. L., *Phytochemistry*, **49**, 745–750 (1998).
- 9) Tanaka H., Nakamura T., Ichino K., Ito K., Tanaka T., *Phytochemistry*, **29**, 857–859 (1990).
- 10) Martinez J. C., Yoshida M., Gottlieb O. R., *Phytochemistry*, **20**, 459–464 (1981).
- 11) Takeda K., Sakurawi K., Ishi H., *Tetrahedron*, **28**, 3757–3766 (1972).
- 12) Abrell L. M., Borgeson B., Crews P., *Tetrahedron Lett.*, **37**, 2331–2334 (1996).
- 13) Magri F. M., Kato M. J., Yoshida M., *Phytochemistry*, **43**, 669–671 (1996).
- 14) Skehan P., Storeng R., Scudiero D., Monks A., McMahon J., Vistica D., Warren J. T., Bokesch H., Kenney S., Boyd M. R., *J. Natl. Cancer Inst.*, **82**, 1107–1112 (1990).

Modification of the Physicochemical Properties of Minocycline Hydrochloride Ointment with Cyclodextrins for Optimum Treatment of Bedsore

Masato SHIGEYAMA,^{*,a} Toyoaki OHGAYA,^a Yoshiaki KAWASHIMA,^b Hirofumi TAKEUCHI,^b and Tomoaki HINO^{b,1)}

Department of Pharmacy, Takayama Red Cross Hospital,^a 3–11 Tenman-cho, Takayama, Gifu 506–8550, Japan, and Department of Pharmaceutical Engineering Gifu Pharmaceutical University,^b 5–6–1 Mitahora-higashi, Gifu 502–0003, Japan. Received October 25, 1999; accepted January 10, 2000

Modification to find the best physicochemical properties of minocycline hydrochloride ointment for optimum treatment of bedsore was investigated by coformulating various types of cyclodextrins (CyD) in the ointment base. It was found that the drug release rate from the ointment base was modified according to the preparation method of ointment base and the type of CyD admixed. The physicochemical properties, such as viscosity, elution volume, water absorption of ointment base were also modified by those factors. The mechanism of physicochemical modification with CyD was explained by the structural change of ointment base and the change of surface tension of emulsifying agent solution with the CyD. The stability of ointment was investigated by confirming the reproducibility of drug release rate after storage at ambient and cooled temperature conditions. In conclusion, a fused mixed ointment with β -CyD was found to be preferable for treatment of bedsore, because of the improved drug release rate, lowered viscosity and increased elution volume of the resultant ointment.

Key words minocycline hydrochloride; release rate constant; viscosity; elution volume; cyclodextrin; surface tension

We have been developing ointment bases of minocycline hydrochloride (MH) used in the medical treatment of bedsores and refractory skin ulcers to improve therapeutic effects. In our previous report,²⁾ the water absorption, the elution, the viscosity and the release of drug of various types of ointment base were investigated. We found that by adding purified lanolin (PL) into the hydrophilic ointment (HO), the amount of penetration of the drug into the epidermis was increased with the improvement of drug release rate and water absorption capacity of the base. In the present study, further modification of physicochemical properties of this ointment base for better treatment of bedsore was sought.

In our hospital, bedsore treatment has been conducted using only a lipophilic ointment base admixed with antibiotics, irrespective of disease stage including the infectious period, necrosis and agglutination period, proliferation period of granulation and the formative period of epidermis. The treatment, therefore, has not always been ideal. We wanted to develop a desirable ointment base having a high water absorbing capacity and improved drug releasing property for the incipient stages of bedsores: the infectious period and necrosis and agglutination periods. In the infectious period, an antibiotic substance is applied to lower the degree of infection, where it is necessary to enhance the drug release rate in order to shorten the period of treatment and avoid creating tolerant bacteria.³⁾ Identification of bedsore bacteria made during our treatment showed that MH had the highest efficacy, so MH was chosen for the present study.

It is known that the physicochemical properties of the ointment base can be modified by formulating various kinds of additives.^{4–9)} As an additive candidate cyclodextrins (CyDs) were chosen because of their characteristic to form inclusion complexes with the lipophilic constituents in the ointment base. This interaction was assumed to occur at the interface of the emulsion droplet, modifying the physicochemical property of the ointment base. This event might change the

fluidity, *i.e.* viscosity, of the ointment base for better dispensing. Furthermore, the drug release behavior might be changed according to the modification of the ointment structure. In this study, the effects of the type of CyD derivative used as the additive on the physicochemical properties of the resultant ointment base and their modification mechanism were elucidated to find the best formulation for optimum treatment of bedsore.

Experimental

Materials Powdered MH, (Japan Lederle) for injection, passed through a JIS sifter of 180 μ m opening was used as the model drug. Ointment bases used were HO, (Maruishi Pharm. Co.), and PL (Yoshida Pharm. Co.). Lactated Ringer's injection (Lactec[®]) as a medium for the release tests (Otsuka Pharm. Co.) was used as received. We used α -cyclodextrin (α -CyD, Nakalai Tesque Co.), β -cyclodextrin (β -CyD, Wako Pure Chemicals Ind. Co.), γ -cyclodextrin (γ -CyD, Sanraku Ocean Co.), heptakis (2,6-di-*O*-methyl)- β -cyclodextrin (DM- β -CyD), heptakis (2,3,6-tri-*O*-methyl)- β -cyclodextrin (TM- β -CyD, Toshin Chemical Co.), and dextrin made at Mitsui Chemical Drug Co., as additives.

Preparation of Ointment Containing MH The ointment bases and MH were kneaded and homogenized with an ointment spatula on a ceramic slab. The kneaded mixture was homogeneously mixed with CyD when required and dispersed in a warmed water bath at 80 °C and the system was then cooled to room temperature. The concentrations of MH and CyD (or dextrin) in ointment were 1% and 5%, respectively (Fusing method).

Release Test of MH from Ointment A Franz diffusion cell with membrane installed horizontally was used to evaluate the drug release from the ointment.¹⁰⁾ Seamless cellulose tubing (Visking Co., size 30/32) was used as the membrane after washing for 2 h in distilled water at 80 °C. Five grams of ointment were mounted on the cellulose membrane placed on the receiver cell (the area of the membrane in contact with the ointment, 8.03 cm²; volume of the cell, 45 ml). Then, 50 ml of distilled water or lactated Ringer's injection solution was introduced into the receiver cell and stirred with a magnetic stirrer. The assembled cell was placed in the water bath thermally controlled at 37 °C. Every 30 min for 3 h, 1 ml of the solution was withdrawn and was replaced by 1 ml of the dissolution medium. The MH released in the medium was measured spectrophotometrically at 349 nm (105-40 type, ultraviolet spectrophotometer, Hitachi, Japan). The data of the drug release test are represented by the mean value of triplicate runs.

Observation of Ointment Structure We observed the structure of emulsion fabricated in ointment base with an optical microscope (Olympus,

* To whom correspondence should be addressed.

BH-2). About 200 mg of ointment base containing various types of CyDs, was spread smoothly on a slide glass with 0.3 mm in thickness, and covered with the cover glass for the microscopic observation.

Measurement of Apparent Viscosity The apparent viscosity of ointment was measured by a rheometer (NRM 100-0 model type, Japan Rheology Co.). The radius and edge angle of corn were 6.4 cm and 20', respectively. The maximum shear rate applied during the measurement was 1800 s^{-1} , and the acceleration and deceleration of corn speed was programmed to be constant within 60 s. The shear rate vs. stress curve of all tested ointment bases exhibited almost a straight line as found by Oishi *et al.*¹¹⁾ The apparent viscosity of the ointment base at room temperature was determined by calculating the ratio of its slope of straight line to that of standard calibration liquid.

Water Absorption and Elution of Ointment Five grams of the ointment sample were applied to the cellulose membrane mounted on the Franz diffusion cell and 50 ml of the medium was introduced into the receiver cell. The system was placed in a water bath thermally controlled at 37°C. After 3 h, the ointment absorbed water was removed from the membrane and weighed (W_1). The ointment completely desiccated with silica gel was weighed (W_2). The eluted ointment base (E) and absorbed water (A) were calculated from the following equations.

$$E = 5.0 - W_2 \quad (1)$$

$$A = W_1 - W_2 \quad (2)$$

Measurement of Surface Tension The surface tensions of the solution of 0–10% HCO-60 containing 5% β -CyD or DM- β -CyD, and the solution of 0–10% β -CyD or DM- β -CyD containing 10% HCO-60 were measured by a surfacetensionmeter (A3 type, Wilhelmy surfacetensionmeter, Kyowa Japan).

Stability of Emulsion Physical stability of emulsion of fused ointment base containing 5% β -CyD was examined with the microscope after standing at cooled or room temperature. The drug release behavior from the ointment base fused with β -CyD was investigated. The release rate constant was calculated by fitting the data to the Higuchi model.¹²⁾

Results and Discussion

Drug Release from Ointment Base In our previous study, it was found that a mixed base of HO and PL at the formulating ratio of 7:3 showed a good high drug release rate and sufficient water absorption capacity. Therefore, we selected this formulation as a reference formulation to examine the influence of various CyDs or dextrin on the release behavior of the drug, MH. As shown in Fig. 1, a linear correlation was observed between the amount of released MH from the ointment base with various CyDs and the square root of time plotted according to the Higuchi model.¹²⁾ This finding suggested that the drug release rate from the ointment base was determined by the diffusion of the drug in the matrix base. Table 1 lists the apparent release rate constant (k) of MH from the ointment base calculated from the slope of straight line determined by the least squares method in Fig. 1. The release rate varied with the type of CyD and the preparation of the ointment base. The order of drug release

rate constants of fused ointment base according to the type of CyD formulated was as follows: dextrin < TM- β -CyD < DM- β -CyD < γ -CyD < none < α -CyD < β -CyD. The release of MH was promoted by adding β -CyD ($p < 0.05$), whereas it was retarded by adding γ -CyD ($p < 0.05$), DM- β -CyD ($p < 0.01$), TM- β -CyD ($p < 0.05$) and dextrin ($p < 0.05$). However, the CyDs admixed physically in the ointment base did not affect or reduce the drug release rate. There was a significant difference in the release rate constant of drug between the physical mixture of CyDs and ointment base and the fused mixture. In the fused mixture of ointment base with α -CyD ($p < 0.01$) or β -CyD ($p < 0.01$), a higher release rate than in the physical mixture was found. There was little difference in the cases of γ -CyD, DM- β -CyD and TM- β -CyD.

Physicochemical Properties (Water Absorption, Elution, Apparent Viscosity) The changes in viscosity, elution volume and water absorption of the ointment base by adding the CyDs were investigated to correlate the drug release rate with those changes. The apparent viscosity of the fused mixture of CyDs is listed in Table 1. The effect of addition of CyDs on the apparent viscosity was found and the order was β -CyD < α -CyD < none < γ -CyD < DM- β -CyD < TM- β -CyD < dextrin. The diffusion rate constant of drug in the ointment base was reduced with increasing the apparent viscosity of the ointment base as shown in Fig. 2. By adding DM- β -CyD, TM- β -CyD and dextrin to the ointment base,

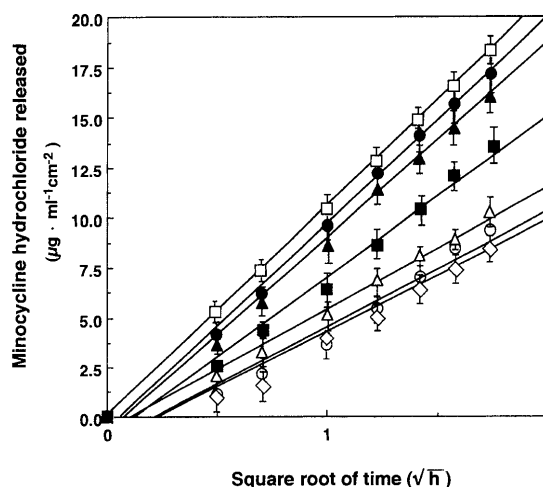


Fig. 1. Higuchi Plots of Release Profiles of Minocycline Hydrochloride from Ointment Containing Various Cyclodextrins Prepared by Fusing Method

●, α -CyD; □, β -CyD; ■, γ -CyD; △, DM- β -CyD; ○, TM- β -CyD; ◇, dextrin; ▲, none. Data represent the mean \pm S.E. of three experiments.

Table 1. Apparent Release Rate Constant and Viscosity of MH Ointment Containing Various Additives

Additives	k^a	k^b	ν^c	Solubility (g/100 ml) ^{13,14)}
None	9.72 ± 0.53	9.38 ± 0.49	0.93 ± 0.11	—
α -CyD	10.16 ± 0.22	7.12 ± 0.18^d	0.90 ± 0.18	14.5
β -CyD	10.93 ± 0.31^e	5.22 ± 0.35^d	0.89 ± 0.11	2.0
γ -CyD	8.05 ± 0.49^e	7.93 ± 0.39	1.02 ± 0.22	23.2
DM- β -CyD	6.06 ± 0.59^f	6.19 ± 0.46	1.09 ± 0.16	57
TM- β -CyD	5.79 ± 0.67^e	5.86 ± 0.62	1.18 ± 0.13	31
Dextrin	5.37 ± 0.69^e	5.31 ± 0.67	1.66 ± 0.23	—

^{a)} k , apparent release rate constant (fused mixture) ($\mu\text{g} \cdot \text{ml}^{-1} \text{cm}^{-2} \text{h}^{-1/2}$). ^{b)} k , apparent release rate constant (physical mixture) ($\mu\text{g} \cdot \text{ml}^{-1} \text{cm}^{-2} \text{h}^{-1/2}$). ^{c)} ν , viscosity (Pa · s) of fused mixture. Composition of ointment base: HO 70: PL 30. Data represent the mean \pm S.E. of three experiments. ^{d)} $p < 0.01$ vs. fused mixture. ^{e)} $p < 0.05$ vs. none. ^{f)} $p < 0.01$ vs. none.

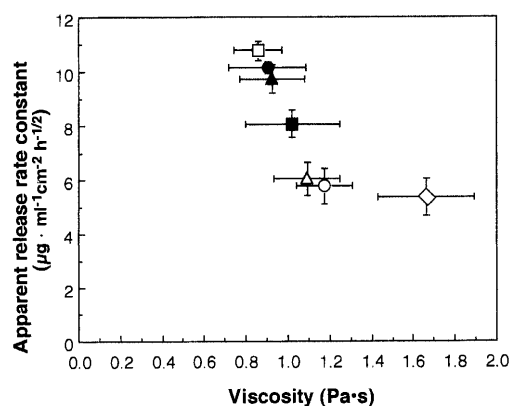


Fig. 2. Relationship between Viscosity and Release Rate

●, α -CyD; □, β -CyD; ■, γ -CyD; △, DM- β -CyD; ○, TM- β -CyD; ◇, dextrin; ▲, none. Data represent the mean \pm S.E. of three experiments.

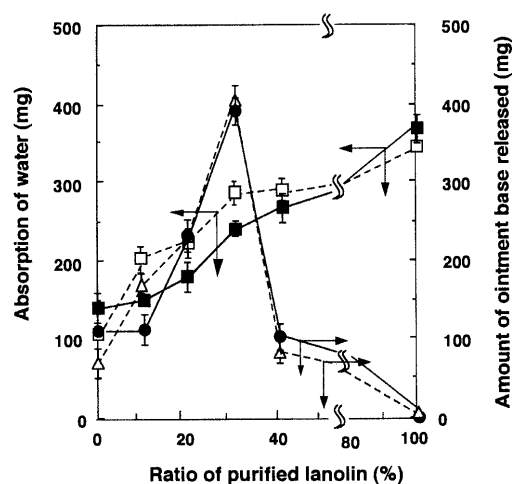


Fig. 3a. Effect of Concentration of Purified Lanolin on Absorption of Water and Amount of Released Ointment Base with DM- β -CyD

●, DM- β -CyD; ■, DM- β -CyD (— fused mixture); △, DM- β -CyD; □, DM- β -CyD (--- Physical mixture). Data represent the mean \pm S.E. of three experiments.

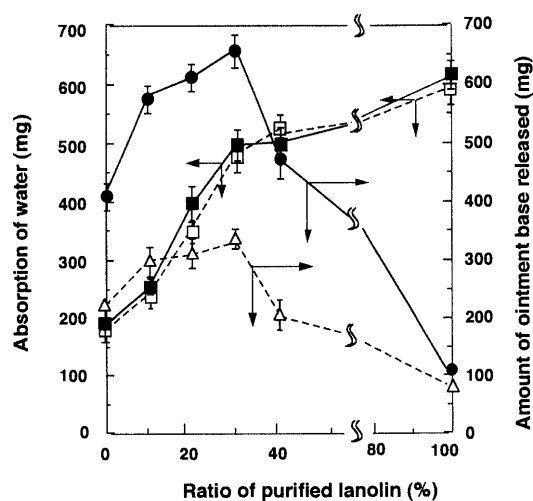


Fig. 3b. Effect of Concentration of Purified Lanolin on Absorption of Water and Amount of Released Ointment Base with β -CyD

●, β -CyD; ■, β -CyD (— fused mixture); △, β -CyD; □, β -CyD (--- physical mixture). Data represent the mean \pm S.E. of three experiments.

the drug release was reduced because of decreasing the diffusion coefficient of drug in the matrix base due to their higher viscosity. On the contrary, β -CyD promoted the drug release rate because of reduced viscosity. It was confirmed that the solubility of MH in water at 37 °C was not changed with addition of β -CyD. This finding indicated that there was no possibility of complex formation between the drug and β -CyD in the ointment base to promote the drug release rate. The amounts of elution and water absorption of the bases with fused mixture and physical mixture of β -CyD or DM- β -CyD were investigated by the elution test. With the DM- β -CyD added ointment base, there was no significant difference between the fused mixture and the physical mixture, as shown in Fig. 3a. However, with the β -CyD added ointment base, there was a significant difference of the elution of the base between the fused mixture and the physical mixture, as shown in Fig. 3b. The elution amount of base was maximum when the base contained 30% PL as found in the previous study. The absorption of water in ointment increased gradually with increasing concentration of PL in the ointment base. However, the amount of elution of ointment base decreased when the concentration was greater than 30% PL. Therefore, the water absorbed with PL in the ointment base swelled the matrix structure of the base, promoting the elution of water soluble ointment base from the base as well as the diffusion of drug. The water absorption capacity of ointment base increased with increasing content of purified lanolin without discrimination between the preparation methods. The reduced viscosity and increased elution and water absorption capacities of fused ointment base with 30% PL and β -CyD might be preferable for better treatment of bedsore because it reduces the stimulation of the skin and is easily washable.

Ointment Structure Structural changes in the ointment base prepared by the fusing method modified with CyDs were investigated to clarify the mechanism of the resultant physicochemical modification by using an optical microscopy. As shown in Fig. 4, coarse liquid droplets were found in the fused ointment base with α -CyD or β -CyD promoting the drug release rates, whereas no visible structural changes with DM- β -CyD or TM- β -CyD were found. In a coloring examination with the water soluble coloring Amalance and hydrophobic coloring sudan III, the drops were distinguished as oil droplets. Therefore, the fused mixture with α -CyD and β -CyD liberated oil droplets, and they coalesced. As a result of this change in structure, it was assumed that the viscosity of the ointment was lowered, due to the decreased interfacial area of ointment base. The schematic representation of the presence or absence of oil droplets is summarized in Fig. 5. In the fused mixture base of 70% HO and 30% PL with α -CyD or β -CyD and without CyD, the oil droplets were produced, whereas DM- β -CyD, TM- β -CyD and dextrin did not produce droplets. In the case of the physical mixture of CyDs and dextrin added to the ointment base, oil droplets were not produced in any ointment. These findings suggest that during the fusion process the emulsifying agent, HCO-60, might interact with α -CyD and β -CyD. Therefore, the interfacial tension of the oil droplets in the fused ointment is reduced, leading to liberation of oil droplets from the system. DM- β -CyD and TM- β -CyD were much more hydrophilic as suggested by their

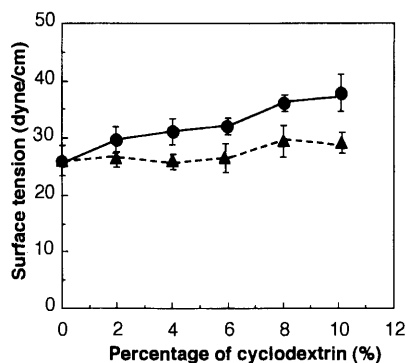


Fig. 6a. Effect of Concentration of Cyclodextrin on Surface Tension
●, β -CyD; ▲, DM- β -CyD. Concentration of HCO-60, 10%. Data represent the mean \pm S.E. of three experiments.

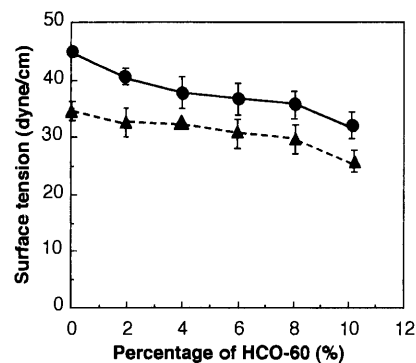
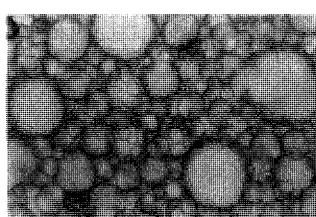
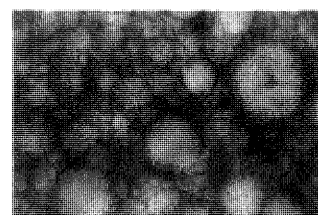


Fig. 6b. Effect of Concentration of HCO-60 on Surface Tension
●, β -CyD; ▲, DM- β -CyD. Concentration of cyclodextrins, 5%. Data represent the mean \pm S.E. of three experiments.

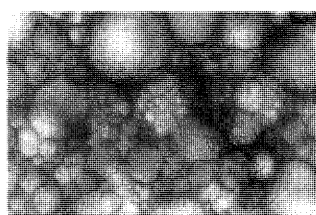


(a) before storage

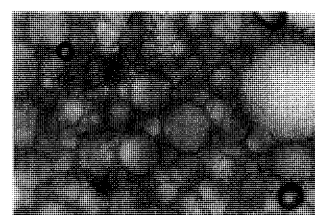


(b) after 7 days $20\mu\text{m}$

Fused mixture : 5% β -CyD (w/w), 1% Minocycline Hydrochloride
Ointment base : HO 70 : PL 30
Stored at room temperature



(a) before storage



(b) after 7 days

Fused mixture : 5% β -CyD (w/w), 1% Minocycline Hydrochloride
Ointment base : HO 70 : PL 30
Storage temperature : 5°C

Fig. 7. Photomicrographs of (a) Freshly Prepared Ointment and (b) Stored Ointment for 7 d

tively. This stability is satisfactory for clinical usage, because they are usually used immediately after preparation in the hospital pharmacy.

Conclusion

The drug (MH) release rate from the HO (70%) and PL (30%) mixed ointment base for treatment of bedsore was desirably improved by coformulating with β -CyD by the fusing method.

The viscosity and the elution amount of the resultant ointment base was reduced and increased, respectively, for better treatment because it is less stimulating to the skin and is easily washable on application. The modification of the physicochemical properties of the ointment base with β -CyD was explained by the interaction of β -CyD with the emulsifying agent (HCO-60) at the interface of oil droplets in the ointment base, leading to the liberation and coalescence of oil droplets in the ointment base. This phenomenon was con-

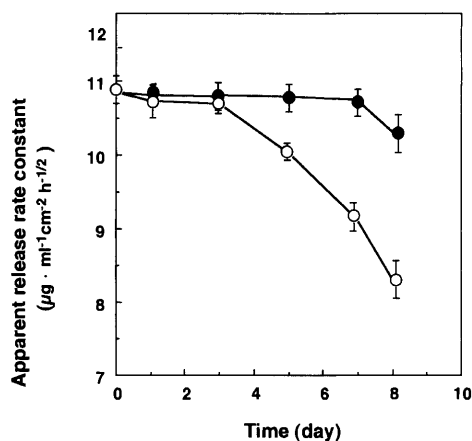


Fig. 8. Changes in Apparent Release Rate Constant of Fused Ointments with β -CyD during Storage

Storage temperature: ●, 5°C; ○, room temperature. Data represent the mean \pm S.E. of three experiments.

firmed by an increase in the surface tension of HCO-60 solution with increasing concentration of β -CyD admixed. The reproducible drug release rate after storage of the ointment base at room temperature for 3 d was confirmed for the clinical usage. In conclusion, the ointment base was preferably modified with β -CyD for better treatment of bedsore and supplied to test clinically.

References and Notes

- 1) Present address: Faculty of Pharmaceutical Sciences, University of Tokushima 1-78-1, Shoumachi, Tokushima 770-0044, Japan.
- 2) Shigeyama M., Ohgaya T., Kawashima Y., Takeuchi H., Hino T., *Chem. Pharm. Bull.*, **47**, 744—748 (1999).
- 3) Miyachi Y., *Ther. Research*, **16**, 4139—4145 (1995).
- 4) Suzuki H., Ootake K., Takahashi T., *Yakuzaigaku*, **50**, 341—346 (1990).
- 5) Tanabe K., Yoshida S., Yamamoto K., Itoh S., Yamazaki M., *Yakuzaigaku*, **48**, 262—269 (1988).
- 6) Uekama K., Masaki K., Arimori A., Irie T., Hirayama F., *Yakugaku Zasshi*, **107**, 449—456 (1987).
- 7) Tomono K., Gotoh H., Okamura M., Horioka M., Ueda H., Nagai T., *Yakuzaigaku*, **51**, 22—28 (1991).
- 8) Uekama K., *Yakugaku Zasshi*, **101**, 857—873 (1981).
- 9) Uekama K., Kurihara M., Hirayama F., *Chem. Soc. Jpn.*, **10**, 1195—1199 (1990).
- 10) Vlachou M. D., Rekkas D. M., Dallas P. P., Choulis N. H., *Int. J. Pharm.*, **82**, 47—52 (1992).
- 11) Oishi H., Takehara M., Koike M., *Yakuzaigaku*, **32**, 110—118 (1972).
- 12) Higuchi T., *J. Soc. Cosmetic Chemists*, **11**, 85—97 (1960).
- 13) Kobayashi S., Kainuma K., *Kagaku To Seibutsu*, **20**, 453—459 (1982).
- 14) Uekama K., Irie T., *Pharm. Factory*, **5**, 20—23 (1985).

Synthesis and Serotonin 2 (5-HT₂) Receptor Antagonist Activity of 5-Aminoalkyl-Substituted Pyrrolo[3,2-*c*]azepines and Related Compounds

Akira MIZUNO,* Atsuto OGATA, Tomoe KAMEI, Makoto SHIBATA, Tetsuo SHIMAMOTO, Yasuhiro HAYASHI, Kyoko NAKANISHI, Chikako TAKIGUCHI, Naomi OKA, and Norio INOMATA

Suntory Institute for Biomedical Research, 1-1-1, Wakayamadai, Shimamoto-cho, Mishima-gun, Osaka 618-8503, Japan.

Received November 1, 1999; accepted January 28, 2000

A series of 5-aminoalkylpyrrolo[3,2-*c*]azepine derivatives was synthesized and their serotonin 2 (5-HT₂) receptor antagonist and antiplatelet aggregation activities were evaluated. 5-HT₂ receptor antagonist activity was largely determined by the nature of the substituent at the 8-position as well as the aminoalkyl group at the 5-position of the pyrrolo[3,2-*c*]azepine ring.

Compound 18a, 5-[3-[4-(4-fluorophenyl)piperazin-1-yl]propyl]-8-hydroxy-1-methyl-1,4,5,6,7,8-hexahydropyrrolo[3,2-*c*]azepin-4-one, was recognized as having potent 5-HT₂ receptor antagonist activity with weak α_1 adrenoceptor blocking activity and no significant D₂ receptor binding affinity, while the corresponding isomeric pyrrolo[3,4-*c*]azepine derivative (22) displayed only weak 5-HT₂ receptor antagonist activity. After racemic 18a was resolved directly *via* diastereomeric salt formation, each enantiomer was evaluated precisely. The 5-HT₂ receptor antagonist activity of 18a was found to reside primarily in (–)-18a (which was about 14-fold more potent than (+)-18a in isolated guinea pig arteries). Consequently, (S)-(–)-18a (SUN C5174) displayed the overall best profile with potent 5-HT₂ receptor antagonist activity ($pA_2=8.98\pm0.06$) and high selectivity *versus* other receptors.

SUN C5174 showed a marked inhibitory effect on the platelet aggregation induced by serotonin in combination with collagen and adenosine diphosphate (ADP) in canine or human platelet-rich plasma ($IC_{50}=6.5$ to 16 nM). Moreover, this compound significantly inhibited the mortality rate in mouse acute pulmonary thromboembolic death induced by collagen and serotonin at oral doses of 0.3 mg/kg or higher.

SUN C5174 is currently undergoing clinical evaluation.

Key words serotonin 2 receptor antagonist; pyrrolo[3,2-*c*]azepine; SUN C5174; antiplatelet aggregation

Arterial thromboembolic events and their ischemic complications give rise to a variety of vasoocclusive disorders such as unstable angina, myocardial infarction, stroke, or peripheral arterial diseases.¹⁾ As such diseases still remain the leading cause of human morbidity and mortality,²⁾ new antithrombotic therapeutic agents are needed.

Serotonin is accumulated into platelets, stored, and later released from platelets activated by collagen, norepinephrine (NE), thromboxan A₂ (TXA₂), adenosine diphosphate (ADP) and other endogenous products. Serotonin only weakly induces platelet aggregation, but synergistically potentiates the effects of the above vasoactive and platelet aggregative substances.³⁾

Since these activities have been demonstrated to be mediated through the serotonin 2 (5-HT₂) receptor,⁴⁾ 5-HT₂ receptor selective antagonists are expected to be useful in the treatment of peripheral circulatory disorders involving vasoconstriction and platelet aggregation.⁵⁾

The 5-HT₂ receptor antagonist ketanserin (1, Fig. 1) has been shown to be beneficial in the treatment of some circula-

tory diseases.^{4a,6)} It is well known that this compound has not only potent 5-HT₂ receptor antagonist activity but also considerable α_1 -adrenoceptor blocking activity which has been confirmed to be responsible for the blood pressure reduction.⁷⁾ Due to adverse effects such as hypotension based on α_1 -adrenoceptor blocking activity, compounds with less potent α_1 blocking activity are preferable. The selective 5-HT₂ receptor antagonist, sarpgregrelate (2a), was recently reported as a therapeutic agent for treatment of peripheral circulatory disturbance.⁸⁾

We are interested in preparing agents with new pharmacological profiles based on utilization of unique skeletons. Previously, we reported the structure–activity relationships (SAR) of pyrrolo[2,3-*c*]azepine derivatives containing a unique bicyclic ring found in certain marine sponges.⁹⁾ The ring system was found to be a useful component in eliciting α_1 - and/or 5-HT₂-receptor antagonist activities, which were markedly affected by the nature of the functional group at the 4-position of the pyrroloazepine ring. Certain compounds, especially (E)-1-[4-[4-(4-fluorobenzoyl)piperidino]butyl]-4-

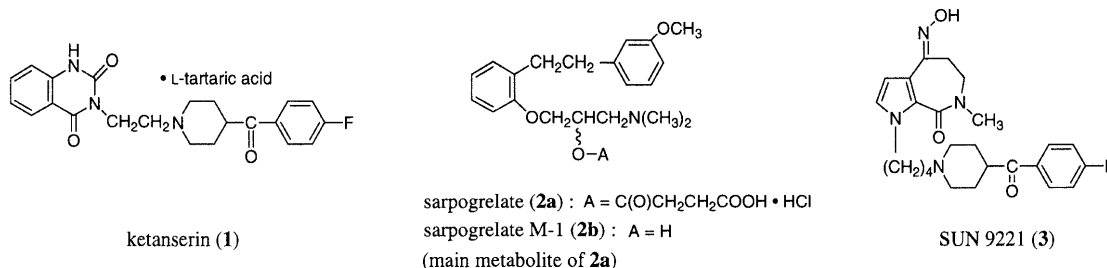


Fig. 1

* To whom correspondence should be addressed.

hydroxyimino-7-methyl-1,4,5,6,7,8-hexahydropyrrolo[2,3-*c*]azepin-8-one (**3**, SUN9221), were potent antihypertensive agents with potent α_1 - and 5-HT₂-receptor antagonist activities. These results suggested that further modification of this ring may produce a selective 5-HT₂ receptor antagonist, and therefore we synthesized and evaluated pyrrolo[3,2-*c*]azepine derivatives (Fig. 2, I) and related compounds.

In this paper, we describe the SAR within a series of these compounds that led to the discovery of SUN C5174 (compound (–)-**18a**), a potent and selective 5-HT₂ receptor antagonist.

Chemistry Synthetic pathways for preparation of the key intermediates (**7**, **12** and **13**) are shown in Chart 1. (1-Substituted)-3-pyrrolicarboxylic acids (**4**) were condensed with β -alanine benzyl ester *p*-toluenesulfonate in the presence of diethyl phosphorocyanidate (DEPC),¹⁰ followed by hydrogenolysis of the benzyl group affording 3-(3-pyrrolicarboxamido)propionic acids (**6**) in good yields. Cyclization of the resultant **6** with 80% polyphosphoric acid (PPA) at 100 °C produced predominantly pyrrolo[3,2-*c*]azepine com-

pounds (**7**) over pyrrolo[3,4-*c*]azepine compounds (**8**) in the range of approximately 2.3 : 1, and whose structures were determined by comparison of NMR data of both compounds (method A).¹¹ Compounds **7c** and **7d** were prepared by alkylation of **7a** in high yields (method B). Subsequently, the reaction of **7** with α -bromo- ω -chloroalkane in the presence of *tert*-BuOK afforded the ω -chloro derivatives (**12**), but yields were poor (method C). As this route was not satisfactory, a more expedient route was investigated. Condensation of **4** with *N*-substituted β -alanine ester derivative (**9**), followed by alkaline hydrolysis of the ester group and cyclization with a mixture of methanesulfonic acid and P₂O₅, directly afforded predominantly the pyrrolo[3,2-*c*]azepine derivatives (**12**) in better yields accompanied by small amounts of isomeric **13** (method D).

The target compounds indicated in Tables 1–4 were synthesized as outlined in Charts 2–3. The ω -chloro derivatives (**12**) were reacted with the appropriate amine in the presence of base (K₂CO₃ or NaHCO₃) and NaI to give the 8-aminoalkyl compounds (**14**) in good yields (method E). As introduction of the chloroethyl group into **7b** by method C was unsuccessful, an alternative approach was adopted for preparation of **14n**. Direct introduction of an aminoethyl moiety into the 5-position of **7b** using 1-(2-chloroethyl)-4-(4-fluorophenyl)piperazine in the presence of NaH gave **14n** in 18% yield (method F). Reduction of **14** with NaBH₄ afforded the desired 8-hydroxy compounds (**18**) (method G). Compound **18b**, with a carbonyl group in the amino moiety at the 5-position, was prepared by initial reduction of **12** and subsequent replacement of chlorine atom by amination (method H) (Chart 2). The derivatives (**15**, **16**, **19** and **20**) with various groups at the 8-position were synthesized from **14a** and **18a**. Treatment of **14a** with hydroxylamine hy-

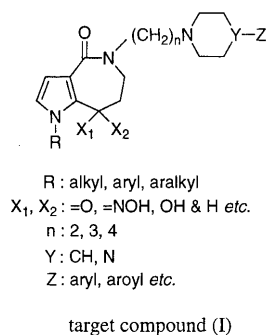


Fig. 2

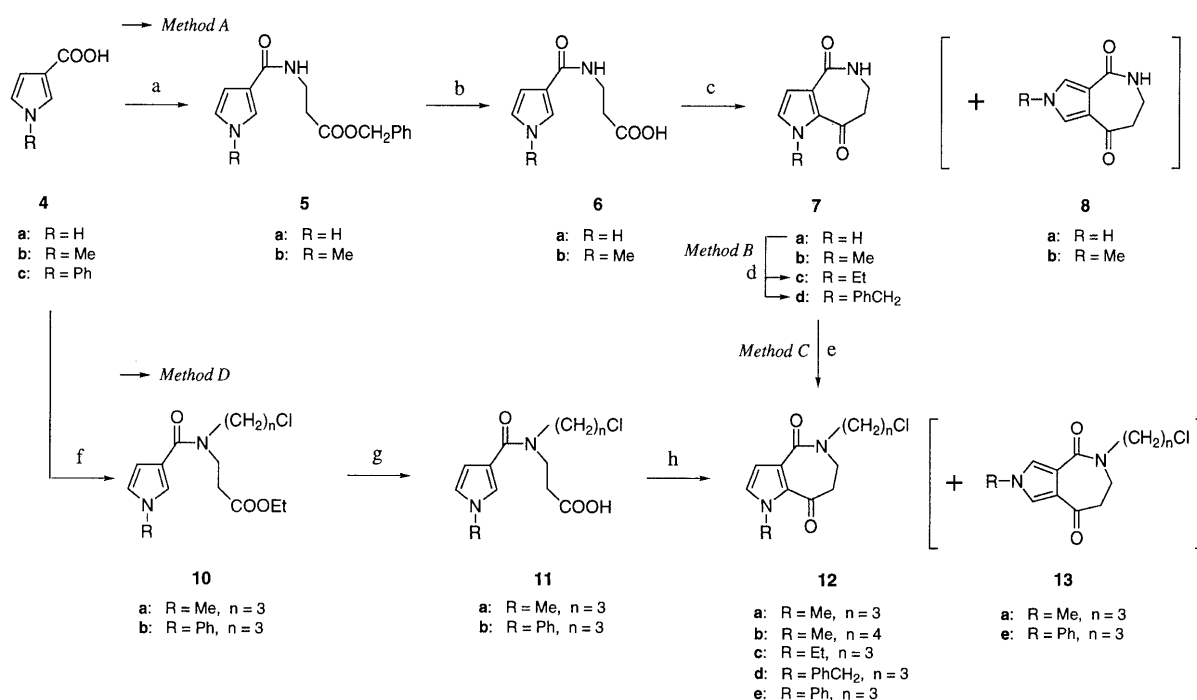
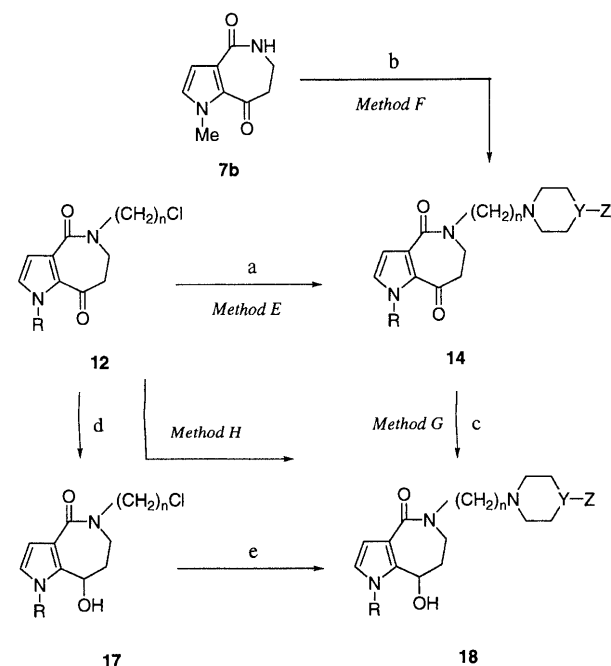


Chart 1



Compounds 14 and 18

14, 18	R	n	Y	Z
a	Me	3	N	4-F-Ph
b ^{a)}	Me	3	CH	4-F-benzoyl
c	Me	3	CH	Ph
d	Me	3	N	Ph
e	Me	3	N	2-F-Ph
f	Me	3	N	3-F-Ph
g	Me	3	N	4-Cl-Ph
h	Me	3	N	4-OH-Ph
i	Me	3	N	4-NO ₂ -Ph
j	Me	3	N	4-MeO-Ph
k	Me	3	N	Ph ₂ CH
l	Me	3	N	2-pyrimidinyl
m	Me	3	N	3-(1,2-BIT) ^{b)}
n	Me	2	N	4-F-Ph
o	Me	4	N	4-F-Ph
p	Et	3	N	4-F-Ph
q	PhCH ₂	3	N	4-F-Ph
r	Ph	3	N	4-F-Ph

a) 14b is absent, as Method H was used

b) 3-(1,2-benzisothiazolyl)



Chart 2

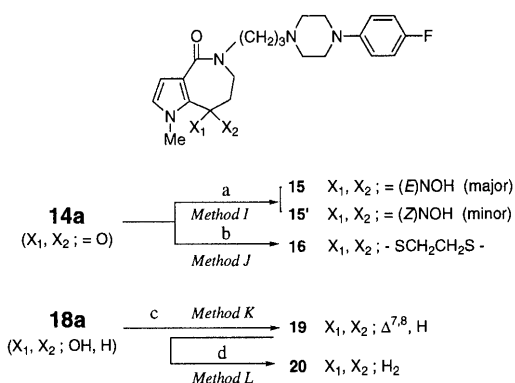
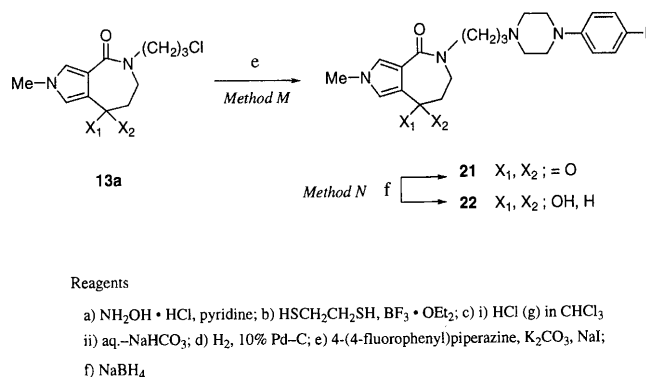


Chart 3

drochloride in basic medium afforded exclusively the (*E*)-oxime (**15**) accompanied by a very small amount of the (*Z*)-oxime (**15'**), which could be easily separated by column chromatography (method I).¹²⁾ Thioacetal compound (**16**) was obtained by reaction of **14a** with ethanedithiol and boron trifluoride etherate (method J). Compound **18a** was dehydrated with hydrogen chloride in CHCl_3 to give the 7,8-unsaturated compound (**19**) (method K), which was reduced by catalytic hydrogenation on Pd on carbon to give the 8-methylene compound (**20**) (method L). The isomeric pyrrolo[3,4-*c*]azepine derivatives (**21** and **22**) were prepared from **13a** in a manner similar to preparation of **14a** and **18a**, respectively (methods M, N) (Chart 3).

Optical resolution of **18a** was performed by diastereomeric salt formation with optically active tartaric acid, followed by fractional recrystallization. Treatment of the resolved-amine tartaric acid salts with aqueous NaOH and subsequent recrystallization produced free bases, (*-*)-**18a** and (*+*)-**18a**



(Chart 4). The enantiomeric purities of (*-*)-**18a** and (*+*)-**18a** were over 99% ee, as determined by HPLC using a chiral column. The absolute configuration of (*-*)-**18a** was established as 8*S* on the basis of X-ray crystallographic analysis of (*-*)-**18a** \cdot L-(+)-tartaric acid salt (Fig. 3).

The chemical structures of the synthesized compounds were confirmed from spectroscopic data (IR, ¹H-NMR, MS) and elemental analyses.

Results and Discussion

It has been reported that the contractions induced by serotonin and NE in the isolated mesenteric artery and aorta of the guinea pig are mainly caused by activation of 5-HT₂ receptors and α_1 -adrenergic receptors, respectively.¹³⁾ Therefore, antagonistic effects of compounds on 5-HT₂ receptors and α_1 -adrenergic receptors were evaluated in terms of the ability to block 10⁻⁵ M serotonin-induced contractions and 10⁻⁵ M NE-induced contractions of isolated guinea pig arter-

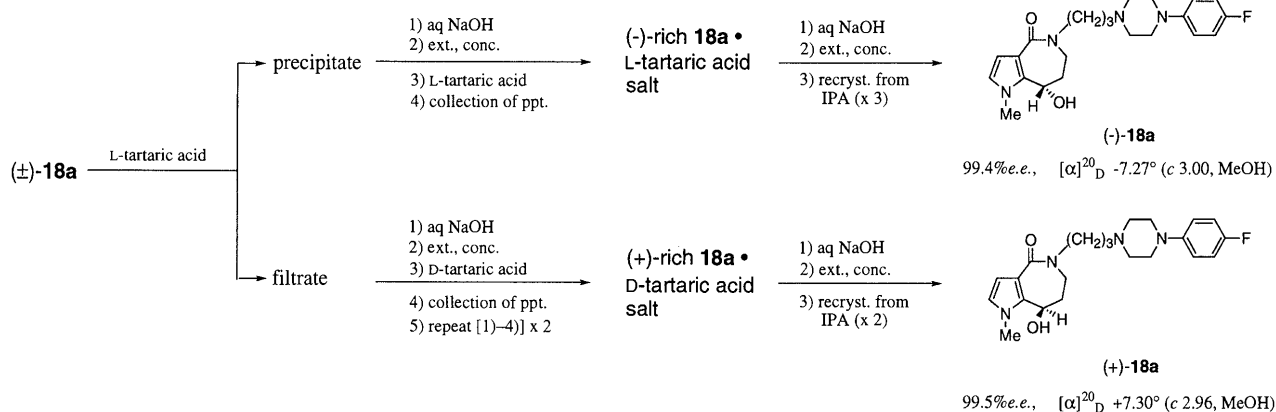


Chart 4

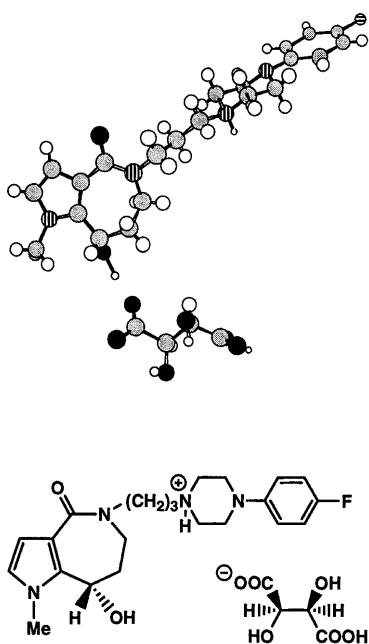


Fig. 3. Molecular Structure of Compound $(-)\text{-18a} \bullet \text{L-(+)-Tartrate}$ as Determined by X-Ray Crystal Analysis

ies, respectively. Details concerning the test methods are described in the Experimental Section.

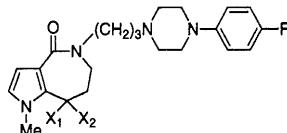
Initially, we investigated the influence of various groups at the 8-position of 1-methylpyrrolo[3,2-*c*]azepine derivatives, as shown in Table 1. 5-HT₂ receptor antagonist activity and selectivity were largely affected by the nature of this group. While a carbonyl derivative (**14a**) and a (*E*)-hydroxyimino compound (**15**) exhibited only weak 5-HT₂ receptor antagonist activity, the hydroxy compound (**18a**) showed very potent activity. Compounds **16** and **19** had potent 5-HT₂ receptor antagonist activity comparable to that of **18a**, but at the expense of higher α_1 blocking and D₂ receptor binding activities. Furthermore, methylene compound (**20**) exhibited the same or slightly more potent 5-HT₂ receptor antagonist activity, but had low selectivity since α_1 blocking activity was rather more potent than that of **18a**. The hydroxy group must be an important factor for manifestation of the potent and selective 5-HT₂ receptor antagonist activity.

Subsequently, the effects of various amines were examined with compounds containing a hydroxy group at the 8-posi-

tion. As shown in Table 2, the amine moieties markedly affected the 5-HT₂ blocking activity. The compounds with a "ketanserin side chain" (**18b**) and 4-phenylpiperidine (**18c**) did not exhibit potent activity. Compound **18d**, which has a piperazine moiety instead of piperidine, showed improved potency, but the selectivity was not sufficient. The effects of substituents on the benzene ring on activity were further explored in a piperazine series. 4-Fluoro substitution (**18a**) led to marked improvement of both 5-HT₂ receptor antagonist activity and selectivity, whereas 2-fluoro (**18e**) or 3-fluoro (**18f**) substitution diminished the activity, in comparison with the unsubstituted compound **18d**. 4-Chloro (**18g**) and 4-hydroxy (**18h**) compounds exhibited less potent activity than the 4-fluoro compound (**18a**), and comparably weak α_1 blocking and D₂ receptor binding activities as the 4-fluoro compound. The results with compounds **18a** and **18d-h** suggested that the presence of a substituent in the 4-position of the benzene ring was important for suppressing α_1 blocking activity and D₂ receptor binding affinity. Both 4-nitro (**18i**) and 4-methoxy (**18j**) compounds showed negligible 5-HT₂ receptor antagonist activity. These observations suggested that the 5-HT₂ receptor antagonist activity was influenced by both the electronic and steric effects of the substituents at the 4-position. Larger groups such as methoxy and nitro groups at the 4-position interfere with the interaction, and serve to reduce activity. Replacement of the phenyl group with other groups such as a benzhydryl (**18k**), 2-pyrimidinyl (**18l**) and 3-(1,2-benzisothiazolyl) group (**18m**) markedly diminished activity.

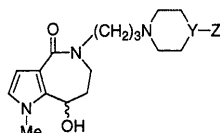
The next step was optimization of the alkylene chain length (*n*) at the 5-position and the substituent at the 1-position of the pyrrolo[3,2-*c*]azepine skeleton, whilst maintaining the optimal amine moiety of **18a**. The results of this study are summarized in Table 3. Alteration of the alkyl chain between the 5-position of pyrrolo[3,2-*c*]azepine and the 4-(4-fluorophenyl)piperazine moiety from propylene (**18a**) to either ethylene (**18n**) or tetramethylene (**18o**), reduced the 5-HT₂ receptor antagonist activity by more than 10-fold. The length of the alkyl side chain was critical for selectivity against α_1 blocking activity as well as 5-HT₂ receptor antagonist activity, and was optimal with *n* = 3.

Subsequently, the effects of the substituent at the 1-position were examined. Substitution of the methyl group by larger groups such as an ethyl (**18p**), benzyl (**18q**) and

Table 1. Biological Activities of Pyrrolo[3,2-*c*]azepine Derivatives with Various Groups at the 8-Position

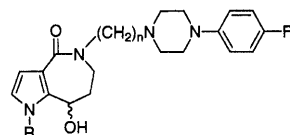
Compound	X_1, X_2	5-HT ₂ -blocking activity ^{a)} (% inhibition)			α_1 -blocking activity ^{b)} (% inhibition)		D ₂ receptor binding affinity ^{c)} IC ₅₀ (nM)
		10 ⁻⁸ M	10 ⁻⁷ M	10 ⁻⁶ M	10 ⁻⁸ M	10 ⁻⁷ M	
14a	=O		23	74	1	9	3260
15	=NOH(<i>E</i>)		13	52	14	40	1410
16	-SCH ₂ CH ₂ S-	25	79		3	24	721
18a	-OH, H	45	88	93	1	10	3110
19	$\Delta^{7,8}$, H	44	79		38	79	1710
20	H ₂	65	92		12	62	3900
Ketanserin (1)		43	93	100	3	47	831
Sarpogrelate (2a)			12	27	1	3	>10000
Sarpogrelate M-1 (2b)			23	69	3	7	8660

a) % inhibition of 10⁻⁵ M serotonin-induced contraction in guinea pig mesenteric artery. b) % inhibition of 10⁻⁵ M norepinephrine-induced contraction in guinea pig aorta. c) IC₅₀ value in [³H]-raclopride binding to rat striatum membrane preparations.

Table 2. Biological Activities of 8-Hydroxypyrrolo[3,2-*c*]azepine Derivatives with Various Amine Moieties (**18**)

Compound	Y	Z	5-HT ₂ -blocking activity ^{a)} (% inhibition)			α_1 -blocking activity ^{b)} (% inhibition)		D ₂ receptor binding affinity ^{c)} IC ₅₀ (nM)
			10 ⁻⁸ M	10 ⁻⁷ M	10 ⁻⁶ M	10 ⁻⁸ M	10 ⁻⁷ M	
18a	N	4-F-Ph	45	88	93	1	10	3110
18b	CH	4-F-benzoyl		28	75	2	30	>10000
18c	CH	Ph	9	45	85	1	6	3010
18d	N	Ph	33	84		3	27	2000
18e	N	2-F-Ph		30	81	5	36	2590
18f	N	3-F-Ph		52	88	1	28	2400
18g	N	4-Cl-Ph	18	53	93	1	7	5800
18h	N	4-OH-Ph		59	89	1	12	8560
18i	N	4-NO ₂ -Ph		2	11	2	5	>10000
18j	N	4-MeO-Ph		2	16	2	5	>10000
18k	N	benzhydryl		12	48	0	0	6420
18l	N	2-Pyrimidinyl		7	13	1	2	>10000
18m	N	3-(1,2-BIT) ^{d)}		49	89	5	68	1100

a)–c) see corresponding footnotes of Table 1. d) 3-(1,2-benzisothiazolyl).

Table 3. Biological Activities of 8-Hydroxypyrrolo[3,2-*c*]azepine Derivatives **18n–r**

Compound	R	<i>n</i>	5-HT ₂ -blocking activity ^{a)} (% inhibition)			α_1 -blocking activity ^{b)} (% inhibition)		D ₂ receptor binding affinity ^{c)} IC ₅₀ (nM)
			10 ⁻⁸ M	10 ⁻⁷ M	10 ⁻⁶ M	10 ⁻⁸ M	10 ⁻⁷ M	
18a	Me	3	45	88	93	1	10	3110
18n	Me	2		10	52	3	29	8490
18o	Me	4		22	62	1	41	162
18p	Et	3	15	70		14	53	4470
18q	PhCH ₂	3		49	89	5	68	483
18r	Ph	3		26	63	4	61	993

a)–c) see corresponding footnotes of Table 1.

phenyl (**18r**) groups resulted in a decrease in the 5-HT₂ receptor antagonist activity, suggesting some steric effects around this position. The best result was obtained with compound **18a** with the methyl group at the 1-position.

We prepared the isomeric pyrrolo[3,4-*c*]azepine analog of **18a** in order to clarify the pharmacological significance of the pyrrolo[3,2-*c*]azepine skeleton. As shown in Table 4, the isomeric compound **22** exhibited less than one tenth of the 5-HT₂ receptor antagonist activity of the corresponding compound **18a**, indicating that combination of the pyrrolo[3,2-*c*]azepine skeleton and the 8-hydroxy group of **18a** is important for manifestation of the potent 5-HT₂ receptor antagonist activity.

Consequently, we selected compound **18a** for further studies. Compound **18a** was a racemic compound possessing an asymmetric center at the 8-position in the pyrroloazepine ring. Since Pfeiffer's rule states that highly potent chiral compounds display a large difference in potency between their enantiomers,¹⁴ we resolved **18a** via a diastereomeric salt to separate (+)-**18a** and (–)-**18a**, and subsequently elucidated their pharmacological properties. In the experiment using

isolated guinea pig arteries, the 5-HT₂ receptor antagonist activity of **18a** was found to reside primarily in (–)-**18a**, which was about 14-fold more potent than that of (+)-**18a**. In contrast, the α₁ blocking activity of (–)-**18a** was equivalent to or less than that of (+)-**18a** (Table 5). (–)-**18a** displayed high 5-HT₂ receptor binding affinity (IC₅₀=4.26 nM), which was 60-fold or more than 100-fold higher than its affinity for α₁ receptors (IC₅₀=254 nM) or 5-HT_{1A} receptors (IC₅₀=480 nM) respectively, and more than 400-fold higher for other receptors such as α₂ (IC₅₀=2380 nM), β (IC₅₀>10000 nM), D₂ (IC₅₀=2380 nM), muscarinic cholinergic (mACh) (IC₅₀>10000 nM), H₁ (IC₅₀=1730 nM) and H₂ (IC₅₀=7790 nM) receptors in receptor binding assays.

In human and canine platelet-rich plasma (PRP), collagen- or ADP-induced platelet aggregation potentiated by serotonin was markedly inhibited by (–)-**18a** (IC₅₀=6.5–16 nM) (Table 6). This antiplatelet aggregation effect by (–)-**18a** was more than 20-fold stronger than that by (+)-**18a**, and more than 2- and 100-fold stronger than those by ketanserin and sarpogrelate, respectively.

Next, we evaluated both enantiomers in an *in vivo* study. In the acute pulmonary thromboembolic death model in mice, (–)-**18a** (0.03 to 1 mg/kg) inhibited the mortality in a dose-dependent manner by oral administration before induction of platelet aggregation, and its inhibitory effect was significant at doses of 0.3 mg/kg or higher (Fig. 4). In addition, (+)-**18a** and ketanserin significantly inhibited mortality at 3 and 1 mg/kg, respectively. In contrast, sarpogrelate showed no significant inhibitory effect even at 30 mg/kg. From the results of *in vitro* and *in vivo* experiments, it was suggested that (–)-**18a** showed much more potent and selective 5-HT₂ receptor antagonist activity than (+)-**18a**.

In conclusion, several 5-aminoalkylpyrrolo[3,2-*c*]azepine derivatives showed potent 5-HT₂ receptor antagonist activity. Among these, (S)-(–)-5-[3-[4-(4-fluorophenyl)piperazin-1-

Table 4. Biological Activities of Pyrrolo[3,2-*c*]azepine Derivatives (**14a**, **18a**) and Pyrrolo[3,4-*c*]azepine Derivatives (**21**, **22**)

Compound	5-HT ₂ -blocking activity ^{a)}			α ₁ -blocking activity ^{b)}		D ₂ receptor binding affinity ^{c)} IC ₅₀ (nM)
	(% inhibition)			(% inhibition)		
	10 ^{−8} M	10 ^{−7} M	10 ^{−6} M	10 ^{−8} M	10 ^{−7} M	
14a		23	74	1	9	3260
18a	45	88	93	1	10	3110
21		31	75	2	19	NT ^{d)}
22		20	75	1	7	6340

a)–c) see corresponding footnotes of Table 1. d) Not tested.

Table 5. Comparison of Biological Activities of Racemic and Optically Active **18a**

Compound	5-HT ₂ -blocking activity ^{a)}						α ₁ -blocking activity ^{b)}					D ₂ receptor binding affinity ^{c)}
	(% inhibition)						(% inhibition)					
	10 ⁻⁹ M	3×10 ⁻⁹ M	10 ⁻⁸ M	10 ⁻⁷ M	10 ⁻⁶ M	pA ₂ ^{d)}	10 ⁻⁹ M	10 ⁻⁸ M	10 ⁻⁷ M	10 ⁻⁶ M	pA ₂ ^{d)}	IC ₅₀ (nM)
(±)- 18a		11	45	88	93	8.65±0.05	0	1	10	59	6.59±0.08	3110
(-)- 18a (SUN C5174)	7	31	58	91		8.98±0.06	0	0	7	54	6.51±0.12	2380
(+)- 18a			18	38	88	7.83±0.07	0	0	8	59	6.76±0.04	4750

a)–c) see corresponding footnotes of Table 1. d) Each value indicates the mean±S.E. of 3–5 experiments.

Table 6. Antiplatelet Aggregation Effects of (–)-**18a** and Reference Drugs in Canine and Human Platelet-rich Plasma

Species		Dog		Human	
Compound/inducer		Collagen (0.3–1 μg/ml)+ Serotonin (1 μM)	ADP (0.3–2 μM)+ Serotonin (1 μM)	Collagen (0.03–0.1 μg/ml)+ Serotonin (1 μM)	ADP (0.5–1 μM)+ Serotonin (10 μM)
IC ₅₀ (nM)	(–)- 18a (SUN C5174)	6.5	13	6.6	16
	(+)- 18a	305	274	617	2559
	Ketanserin	19	29	54	43
	Sarpogrelate	>1000	1679	>1000	>10000
	Sarpogrelate M-1	218	159	356	2259

IC₅₀ is the mean concentration that produced 50% inhibition estimated from the concentration-response curve in 4–6 experiments.

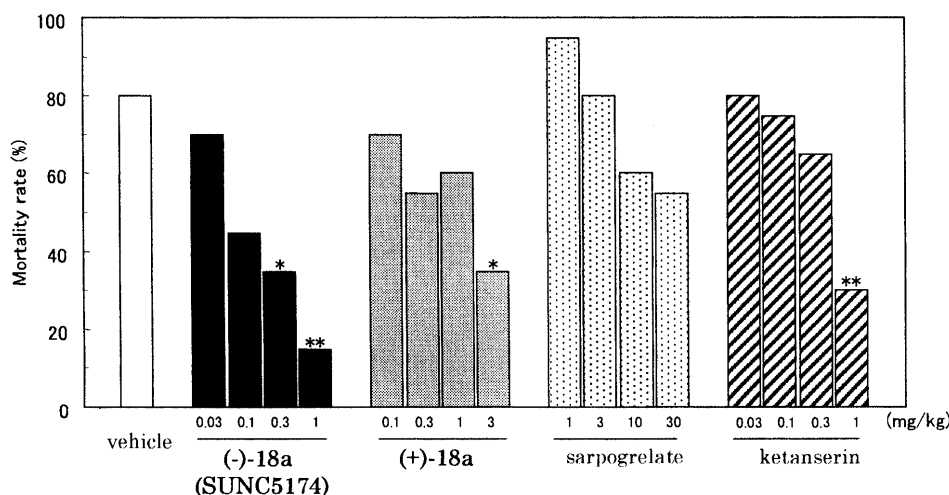


Fig. 4. Inhibitory Effects of Oral (-)-18a and Reference Drugs on Pulmonary Thromboembolic Death in Mice

Each column shows the percentage mortality rate due to pulmonary embolism induced by the intravenous dosing of collagen (5 mg/kg) and serotonin (1 mg/kg) 1 h after oral administration of the test drugs. Twenty mice were used in each group. Statistical differences in the results between vehicle control group and test drug treatment groups were analyzed using Fisher's exact test. *, $p < 0.05$; **, $p < 0.01$.

yl]propyl]-8-hydroxy-1-methyl-1,4,5,6,7,8-hexahydropyrrolo[3,2-*c*]azepin-4-one ((-)-18a, SUN C5174) displayed the best overall profile with potent and selective 5-HT₂ receptor antagonist activity. This property was confirmed by *in vivo* evaluation. These results indicated that the pyrrolo[3,2-*c*]azepine ring system is a useful scaffold for 5-HT₂ receptor antagonists.

Compound (-)-18a (SUN C5174) is currently undergoing clinical evaluation for treatment of peripheral circulatory diseases. Further pharmacological evaluation of (-)-18a will be reported elsewhere.

Experimental

Melting points were determined in open capillaries with a Büchi 535 digital melting point apparatus, and are uncorrected. The ¹H-NMR spectra were recorded on a JEOL JNM-GX270 or Bruker ARX 400 FT NMR spectrometer, and the chemical shifts were expressed in δ (ppm) values with tetramethylsilane as an internal standard. IR spectra were recorded on a Perkin-Elmer 1640 instrument. High resolution fast atom bombardment mass spectra (HR-FAB-MS) were measured on a JEOL JMS-HX110A instrument. Elemental analyses were performed on a Perkin-Elmer 240B elemental analyzer. Optical rotations were measured on a JASCO DIP-360 polarimeter.

In general, all organic extracts were dried over anhydrous sodium sulfate and the solvent was removed with a rotary evaporator under reduced pressure. Analytical TLC was carried out using Silica gel 60 F₂₅₄ plates (Merck Art 5715). Column chromatography was performed on Silica gel 60 (Merck Art 9385, 230–400 mesh).

The following known materials were prepared as described in the literature: methyl pyrrole-3-carboxylate;¹⁵ pyrrole-3-carboxylic acid;^{15b} 1-phenyl-1H-pyrrole-3-carboxylic acid;¹⁶ 1-(4-hydroxyphenyl)piperazine hydrobromide;¹⁷ 1-(1,2-benzisothiazol-3-yl)piperazine;¹⁸ 1-(2-chloroethyl)-4-(4-fluorophenyl)piperazine.¹⁹ 1-(3-Fluorophenyl)piperazine was prepared according to a procedure similar to that described in the literature.¹⁷

Methyl 1-Methyl-1H-pyrrole-3-carboxylate The method of Guida and Mathre²⁰ was employed with minor modification. Potassium *tert*-butoxide (49.8 g, 444 mmol) and 18-crown-6 (7.82 g, 29.6 mmol) were added successively to a stirred solution of methyl pyrrole-3-carboxylate (37.0 g, 296 mmol) in Et₂O (370 ml) at 0 °C. To the resultant suspension was added dropwise a solution of MeI (84.0 g, 592 mmol) in Et₂O (30 ml) under vigorous stirring and ice-cooling, followed by stirring at room temperature for 1 h. The reaction mixture was poured into half-saturated NaCl (200 ml), and the layers were separated. The aqueous layer was extracted with Et₂O (2 × 50 ml). The combined organic layers were washed with brine, dried, and evaporated to give an oil, which was distilled to afford the title compound (32.1 g, 78%) as a colorless oil, bp₄ 93.0–96.0 °C. IR (film): 1705 cm⁻¹. ¹H-NMR (CDCl₃) δ : 3.65 (3H, s), 3.78 (3H, s), 6.51–6.58 (2H, m), 7.22

(1H, m).

1-Methyl-1H-pyrrole-3-carboxylic Acid (4b) A mixture of methyl 1-methyl-1H-pyrrole-3-carboxylate (13.0 g, 93.4 mmol), 1 N NaOH (156 ml) and MeOH (156 ml) was stirred under reflux for 6 h. The reaction mixture was concentrated, and the residue was partitioned between water and Et₂O (150 ml each). The aqueous layer was acidified with 6 N HCl and extracted with EtOAc (3 × 150 ml). The combined extracts were washed with brine (150 ml), dried, and concentrated to give a solid which was recrystallized from EtOAc-diisopropyl ether (IPE) to afford **4b** (9.29 g, 79%) as pale brown crystals, mp 144.0–145.5 °C (lit.²¹ 145.0–145.5 °C). IR (KBr): 3300–2200, 1671 cm⁻¹. ¹H-NMR (CDCl₃) δ : 3.68 (3H, s), 6.56 (1H, m), 6.62 (1H, m), 7.31 (1H, m).

Ethyl 3-(3-Chloropropyl)aminopropionate Hydrochloride (9) 3-Chloropropylamine hydrochloride (130 g, 1 mol) was added to a stirred solution of 5 N NaOH (200 ml) at 0 °C. To the resultant solution was added *N,N*-dimethylformamide (DMF) (400 ml) and ethyl acrylate (120 g, 1.20 mol) successively below 10 °C. After stirring at room temperature for 16 h, the reaction mixture was poured into water (600 ml) and then extracted with EtOAc (4 × 200 ml). The combined extracts were washed with water (3 × 200 ml) and brine (200 ml), dried, and concentrated to afford a yellow oil (195 g). 4 N hydrogen chloride solution in EtOAc (252 ml) was added dropwise to a solution of the resultant oil in EtOAc (974 ml) below 15 °C under stirring, and stirring was continued at 0 °C for 30 min. The precipitates were filtered and washed twice with EtOAc to give **9** (148 g, 64%), mp 138.0–141.0 °C (acetone), colorless crystals. IR (KBr): 2850–2600, 1724 cm⁻¹. ¹H-NMR (CDCl₃) δ : 1.28 (3H, t, $J = 7.1$ Hz), 2.41 (2H, m), 3.02 (2H, t, $J = 7.2$ Hz), 3.19 (2H, m), 3.30 (2H, t, $J = 7.2$ Hz), 3.72 (2H, m), 4.19 (2H, q, $J = 7.1$ Hz), 9.75 (2H, brs). *Anal.* Calcd for C₈H₁₆ClNO₂·HCl: C, 41.75; H, 7.45; N, 6.09. Found: C, 41.85; H, 7.46; N, 6.21.

Method A: 1-Methyl-1,4,5,6,7,8-hexahydropyrrolo[3,2-*c*]azepine-4,8-dione (7b) and 2-Methyl-2,4,5,6,7,8-hexahydropyrrolo[3,4-*c*]azepine-4,8-dione (8b) To a stirred solution of **4b** (9.29 g, 74.2 mmol) and β -alanine benzyl ester *p*-toluenesulfonate (31.3 g, 89.1 mmol) in DMF (400 ml) at 0 °C were added dropwise and successively a solution of DEPC (14.5 g, 89.1 mmol) in DMF (50 ml) and a solution of Et₃N (18.0 g, 178 mmol) in DMF (50 ml). After stirring at room temperature for 16 h, the reaction mixture was concentrated. The residue was dissolved in EtOAc–benzene (2 : 1 v/v, 600 ml), washed successively with half-saturated K₂CO₃, water, 10% citric acid, water and brine (300 ml each). The organic layer was dried and concentrated to give a brown solid, which was recrystallized from EtOAc–hexane to afford **5b** (19.1 g, 90%) as colorless crystals. This material was used immediately in the next step, mp 109.0–110.0 °C. IR (KBr): 3270, 1732, 1623, 1558 cm⁻¹. ¹H-NMR (CDCl₃) δ : 2.66 (2H, t, $J = 5.9$ Hz), 3.64 (3H, s), 3.66 (2H, m), 5.14 (2H, s), 6.28 (1H, dd, $J = 2.0, 2.6$ Hz), 6.33 (1H, brs), 6.53 (1H, dd, $J = 2.0, 2.6$ Hz), 7.11 (1H, t, $J = 2.0$ Hz), 7.29–7.41 (5H, m).

A suspension of **5b** (19.0 g, 66.4 mmol) and 5% Pd–C (1.90 g, 10% wt eq) in tetrahydrofuran (THF) (500 ml) was vigorously stirred under an atmos-

phere of hydrogen for 21 h at room temperature. The catalyst was filtered through celite and washed thoroughly with MeOH. The combined filtrate and washings were concentrated to give a solid, which was recrystallized from CH₃CN to afford **6b** (12.3 g, 95%) as colorless crystals. This material was used immediately in the next step, mp 136.0–138.5 °C. IR (KBr): 3357, 1715, 1574 cm⁻¹. ¹H-NMR (DMSO-*d*₆) δ: 2.44 (2H, t, *J*=7.2 Hz), 3.35 (2H, m), 3.61 (3H, s), 6.39 (1H, m), 6.66 (1H, m), 7.21 (1H, m), 7.54 (1H, t, *J*=5.5 Hz).

A mixture of **6b** (11.0 g, 56.1 mmol) and approximately 80% PPA (550 g) was mechanically stirred at 100 °C for 1 h and then 120 °C for 10 min. The reaction mixture was poured into ice-water, and the pH of the solution was adjusted to 4 with K₂CO₃. The resultant solution was extracted with CHCl₃ (2 × 1 l, 2 × 500 ml). The extracts were washed with brine, dried, and concentrated to give a solid, which contained **7b** and **8b**. The mixture was subjected to column chromatography (eluent, EtOAc:MeOH=97:3, then CHCl₃:MeOH=19:1) to give **7b** (6.29 g, 63%) from the first fraction. The second fraction yielded **8b** (2.58 g, 26%). **7b**: mp 174.0–176.0 °C (CH₃CN), colorless crystals. IR (KBr): 3349, 1652, 1522 cm⁻¹. ¹H-NMR (CDCl₃) δ: 2.86 (2H, m), 3.52 (2H, m), 3.97 (3H, s), 6.78 (1H, d, *J*=2.6 Hz), 6.87 (1H, d, *J*=2.6 Hz), 7.98 (1H, brs). *Anal.* Calcd for C₉H₁₀N₂O₂: C, 60.67; H, 5.66; N, 15.72. Found: C, 60.79; H, 5.61; N, 15.97. **8b**: mp 218.0–222.0 °C (CH₃CN-IPE), colorless crystals. IR (KBr): 3176, 1652, 1547, 1519 cm⁻¹. ¹H-NMR (CDCl₃) δ: 2.82 (2H, m), 3.52 (2H, m), 3.74 (3H, s), 6.90 (1H, brs), 7.34–7.36 (2H, m). *Anal.* Calcd for C₉H₁₀N₂O₂: C, 60.67; H, 5.66; N, 15.72. Found: C, 60.67; H, 5.63; N, 15.90.

Compounds **7a** and **8a** were synthesized from **4a** using the 3-step procedure described above. **7a**: 52% overall yield, colorless crystals, mp >250 °C (MeOH-IPE). ¹H-NMR (CDCl₃) δ: 2.71 (2H, m), 3.33 (2H, m), 6.57 (1H, s), 7.11 (1H, d, *J*=2.4 Hz), 8.29 (1H, brs), 12.13 (1H, brs). *Anal.* Calcd for C₈H₈N₂O₂: C, 58.53; H, 4.91; N, 17.06. Found: C, 58.23; H, 4.86; N, 16.89. **8a**: 23% overall yield, colorless crystals, mp >250 °C (MeOH-IPE). ¹H-NMR (CDCl₃) δ: 2.65 (2H, m), 3.29 (2H, m), 7.34 (1H, s), 7.43 (1H, s), 7.80 (1H, brs), 11.97 (1H, brs). *Anal.* Calcd for C₈H₈N₂O₂: C, 58.53; H, 4.91; N, 17.06. Found: C, 58.38; H, 4.92; N, 16.90.

Method B: 1-Ethyl-1,4,5,6,7,8-hexahydropyrrolo[3,2-*c*]azepine-4,8-dione (7c) A suspension of **7a** (164 mg, 1 mmol), iodoethane (312 mg, 2 mmol) and K₂CO₃ (276 mg, 2 mmol) in 2-butanone (40 ml) was stirred under reflux for 15 h. The reaction mixture was filtered, the residue was washed with CHCl₃, and the combined filtrate and washings were concentrated. The residue was purified by column chromatography (eluent, CHCl₃:MeOH=9:1) to afford **7c** (184 mg, 96%), which was used immediately in the next step. A pure sample was obtained by recrystallization, mp 155.0–156.0 °C (EtOAc-IPE), colorless crystals. IR (KBr): 3185, 1668, 1643, 1526 cm⁻¹. ¹H-NMR (CDCl₃) δ: 1.40 (3H, t, *J*=7.1 Hz), 2.87 (2H, m), 3.50 (2H, m), 4.39 (2H, q, *J*=7.1 Hz), 6.29 (1H, brs), 6.82 (1H, d, *J*=2.7 Hz), 6.94 (1H, d, *J*=2.7 Hz). *Anal.* Calcd for C₁₀H₁₂N₂O₂: C, 62.49; H, 6.29; N, 14.57. Found: C, 62.53; H, 6.28; N, 14.52.

Compound **7d** was prepared in a similar manner to that described for **7c**, and used immediately in the next step. **7d**: 93% yield, colorless crystals, mp 170.5–171.5 °C (EtOAc-hexane). ¹H-NMR (CDCl₃) δ: 2.83 (2H, m), 3.49 (2H, m), 5.60 (2H, s), 6.78 (1H, brs), 6.87 (1H, d, *J*=2.7 Hz), 6.97 (1H, d, *J*=2.7 Hz), 7.11 (2H, m), 7.24–7.34 (3H, m).

Method C: 5-(3-Chloropropyl)-1-methyl-1,4,5,6,7,8-hexahydropyrrolo[3,2-*c*]azepine-4,8-dione (12a) To a stirred solution of potassium *tert*-butoxide (1.68 g, 15 mmol) in THF (40 ml) was added **7b** (1.34 g, 7.5 mmol) at 0 °C followed by stirring at the same temperature for 1 h. A solution of 1-bromo-3-chloropropane (5.90 g, 37.5 mmol) in THF (40 ml) was added dropwise to the reaction mixture at 0 °C and stirring was continued at room temperature for 93 h. An aqueous solution of citric acid (1.58 g, 8.2 mmol) was then added, and the mixture was concentrated. The residue was diluted with water (100 ml), and extracted with CHCl₃ (2 × 100 ml). The combined extracts were washed with brine, dried, and concentrated to give an oil, which was purified by column chromatography (eluent, EtOAc:hexane=2:1) to afford **12a** (628 mg, 33%), which was used immediately in the next step. A pure sample was obtained by recrystallization, mp 116.5–118.0 °C (EtOAc-IPE), colorless crystals. IR (KBr): 1660, 1626, 1524 cm⁻¹. ¹H-NMR (CDCl₃) δ: 2.14 (2H, quintet, *J*=6.7 Hz), 2.85 (2H, dd, *J*=4.0, 6.6 Hz), 3.62 (2H, t, *J*=6.7 Hz), 3.69 (2H, m), 3.75 (2H, t, *J*=6.7 Hz), 3.95 (3H, s), 6.77 (1H, d, *J*=2.6 Hz), 6.84 (1H, d, *J*=2.6 Hz). *Anal.* Calcd for C₁₂H₁₅ClN₂O₂: C, 56.59; H, 5.94; N, 11.00. Found: C, 56.68; H, 5.90; N, 11.04.

Compounds **12b–d** were prepared in a similar manner to that described for **7c**, and was used without further purification. **12b**: 49% yield, colorless

crystals, mp 100.0–102.0 °C (EtOAc-hexane). ¹H-NMR (CDCl₃) δ: 1.76–1.91 (4H, m), 2.83 (2H, dd, *J*=4.0, 6.4 Hz), 3.57–3.69 (6H, m), 3.95 (3H, s), 6.76 (1H, d, *J*=2.6 Hz), 6.83 (1H, d, *J*=2.6 Hz). **12c**: 29% yield, colorless oil. ¹H-NMR (CDCl₃) δ: 1.39 (3H, t, *J*=7.1 Hz), 2.14 (2H, quintet, *J*=6.7 Hz), 2.85 (2H, m), 3.61 (2H, t, *J*=6.7 Hz), 3.68 (2H, m), 3.74 (2H, t, *J*=6.7 Hz), 4.36 (2H, q, *J*=7.1 Hz), 6.78 (1H, d, *J*=2.7 Hz), 6.92 (1H, d, *J*=2.7 Hz). **12d**: 22% yield, colorless oil. ¹H-NMR (CDCl₃) δ: 2.13 (2H, m), 2.81 (2H, m), 3.61 (2H, t, *J*=6.4 Hz), 3.66 (2H, m), 3.74 (2H, t, *J*=6.9 Hz), 5.57 (2H, s), 6.83 (1H, d, *J*=2.7 Hz), 6.95 (1H, d, *J*=2.7 Hz), 7.10 (2H, m), 7.23–7.34 (3H, m).

Method D: 5-(3-Chloropropyl)-1-methyl-1,4,5,6,7,8-hexahydropyrrolo[3,2-*c*]azepine-4,8-dione (12a) and 5-(3-Chloropropyl)-2-methyl-2,4,5,6,7,8-hexahydropyrrolo[3,4-*c*]azepine-4,8-dione (13a) To a stirred solution of **4b** (12.5 g, 100 mmol) and **9** (27.6 g, 120 mmol) in CH₂Cl₂ (450 ml) at 0 °C were added successively a solution of Et₃N (12.1 g, 120 mmol) in CH₂Cl₂ (50 ml), powdered 1-ethyl-3-(3-dimethylamino-propyl)carbodiimide hydrochloride (WSCD·HCl) (23.0 g, 120 mmol) and powdered 4-dimethylaminopyridine (4-DMAP) (2.93 g, 24 mmol). After stirring at room temperature for 5 h, the reaction mixture was washed sequentially with water, 1 N HCl, water, half-saturated NaHCO₃, water and brine (250 ml each), dried, and concentrated. The residue was purified by column chromatography (eluent, EtOAc:hexane=1:1) to afford **10a** (26.1 g, 87%) as a colorless oil. IR (film): 1730, 1611, 1540 cm⁻¹. ¹H-NMR (CDCl₃) δ: 1.26 (3H, t, *J*=7.1 Hz), 2.12 (2H, m), 2.68 (2H, t, *J*=7.3 Hz), 3.57 (2H, t, *J*=6.4 Hz), 3.62–3.68 (5H, m), 3.80 (2H, t, *J*=7.3 Hz), 4.15 (2H, q, *J*=7.1 Hz), 6.33 (1H, m), 6.54 (1H, t, *J*=2.5 Hz), 7.05 (1H, m). HR-FAB-MS Calcd for C₁₄H₂₂³⁵ClN₂O₃: 301.1319 [M]⁺. Found: 301.1322.

To a stirred solution of ester **10a** (1.50 g, 5 mmol) in THF (2.6 ml) was added dropwise 2 N NaOH (2.6 ml, 5.2 mmol) under ice-cooling followed by stirring at room temperature for 30 min. The resultant solution was acidified (pH ca. 3) with 6 N HCl under ice-cooling, and then extracted with CH₂Cl₂ (3 × 50 ml). The combined extracts were washed with brine, dried, and concentrated to afford crude carboxylic acid **11a** (1.36 g). This material was immediately used in the next step without further purification.

To crude **11a** (1.36 g) was added a solution (5.82 g) which was prepared by stirring a mixture of P₂O₅ and methanesulfonic acid (1:6.1 w/w) at 90 °C until homogeneity (approximately 2 h) in another vessel, and the resultant mixture was stirred at 90 °C for 30 min. The reaction mixture was poured into ice-water, and extracted with CHCl₃ (3 × 100 ml). The organic extracts were washed with brine, dried, and concentrated to give a solid, which contained **12a** and **13a**. The mixture was subjected to column chromatography (eluent, EtOAc) to give **12a** (945 mg, 74%) as colorless crystals from the first fraction. The second fraction yielded **13a** (107 mg, 8.4%). **12a**: Physical data were identical with those of the compound prepared by method C. **13a**: mp 123.0–124.5 °C (EtOAc), colorless crystals. IR (KBr): 1653, 1625, 1520 cm⁻¹. ¹H-NMR (CDCl₃) δ: 2.13 (2H, quintet, *J*=6.6 Hz), 2.80 (2H, m), 3.62 (2H, t, *J*=6.6 Hz), 3.66 (2H, m), 3.71 (2H, t, *J*=6.6 Hz), 3.73 (3H, s), 7.28–7.31 (2H, m). *Anal.* Calcd for C₁₂H₁₅ClN₂O₂: C, 56.59; H, 5.94; N, 11.00. Found: C, 56.54; H, 6.00; N, 10.83.

Compounds **12e** and **13e** were synthesized from **4c** in a similar manner described for **12a** and **13a**, and used immediately in the next step. **12e**: 51% overall yield, mp 97.0–98.5 °C (EtOAc-hexane), colorless crystals. ¹H-NMR (CDCl₃) δ: 2.16 (2H, m), 2.81 (2H, m), 3.64 (2H, t, *J*=6.4 Hz), 3.75–3.81 (4H, m), 6.92 (1H, d, *J*=2.8 Hz), 6.99 (1H, d, *J*=2.8 Hz), 7.22–7.27 (2H, m), 7.40–7.46 (3H, m). **13e**: 5.8% overall yield, mp 116.5–118.0 °C (EtOAc-hexane), colorless crystals. ¹H-NMR (CDCl₃) δ: 2.16 (2H, m), 2.87 (2H, m), 3.64 (2H, t, *J*=6.4 Hz), 3.71–3.79 (4H, m), 7.37–7.52 (5H, m), 7.73 (1H, d, *J*=2.6 Hz), 7.75 (1H, d, *J*=2.6 Hz).

Method E: 5-[3-[4-(4-Fluorophenyl)piperazin-1-yl]propyl]-1-methyl-1,4,5,6,7,8-hexahydropyrrolo[3,2-*c*]azepine-4,8-dione (14a) A mixture of chloride **12a** (611 mg, 2.4 mmol), 1-(4-fluorophenyl)piperazine (649 mg, 3.6 mmol), K₂CO₃ (498 mg, 3.6 mmol) and NaI (720 mg, 4.8 mmol) in CH₃CN (30 ml) was stirred under reflux for 38 h. After the solvent was removed, the residue was diluted with half-saturated K₂CO₃ (50 ml), and then extracted with CHCl₃ (2 × 100 ml). The combined extracts were washed with brine, dried, and concentrated to give an oil, which was purified by column chromatography (eluent, EtOAc:MeOH=9:1) to afford **14a** (960 mg, quant.) as a pale yellow oil. IR (film): 1654, 1624 cm⁻¹. ¹H-NMR (CDCl₃) δ: 1.88 (2H, quintet, *J*=7.3 Hz), 2.48 (2H, t, *J*=7.3 Hz), 2.62 (4H, m), 2.84 (2H, m), 3.12 (4H, m), 3.58–3.74 (4H, m), 3.95 (3H, s), 6.77 (1H, d, *J*=2.6 Hz), 6.81–7.02 (5H, m). HR-FAB-MS Calcd for C₂₂H₂₈FN₄O₂: 399.2196 [M]⁺. Found: 399.2220.

Compounds **14c–m** and **14o–r** were prepared in a similar manner to

14a, except that in the syntheses of **14c**, **14i**, **14k** and **14m**, amine (1 eq) and NaHCO_3 (2 eq) were used instead of amine (1.5 eq) and K_2CO_3 (1.5 eq): in the syntheses of **14e** and **14g**, amine hydrochloride (1 eq) and NaHCO_3 (4 eq) were used; in the syntheses of **14f** and **14h**, amine hydrobromide (1 eq) and NaHCO_3 (4 eq) were used; in the syntheses of **14j** and **14l**, amine dihydrochloride (1 eq) and NaHCO_3 (6 eq) were used. These compounds were immediately transformed to the corresponding alcohol **18** by method G.

Method F: 5-[2-[4-(4-Fluorophenyl)piperazin-1-yl]ethyl]-1-methyl-1,4,5,6,7,8-hexahydropyrrolo[3,2-c]azepine-4,8-dione (14n) To a stirred suspension of NaH (1.92 g of a 60% oil dispersion, 48 mmol) in DMF (100 ml) was added a solution of **7b** (7.13 g, 40 mmol) in DMF (150 ml) at 0 °C over a period of 30 min. The mixture was stirred at 0 °C for 30 min and at room temperature for 90 min, and then cooled again to 0 °C. A solution of 1-(2-chloroethyl)-4-(4-fluorophenyl)piperazine (14.6 g, 60 mmol) in DMF (150 ml) was added to the mixture over a period of 30 min, and stirring was continued at room temperature for 16 h. The title compound **14n** (2.77 g, 18%) was obtained as a yellow oil by the same work-up and purification procedure as described for the preparation of **14a**. IR (film): 1652, 1626 cm^{-1} . $^1\text{H-NMR}$ (CDCl_3) δ : 2.63–2.72 (6H, m), 2.93 (2H, m), 3.10 (4H, m), 3.67 (2H, m), 3.78 (2H, m), 3.95 (3H, s), 6.77 (1H, d, $J=2.6$ Hz), 6.83 (1H, d, $J=2.6$ Hz), 6.85 (2H, m), 6.95 (2H, m). HR-FAB-MS Calcd for $\text{C}_{21}\text{H}_{26}\text{FN}_4\text{O}_2$: 385.2039 [MH] $^+$. Found: 385.2032.

Method G: 5-[3-[4-(4-Fluorophenyl)piperazin-1-yl]propyl]-8-hydroxy-1-methyl-1,4,5,6,7,8-hexahydropyrrolo[3,2-c]azepin-4-one (18a) To a stirred solution of ketone **14a** (797 mg, 2 mmol) in EtOH (30 ml) was added portionwise NaBH_4 (757 mg, 20 mmol) at 0 °C, and stirring was continued at 0 °C for 1 h and at room temperature for 16 h. Water (20 ml) was added, and the resultant mixture was stirred at room temperature for 1 h. After the solvent was removed, the residue was diluted with brine (100 ml) and then extracted with CHCl_3 (3 \times 100 ml). The combined extracts were washed with brine, dried, and concentrated. The residue was purified by column chromatography (eluent, EtOAc:MeOH=4:1) to afford **18a** (710 mg, 89%) as colorless crystals. Compound **18n** was synthesized similarly from **14n**. Compounds **18c–m** and **18o–r** were prepared by amination of chloride **12** (method E) and successive reduction of crude **14** (method G) in a similar manner to that described above. The physical data for compounds **18a** and **18c–r** are listed in Table 7.

Method H: 5-[3-[4-(4-Fluorobenzoyl)piperidino]propyl]-8-hydroxy-1-methyl-1,4,5,6,7,8-hexahydropyrrolo[3,2-c]azepin-4-one (18b) To a stirred suspension of ketone **12a** (255 mg, 1 mmol) in EtOH (10 ml) was added portionwise NaBH_4 (85 mg, 2.25 mmol) at 0 °C, followed by stirring at room temperature for 6 h. The work-up was performed in a similar manner to that described in method G to give crude **17** (256 mg) as a colorless solid. This material was sufficiently pure to be used without further purification in the next step. A pure sample was obtained by recrystallization from EtOAc–hexane, mp 107.0–108.5 °C, colorless crystals. IR (KBr): 3328, 1586, 1542, 1513 cm^{-1} . $^1\text{H-NMR}$ (CDCl_3) δ : 2.05 (2H, quintet, $J=6.7$ Hz), 2.22 (2H, m), 2.61 (1H, d, $J=7.8$ Hz), 3.33 (1H, m), 3.52–3.69 (5H, m), 3.72 (3H, s), 4.85–4.93 (1H, m), 6.60 (1H, d, $J=2.9$ Hz), 6.66 (1H, d, $J=2.9$ Hz). Anal. Calcd for $\text{C}_{12}\text{H}_{17}\text{ClN}_2\text{O}_2$: C, 56.14; H, 6.67; N, 10.91. Found: C, 56.08; H, 6.73; N, 10.86.

A suspension of crude **17** (256 mg), 4-(4-fluorobenzoyl)piperidine hydrochloride (244 mg, 1 mmol), NaHCO_3 (336 mg, 4 mmol) and NaI (300 mg, 2 mmol) in CH_3CN (15 ml) was stirred under reflux for 15 h. The work-up and purification was performed in a similar manner to that described in method E to afford **18b** (335 mg, 78% overall) as colorless crystals. The physical data for **18b** are listed in Table 7.

Method I: (E)-5-[3-[4-(4-Fluorophenyl)piperazin-1-yl]propyl]-8-hydroxyimino-1-methyl-1,4,5,6,7,8-hexahydropyrrolo[3,2-c]azepin-4-one (15) and (Z)-5-[3-[4-(4-Fluorophenyl)piperazin-1-yl]propyl]-8-hydroxyimino-1-methyl-1,4,5,6,7,8-hexahydropyrrolo[3,2-c]azepin-4-one (15') A solution of **14a** (797 mg, 2 mmol) and hydroxylamine hydrochloride (556 mg, 8 mmol) in pyridine (40 ml) was stirred at 90 °C for 17 h. After the reaction mixture was evaporated to dryness, the residue was diluted with half-saturated K_2CO_3 (80 ml), and then extracted with CHCl_3 (2 \times 100 ml). The combined extracts were washed with brine, dried, and concentrated to give an oil, which contained mainly **15** (R_f 0.46, CHCl_3 :MeOH=9:1) and a trace amount of the isomer **15'** (R_f 0.35, CHCl_3 :MeOH=9:1). The mixture was subjected to column chromatography (eluent, CHCl_3 :MeOH=19:1) to give (E)-oxime **15** (816 mg, 99%) as a colorless oil from the first fraction. The second fraction yielded (Z)-oxime **15'** (11 mg, 1%) as a colorless oil. **15**: IR (film): 3177, 1615, 1506 cm^{-1} . $^1\text{H-NMR}$ (CDCl_3) δ : 1.89 (2H, m),

2.50 (2H, m), 2.67 (4H, m), 3.05 (2H, m), 3.18 (4H, m), 3.53 (2H, m), 3.61 (2H, t, $J=6.9$ Hz), 3.67 (3H, s), 6.60 (1H, d, $J=3.0$ Hz), 6.64 (1H, d, $J=3.0$ Hz), 6.86 (2H, m), 6.96 (2H, m). HR-FAB-MS Calcd for $\text{C}_{22}\text{H}_{26}\text{FN}_4\text{O}_2$: 414.2305 [MH] $^+$. Found: 414.2294. **15'**: IR (film): 3190, 1614, 1505 cm^{-1} . $^1\text{H-NMR}$ (CDCl_3) δ : 1.86 (2H, m), 2.46 (2H, m), 2.63 (4H, m), 2.93 (2H, m), 3.13 (4H, m), 3.51–3.57 (4H, m), 3.62 (3H, s), 6.59 (1H, d, $J=2.8$ Hz), 6.70 (1H, d, $J=2.8$ Hz), 6.87 (2H, m), 6.96 (2H, m). HR-FAB-MS Calcd for $\text{C}_{22}\text{H}_{26}\text{FN}_4\text{O}_2$: 414.2305 [MH] $^+$. Found: 414.2310.

Method J: 5-[3-[4-(4-Fluorophenyl)piperazin-1-yl]propyl]-1-methyl-1,4,5,6,7,8-hexahydropyrrolo[3,2-c]azepin-4-one-8-spiro-2'-(1',3'-dithiolane) Dihydrochloride (16) To a stirred solution of **14a** (398 mg, 1 mmol) and 1,2-ethanedithiol (168 μl , 2 mmol) in acetic acid (15 ml) was added dropwise boron trifluoride etherate (246 μl , 2 mmol), followed by stirring at room temperature. After 24 h, 1,2-ethanedithiol (1.5 ml, 18 mmol) and boron trifluoride etherate (1.97 ml, 18 mmol) were added and the resultant mixture was stirred for an additional 48 h. The reaction mixture was then made basic with 2N NaOH and extracted with CHCl_3 (2 \times 50 ml). The combined extracts were washed with brine, dried, and concentrated. The residue was purified by column chromatography (eluent, EtOAc:MeOH=9:1) to afford **16'** (free base) (373 mg, 79%) as a pale yellow oil. IR (film): 1608 cm^{-1} . $^1\text{H-NMR}$ (CDCl_3) δ : 1.82 (2H, quintet, $J=7.3$ Hz), 2.45 (2H, t, $J=7.3$ Hz), 2.60 (4H, m), 2.69 (2H, d, $J=9.1$ Hz), 3.11 (4H, m), 3.41–3.70 (8H, m), 3.99 (3H, s), 6.64 (1H, d, $J=2.9$ Hz), 6.70 (1H, d, $J=2.9$ Hz), 6.86 (2H, m), 6.94 (2H, m). The free base **16'** was dissolved in CHCl_3 and treated with a solution of hydrogen chloride in Et₂O to give a solid, which was recrystallized from EtOH–Et₂O to afford **16** as pale yellow crystals, mp 196 °C (dec.). Anal. Calcd for $\text{C}_{24}\text{H}_{31}\text{FN}_4\text{OS}_2\cdot 2\text{HCl}\cdot 1/2\text{H}_2\text{O}$: C, 51.79; H, 5.98; N, 10.07. Found: C, 51.88; H, 6.30; N, 9.98.

Method K: 5-[3-[4-(4-Fluorophenyl)piperazin-1-yl]propyl]-1-methyl-1,4,5,6-tetrahydropyrrolo[3,2-c]azepin-4-one (19) To a stirred solution of **18a** (1.60 g, 4 mmol) in CHCl_3 (20 ml) was added a saturated solution of hydrogen chloride in CHCl_3 (120 ml) at room temperature, and stirring was continued at room temperature for 2 h. The mixture was washed with saturated NaHCO_3 (100 ml) and brine (50 ml), dried and concentrated. The residue was purified by column chromatography (eluent, CHCl_3 :MeOH=97:3) to give a solid which was recrystallized from CH_2Cl_2 –hexane to afford **19** (1.36 g, 89%) as colorless crystals, mp 175.5–177.0 °C (CH_2Cl_2 –hexane). IR (KBr): 2822, 1594 cm^{-1} . $^1\text{H-NMR}$ (CDCl_3) δ : 1.82 (2H, quintet, $J=7.3$ Hz), 2.43 (2H, t, $J=7.3$ Hz), 2.59 (4H, m), 3.11 (4H, m), 3.60 (2H, t, $J=7.3$ Hz), 3.61 (3H, s), 3.71 (2H, d, $J=6.9$ Hz), 6.09 (1H, m), 6.64–6.69 (2H, m), 6.75 (1H, d, $J=2.9$ Hz), 6.86 (2H, m), 6.94 (2H, m). Anal. Calcd for $\text{C}_{22}\text{H}_{27}\text{FN}_4\text{O}$: C, 69.09; H, 7.12; N, 14.65. Found: C, 68.80; H, 7.11; N, 14.62.

Method L: 5-[3-[4-(4-Fluorophenyl)piperazin-1-yl]propyl]-1-methyl-1,4,5,6,7,8-hexahydropyrrolo[3,2-c]azepin-4-one (20) A suspension of **19** (210 mg, 0.55 mmol), 10% Pd–C (50 mg) and acetic acid (5 drops) in EtOH (30 ml) was vigorously stirred under an atmosphere of hydrogen at room temperature for 20 h. The catalyst was filtered through celite and washed with CHCl_3 . After the combined filtrate and washings were concentrated, the residue was diluted with NaHCO_3 (50 ml) and extracted with CHCl_3 (3 \times 50 ml). The extracts were washed with brine, dried, and concentrated to give an oil, which was purified by column chromatography (eluent, EtOAc:MeOH=5:1) to afford **20** (210 mg, quant.) as a pale yellow oil. IR (film): 1604, 1509 cm^{-1} . $^1\text{H-NMR}$ (CDCl_3) δ : 1.83 (2H, m), 2.11 (2H, m), 2.46 (2H, m), 2.61 (4H, m), 2.78 (2H, t, $J=6.9$ Hz), 3.12 (4H, m), 3.44 (2H, m), 3.49 (3H, s), 3.58 (2H, t, $J=7.3$ Hz), 6.54 (1H, d, $J=3.0$ Hz), 6.68 (1H, d, $J=3.0$ Hz), 6.82–6.90 (2H, m), 6.90–6.98 (2H, m). HR-FAB-MS Calcd for $\text{C}_{22}\text{H}_{30}\text{FN}_4\text{O}$: 385.2403 [MH] $^+$. Found: 385.2392.

Method M: 5-[3-[4-(4-Fluorophenyl)piperazin-1-yl]propyl]-2-methyl-2,4,5,6,7,8-hexahydropyrrolo[3,4-c]azepine-4,8-dione (21) The title compound was prepared from chloride **13a** by the same procedure as described for the preparation of **14a**, 93% yield, mp 140.0–141.0 °C, colorless crystals (EtOAc–IPE). IR (KBr): 1654, 1615, 1547 cm^{-1} . $^1\text{H-NMR}$ (CDCl_3) δ : 1.87 (2H, quintet, $J=7.3$ Hz), 2.47 (2H, t, $J=7.3$ Hz), 2.62 (4H, m), 2.79 (2H, m), 3.12 (4H, m), 3.60–3.68 (4H, m), 3.72 (3H, s), 6.87 (2H, m), 6.95 (2H, m), 7.27–7.29 (2H, m). Anal. Calcd for $\text{C}_{22}\text{H}_{27}\text{FN}_4\text{O}_2$: C, 66.31; H, 6.83; N, 14.06. Found: C, 66.26; H, 6.88; N, 14.13.

Method N: 5-[3-[4-(4-Fluorophenyl)piperazin-1-yl]propyl]-8-hydroxy-2-methyl-2,4,5,6,7,8-hexahydropyrrolo[3,4-c]azepin-4-one (22) The title compound was prepared from **21** by the same procedure as described for the preparation of **18a**, 99% yield, mp 95.0–97.0 °C, colorless crystals (toluene). IR (KBr): 3500–3200, 1599, 1537 cm^{-1} . $^1\text{H-NMR}$ (CDCl_3) δ : 1.84 (2H, quintet, $J=7.3$ Hz), 2.06–2.26 (3H, m), 2.46 (2H, m), 2.61 (4H,

Table 7. Physical and Spectral Data for Compounds **18a–r**

Compd. No.	Yield (%) ^{a)}	mp (°C) (solvent) ^{b)}	Formula	Analysis (%) or HRMS Calcd (Found)			¹ H-NMR (CDCl ₃) δ	IR (cm ⁻¹)
				C	H	N		
18a	89	166.0—167.5 (EA)	C ₂₂ H ₂₉ FN ₄ O ₂	65.98 (65.92)	7.30 (7.37)	13.99 (14.04)	1.82 (2H, quintet, <i>J</i> =7.3 Hz), 2.15—2.32 (3H, m), 2.44 (2H, t, <i>J</i> =7.3 Hz), 2.60 (4H, m), 3.11 (4H, m), 3.34 (1H, m), 3.52 (1H, m), 3.59—3.70 (2H, m), 3.72 (3H, s), 4.91 (1H, br s), 6.61 (1H, d, <i>J</i> =2.9 Hz), 6.70 (1H, d, <i>J</i> =2.9 Hz), 6.87 (2H, m), 6.95 (2H, m)	3258, 1595, 1509 ^{e)}
18b	78	175.5—178.0 (dec.) (IPA–IPE)	C ₂₄ H ₃₀ FN ₃ O ₃	67.43 (67.14)	7.07 (7.14)	9.83 (9.74)	1.72—1.87 (6H, m), 2.07 (2H, m), 2.21 (2H, m), 2.38 (2H, m), 2.98 (2H, m), 3.18 (1H, m), 3.30 (1H, m), 3.44 (1H, m), 3.56 (1H, m), 3.63 (1H, m), 3.72 (3H, s), 4.88 (1H, t, <i>J</i> =4.8 Hz), 6.58 (1H, d, <i>J</i> =2.9 Hz), 6.65 (1H, d, <i>J</i> =2.9 Hz), 7.13 (2H, m), 7.96 (2H, m)	1677, 1600, 1508 ^{e)}
18c	79	— ^{c)}	C ₂₃ H ₃₁ N ₃ O ₂	382.2494 [MH] ⁺ (382.2529 [MH] ⁺) ^{d)}			1.82—1.93 (6H, m), 2.10—2.31 (4H, m), 2.44—2.59 (3H, m), 3.12 (2H, d, <i>J</i> =11.3 Hz), 3.33 (1H, m), 3.46—3.69 (3H, m), 3.72 (3H, s), 4.90 (1H, t, <i>J</i> =4.6 Hz), 6.59 (1H, d, <i>J</i> =2.9 Hz), 6.66 (1H, d, <i>J</i> =2.9 Hz), 7.17—7.25 (3H, m), 7.25—7.33 (2H, m)	3312, 1591, 1540, 1511 ^{f)}
18d	89	167.5—170.0 (IPA–IPE)	C ₂₂ H ₃₀ N ₄ O ₂	69.08 (68.99)	7.91 (8.07)	14.65 (14.50)	1.81 (2H, quintet, <i>J</i> =7.3 Hz), 2.22 (2H, m), 2.44 (2H, m), 2.61 (4H, m), 3.20 (4H, m), 3.33 (1H, m), 3.48 (1H, m), 3.63 (2H, m), 3.72 (3H, s), 4.89 (1H, t, <i>J</i> =4.3 Hz), 6.59 (1H, d, <i>J</i> =2.9 Hz), 6.64 (1H, d, <i>J</i> =2.9 Hz), 6.84 (1H, d, <i>J</i> =7.3 Hz), 6.91 (2H, d, <i>J</i> =8.1 Hz), 7.25 (2H, m)	3278, 1598, 1508 ^{e)}
18e	73	138.0—140.0 (EA)	C ₂₂ H ₂₉ FN ₄ O ₂	65.98 (65.81)	7.30 (7.30)	13.99 (13.88)	1.82 (2H, quintet, <i>J</i> =7.3 Hz), 2.23 (2H, m), 2.46 (2H, m), 2.63 (4H, m), 3.11 (4H, m), 3.34 (1H, m), 3.52 (1H, m), 3.59—3.70 (2H, m), 3.72 (3H, s), 4.90 (1H, t, <i>J</i> =4.5 Hz), 6.61 (1H, d, <i>J</i> =2.9 Hz), 6.70 (1H, d, <i>J</i> =2.9 Hz), 6.88—7.08 (4H, m)	3312, 1587, 1540, 1501 ^{e)}
18f	81	163.5—168.5 (EA–H)	C ₂₂ H ₂₉ FN ₄ O ₂	65.98 (65.88)	7.30 (7.30)	13.99 (13.91)	1.80 (2H, m), 2.22 (2H, m), 2.43 (2H, m), 2.58 (4H, m), 3.19 (4H, m), 3.32 (1H, m), 3.48 (1H, m), 3.57—3.69 (2H, m), 3.72 (3H, s), 4.89 (1H, t, <i>J</i> =4.4 Hz), 6.51 (1H, dt, <i>J</i> =1.9, 8.2 Hz), 6.57 (1H, m), 6.60 (1H, d, <i>J</i> =2.9 Hz), 6.66 (1H, m), 6.68 (1H, d, <i>J</i> =2.9 Hz), 7.17 (1H, m)	3273, 1596, 1509 ^{e)}
18g	89	181.0—183.0 (C–EA)	C ₂₂ H ₂₉ ClN ₄ O ₂	63.38 (63.29)	7.01 (7.03)	13.44 (13.50)	1.82 (2H, m), 2.22 (2H, m), 2.43 (2H, m), 2.59 (4H, m), 3.15 (4H, m), 3.33 (1H, m), 3.50 (1H, m), 3.56—3.69 (2H, m), 3.72 (3H, s), 4.89 (1H, m), 6.61 (1H, d, <i>J</i> =2.9 Hz), 6.69 (1H, d, <i>J</i> =2.9 Hz), 6.82 (2H, m), 7.19 (2H, m)	3236, 1582, 1538, 1500 ^{e)}
18h	49	— ^{c)}	C ₂₂ H ₃₀ N ₄ O ₃	399.2396 [MH] ⁺ (399.2412 [MH] ⁺) ^{d)}			1.83 (2H, quintet, <i>J</i> =7.3 Hz), 2.21 (2H, m), 2.44 (2H, t, <i>J</i> =7.3 Hz), 2.60 (4H, m), 3.07 (4H, m), 3.34 (1H, m), 3.57—3.71 (3H, m), 3.72 (3H, s), 4.91 (1H, m), 6.63 (1H, d, <i>J</i> =2.6 Hz), 6.72 (1H, d, <i>J</i> =2.6 Hz), 6.75—6.84 (4H, m)	3250, 1585, 1513 ^{f)}
18i	87	177.0—178.5 (C–IPE)	C ₂₂ H ₂₉ N ₅ O ₄	61.81 (61.59)	6.84 (6.79)	16.38 (16.26)	1.81 (2H, quintet, <i>J</i> =7.3 Hz), 2.13—2.31 (3H, m), 2.45 (2H, m), 2.59 (4H, m), 3.33 (1H, m), 3.41 (4H, m), 3.50—3.71 (3H, m), 3.72 (3H, s), 4.91 (1H, br s), 6.62 (1H, d, <i>J</i> =2.9 Hz), 6.70 (1H, d, <i>J</i> =2.9 Hz), 6.81 (2H, m), 8.11 (2H, m)	3299, 1599, 1509 ^{e)}
18j	84	155.0—158.0 (C–IPE)	C ₂₃ H ₃₂ N ₄ O ₃ · 1/4H ₂ O	66.24 (66.29)	7.73 (7.80)	13.43 (13.39)	1.81 (2H, quintet, <i>J</i> =7.3 Hz), 2.22 (2H, m), 2.44 (2H, m), 2.61 (4H, m), 3.09 (4H, m), 3.33 (1H, m), 3.51 (1H, m), 3.57—3.69 (2H, m), 3.72 (3H, s), 3.76 (3H, s), 4.89 (1H, t, <i>J</i> =4.6 Hz), 6.60 (1H, d, <i>J</i> =2.9 Hz), 6.69 (1H, d, <i>J</i> =2.9 Hz), 6.83 (2H, m), 6.89 (2H, m)	3304, 1597, 1513 ^{e)}
18k	67	— ^{c)}	C ₂₉ H ₃₆ N ₄ O ₂	473.2916 [MH] ⁺ (473.2901 [MH] ⁺) ^{d)}			1.76 (2H, m), 2.19 (2H, m), 2.32—2.57 (10H, m), 3.28 (1H, m), 3.47 (1H, m), 3.53—3.66 (2H, m), 3.71 (3H, s), 4.22 (1H, s), 4.88 (1H, t, <i>J</i> =4.5 Hz), 6.59 (1H, d, <i>J</i> =2.9 Hz), 6.67 (1H, d, <i>J</i> =2.9 Hz), 7.16 (2H, t, <i>J</i> =7.3 Hz), 7.26 (4H, m), 7.40 (4H, m)	3319, 1590, 1540, 1509 ^{f)}
18l	80	169.0—172.5 (EA–H)	C ₂₀ H ₂₈ N ₆ O ₂	62.48 (62.48)	7.34 (7.33)	21.86 (21.89)	1.81 (2H, quintet, <i>J</i> =7.3 Hz), 2.22 (2H, m), 2.42 (2H, m), 2.49 (4H, m), 3.33 (1H, m), 3.49 (1H, m), 3.59—3.70 (2H, m), 3.72 (3H, s), 3.81 (4H, m), 4.89 (1H, t, <i>J</i> =4.4 Hz), 6.46 (1H, d, <i>J</i> =4.8 Hz), 6.60 (1H, d, <i>J</i> =2.9 Hz), 6.68 (1H, d, <i>J</i> =2.9 Hz), 8.29 (2H, d, <i>J</i> =4.8 Hz)	3250, 1610, 1584, 1546, 1508 ^{e)}
18m	85	170.0—170.5 (C–EA)	C ₂₃ H ₂₉ N ₅ O ₂ S	62.84 (62.74)	6.65 (6.60)	15.93 (15.94)	1.83 (2H, m), 2.23 (2H, m), 2.37 (1H, br s), 2.49 (2H, m), 2.68 (4H, m), 3.35 (1H, m), 3.51 (1H, m), 3.55 (4H, m), 3.60—3.70 (2H, m), 3.73 (3H, s), 4.91 (1H, m), 6.61 (1H, d, <i>J</i> =2.9 Hz), 6.69 (1H, d, <i>J</i> =2.9 Hz), 7.35 (1H, m), 7.46 (1H, m), 7.80 (1H, d, <i>J</i> =8.2 Hz), 7.89 (1H, d, <i>J</i> =8.2 Hz)	3226, 1583, 1541, 1515 ^{e)}

Table 7. (continued)

Compd. No.	Yield (%) ^{a)}	mp (°C) (solvent) ^{b)}	Formula	Analysis (%) or HRMS Calcd (Found)			¹ H-NMR (CDCl ₃) δ	IR (cm ⁻¹)
				C	H	N		
18n	97 ^{g)}	185.5—187.5 (IPA)	C ₂₁ H ₂₇ FN ₄ O ₂	65.27 (65.24)	7.04 7.12	14.50 14.54	2.31 (2H, m), 2.53—2.65 (3H, m), 2.69—2.84 (3H, m), 3.09 (4H, m), 3.31 (1H, m), 3.47 (1H, m), 3.57 (1H, m), 3.68 (3H, s), 4.03 (1H, br s), 4.22 (1H, m), 4.91 (1H, m), 6.57 (1H, d, <i>J</i> =2.9 Hz), 6.63 (1H, d, <i>J</i> =2.9 Hz), 6.83 (2H, m), 6.92 (2H, m)	3282, 1582, 1512 ^{e)}
18o	85	197.0—198.5 (EtOH)	C ₂₃ H ₃₁ FN ₄ O ₂	66.64 (66.56)	7.54 7.59	13.52 13.53	1.50—1.65 (4H, m), 2.21 (2H, m), 2.42 (2H, m), 2.59 (4H, m), 3.10 (4H, m), 3.28 (1H, m), 3.47 (1H, m), 3.58 (1H, m), 3.71 (3H, s), 4.88 (1H, t, <i>J</i> =4.6 Hz), 6.59 (1H, d, <i>J</i> =2.9 Hz), 6.66 (1H, d, <i>J</i> =2.9 Hz), 6.82—6.91 (2H, m), 6.94 (2H, m)	3316, 1582, 1512 ^{e)}
18p	58	146.0—147.0 (C-H)	C ₂₃ H ₃₁ FN ₄ O ₂ · 1/4H ₂ O	65.93 (65.94)	7.46 7.52	13.37 13.23	1.43 (3H, t, <i>J</i> =7.3 Hz), 1.83 (2H, quintet, <i>J</i> =7.3 Hz), 2.23 (2H, m), 2.45 (2H, t, <i>J</i> =7.3 Hz), 2.60 (4H, m), 3.11 (4H, m), 3.34 (1H, m), 3.52—3.71 (3H, m), 3.98—4.16 (2H, m), 4.93 (1H, t, <i>J</i> =4.4 Hz), 6.70 (1H, d, <i>J</i> =3.0 Hz), 6.75 (1H, d, <i>J</i> =3.0 Hz), 6.86 (2H, m), 6.94 (2H, m)	3298, 1583, 1512 ^{e)}
18q	80	— ^{c)}	C ₂₈ H ₃₃ FN ₄ O ₂	477.2666 [MH] ⁺ (477.2685 [MH] ⁺) ^{d)}			1.82 (2H, m), 2.15 (2H, m), 2.45 (2H, m), 2.60 (4H, m), 3.11 (4H, m), 3.31 (1H, m), 3.53 (1H, m), 3.58—3.73 (3H, m), 4.76 (1H, t, <i>J</i> =4.3 Hz), 5.15 (1H, d, <i>J</i> =16.1 Hz), 5.43 (1H, d, <i>J</i> =16.1 Hz), 6.69 (1H, d, <i>J</i> =2.9 Hz), 6.78 (1H, d, <i>J</i> =2.9 Hz), 6.86 (2H, m), 6.95 (2H, m), 7.04 (2H, m), 7.25—7.35 (3H, m)	3310, 1590, 1540, 1508 ^{f)}
18r	92	190.5—192.0 (C-EE)	C ₂₇ H ₃₁ FN ₄ O ₂	70.11 (69.74)	6.75 6.71	12.11 12.05	1.86 (2H, m), 2.18 (2H, m), 2.48 (2H, m), 2.61 (4H, m), 3.11 (4H, m), 3.37 (1H, m), 3.63 (2H, t, <i>J</i> =7.2 Hz), 3.78 (1H, m), 4.88 (1H, t, <i>J</i> =4.1 Hz), 6.78 (1H, d, <i>J</i> =3.0 Hz), 6.83—6.90 (3H, m), 6.95 (2H, m), 7.39—7.53 (5H, m)	3111, 1610, 1509 ^{e)}

a) Overall yield from **12** unless otherwise noted. b) Recrystallization solvents: C=chloroform, EA=ethyl acetate, EE=diethyl ether, H=hexane. c) Obtained as an oil. d) Determined by high-resolution mass spectrometry. e) KBr. f) Film. g) Based on **14n**.

m), 3.12 (4H, m), 3.33 (1H, m), 3.57 (2H, t, *J*=7.3 Hz), 3.59 (1H, m), 3.63 (3H, s), 4.94 (1H, t, *J*=5.3 Hz), 6.64 (1H, d, *J*=2.6 Hz), 6.83—6.98 (4H, m), 7.22 (1H, d, *J*=2.6 Hz). *Anal.* Calcd for C₂₂H₂₉FN₄O₂·H₂O: C, 63.14; H, 6.98; N, 13.39. Found: C, 63.10; H, 7.32; N, 13.34.

Optical Resolution of Racemic 5-[3-[4-(4-Fluorophenyl)piperazin-1-yl]propyl]-8-hydroxy-1-methyl-1,4,5,6,7,8-hexahydropyrrolo[3,2-c]azepin-4-one [Preparation of (–)-18a** and (+)-**18a**]** To a warm solution of racemic **18a** (20.0 g, 50 mmol) in MeOH (160 ml) was added L-(+)-tartaric acid (7.50 g, 50 mmol). After the mixture was stirred at room temperature overnight and then at 0 °C for 1 h, the precipitate was collected and dried, yielding 12.5 g of a colorless powder. 2 N NaOH (56.5 ml, 113 mmol) was added to this solid, and extracted with CHCl₃ (3×100 ml). The extracts were washed with brine, dried, and evaporated to give the (–)-rich free form. The operations described above, *i.e.* formation of a salt with L-(+)-tartaric acid (1 eq), collection of precipitate, neutralization, extraction and evaporation, were repeated once more. The obtained solid was recrystallized from 2-propanol (IPA) (1 ml/1 g-solid) three times to afford optically pure (–)-**18a** (5.78 g, 29%, 99.4% ee). The filtrate from the first precipitate was concentrated and converted to the free base to give 10.2 g of (+)-rich free form as a colorless solid. The operations described as for (–)-**18a**, *i.e.* formation of a salt with D-(–)-tartaric acid (1 eq), collection of precipitate, neutralization, extraction and evaporation, were repeated three times. The obtained solid was recrystallized from IPA (1 ml/1 g-solid) twice to afford optically pure (+)-**18a** (5.36 g, 27%, 99.5% ee). (–)-**18a**: mp 168.5—170.0 °C, colorless crystals. The IR and ¹H-NMR spectra were identical with those of racemic **18a**, [α]_D²⁰ (*c*=3.00, MeOH)=–7.27°. *Anal.* Calcd for C₂₂H₂₉FN₄O₂: C, 65.98; H, 7.30; N, 13.99. Found: C, 66.18; H, 7.39; N, 13.99. (+)-**18a**: mp 168.5—170.0 °C, colorless crystals. The IR and ¹H-NMR spectra were identical with those of racemic **18a**, [α]_D²⁰ (*c*=2.96, MeOH)=+7.30°. *Anal.* Calcd for C₂₂H₂₉FN₄O₂: C, 65.98; H, 7.30; N, 13.99. Found: C, 65.97; H, 7.49; N, 14.06. The enantiomeric purities of (–)-**18a** and (+)-**18a** were determined by HPLC under the following conditions: column, CHIRALPAK AD (DAICEL, 4.6 mm i.d.×250 mm); column temperature, 40 °C; mobile phase, hexane–MeOH–EtOH–diethylamine (70:20:10:0.1); flow rate, 1.0 ml/min; detector, UV at 254 nm; retention time, (–)-**18a**, 5.6 min; (+)-**18a**, 6.7 min.

Preparation of (–)-18a** L-(+)-Tartrate** A mixture of (–)-**18a**

(200 mg, 0.5 mmol) and L-(+)-tartaric acid (75 mg, 0.5 mmol) in MeOH (7 ml) was gently heated until a clear solution was obtained. The solution was allowed to stand at room temperature for 24 h. The crystals that formed were collected and washed with cold MeOH to afford the title compound (180 mg, 65%). *Anal.* Calcd for C₂₆H₃₃FN₄O₈: C, 56.72; H, 6.41; N, 10.18. Found: C, 56.88; H, 6.35; N, 10.15.

X-Ray Crystallographic Analysis of (–)-18a**·L-(+)-Tartrate** Diffraction measurements were performed on a Rigaku AFC-7R diffractometer using graphite monochromated CuK α radiation (λ =1.54178 Å). Crystals of (–)-**18a**·L-(+)-tartrate were subjected to crystallographic analysis and were found to belong to the orthorhombic space group *P*2₁2₁2₁ with the following unit cell parameters; *a*=18.828(4) Å, *b*=18.829(5) Å, *c*=7.490(6) Å, *V*=2655(2) Å³, *Z*=4. The final *R*-factor and weighted *R*-factor were 0.048 and 0.072, respectively, based on 1765 reflections with *I*>3 σ (*I*).

Serotonin (5-HT₂)- and α_1 -Adrenergic-Receptor Antagonist Activity The functional serotonin (5-HT₂)- and α_1 -adrenergic-receptor antagonist activities against serotonin and NE, respectively, were determined in the isolated guinea pig mesenteric artery and aorta, respectively.¹³⁾ Briefly, male Hartley strain guinea pigs were anesthetized with pentobarbital Na (50 mg/kg, *i.p.*) and killed by decapitation. The mesenteric arterial bed and aorta were rapidly dissected out. Helical strips (2 mm in width, 20 mm in length) of the arteries were prepared using forceps and mounted vertically in a Magnus chamber, filled with warm (37 °C) and oxygenated (95% O₂ and 5% CO₂ gas mixture) Tyrode's solution with the following composition (in mM): NaCl 137, KCl 5.4, CaCl₂ 2.7, MgCl₂ 0.5, NaHPO₄ 0.45, NaHCO₃ 11.9, glucose 5.5. The upper side of the tissue was connected to a force-displacement transducer (Shinkoh U gage, UL-10G) using silk thread. The isometric tension was recorded continuously using a pen-recorder (National, VP-6537). After a 1-h equilibration period with a resting tension of 0.5 g, the mesenteric arterial or aortic preparation was contracted transiently with serotonin (10^{–5} M) or continuously with NE (10^{–5} M), respectively. Test samples at final concentrations of 10^{–9} and 10^{–6} M were added before transient contraction induced by serotonin or under continuous contraction induced by NE. The functional serotonin (5-HT₂)- or α_1 -antagonist activities against serotonin or NE were determined as the reduction in peak contraction.

For selected compounds, the *p*A₂ values were determined to measure the potency of their antagonistic action against 5-HT₂- or α_1 -receptors. Briefly,

cumulative concentration–response curves for serotonin and NE were constructed by stepwise addition of the agonist, using helical strips of isolated femoral or mesenteric guinea pig arteries, respectively. Serotonin or NE was then washed out several times during a 1-h period. The strips were incubated with various concentrations of compounds for 10 min, and a concentration–response curve for serotonin or NE was obtained again. The pA_2 values were determined from Schild plots.

Receptor Binding Assays 5-HT₂ receptor,²²⁾ α_1 -adrenoceptor,²³⁾ 5-HT_{1A} receptor,²⁴⁾ α_2 -adrenoceptor,²⁵⁾ β -adrenoceptor,²⁶⁾ D₂-dopamine receptor,²⁷⁾ mACh receptor,²⁸⁾ H₁-histamine receptor²⁹⁾ and H₂-histamine receptor³⁰⁾ binding assays were performed as previously described with slight modifications.

5-HT₂ Receptor Binding Assay Aliquots (90 μ g of protein) of rat frontal cortex membranes were incubated at 25 °C for 45 min with 1 nM [³H]ketanserin and various concentrations of test compounds in 50 mM Tris–HCl buffer (pH 7.7) with a final incubation volume of 250 μ l. Specific binding was defined as that displaceable by 1 μ M ketanserin.

α_1 -Adrenoceptor Binding Assay Aliquots (90 μ g of protein) of rat cerebral cortex membranes were incubated at 25 °C for 30 min with 0.3 nM [³H]prazosin and various concentrations of test compounds in 50 mM Tris–HCl buffer (pH 7.7), 0.01% ascorbic acid with a final incubation volume of 250 μ l. Specific binding was defined as that displaceable by 10 μ M prazosin.

5-HT_{1A} Receptor Binding Assay Aliquots (80 μ g of protein) of rat hippocampus membranes were incubated at 25 °C for 30 min with 0.4 nM [³H]8-hydroxy-DPAT and various concentrations of test compounds in 50 mM Tris–HCl buffer (pH 7.7), 10 μ M pargyline, 4 mM CaCl₂, 0.1% ascorbic acid with a final incubation volume of 250 μ l. Specific binding was defined as that displaceable by 100 μ M serotonin.

α_2 -Adrenoceptor Binding Assay Aliquots (90 μ g of protein) of rat striatum membranes were incubated at 25 °C for 30 min with 2 nM [³H]rauwolscine and various concentrations of test compounds in 20 mM HEPES–Na buffer (pH 7.4) with a final incubation volume of 250 μ l. Specific binding was defined as that displaceable by 10 μ M yohimbine.

β -Adrenoceptor Binding Assay Aliquots (100 μ g of protein) of rat cerebral cortex membranes were incubated at 25 °C for 30 min with 1.5 nM [³H]dihydroalprenolol and various concentrations of test compounds in 50 mM Tris–HCl buffer (pH 7.7) with a final incubation volume of 250 μ l. Specific binding was defined as that displaceable by 100 μ M propranolol.

D₂-Dopamine Receptor Binding Assay Aliquots (90 μ g of protein) of rat striatum membranes were incubated at 25 °C for 60 min with 1 nM [³H]raclopride and various concentrations of test compounds in 50 mM Tris–HCl buffer (pH 7.4), 0.01% ascorbic acid, 120 mM NaCl, 5 mM KCl, 2 mM CaCl₂, 1 mM MgCl₂ with a final incubation volume of 250 μ l. Specific binding was defined as that displaceable by 1 μ M spiperone.

mACh Receptor Binding Assay Aliquots (9 μ g of protein) of rat cerebral cortex membranes were incubated at 37 °C for 60 min with 0.3 nM [³H]quinuclidinyl benzilate and various concentrations of test compounds in 50 mM Na-phosphate buffer (pH 7.4), 100 mM NaCl, 1 mM MgCl₂ with a final incubation volume of 250 μ l. Specific binding was defined as that displaceable by 10 μ M atropine.

H₁-Histamine Receptor Binding Assay Aliquots (80 μ g of protein) of guinea pig cerebellum membranes were incubated at 25 °C for 30 min with 4 nM [³H]pyrilamine and various concentrations of test compounds in 50 mM Na-K-phosphate buffer (pH 7.5) with a final incubation volume of 250 μ l. Specific binding was defined as that displaceable by 2 μ M triprolidine.

H₂-Histamine Receptor Binding Assay Aliquots (310 μ g of protein) of guinea pig cerebral cortex membranes were incubated at 25 °C for 30 min with 3 nM [³H]tiotidine and various concentrations of test compounds in 50 mM Na-K-phosphate buffer (pH 7.5) with a final incubation volume of 250 μ l. Specific binding was defined as that displaceable by 100 μ M cimetidine.

For all binding assays, incubation was terminated by rapid filtration under vacuum, and the filters were processed for radioactivity determination. The inhibition of binding by the test compound was analyzed to estimate the IC₅₀ (the concentration of the test compound causing 50% inhibition of binding) using Multicalc™ Advanced (wallac, Finland).

Measurement of Platelet Aggregation The platelet donors were five healthy volunteers aged 25–35 years who took no medication that might alter platelet function for at least two weeks before the start of the study. Canine platelets were prepared from six adult Beagle dogs. Venous blood was mixed with a one-tenth volume of trisodium citrate (0.1 M, pH 7.35), and PRP was then obtained by centrifugation at 200 \times *g* for 5 min at room temperature. It was adjusted to a platelet count of about 300000 μ l^{−1} with autol-

ogous platelet-poor plasma, prepared by centrifugation at 900 \times *g* for 20 min. Platelet aggregation was measured by turbidometry in two dual-chamber channel platelet aggregometers (Mevanix, PAM-8C). PRP (200 μ l) was incubated in the aggregation cuvette for 2 min with test sample (10^{−9}–10^{−5} M) and CaCl₂ (1 mM). Serotonin (1 or 10 μ M) in combination with collagen (0.03–1 μ g/ml) or ADP (0.3–2 μ M) was then added. The final volume of PRP+agonist/test samples was 250 μ l. The concentration of serotonin was chosen because it produced a submaximal potentiation effect, and when used alone it caused less than 10% aggregation. The concentrations of collagen and ADP were determined in each preparation as the maximum concentrations that caused less than 10% aggregation. The degree of aggregation at 10 min after the addition of agonists was measured as the percentage of the difference in light transmission between PRP and platelet-poor plasma.

Acute Pulmonary Thromboembolic Death in Mice Male ddY mice weighing about 25 g (5 to 6 weeks-old) were used after overnight fasting. Acute pulmonary thromboembolism was induced by rapid injection of a mixture (0.1 ml/10 g body weight) of serotonin (1 mg/kg) and collagen (5 mg/kg) into the tail vein and the mortality of mice within 10 min was determined. With the exception of sarpogrelate, all compounds were dissolved in saline containing 10% dimethylsulfoxide. Sarpogrelate was dissolved in 0.5% tragacanth in water according to Hara *et al.*³¹⁾ Compounds were administered orally one hour prior to the injection of serotonin and collagen. Twenty mice were used for each group. Results are expressed as mortality rate in animal numbers and percentage. The dose (ED₅₀) producing 50% reduction of mortality was estimated from the dose–response curve.

Acknowledgments We thank Drs. F. Satoh, T. Tanaka, S. Tanaka and T. Nakanishi for their encouragement throughout this study, and Dr. H. Fukami for useful suggestions during the preparation of this manuscript. We are grateful to Dr. M. Shiro, Rigaku Corporation, Mr. S. Matsuki and Mr. Y. Oyama for X-ray crystallographic analyses. Thanks are also due to Mr. T. Fujita and Dr. H. Naoki, Suntory Institute for Bioorganic Research, for the measurement of HR-FAB-MS.

References and Notes

- 1) a) Fitzgerald D. J., Roy L., Catella F., Fitzgerald G. A., *N. Engl. J. Med.*, **315**, 983–989 (1986); b) Fuster V., Steele P. M., Chesebro J. H., *J. Am. Coll. Cardiol.*, **5**, 175B–184B (1985); c) Harrison M. J. G., *Circulation*, **81** (Suppl. 1), I-20–I-21 (1990).
- 2) a) Davies M. J., Thomas A. C., *Br. Heart J.*, **53**, 363–373 (1985); b) Hamm C. W., Kupper W., Lorenz R. L., Weber P. C., Wober W., *J. Am. Coll. Cardiol.*, **10**, 998–1004 (1987).
- 3) a) van Nueten J. M., *Fed. Proc.*, **42**, 223–227 (1983); b) De Clerck, F., David J.-L., Janssen P. A. J., *Agents Actions*, **12**, 388–397 (1982); c) De Clerck, F., Herman A. G., *Fed. Proc.*, **42**, 228–232 (1983).
- 4) a) Vanhoutte P. M., *Fed. Proc.*, **42**, 233–237 (1983); b) Cohen M. L., Fuller R. W., Eiley K. S., *J. Pharmacol. Exp. Ther.*, **218**, 421–425 (1981); c) De Cree J., Leempoels J., Demoen B., Roels V., Verhaegen H., *Agents Actions*, **16**, 313–317 (1985).
- 5) a) Sigal S. L., Gellman J., Sarembock I. J., LaVeau P. J., Chen Q. S., Cabin H. S., Ezekowitz M. D., *Arterioscler. Thromb.*, **11**, 770–783 (1991); b) Golino P., Piscione F., Willerson J. T., Cappelli-Bigazzi M., Focaccio A., Villari B., Indolfi C., Russolillo E., Condorelli M., Chiariello M., *New Eng. J. Med.*, **324**, 641–648 (1991); c) Shimokawa H., Vanhoutte P. M., *J. Am. Coll. Cardiol.*, **17**, 1197–1202 (1991); d) Crowley S. T., Dempsey E. C., Horwitz K. B., Horwitz L. D., *Circulation*, **90**, 1908–1918 (1994).
- 6) a) van de Wal H. J., Wijn P. F., van Lier H. J., Skotnicki S. H., *Microcirc. Endothelium Lymphatics*, **2**, 657–685 (1985); b) Bush L. R., *J. Pharmacol. Exp. Ther.*, **240**, 674–682 (1987).
- 7) a) Fozard J. R., *J. Cardiovasc. Pharmacol.*, **4**, 829–838 (1982); b) Cohen M. L., Fuller R. W., Kurz K. D., *Hypertension* (Dallas), **5**, 676–681 (1983).
- 8) a) Kikumoto R., Hara H., Ninomiya K., Osakabe M., Sugano M., Fukami H., Tamao Y., *J. Med. Chem.*, **33**, 1818–1823 (1990); b) Hara H., Shimada H., Kitajima A., Tamao Y., *Arzneim. Forsch.*, **41**, 616–620 (1991).
- 9) Mizuno M., Inomata N., Miya M., Kamei T., Shibata M., Tatsuoka T., Yoshida M., Takiguchi C., Miyazaki T., *Chem. Pharm. Bull.*, **47**, 246–256 (1999).
- 10) a) Shioiri T., Yokoyama Y., Kasai Y., Yamada S., *Tetrahedron*, **32**, 2211–2217 (1976); b) Takuma S., Hamada Y., Shioiri T., *Chem. Pharm. Bull.*, **30**, 3147–3153 (1982) and references therein.
- 11) The signals of the two aromatic protons of **8** appeared at almost the

- same position, and were lower than those of **7**.
- 12) The geometry of the oxime moiety of **15** was determined by comparison of ¹H-NMR data of both isomers. The signal of the C-7 methylene proton of **15** appeared at δ 3.05 and was shifted to lower field compared to that the (Z)-isomer (δ 2.91) by the anisotropic effect of the oxygen atom on the oxime moiety.
 - 13) a) Buffolo R. R., Waddell J. E., Yaden E. L., *J. Pharmacol. Exp. Ther.*, **221**, 309—314 (1982); b) Jenkin R. A., Baldi M. A., Iwanov V., Moulds R. F. W., *J. Cardiovasc. Pharmacol.*, **18**, 566—573 (1991); c) Itoh T., Kitamura K., Kuriyama H., *J. Physiol. (London)*, **345**, 409—422 (1983); d) Ishikawa S., *Jpn. J. Pharmacol.*, **35**, 19—25 (1984); e) Fujii K., Kuriyama H., *J. Pharmacol. Exp. Ther.*, **235**, 764—770 (1985).
 - 14) a) Pfeiffer C. C., *Science*, **124**, 29—31 (1956); b) Lehmann F. P. A., *Quant. Struct. Act. Relat.*, **6**, 57—65 (1987).
 - 15) a) van Leusen A. M., Siderius H., Hoogenboom B. E., van Leusen D., *Tetrahedron Lett.*, **52**, 5337—5340 (1972); b) Holland G. F., U. S. Patent 4282242 (1981) [*Chem. Abstr.*, **95**, 187068e (1981)].
 - 16) Huisgen R., Laschtuvka E., *Chem. Ber.*, **93**, 65—81 (1960).
 - 17) Otsuka Pharmaceutical Co., Ltd., Jpn. Kokai Tokkyo Koho, JP81 49361 (1981) [*Chem. Abstr.*, **96**, 69027p (1982)].
 - 18) Yevich J. P., New J. S., Smith D. W., Lobeck W. G., Catt J. D., Minielli J. L., Eison M. S., Taylor D. P., Riblet L. A., Temple D. J., Jr., *J. Med. Chem.*, **29**, 359—369 (1986).
 - 19) Berman M.-C., Bonte J.-P., Lesieur-Demarquilly I., Debaert M., Lesieur D., Leinot M., Benoit J., Labrid C., *Eur. J. Med. Chem. Chim. Ther.*, **17**, 85—88 (1982).
 - 20) Guida W. C., Mathre D. J., *J. Org. Chem.*, **45**, 3172—3176 (1980).
 - 21) Anderson H. J., Nagy H., *Can. J. Chem.*, **50**, 1961—1965 (1972).
 - 22) Leysen J. E., Niemegeers C. J. E., van Nueten J. M., Laduron P. M., *Mol. Pharmacol.*, **21**, 301—314 (1982).
 - 23) Greengrass P., Bremner R., *Eur. J. Pharmacol.*, **55**, 323—326 (1979).
 - 24) Peroutka S. J., *J. Neurochem.*, **47**, 529—540 (1986).
 - 25) Broadhurst A. M., Alexander B. S., Wood M. D., *Life Sci.*, **43**, 83—92 (1988).
 - 26) Bylund D. B., Snyder S. H., *Mol. Pharmacol.*, **12**, 568—580 (1976).
 - 27) Köhler C., Hall H., Ögren S.-O., Gawell L., *Biochem. Pharmacol.*, **34**, 2251—2259 (1985).
 - 28) Yamamura H. I., Snyder S. H., *Proc. Natl. Acad. Sci. U.S.A.*, **71**, 1725—1729 (1974).
 - 29) Tran V. T., Chang R. S. L., Snyder S. H., *Proc. Natl. Acad. Sci. U.S.A.*, **75**, 6290—6294 (1978).
 - 30) Gajtkowski G. A., Norris D. B., Rising T. J., Wood T. P., *Nature (London)*, **304**, 65—67 (1983).
 - 31) Hara H., Kitajima A., Shimada H., Tamano Y., *Thromb. Haemostas.*, **66**, 484—488 (1991).

Benzaldehyde, 2-Hydroxybenzoyl Hydrazone Derivatives as Inhibitors of the Corrosion of Aluminium in Hydrochloric Acid

A. S. FOUDA,^a M. M. GOUDA,^b and S. I. Abd EL-RAHMAN^a

Chemistry Department, Faculty of Science, El-Mansoura University,^a El-Mansoura, Egypt and Chemistry Department, Faculty of Science, El-Menoufia University,^b El-Menoufia, Egypt.

Received November 1, 1999; accepted January 17, 2000

The effect of benzaldehyde, 2-hydroxybenzoyl hydrazone derivatives on the corrosion of aluminium in hydrochloric acid has been investigated using thermometric and polarization techniques. The inhibitive efficiency ranking of these compounds from both techniques was found to be: 2>3>1>4. The inhibitors acted as mixed-type inhibitors but the cathode is more polarized. The relative inhibitive efficiency of these compounds has been explained on the basis of structure of the inhibitors and their mode of interaction at the surface. Results show that these additives are adsorbed on an aluminium surface according to the Langmuir isotherm. Polarization measurements indicated that the rate of corrosion of aluminium rapidly increases with temperature over the range 30–55 °C both in the absence and in the presence of inhibitors. Some thermodynamic data of the adsorption process are calculated and discussed.

Key words benzaldehyde; 2-hydroxybenzoyl hydrazone derivative; corrosion; inhibitor; aluminium; hydrochloric acid

Research on the many important applications of aluminium and its alloys has narrowed down to its electrochemical behaviour and corrosion resistance in a wide variety of media, including investigation of the properties of the surface oxide film, formed naturally or by anodization.¹⁾ Generally, this consists of a thin barrier film adjacent to the metal (*ca.* 25 nm thick) covered by a thicker porous oxide layer. In aggressive media, such as chloride solution, localized corrosion can occur leading to the breakdown of the passive layer and pit formation.

The electrochemistry of aluminium in chloride solutions has been widely investigated.^{2–10)} The effect of the presence of different ions in solutions on the electrochemical behaviour, inhibiting or enhancing corrosion, has also been studied.^{11–16)}

The aim of the present work was to examine the inhibitive action of the above mentioned inhibitors towards the corrosion of aluminium in acidic solutions. The choice of the inhibitors was based on two factors. First, it can be conveniently synthesized from relatively cheap raw materials. Secondly, the presence of an electron cloud on the aromatic ring and the high solubility of these compounds in acid medium induce greater adsorption of the compounds on the surface of aluminium which can lead to effective inhibition.

Experimental

Materials and Test Solutions Aluminium strips 100×10×0.5 mm in size (composition in Table 1) were used for thermometric measurements. For galvanostatic polarization studies, a wire 1 cm in length and ϕ 0.5 mm of the composition shown in Table 1 and embedded in araldite was used. The aluminium electrodes were mechanically polished with emery papers of 1/0, 2/0, 3/0 and 4/0 grade and degreased with alkaline solution (15 g Na₂CO₃ + 15 g Na₃PO₄ per litre). AR grade HCl (BDH) was used for preparing solutions. Double distilled water was used to prepare solutions of 2 N HCl for all experiments.

The inhibitors benzaldehyde, 2-hydroxybenzoyl hydrazone derivatives

were synthesized in the laboratory following the known procedures; their structures were characterized by NMR, IR, mp and elementary analysis and are shown in Chart 1.

Apparatus and Working Procedures The reaction vessel used was basically the same as that described by Mylius.¹⁷⁾ The reaction number (RN) is:

$$RN = (T_m - T_i)/t, \text{ } ^\circ\text{C min}^{-1} \quad (1)$$

where T_m and T_i are the maximum and initial temperatures, and t is the time in minutes taken to reach T_m . All experiments were started at $30 \pm 0.1^\circ\text{C}$ (T_i). The extent of corrosion inhibition by a certain concentration of a particular additive is evaluated from the percentage decrease in RN, *viz.*

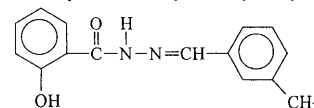
$$\frac{(RN)_{\text{free}} - (RN)_{\text{add}}}{(RN)_{\text{free}}} \times 100 \quad (2)$$

The galvanostatic method used for steady state polarization studies consisted of a constant current device and digital ionalyzer model 701 A for measuring corrosion potentials. All experiments were carried out at $30 \pm 0.1^\circ\text{C}$. The inhibitive efficiency was calculated employing the formula:

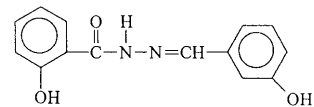
$$\% \text{Inhibition efficiency} = \frac{I - I'}{I} \times 100 \quad (3)$$

where I and I' are the corrosion currents without and with inhibitor, respectively.

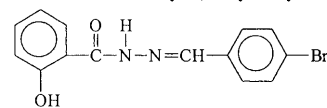
3-methyl benzaldehyde, 2-hydroxy benzoyl-hydrazone (1)



3-hydroxybenzaldehyde, 2-hydroxy benzoyl-hydrazone (2)



4-bromo benzaldehyde, 2-hydroxy benzoyl-hydrazone (3)



benzaldehyde, 2-hydroxy benzoyl-hydrazone (4)

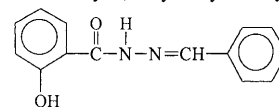


Chart 1

Table 1. Aluminium Composition (wt%)

Si	Fe	Mn	Mg	Cu	Al
0.15	0.19	0.005	0.1	0.02	Rest

* To whom correspondence should be addressed. e-mail: scimchdept@mum.mans.eun.eg

Results and Discussion

Thermometric Measurements In this method the temperature change was followed in the absence and in the presence of different concentrations of the benzaldehyde, 2-hydroxybenzoyl hydrazone derivatives as inhibitors.

Curves of Fig. 1 represent the behaviour observed in the presence of different concentrations of inhibitor **2**. All curves of the tested materials are characterized by an initial slow rise (due to the oxide film originally present on the metal surface¹⁸) followed by a sharp rise and finally by a decrease in temperature after attaining a maximum value. The curves for additive containing systems fall below that of the free acid. This indicates that the additives behave as inhibitors over the concentration range studied. The percentage reduction in RN

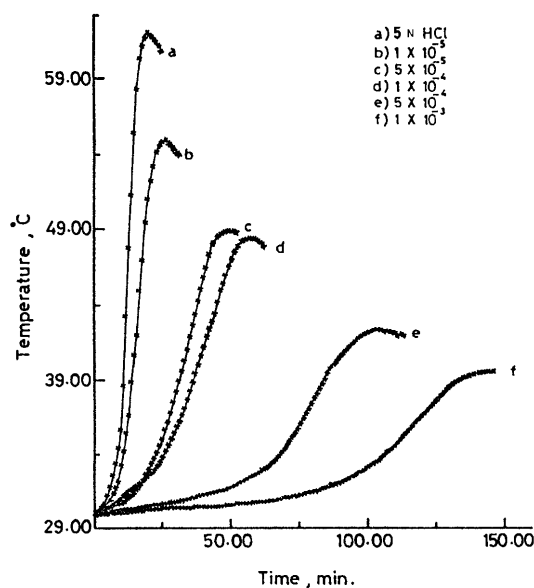


Fig. 1. Temperature-Time Curves Obtained in Absence and Presence of Different Concentrations of Compound **2**

of the studied compounds is presented in Table 2.

The results compiled in Table 2 revealed that the efficiency of corrosion inhibition as determined from the percentage reduction in RN varies with both the concentration and the type of the inhibitor. The inhibitive efficiency of additives is in the order: **2** > **3** > **1** > **4**.

Polarization Measurements The polarization curves for the system involving inhibitor **2** are shown in Fig. 2 and the electrochemical parameters in these media are given in Table 3. The corrosion current density for aluminium in 2 N HCl is: $i_{\text{corr.}} 19 \text{ mA cm}^{-2}$. Addition of inhibitor molecules causes a decrease in $i_{\text{corr.}}$. The decrease in $i_{\text{corr.}}$ and the increase in θ with increasing concentration in the range 1×10^{-5} — $1 \times 10^{-3} \text{ M}$ demonstrate the efficiency of the additive compounds as corrosion inhibitors of aluminium. Also, the slopes of anodic and cathodic Tafel slopes are approximately constant, independent of the concentration of inhibitor. This indicates that the inhibition of the dissolution of aluminium takes place without affecting the mechanism.

A correlation between θ and $\log C$ of adsorbate is given by Frumkin adsorption isotherm. The experimental results (Fig. 3) are in good agreement with the following equation:

$$KC = \left[\frac{\theta}{1-\theta} \right] \exp(-f\theta) \quad (4)$$

Table 2. The Inhibitor Efficiencies of Hydrazone Derivatives at 30 °C

Substance	% Reduction in RN			
	1	2	3	4
1×10^{-5}	32.1	37.5	32.5	31.5
5×10^{-5}	68.0	73.4	72.6	66.7
1×10^{-4}	79.5	77.6	84.8	78.2
5×10^{-4}	92.3	92.8	92.5	91.7
1×10^{-3}	93.4	96.2	94.6	92.7

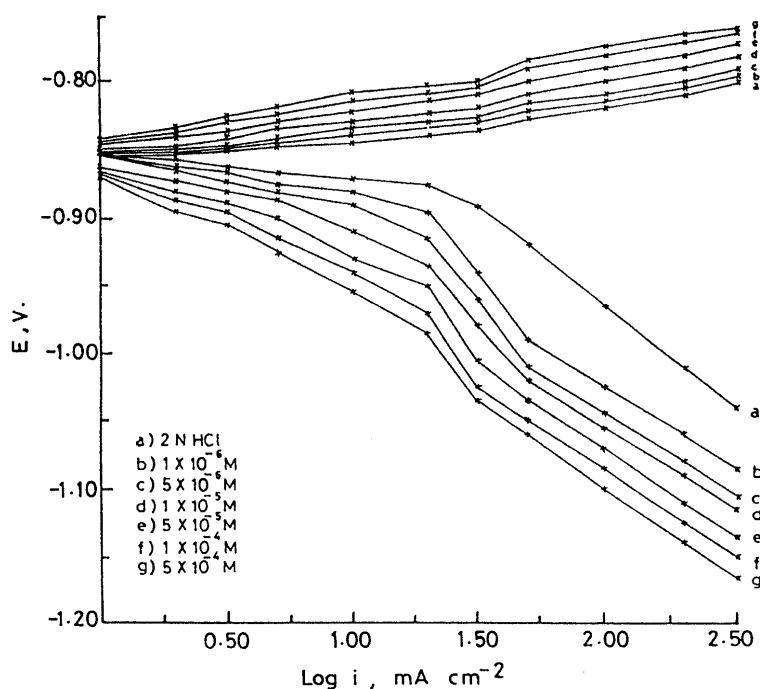


Fig. 2. Effect of Concentration of Compound **2** on the Current Potential Relations of Aluminium Dissolution in 2 N HCl

The inhibition efficiency of additives decreases in the order: **2** > **3** > **1** > **4**.

Table 3. The Effect of Compound 2 Concentrations on the Free Corrosion Potential (E_{corr}), Corrosion Current Density (i_{corr}), Tafel Slopes (β_a , β_c) Inhibition Efficiency (P_i) and Degree of Surface Coverage (θ) of Aluminium in 2 N HCl at 30 °C

Conc. (M)	$-E_{\text{corr}}$ (mV)	i_{corr} (mA cm) ⁻²	β_a (mV/dec.)	β_c (mV/dec.)	% P_i	θ
0.0	848	19.0	38	164	—	—
1×10^{-6}	850	4.5	35	168	75.3	0.75
5×10^{-6}	855	3.3	36	165	83.0	0.83
1×10^{-5}	856	2.9	39	150	85.0	0.85
5×10^{-5}	835	2.2	40	136	88.0	0.88
1×10^{-4}	857	1.7	50	130	91.0	0.91
5×10^{-4}	856	1.5	52	134	92.0	0.92

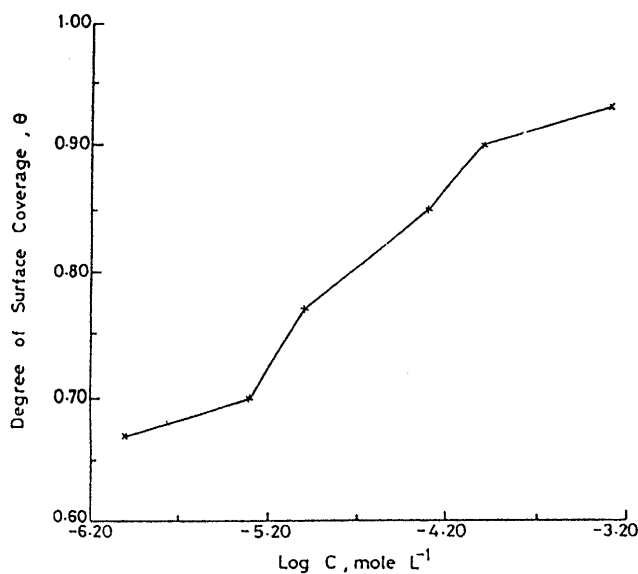


Fig. 3. Effect of Compound 3 concentration on the Degree of Surface Coverage for Al in 2 N HCl

where C is the concentration of adsorbed substance in the bulk of the solution and f is a constant depending on intermolecular interaction in the adsorbed layer and on the heterogeneity of the surface. K is the modified equilibrium constant of the adsorption process, which is related to the standard free energy of adsorption according to the following equation:

$$K = \exp(\Delta G_{\text{ads}}^0 / RT) \cdot \frac{1}{55.5} \quad (5)$$

The effect of temperature on the rate of dissolution of aluminium in 2 N HCl was studied by galvanostatic polarization in the temperature range 30–60°C. For all the additives tested, the logarithm of i_{corr} is a linear function of $1/T$ (Figs. 4, 5). The activation energy values E_a^* (Table 4) increase with increasing inhibition efficiency of the compounds. Compound 2 which gives maximum inhibition efficiency yields the highest activation energy and the opposite is true for compound 4. The similar values of E_a^* suggest that the inhibitors are similar in their mechanism of action and that the order of efficiency may be related to the pre-exponential factor A by the equation:

$$\log R = \log A - \frac{E}{RT} \quad (6)$$

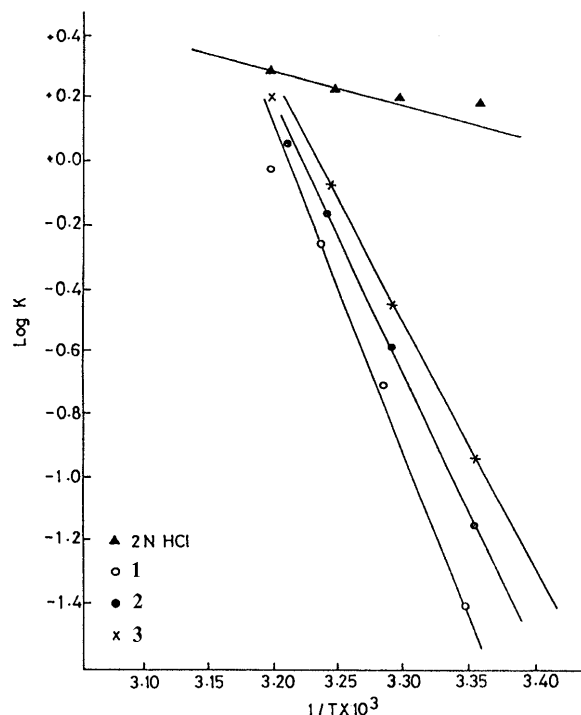


Fig. 4. Log K - $1/T$ Plots for Aluminium Dissolution in Presence and Absence of Compounds 1, 2 and 3

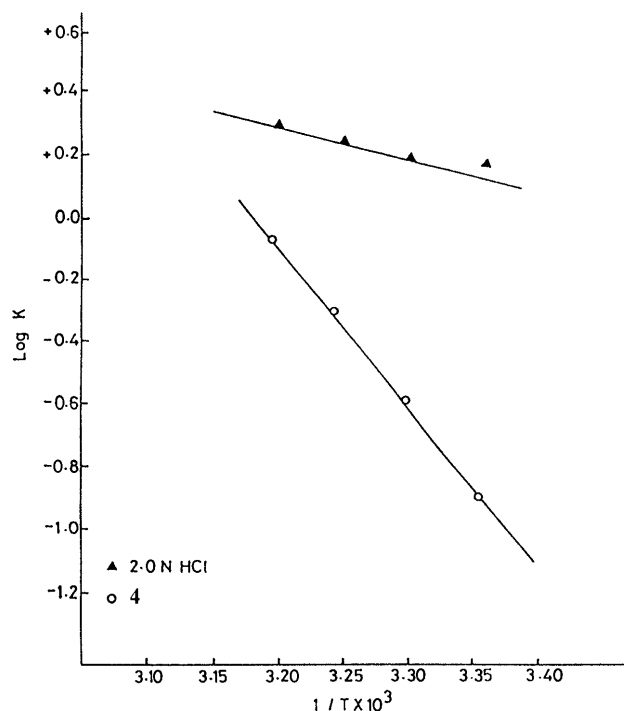


Fig. 5. Log K - $1/T$ Plots for Aluminium Dissolution in Presence and Absence of Compound 4

This is further related to concentration, steric effects, metal surface characteristics, etc. Also, the results show that compound 2 gives maximum efficiency and exhibits the highest negative ΔG_{ads}^0 , indicating that it is strongly adsorbed on the aluminium surface.

Table 5 summarizes the inhibition efficiency of the additives at various concentrations from polarization measurements.

Table 4. Energy of Activation, Free Energy of Adsorption and Modified Equilibrium Constant of Hydrazone Derivatives During Corrosion of Aluminium in 2 N HCl

Inhibitor	% Inhibition	E^* (kcal mol ⁻¹)	$-\Delta G_a^0$ (kcal mol ⁻¹)	B
1	76.0	8.0	10.1	3.2×10^5
2	85.0	10.6	10.6	7.0×10^5
3	77.0	9.1	10.2	3.4×10^5
4	73.7	5.3	10.0	2.9×10^5
Free	—	4.8	—	—

Table 5. Inhibition Efficiency of Different Inhibitors at Various Concentrations at 30 °C

Conc. (M)	% Inhibition efficiency			
	1	2	3	4
1×10^{-6}	66.3	75.3	67.4	67.0
5×10^{-6}	70.0	83.0	70.3	68.4
1×10^{-5}	76.0	85.0	77.0	73.7
5×10^{-5}	84.0	88.0	85.0	83.7
1×10^{-4}	89.0	91.0	90.0	86.0
5×10^{-4}	90.5	92.0	92.0	88.0

Chemical Structure and Corrosion Inhibition of Aluminium Inhibition efficiency was shown,¹⁹⁾ to depend on the number of adsorption active centers in the molecule and their charge density, molecular size, mode of adsorption and formation of metallic complexes.

Variation in structure of the inhibitor molecules (1–4) takes place through the phenyl group of benzaldehyde side chain. Thus variation in inhibition efficiency would probably originate from this part of the molecule.

Vertical adsorption of the additive molecules on the aluminium surface is suggested as evidenced by the presence of the substituent effect on inhibition action. Skeletal representation of the mode of adsorption of the inhibitor molecules is shown in Chart 2.

Adsorbed molecules on the surface of the corroding metal interfere with cathodic and/or anodic reactions.²⁰⁾ Inhibition of these reactions would obviously depend on the degree of coverage of the metal with the adsorbate. Competitive adsorption is assumed to occur on the surface of the metal between the aggressive Cl⁻ ions on one hand and the inhibitor molecules on the other. Experimental results indicated that the decrease inhibition efficiency of the additives used for aluminium dissolution in hydrochloric acid over the concentration range 1×10^{-6} – 5×10^{-4} M is in the order $2 > 3 > 1 > 4$.

In the *p*-substitutions the inductive effects are small due to the great distance that separates the substituent from the reaction center. In *m*-substitution, inductive effects are more significant than resonance effects. In *o*-substitution both a strong inductive effect and resonance are observed. Compound 2 is the most efficient inhibitor due to the presence of three active centers (one C=O and two –OH groups). Compound 3 comes after compound 2 in spite of the fact that it contains the same number of active centers (one –OH, one C=O and one Br atom). This is because the OH group in compound 2 increases the electron charge density on the molecule more than Br atom in compound 3 and hence it in-

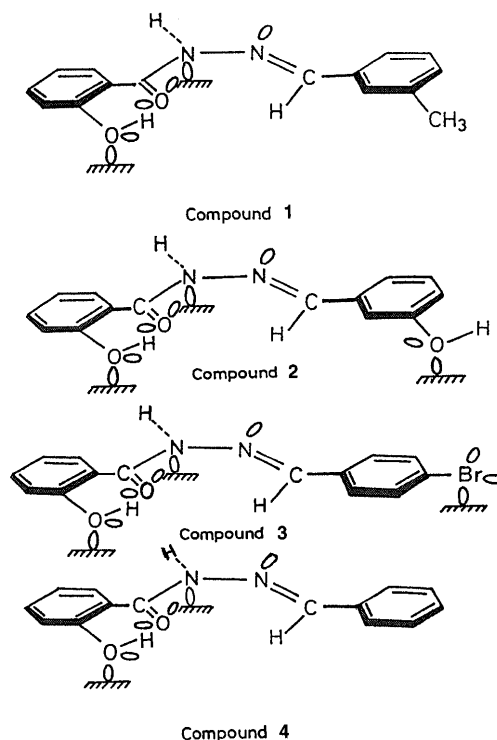


Chart 2. Skeletal Representation of the Mode of Adsorption of the Inhibitor Molecules

creases the inhibition efficiency. Compounds 1 and 4 have the same number of active centers, but in compound 1 the *m*-substituent in the phenyl group of benzaldehyde (*m*-CH₃) has some inductive and resonance effects which increase the electron charge density on the molecule, and hence increase the inhibition efficiency. So, compound 1 is superior to compound 4 in inhibition efficiency. The higher inhibition efficiency values of the compounds used can be attributed to their large surface coverage of the aluminium surface, and to the presence of electrodonating groups in *m*- or *p*-substitution in the phenyl group of benzaldehyde.

Conclusions

The tested benzaldehyde, 2-hydroxybenzoyl hydrazone derivatives act as mixed type inhibitors but the cathode is more polarized against pure aluminium in 2 N hydrochloric acid at 30 °C. All the compounds are adsorbed on the metal surface following the Langmuir adsorption isotherm. Inhibition efficiency increases with increase in the concentration of the inhibitor as well as its electron donor character.

References

- 1) Despic A., Parkhutik V., "Modern Aspects of Electrochemistry," ed. by Bockris J. O'M., White R. E., Conway B. E., Vol. 20, Ch. 6, Plenum, N.Y., 1989.
- 2) Dibari G. A., Read H. J., *Corrosion*, **27**, 483–488 (1971).
- 3) Moore W. M., Chen C. T., Shirn G. A., *Corrosion*, **49**, 644–650 (1984).
- 4) Ovari F., Tamsanyi L., Turmezey T., *Electrochim. Acta*, **33**, 323–328 (1988).
- 5) Tamsanyi L., Varga K., Bartik I., Horanyi G., Maleczki E., *Electrochim. Acta*, **34**, 855–860 (1989).
- 6) Stevanovic R. M., Despic A. R., Drazic D. M., *Electrochim. Acta*, **33**, 397–401 (1988).
- 7) Frers S. E., Stefenel M. M., Chierche T., *J. Appl. Electrochem.*, **20**, 996–1002 (1990).
- 8) Brett C. M. A., *J. Appl. Electrochem.*, **20**, 1000–1006 (1990).

- 9) Cabot P. L., Centellas F. A., Garrido J. A., Perez E., Vidol H., *Electrochim. Acta*, **36**, 179—182 (1991).
- 10) Brett C. M. A., *Corros. Sci.*, **33**, 203—208 (1992).
- 11) Drazic D. M., Zecevic S. K., Atanosoki R. T., Despic A. R., *Electrochim. Acta*, **28**, 751—759 (1983).
- 12) Khedr M. G. A., Lashien M. S., *J. Electrochem. Soc.*, **136**, 968—973 (1989).
- 13) Khedr M. G. A., Lashien M. S., *Corros. Sci.*, **33**, 137—140 (1992).
- 14) Burri G., Luedi W., Haas O., *J. Electrochem. Soc.*, **136**, 2167—2171 (1989).
- 15) Equey J. F., Muller S., Desivestro J., Hass O., *J. Electrochem. Soc.*, **139**, 1499—1506 (1992).
- 16) Breslin C. B., Carroll W. M., *Corros. Sci.*, **34**, 327—331 (1993).
- 17) Mylius F., *Z. Metall.*, **14**, 233 (1948).
- 18) Streicher M. A., *Trans. Electrochem. Soc.*, **43**, 285—290 (1948).
- 19) Fouda A. S., Moussa M. N., Taha F. I., Elnenaa A. I., *Corros. Sci.*, **26**, 719—725 (1985).
- 20) Mohamed A. K., Bekhiet M. M., Fouda A. S., *Bull. Soc. Chim. Fr.*, **128**, 331—337 (1991).

Lupin Alkaloids from Chinese *Maackia amurensis*

Yong-Hong WANG,^a Jia-Shi LI,^b Ze-Rong JIANG,^c Hajime KUBO,^a Kimio HIGASHIYAMA,^a and Shigeru OHMIYA^{*,a}

^aInstitute of Medicinal Chemistry, Hoshi University,^a Ebara 2-4-41, Shinagawa-ku, Tokyo 142-8501, Japan, ^bBeijing University of Traditional Chinese Medicine,^b 11, Beisan Huan Dong Ave, Beijing 100029, People's Republic of China, and ^cShenyang Pharmaceutical University,^c Liaoning 110015, People's Republic of China.

Received November 4, 1999; accepted January 22, 2000

Two new alkaloids were isolated together with 16 known lupin alkaloids from the leaves and stems of Chinese *Maackia amurensis*. Their structures were determined by spectroscopic methods to be (–)-6 α -methoxylupanine and (–)-5 α -(12-cytisinylmethyl)-6 α -hydroxylupanine and identified by comparison with synthetic samples. The structures of lupin alkaloids were also related to the geographical distributions of the *Maackia* plants.

Key words *Maackia amurensis*; Leguminosae; (–)-6 α -methoxylupanine; (–)-5 α -(12-cytisinylmethyl)-6 α -hydroxylupanine; (–)-6 α -hydroxylupanine; chemotaxonomy

In our recent phytochemical study of *Maackia* (*M.*) (Leguminosae) plants native in Japan, we discovered that the structural types of lupin alkaloids are related to geographical distribution of the plants. *M. amurensis* is found in northern Japan and contains sparteine-type lupin alkaloids but not lupinine-type alkaloids. *M. tashiroi*, *M. floribunda* and *M. floribunda* f. *pubescens*, all of which grow in southern Japan, produce lupinine-type alkaloids, and sparteine-type alkaloids are not found.¹⁾ *Maackia* plants produce alkaloids having a >N–CH₂–Y moiety such as (–)-*N*-(2-oxopyrrolidinomethyl)cytisine and (–)-*N*-(*N*-acetylaminomethyl)cytisine.²⁾ The above phenomena are interesting when the chemotaxonomy of leguminous plants and biosynthesis of lupin alkaloids are considered. This report describes the isolation and structural determination of 18 alkaloids from Chinese *M. amurensis*, which also occurs in northern China. (–)-6 α -Hydroxylupanine (**1**) was isolated for the first time from *Maackia* plants. (–)-6 α -Methoxylupanine (**2**) and (–)-5 α -(12-cytisinylmethyl)-6 α -hydroxylupanine (**3**) are new alkaloids. The relations between the geographical distributions and the structural types of lupin alkaloids, and a comparison of alkaloidal constituents of Chinese *Maackia* plants with Japanese ones are also discussed.

Results and Discussion

The total alkaloid mixture (11.0 g) obtained from 75% methanol extracts of air-dried stems (2.0 kg) of *M. amurensis* was separated repeatedly by silica gel column chromatography to yield 18 lupin alkaloids: **1**, **2**, **3**, (–)-*N*-methylcytisine (**4**), (+)-5,6-dehydrolupanine (**5**), (–)-lupanine (**6**), (–)-anagyrine, (–)-epibaptifoline, (–)-cytisine, (–)-12,12'-methylenedicytisine, (–)-*N*-formylcytisine, (–)-*N*-(3-oxobutyl)cytisine, (–)-lusitanine, (–)-tenuamine, (–)-rhombifoline, (–)-camoensidine, (+)-ammodendrine and (+)-maackiamine. Compounds **2** and **3** are new alkaloids (Chart 1). The known alkaloids were identified by direct comparison with authentic samples (co-TLC, mp, [α]_D, IR, ¹H-NMR, ¹³C-NMR and mass spectrometry) as described in our previous reports.^{2–4)}

The total base (11.7 g) obtained from the *M. amurensis* leaves (3.5 kg) was treated similarly to yield 16 alkaloids, which are the same as the constituents of the stems except (–)-*N*-(3-oxobutyl)cytisine and (–)-rhombifoline. It is char-

acteristic of *Maackia* species that unusual lupin alkaloids containing a pyrrolidine or an indolizidine ring and common lupin alkaloids with a piperidine or quinolizidine ring coexist in the plants.^{2,3)} It is surprising that three couples of unusual and common lupin alkaloids, namely (–)-camoensidine and (–)-lupanine, (–)-tenuamine and (–)-lusitanine, and (+)-maackiamine and (+)-ammodendrine, were isolated together from Chinese *M. amurensis* (Chart 1).

The molecular formula of alkaloid **1** was determined to be C₁₅H₂₄N₂O₂ by ¹³C-NMR and high resolution electron impact MS (HR-EI-MS) spectrometry. The presence of a hydroxy group was indicated by the absorption at 3280 cm^{–1} in the IR spectrum and by fragment ions at *m/z* 247 (M⁺–OH) and 246 (M⁺–H₂O) in the EI-MS spectrum. The down-field signal at δ 85.7 (s) in the ¹³C-NMR spectrum suggested the presence of a >N–C–OH group in the molecule (Table 1). When the acidic solution of **1** in CH₂Cl₂ was stirred for 8 h at room temperature, a dehydrated product, **5**,⁴⁾ was obtained. This indicates the presence of a hydroxy group at position 6 in **6**. The [α]_D²³, mp, IR, ¹H-NMR, ¹³C-NMR and MS data for alkaloid **1** coincided with the reported values for (–)-6 α -hydroxylupanine;⁵⁾ therefore the structure of **1** was determined to be (–)-6 α -hydroxylupanine.

The HR-EI-MS and ¹³C-NMR spectra of alkaloid **2** yielded the molecular formula C₁₆H₂₆N₂O₂. The presence of a –OCH₃ group was indicated by the signal at δ 3.48 (3H, s) in the ¹H-NMR spectrum and the signal at δ 49.3 (q) in the ¹³C-NMR spectrum. The signal at δ 89.5 in the ¹³C-NMR spectrum suggested the presence of a >N–C–O group in the structure of **2**. All of the ¹³C signals, except for C-6 (+3.8 ppm), C-7 (–2.2 ppm) and C-4 signals (+1.3 ppm) effected by –OCH₃ group, agreed with those of **1** (Table 1), indicating that **2** is 6-methoxylupanine, which has the same relative stereochemistry as that of **1**. When **2** was stirred in CH₂Cl₂ solution at room temperature for 48 h, it was transformed into **5**, whose absolute configuration is known.⁴⁾ The spectroscopic data and the results of transformation into **5** suggested that **1** and **2** have the same absolute stereochemistry. Thus, alkaloid **2** was determined to be (–)-6 α -methoxylupanine that had the absolute configuration 6*R*, 7*R*, 9*R*, 11*R*, which is the same as that of **1**.

The IR spectrum of alkaloid **3**, colorless oil and [α]_D²³ –31.5° (*c*=0.26, EtOH), showed absorptions at 3400 cm^{–1}

* To whom correspondence should be addressed. e-mail: ohmiya@hoshi.ac.jp

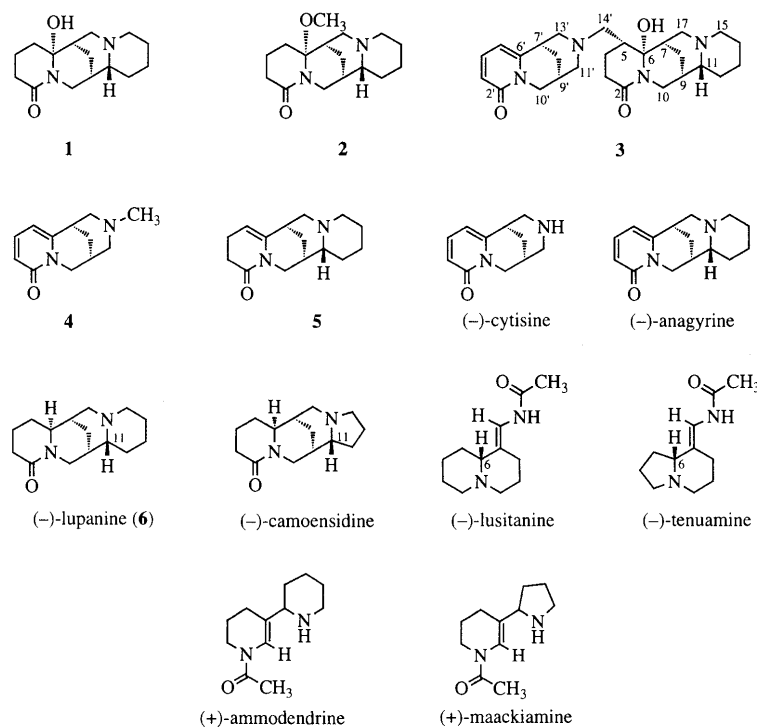
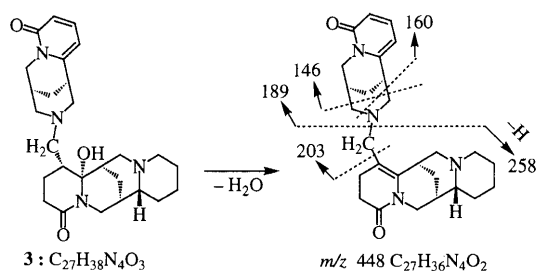


Chart 1

Fig. 1. Diagnostic EI-MS Fragment Ions (m/z) of 3

(OH) and 1640 cm^{-1} ($\text{C}=\text{O}$). The ^{13}C -NMR spectrum of 3 revealed the presence of 27 carbons. The EI-MS spectrum showed the highest MS ion at m/z 448 ($\text{C}_{27}\text{H}_{38}\text{N}_4\text{O}_3$) and the next MS ion at m/z 258 ($\text{C}_{16}\text{H}_{22}\text{N}_2\text{O}$) (Fig. 1), suggesting that 3 might consist of two alkaloid units. The characteristic fragment ions at m/z 203, 189, 160 and 146 indicated the presence of an *N*-alkylcytisine moiety in the structure of 3 such as (–)-rhombifoline and (–)-*N*-(3-oxobutyl)cytisine.^{2,7)} The signal at δ 87.1 (s) in the ^{13}C -NMR spectrum and the characteristic signal at δ 4.20 (1H, dd, $J=13.0, 2.0\text{ Hz}$, 10-H β) in the ^1H -NMR spectrum suggested the presence of a lupanine moiety having a $>\text{N}-\text{C}-\text{OH}$ group. Subtraction of the 11 peaks corresponding to (–)-cytisine from the 27 ^{13}C -NMR signals of 3 left the 15 peaks that were very similar to those of 1 except for signals due to 4-C—7-C and one methylene carbon signal at δ 58.0 which was presumed to be adjacent to a nitrogen (Table 1). The above results suggest that alkaloid 3 contains a cytisine and a 6 α -hydroxylupanine, which are linked by a methylene group. Differences in the chemical shifts of 4-C—7-C between 1 and 3 indicated that the 12-cytisinylmethyl group is located in position 5 of 1 and oriented equatorially (α -configuration). Compared with shifts in alkaloid 1, down-field shifts of C-4 (+4.7 ppm), C-5

Table 1. ^{13}C -NMR Spectral Data for Alkaloids 1–4 and 6 (in CDCl_3)⁶⁾

C	1	(1–6)	2 (2–1)	3 (3–1)	4	6
2	171.6 (+0.1)	172.3 (+0.7)	171.2 (–0.4)			171.5
3	33.1 (+0.1)	32.8 (–0.3)	33.0 (–0.1)			33.0
4	15.9 (–3.7)	17.2 (+1.3)	20.6 (+4.7)			19.6
5	32.5 (+5.8)	32.0 (–0.5)	38.1 (+5.6)			26.7
6	85.7 (+24.0)	89.5 (+3.8)	87.1 (+1.4)			61.7
7	38.0 (+3.1)	35.8 (–2.2)	32.3 (–5.7)			34.9
8	19.4 (–7.9)	19.8 (+0.4)	19.4 (0.0)			27.3
9	34.2 (+1.8)	34.3 (+0.1)	35.1 (+0.9)			32.4
10	42.8 (–3.8)	42.9 (+0.1)	42.9 (+0.1)			46.6
11	63.9 (+0.1)	63.6 (–0.3)	63.8 (–0.1)			63.8
12	34.1 (+0.6)	34.1 (0.0)	34.3 (+0.2)			33.5
13	24.5 (0.0)	24.2 (–0.3)	24.4 (–0.1)			24.5
14	24.6 (–0.7)	24.6 (0.0)	24.7 (+0.1)			25.3
15	55.2 (–0.1)	55.1 (–0.1)	55.2 (0.0)			55.3
17	54.4 (+1.6)	53.6 (–0.8)	54.4 (0.0)			52.8
–OCH ₃	—	49.3	—			—
2'				162.9	163.3	
3'				116.9	116.6	
4'				138.8	138.4	
5'				104.6	104.4	
6'				150.5	151.3	
7'				35.3	35.3	
8'				25.7	25.8	
9'				28.3	27.9	
10'				49.9	49.8	
11'				62.1	62.4	
13'				61.0	62.1	
14'				58.0	46.1	

(+5.6 ppm) and C-6 signals (+1.4 ppm) are explained by a substitution effect through a bond, and an up-field shift of the C-7 signal (–5.7 ppm) occurs through a γ -effect through space. Both effects are caused by the equatorial alkyl group at position 5. Therefore, alkaloid 3 was presumed to be 5 α -(12-cytisinylmethyl)-6 α -hydroxylupanine. The structure was confirmed by comparison with a synthetic sample, which was

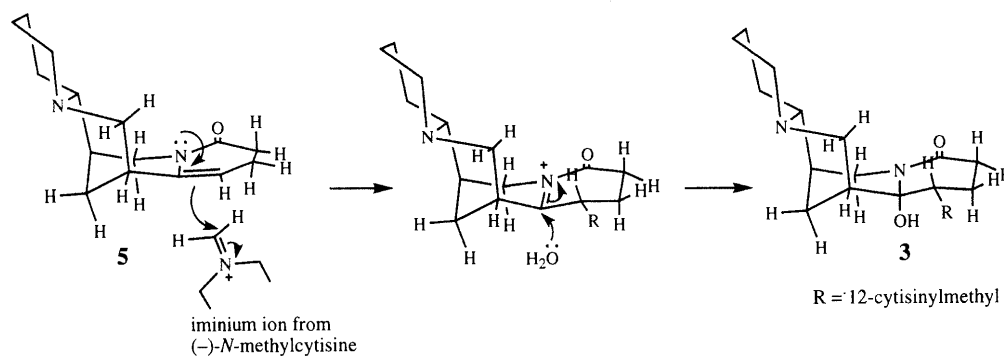


Chart 2

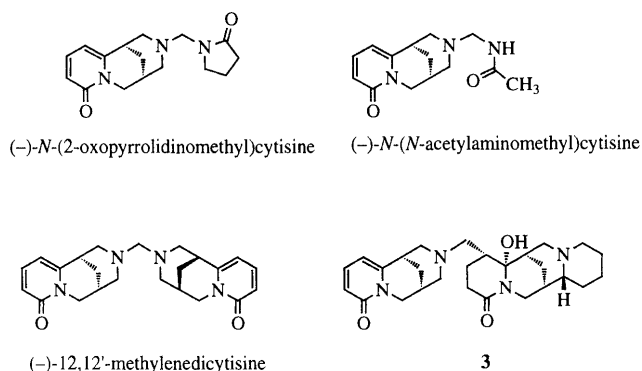


Chart 3

synthesized in a 12% yield by stirring a solution of (–)-cytisine, **5** and HCHO in H₂O for 12 h. Consideration of the reaction mechanism suggested α -configuration of the cytisinylmethyl group of the product (Chart 2). The molecular formula of alkaloid **3** should be C₂₇H₃₈N₄O₃, but in high resolution chemical ionization MS (HR-CI-MS), the highest MS ion at m/z 449.2906 suggested the formula C₂₇H₃₇N₄O₂ (Calcd for 449.2916, base peak), which corresponds to [(M+H)⁺–H₂O] (Fig. 1). We consider this to be attributable to dehydration of **3** during MS measurement process because **3** is a large molecule and contains a tertiary hydroxy group. The structure of **3** was confirmed to be (–)-5 α -(12-cytisinylmethyl)-6 α -hydroxylupanine.

Compound **5** is considered to be an important intermediate in the metabolic pathway from **6** to (–)-anagyrine.⁴ In this report, two unstable alkaloids, **1** and **2**, were identified. These may be biosynthetic intermediates between **5** and **6**.

The conjugate of (–)-cytisine and **1**, **3**, also contains a >N–CH₂–Y (Y=C) moiety in its structure. Four alkaloids including **3**, (–)-N-(2-oxopyrrolidinomethyl)cytisine,² (–)-N-(N-acetylaminoethyl)cytisine² and (–)-12,12'-methylenedicytisine,⁸ have so far been isolated from *Maackia* species (Chart 3). The alkaloids having a >N–CH₂–Y moiety in their structures are rarely found in plants, at least in lupin alkaloids, though the berberine bridge in the alkaloid berberine is well known as an example of such a group.⁹ The methylene bridge of the above lupin alkaloids is presumed to be formed by Mannich-like reaction *via* an oxidative process in which the *N*-methyl group of **4** is oxidized to a iminium ion analogous with the formation of the berberine bridge in the biosynthesis of berberine from reticuline. The lupin alkaloids containing the methylene bridge consist of two mole-

cules, one of which is (–)-cytisine. Thus, *Maackia* plants are characterized by production of these alkaloids.

In our phytochemical study of Chinese *Maackia* plants, the components of three species (*M. hupehensis*, *M. tenuifolia* and *M. amurensis*) were investigated. *M. hupehensis* and *M. tenuifolia*, which are native to southern China, produce lupinine-type alkaloids such as (–)-lupanine and (+)-epilupanine but not sparteine-type alkaloids. *M. amurensis*, which grows in northern China, produces sparteine-type alkaloids but not lupinine-type alkaloids. The anagyrine-type, cytisine-type alkaloids and lusitanine alkaloid are common in the plants of the above two groups. (–)-Lusitanine¹⁰ is similar to (–)-lupanine. However, (–)-lupanine¹¹ comes directly from lysine. (–)-Lusitanine is thought to come from the C, D-ring of tetracyclic lupin alkaloids because its configuration at position 6 agrees with that of position 11 in (–)-lupanine and (–)-anagyrine (Chart 1). The absolute configuration of (–)-tenuamine² is not clear; (–)-tenuamine may also come from the C, D-ring of camoensidine in analogy with (–)-lusitanine.

Unusual alkaloids with a pyrrolidine or an indolizidine ring and common alkaloids with a piperidine or quinolizidine ring such as (–)-camoensidine and (–)-lupanine, and (–)-tenuamine and (–)-lusitanine, occur in pairs and coexist in all *Maackia* plants (Chart 1). This is characterized for *Maackia* species and suggests that *Maackia* plants might have the biosynthetic ability to use ornithine instead of lysine as the precursor amino acid for the alkaloids.

The above phenomena of Chinese *Maackia* plants are the same as those for Japanese *Maackia* species (Table 2). This is interesting from the perspectives of both the chemotaxonomy of *Maackia* plants and the biosynthesis of lupin alkaloids.

Experimental

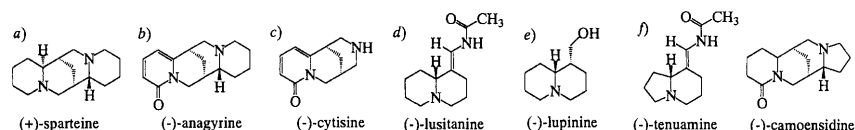
Melting points were determined on a Yanagimoto micro melting point apparatus and are uncorrected. Optical rotations were measured on a JASCO DIP-1000 polarimeter. IR spectra were measured with a JASCO FT/IR-200 fourier transform infrared spectrometer. High and low resolution MS were measured at 70 eV using a direct inlet system with a JEOL JMS-600W spectrometer. The NMR (¹H, 500 MHz, ¹³C, 125 MHz) spectra were recorded using tetramethylsilane (TMS) as an internal standard with a JEOL NMR instruments. TLC were conducted on precoated silica gel plates (Merck 60 F₂₅₄). Column chromatography was performed on silica gel with the following solvent systems: A, Et₂O–CH₂Cl₂–MeOH–25%NH₄OH (4:4:6 6:0.1) for separation of alkaloids **1**, **2** and **3**; B, CH₂Cl₂–MeOH–25% NH₄OH (90:9:1) for anagyrine, 5,6-dehydrolupanine, lupanine and ammodendrine; and C, CH₂Cl₂–MeOH (4:1) for cytisine, epibaptifoline and lusitanine.

Plant Material The leaves and stems of *M. amurensis* were collected in

Table 2. Components of the Chinese and Japanese *Maackia* Plants

Country	Plants	Sparteine-type ^{a)}	Anagyrine-type ^{b)}	Cytisine-type ^{c)}	Lusitanine ^{d)}	Lupinine-type ^{e)}	Unusual-type ^{f)}
Japan	<i>M. tashioi</i>		+	+++	++	++	+
	<i>M. floribunda</i>		+	++	+	+	+
	<i>M. floribunda</i> <i>f. pubescens</i>		+	+++	++	+++	+
	<i>M. amurensis</i>	+++	+	+++	+		+
China	<i>M. hupehensis</i>		++	+++	+	++	+
	<i>M. tenuifolia</i>		+	+++	+	+	+
	<i>M. amurensis</i>	++	++	+++	++		++

(+++ , <30%; ++ , <20%; + , <10%)



Liaoning province, northern China, during July 1998 and identified by Prof. Ze-Rong Jiang, Department of Pharmacognosy, Shenyang Pharmaceutical University. A voucher specimen (No. 1269358) is deposited in the Herbarium Institute of Botany, Chinese Academy of Sciences, Xiangshan.

Extraction and Isolation The air-dried stems of *M. amurensis* (2.0 kg) were extracted with 75% MeOH for 24 h at room temperature (3 times). The combined extracts were concentrated and acidified with 10% HCl to pH 3. The acidic phase was washed quickly with Et₂O (3 times), basified with 25% NH₄OH to pH 11 and then extracted with CH₂Cl₂ (3 times). The basic phase was saturated with K₂CO₃ and then extracted with CH₂Cl₂ repeatedly until it became negative to Dragendorff's reagent. The CH₂Cl₂ extracts were combined, dried over Na₂SO₄ and evaporated to dryness. The crude alkaloid (11.0 g, 0.55%) obtained was subjected to silica gel column chromatography (230–400 mesh, 550 g) with CH₂Cl₂–MeOH–25%NH₄OH (30:1.5:0.1), monitoring with TLC, to give 15 frs., which were further separated to give (–)-anagyrine (0.7 g), (–)-*N*-(3-oxobutyl)cytisine (85 mg), (–)-rhombifoline (76 mg), (–)-*N*-methylcytisine (4, 0.4 g), (–)-*N*-formylcytisine (0.3 g), (+)-5,6-dehydrolupanine (5, 0.6 g), (–)-6- α -methoxylupanine (2, 98 mg), (–)-lupanine (1.0 g), (–)-6- α -hydroxylupanine (1, 74 mg), (–)-cytisine (1.6 g), (–)-5- α -(12-cytisinylmethyl)-6- α -hydroxylupanine (3, 52 mg), (–)-12,12'-methylenedicytisine (0.6 g), (–)-epibaptifoline (0.6 g), (+)-ammodendrine (0.2 g), (+)-maackiamine (0.1 g), (–)-lusitanine (0.4 g), (–)-tenuamine (0.2 g), and (–)-camoensidine (0.5 g).

The crude alkaloid (11.7 g) from the *M. amurensis* leaves was treated in the similar manner as described above to yield (–)-anagyrine (0.8 g), (–)-*N*-methylcytisine (4, 0.45 g), (–)-*N*-formylcytisine (0.4 g), (+)-5,6-dehydrolupanine (5, 0.8 g), (–)-6- α -methoxylupanine (2, 0.11 g), (–)-lupanine (1.0 g), (–)-6- α -hydroxylupanine (1, 86 mg), (–)-cytisine (2.0 g), (–)-5- α -(12-cytisinylmethyl)-6- α -hydroxylupanine (3, 46 mg), (–)-12,12'-methylenedicytisine (0.7 g), (–)-epibaptifoline (1.0 g), (+)-ammodendrine (0.2 g), (+)-maackiamine (0.2 g), (–)-lusitanine (0.6 g), (–)-tenuamine (0.4 g), and (–)-camoensidine (0.7 g) in order of elution.

1: Colorless crystals, mp 115–117°C, [α]_D²³ –69.2° (*c*=0.34, EtOH). IR (KBr) cm^{–1}: 3280 (OH), 2850, 2800, 2750 (Bohlmann bands), 1640 (lactam C=O). HR-EI-MS: 264.1821 (M⁺, Calcd for C₁₅H₂₄N₂O₂: 264.1828). EI-MS *m/z* (ret. int. %): 264 (35), 247 (30), 246 (100), 217 (8), 203 (10), 189 (9), 163 (10), 150 (25), 136 (45), 110 (45). ¹H-NMR (CDCl₃) δ : 4.22 (1H, dd, *J*=13.2, 2.1 Hz, 10-H β), 2.95 (1H, d, *J*=13.2 Hz, 10-H α), 2.92 (1H, dd, *J*=11.8, 7.8 Hz, 17-H α), 2.76 (1H, m, 15-H α), 2.48 (1H, ddd, *J*=13.1, 6.8, 5.4 Hz, 3-H α), 2.35 (1H, ddd, *J*=13.1, 2.5, 2.5 Hz, 3-H β), 2.09 (1H, m, 7-H). ¹³C-NMR: see Table 1.

Dehydration of 1 (–)-6- α -Hydroxylupanine (1, 30 mg) was dissolved in 3 ml of CH₂Cl₂, and 30 μ l of 0.1% HCl–MeOH was added to the solution. The acidic solution was stirred at room temperature for 8 h. The reaction mixture was concentrated, basified with 25% NH₄OH and then extracted with CH₂Cl₂ (3 times). The CH₂Cl₂ extract was evaporated to dryness, and the residue was purified by silica gel column chromatography (20 g) with solvent B to give an oily substance (16 mg) that was identified as (+)-5,6-dehydrolupanine (5), [α]_D²³ +35.4° (*c*=0.12, EtOH). HR-EI-MS: 246.1731 (M⁺, Calcd for C₁₅H₂₂N₂O: 246.1733). ¹H-NMR (CDCl₃) δ : 4.90 (1H, dd, *J*=5.6, 3.6 Hz, 5-H), 3.97 (1H, d, *J*=13.2 Hz, 10-H β). ¹³C-NMR (CDCl₃) δ : 19.2 (t, 4-C), 21.4 (t, 13-C), 22.8 (t, 14-C), 25.1 (t, 8-C), 27.4 (t, 12-C), 31.8

(t, 3-C), 33.2 (d, 9-C), 34.2 (d, 7-C), 48.2 (t, 10-C), 54.7 (t, 17-C), 56.5 (t, 15-C), 63.3 (d, 11-C), 102.2 (d, 5-C), 143.0 (s, 6-C), 170.8 (s, 2-C).

2: Colorless oil, [α]_D²³ –16.5° (*c*=0.42, EtOH). HR-EI-MS: 278.2002 (M⁺, Calcd for C₁₆H₂₆N₂O₂: 278.1994), 263.1751 (Calcd for C₁₅H₂₃N₂O₂: 263.1759), 246.1725 (Calcd for C₁₅H₂₃N₂O: 246.1732). EI-MS *m/z* (ret. int. %): 278 (20), 263 (100), 246 (30), 150 (16), 136 (15), 122 (8), 98 (75). ¹H-NMR (CDCl₃) δ : 4.30 (1H, dd, *J*=12.8, 2.0 Hz, 10-H β), 3.48 (3H, s, –OCH₃), 2.95 (1H, dd, *J*=12.8, 2.3 Hz, 10-H α), 2.82 (1H, ddd, *J*=13.2, 7.4, 2.9 Hz, 17-H α), 2.75 (1H, d, *J*=11.5 Hz, 15-H α), 2.46 (1H, m, 3-H α), 2.38 (1H, m, 3-H β), 2.20 (1H, m, 7-H). ¹³C-NMR: see Table 1.

Conversion of 2 to 5 (–)-6- α -Methoxylupanine (2, 40 mg) was stirred in CH₂Cl₂ (5.0 ml) at room temperature for 48 h. The solution was evaporated and the residue was separated by silica gel column chromatography (30 g) with solvent A to give 5 (15 mg) and recovered 2 (20 mg).

3: Colorless oil, [α]_D²³ –31.5° (*c*=0.26, EtOH). IR (KBr) cm^{–1}: 3400 (OH), 1640 (C=O). HR-ESI-MS: 449.2906 {[M+H]⁺–H₂O}, Calcd for C₂₇H₃₇N₄O₄: 449.2916}. HR-EI-MS: 258.1739 (Calcd for C₁₆H₂₂N₂O: 258.1732). EI-MS *m/z* (ret. int. %): 448 (8), 258 (100), 203 (15), 189 (20), 160 (33), 146 (80), 134 (40). ¹H-NMR (CDCl₃) δ : 7.29 (1H, dd, *J*=9.1, 6.9 Hz, 4'-H), 6.41 (1H, dd, *J*=9.1, 1.3 Hz, 3'-H), 5.99 (1H, dd, *J*=6.9, 1.3 Hz, 5'-H), 4.20 (1H, dd, *J*=13.0, 2.0 Hz, 10-H β), 4.05 (1H, d, *J*=15.5 Hz, 10'-H β), 3.85 (1H, dd, *J*=15.5, 6.3 Hz, 10'-H α). ¹³C-NMR: see Table 1.

Synthesis of 3 To a stirred solution of 5 (130 mg, 0.51 mmol) in 10 ml of H₂O was added 2 ml of 37% HCHO (0.52 mmol) and (–)-cytisine (100 mg, 0.55 mmol). After it was stirred at room temperature for 12 h, the solution was extracted with CH₂Cl₂. The CH₂Cl₂ extract was evaporated to dryness and then purified by silica gel column chromatography (25 g) with CH₂Cl₂–MeOH–25% NH₄OH (65:5:0.8) to yield 3 (30 mg, 0.06 mmol).

Acknowledgements We would like to express our thanks to Dr. Fumio Ikegami, Research Center of Medicinal Resources, Faculty of Pharmaceutical Sciences, Chiba University, Japan, for collecting the corresponding materials of Japanese *M. amurensis*.

References and Notes

- Kubo H., *The Proceedings of the Hoshi University*, **39**, 11–19 (1997); *idem*, *Chem. Abstr.*, **128**, 34912a (1998).
- Wang Y. H., Li J. S., Kubo H., Higashiyama K., Komiya H., Ohmiya S., *Chem. Pharm. Bull.*, **47**, 1308–1310 (1999); Wang Y. H., Higashiyama K., Kubo H., Li J. S., Ohmiya S., *Heterocycles*, **51**, 3001–3004 (1999).
- Saito K., Yoshino T., Sekine T., Ohmiya S., Kubo H., Otomatsu H., Murakoshi I., *Phytochemistry*, **42**, 2533–2534 (1989); Ohmiya S., Kubo H., Otomatsu H., Saito K., Murakoshi I., *Heterocycles*, **30**, 537–542 (1990).
- Saito K., Takamatsu S., Sekine T., Ikegami F., Ohmiya S., Kubo H., Otomatsu H., Murakoshi I., *Phytochemistry*, **28**, 958–959 (1989).
- Abdel-Halim O. B., *Phytochemistry*, **40**, 1323–1325 (1995).
- The ¹³C-NMR spectrum was assigned on the basis of homo- and hetero-correlation spectroscopy (¹H–¹H, and ¹H–¹³C COSY). The assignments to 4-C and 8-C were inverted to the reported values.⁵⁾ We con-

- sider our assignment appropriate because it reflects properly the substituent effects of the hydroxy group at position 6.
- 7) Cordell G. A. (ed), "The Alkaloids," Vol. 47, Academic Press, New York, 1995, pp. 44—50.
 - 8) Kubo H., Ohmiya S., Saito K., Murakoshi I., *Thai J. Pharm. Sci.*, **17**, 171—173 (1993).
 - 9) Dewick P. M., "Medicinal Natural Products," John Wiley and Sons Ltd., London, 1997, pp. 5—31.
 - 10) Saito K., Yoshino T., Tsai S., Ohmiya S., Kubo H., Otomasu H., Murakoshi I., *Chem. Pharm. Bull.*, **35**, 1308—1310 (1987).
 - 11) Suzuki H., Koike Y., Murakoshi I., Saito K., *Phytochemistry*, **42**, 1557—1562 (1996).

Effects of Aging on Crystallization, Dissolution and Absorption Characteristics of Amorphous Tolbutamide–2-Hydroxypropyl- β -cyclodextrin Complex

Kenya KIMURA, Fumitoshi HIRAYAMA, Hidetoshi ARIMA, and Kaneto UEKAMA*

Faculty of Pharmaceutical Sciences, Kumamoto University, 5-1 Oe-honmachi, Kumamoto 862-0973, Japan.

Received November 11, 1999; accepted January 16, 2000

The effects of storage on the crystallization, dissolution and absorption of tolbutamide from amorphous tolbutamide–2-hydroxypropyl- β -cyclodextrin (HP- β -CyD) complex were investigated, in comparison with those of polyvinylpyrrolidone (PVP) solid dispersion. The amorphous solid complex of tolbutamide with HP- β -CyD and the solid dispersion of tolbutamide with PVP were prepared by a spray-drying method. During storage, a stable form of tolbutamide (form I) was crystallized from the amorphous PVP dispersion, whereas a metastable form of tolbutamide (form II) was crystallized from the HP- β -CyD complex. The dissolution rate of tolbutamide from both HP- β -CyD complex and PVP dispersion was significantly faster than that of tolbutamide alone. However, the dissolution rate from the PVP dispersion markedly decreased with storage, because of the formation of slow dissolving form I crystals. On the other hand, the dissolution rate from the HP- β -CyD complex was only slightly decreased due to the formation of fast dissolving form II crystals. These *in vitro* dissolution characteristics were clearly reflected in the *in vivo* absorption of tolbutamide and the glucose plasma level after oral administration in dogs. The results suggested that HP- β -CyD is useful not only for converting crystalline tolbutamide to an amorphous substance, but also for maintaining the fast dissolution rate of the drug over a long period. Furthermore, the crystallization of drugs from CyD complexes, with storage, seemed to be different from that involving polymer excipients such as PVP.

Key words tolbutamide; 2-hydroxypropyl- β -cyclodextrin; amorphous complex; crystallization; dissolution; absorption

Crystal modifications significantly affect various pharmaceutical properties such as the solubility, dissolution rate, stability and bioavailability of drugs.^{1–3)} As a consequence, the rational control of crystal growth, habit and polymorphic transition, using pharmaceutical additives, becomes an attractive and intriguing area of drug research and development. Cyclodextrins (CyDs), cyclic oligosaccharides consisting 6–8 glucose units linked through α -1,4 glycosidic bonds, form inclusion complexes with various drug molecules in solution and in solid state and have been utilized successfully to improve certain properties such as the solubility, stability and bioavailability of drugs.^{4–6)} Many reports have shown that crystalline drugs can be converted to an amorphous form by complexation with amorphous CyDs such as 2-hydroxypropyl- β -CyD (HP- β -CyD), and their aqueous solubility and dissolution rates thus markedly increased.^{7–9)} However, the effects of storage on pharmaceutical properties of amorphous CyD complexes, such as crystallization, dissolution and absorption behavior, *etc.*, have not fully been elucidated.¹⁰⁾ In the present study, we studied the effects of aging on the crystallization, dissolution and absorption of the HP- β -CyD complex with an oral hypoglycemic agent, tolbutamide (Fig. 1), in comparison with those of the solid dispersion of tolbutamide with polyvinylpyrrolidone, because HP- β -CyD can convert crystalline drugs such as nifedipine to amorphous solids.^{11,12)} Tolbutamide was chosen because it has several polymorphic forms, such as a stable form (form I) and metastable forms (forms II, III, IV).^{13–16)}

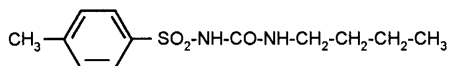


Fig. 1. Structure of Tolbutamide

Experimental

Materials Tolbutamide and chlorpropamide were donated by Nippon Hoechst–Marion–Roussel, Ltd. (Tokyo, Japan) and Ono Pharmaceutical Co., Ltd. (Osaka, Japan), respectively. HP- β -CyD (DS 4.8, average molecular weight 1413) was supplied from Japan Maize Co. (Tokyo, Japan). Polyvinylpyrrolidone K-30 (PVP, average molecular weight 40000) was purchased from Nacalai Tesque, Inc. (Kyoto, Japan). Other chemicals and solvents were of analytical reagent grade, and deionized double-distilled water was used throughout the study.

Apparatus Powder X-ray diffractograms were measured using a Rigaku Rint-2500 diffractometer under the following conditions: Ni-filtered Cu- K_{α} radiation (1.542 Å), a voltage of 40 kV, a current of 40 mA, a divergent slit of 1.74 mm (1°), a scattering slit of 0.94 mm (1°), a receiving slit of 0.15 mm, and a goniometer angular increment of 1°/min. The differential scanning calorimetry (DSC) analyses were carried out using a Perkin–Elmer DSC-7 thermal analyzer (Norwalk, CT) with a data analysis system (DEC station 325 computer, U.S.A.), operated with sample weights of 5 mg and a scanning rate of 10°/min. The heat fusion was calibrated with indium (purity 99.999%; melting point 156.4 °C, ΔH 28.47 J/mg). Viscosity of HP- β -CyD and PVP solutions was measured using a Low Shear 30 rotational rheometer (Contraves AG, Zurich, Switzerland) with an accuracy of $\pm 0.05\%$. Water contents of HP- β -CyD and PVP were measured using a Perkin–Elmer TGA7 thermal gravimeter (Norwalk, CT, U.S.A.), *i.e.*, samples (1.0 g) were stored at 60 °C and 75% relative humidity (R.H.), and at appropriate intervals a small amount (5 mg) of the samples was subjected to the thermogravimetric (TG) analysis. The weight decrease due to evaporation of water was read from the change at about 100 °C in TG curves. The water content determined by this method was in agreement with the results as measured by changes in weight.

Preparation of Tolbutamide Polymorphs, HP- β -CyD Complex and PVP Solid Dispersion The stable form of tolbutamide (form I) was prepared by recrystallization from benzene at room temperature according to the method of Simons.¹³⁾ Form II crystals of tolbutamide were obtained by keeping form IV, a metastable polymorph of tolbutamide prepared by the spray-drying method reported previously,¹⁶⁾ at 60 °C and 75% R.H. for 10 min. Form IV of tolbutamide was prepared by the spray-drying method, *i.e.*, the drug was dissolved in a mixed solvent of ethanol–dichloromethane (1.2 : 1 v/v, 150 ml) and subjected to spray-drying using a Pulvis GA32 Yamato spray-drier (Tokyo, Japan) under the following conditions: an air flow rate of 0.4 m³/min, an air pressure of 1.0 kgf/cm², inlet and outlet temperatures of 85 and 55 °C, respectively. The solid tolbutamide–HP- β -CyD com-

* To whom correspondence should be addressed.

plex in a molar ratio of 1 : 1 (weight ratio of 1 : 5.2) and the solid tolbutamide-PVP dispersion in a weight ratio of 1 : 5.2 were obtained by dissolving the components in a mixed solvent of ethanol-dichloromethane, followed by spray-drying under the above condition.

Agging Studies The test powder (3–5 g <100 mesh) was placed in glass containers in desiccators at a constant humidity of 75% R.H. (solution saturated with sodium chloride),^{16–18} then stored in incubators at constant temperatures (40–70 °C). At appropriate time intervals, samples were withdrawn, dried under reduced pressure for about 1 d at room temperature, and subjected to powder X-ray diffractometry and DSC analysis. The content of tolbutamide polymorphs (form I and form II) in matrices was calculated from areas of the diffraction peaks at $2\theta = 19.9^\circ$ and 10.3° characteristic of the former and the latter crystals, respectively. The standard calibration curve was made by mixing the polymorphs and HP- β -CyD or PVP (<100 mesh) in appropriate ratios and measuring the areas of above diffraction peaks (minimum content for the detection of forms I and II was about 3.0%). The content of form II crystals determined by X-ray diffractometry was in agreement with that calculated from the endothermic peak (ΔH 1.5 kJ/mol) at 100 °C, characteristic of the transition of form II to form I in DSC curves.

Dissolution Studies The dissolution rate was measured according to the dispersed amount method.¹⁹ A fixed amount (tolbutamide 100 mg <100 mesh) of test powders was put into 25 ml of Japanese Pharmacopoeia XIII (JP XIII) second fluid (pH 6.8) and stirred at 91 rpm at 37 °C. At appropriate intervals, an aliquot (1.0 ml) was withdrawn with a cotton-plugged pipette and spectrophotometrically analyzed for tolbutamide at 230 nm. A constant volume of dissolution medium was maintained by adding an equal volume of the original medium.

Absorption Studies *In vivo* absorption studies were carried out using male beagle dogs (9–11 kg) that were fasted for 24 h before drug administration. The sample (equivalent to 100 mg tolbutamide/body) was wafer wrapped and administered orally with water (50 ml), using a catheter. Blood samples (1 ml) were withdrawn from the cephalic vein using a heparinized injection syringe and centrifuged at $1100 \times g$ for 10 min. The plasma (0.2 ml) was added to the acetonitrile solution of an internal standard, chlorpropamide (1.0 mg/ml, 0.5 ml), and extracted with ethyl ether (4.0 ml). The organic phase (3.0 ml) was evaporated, the residue was dissolved in acetonitrile (0.1 ml), and tolbutamide was determined by HPLC with a Hitachi L-600 pump and a 635A UV detector (Tokyo, Japan), a Yamamura YMC AQ-312 ODS column (5 μ m, 6 \times 150 mm, Kyoto, Japan), a mobile phase of acetonitrile–0.05 M NaH_2PO_4 solution (45 : 55 v/v), a flow rate of 1.6 ml/min, and detection at 230 nm. Plasma levels of glucose were determined using a glucose measuring kit (Glucose CII Test Wako, Wako Pure Chemical, Ltd., Osaka, Japan), *i.e.*, the plasma (0.02 ml) was mixed with the kit solution (3.0 ml) and incubated at 37 °C for 5 min and the UV absorption was measured at 505 nm.

Results and Discussion

Crystallization of Tolbutamide during Storage Tolbutamide is known to form a 1 : 2 complex with β -CyDs in aqueous solution. However, our previous study using nuclear

magnetic resonance spectroscopy indicated that tolbutamide predominantly forms a 1 : 1 inclusion complex with HP- β -CyD in aqueous solution and in the solid state, and the toluene moiety is preferentially included in the cavity (stability constants of the 1 : 1 and 1 : 2 complexes: 225 and 25 M^{-1} , respectively).²⁰ Therefore, the complex was prepared by spray-drying the drug and the host in a molar ratio of 1 : 1 (weight ratio of 1 : 5.2). The solid dispersion of tolbutamide with PVP was prepared in a weight ratio of 1 : 5.2. Figure 2 shows changes in the powder X-ray diffraction pattern of tolbutamide-HP- β -CyD complex and tolbutamide-PVP solid dispersion during storage at 60 °C, 75% R.H. The complex and the PVP dispersion gave a halo-pattern in the powder X-ray diffractogram, indicating that they are in an amorphous state. On the storage of the complex and the PVP dispersion, X-ray diffraction peaks appeared due to tolbutamide crystals formed in HP- β -CyD and PVP amorphous matrices. The HP- β -CyD and PVP matrices spray-dried without tolbutamide showed no diffraction peaks under the present storage conditions. The PVP dispersion gave diffraction peaks characteristic of a stable crystal form (form I) of tolbutamide at $2\theta = 8.7^\circ$, 12.1° , 12.9° , 14.1° , 15.3° , 17.1° , and 19.9° .¹⁶ On the other hand, the HP- β -CyD complex gave diffraction peaks at 10.3° , 11.3° , 15.5° , 19.6° and 21.3° , characteristic of form II, and no form I peaks were observed for at least one month. On further storage of the HP- β -CyD complex, the form II diffraction peaks disappeared and the diffraction pattern changed to that of form I. The crystallization rate of tolbutamide from the complex and the PVP dispersion was measured by monitoring the change in peak areas at 19.9° and 10.3° , characteristic of form I and form II, respectively, and the results are shown in Fig. 3. In the PVP matrix, tolbutamide crystallized exclusively to form I, and the crystallization was completed within about 2 d under the experimental conditions. In sharp contrast, the HP- β -CyD complex gave predominantly form II crystals which were stable in the matrix and began to convert to form I crystals from about 2 months after the storage. The crystallization of tolbutamide to form II in the HP- β -CyD matrix was about 75% of the original amount of the drug, and the remaining tolbutamide (about 25%) may exist as a stable amorphous complex. The crystallization-time profiles of tolbutamide in these matrices were analyzed according to the Hancock and Sharp equation

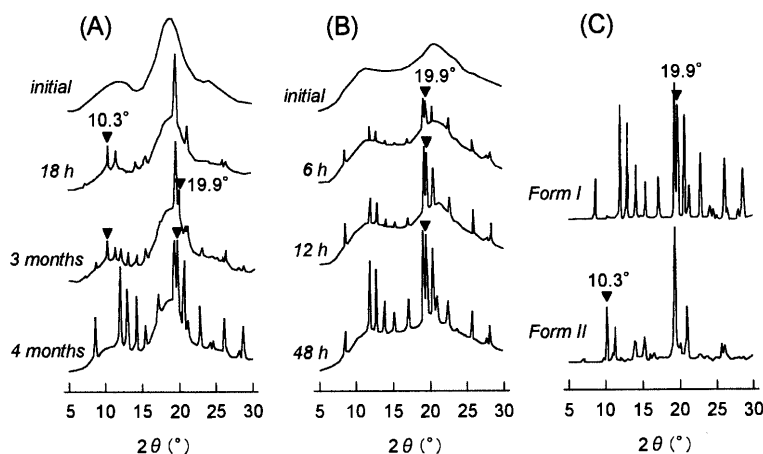


Fig. 2. Changes in Powder X-Ray Diffraction Patterns of HP- β -CyD Complex (A) and PVP Dispersion (B) during Storage at 60 °C and 75% R.H. and Powder X-Ray Diffraction Patterns of Forms I and II of Tolbutamide (C)

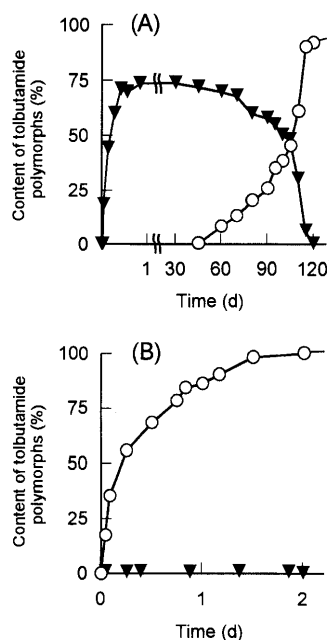


Fig. 3. Time Courses for Crystallization of Tolbutamide Polymorphs (Form I (○) and Form II (▼)) in HP-β-CyD (A) and PVP (B) Matrices during Storage at 60 °C and 75% R.H.

Each point represents the mean \pm S.E. of 2–3 experiments.

(Eq. 1)²¹:

$$\ln[-\ln(1-\alpha)] = m \ln t + \ln B \quad (1)$$

where m is the intrinsic value for various theoretical equations of solid-state decomposition, α is the fraction of the total sample crystallized to tolbutamide, t is the storage time, and B is a constant. The plot of $\ln[-\ln(1-\alpha)]$ versus $\ln t$ using data of $\alpha=0.0$ —about 0.7 gave straight lines of $m=0.99 \pm 0.03$ (mean \pm standard error (S.E.), $n=3$, correlation coefficient $r=0.99$) for the crystallization to form II in the HP-β-CyD matrix at 60 °C and 75% R.H. The m value of 0.99 indicates that a random nucleation on each particle is a rate-determining step for the crystallization of form II in the HP-β-CyD matrix (a criterion for this conversion is $m=1.0$),²¹ and the rate obeys the equation $-\ln(1-\alpha)=kt$. On the other hand, the PVP system gave an m value of 0.63 ± 0.02 ($n=3$, $r=0.99$). The m value of 0.63 for the PVP system indicates a one-dimensional diffusion-controlled crystallization (a criterion for this conversion is 0.62),²¹ and its rate obeys $\alpha^2=kt$. Therefore, the crystallization rates of tolbutamide from the HP-β-CyD complex and the PVP dispersion were analyzed, respectively, according to the aforementioned equations, and the plots of results at various temperatures are shown in Fig. 4. The plots of $-\ln(1-\alpha)$ or α^2 versus t were linear, and crystallization rate constants (k) were obtained from the slopes: crystallization of form II from the HP-β-CyD complex, $k=1.28 (\pm 0.06) \times 10^{-2} \text{ h}^{-1}$ (40 °C), $1.81 (\pm 0.04) \times 10^{-2} \text{ h}^{-1}$ (45 °C), $2.55 (\pm 0.03) \times 10^{-2} \text{ h}^{-1}$ (50 °C), $3.30 (\pm 0.04) \times 10^{-2} \text{ h}^{-1}$ (55 °C), $6.62 (\pm 0.01) \times 10^{-2} \text{ h}^{-1}$ (60 °C), and $1.19 (\pm 0.02) \times 10^{-1} \text{ h}^{-1}$ (70 °C), and crystallization of form I from the PVP dispersion, $k=5.14 (\pm 0.02) \times 10^{-3} \text{ h}^{-1}$ (40 °C), $6.32 (\pm 0.02) \times 10^{-3} \text{ h}^{-1}$ (45 °C), $8.09 (\pm 0.02) \times 10^{-3} \text{ h}^{-1}$ (50 °C), $1.32 (\pm 0.03) \times 10^{-2} \text{ h}^{-1}$ (55 °C), $2.49 (\pm 0.03) \times 10^{-2} \text{ h}^{-1}$ (60 °C), and $6.64 (\pm 0.05) \times 10^{-2} \text{ h}^{-1}$ (70 °C). The Arrhenius plots of

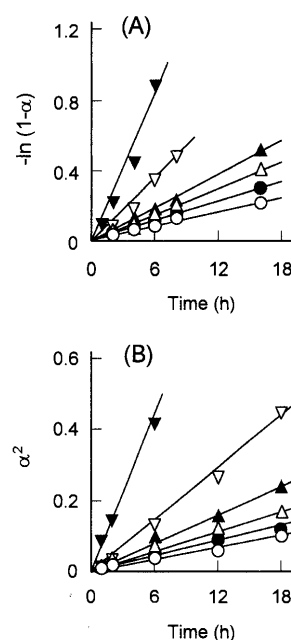


Fig. 4. Plots of $[-\ln(1-\alpha)]$ or α^2 versus Time for Crystallization to Tolbutamide Polymorphs at 75% R.H. and Various Temperatures

(A) to Form II in HP-β-CyD matrix, (B) to Form I in PVP matrix. (○), 40 °C; (●), 45 °C; (△), 50 °C; (▲), 55 °C; (▽), 60 °C; (▼), 70 °C. Each point represents the mean \pm S.E. of 2–3 experiments.

these rate constants gave straight lines ($r=0.999$), from which the activation parameters of 68 (± 1) and 78 (± 2) kJ/mol were obtained for the crystallization of form II from the HP-β-CyD complex and form I from the PVP dispersion, respectively. The diffusion-controlled crystallization of tolbutamide in the PVP matrix may be attributable at least partly to the high water absorption property of the excipient, because its water content and viscosity were much higher than those of HP-β-CyD, *i.e.*, the water content of PVP and HP-β-CyD at equilibrium (stored at 60 °C, 75% R.H. for 1 d) was about 15.2% and 3.4%, respectively, and the viscosities of the former and latter excipients (15% solution, for example) were about 7.1 cp and 1.3 cp, respectively. Therefore, stable form I of tolbutamide may crystallize from viscous PVP solution after dissolution in adsorbed water. Similar diffusion-controlled crystallization in a PVP matrix was observed for nifedipine, as reported previously.¹² On the other hand, the crystallization of tolbutamide form II from the HP-β-CyD complex cannot be ascribed merely to such environmental factors. Although further studies should be done in order to elucidate its crystallizing mechanism, the inclusion effect of the host molecule seems to be operative in the form II crystallization, because the same phenomenon was also observed in the crystallization from aqueous HP-β-CyD solutions (data not shown here). The detailed crystallizing mechanism of tolbutamide from CyD complexes will be reported elsewhere.

Dissolution and Absorption Behavior The different crystallization of tolbutamide from the HP-β-CyD complex and the PVP dispersion on storage will affect the dissolution of tolbutamide. Figure 5 shows dissolution profiles of tolbutamide-HP-β-CyD complex and tolbutamide-PVP solid dispersion immediately after the preparation, in addition to profiles of samples stored for one week at 60 °C, 75% R.H. The

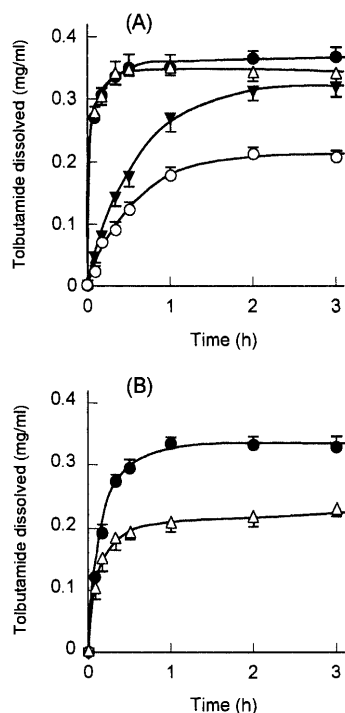


Fig. 5. Dissolution Profiles of Tolbutamide (Form I (○) and Form II (▼)) and Tolbutamide from HP- β -CyD Complex (●) and PVP Dispersion (△) Containing Amounts Equivalent to 100 mg Drug, in JP XIII Second Fluid (pH 6.8) at 37 °C, Measured by Dispersed Amount Method

(A) before storage, (B) after storage for one week at 60 °C and 75% R.H. Each point represents the mean \pm S.E. of 2–3 experiments.

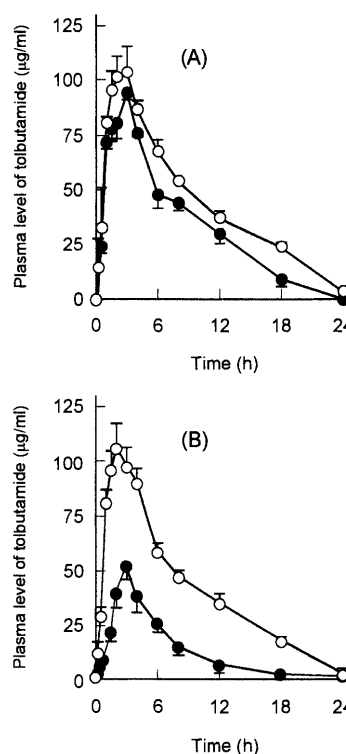


Fig. 6. Plasma Levels of Tolbutamide after Oral Administration of Tolbutamide-HP- β -CyD Complex (A) or Tolbutamide-PVP Dispersion (B) (Equivalent to 100 mg Drug/Body) in Dogs

(○), immediately after preparation; (●), after storage for one week at 60 °C and 75% R.H. Each point represents the mean \pm S.E. of 3–4 experiments.

Table 1. Bioavailability Parameters of Tolbutamide after Oral Administration of Tolbutamide-HP- β -CyD Complex or Tolbutamide-PVP Dispersion (Equivalent to 100 mg Drug/Body) in Dogs^{a)}

System	t_{\max} (h) ^{b)}	C_{\max} (μg/ml) ^{c)}	AUC (h·μg/ml) ^{d)}	MRT (h) ^{e)}	F (%) ^{f)}
HP- β -CyD complex					
Before storage	3.3 \pm 0.4	105.8 \pm 11.4	1043.8 \pm 23.7	7.5 \pm 0.3	88.8 \pm 2.6
After storage	2.8 \pm 0.3	95.1 \pm 3.1	811.0 \pm 15.9	7.1 \pm 0.2*	69.0 \pm 1.4
PVP dispersion					
Before storage	2.9 \pm 0.4	107.4 \pm 9.0	989.2 \pm 16.7	7.7 \pm 0.4	84.2 \pm 2.1
After storage	3.1 \pm 0.3	52.4 \pm 4.2**	259.0 \pm 11.3***	6.9 \pm 0.3*	22.0 \pm 1.3**

Each value represents the mean \pm S.E. of 3–4 dogs; significant differences from HP- β -CyD complex or PVP dispersion before storage are noted as follows: * p < 0.05; ** p < 0.01; *** p < 0.001. b) The time required to reach the maximum plasma level. c) The maximum plasma level. d) The area under the plasma level versus time curve up to 24 h post-administration. e) The mean residence time in plasma. f) The extent of bioavailability compared with the AUC value of intravenously administered tolbutamide.

dissolution rates of these amorphous complexes and PVP dispersion were fast, and there was insignificant difference in the dissolution rate between them. With storage, however, the dissolution rate from the PVP dispersion significantly decreased, whereas that of the HP- β -CyD complex only slightly decreased. Under the above storage conditions, tolbutamide had crystallized to form I in PVP matrix and to form II in the HP- β -CyD matrix. The dissolution rate of tolbutamide polymorphs was in the order of form IV = form II \gg form III $>$ form I, as reported previously.¹⁶⁾ Therefore, the large deceleration of the PVP system as a result of storage is attributable to the formation of form I crystals with a slow dissolution characteristic, whereas the slight deceleration is attributable to the formation of form II crystals with a fast dissolution characteristic. The insignificant decrease in dissolution rate of the tolbutamide-HP- β -CyD complex was reflected in the *in vivo* absorption behavior of the drug. Figure 6 shows plasma levels of tolbutamide after oral administration in dogs

of a tolbutamide-HP- β -CyD complex, tolbutamide-PVP dispersion immediately after the preparation, or those after storage for one week at 60 °C, 75% R.H. Table 1 summarizes their bioavailability parameters. No appreciable aging effect on the plasma tolbutamide levels was observed when the HP- β -CyD complex was administered, whereas the aged PVP dispersion significantly lowered the level, *i.e.*, the area under the curve (AUC) was 1/4 that of the drug alone. As shown in Fig. 7, the plasma glucose levels also decreased when the aged PVP dispersion was administered, whereas the aged HP- β -CyD complex showed an insignificant decrease in the glucose level.

The present results suggest that HP- β -CyD is useful not only for converting crystalline tolbutamide to an amorphous substance, but also for maintaining the fast dissolution rate of the drug for a long period. Furthermore, it is to be emphasized that the crystallization of drugs from CyD complexes on storage may be different from complexes with polymer

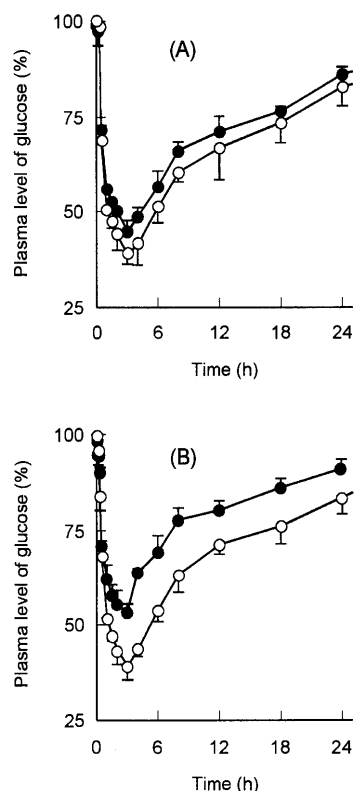


Fig. 7. Plasma Glucose Levels after Oral Administration of Tolbutamide-HP- β -CyD Complex (A) or Tolbutamide-PVP Dispersion (B) (Equivalent to 100 mg Drug/Body) in Dogs

(○), immediately after preparation; (●), after storage for one week at 60 °C and 75% R.H. Each point represents the mean \pm S.E. of 3–4 experiments.

excipients such as PVP, and attention should be given to the crystallization of drugs from CyD complexes, particularly drugs with many polymorphs.

References

- 1) Haleblan J., McCrone W., *J. Pharm. Sci.*, **58**, 911–929 (1969).
- 2) Brittain H. G., Bogdanowich S. J., Bugay D. E., Vincentis J. D., Lewen G., Newman A. W., *Pharm. Res.*, **8**, 963–973 (1991).
- 3) Borka L., *Pharm. Acta Helv.*, **66**, 16–22 (1991).
- 4) Bender M. L., Komiyama M., "Cyclodextrin Chemistry," Springer-Verlag, Berlin, 1978.
- 5) Hirayama F., Uekama K., "Cyclodextrins and Their Industrial Uses," ed. by Duchêne D., Edition de Santé, Paris, 1987, pp. 133–172.
- 6) Connors K. A., *Chem. Rev.*, **97**, 1325–1357 (1997).
- 7) Müller B. W., Brauns U., *Int. J. Pharm.*, **26**, 77–88 (1985).
- 8) Pitha J., Pitha J., *J. Pharm. Sci.*, **74**, 987–990 (1985).
- 9) Antoniadou-Vyza E., Buckton G., Michaleas S. G., Loukas Y. L., Efentakis M., *Int. J. Pharm.*, **158**, 233–239 (1997).
- 10) Hirayama F., Usami M., Kimura K., Uekama K., *Eur. J. Pharm. Sci.*, **5**, 23–30 (1997).
- 11) Suzuki H., Sunada H., *Chem. Pharm. Bull.*, **46**, 482–487 (1998).
- 12) Uekama K., Ikegami K., Wang Z., Horiuchi Y., Hirayama F., *J. Pharm. Pharmacol.*, **44**, 73–78 (1992).
- 13) Simmons D. L., Ranz R. J., Gyanchandani N. D., Picotte P., *Can. J. Pharm. Sci.*, **43**, 121–123 (1972).
- 14) Al-Saieq S. S., Riley G. S., *Pharm. Acta Helv.*, **56**, 125–129 (1981).
- 15) Leary J. R., Ross S. D., Thomas M. J. K., *Pharm. Weekblad. Sci. Ed.*, **3**, 62–66 (1981).
- 16) Kimura K., Hirayama F., Uekama K., *J. Pharm. Sci.*, **88**, 385–391 (1999).
- 17) Carr D. S., Hariss B. L., *Ind. Eng. Chem.*, **41**, 2014–2015 (1949).
- 18) Hyqvist H., *Int. J. Pharm. Technol. Prod. Mfr.*, **4**, 47–48 (1983).
- 19) Nogami H., Nagai T., Yotsuyanagi Y., *Chem. Pharm. Bull.*, **17**, 499–509 (1969).
- 20) Kimura K., Hirayama F., Arima H., Uekama K., *Pharm. Res.*, **16**, 1729–1734 (1999).
- 21) Hancock J. D., Sharp J. H., *J. Am. Ceram. Soc.*, **55**, 74–77 (1972).

Medicinal Flowers. II.¹⁾ Inhibitors of Nitric Oxide Production and Absolute Stereostructures of Five New Germacrane-Type Sesquiterpenes, Kikkanols D, D Monoacetate, E, F, and F Monoacetate from the Flowers of *Chrysanthemum indicum* L.

Masayuki YOSHIKAWA,* Toshio MORIKAWA, Iwao TOGUCHIDA, Shoichi HARIMA, and Hisashi MATSUDA

Kyoto Pharmaceutical University, Misasagi, Yamashina-ku, Kyoto 607–8412, Japan.

Received November 17, 1999; accepted January 19, 2000

The methanolic extract and ethyl acetate-soluble portion from the flowers of *Chrysanthemum indicum* L., *Chrysanthemi Indici* Flos, were found to show inhibitory activity against nitric oxide (NO) production in lipopolysaccharide-activated macrophages. Five new germacrane-type sesquiterpenes, kikkanols D, D monoacetate, E, F, and F monoacetate, were isolated from the ethyl acetate-soluble portion. Their absolute stereostructures were elucidated on the basis of chemical and physicochemical evidence, which included application of the modified Mosher's method. The effects of fifteen principal components from the ethyl acetate-soluble portion of this medicinal flower against NO production were examined and, among them, acetylenic compounds and flavonoids were found to show potent inhibitory activity.

Key words kikkanol; *Chrysanthemum indicum*; NO production inhibitor; germacrane-type sesquiterpene; medicinal flower; Compositae

In the course of our studies on bioactive principles of natural medicines,²⁾ we have found that the methanolic extract from a medicinal flower *Chrysanthemi Indici* Flos, the flower of *Chrysanthemum* (*C.*) *indicum* L. (Compositae), exhibited potent inhibitory activity against rat lens aldose reductase. In the preceding paper,¹⁾ we reported the isolation and structural elucidation of three eudesmane-type sesquiterpenes, termed kikkanols A (6), B (7), and C (8), from the ethyl acetate-soluble portion with the inhibitory activity on aldose reductase. Several active components: luteolin (14), eupatilin (15), luteolin 7-*O*- β -D-glucopyranoside, luteolin 7-*O*- β -D-glucopyranosiduronic acid, acacetin 7-*O*-(6"- α -L-rhamnopyranosyl)- β -D-glucopyranoside, and chlorogenic acid, were isolated through bioassay-guided separation using the inhibitory activity against rat lens aldose reductase. As a continuation of the characterization study of the flowers of *C. indicum*, we have also found that the methanolic extract and the ethyl acetate-soluble portion showed inhibitory effect against nitric oxide (NO) production in lipopolysaccharide (LPS)-activated macrophages. We recently isolated five new germacrane-type sesquiterpenes called kikkanols D (1), D monoacetate (2), E (3), F (4), and F monoacetate (5) from the ethyl acetate-soluble portion. This paper deals with the isolation and absolute stereostructure elucidation of new kikkanols (1–5) from the flowers of *C. indicum*. In addition, we describe the inhibitory effect of the principal components from the ethyl acetate-soluble portion of this medicinal flower against NO production.³⁾

The methanolic extract of the flowers of Chinese *C. indicum*, which showed an inhibitory effect against NO production as shown in Table 1, was partitioned into a mixture of ethyl acetate and water to furnish the ethyl acetate-soluble portion and an aqueous phase. The aqueous phase was further extracted with 1-butanol to give a 1-butanol-soluble portion and a water-soluble portion as described.¹⁾ The ethyl acetate-soluble portion was found to show inhibitory effect against NO production, while the 1-butanol-soluble and water-soluble portions lacked the activity. The ethyl acetate-

soluble portion was subjected to silica gel and octadecyl silica (ODS) column chromatography and, finally, HPLC to furnish 1 (0.002% from the natural medicine), 2 (0.001%), 3 (0.003%), 4 (0.0024%), and 5 (0.0044%) together with 6, 7, and 8, three sesquiterpene (9, 10, 11), two polyacetylenes (12, 13), and two flavones (14, 15).¹⁾

Absolute Stereostructures of 1–3 Kikkanol D (1) was isolated as a colorless oil with negative optical rotation ($[\alpha]_D^{25} -60.0^\circ$). The electron impact (EI)-MS of 1 showed a molecular ion (M^+) peak at m/z 254 in addition to fragment ion peaks at m/z 236 ($M^+ - H_2O$) and m/z 95 (base peak). The molecular formula $C_{15}H_{26}O_3$ of 1 was determined from the molecular ion peak observed in the EI-MS and by high-resolution MS measurement. The IR spectrum of 1 showed absorption bands ascribable to hydroxyl and olefin functions at 3417 and 1646 cm^{-1} , respectively. The 1H -NMR (CD_3OD) and ^{13}C -NMR (Table 2) spectra of 1 showed signals assignable to two secondary methyls [δ 0.94, 0.96 (both d, $J=7.0$ Hz, 12 and 13- H_3)], a methylene [δ 3.84, 3.95 (ABq, $J=13.1$ Hz, 15- H_2)] and two methines bearing a hydroxyl group [δ 3.92 (br d, $J=ca.$ 10 Hz, 8- H), 4.09 (d, $J=9.8$ Hz, 9- H)], an *exo*-methylene [δ 4.89, 4.94 (both s, 14- H_2)], and an olefin [δ 5.44 (dd, $J=6.1, 11.0$ Hz, 3- H)] together with four methylenes (1, 2, 5, 6- H_2), two methines (7, 11- H), and two quaternary carbons (4, 10-C).

The plane structure of 1 was constructed on the basis of 1H - 1H correlation spectroscopy (H-H COSY) and heteronuclear multiple bond correlation (HMBC) experiments. Thus, the H-H COSY experiment on 1 indicated the presence of two partial structures written in bold lines as shown in Fig. 1: from 1-C–3-C, 5-C–9-C, and 7-C–13-C. In the HMBC experiment, long-range correlations were observed between the following protons and carbons of 1 (5- H_2 , 15- H_2 and 4-C; 1- H_2 , 9- H and 10-C), so that the connectivities of the quaternary carbons (4, 10-C) in 1 were clarified. The abovementioned evidence led us to confirm the skeleton of 1 to be 3,10(14)-germacradien-8,9,15-triol.

Kikkanol D monoacetate (2) was isolated as a colorless oil

* To whom correspondence should be addressed. e-mail: shoyaku@mb.kyoto-phu.ac.jp



	IC ₅₀ (μg/ml)
MeOH extract	89.2
AcOEt-soluble portion	17.3
1-Butanol-soluble portion	>300
H ₂ O-soluble portion	>300

Figure 1 displays the chemical structures of compounds 1, 2, and 3, along with their corresponding H-H COSY and HMBC correlations. The structures are numbered 1, 2, and 3. Compound 1 is a bicyclic molecule with multiple hydroxyl groups. Compound 2 is a bicyclic molecule with a ketone group. Compound 3 is a bicyclic molecule with a ketone group and a hydroxyl group. The correlations are indicated by arrows: solid lines for H-H COSY and dashed lines for HMBC.

Legend:

- H-H COSY
- - - HMBC

methoxide (NaOMe)–methanol and the HMBC experiment showed long-range correlation between the acetyl proton and the 15-carbon. On the basis of this evidence, **2** was determined to be the 15-acetate of **1**.

Kikkanol E (**3**) was isolated as a colorless oil with negative optical rotation ($[\alpha]_D^{22} -94.4^\circ$). The molecular formula $C_{15}H_{24}O_3$ of **3** has been determined from the molecular ion peak at m/z 252 (M^+) in the EI-MS of **3** and by high-resolution MS measurement. In the UV spectrum of **3**, an absorption maximum was observed at 232 nm ($\log \epsilon$ 3.89), suggestive of an α,β -unsaturated carbonyl function. The IR spec-

Table 2. ^{13}C -NMR Data for 1–5

Position	1 ^{a)}	2 ^{b)}	3 ^{a)}	4 ^{a)}	5 ^{b)}
C-1	37.4	35.9	36.6	36.2	35.1
C-2	25.3	24.6	27.2	28.2	27.6
C-3	126.7	129.6	156.9	129.0	130.9
C-4	140.1	134.5	144.5	140.8	135.1
C-5	26.4	26.0	23.7	33.4	32.6
C-6	22.8	21.9	22.7	28.4	27.1
C-7	41.7	40.3	42.3	44.2	42.7
C-8	76.5	75.5	76.5	73.6	72.7
C-9	72.8	72.1	73.0	77.7	77.0
C-10	150.3	148.7	149.6	151.1	149.5
C-11	35.3	34.2	34.2	33.5	32.2
C-12	21.1 ^{c)}	20.5 ^{c)}	20.9 ^{c)}	21.5 ^{c)}	21.0 ^{c)}
C-13	21.3 ^{c)}	20.8 ^{c)}	21.4 ^{c)}	21.8 ^{c)}	21.3 ^{c)}
C-14	115.1	115.0	115.6	113.8	113.9
C-15	66.3	67.6	197.1	61.9	63.6
$\text{CH}_3\text{-CO-}$		21.0			21.0
$\text{CH}_3\text{-CO-}$		170.9			171.2

Measured in a) CD_3OD , b) CDCl_3 at 125 MHz. c) Assignments may be interchangeable within the same column.

trum of **3** showed absorption bands ascribable to hydroxyl, α,β -unsaturated carbonyl, and olefin functions at 3417, 1688, and 1640 cm^{-1} . The ^1H -NMR (CD_3OD) and ^{13}C -NMR (Table 2) spectra of **3** showed signals assignable to two secondary methyls [δ 0.74, 0.77 (both d, $J=6.7\text{ Hz}$, 12 and 13- H_3)], two methines bearing a hydroxyl group [δ 3.78 (br d, $J=ca. 10\text{ Hz}$, 8-H), 3.90 (d, $J=9.8\text{ Hz}$, 9-H)], an *exo*-methylene [δ 4.80, 4.95 (both d, $J=1.2\text{ Hz}$, 14- H_2)], an olefin [δ 6.54 (dd, $J=5.8, 11.9\text{ Hz}$, 3-H)], and an aldehyde [δ 9.22 (brs, 15-H)] together with four methylenes (1, 2, 5, 6- H_2), two methines (7, 11-H), and two quaternary carbons (4, 10-C). The partial structures of **3** written in bold lines were clarified by H–H COSY and long-range correlations were observed between the following protons and carbons of **3** (3-H and 15-C; 5- H_2 , 15-H and 4-C; 1- H_2 , 9-H and 10-C) in the HMBC experiment (Fig. 1). The proton and carbon signals in the NMR spectra of **3** were superimposable on those of **1**, except for the signals due to the 15-aldehyde function. Finally, reduction of **3** with sodium borohydride (NaBH_4) in the presence of cerium chloride (CeCl_3) in MeOH furnished **1** quantitatively. Thus, **3** was characterized to be the 15-aldehyde derivative of **1**.

Next, the absolute stereostructures and the geometric structures of **1**–**3** were determined by the following procedure. In order to characterize the relative stereostructure of the 7-, 8-, and 9-positions, **3** was converted to the 8,9-acetonide derivative (**3a**) by treatment of **3** with 2,2-dimethoxypropane and Dowex HCR-W2 (H^+ form). In the nuclear Overhauser effect spectroscopy (NOESY) experiment on **3a**, the nuclear Overhauser effect (NOE) correlations were observed between the signals of the following proton pairs (3-H and 15-H, 7-H and 8-H) as shown in Fig. 2. Since the NOE correlation was observed between the 3-olefin proton and the 15-aldehyde proton, the geometry of the olefin group in **3** was confirmed to be *E*-form. The NOE correlation between the 7-proton and the 8-proton and the coupling patterns of the 8-proton (dd, $J=3.5, 9.5\text{ Hz}$) and 9-proton (d, $J=9.5\text{ Hz}$) of **3a** led us to confirm the relative structure of **3a** as having 7 α -isopropyl, 8 α -hydroxyl, and 9 β -hydroxyl groups.

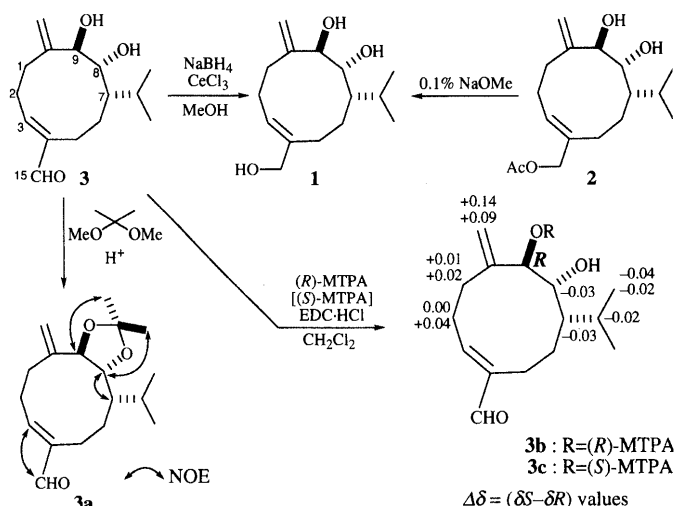


Fig. 2

The absolute configuration of **3** was determined by application of the modified Mosher's method⁴⁾ for the 9-mono-(*R*)- and (*S*)-2-methoxy-2-trifluorophenylacetate (MTPA esters, **3b** and **3c**), which were prepared by selective esterification of the 9-hydroxyl group in **3** with (*R*)- and (*S*)-2-methoxy-2-trifluoromethylphenylacetic acid in the presence of 1-ethyl-3-(3-dimethylaminopropyl)carbodiimide hydrochloride (EDC·HCl) and 4-dimethylaminopyridine (4-DMAP). As shown in Fig. 2, the signals due to protons attached to the 1, 2, and 14-carbons in the (*S*)-MTPA ester (**3c**) were observed at a lower field than those of the (*R*)-MTPA ester (**3b**) ($\Delta\delta$, positive), while the signals due to protons on the 7, 8, 11, 12 and 13-carbons in **3c** were observed at higher fields than those of **3b** ($\Delta\delta$, negative). Thus, the absolute configuration at the 9-carbon in **3** has been shown to be *R*. Consequently, the absolute stereostructures of **1**–**3** were determined.

Absolute Stereostructures of 4 and F 5 Kikkanol F (**4**) was isolated as a colorless oil with negative optical rotation ($[\alpha]_D^{25} -95.7^\circ$). The IR spectrum of **4** showed absorption bands due to hydroxyl and olefin functions at 3360 and 1651 cm^{-1} . The EI-MS of **4** showed a molecular ion peak at m/z 254 (M^+), 236 ($\text{M}^+ - \text{H}_2\text{O}$), and 95 (base peak) and the molecular formula $\text{C}_{15}\text{H}_{26}\text{O}_3$, which is the same as that of **1**, was determined by high-resolution MS measurement. The proton signals in the ^1H -NMR (CD_3OD) spectrum of **4** were also found to be similar to those of **1** and indicated the presence of the same functional groups: two secondary methyls [δ 0.99, 1.01 (both d, $J=6.4\text{ Hz}$, 12 and 13- H_3)], a methylene [δ 3.92, 4.17 (ABq, $J=11.9\text{ Hz}$, 15- H_2)] and two methines bearing a hydroxyl group [δ 3.44 (d, $J=10.1\text{ Hz}$, 9-H), 3.92 (br d, $J=ca. 10\text{ Hz}$, 8-H)], an *exo*-methylene [δ 4.93, 5.00 (both s, 14- H_2)], and an olefin [δ 5.38 (dd, $J=7.9, 7.9\text{ Hz}$, 3-H)]. In addition, the connectivities of the ^1H - ^1H and the quaternary carbons in **4** was clarified by H–H COSY and HMBC experiments as shown in Fig. 3. The geometric structure of **4** was characterized by comparison of the carbon signals (2-C, 5-C, 15-C) around the olefin group in the ^{13}C -NMR (Table 2) data for **4** with those for **1**. Namely, the signal due to the 5-carbon of **4** was observed at a lower field than that of **1** (δ_C 33.4 for **4**, δ_C 26.4 for **1**), while the 15-carbon signal of **4** was observed at a higher field than that of **1** (δ_C 61.9 for **4**,

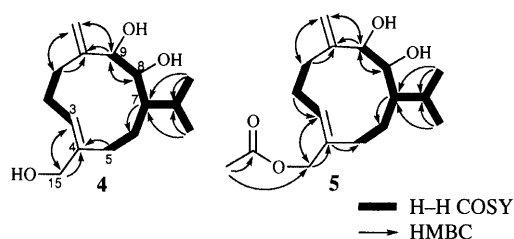


Fig. 3

δ_C 66.3 for **1**). On the basis of this evidence, **4** has been identified as the Z-isomer of **1**.

Kikkanol F monoacetate (**5**) was also isolated as a colorless oil with negative optical rotation ($[\alpha]_D^{22} -59.6^\circ$). The molecular formula $C_{17}H_{28}O_4$ of **5** has been determined for the molecular ion peak m/z 296 (M^+) in the EI-MS and by high-resolution MS measurement. The IR spectrum of **5** showed absorption bands at 3436, 1738, and 1651 cm^{-1} ascribable to hydroxyl, carbonyl, and olefin functions. The ^1H -NMR (CDCl_3) and ^{13}C -NMR (Table 2) spectra of **5** showed signals due to an acetyl methyl [δ 2.06 (s, 15-OAc)] and a methylene bearing an acetoxyl group [δ 4.49, 4.59 (ABq, $J=12.2\text{ Hz}$, 15- H_2)] together with two secondary methyls, two methines bearing a hydroxyl group, an *exo*-methylene, and an olefin. Alkaline treatment of **5** furnished **4** and the HMBC experiment showed a long-range correlation between the acetyl proton and the 15-carbon (Fig. 3). Therefore, **5** was confirmed to be the 15-acetate of **4**.

The relative stereostructures and geometric structures of **4** and **5** were also determined by the NOE experiment on the 8,9-acetonide derivative (**5a**), which was prepared by acid treatment of **5** in 2,2-dimethoxypropane. Thus, the NOE correlations were observed between the signals of the following proton pairs (2- H_2 and 15- H_2 , 3-H and 5- H_2 , 7-H and 8-H) as depicted in Fig. 4. This evidence led us to confirm the geometry of the olefin group in **5a** as Z-form. Furthermore, on the basis of the NOE correlations between the 7-proton and the 8-proton and the coupling patterns of the 8-proton (dd, $J=1.8, 9.1\text{ Hz}$) and 9-proton (d, $J=9.1\text{ Hz}$), the configurations of **5a** at the 7, 8, and 9-positions were confirmed to be the same as those of **3a**.

Finally, the absolute configuration of **5** was determined by application of the modified Mosher's method. As shown in Fig. 4, the signals due to protons attached to the 1, 2, and 14-carbons in the 9-mono-(*S*)-MTPA ester (**5c**) were observed at a lower field than those of the 9-mono-(*R*)-MTPA ester (**5b**) ($\Delta\delta$, positive), while the signals due to protons on the 5, 6, 7, 8, 11, 12 and 13-carbons in **5c** were observed at higher fields than those of **5b** ($\Delta\delta$, negative). Consequently, the absolute configuration at the 9-position of **5** has been shown to be *R*, and the absolute stereostructures of **4** and **5** were determined to be as shown.

Inhibitory Activity of Constituents from Flowers of *C. indicum* against NO Production in LPS-Activated Mouse Peritoneal Macrophages NO, an inorganic free radical, has been implicated in physiological and pathological processes, such as vasodilation, nonspecific host defense, ischemia reperfusion injury, and chronic or acute inflammation. NO is produced by the oxidation of L-arginine by a NO synthase (NOS). In the family of NOS, inducible NOS in particular is involved in a pathological aspect with overpro-

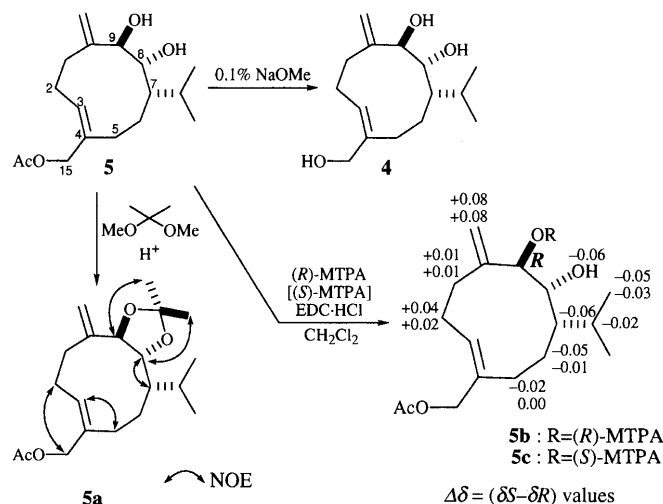


Fig. 4

Table 3. Inhibitory Activity of Constituents from *C. indicum* against NO Production in LPS-Activated Macrophages

Compounds	IC ₅₀ (μM)
Kikkanol A (6)	>100 (19.5)
Kikkanol B (7)	>100 (49.8)
Kikkanol C (8)	>100 (16.5)
Kikkanol D (1)	>100 (18.3)
Kikkanol D monoacetate (2)	>100 (29.8)
Kikkanol E (3)	>100 (36.2)
Kikkanol F (4)	>100 (14.0)
Kikkanol F monoacetate (5)	91.3
Oplopanone (9)	>100 (36.5)
Clovanediol (10)	>100 (27.4)
Caryolane 1,9 β -diol (11)	>100 (40.7)
<i>cis</i> -Spiroketalenoether polyynes (12)	38.3
<i>trans</i> -Spiroketalenoether polyynes (13)	59.5
Luteolin (14)	19.7 ^a
Eupatilin (15)	42.4
L-NMMA	27.9

Values in parentheses represent the (%) inhibition at 100 μM . ^a Cytotoxic effect was observed at 100 μM .

duction of NO, and can be expressed in response to pro-inflammatory agents such as interleukin-1 β , tumor necrosis factor- α , and LPS in various cells including macrophages, endothelial cells, and smooth muscle cells.

As a part of our characterization studies on bioactive components of natural medicines,²⁾ we previously reported several NO production inhibitors: higher unsaturated fatty acids,⁵⁾ polyacetylenes,⁶⁾ coumarins,⁶⁾ stilbenes,⁷⁾ sesquiterpenes,⁸⁾ and triterpenes.⁹⁾ In the course of our continuing survey on NO production inhibitors from natural medicines, we have found that the methanolic extract and the ethyl acetate-soluble portion from the flowers of *C. indicum*, which is prescribed for antiinflammatory, analgesic, and antipyretic purposes and the treatment of eye disease in Chinese traditional preparations, showed inhibitory activity against NO production in LPS-activated macrophages (Table 1). Next, we examined the inhibitory activity of principal components (**1**—**15**) from the ethyl acetate-soluble portion of this natural medicine. As shown in Table 3, two acetylenic compounds, *cis*-spiroketalenoether polyynes (**12**) and *trans*-spiroketalenoether polyynes (**13**), and two flavones, **14**, and **15**, were found

to inhibit the NO production. The inhibitory activity of these components and the extract from the flower of *C. indicum* against NO production may be important evidence substantiating the traditional effects of this medicinal flower.

Experimental

The following instruments were used to obtain physical data: specific rotations, Horiba SEPA-300 digital polarimeter ($l=5$ cm); UV spectra, Shimadzu UV-1200 spectrometer; IR spectra, Shimadzu FTIR-8100 spectrometer; EI-MS and high-resolution MS, JEOL JMS-GCMATE mass spectrometer; FAB-MS and high-resolution MS, JEOL JMS-SX 102A mass spectrometer; ^1H -NMR spectra, JNM-LA500 (500 MHz) spectrometer; ^{13}C -NMR spectra, JNM-LA500 (125 MHz) spectrometer with tetramethylsilane as an internal standard.

The following experimental conditions were used for chromatography: ordinary-phase silica gel column chromatography, Silica gel BW-200 (Fuji Silysia Chemical, Ltd., 150–350 mesh); reversed-phase silica gel column chromatography, Chromatorex ODS DM1020T (Fuji Silysia Chemical, Ltd., 100–200 mesh); TLC, pre-coated TLC plates with Silica gel 60F₂₅₄ (Merck, 0.25 mm) (ordinary phase) and Silica gel RP-18 60F₂₅₄ (Merck, 0.25 mm) (reversed phase); reversed-phase HPTLC, pre-coated TLC plates with Silica gel RP-18 60WF_{254S} (Merck, 0.25 mm); detection was achieved by spraying with 1% Ce(SO₄)₂–10% aqueous H₂SO₄ and heating.

Isolation of Kikkanols D (1), D Monoacetate (2), E (3), F (4), and F Monoacetate (5) from the Flowers of *C. indicum* L. Fraction 8 (3.7 g) obtained from the ethyl acetate-soluble portion of the flowers of *C. indicum* L. (5.8 kg, cultivated in China and purchased from Koshiro Co., Ltd., Osaka) and isolated kikkanols A–C (6–8), oplopanone (9), and eupatilin (15) as reported previously,¹⁾ was further separated by reversed-phase silica gel column chromatography (100 g, MeOH–H₂O) and HPLC [YMC-Pack ODS-A, MeOH–H₂O (70:30, v/v)] to furnish kikkanols D monoacetate (2, 19 mg), and F monoacetate (5, 86 mg). Fraction 10 (6.3 g), from which clovanediol (10), caryolane 1,9 β -diol (11), and luteolin (14) were previously isolated,¹⁾ was subjected to reversed-phase silica gel column chromatography (300 g, MeOH–H₂O) and HPLC [YMC-Pack ODS-A, MeOH–H₂O (50:50, v/v)] to furnish kikkanols D (1, 38 mg), E (3, 57 mg), and F (4, 46 mg).

Kikkanol D (1): Colorless oil, $[\alpha]_D^{25} -60.0^\circ$ ($c=0.7$, CHCl₃). High-resolution EI-MS: Calcd for C₁₅H₂₆O₃ (M⁺): 254.1882. Found: 254.1889. IR (film): 3417, 2958, 1646, 909 cm⁻¹. ^1H -NMR (CD₃OD) δ : 0.94, 0.96 (3H each, both d, $J=7.0$ Hz, 12 and 13-H₃), 1.42 (1H, m, 6 β -H), 1.55 (1H, br ddd, $J=ca. 2, 7, 9$ Hz, 7-H), 1.64 (1H, dq, $J=1.8, 7.0$ Hz, 11-H), 1.90 (1H, dddd, $J=4.3, 5.2, 6.8, 14.4$ Hz, 6 α -H), 2.04 (1H, m, 2-H), 2.07 (1H, m, 5-H), 2.21 (1H, ddd, $J=4.3, 13.4, 15.4$ Hz, 1 β -H), 2.45 (1H, ddd, $J=5.2, 12.5, 14.4$ Hz, 5-H), 2.58 (1H, m, 1 α -H), 2.64 (1H, m, 2-H), 3.84, 3.95 (ABq, $J=13.1$ Hz, 15-H₂), 3.92 (1H, br d, $J=ca. 10$ Hz, 8-H), 4.09 (1H, d, $J=9.8$ Hz, 9-H), 4.89, 4.94 (1H each, both s, 14-H₂), 5.44 (1H, dd, $J=6.1, 11.0$ Hz, 3-H). ^{13}C -NMR (CD₃OD) δ_C : given in Table 2. EI-MS m/z (%): 254 (M⁺, 1), 236 (M⁺–H₂O, 8), 95 (100).

Kikkanol D Monoacetate (2): Colorless oil, $[\alpha]_D^{24} -138.1^\circ$ ($c=0.1$, CHCl₃). High-resolution positive-ion FAB-MS: Calcd for C₁₇H₂₈O₄Na (M+Na)⁺: 319.1886. Found: 319.1895. IR (film) 3436, 2957, 1717, 1648, 909 cm⁻¹. ^1H -NMR (CDCl₃) δ : 0.96, 0.98 (3H each, both d, $J=7.1$ Hz, 12 and 13-H₃), 1.40 (1H, m, 6 β -H), 1.51 (1H, br ddd, $J=ca. 2, 6, 10$ Hz, 7-H), 1.68 (1H, dq, $J=2.4, 7.1$ Hz, 11-H), 1.97 (1H, dddd, $J=2.7, 5.2, 9.8, 15.3$ Hz, 6 α -H), 2.06 (3H, s, CH₃–CO–), 2.06 (1H, m, 5-H), 2.10 (1H, m, 2-H), 2.21 (1H, m, 1 β -H), 2.46 (1H, ddd, $J=5.2, 12.5, 16.6$ Hz, 5-H), 2.61 (1H, m, 2-H), 2.63 (1H, m, 1 α -H), 3.95 (1H, br d, $J=ca. 10$ Hz, 8-H), 4.10 (1H, d, $J=10.0$ Hz, 9-H), 4.33, 4.52 (ABq, $J=12.3$ Hz, 15-H₂), 4.94 (1H, brs, 14-H), 5.01 (1H, d, $J=1.2$ Hz, 14-H), 5.50 (1H, dd, $J=8.8, 13.0$ Hz, 3-H). ^{13}C -NMR (CDCl₃) δ_C : given in Table 2. Positive-ion FAB-MS m/z : 319 (M+Na)⁺.

Kikkanol E (3): Colorless oil, $[\alpha]_D^{22} -94.4^\circ$ ($c=0.1$, MeOH). High-resolution EI-MS Calcd for C₁₅H₂₄O₃ (M⁺): 252.1725. Found: 252.1731. UV [MeOH, nm, (log ϵ): 232 (3.89)]. IR (film): 3417, 2952, 1688, 1640, 912 cm⁻¹. ^1H -NMR (CD₃OD) δ : 0.74, 0.77 (3H each, both d, $J=6.7$ Hz, 12 and 13-H₃), 1.17 (1H, m, 7-H), 1.48 (1H, dq, $J=0.6, 6.7$ Hz, 11-H), 1.55 (1H, dddd, $J=3.3, 6.4, 9.7, 13.8$ Hz, 6 β -H), 1.76 (1H, dddd, $J=5.8, 8.0, 11.6, 13.8$ Hz, 6 α -H), 2.25 (1H, m, 5-H), 2.28 (1H, m, 2-H), 2.34 (1H, m, 1 β -H), 2.37 (1H, m, 5-H), 2.64 (1H, br d-like, 1 α -H), 2.82 (1H, dddd, $J=4.3, 8.9, 11.9, 12.8$ Hz, 2-H), 3.78 (1H, br d, $J=ca. 10$ Hz, 8-H), 3.90 (1H, d, $J=9.8$ Hz, 9-H), 4.80, 4.95 (1H each, both d, $J=1.2$ Hz, 14-H₂), 6.54 (1H, dd, $J=5.8, 11.9$ Hz, 3-H), 9.22 (1H, brs, 15-CHO). ^{13}C -NMR (CD₃OD) δ_C : given in Table 2. EI-MS: m/z (%): 252 (M⁺, 4), 234 (M⁺–H₂O, 8), 96 (100).

Kikkanol F (4): Colorless oil, $[\alpha]_D^{25} -95.7^\circ$ ($c=0.5$, CHCl₃). High-resolution EI-MS: Calcd for C₁₅H₂₆O₃ (M⁺): 254.1882. Found: 254.1885. IR (film): 3360, 2930, 1651, 904 cm⁻¹. ^1H -NMR (CD₃OD) δ : 0.99, 1.01 (3H each, both d, $J=6.4$ Hz, 12 and 13-H₃), 1.30 (1H, m, 7-H), 1.36 (1H, dddd, $J=1.5, 3.7, 7.3, 14.3$ Hz, 6 β -H), 1.66 (1H, dddd, $J=1.8, 4.0, 13.4, 14.3$ Hz, 6 α -H), 1.75 (1H, dq, $J=1.5, 6.4$ Hz, 11-H), 1.85 (1H, ddd-like, 5-H), 2.19 (1H, ddd, $J=8.5, 11.3, 12.0$ Hz, 1 α -H), 2.37 (1H, m, 5-H), 2.40, 2.41 (1H each, both m, 2-H₂), 2.44 (1H, m, 1 β -H), 3.44 (1H, d, $J=10.1$ Hz, 9-H), 3.92 (1H, br d, $J=ca. 10$ Hz, 8-H), 3.92, 4.17 (ABq, $J=11.9$ Hz, 15-H₂), 4.93, 5.00 (1H each, both s, 14-H₂), 5.38 (1H, dd, $J=7.9, 7.9$ Hz, 3-H). ^{13}C -NMR (CD₃OD) δ_C : given in Table 2. EI-MS m/z (%): 254 (M⁺, 1), 236 (M⁺–H₂O, 9), 95 (100).

Kikkanol F Monoacetate (5): Colorless oil, $[\alpha]_D^{22} -59.6^\circ$ ($c=0.8$, CHCl₃). High-resolution EI-MS: Calcd for C₁₇H₂₈O₄ (M⁺): 296.1987. Found: 296.1993. IR (film) 3436, 2977, 1738, 1651, 903 cm⁻¹. ^1H -NMR (CDCl₃) δ : 1.00, 1.00 (3H each, both d, $J=6.8$ Hz, 12 and 13-H₃), 1.27 (1H, m, 7-H), 1.41 (1H, dddd, $J=3.7, 4.1, 8.6, 15.0$ Hz, 6 β -H), 1.66 (1H, dddd, $J=2.1, 4.1, 4.1, 15.0$ Hz, 6 α -H), 1.78 (1H, dq, $J=1.8, 6.8$ Hz, 11-H), 1.81 (1H, ddd, $J=4.1, 4.1, 13.9$ Hz, 5-H), 2.06 (3H, s, CH₃–CO–), 2.23 (1H, m, 1 α -H), 2.37 (1H, m, 5-H), 2.43, 2.46 (1H each, both m, 2-H₂), 2.50 (1H, m, 1 β -H), 3.50 (1H, d, $J=9.8$ Hz, 9-H), 3.94 (1H, br d, $J=ca. 10$ Hz, 8-H), 4.49, 4.59 (ABq, $J=12.2$ Hz, 15-H₂), 4.99, 5.04 (1H each, both s, 14-H₂), 5.51 (1H, dd, $J=6.7, 10.4$ Hz, 3-H). ^{13}C -NMR (CDCl₃) δ_C : given in Table 2. EI-MS m/z : 296 (M⁺, 1), 278 (M⁺–H₂O, 3), 95 (100).

Deacetylation of 2, and 5 A solution of 2 (1.2 mg, 4.1 μmol) or 5 (3.5 mg, 11.8 μmol) in 0.1% NaOMe–MeOH (1.0 ml) was stirred at 40 $^\circ\text{C}$ for 1 h. The reaction mixture was neutralized with Dowex HCR-W2 (H⁺ form) and the resin was removed by filtration. Evaporation of the solvent from the filtrate under reduced pressure gave a residue, which was purified by silica gel column chromatography (0.2 g, *n*-hexane–acetone=3:1) to furnish 1 (0.9 mg, 87%) or 4 (3.0 mg, quant.).

NaBH₄–CeCl₃ Reduction of 3 A solution of 3 (2.0 mg, 7.9 μmol) in MeOH (2.0 ml) was treated with NaBH₄ (1.5 mg) in the presence of CeCl₃ (10 mg) and the mixture was stirred at 0 $^\circ\text{C}$ for 45 min. The reaction mixture was quenched at acetone (1.0 ml), then poured into ice-water and the whole was extracted with AcOEt. The AcOEt extract was washed with brine, then dried over MgSO₄ powder and filtered. Removal of the solvent from the filtrate under reduced pressure furnished a residue, which was purified by silica gel column chromatography (0.2 g, *n*-hexane–acetone=2:1) to give 1 (2.1 mg, quant.).

Preparation of Acetonide Derivatives 3a and 5a from 3 and 5 A solution of 3 (0.9 mg, 3.6 μmol) or 5 (2.5 mg, 8.4 μmol) in 2,2-dimethoxypropane (1.0 ml) was treated with Dowex HCR-W2 (H⁺ form, 10 mg) and the mixture was stirred at room temperature for 2 h. The resin was removed by filtration. Removal of the solvent from the filtrate under reduced pressure yielded a residue, which was subjected to silica gel column chromatography (0.2 g, *n*-hexane–AcOEt=5:1) to give 3a (1.1 mg, quant.) or 5a (2.9 mg, quant.).

3a: Colorless oil. ^1H -NMR (CDCl₃) δ : 0.88, 0.90 (3H each, both d, $J=7.0$ Hz, 12 and 13-H₃), 1.25 (1H, m, 7-H), 1.40, 1.43 (3H each, both s, (CH₃)₂–C), 1.49 (1H, m, 6 β -H), 1.76 (1H, dq, $J=1.6, 7.0$ Hz, 11-H), 1.82 (1H, dddd, $J=2.2, 10.1, 10.6, 12.6$ Hz, 6 α -H), 2.27, 2.54 (1H each, both m, 5-H₂), 2.57 (1H, m, 2-H), 2.60, 2.62 (1H each, both m, 1-H₂), 2.70 (1H, dddd, $J=5.8, 6.4, 8.5, 12.5$ Hz, 2-H), 4.03 (1H, dd, $J=3.5, 9.5$ Hz, 8-H), 4.29 (1H, d, $J=9.5$ Hz, 9-H), 5.09, 5.21 (1H each, both s, 14-H₂), 6.51 (1H, dd, $J=8.5, 8.6$ Hz, 3-H), 9.39 (1H, s, 15-CHO). EI-MS m/z : 292 (M⁺, 5), 252 (M⁺–C₃H₄, 5), 234 (M⁺–C₃H₄–H₂O, 19), 148 (100).

5a: Colorless oil. ^1H -NMR (CDCl₃) δ : 0.98, 1.00 (3H each, both d, $J=6.4$ Hz, 12 and 13-H₃), 1.18 (1H, m, 7-H), 1.35, 1.38 (3H each, both s, (CH₃)₂–C), 1.43 (1H, m, 6 β -H), 1.64 (1H, dddd, $J=3.0, 3.7, 6.7, 13.8$ Hz, 6 α -H), 1.73 (1H, dq, $J=2.7, 6.4$ Hz, 11-H), 1.81 (1H, ddd, $J=3.3, 3.4, 13.4$ Hz, 5-H), 2.08 (3H, s, CH₃–CO–), 2.20 (1H, m, 2-H), 2.26 (1H, m, 1 α -H), 2.37 (1H, ddd, $J=3.6, 3.7, 13.4$ Hz, 5-H), 2.46 (1H, m, 1 β -H), 2.49 (1H, m, 2-H), 3.73 (1H, d, $J=9.1$ Hz, 9-H), 3.97 (1H, dd, $J=1.8, 9.1$ Hz, 8-H), 4.50, 4.64 (ABq, $J=12.2$ Hz, 15-H₂), 5.22, 5.26 (1H each, both s, 14-H₂), 5.56 (1H, dd, $J=3.9, 4.0$ Hz, 3-H). EI-MS m/z : 336 (M⁺, 38), 120 (100).

Preparation of the (R)-MTPA Ester (3b) and the (S)-MTPA Ester (3c) from 3 A solution of 3 (1.2 mg, 4.8 μmol) in CH₂Cl₂ (1.0 ml) was treated with (R)-MTPA (5.6 mg, 24 μmol) in the presence of EDC·HCl (4.9 mg, 24 μmol) and 4-DMAP (1.7 mg, 15 μmol) and the mixture was stirred at room temperature for 24 h. The reaction mixture was poured into ice-water and the whole was extracted with AcOEt. The AcOEt extract was treated in the usual manner to give a residue, which was purified by silica gel column chromatography (0.2 g, *n*-hexane–AcOEt=5:1) to give 3b (1.5 mg, 67%).

Through a similar procedure, **3c** (1.4 mg, 63%) was prepared from **3** (1.2 mg) using (*S*)-MTPA (5.6 mg), EDC·HCl (4.9 mg) and 4-DMAP (1.7 mg).

3b: Colorless oil. $^1\text{H-NMR}$ (CDCl_3) δ : 0.83, 0.85 (3H each, both d, $J=7.0$ Hz, 12 and 13- H_3), 1.36 (1H, m, 7-H), 1.60 (1H, dq, $J=1.5$, 7.0 Hz, 11-H), 1.69 (1H, m, 6 β -H), 1.95 (1H, m, 6 α -H), 2.42 (1H, m, 5-H), 2.44 (1H, m, 1 β -H), 2.46 (1H, m, 2-H), 2.60 (1H, ddd, $J=5.8$, 6.7, 14.4 Hz, 5-H), 2.91 (1H, br d-like, 1 α -H), 3.04 (1H, dddd, $J=1.2$, 8.9, 11.6, 14.6 Hz, 2-H), 3.54 (3H, s, $-\text{OCH}_3$), 4.09 (1H, dd, $J=3.6$, 10.4 Hz, 8-H), 4.94, 5.17 (1H each, both s, 14- H_2), 5.47 (1H, d, $J=10.4$ Hz, 9-H), 6.55 (1H, dd, $J=5.8$, 11.6 Hz, 3-H), 7.40—7.54 (5H, m, Ph), 9.38 (1H, s, 15-CHO).

3c: Colorless oil. $^1\text{H-NMR}$ (CDCl_3) δ : 0.79, 0.83 (3H each, both d, $J=7.0$ Hz, 12 and 13- H_3), 1.33 (1H, m, 7-H), 1.58 (1H, dq, $J=1.8$, 7.0 Hz, 11-H), 1.69 (1H, m, 6 β -H), 1.95 (1H, m, 6 α -H), 2.42 (1H, m, 5-H), 2.45 (1H, m, 1 β -H), 2.46 (1H, m, 2-H), 2.59 (1H, ddd, $J=5.8$, 6.8, 12.5 Hz, 5-H), 2.93 (1H, br d-like, 1 α -H), 3.08 (1H, dddd, $J=5.7$, 11.4, 11.7 Hz, 2-H), 3.56 (3H, s, $-\text{OCH}_3$), 4.06 (1H, dd, $J=3.2$, 10.1 Hz, 8-H), 5.08, 5.26 (1H each, both s, 14- H_2), 5.49 (1H, d, $J=10.1$ Hz, 9-H), 6.54 (1H, dd, $J=6.2$, 11.7 Hz, 3-H), 7.39—7.54 (5H, m, Ph), 9.38 (1H, s, 15-CHO).

Preparation of the (*R*)-MTPA Ester (5b**) and the (*S*)-MTPA Ester (**5c**) from **5**** A solution of **5** (2.0 mg, 6.8 μmol) in CH_2Cl_2 (1.0 ml) was treated with (*R*)-MTPA (7.9 mg, 34 μmol) in the presence of EDC·HCl (7.0 mg, 34 μmol) and 4-DMAP (2.5 mg, 20 μmol) and the mixture was heated under reflux for 6 h. The reaction mixture was poured into ice-water and the whole was extracted with AcOEt. Work-up of the AcOEt extract as described above gave a product which was purified by silica gel column chromatography (0.5 g, *n*-hexane–AcOEt=5:1) to furnish **5b** (1.0 mg, recovered **5**, 0.4 mg, 23%). Through a similar procedure, **5c** (1.8 mg, recovered **5**, 0.4 mg, 33%) was obtained from **5** (2.5 mg) using (*S*)-MTPA (10 mg), EDC·HCl (8.8 mg) and 4-DMAP (3.1 mg) by the same procedure.

5b: Colorless oil. $^1\text{H-NMR}$ (CDCl_3) δ : 0.97, 0.99 (3H each, both d, $J=6.7$ Hz, 12 and 13- H_3), 1.42 (1H, m, 7-H), 1.48 (1H, m, 6 β -H), 1.75 (1H, m, 11-H), 1.77 (1H, m, 6 α -H), 1.84 (1H, ddd, $J=3.3$, 3.4, 13.8 Hz, 5-H), 2.07 (3H, s, $\text{CH}_3\text{-CO-}$), 2.33 (1H, m, 2-H), 2.39 (1H, m, 5-H), 2.40, 2.42 (1H each, both m, 1- H_2), 2.53 (1H, m, 2-H), 3.52 (3H, s, $-\text{OCH}_3$), 4.16 (1H, dd, $J=4.9$, 9.7 Hz, 8-H), 4.61, 4.66 (ABq, $J=12.2$ Hz, 15- H_2), 5.08, 5.16 (1H each, both s, 14- H_2), 5.20 (1H, d, $J=9.7$ Hz, 9-H), 5.58 (1H, dd, $J=7.0$, 7.0 Hz, 3-H), 7.39—7.54 (5H, m, Ph).

5c: Colorless oil. $^1\text{H-NMR}$ (CDCl_3) δ : 0.92, 0.96 (3H each, both d, $J=6.7$ Hz, 12 and 13- H_3), 1.36 (1H, m, 7-H), 1.43 (1H, m, 6 β -H), 1.73 (1H, m, 11-H), 1.76 (1H, m, 6 α -H), 1.82 (1H, m, 5-H), 2.07 (3H, s, $\text{CH}_3\text{-CO-}$), 2.37 (1H, ddd, $J=4.3$, 7.0, 12.2 Hz, 2-H), 2.39 (1H, m, 5-H), 2.41 (1H, m, 1-H), 2.43 (1H, ddd, $J=5.8$, 7.3, 14.7 Hz, 1-H), 2.55 (1H, m, 2-H), 3.54 (3H, s, $-\text{OCH}_3$), 4.10 (1H, dd, $J=4.3$, 9.4 Hz, 8-H), 4.65, 4.66 (ABq, $J=12.5$ Hz, 15- H_2), 5.16, 5.24 (1H each, both s, 14- H_2), 5.21 (1H, d, $J=9.4$ Hz, 9-H), 5.58 (1H, dd, $J=7.7$, 9.8 Hz, 3-H), 7.39—7.54 (5H, m, Ph).

Bioassay: NO Production from Macrophages Stimulated by LPS Peritoneal exudate cells were collected from the peritoneal cavities of male ddY mice by washing with 6—7 ml of ice-cold phosphate buffered saline (PBS), and cells (5×10^5 cells/well) were suspended in 200 μl of RPMI 1640 supplemented with 5% fetal calf serum (FCS), penicillin (100 units/ml) and streptomycin (100 μg /ml), and pre-cultured in 96-well microplates at 37 °C in 5% CO_2 in air for 1 h. Nonadherent cells were removed by washing the cells with PBS, and the adherent cells (more than 95% macrophages as determined by Giemsa staining) were cultured in fresh medium containing 10 μg /ml LPS and test compound (1, 3, 10, 30 and 100 μM) for 20 h. NO production in each well was assessed by measuring the accumulation of nitrite in the culture medium using Griess reagent. Cytotoxicity was deter-

mined by 3-(4,5-dimethyl-2-thiazolyl)-2,5-diphenyl-2H-tetrazolium bromide (MTT) colorimetric assay. Briefly, after 20 h incubation with test compounds, MTT (10 μl , 5 mg/ml in PBS) solution was added to the wells. After 4 h culture, the medium was removed, and isopropanol containing 0.04 N HCl was then added to dissolve the formazan produced in the cells. The optical density of the formazan solution was measured with a microplate reader at 570 nm (reference, 655 nm). N^G -monomethyl-L-arginine (L-NMMA), was used as a reference compound. Each test compound was dissolved in dimethyl sulfoxide (DMSO), and the solution was added to the medium (final DMSO concentration was 0.5%). Inhibition (%) was calculated by the following formula and IC_{50} was determined graphically ($N=4$):

$$\text{inhibition (\%)} = \frac{A-B}{A-C} \times 100$$

$A-C$: NO_2^- concentration (μM) [A : LPS (+), sample (–); B : LPS (+), sample (+); C : LPS (–), sample (–)].

References

- 1) Part I: Yoshikawa M., Morikawa T., Murakami T., Toguchida I., Harima S., Matsuda H., *Chem. Pharm. Bull.*, **47**, 340—345 (1999).
- 2) a) Yoshikawa M., Murakami T., Ueda T., Shimoda H., Yamahara J., Matsuda H., *Heterocycles*, **50**, 411—418 (1999); b) Yoshikawa M., Ueda T., Shimoda H., Murakami T., Yamahara J., Matsuda H., *Chem. Pharm. Bull.*, **47**, 383—387 (1999); c) Matsuda H., Li Y., Murakami T., Yamahara J., Yoshikawa M., *Bioorg. Med. Chem.*, **7**, 323—327 (1999); d) Li Y., Matsuda H., Yoshikawa M., *ibid.*, **7**, 1201—1205 (1999); e) Matsuda H., Shimoda H., Yoshikawa M., *ibid.*, **7**, 1445—1450 (1999); f) Li Y., Matsuda H., Wen S., Yamahara J., Yoshikawa M., *Bioorg. Med. Chem. Lett.*, **9**, 2473—2478 (1999); g) Matsuda H., Shimoda H., Yamahara J., Yoshikawa M., *Biol. Pharm. Bull.*, **22**, 870—872 (1999); h) Matsuda H., Shimoda H., Kageura T., Yoshikawa M., *ibid.*, **22**, 925—931 (1999); i) Matsuda H., Li Y., Yoshikawa M., *Bioorg. Med. Chem.*, **7**, 1737—1741 (1999); j) Matsuda H., Li Y., Yoshikawa M., *Eur. J. Pharm.*, **373**, 63—70 (1999); k) Matsuda H., Li Y., Murakami T., Yamahara J., Yoshikawa M., *ibid.*, **368**, 237—243 (1999); l) Matsuda H., Li Y., Yamahara J., Yoshikawa M., *J. Pharm. Exp. Ther.*, **289**, 729—734 (1999); m) Matsuda H., Li Y., Yoshikawa M., *Life Sci.*, **65**, PL 27—32 (1999).
- 3) Yoshikawa M., Morikawa T., Murakami T., Matsuda H., Harima S., Abstract of Papers, the 43rd Symposium on the Chemistry of Terpenes, Essential Oils, and Aromatics, Oita, **October 1999**, pp. 250—252.
- 4) Ohtani I., Kusumi T., Kashman H., Kakisawa H., *J. Am. Chem. Soc.*, **113**, 4092—4096 (1991).
- 5) Yoshikawa M., Murakami T., Shimada H., Yoshizumi S., Saka M., Yamahara J., Matsuda H., *Chem. Pharm. Bull.*, **46**, 1008—1014 (1998).
- 6) Matsuda H., Murakami T., Kageura T., Ninomiya K., Toguchida I., Nishida N., Yoshikawa M., *Bioorg. Med. Chem. Lett.*, **8**, 2191—2196 (1998).
- 7) Matsuda H., Kageura T., Morikawa T., Toguchida I., Harima S., Yoshikawa M., *Bioorg. Med. Chem. Lett.*, **10**, 323—327 (2000).
- 8) Matsuda H., Ninomiya K., Morikawa T., Yoshikawa M., *Bioorg. Med. Chem. Lett.*, **8**, 339—344 (1998).
- 9) Matsuda H., Kageura T., Toguchida I., Murakami T., Kishi A., Yoshikawa M., *Bioorg. Med. Chem. Lett.*, **9**, 3081—3086 (1999).

Three New Sesquiterpene Lactones from the Pericarps of *Illicium merrillianum*

Jian-mei HUANG,^a Yoshiyasu FUKUYAMA,^{*a} Chun-shu YANG,^b Hiroyuki MINAMI,^a and Masami TANAKA^a

Institute of Pharmacognosy, Faculty of Pharmaceutical Sciences, Tokushima Bunri University,^a Yamashiro-cho, Tokushima 770–8514, Japan, and Faculty of Pharmaceutical Sciences, Beijing University of Chinese Medicine,^b Beijing, 100029, China. Received November 17, 1999; accepted January 5, 2000

Structures of three new sesquiterpene lactones 1–3, isolated from the pericarps of *Illicium merrillianum*, have been assigned as 14-*O*-benzoylfloridanolide, 2,10-epoxy-3-dehydroxypseudoanisatin and 7-*O*-methylpseudo-majucin on the basis of spectroscopic data and chemical transformation. The structure of 2, having an ether linkage between C-2 and C-10, has been confirmed by X-ray crystallographic analysis.

Key words *Illicium merrillianum*; sesquiterpene lactone; 14-*O*-benzoylfloridanolide; 2,10-epoxy-3-dehydroxypseudoanisatin; 7-*O*-methylpseudo-majucin

Illicium (*I.*) *merrillianum* is native to the southwest of China and Myanmar, and its root bark, bark and fruit have been used as anti-rheumatism in Chinese folk medicine. From the pericarps of this plant, we isolated some interesting sesquiterpenes such as merrillianone and cycloparvifloralane,¹⁾ which possess a cage-like acetal and hemiacetal structure. As part of our continuous studies on the chemical constituents of the pericarps of *I. merrillianum*, we have isolated three new sesquiterpene lactones, 1–3, along with tashironin,²⁾ as well as an inseparable mixture of parviflorolide (7) and cycloparviflorolide (8).³⁾ Compound 1 has a carbon skeleton similar to 13-acetoxy-14-(*n*-butyryloxy)floridanolide (4)⁴⁾ and minwanensin (6),⁵⁾ whereas compound 3 is closely related to pseudomajucin-type sesquiterpene lactone.⁶⁾ Compound 2, in particular, belongs to pseudoanisatin-type sesquiterpene⁷⁾ and features the presence of an additional 2,10-ether linkage. In this paper, we deal with the isolation and structural elucidation of these three new compounds 1–3.

Compound 1 has the molecular formula C₂₂H₂₈O₇, established by high resolution FAB mass at *m/z* 427.1762 [M+Na]⁺. Its ¹H- and ¹³C-NMR spectral data (Tables 1 and 2) showed the presence of a benzoyl group [δ_{H} 8.00 (2H, dd), 7.57 (1H, td) and 7.44 (2H, t), δ_{C} 166.0, 133.0, 130.0, 129.6 and 128.4]. The remaining signals in the ¹H- and ¹³C-NMR spectra suggested that 1 was closely related to anisatin.⁸⁾ However, its IR spectrum showed no absorption (about 1820 cm⁻¹) due to a β -lactone carbonyl group, and a large AB-type coupling constant (12.0 Hz) for H-14 in 1 was observed instead of 6.6 Hz for H-14 in anisatin. Considering the coupling constant of H-14 and the presence of an extra tertiary methyl group at δ_{H} 1.36, 1 was deduced to be a structure which consists of a carbon skeleton similar to that of 13-acetoxy-14-(*n*-butyryloxy)floridanolide (4)⁴⁾ and minwanensin (6).⁵⁾ The benzoyl group was assigned to connect to C-14 on the basis of a cross peak between H-14 (δ_{H} 4.34 d and 4.39 d) and the carbonyl carbon (δ_{C} 166.0) of the benzoyl group in the heteronuclear multiple quantum coherence (HMBC) spectrum. All the ¹H- and ¹³C-NMR signals were unambiguously assigned by analyses of the various two-dimensional (2D)-NMR spectra (Tables 1 and 2).

The relative configuration on C-1, 5, 6 and 10 was clarified

by the nuclear Overhauser enhancement and exchange spectroscopy (NOESY) experiment, as shown in Fig. 2. Thus, the structure of 1 was represented as 14-*O*-benzoylfloridanolide.

Compound 2, colorless grains, showed *m/z* 319.1131 [M+Na]⁺ for C₁₅H₂₀O₆Na in HR-FAB-MS. Its molecular formula, C₁₅H₂₀O₆, was equivalent to six degrees of unsaturation. The spectral data of 2 indicated the presence of a δ -lactone group (1721 cm⁻¹ and δ_{C} 170.6) and a ketone (1710 cm⁻¹ and δ_{C} 205.9) group. The IR spectrum revealed the presence of hydroxyl groups at 3380 cm⁻¹. The ¹H-NMR resonances for three methyl groups at δ_{H} 0.88 (d), δ_{H} 1.63 and 1.28 (each s), two isolated methylenes at δ_{H} 2.44 and 3.78, and δ_{H} 4.03 and 4.63, in addition to two carbonyl groups described above, indicated that 2 resembled pseudoanisatin. The ¹H- and ¹³C-NMR data of 2 (Tables 1 and 2) showed that C-2, C-4, C-6 and C-10 attached an oxygen atom, respectively. Among them, C-4 and C-6 were verified to bear hydroxyl groups (δ_{H} 6.94 and 8.97) on the basis of HMBC correlations (Fig. 3). In consideration of the degree of unsaturation, an ether linkage should be formed between C-2 and C-10. In fact, the C-2 and C-10 carbons in 2 resonated at δ_{C} 82.4 and 81.3 lower than pseudomajucin⁶⁾ and pseudoanisatin⁷⁾ with hydroxyl groups on the C-2 and

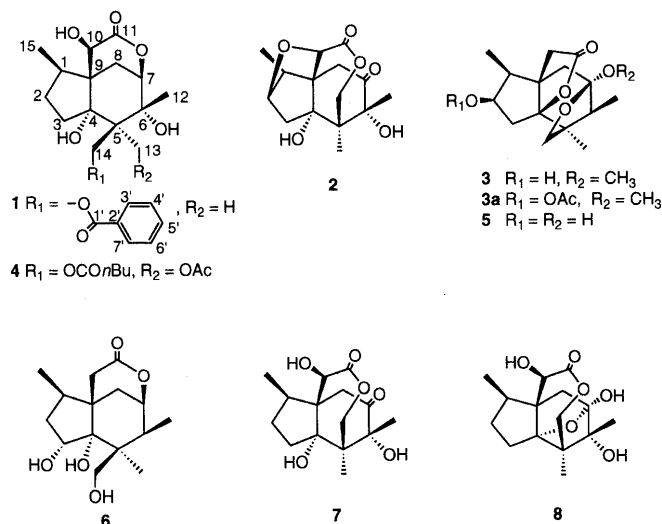


Fig. 1

* To whom correspondence should be addressed. e-mail: fukuyama@ph.bunri-u.ac.jp

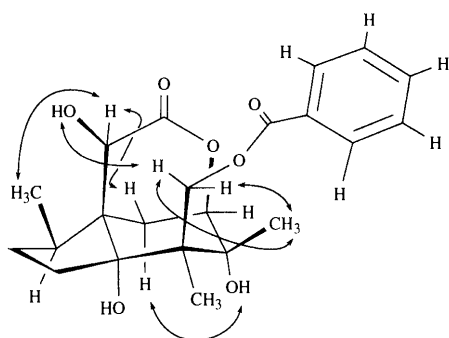


Fig. 2. Representative NOESY Correlations of 1

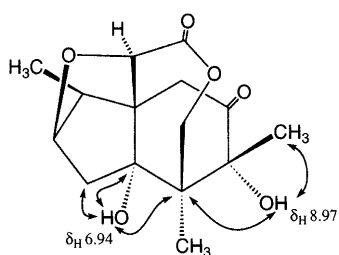


Fig. 3. HMBC Correlations from Hydroxyl Protons of 2

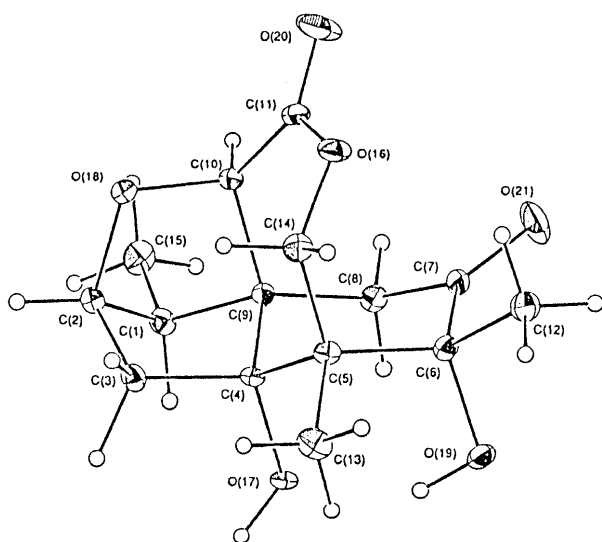


Fig. 4. ORTEP Drawing of 2

C-10 position, respectively. This also substantiated the ether bond formation between C-2 and C-10. The relative stereochemistry of **2** was deduced to be the same as pseudoanisatin, according to NOESY. Thus, the structure of **2** was elucidated to be that shown in Fig 1. Finally, X-ray crystallographic analysis of **2** [the Oak Ridge thermal ellipsoid plot program (ORTEP) drawing of **2** is showed in Fig. 4] confirmed this structure as elucidated by NMR spectroscopic data.

Compound **3** had the molecular formula, $C_{16}H_{24}O_5$, according to the HR-FAB-MS (m/z 297.1714 $[M+H]^+$). The NMR spectra suggested the presence of a methoxyl group at δ_H 3.40 and δ_C 50.7. The remaining 1H - and ^{13}C -NMR spectra implied that **3** was closely related to pseudomajucin (**5**).⁶⁾ Acetylation of **3** yielded **3a**, in which H-2 (δ_H 5.23) shifted downfield by around 1.0 ppm, suggesting the presence of a hydroxyl group at the C-2 position. The presence of a γ -lac-

Table 1. 1H -NMR (600 MHz) Spectral Data of **1**–**3**

Proton	1 ^{a)}	2 ^{b)}	3 ^{b)}
1	2.45 qdd (12.6, 8.4, 7.2) ^{c)}	2.90 q (7.2)	1.89 qd (7.2, 3.6)
2 β	1.54 dddd (12.6, 12.0, 8.4, 2.4)		
2 α	2.01 dddd (12.6, 12.6, 9.6, 7.2)	4.22 br s	4.36 ddd (4.2, 3.6, 1.8)
3 β	1.62 ddd (13.8, 9.6, 2.4)	2.31 d (14.4)	2.33 dd (14.4, 1.8)
3 α	2.60 ddd (13.8, 12.0, 7.2)	1.76 dd (14.4, 2.4)	2.07 dd (14.4, 4.2)
6			1.86 q (7.2)
7	4.33 dd (3.6, 2.4)		
8 β	1.80 dd (15.0, 3.6)	2.44 d (14.4)	2.54 d (13.2)
8 α	2.54 dd (15.0, 2.4)	3.78 d (14.4)	1.62 d (13.2)
10 β			3.20 d (18.6)
10 α	4.19 s	4.76 s	2.78 d (18.6)
12	1.44 s	1.63 s	1.03 d (7.2)
13	1.36 s	1.28 s	0.91 s
14	4.34 d (12.0)	4.63 d (13.8)	4.10 d (9.0)
	4.39 d (12.0)	4.03 d (13.8)	3.66 d (9.0)
15	1.05 d (7.2)	0.88 d (7.2)	1.16 d (7.2)
3',7'	8.00 dd (7.5, 1.9)		
4',6'	7.44 t (7.5, 7.5)		
5'	7.57 td (7.5, 1.9)		
4-OH		6.94 s	
6-OH	4.65 s	8.97 s	
OCH ₃			3.40 s

a) In $CDCl_3$. b) In C_5D_5N . c) Coupling constants (J) in Hz are given in parentheses.

Table 2. ^{13}C -NMR (150 MHz) Spectral Data of **1**–**3**

Carbon	1 ^{a)}	2 ^{b)}	3 ^{b)}
1	38.8	44.3	55.1
2	29.4	82.4	73.6
3	32.9	42.6	43.9
4	89.5	81.3	100.4
5	46.9	49.1	50.9
6	76.5	79.5	44.1
7	83.6	205.9	108.8
8	27.4	35.2	49.4
9	49.3	56.0	48.6
10	71.1	81.3	41.6
11	175.3	170.6	176.7
12	21.7	18.1	8.7
13	14.7	14.6	14.0
14	65.9	70.0	71.8
15	14.1	8.3	10.1
1'	166.0		
2'	130.0		
3',7'	129.6		
4',6'	128.4		
5'	133.0		
OCH ₃			50.7

a) In $CDCl_3$. b) In C_5D_5N .

tone moiety was also deduced from IR absorption at 1759 cm^{-1} , as well as by carbon resonance at δ_C 176.7. The 1H -NMR spectrum of **3** exhibited one tertiary methyl signal at δ_H 0.91, two secondary methyl signals at δ_H 1.03 and 1.16, and three isolated methylene signals at δ_H 1.62 and 2.54, δ_H 2.78 and 3.20, and δ_H 3.66 and 4.10. The coupling constants of H-8, H-10 and H-14 were 13.2, 9.0 and 18.6 Hz, respectively, which were almost the same as those of **5**. These spec-

tral data suggested that **3** was a pseudomajucin with an extra methoxyl group. In fact, the ^{13}C -NMR spectra of **3** showed that only C-7 and C-8 signals for **3** were shifted to a low field and high field, respectively, in comparison with those of **5**. This meant that **3** had a methoxyl group at the C-7 position, which replaced the hydroxyl group existing in **5**. This was confirmed by the presence of a HMBC correlation between OCH_3 (δ_{H} 3.40) and C-7 (δ_{C} 108.8).

The relative configuration for **3** was determined to be the same as that of **5** by NOESY and by the following chemical transformation. Treatment of **5** with anhydrous methanol in the presence of Amberlyst-15 gave a methylated product, whose ^1H -NMR data and specific optical rotation were identical with those of **3**. Thus, the structure of **3** was determined to be 7-*O*-methylpseudomajucin.

Among three new compounds, **1**–**3**, compound **2** possesses an ether linkage between C-2 and C-10, such as 1,4-epoxy-6-deoxypseudoanisatin⁹ isolated from *I. dunnianum*. To the best of our knowledge, only these two *Illicium* sesquiterpene lactones have this kind of ether linkage, and all oxygen bridges in the other *Illicium* sesquiterpenes, such as **8**,² **5**⁷ and neodunnianin,⁹ exist as hemiacetal or acetal groups.

Experimental

Melting points were determined on a Yanagimoto micro melting point apparatus. Optical rotations were measured on a Jasco DIP-1000 digital polarimeter. IR spectra were measured on a Jasco FT-IR 5300 infrared spectrophotometer. NMR spectra were recorded on a Varian Unity 600 instrument. Chemical shifts were given as δ (ppm) with tetramethylsilane as an internal standard. The MS were recorded on a JEOL AX-500 instrument. Column chromatography was carried out on Kieselgel 60 (70–230 mesh and 230–400 mesh) and Sephadex LH-20.

Plant Material The ripe fruits of *I. merrillianum* A. C. SMITH were collected in Yunnan, China in September 1998, and voucher specimen 94041 has been deposited in the Herbarium of Beijing University of Chinese Medicine.

Extraction and Purification The pericarps of *I. merrillianum* (3.7 kg) were powdered and extracted with methanol at room temperature to give 1 kg of pale yellow extract. The extract (430 g) was chromatographed on 400 g silica gel (70–230 mesh) and eluted successively with CH_2Cl_2 , CH_2Cl_2 –EtOAc (9:1, 1:1), EtOAc, EtOAc–MeOH (7:3) and MeOH to yield seven fractions (A–G). Fraction B was further divided by silica gel column chromatography with *n*-hexane–EtOAc (3:2) as an eluent to give 7 fractions. Fraction 3 was chromatographed on Sephadex LH-20 (MeOH), and silica gel eluted by CHCl_3 –MeOH (40:1) to give tashironin (9 mg). Fraction 6 was subjected to column chromatography on Sephadex LH-20 to afford frs. 8–12. Of these fractions, 14-*O*-benzoylfloridanolide (**1**), (10 mg) was obtained from fr. 11 by chromatography on silica gel [CHCl_3 –EtOAc (3:2)], RP-8 [Lichroprep RP-8 (40–63 μm) B, MeOH– H_2O (3:2, 2 ml/min)] and HPLC [Cosmosil 5C18-AR, 10 \times 250 mm, i.d., MeOH– H_2O (3:2, 2 ml/min)]. Fraction C was divided by chromatography on silica gel eluting with hexane–EtOAc (1:1) to give frs. 13–23. Anisatin (12 mg) and a mixture of cycloparviflorolide (**8**) and parviflorolide (**7**, 510 mg) were isolated by crystallization from fr. 18. Fraction 21 was separated by chromatography on silica gel using CH_2Cl_2 –MeOH (15:1) as eluent to give frs. 24–28. 7-*O*-Acetylanisatin (8 mg), 2,10-epoxy-3-dehydroxypseudoanisatin (**2**), (16 mg) and 7-*O*-methylpseudomajucin (**3**), (7 mg) were isolated by HPLC [Cosmosil 5C18-AR-II, 10 \times 50 mm, i.d., MeOH– H_2O (2:3, 2 ml/min)] from fr. 24.

14-*O*-Benzoylfloridanolide (**1**): mp 180–181 °C, $[\alpha]_{\text{D}}^{24}$ –5.97° (c =0.94, CHCl_3). HR-FAB-MS m/z : 427.1762 $[\text{M}+\text{Na}]^+$ (Calcd for $\text{C}_{22}\text{H}_{28}\text{NaO}_7$: 427.1733). IR (film) cm^{-1} : 3376 (OH), 1724 (C=O). ^1H - and ^{13}C -NMR: Tables 1 and 2.

2,10-Epoxy-3-dehydroxypseudoanisatin (**2**): Colorless grains (from MeOH), mp 260–261 °C, $[\alpha]_{\text{D}}^{25}$ +11.6° (c =0.22, CHCl_3). HR-FAB-MS m/z : 319.1131 $[\text{M}+\text{Na}]^+$ (Calcd for $\text{C}_{15}\text{H}_{20}\text{NaO}_5$: 319.1158). IR (film) cm^{-1} : 3379 (OH), 1721 and 1710 (C=O). ^1H - and ^{13}C -NMR: Tables 1 and 2.

X-Ray Crystallographic Analysis of **2**: Crystal data: orthorhombic space group $P2_1P2_1P2_1$ (Z =4), a =8.011(0) Å, b =8.535(0) Å, c =20.121(0) Å, radiation=Mo K_{α} (λ =0.71073 Å), final R =0.031, R_w =0.094; data collection: MXC DIP2000 (MAC Science); cell refinement: CRYSTAN; data reduction: CRYSTAN; program(s) used to solve structure: CRYSTAN SIR92,¹⁰ program(s) used refine structure: CRYSTAN; software used to prepare material for publication: CRYSTAN (crystallographic details and data have been deposited with the Cambridge Crystallographic Data Center).

7-*O*-Methylpseudomajucin (**3**): $[\alpha]_{\text{D}}^{25}$ –35.6° (c =1.08, MeOH). HR-FAB-MS m/z : 297.1714 $[\text{M}+\text{H}]^+$ (Calcd $\text{C}_{16}\text{H}_{25}\text{O}_5$ for 297.1702). EI-MS m/z (rel. int.): 127 (100). IR (film) cm^{-1} : 3441 (OH), 1759 (C=O). ^1H - and ^{13}C -NMR: Tables 1 and 2.

Acetylation of **3**: To a solution of **3** (1 mg) in 0.25 ml of pyridine, 0.25 ml of Ac_2O was added. This solution was kept at room temperature overnight and concentrated under reduced pressure to give a residue, which was purified by TLC [CH_2Cl_2 –EtOAc (1:2)] to give the acetate **3a** (0.5 mg). **3a**: ^1H -NMR (600 MHz, pyridine- d_5) δ : 0.86 (3H, s, 13- H_3), 0.96 (3H, d, J =7.2 Hz, 15- H_3), 1.00 (3H, d, J =7.2 Hz, 12- H_3), 1.55 (1H, d, J =13.2 Hz, 8-H), 1.85 (1H, q, J =7.2 Hz, 6-H), 2.06 (3H, s, COCH_3), 2.10 (1H, dq, J =7.2, 4.2 Hz, 1-H), 2.16 (1H, dd, J =15.0, 4.2 Hz, 3-H), 2.36 (1H, dd, J =15.0, 1.2 Hz, 3-H), 2.55 (1H, d, J =13.2 Hz, 8-H), 2.82 (1H, d, J =18.6 Hz, 10-H), 3.00 (1H, d, J =18.6 Hz, 10-H), 3.37 (3H, s, OCH_3), 3.64 (1H, d, J =9.0 Hz, 14-H), 4.00 (1H, d, J =9.0 Hz, 14-H), 5.23 (1H, ddd, J =4.2, 4.2, 1.2 Hz, 2-H).

Methylation of Pseudomajucin (**5**): A mixture of **5** (2 mg) in 0.2 ml of anhydrous methanol containing two pieces of Amberlyst-15 was stirred at room temperature overnight. The product was separated by silica gel TLC [CH_2Cl_2 –EtOAc (1:2)]. The specific optical rotation and ^1H -NMR data of this product were identical with those of **3**.

Acknowledgements We are indebted to Dr. Shigeru Takaoka and Miss Yasuko Okamoto for carrying out X-ray crystallographic analysis, and measuring MS spectra, respectively. One of the authors (J.-M. Huang) thanks the High Tech-Research Center Fund from the Promotion and Mutual Aid Corporation for Private Schools of Japan for a postdoctoral fellowship.

References

- Huang J.-M., Yang C.-S., Wang H., Wu Q.-M., Wang J.-L., Fukuyama Y., *Chem. Pharm. Bull.*, **47**, 1749–1752 (1999).
- Fukuyama Y., Shida N., Kodama M., *Tetrahedron Lett.*, **36**, 583–586 (1995).
- Schmidt T. J., *J. Nat. Prod.*, **62**, 684–687 (1999).
- Schmidt T. J., Schmidt H. M., Müller E., Peters W., Fronczek F. R., Truesdale A., Fischer N. H., *J. Nat. Prod.*, **61**, 230–236 (1998).
- Wang J.-L., Yang C.-S., Yan R.-N., Yao B., Yang X.-B., *Acta Pharm. Sinica*, **29**, 693–696 (1994).
- Kouno I., Baba N., Hashimoto M., Kawano N., Yang C.-S., Sato S., *Chem. Pharm. Bull.*, **37**, 2427–2430 (1989).
- Kouno I., Irie H., Kawano N., *J. Chem. Soc., Perkin Trans. 1*, **1984**, 2511–2515.
- Yang C.-S., Kouno I., Kawano N., Sato S., *Tetrahedron Lett.*, **29**, 1165–1168 (1988).
- Huang J.-M., Wang J.-L., Yang C.-S., *Phytochemistry*, **46**, 777–780 (1997).
- Scheldrick G. M., "Crystallographic Computing 3," ed by Scheldrick G. M., Kruger C., Goddard R., Oxford University Press, Oxford, 1985, pp. 175–189.

Application of Liquid Chromatography–Atmospheric Pressure Chemical Ionization Mass Spectrometry to the Differentiation of Stereoisomeric C₁₉-Norditerpenoid Alkaloids

Koji WADA,* Takao MORI, and Norio KAWAHARA

Hokkaido College of Pharmacy, 7-1, Katsuraoka-cho, Otaru 047-0264, Japan.

Received November 24, 1999; accepted February 16, 2000

High-performance liquid chromatography–atmospheric pressure chemical ionization mass spectrometry (HPLC–APCI–MS) was successfully applied to stereoisomeric C₁₉-norditerpenoid alkaloids at position 1. APCI–MS allowed the easy and precise control of the energy deposition by varying the drift voltage. Comparison of the breakdown curves, observed by changing the potential difference between the first electrode and the second electrode of the APCI ion source, revealed stereochemical dependence of different fragmentations. The APCI spectra of alkaloids were predominantly the $[M+H]^+$ ion and major fragment ion, corresponding to the $[M+H-H_2O]^+$ ion or the $[M+H-CH_3COOH]^+$ ion, and comparison of the spectra showed that the abundance of fragment ions was significantly higher for C-1 β -form alkaloids than for C-1 α -form alkaloids. The characteristic fragment ions were formed by the loss of a water, acetic acid or methanol molecule at position 8. The fragmentation mechanisms depending on the stereochemistry of the precursor ion could be discerned by recording the spectra in a deuterated solvent system of 0.05 M ammonium acetate in D₂O–acetonitrile–tetrahydrofuran. Loss of D₂O from the precursor ion gave the fragment ion. This result indicated that the proton of protonation was included in the leaving water molecule. The peak intensity ratio $R=[M+H]^+/[M+H-H_2O]^+$ manifested the stereochemical differentiation of alkaloids at position 1.

Key words atmospheric pressure chemical ionization; C₁₉-norditerpenoid alkaloid; 1-*epi*-neoline; 1-*epi*-delcosine

The structural elucidation of organic compounds of natural and synthetic origin has been one of the major analytical applications of mass spectrometry (MS). In general, the mass spectra provide useful information on the stereochemistry of the compound under investigation, and the stereochemical information arises from sterically controlled ionic fragmentations.¹⁾ The fragmentation pattern manifested in a conventional mass spectrum is a direct reflection of the internal energy distribution of precursor ions. Consequently, the stereochemical differentiation, which generally depends on one particular fragmentation pathway among various dissociation channels, is very sensitive to the experimental conditions of ionization. Several analytical methods have been developed in order to control the amount of internal energy deposited on the precursor ion of interest with regard to the fragment ion yield.^{2–4)} A number of reports on the stereochemistry of indoloquinolizine alkaloids,⁵⁾ quinolizine alkaloids,⁶⁾ eburnane-type alkaloids,⁷⁾ and indoloquinolizine⁸⁾ and indole⁹⁾ alkaloids by electrospray ionization have appeared in recent years.

Various *Aconitum* (Ranunculaceae) plants produce C₁₉-norditerpenoid and C₂₀-diterpenoid alkaloids.¹⁰⁾ Previous structure studies of diterpenoid alkaloids involving MS have been carried out essentially by electron impact (EI) ionization and conventional analysis.^{11–16)} In particular, the fragmentation pathways of the presence of a C-6(OCH₃)–C-7(OH)–C-8(OH) grouping in C₁₉-norditerpenoid alkaloids have been extensively investigated, the structures of the fragment ions being supported by deuterium labeling at C-6 (OCD₃).¹⁷⁾ To our knowledge, previous investigation of the stereochemical differentiation of diterpenoid alkaloids has been performed using only EI.¹⁸⁾ Earlier reports have shown the optimum conditions for determination of C₁₉-norditerpenoid and C₂₀-diterpenoid alkaloids in plant extracts using high-performance liquid chromatography–atmospheric pres-

sure chemical ionization MS (HPLC–APCI–MS).^{19–21)} In a previous study,²²⁾ we demonstrated that HPLC–APCI–MS could be used in experiments on the energy-dependence of ion abundances with a view to differentiating stereoisomeric pairs of C₁₉-norditerpenoid alkaloids at position 6.

In the present paper, we report the results of an HPLC–APCI–MS study of C₁₉-norditerpenoid neoline-type alkaloids, neoline (1), 1-*epi*-neoline (2),²³⁾ 14-acetylneoline (3), 14-acetyl-1-*epi*-neoline (4),²⁴⁾ 8-acetyl-14-benzoylneoline (5) and 8-acetyl-14-benzoyl-1-*epi*-neoline (6), and delcosine-type alkaloids, delcosine (13), 1-*epi*-delcosine (14), 14-acetyl-1-*epi*-delcosine (15) and 14-acetyl-1-*epi*-delcosine (16), for resolving structural problems related to the differentiation of stereoisomers. These alkaloids differ only in the stereochemistry at position 1, alkaloids 2, 4, 6, 14 and 16 being characterized by a β -hydroxyl group and alkaloids 1, 3, 5, 13 and 15 by an α -hydroxyl group.

Results and Discussion

In our previous studies,^{19–21)} it was demonstrated that HPLC–APCI–MS permitted the observation of clearly protonated molecule ($[M+H]^+$) species of *Aconitum* alkaloids. The APCI mass spectra of *Aconitum* alkaloids showed predominantly the $[M+H]^+$ ion together with most major fragment ions. We previously reported that HPLC–APCI–MS was useful for the structural elucidation of six stereoisomeric C₁₉-norditerpenoid alkaloids at position 6.²²⁾ Comparison of the APCI spectra showed that the abundance of fragment ions was significantly higher for C-6 β -form alkaloids than for C-6 α -form alkaloids.

In the present study, we applied an HPLC–APCI–MS method to the investigation of stereochemical differentiation of C₁₉-norditerpenoid neoline-type alkaloids 1–6 and delcosine-type alkaloids 13–16. At first, the APCI mass spectra obtained in the HPLC–APCI–MS of neoline-type alkaloids

* To whom correspondence should be addressed. e-mail: kowada@hokuyakudai.ac.jp

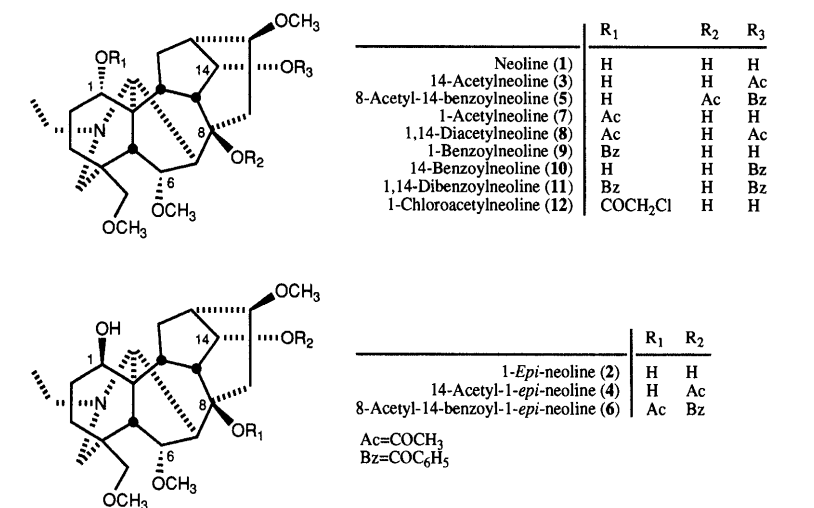


Chart 1

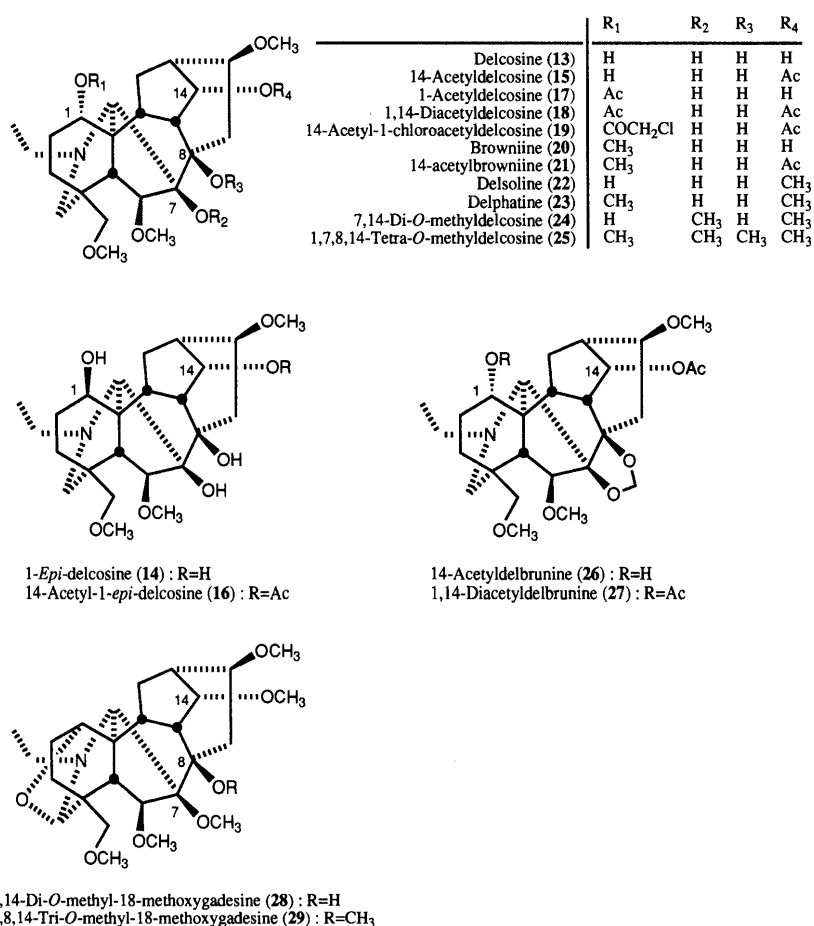


Chart 2

1—6 were examined (Fig. 1). When HPLC–APCI–MS of alkaloids 1—6 were measured at the drift voltage of 140 V between the first electrode and the second electrode of the APCI ion source, the $[M+H]^+$ ion and a characteristic product ion were obtained (Table 1). The spectra of neoline (1)²²⁾ and 1-*epi*-neoline (2) showed a very intense ion peak at m/z 438, corresponding to the $[M+H]^+$ ions, and a fragment ion at m/z 420, which was formed by the loss of a water molecule. Similarly, the spectra of 14-acetylneoline (3)²²⁾ and 14-acetyl-1-*epi*-neoline (4) revealed a strong $[M+H]^+$ ion at m/z

480 and a fragment ion at m/z 462, which was formed by the loss of a water molecule. The spectra of both 8-acetyl-14-benzoylneoline (5) and 8-acetyl-14-benzoyl-1-*epi*-neoline (6) exhibited an ion at m/z 584, corresponding to an $[M+H]^+$ ion, and a fragment ion at m/z 524. The fragment ion at m/z 524 was attributed to the loss of an acetic acid molecule from the $[M+H]^+$ ion. The $[M+H]^+$ ion of these alkaloids clearly appeared to be more stable, undergoing a much more limited fragmentation. As we have reported,²²⁾ the site of protonation in the alkaloids was at a nitrogen atom, and proton chelation

Table 1. m/z and Relative Abundance (%) of the Mass Spectral Fragments of Norditerpenoid Neoline-Type Alkaloids

Compd.	$[M+H]^+$	$[M+H-H_2O]^+$	$[M+H-RCOOH]^+$	$[M-d_n+D]^+$	$[M-d_n+D-D_2O]^+$	$[M-d_n+D-CH_3COOD]^+$
1	438 (100%)	420 (10%)	—	442 (100%)	422 (12%)	—
2	438 (100%)	420 (18%)	—	442 (100%)	422 (28%)	—
3	480 (100%)	462 (6%)	—	483 (100%)	463 (8%)	—
4	480 (100%)	462 (14%)	—	—	—	—
5	584 (100%)	—	524 (23%)	587 (100%)	—	525 (7%)
6	584 (100%)	—	524 (72%)	—	—	—
7	480 (100%)	462 (8%)	420 (11%)	483 (84%)	463 (9%)	422 (18%)
8	522 (100%)	504 (17%)	462 (8%)	524 (100%)	504 (10%)	463 (18%)
9	542 (100%)	524 (5%)	420 (5%)	—	—	—
10	542 (100%)	524 (14%)	—	—	—	—
11	646 (100%)	628 (9%)	524 (35%)	—	—	—
12	514 (19%)	496 (10%)	420 (38%)	—	—	—

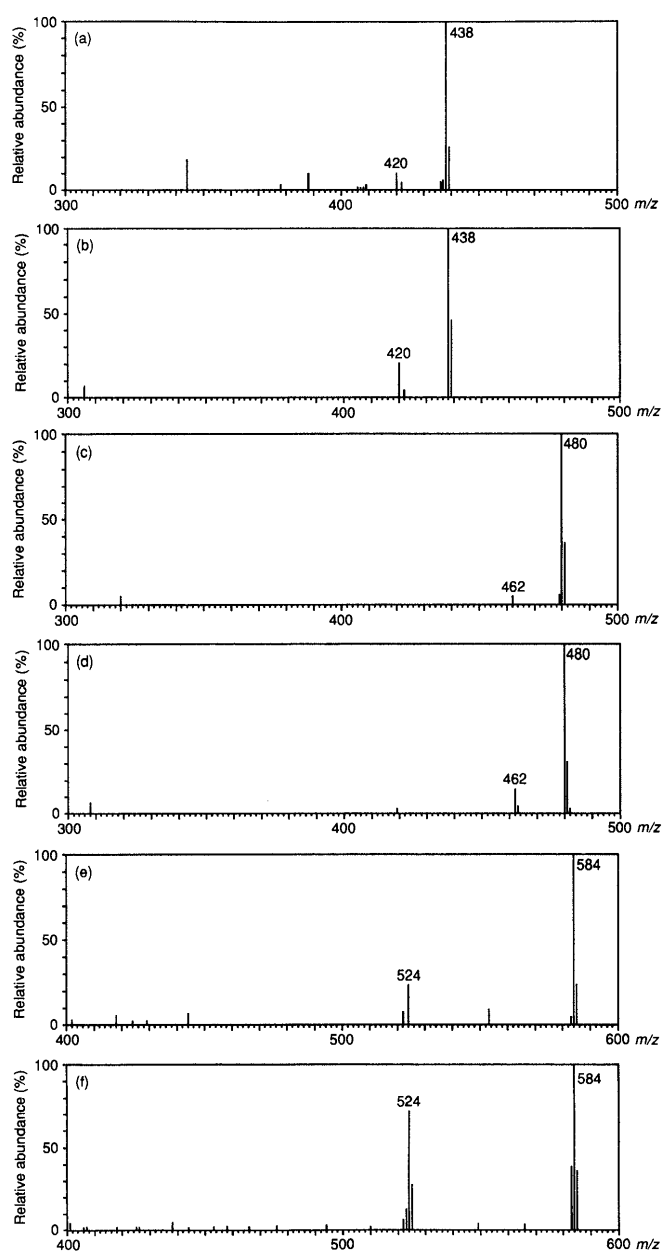


Fig. 1. APCI Mass Spectra of Alkaloids

(a) Neoline (1), (b) 1-*epi*-neoline (2), (c) 14-acetylneoline (3), (d) 14-acetyl-1-*epi*-neoline (4), (e) 8-acetyl-14-benzoylneoline (5) and (f) 8-acetyl-14-benzoyl-1-*epi*-neoline (6). The drift voltage between the first and the second electrodes was 140 V.

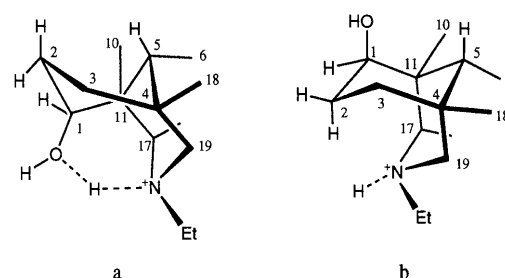


Chart 3

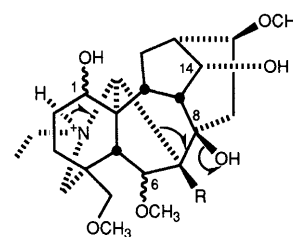


Chart 4

occurred between the amino group and the C-1 hydroxyl group (Chart 3a), with the proton being transferred to the C-8 hydroxyl group and fragmented as a water molecule (Chart 4).

In order to compare the stabilities of $[M+H]^+$ ions **1** and **2** towards the fragmentation processes, we proceeded to the study of energy dependence of the ion abundances.²²⁾ The results for the ions at m/z 438 and 420 are shown in Fig. 2. Conditions for the formation of the ion at m/z 420 appeared to be closely related to the stereochemistry of the alkaloids under investigation and were sensitive to energy variation. The curves of the ion at m/z 420 were completely different. The top of the m/z 420 ion curves corresponding to **2** seemed to be located at voltage values lower than **1**. For comparison, energy dependence of the fragmentation pathway in relation to the stereochemistry of the protonated molecules was examined (Fig. 3). The formation of the ion at m/z 420 clearly required a greater amount energy in the case of **1** than **2**. The two curves obtained were separated by 30–35 V, evidently corresponding to the stability difference between the $[M+H]^+$ ions **1** and **2** towards the fragmentation pathway.

Comparison of the spectra of **1** and **2** showed a remarkable increase in the relative abundance of the ion peak at m/z 420 in the case of **2**. Also, the abundance of the fragment ion at

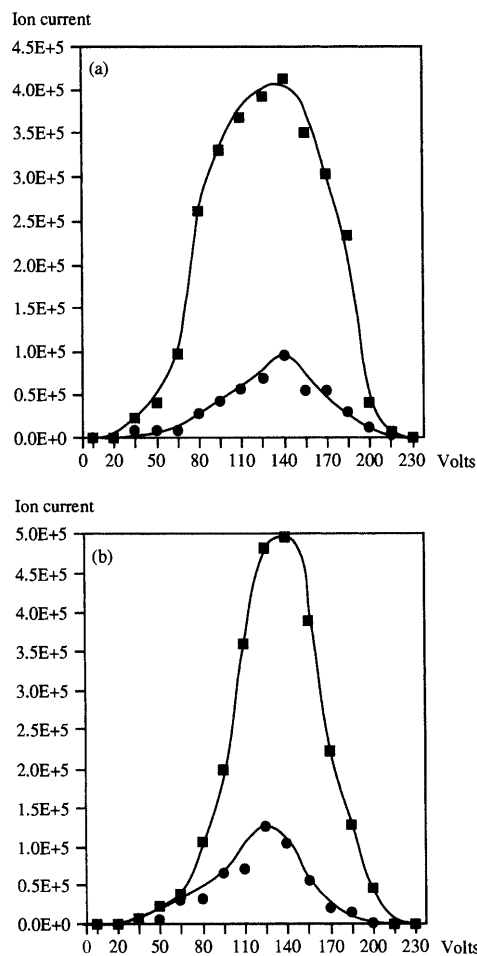


Fig. 2. Ion Currents of the Protonated Molecule at m/z 438 (■) and the Fragment Ion at m/z 420 (●) Arising from Alkaloids Neoline (1; a) and 1-Epi-neoline (2; b) as a Function of the Drift Voltage between the First and the Second Electrodes of the APCI Ion Source

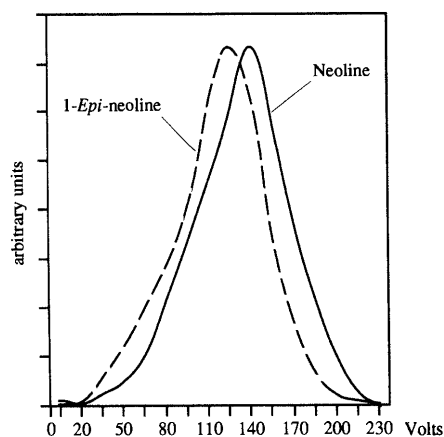


Fig. 3. Ion Currents of the Fragment Ion m/z 420 Arising from Alkaloids Neoline (1, Solid Line) and 1-Epi-neoline (2, Dashed Line) as a Function of the Drift Voltage between the First and the Second Electrodes of the APCI Ion Source

For a better comparison, the tops of the curves were equalized in the figure.

m/z 462, similar to that of the m/z 420 fragment ion in 2, was larger for 4 than for its epimer 3. Clearly, the abundance of the ion peak at m/z 524 was significantly higher for 6 than for its epimer 5. These results appeared as a stereospecific fragmentation process. Examination of drift collision-induced

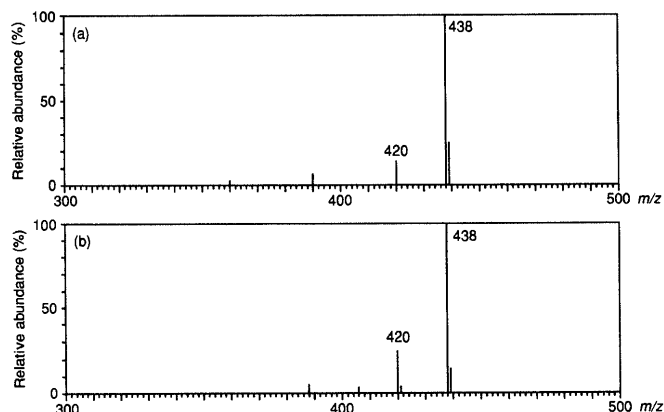


Fig. 4. APCI Mass Spectra of Alkaloids Neoline (1; a) and 1-Epi-neoline (2; b)

The drift voltage between the first and the second electrodes was 180 V.

dissociation (CID) analysis^{25,26} (drift voltage of 180 V) of 1–4 clearly showed that there was a loss of water from the $[M+H]^+$ ion and that the abundance of the $[M+H-H_2O]^+$ ion increased (Fig. 4). In the drift CID spectra of alkaloids 5 and 6, the abundance of the $[M+H-CH_3COOH]^+$ ion increased. The spectra of alkaloids 5 and 6 did not show a fragment ion at m/z 566 corresponding to the $[M+H-H_2O]^+$ ion. Because of an intramolecular H-bonded system between the amino group and the C-1 hydroxyl group (Chart 3a), the $[M+H]^+$ ion of alkaloid 5 was stabilized. Similarly, the $[M+H]^+$ ions of alkaloids 1 and 3 were stabilized. In the case of alkaloids 2, 4 and 6, proton chelation cannot occur (Chart 3b), and proton transfer therefore occurred more easily in alkaloids 2, 4 and 6 than in alkaloids 1, 3 and 5. We considered that the peak intensity ratio for alkaloids 1–4 is $R = [M+H]^+ / [M+H-H_2O]^+$ and that for alkaloids 5 and 6 is $R' = [M+H]^+ / [M+H-CH_3COOH]^+$. The R values of alkaloids 1 and 3, which contain C-1 α -hydroxyl groups, were 10–17, whereas those of alkaloids 2 and 4, which contain C-1 β -hydroxyl groups, were 5.6–7.1. The R' value of alkaloid 5, which contains a C-1 α -hydroxyl group, was 4.4, whereas that of alkaloid 6, which contains a C-1 β -hydroxyl group, was 1.4. These results indicated that the R and R' values showed stereochemical differentiation of alkaloids at position 1.

The fragmentation mechanisms depending on the stereochemistry of the precursor ion could be discerned by recording the spectra of alkaloids 1 and 2 in a deuterated solvent system of 0.05 M ammonium acetate in D_2O –acetonitrile–tetrahydrofuran.²² These spectra showed a major ion peak at m/z 442 corresponding to the $[M-d_3+D]^+$ ions formed by deuterium exchange of hydroxyl hydrogens and addition of D^+ on the molecules (Fig. 5). Loss of D_2O from this precursor ion gave the fragment ion at m/z 422. This result indicated that the proton of protonation was included in the leaving water molecule, irrespective of the stereochemistry at position 1. Furthermore, the fragment ion at m/z 525 in 5 was formed by the loss of CH_3COOD from the precursor ion at m/z 587 corresponding to the $[M-d+D]^+$ ion. These results revealed that the site of the leaving hydroxyl or acetyl group was position 8.

The study of fragmentation behavior of alkaloids 1-acetylneoline (7),²² 1,14-diacetylneoline (8),²² 1-benzoylneoline

(9),²⁷⁾ 14-benzoylneoline (10),²⁷⁾ 1,14-dibenzoylneoline (11)²⁷⁾ and 1-chloroacetylneoline (12) showed an $[M+H]^+$ ion peak and a characteristic fragment ion peak corresponding to the $[M+H-H_2O]^+$ and the $[M+H-R_1OH]^+$ ions. The common substitution feature of alkaloids 7–9 and 11–12 corresponds to the presence of an ester group at C-1 and a hydroxyl group at C-8. The spectra of 7 and 8 showed a fragment ion peak corresponding to the $[M+H-CH_3COOH]^+$ ion, and the spectra of 9 and 11 showed a fragment ion peak corresponding to the $[M+H-C_6H_5COOH]^+$ ion. Also, the spectra of 12 showed a major fragment ion at m/z 420 corresponding to the $[M+H-ClCH_2COOH]^+$ ion. In the spectra of 10, fragment ion peaks other than that of the $[M+H-H_2O]^+$ ion were not observed. These results indicated that the characteristic fragment ion $[M+H-H_2O]^+$ was formed by the loss of a water molecule at the above-mentioned position 8. In addition, in the case of the presence of an ester group at C-1, the characteristic fragment ions were

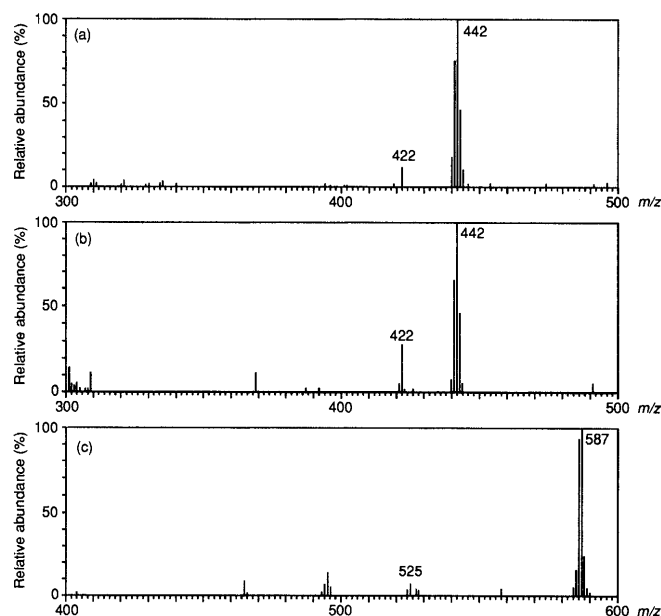


Fig. 5. APCI Mass Spectra of Alkaloids Recorded by the Solvent System of 0.05 M Ammonium Acetate in D_2O -Acetonitrile-Tetrahydrofuran

(a) Neoline (1), (b) 1-*epi*-neoline (2) and (c) 8-acetyl-14-benzoylneoline (5). The drift voltage between the first and the second electrodes was 140 V.

formed by the loss of R_1OH at position 1. Furthermore, the deuterated spectra of 7 and 8 showed fragment ions at m/z 422 and 463, respectively, corresponding to the $[M-d_n+D-CH_3COOD]^+$ ion from the $[M-d_n+D]^+$ ion. This result revealed that the site of the leaving acetyl group was the above-mentioned position 1.

Next, the APCI mass spectra obtained in the HPLC-APCI-MS of delcosine-type alkaloids 13–16 were examined and were first recorded at the drift voltage of 140 V (Fig. 6). The spectra of delcosine (13) and 1-*epi*-delcosine (14) showed a highly intense ion peak at m/z 454, corre-

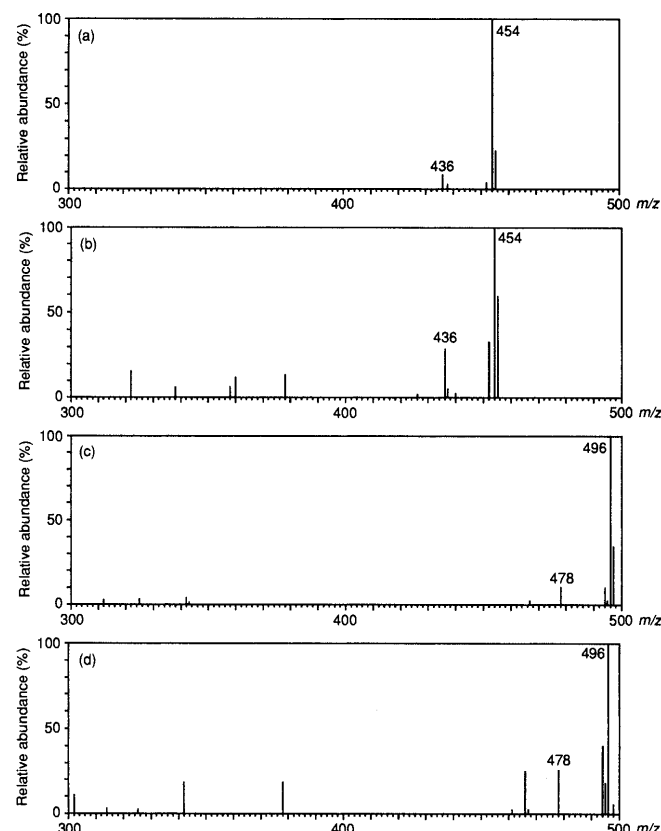


Fig. 6. APCI Mass Spectra of Alkaloids

(a) Delcosine (13), (b) 1-*epi*-delcosine (14), (c) 14-acetyl-1-*epi*-delcosine (15) and (d) 14-acetyl-1-*epi*-delcosine (16). The drift voltage between the first and the second electrodes was 140 V.

Table 2. m/z and Relative Abundance (%) of the Mass Spectral Fragments of Norditerpenoid Delcosine-Type Alkaloids

Compd.	$[M+H]^+$	$[M+H-H_2O]^+$	$[M+H-CH_3OH]^+$	$[M+H-CH_3COOH]^+$
13	454 (100%)	436 (9%)	—	—
14	454 (100%)	436 (29%)	—	—
15	496 (100%)	478 (10%)	—	—
16	496 (100%)	478 (26%)	—	—
17	496 (100%)	478 (18%)	—	—
18	538 (100%)	520 (5%)	—	—
19	572 (100%)	554 (11%)	—	—
20	468 (100%)	450 (26%)	—	—
21	510 (100%)	492 (7%)	—	—
22	468 (100%)	450 (16%)	—	—
23	482 (100%)	464 (27%)	—	—
24	482 (100%)	464 (57%)	—	—
25	510 (21%)	—	478 (100%)	—
26	508 (100%)	—	—	—
27	550 (100%)	—	—	490 (30%)
28	480 (77%)	462 (100%)	—	—
29	494 (9%)	—	462 (100%)	—

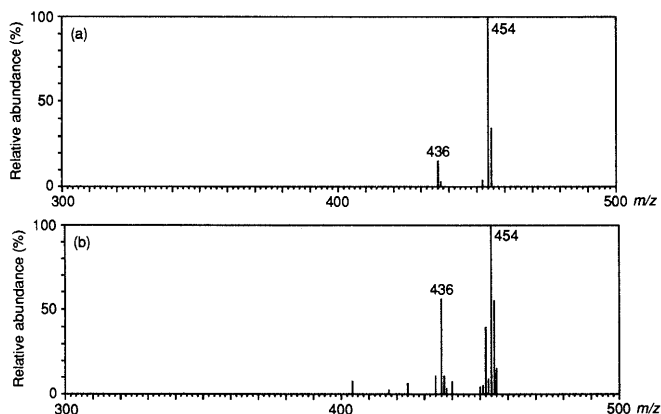


Fig. 7. APCI Mass Spectra of Alkaloids Delcosine (**13**; a) and 1-Epi-delcosine (**14**; b)

The drift voltage between the first and the second electrodes was 180 V.

sponding to the $[M+H]^+$ ions, and a fragment ion at m/z 436, which was formed by the loss of a water molecule. Similarly, the spectra of 14-acetyldelcosine (**15**) and 14-acetyl-1-*epi*-delcosine (**16**) exhibited a strong $[M+H]^+$ ion at m/z 496 and a fragment ion at m/z 478, which was formed by the loss of a water molecule.

Evidence of fragmentation mechanisms depending on the precursor ion was provided by the study of fragmentation behavior of alkaloids 1-acetyldelcosine (**17**),²⁸ 1,14-diacetyldelcosine (**18**),²⁹ 14-acetyl-1-chloroacetyldelcosine (**19**), browniine (**20**),³⁰ 14-acetylbrowniine (**21**),³⁰ delsoline (**22**),³¹ delphatine (**23**),³¹ 7,14-di-*O*-methylidelcosine (**24**), 1,7,8,14-tetra-*O*-methylidelcosine (**25**), 14-acetyldelbrunine (**26**),³² 1,14-diacetyldelbrunine (**27**), 7,14-di-*O*-methyl-18-methoxygadesine (**28**) and 7,8,14-tri-*O*-methyl-18-methoxygadesine (**29**). The common substitution feature of alkaloids **17**–**24** corresponds to the presence of a hydroxyl group at C-8 and **28** corresponds to only the presence of a hydroxyl group at C-8. The spectra of **17**–**24** and **28** showed a major fragment ion peak corresponding to the $[M+H-H_2O]^+$ ion. Also, the spectra of **25** and **29**, in the presence of a methoxyl group at C-8, showed a major fragment ion peak corresponding to the $[M+H-CH_3OH]^+$ ion. The spectra of **27**, in the presence of acetyl group at C-1, showed a major fragment ion peak corresponding to the $[M+H-CH_3COOH]^+$ ion. These results indicated that the characteristic fragment ions were formed by the loss of H_2O or CH_3OH at position 8, as previously reported for neoline-type alkaloids²²⁾ (Chart 4), and by the loss of CH_3COOH at position 1, as in the above-mentioned neoline-type alkaloids.

Comparison of the spectra of **13** and **14** showed a remarkable increase in the relative abundance of the ion peak at m/z 436 in the case of **14**. Also, the abundance of the fragment ion at m/z 478 was larger for **16** than for its epimer **15**. These results appeared as a stereospecific fragmentation process. The drift CID spectrum of **13**–**16** clearly showed a characteristic fragment ion, and the abundance of the $[M+H-H_2O]^+$ ion increased (Fig. 7). We considered that the peak intensity ratio for alkaloids **13**–**16** is $R=[M+H]^+/[M+H-H_2O]^+$. The R values of alkaloids **13** and **15**, which contain C-1 α -hydroxyl groups, were 10–11, whereas those of alkaloids **14** and **16**, which contain C-1 β -hydroxyl groups, were 3.5–3.9. These results indicated that the R value

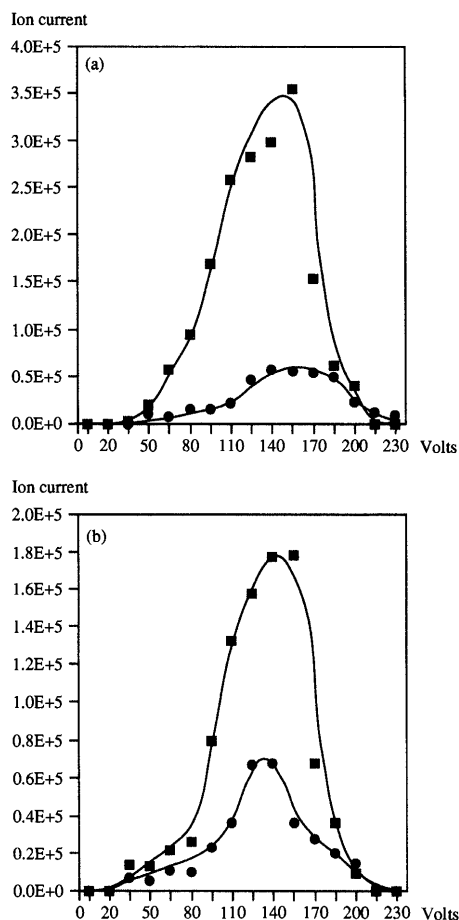


Fig. 8. Ion Currents of the Protonated Molecule at m/z 454 (■) and the Fragment Ion at m/z 436 (●) Arising from Alkaloids Delcosine (**13**; a) and 1-Epi-delcosine (**14**; b) as a Function of the Drift Voltage between the First and the Second Electrodes of the APCI Ion Source

showed stereochemical differentiation of alkaloids at position 1.

In order to compare the stabilities of the $[M+H]^+$ ions of **13** and **14** towards the fragmentation processes, we proceeded to the study of energy dependence of the ion intensities.²²⁾ The results for the ions at m/z 454 and 436 are shown in Fig. 8. The curves of the ion at m/z 436 were completely different. For the sake of comparison, energy dependence of the fragmentation pathway in relation to the stereochemistry of the protonated molecules was examined (Fig. 9). The formation of the ion m/z 436 clearly required a greater amount of energy in the case of **13** than **14**. The two curves obtained were separated by 10–15 V, evidently corresponding to the stability difference between $[M+H]^+$ ions of **13** and **14** towards this fragmentation pathway.

The fragmentation mechanisms depending on the stereochemistry of the precursor ion could be perceived by recording the spectra of alkaloids **13** and **14** in a deuterated solvent system of 0.05 M ammonium acetate in D_2O -acetonitrile-tetrahydrofuran.²²⁾ These spectra showed a major ion peak at m/z 459 corresponding to the $[M-d_4+D]^+$ ions formed by deuterium exchange of hydroxyl hydrogens and addition of D^+ on the molecules (Fig. 10). The fragment ion at m/z 439 was attributed to the loss of D_2O from this precursor ion. This result indicated that the proton of protonation was included in the leaving water molecule, irrespective of the

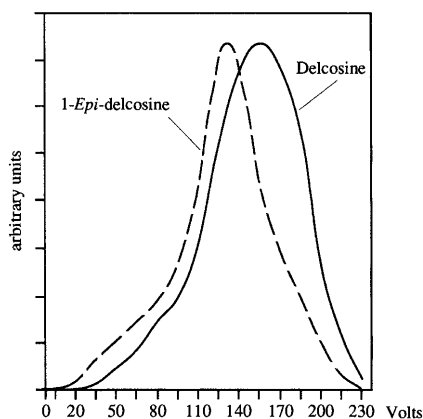


Fig. 9. Ion Currents of the Fragment Ion m/z 436 Arising from Alkaloids Delcosine (**13**, Solid Line) and 1-*Epi*-delcosine (**14**, Dashed Line) as a Function of the Drift Voltage between the First and the Second Electrodes of the APCI Ion Source

For a better comparison, the tops of the curves were equalized in the figure.

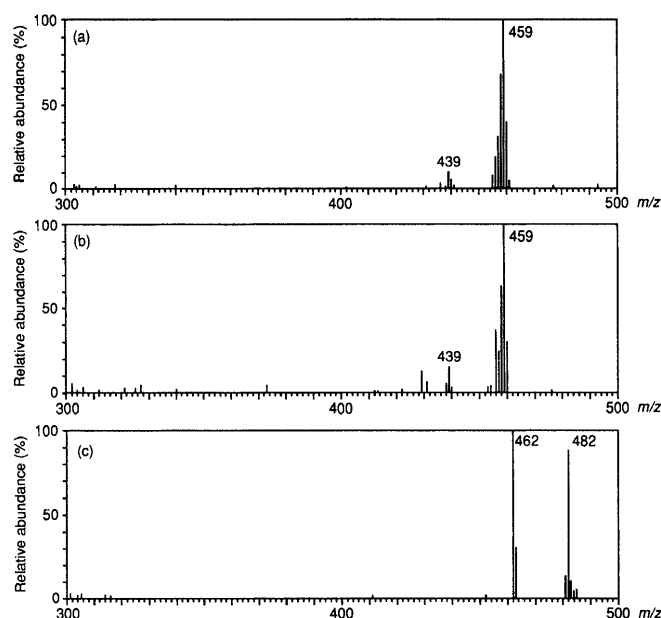


Fig. 10. APCI Mass Spectra of Alkaloids Recorded by the Solvent System of 0.05 M Ammonium Acetate in D_2O -Acetonitrile-Tetrahydrofuran

Delcosine (**13**; a), 1-*epi*-delcosine (**14**; b) and 7,14-di-*O*-methyl-18-methoxygadesine (**28**; c). The drift voltage between the first and the second electrodes was 140 V.

stereochemistry at position 1. Furthermore, the fragment ion at m/z 462 in **28** was formed by the loss of D_2O from the precursor ion at m/z 482 corresponding to the $[M-d+D]^+$ ion. These results revealed that the site of the leaving hydroxyl group was position 8, as in neoline-type alkaloids. Proton chelation occurred between the amino group and the C-1 hydroxyl group (Chart 3a), and the proton was transferred to the C-8 hydroxyl group and fragmented as a water molecule (Chart 4). In the case of alkaloids **14** and **16**, proton chelation cannot occur (Chart 3b), and proton transfer therefore occurred more easily in alkaloids **14** and **16** than in alkaloids **13** and **15**.

In conclusion, the APCI mass spectra of the C_{19} -norditerpenoid neoline-type and delcosine-type alkaloids were remarkably simple and very similar with respect to characteristic fragments. In the APCI mass spectra of the C_{19} -norditerpenoid neoline-type and delcosine-type alkaloids, the charac-

teristic fragment ions were formed by loss of substituents at position 8. In addition, in the presence of an ester group at C-1, the site of elimination of ester molecules was position 1. Comparison of the characteristic fragment ion abundance showed a complementarity for structural investigations of stereochemical differentiation. Information obtained from energy dependence experiments can be very valuable for the detection of subtle structural characteristics of organic molecules, including stereochemical differentiation.

Experimental

All melting points were measured on a Yanagimoto micromelting points apparatus without correction. IR spectra were recorded using a model FT/IR 7000 spectrometer (Jasco, Tokyo, Japan). 1H -NMR spectra were measured in deuterated trichloromethane solution with a model GX-270 spectrometer (JEOL, Tokyo, Japan) using tetramethylsilane (TMS) as an internal standard. MS was performed with a model M-2000 mass spectrometer (Hitachi, Tokyo, Japan).

Materials Neoline (**1**), delcosine (**13**), 14-acetyldelcosine (**15**), browniine (**20**) and 14-acetylbrowniine (**21**) were purified from *Aconitum japonicum* roots²⁷⁾ and *Aconitum yessoense* var. *macrotyosense* (NAKAI) TAMURA roots,³⁰⁾ respectively, and identified as described previously. 14-Acetylneoline (**3**),²²⁾ 1,14-diacetylneoline (**8**),²⁷⁾ 1-benzoylneoline (**9**),²⁷⁾ 14-benzoylneoline (**10**),²⁷⁾ 1,14-dibenzoylneoline (**11**)²⁷⁾ and 1-acetyldelcosine (**17**)²⁸⁾ were synthesized as described previously. 1-*Epi*-neoline (**2**),²³⁾ 14-acetyl-1-*epi*-neoline (**4**),²⁴⁾ 8-acetyl-14-benzoylneoline (**5**), 8-acetyl-14-benzoyl-1-*epi*-neoline (**6**), 1-acetylneoline (**7**), 1-chloroacetylneoline (**12**), 1-*epi*-delcosine (**14**), 14-acetyl-1-*epi*-delcosine (**16**), 1,14-diacetyldelcosine (**18**),²⁹⁾ 14-acetyl-1-chloroacetyldelcosine (**19**), delsoline (**22**),³¹⁾ delphatine (**23**),³¹⁾ 7,14-di-*O*-methyl-18-methoxygadesine (**24**), 7,14-di-*O*-methyl-18-methoxygadesine (**25**), 14-acetyldelbrunine (**26**),³²⁾ 1,14-diacetyldelbrunine (**27**), 7,14-di-*O*-methyl-18-methoxygadesine (**28**) and 7,8,14-tri-*O*-methyl-18-methoxygadesine (**29**) were synthesized from neoline (**1**), 14-acetylneoline (**3**), 14-acetyl-1-*epi*-neoline (**4**), 14-benzoylneoline (**10**), delcosine (**13**), 14-acetyldelcosine (**15**), browniine (**20**), delsoline (**22**) and 14-acetyldelbrunine (**26**), respectively. Ammonium acetate of reagent grade was purchased from Kanto Chemicals (Tokyo, Japan), and acetonitrile and tetrahydrofuran of HPLC grade and deuterium oxide (99.9%) were purchased from Wako Pure Chemical Industries (Osaka, Japan).

Preparation of 14-Acetyl-1-*epi*-neoline (4) 1) Oxidation of 14-acetylneoline. A solution of 14-acetylneoline (**3**; 134.8 mg) in dichloromethane (39 ml) was mixed with pyridinium dichromate (PDC; 317.7 mg). The mixture was stirred at room temperature for 1 h. The reaction mixture was passed through a short column of florisil to give 14-acetyl-1-dehydroneoline (83.3 mg, 62%) and starting material (19.4 mg). Amorphous. IR ($CHCl_3$) cm^{-1} : 3588, 1744, 1212, 1135. 1H -NMR δ : 1.10 (3H, t, $J=7.0$ Hz, $N-CH_2CH_3$), 2.06 (3H, s, $OCOCH_3$), 3.23, 3.29, 3.37 (each 3H, s, OCH_3), 4.07 (1H, d, $J=6.3$ Hz, 6β -H), 4.88 (1H, t, $J=4.6$ Hz, 14β -H). HR-ESI-MS m/z : 477.2718 (Calcd for $C_{26}H_{39}NO_7$: 477.2725). EI-MS m/z : 477 (M^+), 462 (M^+-CH_3 , base peak), 446 (M^+-OCH_3).

2) 14-Acetyl-1-*epi*-neoline. 14-Acetyl-1-dehydroneoline (83.3 mg), dissolved in MeOH-absolute EtOH (1 : 1, 16 ml), was treated with $NaBH_4$ (20 mg). The resulting solution was stirred at room temperature for 2 h 15 min. Water was added, and the mixture was extracted with $CHCl_3$. The $CHCl_3$ extract was evaporated to dryness after being washed with 5% sodium hydrogencarbonate and brine and then dried with anhydrous magnesium sulfate and purification by column chromatography on silica gel (1% hexane-ethyl acetate) gave 14-acetylneoline (**3**; 17.1 mg, 21%) and 14-acetyl-1-*epi*-neoline (**4**; 50.0 mg, 60%).

4: Amorphous. IR (KBr) cm^{-1} : 3454, 1742, 1247, 1096. 1H -NMR δ : 1.05 (3H, t, $J=7.0$ Hz, $N-CH_2CH_3$), 2.06 (3H, s, $OCOCH_3$), 3.26, 3.31, 3.34 (each 3H, s, OCH_3), 3.88 (1H, br s, 1α -H), 4.07 (1H, d, $J=6.6$ Hz, 6β -H), 4.88 (1H, t, $J=4.6$ Hz, 14β -H). HR-ESI-MS m/z : 479.2857 (Calcd for $C_{26}H_{41}NO_7$: 479.2880). EI-MS m/z : 479 (M^+), 464 (M^+-CH_3 , base peak), 462 (M^+-OH), 448, 446.

Preparation of 1-*Epi*-neoline (2) A mixture of 14-acetyl-1-*epi*-neoline (**4**; 20.0 mg) and 5% KOH-aq.MeOH (5 ml) was kept at room temperature for 15.5 h. The resulting solution was evaporated and after the addition of water, the solution was extracted with $CHCl_3$. Then the usual work-up afforded an amorphous powder (18.1 mg, 99%). Amorphous. IR (KBr) cm^{-1} : 3450, 1100. 1H -NMR δ : 1.46 (3H, t, $J=7.3$ Hz, $N-CH_2CH_3$), 3.30, 3.33, 3.34 (each 3H, s, OCH_3), 3.83 (1H, br s, 1α -H), 4.14 (1H, d, $J=6.5$ Hz, 6β -H),

4.24 (1H, t, $J=4.6$ Hz, 14β -H). HR-EI-MS m/z : 437.2763 (Calcd for $C_{24}H_{39}NO_6$: 437.2775). EI-MS m/z : 437 (M^+), 422 (M^+-CH_3 , base peak), 420 (M^+-OH), 406, 404.

Preparation of 8-Acetyl-14-benzoylneoline (5) and 8-Acetyl-14-benzoyl-1-*epi*-neoline (6) 1) Oxidation of 14-benzoylneoline. A solution of 14-benzoylneoline (**10**: 239.3 mg) in dichloromethane (68 ml) was mixed with PDC (499.4 mg). The mixture was stirred at room temperature for 1 h. The reaction mixture was passed through a short column of florisil and then purified on column chromatography of silica gel (25–10% hexane–ether saturated with 28% ammonia) to give 14-benzoyl-1-dehydroneoline (67.4 mg, 28%) and starting material (20.8 mg). Amorphous. IR ($CHCl_3$) cm^{-1} : 3622, 1717, 1218, 1133. 1H -NMR δ : 1.11 (3H, t, $J=7.0$ Hz, $N-CH_2CH_3$), 3.22, 3.30, 3.36 (each 3H, s, OCH_3), 4.09 (1H, d, $J=6.5$ Hz, 6β -H), 5.21 (1H, t, $J=4.6$ Hz, 14β -H), 7.43 (2H, t, $J=7.0$ Hz, aromatic-H), 7.55 (1H, t, $J=7.3$ Hz, aromatic-H), 8.00 (2H, d, $J=6.8$ Hz, aromatic-H). HR-EI-MS m/z : 539.2894 (Calcd for $C_{31}H_{41}NO_7$: 539.2882). EI-MS m/z : 539 (M^+), 522 (M^+-OH), 509, 494, 423, 105 [$[COC_6H_5]^+$, base peak].

2) Acetylation of 14-benzoyl-1-dehydroneoline. A mixture of 14-benzoyl-1-dehydroneoline (67.4 mg), acetic anhydride (1 ml) and *p*-toluenesulfonic acid monohydrate (36.7 mg) was kept at 90–100 °C for 2.5 h. The usual work-up and purification by column chromatography on silica gel (40% hexane–ether saturated with 28% ammonia) afforded 8-acetyl-14-benzoyl-1-dehydroneoline (48.0 mg, 66%). Amorphous. IR ($CHCl_3$) cm^{-1} : 1719, 1222, 1135. 1H -NMR δ : 1.11 (3H, t, $J=7.0$ Hz, $N-CH_2CH_3$), 1.42 (3H, s, $OCOCH_3$), 3.22, 3.28, 3.36 (each 3H, s, OCH_3), 4.00 (1H, d, $J=7.5$ Hz, 6β -H), 5.12 (1H, t, $J=4.2$ Hz, 14β -H), 7.43 (2H, t, $J=7.0$ Hz, aromatic-H), 7.55 (1H, t, $J=7.3$ Hz, aromatic-H), 8.05 (2H, d, $J=7.0$ Hz, aromatic-H). HR-EI-MS m/z : 581.3005 (Calcd for $C_{33}H_{43}NO_8$: 581.2987). EI-MS m/z : 581 (M^+), 566 (M^+-CH_3 , base peak), 550 (M^+-OCH_3), 522 ($M^+-OCOCH_3$).

3) Reduction of 8-acetyl-14-benzoyl-1-dehydroneoline. 8-Acetyl-14-benzoyl-1-dehydroneoline (48.0 mg), dissolved in MeOH–absolute EtOH (1 : 1, 10 ml), was treated with $NaBH_4$ (11 mg). The resulting solution was stirred at room temperature for 2 h. Water was added, and the mixture was extracted with $CHCl_3$. Then the usual work-up and purification by column chromatography on silica gel (50% hexane–ethyl acetate) gave 8-acetyl-14-benzoylneoline (**5**: 10.2 mg, 21%) and 8-acetyl-14-benzoyl-1-*epi*-neoline (**6**: 25.0 mg, 52%).

5: Amorphous. IR (KBr) cm^{-1} : 3438, 1725, 1280, 1118. 1H -NMR δ : 1.16 (3H, t, $J=7.0$ Hz, $N-CH_2CH_3$), 1.42 (3H, s, $OCOCH_3$), 3.20, 3.31, 3.39 (each 3H, s, OCH_3), 3.74 (1H, s, 1β -H), 4.06 (1H, d, $J=5.6$ Hz, 6β -H), 5.09 (1H, t, $J=4.6$ Hz, 14β -H), 7.44 (2H, t, $J=7.3$ Hz, aromatic-H), 7.56 (1H, t, $J=7.3$ Hz, aromatic-H), 8.05 (2H, d, $J=7.0$ Hz, aromatic-H). HR-EI-MS m/z : 583.3141 (Calcd for $C_{33}H_{45}NO_8$: 583.3143). EI-MS m/z : 583 (M^+), 568 (M^+-CH_3), 566 (M^+-OH , base peak), 524 ($M^+-OCOCH_3$), 105 [$[COC_6H_5]^+$].

6: mp 169–171.5 °C. IR (KBr) cm^{-1} : 3516, 1723, 1278, 1164. 1H -NMR δ : 1.06 (3H, t, $J=7.0$ Hz, $N-CH_2CH_3$), 1.43 (3H, s, $OCOCH_3$), 3.19, 3.29, 3.37 (each 3H, s, OCH_3), 3.93 (1H, br s, 1α -H), 4.03 (1H, d, $J=6.5$ Hz, 6β -H), 5.13 (1H, t, $J=4.6$ Hz, 14β -H), 7.43 (2H, t, $J=7.0$ Hz, aromatic-H), 7.55 (1H, t, $J=7.5$ Hz, aromatic-H), 8.05 (2H, d, $J=7.0$ Hz, aromatic-H). HR-EI-MS m/z : 583.3168 (Calcd for $C_{33}H_{45}NO_8$: 583.3143). EI-MS m/z : 583 (M^+), 568 (M^+-CH_3), 566 (M^+-OH), 524 ($M^+-OCOCH_3$, base peak), 105 [$[COC_6H_5]^+$].

Preparation of 1-Acetylneoline (7) A mixture of neoline (**1**: 30.5 mg), pyridine (0.5 ml) and acetic anhydride (0.5 ml) was kept at 0 °C for 2 h. The usual work-up and purification by column chromatography on silica gel (ether saturated with 28% ammonia) afforded 1-acetylneoline (20.7 mg, 62%). Amorphous. IR (KBr) cm^{-1} : 3444, 1738, 1247, 1112. 1H -NMR δ : 1.10 (3H, t, $J=7.0$ Hz, $N-CH_2CH_3$), 2.01 (3H, s, $OCOCH_3$), 3.30, 3.31, 3.35 (each 3H, s, OCH_3), 4.09 (1H, t, $J=4.8$ Hz, 14β -H), 4.21 (1H, d, $J=6.8$ Hz, 6β -H), 4.81 (1H, dd, $J=6.8$, 10.5 Hz, 1β -H). HR-EI-MS m/z : 479.2879 (Calcd for $C_{26}H_{41}NO_7$: 479.2882). EI-MS m/z : 479 (M^+), 462 (M^+-OH), 437, 420 ($M^+-OCOCH_3$, base peak).

Preparation of 1-Chloroacetylneoline (12) A mixture of neoline (**1**: 51.0 mg), pyridine (0.8 ml) and chloroacetic anhydride (60.4 mg) was kept at room temperature for 12.5 h. The usual work-up afforded 1-chloroacetylneoline (37.5 mg, 63%). Amorphous. IR (KBr) cm^{-1} : 3432, 1750, 1243, 1112. 1H -NMR δ : 1.10 (3H, t, $J=7.0$ Hz, $N-CH_2CH_3$), 3.30, 3.31, 3.35 (each 3H, s, OCH_3), 4.02 (2H, s, $OCOCH_2Cl$), 4.11 (1H, t, $J=4.6$ Hz, 14β -H), 4.22 (1H, d, $J=6.8$ Hz, 6β -H), 4.90 (1H, dd, $J=6.8$, 10.2 Hz, 1β -H). HR-EI-MS m/z : 513.2427 (Calcd for $C_{26}H_{40}ClNO_7$: 513.2491). EI-MS m/z : 515 (M^++2), 513 (M^+), 498, 496 (M^+-OH), 420 ($M^+-OCOCH_2Cl$, base peak).

Preparation of 1-Epi-delcosine (14) 1) Oxidation of 14-acetyldelecosine. A solution of 14-acetyldelecosine (**15**: 200.3 mg) in dichloromethane (60 ml) was mixed with PDC (457.2 mg). The mixture was stirred at 0 °C for 5 h. The reaction mixture was passed through a short column of florisil and afforded 14-acetyl-1-dehydrodelecosine (101.5 mg, 51%) and the starting material (10.4 mg). Amorphous. IR ($CHCl_3$) cm^{-1} : 3622, 1736, 1218, 1135. 1H -NMR δ : 1.01 (3H, t, $J=7.0$ Hz, $N-CH_2CH_3$), 2.04 (3H, s, $OCOCH_3$), 3.29 (6H, s, OCH_3), 3.37 (3H, s, OCH_3), 3.98 (1H, s, 6α -H), 4.78 (1H, t, $J=4.6$ Hz, 14β -H). HR-EI-MS m/z : 493.2676 (Calcd for $C_{26}H_{39}NO_8$: 493.2674). EI-MS m/z : 493 (M^+), 478 (M^+-CH_3 , base peak), 475, 460.

2) 1-Epi-delcosine. 14-acetyl-1-dehydrodelecosine (56.9 mg), dissolved in tetrahydrofuran (20 ml), was treated with $LiAlH_4$ (60 mg). The resulting solution was stirred at room temperature for 2 h. Water was added, and the mixture was filtrated with a glass filter. Then the solution was evaporated, and then purification by column chromatography on silica gel (0.3% MeOH– $CHCl_3$ saturated with 28% ammonia) gave delcosine (**13**: 19.0 mg, 36%) and 1-*epi*-delcosine (**14**: 24.2 mg, 46%).

14: Amorphous. IR (KBr) cm^{-1} : 3454, 1091. 1H -NMR δ : 1.02 (3H, t, $J=7.0$ Hz, $N-CH_2CH_3$), 3.31, 3.36, 3.38 (each 3H, s, OCH_3), 3.81 (1H, br s, 1α -H), 3.95 (1H, s, 6α -H), 4.14 (1H, dd, $J=4.6$, 8.5 Hz, 14β -H). HR-EI-MS m/z : 453.2707 (Calcd for $C_{24}H_{39}NO_7$: 453.2714). EI-MS m/z : 453 (M^+), 438 (M^+-CH_3), 436 (M^+-OH), 422, 420 (base peak).

Preparation of 14-Acetyl-1-*epi*-delcosine (16) 14-Acetyl-1-dehydrodelecosine (44.6 mg), dissolved in MeOH (8 ml), was treated with $NaBH_4$ (10 mg). The resulting solution was stirred at room temperature for 1 h 50 min. Water was added, and the mixture was extracted with $CHCl_3$. Then the usual work-up and purification by column chromatography on silica gel (ethyl acetate) gave 14-acetyldelecosine (**15**: 20.4 mg, 46%) and 14-acetyl-1-*epi*-delcosine (**16**: 19.7 mg, 44%).

16: mp, 112 °C (dec.). IR (KBr) cm^{-1} : 3452, 1738, 1253, 1091. 1H -NMR δ : 1.02 (3H, t, $J=7.0$ Hz, $N-CH_2CH_3$), 2.06 (3H, s, $OCOCH_3$), 3.30, 3.32, 3.37 (each 3H, s, OCH_3), 3.87 (1H, br s, 1α -H), 3.94 (1H, s, 6α -H), 4.83 (1H, t, $J=4.6$ Hz, 14β -H). HR-EI-MS m/z : 495.2851 (Calcd for $C_{26}H_{41}NO_8$: 495.2830). EI-MS m/z : 495 (M^+ , base peak), 480 (M^+-CH_3), 478 (M^+-OH), 462.

Preparation of 1,14-Diacetyldelecosine (18) A mixture of delcosine (**13**: 200 mg), pyridine (3 ml) and acetic anhydride (3 ml) was kept at 80 °C for 1 h. The usual work-up and purification by column chromatography on silica gel (20% hexane–ether saturated with 28% ammonia) afforded 1,14-diacetyldelecosine (89.1 mg, 38%). mp, 83 °C (dec.). IR (KBr) cm^{-1} : 3450, 1725, 1245. 1H -NMR δ : 1.08 (3H, t, $J=7.2$ Hz, $N-CH_2CH_3$), 2.04, 2.05 (each 3H, s, $OCOCH_3$), 3.28, 3.31, 3.41 (each 3H, s, OCH_3), 3.92 (1H, s, 6α -H), 4.71 (1H, t, $J=4.6$ Hz, 14β -H), 4.72 (1H, dd, $J=8.2$, 9.8 Hz, 1β -H). HR-EI-MS m/z : 537.2909 (Calcd for $C_{28}H_{43}NO_9$: 537.2935). EI-MS m/z : 537 (M^+), 522 (M^+-CH_3), 479 (base peak).

Preparation of 14-Acetyl-1-chloroacetyldelecosine (19) A mixture of 14-acetyldelecosine (**15**: 31.0 mg), pyridine (0.5 ml) and chloroacetic anhydride (34.5 mg) was kept at room temperature for 1.5 h. The usual work-up and purification by column chromatography on silica gel (5% hexane–ether saturated with 28% ammonia) afforded 14-acetyl-1-chloroacetyldelecosine (20.3 mg, 57%) and the starting material (11.4 mg). Amorphous. IR (KBr) cm^{-1} : 3460, 1738, 1251, 1093. 1H -NMR δ : 1.08 (3H, t, $J=7.0$ Hz, $N-CH_2CH_3$), 2.05 (3H, s, $OCOCH_3$), 3.29, 3.31, 3.41 (each 3H, s, OCH_3), 3.93 (1H, s, 6α -H), 4.05 (2H, s, $OCOCH_2Cl$), 4.71 (1H, t, $J=4.8$ Hz, 14β -H), 4.81 (1H, dd, $J=7.8$, 9.7 Hz, 1β -H). HR-EI-MS m/z : 571.2537 (Calcd for $C_{28}H_{42}ClNO_9$: 571.2545). EI-MS m/z : 573 (M^++2), 571 (M^+), 556 (M^+-CH_3), 553 (M^+-OH), 540, 538, 478 ($M^+-OCOCH_2Cl$, base peak).

Preparation of Delsoline (22) A mixture of delcosine (**13**: 50.8 mg), dioxane (5 ml), sodium hydride (NaH; 54.1 mg) and methyl iodide (0.14 ml) was kept at 0 °C for 1 h and then at room temperature for 16 h. The solution was filtrated, and then purification by column chromatography on silica gel (3% MeOH– $CHCl_3$ saturated with 28% ammonia) afforded delsoline (28.6 mg, 54%). mp 216–219 °C. IR (KBr) cm^{-1} : 3458, 1102. 1H -NMR δ : 1.09 (3H, t, $J=7.0$ Hz, $N-CH_2CH_3$), 3.33, 3.41 (each 3H, s, OCH_3), 3.36 (6H, s, OCH_3), 4.06 (1H, s, 6α -H). HR-EI-MS m/z : 467.2854 (Calcd for $C_{25}H_{41}NO_7$: 467.2882). EI-MS m/z : 467 (M^+), 452 (M^+-CH_3 , base peak), 450 (M^+-OH), 436 (M^+-OCH_3).

Preparation of Delphatine (23) A mixture of browniine (**20**: 57.5 mg), 1,2-dimethoxyethane (6 ml), NaH (31.0 mg) and methyl iodide (0.077 ml) was kept at 0 °C for 1 h and then at room temperature for 16 h. The solution was filtrated, and then purification by column chromatography on silica gel ($CHCl_3$ saturated with 28% ammonia) afforded delphatine (31.2 mg, 51%). Amorphous. IR (KBr) cm^{-1} : 3456, 1091. 1H -NMR δ : 1.04 (3H, t, $J=7.0$ Hz, $N-CH_2CH_3$), 3.24, 3.30, 3.33, 3.40, 3.41 (each 3H, s, OCH_3), 4.08 (1H, s,

6 α -H). HR-EI-MS m/z : 481.3014 (Calcd for $C_{26}H_{43}NO_7$: 481.3037). EI-MS m/z : 481 (M^+), 466 ($M^+ - CH_3$), 464 ($M^+ - OH$), 450 ($M^+ - OCH_3$, base peak).

Preparation of 7,14-Di-O-methyldecosine (24) and 7,14-Di-O-methyl-18-methoxygadesine (28) A mixture of delcosine (**22**: 15.5 mg), 1,2-dimethoxyethane (2 ml), NaH (16.4 mg) and methyl iodide (0.04 ml) was kept at 0 °C for 1 h and then at room temperature for 20 h. The solution was filtrated, and then purification by column chromatography on silica gel (20% hexane–ether saturated with 28% ammonia) afforded 7,14-di-O-methyldecosine (**24**, 8.8 mg, 55%) and 7,14-di-O-methyl-18-methoxygadesine (**28**, 2.0 mg, 13%).

24: mp 208–209.5 °C. IR (KBr) cm^{-1} : 3486, 1114, 1094. 1H -NMR δ : 1.06 (3H, t, $J=7.0$ Hz, $N-CH_2CH_3$), 3.36, 3.37, 3.39, 3.41, 3.59 (each 3H, s, OCH_3), 4.16 (1H, s, 6 α -H). HR-EI-MS m/z : 481.3015 (Calcd for $C_{26}H_{43}NO_7$: 481.3037). EI-MS m/z : 481 (M^+), 466 ($M^+ - CH_3$, base peak), 464 ($M^+ - OH$).

28: Amorphous. IR ($CHCl_3$) cm^{-1} : 3452, 1135, 1104. 1H -NMR δ : 0.99 (3H, t, $J=7.0$ Hz, $N-CH_2CH_3$), 3.34, 3.35, 3.40, 3.43, 3.67 (each 3H, s, OCH_3), 3.85 (1H, s, 19-H), 4.10 (1H, s, 6 α -H). HR-EI-MS m/z : 479.2881 (Calcd for $C_{26}H_{41}NO_7$: 479.2881). EI-MS m/z : 479 (M^+), 464 ($M^+ - CH_3$, base peak).

Preparation of 1,7,8,14-Tetra-O-methyldecosine (25) and 7,8,14-Tri-O-methyl-18-methoxygadesine (29) A mixture of delcosine (**13**: 81.0 mg), 1,2-dimethoxyethane (8 ml), NaH (87.5 mg) and methyl iodide (0.24 ml) was kept at 0 °C for 1 h and then at room temperature for 2 d. The solution was filtrated, and then purification by column chromatography on silica gel (30% hexane–ether saturated with 28% ammonia) afforded 1,7,8,14-tetra-O-methyldecosine (**25**, 44.2 mg, 44%) and 7,8,14-tri-O-methyl-18-methoxygadesine (**29**, 8.2 mg, 9%).

25: Amorphous. IR ($CHCl_3$) cm^{-1} : 1098. 1H -NMR δ : 1.00 (3H, t, $J=7.0$ Hz, $N-CH_2CH_3$), 3.21, 3.34, 3.36, 3.43, 3.59 (each 3H, s, OCH_3), 3.37 (6H, s, OCH_3), 4.00 (1H, s, 6 α -H). HR-EI-MS m/z : 509.3366 (Calcd for $C_{28}H_{47}NO_7$: 509.3350). EI-MS m/z : 509 (M^+), 494 ($M^+ - CH_3$), 478 ($M^+ - OCH_3$, base peak).

29: Amorphous. IR ($CHCl_3$) cm^{-1} : 1135, 1104. 1H -NMR δ : 1.03 (3H, t, $J=7.0$ Hz, $N-CH_2CH_3$), 3.37, 3.39, 3.41, 3.68 (each 3H, s, OCH_3), 3.38 (6H, s, OCH_3), 3.95 (1H, s, 19-H), 4.19 (1H, s, 6 α -H). HR-EI-MS m/z : 493.3042 (Calcd for $C_{27}H_{43}NO_7$: 493.3038). EI-MS m/z : 493 (M^+), 478 ($M^+ - CH_3$, base peak), 446.

Preparation of 14-Acetyldebrunine (26) A mixture of 14-acetyldebrunine (**15**: 200 mg), water (0.08 ml), paraformaldehyde (400 mg), acetic acid (8 ml) and conc- H_2SO_4 (0.2 ml) was kept at 100 °C for 25 h. Water was added. The usual work-up and purification by column chromatography on silica gel (5% hexane–ether saturated with 28% ammonia) afforded 14-acetyldebrunine (24.7 mg, 55%) and the starting material (68.1 mg). Amorphous. IR (KBr) cm^{-1} : 3454, 1740, 1247, 1094. 1H -NMR δ : 1.11 (3H, t, $J=7.0$ Hz, $N-CH_2CH_3$), 2.06 (3H, s, $OCOCH_3$), 3.29 (6H, s, OCH_3), 3.38 (3H, s, OCH_3), 3.80 (1H, s, 6 α -H), 4.86 (1H, t, $J=4.6$ Hz, 14 β -H), 5.05, 5.10 (each 1H, d, $J=1.0$ Hz, OCH_2O). HR-EI-MS m/z : 507.2836 (Calcd for $C_{27}H_{41}NO_8$: 507.2830). EI-MS m/z : 507 (M^+), 492 ($M^+ - CH_3$), 490 ($M^+ - OH$), 474 (base peak).

Preparation of 1,14-Diacetyldebrunine (27) A mixture of 14-acetyldebrunine (**26**: 17.2 mg), pyridine (0.5 ml) and acetic anhydride (0.5 ml) was kept at 70 °C for 15 h. The usual work-up and purification by column chromatography on silica gel (10% hexane–ether saturated with 28% ammonia) afforded 1,14-diacetyldebrunine (8.8 mg, 47%). Amorphous. IR ($CHCl_3$) cm^{-1} : 1731, 1251, 1133. 1H -NMR δ : 1.09 (3H, t, $J=7.0$ Hz, $N-CH_2CH_3$), 2.05, 2.06 (each 3H, s, $OCOCH_3$), 3.27, 3.29, 3.35 (each 3H, s, OCH_3), 3.73 (1H, s, 6 α -H), 4.75 (1H, t, $J=9.2$ Hz, 1 β -H), 4.79 (1H, t, $J=4.6$ Hz, 14 β -H), 5.08 (2H, s, OCH_2O). HR-EI-MS m/z : 549.2934 (Calcd for $C_{29}H_{43}NO_8$: 549.2935). EI-MS m/z : 549 (M^+), 534 ($M^+ - CH_3$), 518 ($M^+ - OCH_3$), 504, 490 ($M^+ - OCOCH_3$, base peak).

HPLC–APCI-MS Conditions A model M-2000 mass spectrometer (Hitachi, Tokyo, Japan) through an APCI interface was used as the HPLC–APCI-MS system. The HPLC system consisted of a Model L-6200 chromatographic pump (Hitachi, Tokyo, Japan) and a Rheodyne (Cotati, CA, U.S.A.) Model 7125 injector with a 20- μ l loop. Direct injection analysis was performed without HPLC columns. The eluent was transferred at the flow rate of 0.8 ml/min directly to the APCI interface. The solvent consisted

of 0.05 M ammonium acetate–acetonitrile–tetrahydrofuran (60:25:15, v/v). The mass spectrometer interface consisted of nebulizing and vaporizing units. The temperature of the nebulizer was set to 280 °C to give optimum abundance of the target ions. The desolvation temperature was set to 400 °C. The vaporized sample and solvent molecules were passed into the ion source of the APCI-MS system. The solvent molecules were ionized by corona discharge, and then the sample molecules and ionized solvent molecules underwent ion-molecule reactions.

Deuterium Exchange Studies Sample solution dissolved in deuterated methanol. The solvent consisted of 0.05 M ammonium acetate in D_2O –acetonitrile–tetrahydrofuran (60:25:15, v/v). The conditions were the same as those stated above.

References

- 1) Splitter J. S., Turecek F. (ed.), "Application of Mass Spectrometry of Organic Stereochemistry," VCH, New York, 1994.
- 2) Fetterolf D. D., Yost R. A., *Int. J. Mass Spectrom. Ion Phys.*, **44**, 37–50 (1982).
- 3) McLuckey S. A., Cooks R. G., "Tandem Mass Spectrometry," ed. by McLaffey F. W., Wiley-Intersciences, New York, 1983, pp. 303–320.
- 4) Hayes R. N., Gross M. L., *Methods Enzymol.*, **193**, 237–263 (1990).
- 5) Beckett A. H., Dwuuma-Badu D., Haddock R. E., *Tetrahedron*, **25**, 5961–5969 (1969).
- 6) Fujisawa H., *Chem. Pharm. Bull.*, **36**, 4136–4143 (1988).
- 7) Czira G., Tamás J., Kalas G., *Org. Mass Spectrom.*, **19**, 555–562 (1984).
- 8) Laprèvote O., Ducrot P., Thal C., Serani L., Das B. C., *J. Mass Spectrom.*, **31**, 1149–1155 (1996).
- 9) Laprèvote O., Serani L., Das B. C., *J. Mass Spectrom.*, **32**, 339–340 (1997).
- 10) Amiya T., Bando H., "The Alkaloids," Vol. 34, ed. by Brossi A., Academic Press, San Diego, 1988, pp. 95–179.
- 11) Edwards O. E., "The Alkaloids," Vol. 1, ed. by Saxton J. E., The Chemical Society, London, 1971, pp. 343–381.
- 12) Pelletier S. W., Page S. W., "The Alkaloids," Vol. 3, ed. by Saxton J. E., The Chemical Society, London, 1973, pp. 232–257.
- 13) Pelletier S. W., Page S. W., "The Alkaloids," Vol. 8, ed. by Grudon M. F., The Chemical Society, London, 1978, pp. 219–245.
- 14) Pelletier S. W., Page S. W., "The Alkaloids," Vol. 10, ed. by Grudon M. F., The Chemical Society, London, 1981, pp. 211–226.
- 15) Yunusov M. S., *Natural Product Reports*, **8**, 499–526 (1991).
- 16) Yunusov M. S., *Natural Product Reports*, **10**, 471–486 (1993).
- 17) Yunusov M. S., Rashkes Ya. V., Salimov B. T., Ametova E. F., Yunusov S. Yu., *Khim. Priir. Soedin.*, **1985**, 525–536.
- 18) Yunusov M. S., Rashkes Ya. V., Yunusov S. Yu., *Khim. Priir. Soedin.*, **8**, 85–87 (1972).
- 19) Wada K., Bando H., Kawahara N., *J. Chromatogr.*, **644**, 43–48 (1993).
- 20) Wada K., Bando H., Kawahara N., Mori T., Murayama M., *Biol. Mass Spectrom.*, **23**, 97–102 (1994).
- 21) Wada K., Bando H., Kawahara N., *Natural Medicines*, **51**, 37–39 (1997).
- 22) Wada K., Mori T., Kawahara N., *J. Mass Spectrom.*, **35**, in press.
- 23) Pelletier S. W., Djarmati Z., Lajsic D., Camp W. H. De, *J. Am. Chem. Soc.*, **98**, 2617–2625 (1976).
- 24) Pelletier S. W., Etse J. T., *J. Nat. Prod.*, **52**, 145–152 (1989).
- 25) Kambara H., Kanomata I., *Anal. Chem.*, **49**, 270–275 (1977).
- 26) Sakairi M., Kambara H., *Anal. Chem.*, **60**, 774–780 (1988).
- 27) Wada K., Bando H., Mori T., Wada R., Kanaiwa Y., Amiya T., *Chem. Pharm. Bull.*, **33**, 3658–3661 (1985).
- 28) Wada K., Ishizuki S., Mori T., Bando H., Murayama M., Kawahara N., *Biol. Pharm. Bull.*, **20**, 978–982 (1997).
- 29) Joshi B. S., Glisk J. A., Choksi H. P., Chen S. Y., Srivastava S. K., Pelletier S. W., *Heterocycles*, **22**, 2037–2042 (1984).
- 30) Bando H., Wada K., Amiya T., *Heterocycles*, **26**, 2623–2637 (1987).
- 31) Benn M. H., Jacyno J. M., "Alkaloids; Chemical and Biological Perspectives," Vol. 1, ed. by Pelletier S. W., Wiley-Interscience, New York, 1983, pp. 153–210.
- 32) Deng W., Sung W., *Heterocycles*, **24**, 873–876 (1986).

The Cyclization Reaction of *Ortho*-Ethynylbenzaldehyde Derivatives into Isoquinoline Derivatives

Takao SAKAMOTO,* Atsushi NUMATA, and Yoshinori KONDO

Graduate School of Pharmaceutical Sciences, Tohoku University, Aramaki-aza-Aoba, Aoba-ku, Sendai 980–8578, Japan.

Received December 1, 1999 ; accepted January 28, 2000

In order to elucidate the reaction mechanism of the cyclization between an ethynyl group and an imino group at the *ortho*-position on an aromatic ring to afford isoquinolines, reaction of 2-ethynylbenzaldehydes under various conditions was examined. It is concluded that reaction proceeds *via* an ionic process and the isoquinoline 4-hydrogen atom derives from the solvent. In addition, it was found that 2-ethynylbenzaldehyde *O*-methyloximes underwent cyclization in the presence of primary and secondary alcohols to give 3-substituted isoquinolines.

Key words 2-ethynylbenzaldehyde; isoquinoline; *N*-oxide; cyclization; palladium-catalyzed reaction

The cyclization reaction which occurs between two *ortho*-positioned functional groups on aromatic or heteroaromatic rings is a useful construction method for aromatic- or heteroaromatic-condensed rings, because the method is considered to be independent of the electronic character of the aromatic ring component.¹⁾ One example is the synthesis of condensed heterocycles containing an isoquinolinic nitrogen from *ortho*-ethynylarylaldehydes which can be easily prepared by palladium-catalyzed reaction of *ortho*-halo(or trifluoromethylsulfonyloxy)arylaldehydes with terminal alkynes.

Based on this concept, a facile method for the synthesis of isoquinoline 2-oxides from 2-ethynylbenzaldehyde oximes has already been reported by us.²⁾ As an extension of the method, we have also reported the synthesis of naphthyridines, carbolines, and their *N*-oxides from *ortho*-ethynylpyridinecarbaldehydes, *ortho*-ethynylindolecarbaldehydes, and their oximes.^{3,4)}

Our attention has been now turned to the cyclization reaction process which consists of the interaction between an ethynyl group and an imino group at the *ortho*-position of the aromatic or heteroaromatic rings. We now report a mechanistic investigation of the isoquinoline cyclization reaction from 2-ethynylbenzaldehydes, their oximes, and their *O*-methyl-oximes as substrates.

Initially, the cyclization reaction of 2-ethynylbenzaldehydes (**1a–d**), prepared by the palladium-catalyzed reaction of 2-bromobenzaldehyde with terminal alkynes under conventional conditions,²⁾ to the 3-substituted isoquinolines (**2a–d**) was examined. We have not previously reported this type of reaction, although the cyclization reaction of *ortho*-ethynylpyridinecarbaldehydes and *ortho*-ethynylindolecarbaldehydes to naphthyridines and carbolines has been reported.^{3,4)}

Using 2-(oct-1-yn-1-yl)benzaldehyde (**1a**) as a substrate, it was found that the cyclization reaction proceeded under several conditions shown in Table 1, and the conditions, using ammonia in ethanol gave relatively good results with respect to the yield of the isoquinolines (**2a–d**), *i.e.*, in 45–95% yields as shown in Table 1.

The isoquinoline cyclization reaction of 2-ethynylbenzaldehydes with ammonia or equivalent sources is presumed to proceed *via* the corresponding aldimine intermediates. However, since aldimines are generally unstable and the preparation of aldimines by another route is difficult, we

chose the corresponding oximes as substrates to elucidate the course of the cyclization reaction. Although it is difficult to affirm in a strict sense that the reaction courses of 2-ethynylbenzaldehydes with ammonia or its equivalent to isoquinolines and of 2-ethynylbenzaldehyde oximes to isoquinoline 2-oxides are the same, we presume that the two cyclization reactions proceed principally *via* the same process.

Before considering the cyclization reaction courses of oximes, elucidation of the oxime stereochemistry is necessary, since the stereochemistry sometimes plays an important role. The ¹H-NMR spectra of the 2-(ethynyl)benzaldehyde oximes (**3a–d**) showed formyl protons at 8.57–8.65 ppm. Since it is known⁵⁾ that arylaldehyde oximes generally exist as stable *E*-isomers and the ¹H-NMR spectrum of (*E*)-4-bromobenzaldehyde oxime shows the formyl proton at 8.19 ppm, compounds (**3a–d**) which contain an ethynyl substituent at the *ortho*-position probably also exist as the *E*-isomers.

As shown in Chart 2, ionic processes, represented by paths A and B, are considered as possible reaction courses from the oximes to isoquinoline 2-oxides. Although path A is the most probable one between the two possible ionic mechanisms, path B, which involves benzoxazepine intermediates, can not be excluded. If the reaction proceeds according to paths A and B, the hydrogen at the 4-position of the isoquinoline is expected to arise from the starting oximes (H^A) or solvent (H^B). We then tried the cyclization reaction in various solvents as shown in Table 2.

The reaction in the presence of a strong proton donor such as *p*-toluenesulfonic acid (TsOH) or acetic acid gave **4** in high yields and the reaction in the presence of a weak proton donor such as methanol or ethanol also gave **4**. Moreover, the cyclization reaction in monodeuteriomethanol (CH₃OD) gave only 4-deuterio-3-hexylisoquinoline 2-oxide.

It is considered that the benzoxazepine intermediates in

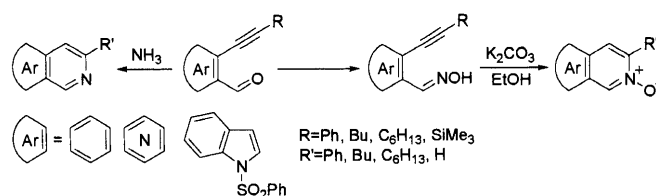


Chart 1

* To whom correspondence should be addressed. e-mail: Sakamoto@mail.pharm.tohoku.ac.jp

Table 1. Cyclization Reaction of 2-Ethynylbenzaldehydes (**1a—d**) to 3-Substituted Isoquinolines (**2a—d**)

Compd. No.	R	Conditions				Compd. No.	R'	Yield (%) [Recovery]
		"NH ₃ " source	Solvent	Temp. (°C)	Time (h)			
1a	C ₆ H ₁₃	NH ₃	EtOH	80 (sealed)	2	2a	C ₆ H ₁₃	60 [7]
1a	C ₆ H ₁₃	HCOONH ₄	EtOH	Reflux	12	2a	C ₆ H ₁₃	13 [74]
1a	C ₆ H ₁₃	HCOONH ₄	EtOH	80 (sealed)	2	2a	C ₆ H ₁₃	40 [49]
1a	C ₆ H ₁₃	(NH ₄) ₂ CO ₃	EtOH	Reflux	2	2a	C ₆ H ₁₃	—[69]
1a	C ₆ H ₁₃	(NH ₄) ₂ CO ₃	EtOH	80 (sealed)	2	2a	C ₆ H ₁₃	40 [29]
1a	C ₆ H ₁₃	H ₂ NCHO	—	100	12	2a	C ₆ H ₁₃	21 [36]
1b	Bu	NH ₃	EtOH	80 (sealed)	2	2b	Bu	95 [—]
1c	Ph	NH ₃	EtOH	80 (sealed)	2	2c	Ph	45 [—]
1d	SiMe ₃	NH ₃	EtOH	80 (sealed)	2	2d	H	50 [—]

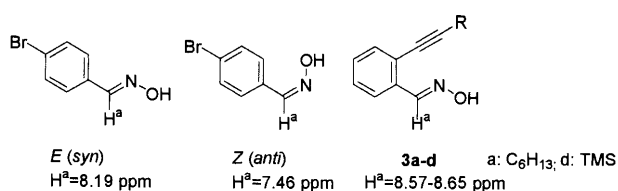


Fig. 1

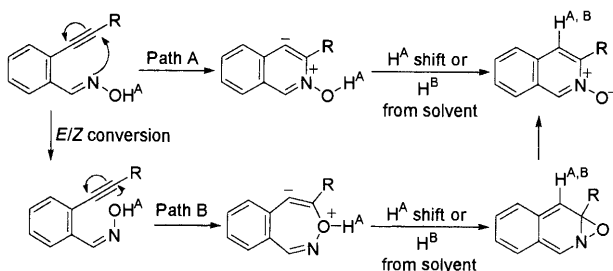


Chart 2

path B rearrange to give oxazirine intermediates which finally afford isoquinoline 2-oxides (**4**). Furthermore, it is presumed that the oxazirine intermediates could be deoxygenated by reaction with triphenylphosphine to give isoquinolines. Since the reaction of 2-(trimethylsilyl-ethynyl)benzaldehyde oximes (**3d**) in the presence of triphenylphosphine gave isoquinoline 2-oxide (**4d**) and no isoquinolines (**2**), we concluded that path B does not operate during the cyclization reaction process.

We next examined the cyclization reaction of 2-(oct-1-yn-1-yl)benzaldehyde *O*-methyloxime (**5**), which has no acidic hydrogen, under the various conditions shown in Table 3 in order to determine whether the hydrogen at the 4-position of the isoquinoline 2-oxides comes from the hydrogen of the oximes or from the solvent used in path A. The cyclization of **5a** in acetic acid gave 3-hexyloisoquinoline 2-oxide (**4a**) in 39% yield together with the starting material (**5a**) (run 1).

These results showed that compound **5a**, which has no acidic hydrogen, can be cyclized to give **4a** in acidic media, and the probable *N*-methoxyisoquinolinium intermediate is demethylated under the given reaction conditions. Concern-

Table 2. Cyclization Reaction of 2-(Oct-1-yn-1-yl)benzaldehyde Oxime (**3a**) to 3-Hexyloisoquinoline 2-Oxide (**4a**)

Run	Reaction conditions				Yield (%)
	Solvent	Additive	Temp. (°C)	Time (h)	
1	PhMe	—	Reflux	48	67
2	PhMe	TsOH	80	48	88
3	AcOH	AcONa	80	48	98
4	AcOH	—	80	48	95
5	EtOH	—	Reflux	24	64
6	EtOH	—	Reflux	48	65
7	MeOH	—	Reflux	48	96

ing the dealkylation reaction of *N*-alkoxyazinium derivatives giving the corresponding *N*-oxides, Katritzky reported⁶⁾ that the reaction of 1-methoxypyridinium *p*-toluenesulfonate with sodium acetate in acetic acid gave pyridine 1-oxide. The demethylation may occur by attack of the acetoxyl anion on the methyl group, but a detailed mechanism is still not presently available.

In addition to the above results, we were also interested in the formation of isoquinoline (**2a**) from **5** although the yields were low (runs 2—4). The reaction of **5** in ethanol in a sealed tube at 180 °C for 48 h gave **2a** in 90% yield (run 5). The reaction in toluene proceeded in 40—78% yields in the presence of primary or secondary alcohols (runs 7—9), but gave **2a** in low yield in the absence of alcohols (run 6). Moreover, the cyclization reaction of **5a** in monodeuteriomethanol (CH₃OD) gave the 4-deuterio-3-hexyloisoquinoline.

Although dealkoxylation of *N*-alkoxyazinium derivatives in the presence of nucleophiles has been reported,⁶⁾ we assumed that the reaction proceeded *via* the course shown in Chart 3. Namely, the betaine intermediate produced by thermal reaction of 2-ethynylbenzaldehyde *O*-methyloximes abstracts a proton from the alcohols, as shown in Table 3 to give the *N*-methoxyisoquinolinium intermediates which react with the resulting alkoxides. The alkoxide adducts eliminate

Table 3. Cyclization Reaction of 2-Ethynylbenzaldehyde *O*-Methyloxime (**5**)

Run	R	Reaction Conditions				Yield (%)		
		Solvent	Additive	Temp. (°C)	Time (h)	4	2a	5
1	C ₆ H ₁₃	AcOH	—	80	48	39	—	52
2	C ₆ H ₁₃	AcOH	AcONa	80	48	64	4	—
3	C ₆ H ₁₃	EtOH	—	80	48	—	3	68
4	C ₆ H ₁₃	EtOH	K ₂ CO ₃	80	12	—	7	89
5	C ₆ H ₁₃	EtOH	—	180 (sealed)	48	—	90	—
6	C ₆ H ₁₃	PhMe	—	180 (sealed)	48	—	27	33
7	C ₆ H ₁₃	PhMe	PhCH ₂ OH (excess)	180 (sealed)	24	—	78	—
8	C ₆ H ₁₃	PhMe	PhCH ₂ CH ₂ OH (1 eq)	180 (sealed)	48	—	40	30
9	C ₆ H ₁₃	PhMe	cyclohexanol (2 eq)	180 (sealed)	48	—	54	23
10	Ph	PhMe	Ph ₂ CHOH (1 eq)	180 (sealed)	48	—	87	—
11	Ph	EtOH	—	180 (sealed)	48	—	98	—
12	Ph	PhMe	MeOH (0.3 eq)	180 (sealed)	48	—	86	14

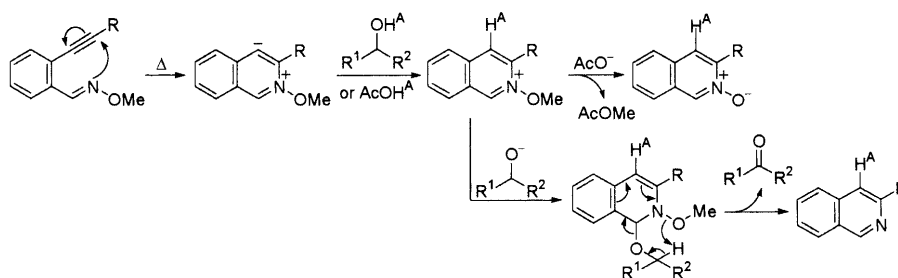


Chart 3

the corresponding carbonyl compound and isoquinolines as shown in Chart 3. Indeed, benzophenone was isolated from the reaction of **5a** with diphenylmethanol.

In conclusion, the cyclization reaction between an ethynyl group and an imino group both existing at the *ortho*-position of aromatic or heteroaromatic rings proceeds through an ionic process, path A shown in Chart 2, and the hydrogen at the 4-position of the isoquinolines come from the protic solvent. Moreover, it was found that 2-ethynylbenzaldehyde oximes underwent cyclization to give 3-substituted isoquinoline 2-oxides in protic media and 2-ethynylbenzaldehyde *O*-methyloximes cyclized in the presence of primary or secondary alcohols to give 3-substituted isoquinolines.

Experimental

General All melting points and boiling points are uncorrected. IR spectra were taken on a JASCO IR-810 spectrophotometer. ¹H-NMR spectra were recorded on Varian Gemini 2000 (300 MHz) and Hitachi R-300 (300 MHz) spectrometers. Chemical shifts are expressed in δ (ppm) values with tetramethylsilane (TMS) as the internal reference, and coupling constants are expressed in hertz (Hz). The following abbreviations are used: s=singlet, d=doublet, t=triplet, m=multiplet, dd=doublet of doublets, br=broad, and br s=broad singlet. Mass spectra (MS) and high resolution mass spectra (HR-MS) were recorded on JMS-DX303 and JMS-AX500 instruments.

General Procedure for Synthesis of 2-Ethynylbenzaldehydes (1) A mixture of 2-bromobenzaldehyde (2 mmol), an alkyne (2.5–4 mmol), Pd(PPh₃)₂Cl₂ (60 mg), CuI (30 mg), Et₃N (300 mg), and *N,N*-dimethylformamide (DMF) (10 ml) was stirred at room temperature –50 °C for 1–15 h. The mixture was diluted with H₂O, and extracted with Et₂O. The residue obtained from the ethereal extract was purified by silica gel column chromatography using AcOEt–hexane (1:10) as eluent. The product was purified

by distillation.

2-(Oct-1-yn-1-yl)benzaldehyde (**1a**): Yellow oil, bp 97 °C (3 mmHg). Yield 80%. IR (liquid) cm⁻¹: 2220, 1700. ¹H-NMR (CDCl₃) δ : 0.91 (3H, t, *J*=7.0 Hz), 1.30–1.44 (4H, m), 1.46–1.49 (2H, m), 1.59–1.67 (2H, m), 2.48 (2H, t, *J*=7.0 Hz), 7.38–7.41 (1H, m), 7.50–7.53 (2H, m), 7.87–7.91 (1H, m), 10.55 (1H, s). MS *m/z*: 214 (M⁺). HR-MS *m/z*: 214.1321 (Calcd for C₁₅H₁₈O: 214.1358).

2-(Hex-1-yn-1-yl)benzaldehyde (**1b**): Yellow oil, bp 105 °C (3 mmHg). Yield 66%. IR (CHCl₃) cm⁻¹: 2210, 1690. ¹H-NMR (CHCl₃) δ : 0.95 (3H, t, *J*=7.0 Hz), 1.20–2.00 (4H, m), 2.50 (2H, t, *J*=7.0 Hz), 7.10–7.60 (3H, m), 7.60–8.00 (1H, m), 10.47 (1H, s).

2-(Phenylethynyl)benzaldehyde (**1c**): Yellow oil, bp 173 °C (3 mmHg). Yield 82%. IR (liquid) cm⁻¹: 2210, 1700. ¹H-NMR (CDCl₃) δ : 7.10–7.60 (8H, m), 7.60–8.00 (1H, m), 10.51 (1H, s).

2-(Trimethylsilylphenylethynyl)benzaldehyde (**1d**): Colorless oil, bp 105 °C (3 mmHg). Yield 88%. IR (liquid) cm⁻¹: 2150, 1690. ¹H-NMR (CDCl₃) δ : 0.27 (9H, s), 7.30–7.70 (3H, m), 7.70–8.10 (1H, m), 10.47 (1H, s).

General Procedure for Synthesis of Isoquinolines (2) A solution of 2-ethynylbenzaldehydes (**1**) (1 mmol) was allowed to react under the conditions shown in Table 1 [“NH₃” source: HCOONH₄ (630 mg, 10 mmol), (NH₄)₂CO₃ (1.141 g, 10 mmol) in EtOH (10 ml); H₂NCHO (5 ml)]. After concentration of the reaction mixture *in vacuo*, saturated aqueous K₂CO₃ solution was added, and the mixture was extracted with CHCl₃. The CHCl₃ extract was washed with saturated aqueous NaCl solution and dried over MgSO₄. The residue was purified by silica gel column chromatography using CHCl₃–EtOH (100:1) as eluent. The product was purified by recrystallization or distillation.

3-Hexyloisoquinoline (**2a**): Colorless liquid, bp 105 °C (3 mmHg). ¹H-NMR (CDCl₃) δ : 0.86 (3H, t, *J*=6.6 Hz), 1.31–1.40 (6H, m), 1.81 (2H, t, *J*=7.5 Hz), 2.93 (2H, t, *J*=7.5 Hz), 7.47 (1H, s), 7.52 (1H, t, *J*=7.5 Hz), 7.65 (1H, t, *J*=8.5 Hz), 7.75 (1H, d, *J*=7.5 Hz), 7.93 (1H, d, *J*=8.5 Hz), 9.21 (1H, s). MS *m/z*: 213 (M⁺). HR-MS *m/z*: 213.1472 (Calcd for C₁₅H₁₉N: 213.1517).

3-Butyloisoquinoline (**2b**): Colorless liquid, bp 150 °C (20 mmHg). ¹H-

NMR (CDCl₃) δ : 0.95 (3H, t, $J=7.0$ Hz), 1.10–2.20 (4H, m), 2.94 (2H, t, $J=7.0$ Hz), 7.30–8.10 (5H, m), 9.20 (1H, s).

3-Phenylisoquinoline (**2c**): Colorless granules from hexane, mp 101–102 °C, (lit.⁸) mp 102.5–103.5 °C. ¹H-NMR (CDCl₃) δ : 7.30–8.30 (10H, m), 9.34 (1H, s).

Isoquinoline (**2d**)⁹: Colorless liquid, bp 70 °C (3 mmHg). ¹H-NMR (CDCl₃) δ : 7.40–8.20 (5H, m), 8.56 (1H, d, $J=6.0$ Hz), 9.28 (1H, s).

General Procedure for Preparation of 2-Ethynylbenzaldehyde Oximes (3) A solution of 2-ethynylbenzaldehyde (**1**) (1 mmol) in EtOH (5 ml) was added to hydroxylamine hydrochloride (104 mg, 1.5 mmol) and AcONa (123 mg, 1.5 mmol). The mixture was stirred at room temperature for 1–15 h, and concentrated *in vacuo*. Saturated aqueous K₂CO₃ solution was added and the mixture extracted with CHCl₃. The CHCl₃ extract was washed with saturated aqueous NaCl solution and dried over MgSO₄. The residue was purified by silica gel column chromatography using CHCl₃–EtOH (100:1) as eluent. The product was purified by recrystallization from hexane.

2-(Oct-1-yn-1-yl)benzaldehyde Oxime (**3a**): Brown oil, bp 115 °C (3 mmHg). Yield 83%. IR (liquid) cm⁻¹: 3300, 2220. ¹H-NMR (CDCl₃) δ : 0.91 (3H, t, $J=7.0$ Hz), 1.31–1.44 (4H, m), 1.46–1.49 (2H, m), 1.58–1.66 (2H, m), 2.46 (2H, t, $J=7.0$ Hz), 7.27–7.30 (2H, m), 7.32–7.44 (1H, m), 7.80 (1H, br), 7.82–7.83 (1H, m), 8.65 (1H, s). MS m/z : 229 (M⁺). HR-MS m/z : 229.1449 (Calcd for C₁₅H₁₉NO: 229.1467).

2-(Trimethylsilyl)ethynylbenzaldehyde Oxime (**3d**): Colorless needles from hexane, mp 87–88 °C (lit.²) mp 87–89 °C. Yield 83%. IR (CHCl₃) cm⁻¹: 2280. ¹H-NMR (CHCl₃) δ : 0.28 (9H, s), 7.10–7.60 (3H, m), 7.60–8.00 (1H, m), 8.57 (1H, s), 9.13 (1H, s).

General Procedure for Cyclization of 2-(Oct-1-yn-1-yl)benzaldehyde Oxime (3a) 2-(Oct-1-yn-1-yl)benzaldehyde oxime (**3a**) (100 mg, 0.44 mmol) in solvent (10 ml) was heated for 12–48 h, as shown in Table 2 [additive: TsOH (172 mg, 1 mmol), AcONa (82 mg, 1 mmol)]. After concentration of the reaction mixture, the residue was partitioned between H₂O and CHCl₃. The CHCl₃ layer was washed with saturated aqueous NaCl solution and dried over MgSO₄. The residue was purified by silica gel column chromatography using CHCl₃–EtOH (100:1) as eluent to give 3-hexylisoquinoline 2-oxide (**4a**) as colorless needles, mp 63–66 °C (recrystallized from hexane). ¹H-NMR (CDCl₃) δ : 0.90 (3H, t, $J=7.3$ Hz), 1.24–1.50 (6H, m), 1.79–1.84 (2H, m), 3.04 (2H, t, $J=7.3$ Hz), 7.52–7.58 (3H, m), 7.67–7.75 (2H, m), 8.85 (1H, s). MS m/z : 229 (M⁺). Anal. Calcd for C₁₅H₁₉NO: C, 78.56; H, 8.35; N, 6.11. Found: C, 78.44; H, 8.38; N, 6.06.

Reaction of 2-(Trimethylsilyl)ethynylbenzaldehyde Oxime (3d) with K₂CO₃ in the Presence of PPh₃ A mixture of 2-(trimethylsilyl)ethynylbenzaldehyde oxime (**3d**) (0.65 g, 3 mmol), K₂CO₃ (0.41 g, 3 mmol), and PPh₃ (0.78 g, 3 mmol) in EtOH (6 ml) was heated at 60 °C for 5 h. After removal of EtOH *in vacuo*, saturated aqueous K₂CO₃ solution was added to the residue, and the mixture was extracted with CHCl₃. The CHCl₃ extract was washed with saturated aqueous NaCl solution and dried over MgSO₄. The residue was purified by silica gel column chromatography using CHCl₃–EtOH (100:1) as eluent to give isoquinoline 2-oxide (**4d**) (0.26 g, 60%), mp 99–101 °C (lit.¹⁰) mp 105–106 °C. ¹H-NMR (CDCl₃) δ (ppm): 7.30–8.00 (5H, m), 8.10 (1H, dd, $J=7.0, 2.0$ Hz), 8.88 (1H, d, $J=2.0$ Hz).

Cyclization Reaction of 2-(Oct-1-yn-1-yl)benzaldehyde Oxime (3a) in CH₃OD A solution of 2-(oct-1-yn-1-yl)benzaldehyde oxime (**3a**) (50 mg, 0.22 mmol) in CH₃OD (5 ml) was refluxed for 48 h. After removal of the solvent *in vacuo*, saturated aqueous K₂CO₃ solution was added to the residue, and the mixture was extracted with CHCl₃. The CHCl₃ extract was washed with saturated aqueous NaCl solution and dried over MgSO₄. The residue was purified by silica gel column chromatography using CHCl₃–EtOH (100:1) as eluent to give 4-deuterio-3-hexylisoquinoline as colorless needles (29 mg, 58%). ¹H-NMR (CDCl₃) δ (ppm): 0.90 (3H, t, $J=7.0$ Hz), 1.26–1.50 (6H, m), 1.81 (2H, t, $J=7.7$ Hz), 3.04 (2H, t, $J=7.3$ Hz), 7.53–7.59 (2H, m), 7.68–7.76 (2H, m), 8.86 (1H, s). The deuteration ratio was estimated by integration of ¹H-NMR signals (D content, 100%).

General Procedure for Preparation of 2-Ethynylbenzaldehyde O-Methyloximes (5) A solution of 2-ethynylbenzaldehyde (**3**) (1 mmol) in

EtOH (5 ml) was added to *O*-methylhydroxylamine hydrochloride (125 mg, 1.5 mmol) and AcONa (123 mg, 1.5 mmol). The mixture was stirred at room temperature for 12 h, then concentrated *in vacuo*. H₂O was added and the mixture was extracted with CHCl₃. The CHCl₃ extract was washed with saturated aqueous NaCl solution and dried over MgSO₄. The residue was purified by silica gel column chromatography using hexane–AcOEt (100:1) as eluent. The product was purified by distillation.

2-(Oct-1-yn-1-yl)benzaldehyde *O*-Methyloxime (**5a**): Yellow oil, bp 140 °C (3 mmHg). Yield 98%. IR (liquid) cm⁻¹: 2210. ¹H-NMR (CDCl₃) δ : 0.91 (3H, t, $J=6.9$ Hz), 1.30–1.64 (8H, m), 2.44 (2H, t, $J=6.9$ Hz), 3.99 (3H, s), 7.25–7.28 (2H, m), 7.38–7.41 (1H, m), 7.84–7.88 (1H, m), 8.57 (1H, s). MS m/z : 243 (M⁺). HR-MS m/z : 243.1635 (Calcd for C₁₆H₂₁NO: 243.1623).

2-Phenylethynylbenzaldehyde *O*-Methyloxime (**5c**): Yellow liquid, bp 140 °C (3 mmHg). Yield 85%. IR (liquid) cm⁻¹: 2210. ¹H-NMR (CDCl₃) δ : 4.01 (3H, s), 7.32–7.38 (5H, m), 7.53–7.57 (3H, m), 7.91–7.94 (1H, m), 8.66 (1H, s). MS m/z : 235 (M⁺). HR-MS m/z : 235.0973 (Calcd for C₁₆H₁₃NO: 235.0997).

General Procedure for Cyclization of 2-Ethynylbenzaldehyde O-Methyloxime (5) A solution of 2-ethynylbenzaldehyde *O*-methyloxime (**5**) (1 mmol) in a solvent (10 ml) under the conditions shown Table 3 was heated at 80–180 °C for 12–48 h [additive: AcONa (82 mg, 1 mmol), K₂CO₃ (138 mg, 1 mmol), benzyl alcohol (198 mg, 1 mmol), 2-phenethyl alcohol (122 mg, 1 mmol), cyclohexanol (100 mg, 1 mmol)]. After concentration of the reaction mixture *in vacuo*, saturated aqueous K₂CO₃ solution was added, and the mixture was extracted with CHCl₃. The CHCl₃ extract was washed with saturated aqueous NaCl solution and dried over MgSO₄. The residue was purified by silica gel column chromatography using hexane–AcOEt (100:1) as eluent. The product was purified by distillation.

Cyclization Reaction of 2-(Oct-1-yn-1-yl)benzaldehyde O-Methyloxime (5a) in CH₃OD A solution of 2-(oct-1-yn-1-yl)benzaldehyde *O*-methyloxime (**5a**) (100 mg, 0.41 mmol) in CH₃OD (10 ml) was heated at 180 °C for 48 h. After removal of the solvent *in vacuo*, saturated aqueous K₂CO₃ solution was added to the residue, and the mixture was extracted with CHCl₃. The CHCl₃ extract was washed with saturated aqueous NaCl solution and dried over MgSO₄. The residue was purified by silica gel column chromatography using hexane–AcOEt (10:1) as eluent to give 4-deuterio-3-hexylisoquinoline as a colorless liquid (75 mg, 85%). ¹H-NMR (CDCl₃) δ (ppm): 0.86 (3H, t, $J=6.6$ Hz), 1.31–1.40 (6H, m), 1.81 (2H, t, $J=7.5$ Hz), 2.93 (2H, t, $J=7.5$ Hz), 7.52 (1H, t, $J=7.5$ Hz), 7.65 (1H, t, $J=8.5$ Hz), 7.75 (1H, d, $J=7.5$ Hz), 7.93 (1H, d, $J=8.5$ Hz), 9.21 (1H, s). The deuteration ratio was determined from by integration of ¹H-NMR signals (D content, 89%).

Acknowledgements The authors thank Mr. Kazuhiko Hayashi for assistance with some of these experiments.

References

- 1) Sakamoto T., Kondo Y., Yamanaka H., *Heterocycles*, **27**, 2225–2249 (1988).
- 2) Sakamoto T., Kondo Y., Miura N., Hayashi K., Yamanaka H., *Heterocycles*, **24**, 2311–2314 (1986).
- 3) Numata A., Kondo Y., Sakamoto T., *Synthesis*, **1999**, 306–311.
- 4) Sakamoto T., Numata A., Saito H., Kondo Y., *Chem. Pharm. Bull.*, **47**, 1740–1743 (1999).
- 5) Fenselau A. H., Hamamura E. H., Moffatt J. G., *J. Org. Chem.*, **35**, 3546–3552 (1970).
- 6) Coats N. A., Katritzky A. R., *J. Org. Chem.*, **24**, 1836–1837 (1959).
- 7) Lehmkuyl J. N., *Chem. Ber.*, **30**, 897 (1897).
- 8) Bradsher C. K., Wallis T. G., *J. Org. Chem.*, **43**, 3817–3820 (1978).
- 9) Pouchert I. C., Behnke J. (ed.), "The Aldrich Library of ¹³C and ¹H FT NMR Spectra," Vol. 3, Aldrich Chemical Co. Ltd., 1993, p. 456.
- 10) Robison M. M., Robison B. L., *J. Org. Chem.*, **21**, 1337–1314 (1956).

Sustained-Release Phenylpropanolamine Hydrochloride Bilayer Caplets Containing the Hydroxypropylmethylcellulose 2208 Matrix.

I. Formulation and Dissolution Characteristics

Shinji OHMORI* and Tadashi MAKINO

Healthcare Research Laboratories, Consumer Healthcare Company, Takeda Chemical Industries, Ltd., 17–85, Jusohonmachi 2-Chome, Yodogawa-ku, Osaka 532–8686, Japan.

Received December 3, 1999; accepted January 29, 2000

The purpose of this study was to develop a new sustained-release phenylpropanolamine hydrochloride (PPA) bilayer caplets that consists of an immediate-release portion and a prolonged-release portion containing a hydroxypropylmethylcellulose 2208 (HPMC2208) matrix. Since PPA is a highly water-soluble drug, incorporation of 60% HPMC2208 level in the matrix was required for giving the product a PPA-slow releasing property. Difference in the viscosity grade of HPMC2208 in the matrices did not greatly influence the PPA dissolution characteristics from the matrices. Therefore, we formulated the prolonged-release portion consisting of 10% PPA, 30% excipients, and 60% HPMC2208 (Metolose 90SH4000) into the sustained-release PPA bilayer caplets. The PPA dissolution characteristics from the formulated bilayer caplets showed the prolonged dissolution profile after rapid dissolution and was close to the targeted profile calculated from PPA pharmacokinetics study. The manufacturing methods of the prolonged-release portion and the filling order of the prolonged-release portion in bilayer compression did not significantly affect the PPA dissolution characteristics from the bilayer caplets. The PPA dissolution characteristics from the bilayer caplets was pH independent. Moreover, the PPA dissolution characteristics from the bilayer caplets was not affected by mechanical shear. The sustained-release PPA bilayer caplets is expected to present constant prolonged-release of PPA after rapid dissolution *in vivo* without dissolution change due to pH and mechanical shear.

Key words bilayer caplet; phenylpropanolamine hydrochloride; hydroxypropylmethylcellulose; dissolution; formulation; hydrophilic matrix

Phenylpropanolamine hydrochloride (PPA), a sympathomimetic drug, is widely used as a nasal decongestant. Although PPA is rapidly and completely absorbed from the gastrointestinal tract after oral administration in humans, its plasma half-life in humans is short, 3.9 h, requiring that the drug be administered three times daily.¹⁾ It is therefore important and desirable to prolong the effective plasma level in order to maintain the clinical efficacy of the drug. Alderman and Hashem *et al.* suggested that hydrophilic polymer matrices incorporated in the drug is an adequate method to maintain a prolonged plasma drug level.^{2,3)} The application of an immediate-release portion to a prolonged-release system can produce the rapid onset of plasma levels for those drugs that are required to show the prompt appearance of the therapeutic effect, followed by a prolonged-release phase at a constant rate. Typical forms containing both an immediate-release portion and a prolonged-release portion are spansule capsules⁴⁾ and bilayer tablets are what is termed spantabs.⁵⁾

Since it was reported that multiple unit was superior in reliability in prolonged gastric emptying time to single unit,⁶⁾ multiple unit, such as spansule capsules, was widely chosen as a sustained-release dosage form. However, in the case that the sustained active ingredient is PPA, single unit is the same utility, such as plasma levels in humans, as reported with respect to multiple unit.⁷⁾

Bilayer caplets are excellent in two respects; firstly, single unit, such as bilayer caplets, excel in unit size than multiple unit, such as spansule capsules, and secondly, tablet shape changes from flat to capsule-like, namely caplets, that improve easiness in swallowing as compared with flat tablets.

Highly water-soluble drugs, such as PPA, play an important role in polymer swelling and contribute to the matrix in-

tegrity in hydrophilic polymer matrices as compared with slightly or poorly water-soluble drugs.⁸⁾ Therefore, it was technologically difficult to slow PPA dissolution from hydrophilic polymer matrices. Thus, there were several reports concerning formulation and dissolution characteristics of prolonged-release PPA granules coated with wax or ethylcellulose.^{9,10)} In contrast, there have been few reports concerning formulation and dissolution characteristics of sustained-release PPA bilayer caplets containing a hydrophilic polymer matrix.

Alderman²⁾ suggested that hydroxypropylmethylcellulose 2208 (HPMC2208) can hydrate rapidly enough to protect the tablets from fast disintegration and dissolution in the matrices than in the cases of HPMC2906, HPMC2910, hydroxypropylcellulose (HPC), and methylcellulose. Hence, HPMC2208 was chosen as a hydrophilic polymer constituting the prolonged-release matrix in bilayer caplets.

The purpose of this study was to develop a new long-acting nasal decongestant oral product (BENZA[®]AL), having bilayer consists of an immediate-release layer and a prolonged-release layer containing a HPMC2208 matrix, to deliver the PPA at controlled rate. In this study, formulation and dissolution characteristics of sustained-release PPA bilayer caplets containing a HPMC 2208 (Metolose 90SH4000) matrix were investigated.

Experimental

Materials PPA (Alps Pharmaceutical Ind. Co.) was used as a sustained-release drug. *d*-Chlorpheniramine maleate (*d*-CP, Kongo Chemical Co.), beladonna total alkaloids (BEA, Alps Pharmaceutical Ind. Co.), anhydrous caffeine (CAF, Shiratori Pharmaceutical Co.), and tranexamic acid (TRA, Daiichi Pharmaceutical Co.) were used as immediate-release drugs.

HPMC 2208 (Metolose 90SH4000, Metolose 90SH15000, Metolose

* To whom correspondence should be addressed. e-mail: Ohmori-Shinji@takeda.co.jp

90SH100000, Shin-Etsu Chemical Co.) were used as hydrophilic polymers of prolonged-release matrices. HPMC 2208 used in the experiments is as follows: median particle size 60–70 μm , moisture content (loss on drying, 1 g, 105 °C, 1 h) 3.5–5.0%. Microcrystalline cellulose (Ceolus KG-801, Asahi Chemical Ind. Co.) and spray-dried anhydrous dibasic calcium phosphate (Fujicalin SG, Fuji Chemical Ind. Co.) were used as diluents in the prolonged-release portion. Corn starch (Cornstarch, Japan Cornstarch Co.) was used as a diluent in the immediate-release portion. A low viscosity grade HPC (HPC-L, Nippon Soda Co.) and low-substituted HPC (L-HPC LH-31, Shin-Etsu Chemical Co.) were used as a binder and a disintegrant, respectively, in the immediate-release portion. Sunset yellow FCF (Yellow No.5, San-Ei Gen F.F.I.) was used as a colorant for the immediate-release portion. Magnesium stearate (Mg-St) and light anhydrous silicic acid (Sylysia 320) were used as a lubricant and a glidant, respectively. All other chemicals were of reagent grade.

Preparation of HPMC2208 Matrix Tablets In the experiment in which the effect of HPMC2208 level in the matrices was investigated, PPA 20mg, HPMC2208, Fujicalin SG were directly compacted with a compression instrument (Autograph AG-5000B, Shimadzu Corporation) using a 8 mm diameter flat-faced punch. The HPMC2208 level was varied from 40 to 120 mg. The quantity of Fujicalin SG was adjusted to maintain a consistent tablet weight of 200 mg. The compression speed was 10 mm/min. The ejection speed was 100 mm/min. The compression pressure was 98 MPa. In the experiment in which the effect of HPMC2208 viscosity grade in the matrices was investigated, PPA 20 mg and HPMC2208 120 mg were directly compacted with the compression instrument using a 7 mm diameter flat-faced punch. The compression speed, the ejection speed, and the compression pressure were the same as that described above.

Manufacturing of the Immediate-Release Portion by Wet Granulation PPA, d-CP, CAF, TRA, Cornstarch, and Sylysia 320 were granulated with BEA ethanol solution and HPC-L aqueous solution using an agitation granulator (vertical granulator FM-VG-25, Powrex Co.). The immediate-release portion was colored with Yellow No. 5. The granules were vacuum dried at 40 °C for 16 h and were size-reduced with a screening mill (power mill, Showa Kagaku Kikai Co.). The size-reduced granules were mixed with LH-31 and Mg-St by a diffusion mixer (tumbler mixer, Showa Kagaku Kikai Co.).

Physical properties of the immediate-release portion are as follows: particle size distribution is that 16 mesh on 1%, 16–30 mesh 14%, 30–60 mesh 22%, 60–100 mesh 36%, 100 mesh pass 27%, median particle size is 214 μm , loose specific volume is 1.8 ml/g, dense specific volume is 1.4 ml/g.

Manufacturing of the Prolonged-Release Portion by Dry Granulation The prolonged-release portion consisting of PPA, Ceolus KG-801, Fujicalin SG, and Metolose 90SH4000 were granulated by a roller compactor (roller compactor mini, Freund Ind. Co.). The compactor was equipped with a concavo-convex roller pair with serration, type DPS.¹¹⁾ The diameter and width of the roller were 100 and 35 mm, respectively. The roller compaction pressure was 46.7 kN. The compacts were size-reduced with a screening mill (power mill, Showa Kagaku Kikai Co.). The size-reduced granules were mixed with Mg-St and Sylysia 320 by a diffusion mixer (tumbler mixer, Showa Kagaku Kikai Co.). Physical properties of the prolonged-release portion by dry granulation are as follows: particle size distribution is that 16 mesh on 1%, 16–30 mesh 23%, 30–60 mesh 20%, 60–100 mesh 24%, 100 mesh pass 32%, median particle size is 225 μm , loose specific volume is 2.1 ml/g, dense specific volume is 1.5 ml/g.

Manufacturing of the Prolonged-Release Portion by Direct Compression The prolonged-release portion consisting of PPA, Ceolus KG-801, Fujicalin SG, and Metolose 90SH4000 were directly mixed with Mg-St and Sylysia 320 by a diffusion mixer (tumbler mixer, Showa Kagaku Kikai Co.). Physical properties of the prolonged-release portion by direct compression are as follows: median particle size is 43 μm , loose specific volume is 2.5 ml/g, dense specific volume is 1.8 ml/g.

Bilayer Compression The rotary bilayer tablets press (aquarius 0512LD2AX, Kikusui Seisakusho Co.) was utilized for bilayer compression. A schematic representation of bilayer compression is illustrated in Fig. 1. We termed the method A: a prolonged-release portion was fed as the first layer and an immediate-release portion was fed as the second layer in bilayer compression, and termed the method B: an immediate-release portion was fed as the first layer and a prolonged-release portion was fed as the second layer in bilayer compression. A pre-compression pressure and main compression pressure were 6.5 and 91 MPa, respectively. Dies were of 13.5 × 6.2 mm size in an oblong shape, and concave punches of 3.8 mm radius of curvature were used. Each of the layer weighed 200 mg. Thickness of bilayer caplets is 5.5 mm ± 6%. Hardness of bilayer caplets is 100–140 N. Unless

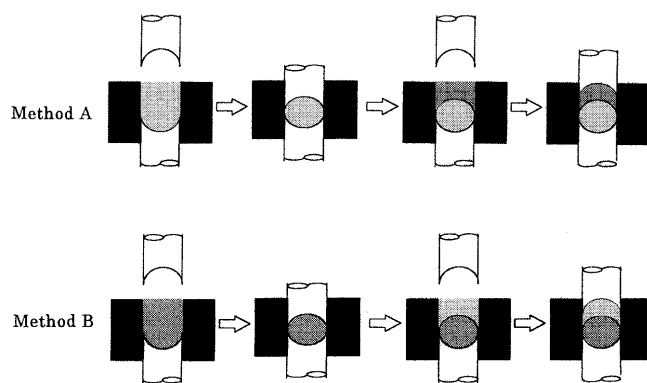


Fig. 1. Schematic Representation of Bilayer Compression

■, Immediate-release portion; □, prolonged-release portion.

otherwise specified, bilayer caplets by method B was used in the experiments.

Dissolution Study on the Paddle Method The matrix tablets and bilayer caplets were subjected to the dissolution test using a JP XIII paddle apparatus (dissolution tester, Toyama Sangyo Co.) in 900 ml of water maintained at 37 ± 0.5 °C, with the paddle rotating at 100 rpm.

In the experiments in which the effect of paddle rotating speed was investigated, the paddle rotating speed was varied from 50 to 200 rpm. In the experiments in which the effect of dissolution medium was investigated, the dissolution medium was changed from water to the JP XIII 1st fluid (pH 1.2) or the JP XIII 2nd fluid (pH 6.8). Measurement of PPA release was performed by HPLC (LC-9A instrument, Shimadzu Corporation) with UV detection at 210 nm. The mobile phase used was 0.013 M sodium lauryl sulfate aqueous solution (pH 2.0): methanol (1:2) at a flow rate of 1.0 ml/min through a C₁₈ column (Wakosil 5C18 AR 6 mm φ × 150 mm). The column temperature was 40 °C.

Dissolution Study on the Paddle-Beads Method On the paddle-beads method,^{12,13)} the apparatus used was the same as that described above. The dissolution medium was water maintained at 37 ± 0.5 °C. The medium volume was 250 ml. A total of 2500 polystyrene beads (diameter 6.5 mm, Wako Pure Chemical Co.) was added to the medium. The paddle rotating speed was 25 rpm. Measurement of released PPA was performed as described above.

Similarity Assessment of Dissolution Profiles Moore and Flanner suggested a simple model independent approach uses a similarity factor to compare dissolution profiles.¹⁴⁾ The similarity factor (f_2) was calculated using the following Eq. 1

$$f_2(\%) = 50 \log \left\{ \left[1 + \frac{1}{n} \sum_{i=1}^n w_i (R_i - T_i)^2 \right]^{-0.5} \right\} \times 100 \quad (1)$$

where log is logarithm to base 10, n is number of sampling time points, Σ is summation over all time points, w_i is an optional weight factor, R_i is dissolution at time point i of the reference, and T_i is dissolution at time point i of the test. For curves to be considered similar, f_2 values should be closed to 100%. An f_2 value between 50% and 100 % suggests the two dissolution profiles are similar. In this study, all the values are to be treated equally. Accordingly, w_i is 1.0. In Fig. 3, the reference dissolution profile is the PPA dissolution profile from the 90SH4000 matrix tablets. In Fig. 4, the reference dissolution profile is the targeted dissolution profile. In Figs. 5–8, the reference dissolution profile is the PPA dissolution profile from the bilayer caplets having the prolonged-release portion manufactured by direct compression in the second layer on the paddle method. The paddle method condition is as follows: dissolution medium is water, paddle rotating speed is 100 rpm.

Results and Discussion

Formulation of the Sustained-Release PPA Bilayer Caplets Effect of PPA: HPMC2208 ratio on PPA dissolution characteristics from the matrices was investigated for the selection of drug: polymer ratio which gives the more pronounced prolonged-release effect with suitable weight of

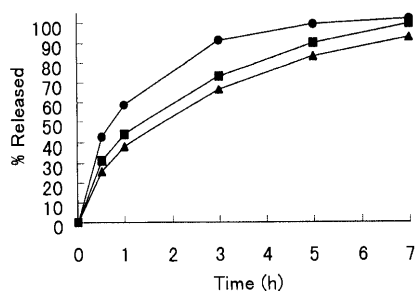


Fig. 2. Effect of PPA : Metolose 90SH4000 Ratio in the Matrices on PPA Dissolution Characteristics ($n=3$)

PPA: Metolose 90SH4000 ratio: ●, 1:2; ■, 1:4; ▲, 1:6.

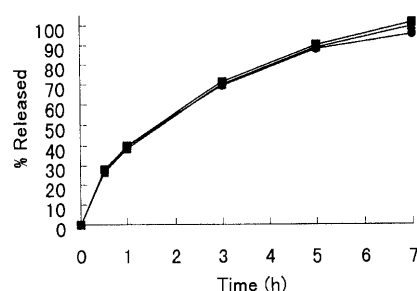


Fig. 3. Effect of HPMC2208 Viscosity Grade in the Matrices on PPA Dissolution Characteristics ($n=6$)

●, Metolose 90SH4000; ■, Metolose 90SH15000; ▲, Metolose 90SH100000.

tablets. Metolose 90SH4000 was chosen as HPMC2208 in this experiment. With an increase in Metolose 90SH4000 ratio in the matrices, the dissolution rate of PPA from the Metolose 90SH4000 matrices decreased. This is shown in Fig. 2. The time to release 90% of PPA from Metolose 90SH4000 matrices were about 3, 5, and 7 h for PPA: Metolose 90SH4000 ratio were 1:2, 1:4, and 1:6, respectively. The ratio of 1:6 was most suitable for the prolonged-release characteristics of PPA. On the ratio of 1:6, the Metolose 90SH4000 level in the matrix with suitable weight was 60%. High Metolose 90SH4000 level in the matrix was required for giving the matrix the prolonged PPA dissolution characteristics. It was due to highly water-soluble property of PPA. Maximally, 405 mg of PPA can be dissolved in 1 ml water at 37 °C.

Alderman²⁾ suggested that increasing viscosity of polymer in a matrix formulation increases the gel layer viscosity and the strength of gels, the resulting gelatinous diffusion layer becomes stronger and more resistant to diffusion or erosion. Therefore, increases in polymer viscosity will generally slow drug release from matrices. He reported the case of riboflavin. The extent of swelling of Metolose 90SH is in the order 90SH100000 > 90SH15000 > 90SH4000.¹⁵⁾ Higher viscosity grade shows a greater swelling volume. However, PPA dissolution characteristics from matrices with differing HPMC2208 viscosity grade showed similar dissolution profiles. This is shown in Fig. 3. The f_2 values were 75.2% for Metolose 90SH15000 matrix tablets and 80.8% for Metolose 90SH100000 matrix tablets. Since overall dissolution profiles were similar and the f_2 values were between 50% and 100%, we confirmed that viscosity grades did not significantly affect PPA dissolution characteristics from the HPMC2208 matrices.

Although riboflavin is a water-insoluble drug, PPA is a

highly water-soluble drug. Accordingly, it was suggested that PPA can easily diffuse through hard gelatinous layer in the matrix. Therefore, viscosity grades did not significantly affect PPA dissolution characteristics from the HPMC2208 matrices. In addition, the gel layers formed might be strong enough to resist erosion due to their high polymer concentration in the matrices.

PPA pharmacokinetics study had previously been conducted for the purpose of the formulation of the bilayer caplets having the most suitable sustained-release characteristics of PPA in humans. The most suitable sustained-release characteristics of PPA from the bilayer caplets, that is a twice daily medicine, have the same maximum plasma concentration (C_{max}), the prolonged mean residence time (MRT), and 1.5 fold area under the plasma concentration-time curve (AUC) as compared with an immediate-release dosage form that is a three times daily medicine. The study was performed using 3 different PPA release formulations that are one immediate-release formulation whose PPA is completely dissolved within 0.5 h, and two prolonged-release formulations ($T_{50}=0.9$ h and $T_{50}=2.3$ h). The 3 different formulations were orally administered in humans in a crossover design. The most suitable sustained-release characteristics of PPA was calculated from the individual PPA plasma concentration data of each formulation in the study. As a result, the targeted PPA dissolution profile *in vitro* was obtained through the calculation of the most suitable sustained-release characteristics of PPA *in vivo*. From the targeted PPA dissolution profile, we decided that PPA content in the immediate-release portion was 5 mg and PPA content in the prolonged-release portion was 20 mg in a bilayer caplet. Therefore, we formulated the prolonged-release portion consisting of 10% PPA, 30% excipients (the diluents, the lubricant, and the glidant), and 60% Metolose 90SH4000 into the sustained-release PPA bilayer caplets.

Effect of Manufacturing Method of the Prolonged-Release Portion on PPA Dissolution Characteristics The specific volume of the prolonged-release portion manufactured by wet granulation became high as compared with the physical mixture because of swelling property of Metolose 90SH4000 and 60% Metolose 90SH 4000 level in the prolonged-release portion. We found that the prolonged-release portion manufactured by wet granulation is unsuitable for compression using the rotary bilayer tablets press. Accordingly, dry granulation and direct compression were chosen for manufacturing methods of the prolonged-release portion.

PPA dissolution characteristics from two types of bilayer caplets, whose prolonged-release portion was manufactured by dry granulation and direct compression, were investigated. This is shown in Fig. 4. The targeted PPA dissolution profile is also shown in Fig. 4. The PPA dissolution characteristics from two types of the formulated bilayer caplets showed the prolonged dissolution profile after rapid dissolution and was close to the targeted profile. The f_2 values were 68.1% for bilayer caplets having the prolonged-release portion manufactured by direct compression and 58.6% for bilayer caplets having the prolonged-release portion manufactured by dry granulation. We confirmed that the dissolution profiles from two types of the formulated bilayer caplets were similar to the targeted profile. Moreover, we confirmed that manufacturing methods of the prolonged-release portion

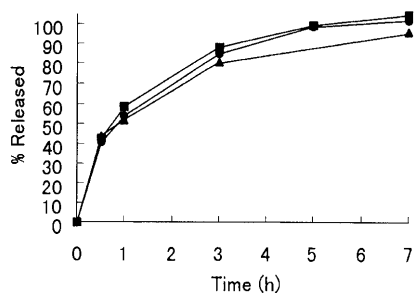


Fig. 4. Effect of Manufacturing Method of the Prolonged-Release Portion on PPA Dissolution Characteristics from Bilayer Caplets ($n=6$)

●, Direct compression; ■, dry granulation; ▲, targeted dissolution profile.

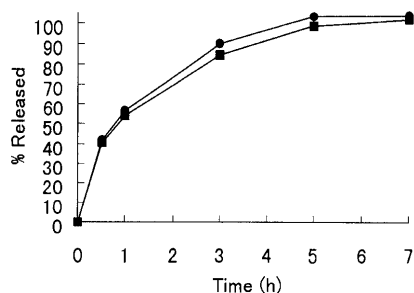


Fig. 5. Effect of Filling Order of the Prolonged-Release Portion in Bilayer Compression on PPA Dissolution Characteristics from Bilayer Caplets ($n=6$)

●, Method A: the prolonged-release portion is the first layer. ■, Method B: the prolonged-release portion is the second layer.

did not significantly affect the PPA dissolution characteristics from the bilayer caplets. It was suggested that the swelling ability of Metolose 90SH4000 is not significantly changed by the mechanical force that is the roller compaction pressure. This result confirms the findings by Sheskey *et al.*¹⁶⁾ that no significant difference in drug release on HPMC matrices was observed regardless of the manufacturing methods in the case that drug is niacinamide which is a highly water-soluble drug and HPMC level is 30%.

Effect of Filling Order of the Prolonged-Release Portion in Bilayer Compression on PPA Dissolution Characteristics The bilayer caplets by method A and method B were chosen in this experiment. Different filling order of the prolonged-release portion in bilayer compression gave different shape of the prolonged-release portion in bilayer caplets. Shape is an important factor for dissolution from matrices. Ford *et al.* investigated the influences of tablet shape on the release rates of promethazine hydrochloride tablets.¹⁷⁾ They concluded that the release rate is proportional to the surface area of tablet since release rates decreased as the tablet surface area decreased. However, PPA dissolution profiles from two types of bilayer caplets showed similar curves. This is shown in Fig. 5. The f_2 value was 71.8%. The filling order of the prolonged-release portion in bilayer compression related to the compressed shape did not significantly affect the PPA dissolution characteristics from bilayer caplets. Since the shape of prolonged-release portion readily changed by swelling of Metolose 90SH4000 in the dissolution test, the shape of prolonged-release portion in the bilayer caplets did not significantly affect PPA dissolution characteristics in this case.

Effect of Dissolution Medium on PPA Dissolution

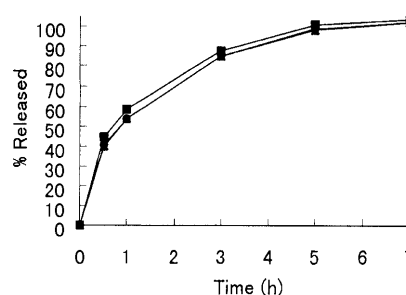


Fig. 6. Effect of Dissolution Medium on PPA Dissolution Characteristics from the Bilayer Caplets ($n=6$)

●, Water; ■, the JP XIII 1st fluid (pH 1.2); ▲, the JP XIII 2nd fluid (pH 6.8).

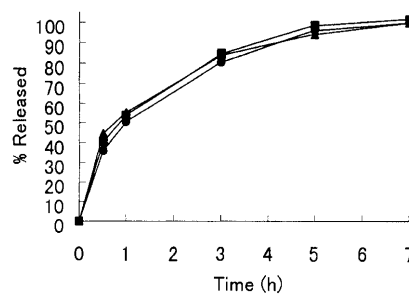


Fig. 7. Effect of Paddle Rotating Speed on PPA Dissolution Characteristics from the Bilayer Caplets ($n=6$)

●, 50 rpm; ■, 100 rpm; ▲, 200 rpm.

Characteristics It is important for the sustained-release product to have pH independent drug release characteristics owing to reliable absorption in the digestive organ. Therefore, the effect of dissolution medium on the PPA dissolution characteristics from the bilayer caplets was investigated. This is shown in Fig. 6. The f_2 values were 74.8% for the JP XIII 1st fluid and 98.7% for the JP XIII 2nd fluid. The dissolution medium did not significantly affect PPA dissolution characteristics from the bilayer caplets. The PPA dissolution characteristic from bilayer caplets was pH independent, because Metolose 90SH4000 is pH independent swelling polymer²⁾ and PPA, 412 and 88 mg, can be dissolved in 1 ml of the JP XIII 1st fluid and the JP XIII 2nd fluid at 37 °C, respectively.

Effect of Paddle Rotating Speed on PPA Dissolution Characteristics The significance of mechanical shear in terms of the *in vivo* drug release has been demonstrated on hydrophilic polymer matrices.¹⁸⁾ Abrahamsson *et al.* suggested that investigation of the effect of paddle rotating speed is meaningful in the test for investigation of prandial effects on hydrophilic matrix tablets.¹⁹⁾ Figure 7 shows that effect of paddle rotating speed on PPA dissolution characteristics from the bilayer caplets. The f_2 values were 71.5% for 50 rpm and 74.8% for 200 rpm. It was found that the dissolution characteristics is not significantly affected by the paddle rotating speed.

PPA Dissolution Characteristics on the Paddle-Beads Method Aoki *et al.* proposed the paddle-beads method to introduce a mechanical impact force into the paddle method for the purpose of simulating the *in vivo* dissolution.^{12,13)} Therefore, the paddle-beads method was performed to examine the effect of mechanical shear on the PPA dissolution characteristics. Figure 8 shows the PPA dissolution characteristics on the paddle-beads method. The f_2 value was 67.7%.

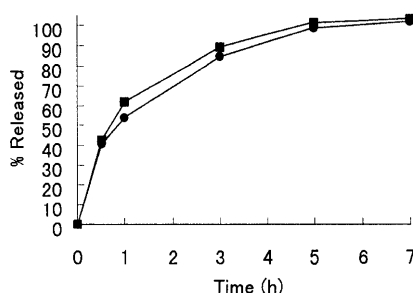


Fig. 8. PPA Dissolution Characteristics from the Bilayer Caplets on the Paddle-Beads Method ($n=6$)

●, the paddle method: dissolution medium, water 900 ml; paddle rotating speed, 100 rpm. ■, the paddle-beads method: dissolution medium, water 250 ml with 2500 beads; paddle rotating speed, 25 rpm.

The PPA dissolution characteristics was not significantly different from those on the paddle method. We found that the PPA dissolution characteristics from the bilayer caplets containing the Metolose 90SH4000 matrix is not significantly affected by mechanical shear that is the combination of the paddle rotating and the beads. This is due to the fact that Metolose 90SH4000 has excellent hydro-gel strength¹⁵ and Metolose 90SH4000 level in the prolonged-release portion is 60%. It was suggested that the PPA dissolution from the formulated bilayer caplets is less susceptible to the influence of mechanical shear arising from digestive actions or friction force between the bilayer caplets and the gastrointestinal mucus.

Conclusions

PPA is a highly water-soluble drug that can easily diffuse through hard gelatinous layer in the matrices. Therefore, we formulated the prolonged-release portion consisting of 10% PPA, 30% excipients, and 60% Metolose 90SH4000 into the sustained-release PPA bilayer caplets. The PPA dissolution characteristics from the formulated bilayer caplets showed the prolonged dissolution profile after rapid dissolution and was close to the targeted profile calculated from PPA pharmacokinetics study. The PPA dissolution characteristics from the formulated bilayer caplets was not significantly affected by manufacturing methods of the bilayer caplets. The PPA

dissolution characteristics from the bilayer caplets was pH independent. Moreover, the PPA dissolution characteristics from the bilayer caplets was not significantly affected by the mechanical shear, such as paddle rotating speed and the beads in the medium. Similarity of dissolution profiles was confirmed by overall profiles and the similarity factor (f_2).

The sustained-release PPA bilayer caplets is expected to present constant prolonged-release of PPA after rapid dissolution *in vivo* without dissolution change due to pH and mechanical shear during the transition in gastrointestinal tract.

References and Notes

- 1) Kanfer I., Haigh J. M., Dowse R., *Analytical Profiles of Drug Substances*, **12**, 357—383 (1983).
- 2) Alderman D. A., *Int. J. Pharm. Tech. & Prod. Mfr.*, **5**, 1—9 (1984).
- 3) Hashem F. M., El-Shaboury M. H., Gabr K. E., *Drug Dev. Ind. Pharm.*, **20**, 1795—1809 (1994).
- 4) Rosen E., Swintosky J. V., *J. Pharm. Pharmacol.*, **12**, 237T—244T (1960).
- 5) El-Khawas M., El-Khordairy K., Samaha M. W., *Pharm. Ind.*, **55**, 392—395 (1993).
- 6) Davis S. S., Stockwell A. F., Taylor M. J., Hardy J. G., Whalley D. R., Wilson C. G., Bechgaard H., Christensen F. N., *Pharm. Res.*, **3**, 208—213 (1986).
- 7) Feely L. C., Davis S. S., *Pharm. Res.*, **6**, 274—278 (1989).
- 8) Panomsuk S. P., Hatanaka T., Aiba T., Katayama K., Koizumi T., *Chem. Pharm. Bull.*, **44**, 1039—1042 (1996).
- 9) Tomida Y., Yokohama S., Maki M., Toguchi H., Shimamoto T., *J. Takeda Res. Lab.*, **36**, 83—89 (1977).
- 10) Yamakawa I., Shimomura M., Hattori T., Watanabe S., Tsutsumi J., Shinoda A., Miyake Y., *J. Pharmacobio-Dyn.*, **9**, 947—952 (1986).
- 11) Funakoshi Y., Asogawa T., Satake E., *Drug Dev. Ind. Pharm.*, **3**, 555—573 (1977).
- 12) Aoki S., Uesugi K., Tatsuishi K., Ozawa H., Kayano M., *Int. J. Pharm.*, **85**, 65—73 (1992).
- 13) Aoki S., Ando H., Tatsuishi K., Uesugi K., Ozawa H., *Int. J. Pharm.*, **95**, 67—75 (1993).
- 14) Moore J. M., Flanner H. H., *Pharm. Technol.*, **20**, 64—74 (1996).
- 15) Metolose technical information, Shin-Etsu Chemical Co., 1993.
- 16) Sheskey P. J., Cabelka T. D., Robb R. T., Boyce B. M., *Pharm. Technol.*, **18**, 132—150 (1994).
- 17) Ford J. L., Rubinstein M. H., McCaul F., Hogan J. E., Edgar P. J., *Int. J. Pharm.*, **40**, 223—234 (1987).
- 18) Shameen M., Katori N., Aoyagi N., Kojima S., *Pharm. Res.*, **12**, 1049—1054 (1995).
- 19) Abrahamsson B., Roos K., Sjögren J., *Drug Dev. Ind. Pharm.*, **25**, 765—771 (1999).

Sustained-Release Phenylpropanolamine Hydrochloride Bilayer Caplets Containing the Hydroxypropylmethylcellulose 2208 Matrix. II. Effects of Filling Order in Bilayer Compression and Manufacturing Method of the Prolonged-Release Layer on Compactibility of Bilayer Caplets

Shinji OHMORI* and Tadashi MAKINO

Healthcare Research Laboratories, Consumer Healthcare Company, Takeda Chemical Industries, Ltd., 17–85, Jusohonmachi 2-Chome, Yodogawa-ku, Osaka 532–8686, Japan. Received December 3, 1999; accepted January 29, 2000

The purpose of this study was to establish the manufacturing method of the formulated bilayer caplets containing the hydroxypropylmethylcellulose 2208 (HPMC2208) matrix without lamination. In manufacturing the bilayer caplets containing the HPMC2208 (Metolose 90SH4000) matrix, some bilayer caplets were cracked. We found that cracking of bilayer caplets is not the separation of two layers, but lamination of the prolonged-release layer. It was assumed that Metolose 90SH4000 causes lamination of the prolonged-release layer.

Two factors, roller compaction pressure on dry granulation of the prolonged-release layer and filling order of the prolonged-release layer in bilayer compression, were related to lamination of bilayer caplets. The compactibility of the prolonged-release layer decrease with an increase in roller compaction pressure on dry granulation. The compactibility of the prolonged-release layer manufactured by direct compression is superior to that manufactured by dry granulation. The compactibility of the prolonged-release layer in the shape of the second layer, convexo-concave, is superior to that in the shape of the first layer, convexo-convex. This is due to the fact that the density distribution inside the compact in the shape of convexo-concave was more uniform than that in the shape of convexo-convex.

The manufacturing method of the formulated bilayer caplets having the prolonged-release layer whose Metolose 90SH4000 content is 60% without lamination is as follows: the prolonged-release layer manufactured by direct compression is fed as the second layer in bilayer compression.

Key words lamination; bilayer caplet; hydroxypropylmethylcellulose 2208; compactibility; convexo-concave; direct compression

In our previous work,¹⁾ we formulated the sustained-release phenylpropanolamine hydrochloride (PPA) bilayer caplets containing the hydroxypropylmethylcellulose 2208 (HPMC2208), Metolose 90SH4000, matrix to expect the prolonged-release characteristics of PPA after rapid dissolution *in vivo* without dissolution change due to pH and mechanical shear.

The bilayer caplets have deep convex face that is 3.8 mm radius of curvature (3.8R) to improve easy of swallowing. It is widely known that deep convex-faced tablets have the tendency of capping and lamination.²⁾ Establishment of the manufacturing method of the formulated bilayer caplets containing the HPMC2208 matrix with an excellent compactibility is important for manufacturing the good-quality product without capping and lamination.

There have been many papers recently on the compactibility of HPMC2208. Nokhodchi *et al.* investigated the effect of particle size and viscosity grade on the compaction properties of HPMC2208,³⁾ the effect of moisture on the compaction of HPMC2208,^{4,5)} and the effects of compression rate and force on the compaction properties of different viscosity grades of HPMC2208.⁶⁾ Malamataris *et al.* investigated the effect of particle size and sorbed moisture on compactibility of tableted HPMC2208.^{7,8)} Furthermore, there are several reports on the compactibility of the formulated matrix tablets whose HPMC2208 content is not more than 30%.^{9–11)}

However, information on multilayer compression is limited. Li *et al.* suggested that the compression force on the first layer was the major factor affecting lamination of bilayer tablets and the compression zone in the die cavity of the sec-

ond layer was the critical factor in controlling tablet capping tendency.¹²⁾ Karehill *et al.* suggested that a high fragmentation tendency of tableting compounds and excipients will facilitate the formation of mechanically strong bilayer tablets.¹³⁾ Yang *et al.* investigated that the compression behavior and compactibility of the triple-layer tablets containing poly (ethylene oxide).¹⁴⁾

Nevertheless, in the above literature and a review of the literature,¹⁵⁾ information concerning the compression characteristics of formulated bilayer caplets containing a HPMC2208 matrix is rarely mentioned.

The purpose of this study was to establish the manufacturing method of the formulated bilayer caplets (BENZA[®]AL) containing the HPMC2208 (Metolose 90SH4000) matrix without lamination. In this study, effects of filling order in bilayer compression and manufacturing method of the prolonged-release layer whose Metolose 90SH4000 content is 60% on the compactibility of bilayer caplets were investigated.

Experimental

Materials PPA (Alps Pharmaceutical Ind. Co.) was used as a sustained-release drug. HPMC 2208 (Metolose 90SH4000, Shin-Etsu Chemical Co.) was used as a hydrophilic polymer of the prolonged-release matrices. Metolose 90SH4000 used in the experiments is as follows; median particle size 60–70 μm , moisture content (loss on drying, 1 g, 105 °C, 1 h) 3.5–5.0%.

Microcrystalline cellulose (Ceolus KG-801, Asahi Chemical Ind. Co.) and spray-dried anhydrous dibasic calcium phosphate (Fujicalin SG, Fuji Chemical Ind. Co.) were used as diluents in the prolonged-release layer. Other excipients used as components of the immediate-release layer and the prolonged-release layer were described in the previous paper.¹⁾ Microcrys-

* To whom correspondence should be addressed. e-mail: Ohmori-Shinji@takeda.co.jp

talline cellulose (Avicel PH101, Asahi Chemical Co.) and directly compressible lactose (Tabletose, Meggle GmbH) were used for measurements of tensile strength. All other chemicals were of reagent grade.

Measurement of Tensile Strength Tablets (350 mg) were directly compacted with a compression instrument (Autograph AG-5000B, Shimadzu Corporation) using a 10 mm diameter flat-faced punch. The compression speed was 10 mm/min. The ejection speed was 100 mm/min. The compression pressure was varied from 98 to 196 MPa. The tablet crushing force was measured by a diametrical compression using the compression instrument. Tensile strength (T) was calculated using the following Eq. 1:

$$T = 2F/\pi DL \quad (1)$$

where F is the crushing force, D is the tablet diameter, and L is the tablet thickness.¹⁶⁾ In the experiment on the effect of roller compaction pressure on the compactibility of the prolonged-release layer, the granules (200 mg), particle size fraction is 100–140 mesh, were directly compacted with the compression instrument using a 8 mm diameter flat-faced punch. The compression pressure was 98 MPa.

Manufacturing of the Immediate-Release Layer by Wet Granulation Manufacturing of the immediate-release layer by wet granulation was described in the previous paper.¹⁾ PPA content in the immediate-release layer was 5 mg in a bilayer caplet.

Manufacturing of the Prolonged-Release Layer by Dry Granulation Manufacturing of the prolonged-release layer consisting of PPA, Ceolus KG-801, Fujicalin SG, and Metolose 90SH4000 by dry granulation was described in the previous paper.¹⁾ PPA content in the prolonged-release layer was 20 mg in a bilayer caplet. The roller compaction pressure was varied from 3.1 to 46.7 kN. Unless otherwise specified, the roller compaction pressure used in the experiments was 46.7 kN.

Manufacturing of the Prolonged-Release Layer by Direct Compression Manufacturing of the prolonged-release layer consisting of PPA, Ceolus KG-801, Fujicalin SG, and Metolose 90SH4000 by direct compression was described in the previous paper.¹⁾ PPA content in the prolonged-release layer was 20 mg in a bilayer caplet.

Bilayer Compression Bilayer compression was described in the previous paper.¹⁾ We termed the method A: a prolonged-release portion was fed as the first layer and an immediate-release portion was fed as the second layer in bilayer compression, and termed the method B: an immediate-release portion was fed as the first layer and a prolonged-release portion was fed as the second layer in bilayer compression. A pre-compression pressure and main compression pressure were 6.5 and 91 MPa, respectively. Dies were of 13.5×6.2 mm size in an oblong shape, and concave punches of 3.8R were used.

Microphotographs of Tablets Microphotographs of tablets were taken using a video microscope (VMS-5000, SCALAR) and a video printer (Mavigraph UP-1800, SONY).

Measurement of Capping Ratio Flat, 14 mm radius of curvature (14R) convexo-convex, 7.5 mm radius of curvature (7.5R) convexo-convex, 7.5R convexo-concave tablets consisting of the prolonged-release layer manufactured by dry granulation were used. Flat tablets were compacted using a flat-faced upper punch and a flat-faced lower punch. Convexo-convex tablets were compacted using a concave-faced upper punch and a concave-faced lower punch. In particular, convexo-concave tablets were compacted using a concave-faced upper punch and a convex-faced lower punch. We assumed that the capping ratio of convexo-concave tablets is the capping ratio of tablets in the shape of second layer on bilayer caplets. The compression pressure was 98 MPa. Other compression condition was the same described in the experiment of measurement of tensile strength. The capping ratio was measured by counting the number of capped tablets in the friability test. The friability test was conducted 30 rpm for 3 min with the special friability tester. The diameter of the tester was 50 cm. The stainless steel board was attached to the tester. The board was where tablets were dropped in the tester.

Evaluation of the Uniformity of Density Distribution inside the Tablets Flat, 7.5R convexo-convex, 7.5R convexo-concave tablets consisting of the prolonged-release layer manufactured by dry granulation were used. The difference in boring speed between the center and the edge on the tablets have been used to evaluate the uniformity of density distribution inside the tablets. Spinalyzer (Japan Electron Optics Laboratory) was utilized for measurement of boring speed. The load was 90 g. The drill diameter was 1 mm. The drill revolving speed was 50 rpm.

Computerized Tomograms (CT) of Bilayer Caplets CT of bilayer caplets were performed by the composite X-ray examination system (Musashi, NS-ELEX Co.).

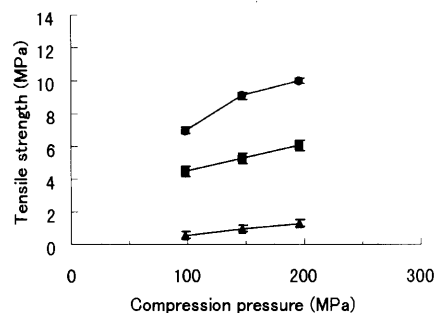


Fig. 1. Relationship between Compression Pressure and Tensile Strength
●, Avicel PH101; ■, Metolose 90SH4000; ▲, Tabletose; mean ± S.D.; $n=5$.

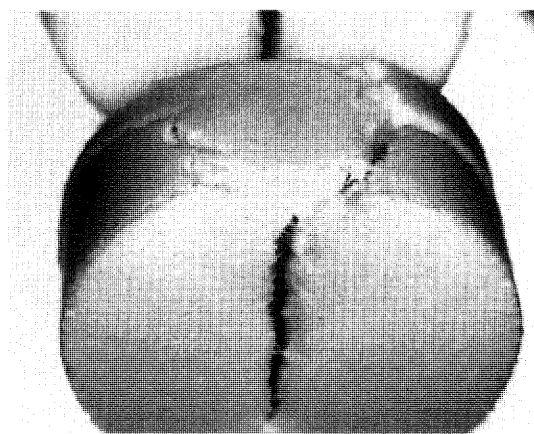


Fig. 2. Microphotograph of Metolose 90SH4000 Tablets after the Diametrical Compression Test

Results and Discussion

The Compactibility of Metolose 90SH4000 The tensile strength of Metolose 90SH4000 tablets was investigated as compared with the tensile strengths of Avicel PH101 tablets and Tabletose tablets. This is shown in Fig. 1. The tensile strength of Metolose 90SH4000 tablets was inferior to the tensile strength of Avicel PH101 tablets, but was superior to the tensile strength of Tabletose tablets. Since Tabletose is a directly compressible material, the compactibility of Metolose 90SH4000 is good.

Figure 2 shows the microphotograph of the Metolose 90SH4000 tablets after the diametrical compression test. The tablets were not only fractured in the diametrical direction but laminated. We found that Metolose 90SH4000 has a tendency of lamination. Nakagawa and co-workers investigated the effects of morphology of aspirin crystals on the preferred orientation in a tablet using an X-ray diffraction method.^{17,18)} They reported that thin, plate-like crystals had the greater tendency to orient preferentially in a tablet and showed a greater tendency of lamination in the compression process. By observation of Metolose 90SH4000 tablets after the diametrical compression test in Fig. 2, it was assumed that the reason why Metolose 90SH4000 has a tendency of lamination that Metolose 90SH4000 is of fibrous structure that would preferentially orient in a tablet during compression.

The above mentioned facts indicate that Metolose 90SH4000 has both a good compactibility and a tendency of lamination.

Cracking of Bilayer Caplets In manufacturing the formulated bilayer caplets having the prolonged-release layer

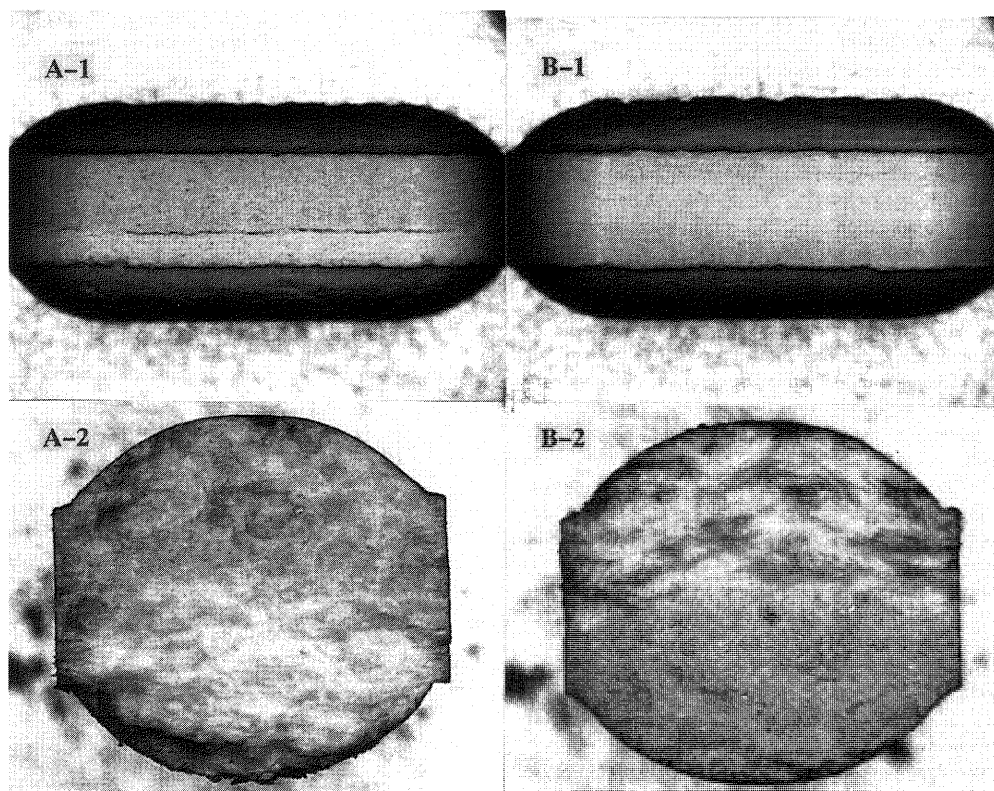


Fig. 3. Microphotographs of Side View and Cross-Section of Cracked Bilayer Caplets

A) Method A: the prolonged-release layer manufactured by dry granulation is the first layer. B) Method B: the prolonged-release layer manufactured by dry granulation is the second layer. 1) Side view. 2) Cross-section.

whose Metolose 90SH4000 content is 60%, some bilayer caplets were cracked. It was usually guessed that cracking would be the separation between the first layer and the second layer due to deficient bonding of the two layers. In order to confirm the cause of cracking of bilayer caplets, side view and cross-section of cracked caplets were observed using a video microscope. The microphotographs of side view and cross-section of cracked caplets are shown in Fig. 3. Cracked caplets have not separated the second layer from the first layer. We found that cracking of bilayer caplets results from lamination in the prolonged-release layer.

From the results shown in Figs. 2 and 3, it was suggested that Metolose 90SH4000, whose content in the prolonged-release layer is 60%, causes lamination of the prolonged-release layer. Moreover, the deep convex face which is 3.8 R on the bilayer caplets promoted lamination.

Relationships between Manufacturing Methods of Bilayer Caplets and Number of Laminated Bilayer Caplets

The relationships between manufacturing methods of bilayer caplets and number of laminated bilayer caplets were investigated. This is shown in Fig. 4. Two factors, roller compaction pressure on dry granulation of the prolonged-release layer and filling order of the prolonged-release layer in bilayer compression, were related to lamination of bilayer caplets. An increase in roller compaction pressure increased the number of laminated bilayer caplets. When filling order of the prolonged-release layer in bilayer compression changed from the first filling (method A) to the second filling (method B), the number of laminated caplets were notably reduced. Almost all the caplets whose the prolonged-release layer manufactured by dry granulation in the first layer were laminated.

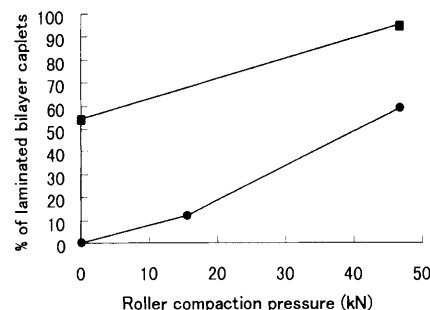


Fig. 4. Relationships between Manufacturing Methods of Bilayer Caplets and Number of Laminated Bilayer Caplets ($n=100$)

■, Method A: the prolonged-release layer is the first layer. ●, Method B: the prolonged-release layer is the second layer.

In contrast, all the caplets whose the prolonged-release layer manufactured by direct compression, *i.e.*, the roller compaction pressure is 0 kN, in the second layer have never laminated.

Effect of Roller Compaction Pressure on Compactibility of the Prolonged-Release Layer Difference between dry granulation and direct compression lies in roller compaction pressure applied. Therefore, effect of roller compaction pressure on the compactibility of the prolonged-release layer was investigated. This is shown in Fig. 5. The results indicate the tensile strength of tablets consisting of the prolonged-release layer notably decrease with an increase in roller compaction pressure on dry granulation even if particle size was the same. The tensile strength of tablets consisting of the prolonged-release layer manufactured by direct compression, *i.e.*, the roller compaction pressure is 0 kN, shows

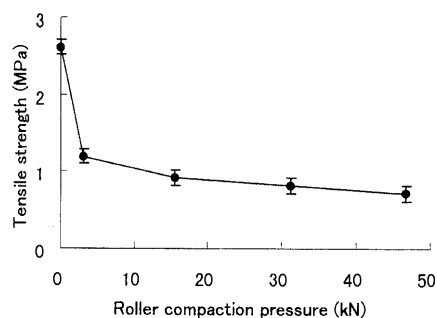


Fig. 5. Effect of Roller Compaction Pressure on the Tensile Strength of Tablets Consisting of the Prolonged-Release Layer

Particle size fraction of the prolonged-release layer: 100–140 mesh, mean \pm S.D.; $n=5$.

the highest tensile strength. Accordingly, the compactibility of the prolonged-release layer manufactured by direct compression is superior to that manufactured by dry granulation. This results confirmed the findings of Sheskey *et al.*^{9,10)}

Mollan, Jr. *et al.* described that microcrystalline cellulose owes most of its high tensile strength to hydrogen bonds.¹⁹⁾ During roller compaction, Metolose 90SH4000 undergoes plastic deformation^{3–8)} which causes an increase in available surface area and this allows an increased number of bonds to be potentially formed. It is possible that the number of hydrogen bonding sites could be saturated and thus would be rigid granules that is unavailable for further bonding on compression as in the case of microcrystalline cellulose.

Effect of Filling Order of the Prolonged-Release Layer in Bilayer Compression on Compactibility of Bilayer Caplets Different filling order of the prolonged-release layer in bilayer compression gave different shape of the prolonged-release layer in bilayer caplets. The compressed shape of the first layer is convexo-convex and the compressed shape of the second layer is convexo-concave. The effect of the compressed shape on the compactibility was investigated by measuring capping ratios of several shape of tablets. Figure 6 shows the capping ratios of tablets consisting of the prolonged-release layer manufactured by dry granulation whose shape was flat, 14R convexo-convex, 7.5R convexo-convex, and 7.5R convexo-concave. An decrease in the punch radius of curvature increased the capping ratio. In other words, deep convex face of tablets promoted capping. The capping ratio of convexo-concave tablets was smaller than that of convexo-convex tablets though the punch radius of curvature was the same. This result has attracted considerable interest.

Sugimori *et al.* suggested a linear relationship expressed by Eq. 2

$$Q_{rc} = Q_{rf} + k \left(\frac{T_v}{T_e} - 1 \right) \quad (2)$$

where Q_{rc} is the extrapolated residual die wall pressure of a convexo-convex tablet, Q_{rf} is that of a flat tablet, k is constant, T_v is the thickness of the flat tablet having the same diameter and the same volume as the convexo-convex tablet, and T_e is the edge thickness of the convexo-convex tablet.²⁰⁾ They reported that an increase in T_v/T_e -value resulted in an increase in extrapolated residual die wall pressure. They concluded that the extrapolated residual die wall pressure coincided with the capping tendency of tablets and T_v/T_e -value

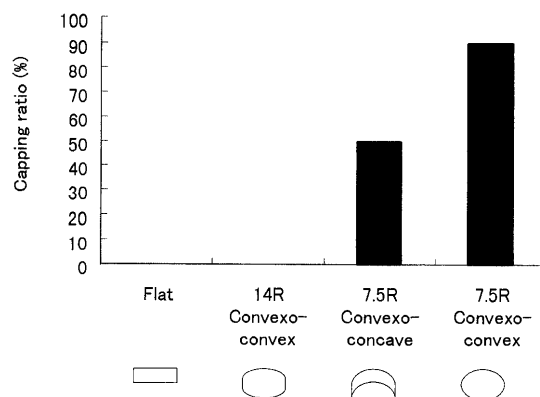


Fig. 6. Effect of Tablet Shape on Capping Ratio ($n=10$)

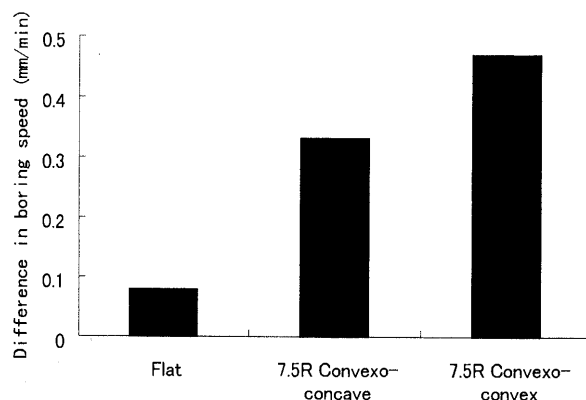


Fig. 7. The Differences in Boring Speed between the Center and the Edge on the Tablets in the Different Shape ($n=3$)

was useful in predicting capping. Since T_v/T_e -value of the convexo-concave tablets was smaller than that of the convexo-convex tablets, the residual die wall pressure per unit area of the convexo-concave tablets would be smaller than that of the convexo-convex tablets. It was assumed that the residual die wall pressure per unit area is one of the reasons why the capping ratio of the convexo-concave tablets were smaller than that of the convexo-convex tablets. However, the capping ratio of the convexo-concave tablets was larger than the flat tablets though T_v/T_e -value was the same. This result suggested another reason would exist.

Matsuno and Okano suggested that capping and lamination resulted from the lack of uniform density distribution inside tablets.²¹⁾ Accordingly, we assumed that the density distribution inside the convexo-concave tablets would be more uniform than that inside the convexo-convex tablets, but less uniform than that inside the flat tablets.

Effect of the Compressed Shape on the Uniformity of Density Distribution inside the Tablets The boring speed measurement is a useful parameter to evaluate the distribution of hardness inside the tablets.^{22–25)} Therefore, we measured the difference in boring speed between the center and the edge on the flat, the convexo-concave, and the convexo-convex tablets to evaluate the uniformity of density distribution inside the tablets. This is shown in Fig. 7. The difference in boring speed on the convexo-concave tablets is smaller than that on the convexo-convex tablets, but larger than that on the flat tablets. We found that the density distribution inside the convexo-concave tablets is more uniform than that inside the convexo-convex tablets, but less uniform than that

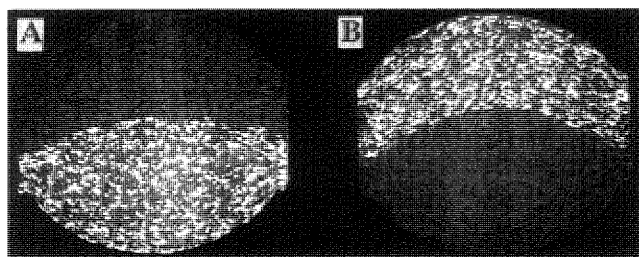


Fig. 8. CT of Cross-Section of Bilayer Caplets

A) Method A: the prolonged-release layer is the first layer. B) Method B: the prolonged-release layer is the second layer.

inside the flat tablets. We concluded that the lack of uniform density distribution inside tablets chiefly causes lamination.

Figure 8 shows CT pictures of cross-section of bilayer caplets having the prolonged-release layer manufactured by direct compression. The white spots of the pictures were calcium of the compressed anhydrous dibasic calcium phosphate (Fujicalin SG) in the prolonged-release layer. On the prolonged-release layer in the shape of convexo-convex, the white spots in the edge were concentrated and the white spots in the center were loose. In contrast, on the prolonged-release layer in the shape of convexo-concave, the white spots were uniformly distributed. Accordingly, we visually concluded that the prolonged-release layer as the second layer in the shape of convexo-concave have more uniform density distribution than the prolonged-release layer as the first layer in the shape of convexo-convex.

Conclusions

Cracking of the formulated bilayer caplets was not the separation of two layers, but lamination of the prolonged-release layer. It was assumed that Metolose 90SH4000 causes lamination of the prolonged-release layer.

When comparing the compactibility of the formulated bilayer caplets manufactured by different methods, we found that:

1. The manufacturing method of the formulated bilayer caplets having the prolonged-release layer whose Metolose 90SH4000 content is 60% without lamination is as follows: the prolonged-release layer manufactured by direct compression is fed as the second layer in bilayer compression.

2. The compactibility of the prolonged-release layer decrease with an increase in roller compaction pressure on dry granulation. The compactibility of the prolonged-release

layer manufactured by direct compression is superior to that manufactured by dry granulation.

3. Excellent compactibility of the second filling of the prolonged-release layer in bilayer compression is due to the compressed shape of the second layer, convexo-concave, that have more uniform density distribution than the compressed shape of the first layer, convexo-convex.

References and Notes

- 1) Ohmori S., Makino T., *Chem. Pharm. Bull.*, **48**, 673—677 (2000).
- 2) Loeffler G. F., *Pharmaceutical Dosage Forms; Tablets Vol. 2*, ed. by Lieberman H. A., Lachman L., Marcel Dekker, Inc., New York and Basel, 1981, pp. 451—484.
- 3) Nokhodchi A., Rubinstein M. H., Ford J. L., *Int. J. Pharm.*, **126**, 189—197 (1995).
- 4) Nokhodchi A., Ford J. L., Rowe P. H., Rubinstein M. H., *J. Pharm. Pharmacol.*, **48**, 1116—1121 (1996).
- 5) Nokhodchi A., Ford J. L., Rowe P. H., Rubinstein M. H., *J. Pharm. Pharmacol.*, **48**, 1122—1127 (1996).
- 6) Nokhodchi A., Ford J. L., Rowe P. H., Rubinstein M. H., *Int. J. Pharm.*, **129**, 21—31 (1996).
- 7) Malamataris S., Karidas T., Goidas P., *Int. J. Pharm.*, **103**, 205—215 (1994).
- 8) Malamataris S., Karidas T., *Int. J. Pharm.*, **104**, 115—123 (1994).
- 9) Sheskey P. J., Cabelka T. D., *Pharm. Technol.*, **16**, 60—74 (1992).
- 10) Sheskey P. J., Cabelka T. D., Robb R. T., Boyce B. M., *Pharm. Technol.*, **18**, 132—150 (1994).
- 11) Sheskey P. J., Robb R. T., Moore R. D., Boyce B. M., *Drug Dev. Ind. Pharm.*, **21**, 2151—2165 (1995).
- 12) Li S. P., Karth M. G., Feld K. M., DiPaolo L. C., Pendharkar C. M., Williams R. O., *Drug Dev. Ind. Pharm.*, **21**, 571—590 (1995).
- 13) Karehill P. G., Glazer M., Nyström C., *Int. J. Pharm.*, **64**, 35—43 (1990).
- 14) Yang L., Venkatesh G., Fassihi R., *Int. J. Pharm.*, **152**, 45—52 (1997).
- 15) Günsel W. C., *Pharmaceutical Dosage Forms; Tablets Vol. 1*, ed. by Lieberman H. A., Lachman L., Marcel Dekker, Inc., New York and Basel, 1980, pp. 187—224.
- 16) Fell J. T., Newton J. M., *J. Pharm. Sci.*, **59**, 688—691 (1970).
- 17) Nakai Y., Fukuoka E., Nakagawa H., *Yakugaku Zasshi*, **98**, 184—190 (1978).
- 18) Nakagawa H., *Chem. Pharm. Bull.*, **30**, 1401—1407 (1982).
- 19) Mollan M. J., Jr., Chang N., Celik M., *Pharm. Technol.*, **19**, 58—70 (1995).
- 20) Sugimori K., Mori S., Kawashima Y., *Powder Technol.*, **58**, 259—264 (1989).
- 21) Matsuno M., Okano H., *Yakugaku Kenkyu*, **29**, 45—47 (1957).
- 22) Nishimura K., Aoki S., Maki T., *Proceedings of Standard Formulation Research Association*, 1997, 38—42.
- 23) Kigasawa K., Iimura H., Sugimura H., Tanizaki A., *Yakugaku Zasshi*, **94**, 1281—1285 (1974).
- 24) Kigasawa K., Iimura H., Sugimura H., Tanizaki A., *Yakugaku Zasshi*, **94**, 1286—1289 (1974).
- 25) Kigasawa K., Iimura H., Tanizaki A., Sugimura H., Shimizu H., *Yakugaku Zasshi*, **95**, 769—773 (1975).

Synthesis of New Synthons for Organofluorine Compounds from Halothane Containing Sulfur Functional Groups¹⁾

Makoto KATO, Kensuke MAEDA, Kazuyuki SATO, Masaaki OMOTE, Akira ANDO, and Itsumaro KUMADAKI*

Faculty of Pharmaceutical Sciences, Setsunan University, 45-1 Nagaotoge-cho, Hirakata, Osaka 573-0101, Japan.

Received December 6, 1999; accepted January 31, 2000

To develop new synthons for the syntheses of organofluorine compounds, the treatment of Halothane, 2-bromo-2-chloro-1,1,1-trifluoroethane, (**1**) with 4-methylbenzenethiol (**2**) in the presence of sodium hydride gave 1-chloro-2,2,2-trifluoroethyl 4-methylphenyl sulfide (**3**), which was oxidized with *m*-chloroperbenzoic acid (*m*-CPBA) to the corresponding sulfoxide (**4**) and sulfone (**5**). Reaction of **3** and **5** with allyltributyltin in the presence of 2,2'-azobis(isobutyronitrile) (AIBN) gave 1-(trifluoromethyl)-3-butenyl compounds (**9**, **11**). Sulfoxide **4** was decomposed in this condition. The treatment of **3** with allyltrimethylsilane in the presence of Lewis acids gave 1-(trifluoromethyl)-3-butenyl compounds (**9**) in good yield. This result suggests that 4-methylphenylthio substituent stabilizes the α -carbocation effectively, though the trifluoromethyl group destabilizes it strongly. Aromatic compounds similarly reacted with **3** in the presence of titanium(IV) chloride to give 2-aryl-1,1,1-trifluoro-2-(4-methylphenylthio)ethanes. Thus, sulfur compounds derived from Halothane were found to be useful new synthons for organofluorine compounds.

Key words Halothane; 2-bromo-2-chloro-1,1,1-trifluoroethane; methylbenzenethiol; radical reaction; allylation; carbocation

Nowadays, organofluorine compounds are attracting much attention in biomedical fields, and many new medicines containing fluorine substituents have been developed.²⁾ New methodologies for organofluorine compounds have been developed, too. However, new methods for syntheses of new types of organofluorine compounds are still required. We are engaged in finding new synthons for the synthesis of organofluorine compounds, especially for trifluoromethyl compounds. In the course of this study, we found Halothane, 2-bromo-2-chloro-1,1,1-trifluoroethane (**1**), to be a useful synthon for organofluorine compounds.³⁾ Now, we would like to report the synthesis of new synthons by modification of the reactivity of **1** introducing sulfur substituents.

Reaction of **1** with 4-methylbenzenethiol (**2**) in the presence of sodium hydride was examined in aprotic solvents. After **2** was treated with sodium hydride in dimethylformamide (DMF), one equivalent of **1** was added at 0 °C and allowed to warm up to room temperature to give 1-chloro-2,2,2-trifluoroethyl 4-methylphenyl sulfide (**3**) in a yield of 32% (Chart 1).

MS of **3** showed a mother ion at *m/z*: 240 and 242 in a ratio of 3 : 1, which revealed the presence of one chlorine atom and no bromine atom. ¹⁹F-NMR showed a doublet at –8.7 ppm. ¹H-NMR showed a quartet at δ 5.20 ($J_{\text{H-F}}$ = 6.6 Hz). The structure of **3** was supported by these spectral data.

Since **1** is highly volatile, two equivalents of **1** were used. The yield of **3** was improved to 55%. To improve the yield of **3** further, reactions in other solvents were examined. Results are summarized in Table 1.

N-Methylpyrrolidone (NMP) gave the best result. These results suggested that a less polar solvent gave a better yield of **3**. Thus, a less polar tetrahydrofuran (THF) was examined,

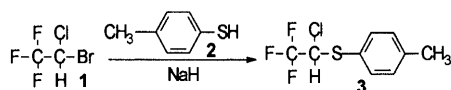


Chart 1

Table 1. Reaction of **1** with **2** in Aprotic Solvents

Entry	1 (eq)	Solvent	Time (h)	Yield (%)
1	1	DMF	3.5	32
2	2	DMF	4.0	55
3	2	DMSO	4.0	21
4	2	DMI	4.0	60
5	1	NMP	3.5	34
6	2	NMP	4.0	73
7	2	THF	—	—

DMSO: dimethyl sulfoxide; DMI: 1,3-dimethyl-2-imidazolidinone.

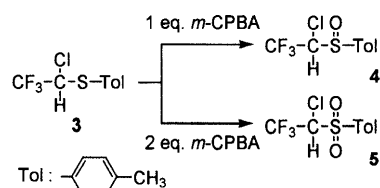


Chart 2

but this did not dissolve the sodium thiolate, and the reaction was not examined further.

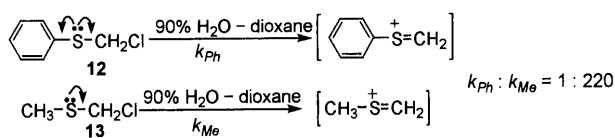
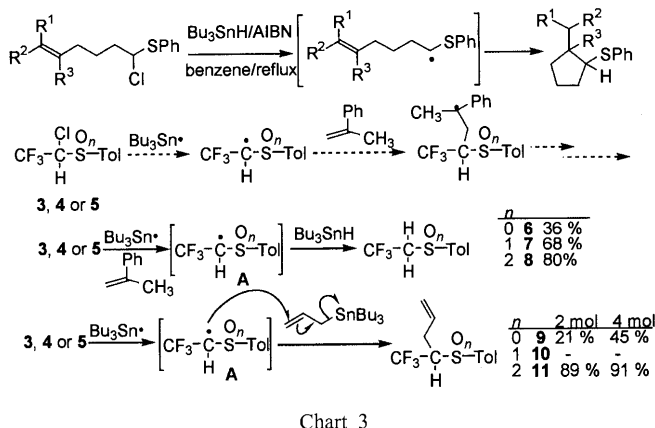
To modify the reactivity of **3**, it was oxidized with one equivalent of *m*-chloroperbenzoic acid (*m*-CPBA) to the corresponding sulfoxide (**4**) and with two equivalents to the sulfone (**5**) (see Chart 2).

Compound **4** has two chiral centers, and its GC and ¹⁹F-NMR spectra showed that it was a mixture of two diastereomers (ratio 3 : 2).

A radical generated from the reaction of α -chlorosulfide with tributyltin hydride was reported to add to a carbon-carbon double bond intramolecularly,⁴⁾ as shown at the top of Chart 3.

If this reaction proceeds with **3**, **4** or **5** intermolecularly, it will provide a new methodology for organic fluorine compounds. Thus, we examined their reaction with α -methylstyrene, expecting the reaction shown in the middle of Chart

* To whom correspondence should be addressed. e-mail: kumadaki@pharm.setsunan.ac.jp



3. When a mixture of **3** and tributyltin hydride was refluxed in benzene with a catalytic amount of 2,2'-azobis(isobutyronitrile) (AIBN), only the reduction product (**6**) was obtained in 36% yield, and the expected product was not obtained at all. Compounds **4** and **5** gave similar results. These facts suggested that radical intermediates were formed. However, they did not react with the olefin, but with tributyltin hydride to give the reduction products (**7** or **8**).

To avoid this undesirable reduction, we examined the reaction of **3** with allyltributyltin, which has no hydrogen and was reported to react through an $SH2'$ mechanism.⁵⁾ A solution of **3** and two equivalents of allyltributyltin in benzene was refluxed with a catalytic amount of AIBN, then an allyl group was introduced in the place of the chlorine atom to give 5,5,5-trifluoro-4-(4-methylphenylthio)-1-pentene (**9**) in the yield of 21%. The use of four equivalents of allyltributyltin improved the yield to 45%. These low yields might be due to the attack by an radical A on the sulfur atom of **3**, since the sulfone **5** gave a much better yield, as shown below.

The same reaction of sulfoxide **4** did not give the objective allyl compound (**10**) at all, even after prolonged reaction time. We could not recover **4**. This suggested that the sulfoxide group is unstable in this reaction condition. On the other hand, the sulfone **5** gave much better yields of the allyl compound (**11**) in a much shorter reaction time than in the case of **3**. These reactions are shown in the bottom of Chart 3.

Finally, cationic reactions of **3** will be discussed. Generally speaking, an α -alkylthio group stabilizes a carbocation. The rate of solvolysis of phenylthiomethyl chloride (**12**) was reported to be 220 times slower than that of methylthiomethyl chloride (**13**), as shown in Chart 4.⁶⁾

This large difference in rates is explained by an electronic effect of the sulfur of the phenylthio group: it stabilizes the carbocation, but is much smaller than that of the methylthio group, since the phenyl group tends to accept the electron pair by resonance, as shown by another arrow in Chart 4. Namely, a change in the structure significantly influences the stability of thioalkyl carbocation.

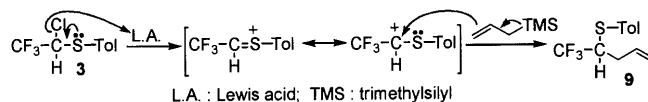


Table 2. Reaction of **3** with Allyltrimethylsilane in the Presence of Lewis Acids

Entry	Allyltrimethylsilane (eq)	Lewis acid (eq)	Time (h)	Yield (%)
1	3	BF ₃ ·Et ₂ O (3)	48	Trace
2	3	SnCl ₄ (3)	48	10
3	3	ZnBr ₂ (3)	48	30
4	1	TiCl ₄ (1)	60	80
5	1	TiCl ₄ (3)	33	70
6	3	TiCl ₄ (3)	18	94

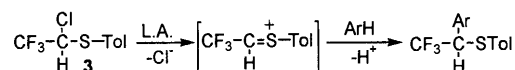
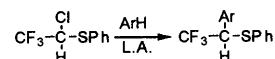


Table 3. Reaction of **3** with Aromatic Compounds in the Presence of TiCl₄

Entry	Aromatic compound	Time (h)	Product %	Ref. ⁷⁾
1	Benzene	24	14 78	66 ^{a)}
2	Toluene	12	15 (o-) 16 16 (p-) 82	6 (o-) ^{a)} 77 (p-) ^{a)}
3	Naphthalene	10	17 (α -) 90	80 (α -) ^{b)}
4	Phenol	3	18 (o-) 15 19 (p-) 24	

a) ZnCl₂/CH₃NO₂/reflux. b) SnCl₄/ClCH₂CH₂Cl/reflux.

Cf. Reaction of 1-chloro-2,2,2-trifluoro-1-(phenylthio)ethane with aromatic compounds.



A trifluoromethyl group is a strong electron-withdrawing group and it destabilizes an α -cation to it. Thus, we were interested in which effect, of the phenylthio group or of the trifluoromethyl group, predominates in the reaction of **3**. We treated **3** with allyltrimethylsilane in the presence of several Lewis acids. The results are shown in Chart 5 and Table 2.

These results suggest that the chlorine atom was abstracted with a Lewis acid to give a carbocation, which reacted with allyltrimethylsilane to give an allylated product (**9**). Titanium(IV) chloride was found to work as the best catalyst. It gave a high yield of **9** in the shortest reaction time.

If the carbocation is produced by the reaction of **3** with titanium(IV) chloride, it will react with aromatic compounds to afford 2,2,2-trifluoro-1-(4-methylphenylthio)ethyl derivatives. At first, benzene was treated with **3** in the presence of titanium(IV) chloride at room temperature. When three molar equivalents of aromatic compounds and titanium(IV) chloride were used, moderate to good yields of 2,2,2-trifluoro-1-(4-methylphenylthio)ethyl compounds were obtained, as shown in Chart 6 and Table 3.

Among the aromatics examined, benzene is the least reactive, and it took 24 h for completion of the reaction. However, it gave a fairly good yield of the product. Toluene and naph-

thalene gave excellent results. Phenol showed the highest reactivity, but the yields of products were not satisfactory due to the difficulty of isolation. The last column of the table shows Uneyama's results of the reaction of a phenylthio homolog of **3** for comparison with ours.⁷⁾ It is clear from the table that the 4-methylphenylthio compound **3** is much more reactive than the phenylthio homolog: the former reacted at a much lower temperature and gave better yields than the latter. This shows that a 4-methylphenylthio group stabilizes an α -cation much better than a phenyl thio group.

In conclusion, **1** reacted with **2** to give a 4-methylphenylthio compound (**3**). This was converted to a sulfoxide (**4**) and sulfone (**5**) selectively using appropriate amounts of *m*-CPBA. Reaction of **3**, **4** or **5** with olefins and tributyltin hydride in the presence of AIBN resulted in the reduction of the chlorine atom to give trifluoroethylsulfur compounds (**6**, **7** or **8**). This suggests that the radical intermediates react more readily with tributyltin hydride than with an olefin. Allyltributyltin reacted with **3** or **5** to give the corresponding allyl compounds (**9** or **11**), while **4** was decomposed in the reaction condition. The reaction of **3** with allyltrimethylsilane in the presence of titanium(IV) chloride gave the allyl compound (**9**) in excellent yield. This result shows that the stabilization of an α -carbocation by a 4-methylphenylthio group exceeded the destabilization by a trifluoromethyl group. The last reaction can be applied to aromatic compounds to give 2,2,2-trifluoro-1-(4-methylphenylthio)ethyl compounds in good yields. Therefore, **3** was found to be useful for the syntheses of organofluorine compounds.

Experimental

General Procedures ¹H-NMR were recorded on JEOL-FX90Q and JNM-GX400 spectrometers. Tetramethylsilane was used as an internal standard. ¹⁹F-NMR were recorded on Hitachi FT-NMR R-1500 and JEOL-FX90Q spectrometers. Benzotrifluoride was used as an internal standard. Mass spectra were obtained by JEOL JMS-DX-300. Melting point was measured on a Yanagimoto melting point apparatus. Gas-liquid chromatography (GLC) was carried out on a Hitachi 263-50 gas chromatograph (column, 5% SE-30 3 mm \times 2 m; carrier, N₂ at 30 ml/min). Peak areas were calculated on a Hitachi D-2000 chromato-integrator.

1-Chloro-2,2,2-trifluoroethyl 4-Methylphenyl Sulfide (3) **1** In an atmosphere of Ar, a solution of 4-methylbenzenethiol (**2**, 1.24 g, 10 mmol) in DMF (3 ml) was added dropwise to a suspension of 60% NaH (402 mg, 10 mmol) in DMF (3 ml) at 0°C. After the mixture was stirred at this temperature for another 10 min, Halothane (**1**, 1.1 ml, 10 mmol) was added, then the mixture was stirred at room temperature for 3.5 h. The whole mixture was poured into ice-water containing 10% HCl, then filtered through a layer of Celite. The Celite layer was washed with Et₂O. All the solutions were combined and extracted with Et₂O. The Et₂O layer was washed with saturated NaHCO₃, then brine, and dried over MgSO₄. After the solvent was removed under a vacuum, the residue was separated by column chromatography (SiO₂, hexane) to give **3** (770 mg, 32%). **3**: A colorless oil. bp 101°C (16 mmHg). MS *m/z*: 240 (M⁺). High resolution MS (HR-MS) Calcd for C₉H₈ClF₃S (M⁺): 239.999. Found: 239.995. ¹⁹F-NMR (CDCl₃) δ : -8.74 (3F, d, *J*=6.6 Hz). ¹H-NMR (CDCl₃) δ : 2.37 (3H, s), 5.20 (1H, q, *J*=6.6 Hz), 7.47 (2H, d, *J*=8.1 Hz), 7.53 (2H, d, *J*=8.1 Hz).

2 In an atmosphere of Ar, a solution of **2** (1.24 g, 10 mmol) in DMF (3 ml) was added slowly to a suspension of 60% NaH (402 mg, 10 mmol) in DMF (3 ml) at 0°C. After the mixture was stirred at this temperature for 10 min, **1** (2.1 ml, 20 mmol) was added dropwise to this mixture. After the mixture was allowed to warm to room temperature, it was stirred for another 4 h. The whole mixture was worked up as above to give **3** (1.32 g, 55%).

3 Solvent effects. To investigate solvent effects, the same reaction as above was carried out using the solvents shown in Table 1. The results are summarized in Table 1.

2-Chloro-1,1,1-trifluoro-2-(4-methylbenzenesulfonyl)ethane (4) In an atmosphere of Ar, **3** (240 mg, 1 mmol) was added drop by drop to a solution of 60% *m*-CPBA (287 mg, 1 mmol) in CH₂Cl₂ (5 ml) at room temperature.

After the mixture was stirred for 1 h, it was treated with 20% NaHSO₃ and extracted with CH₂Cl₂. The CH₂Cl₂ layer was washed with saturated NaHCO₃ and brine, then dried over MgSO₄. After evaporation of the solvent under a vacuum, the residue was purified by column chromatography (SiO₂, hexane-CH₂Cl₂, 3:2) to give **4** (221 mg, 86%). **4** was found to be a mixture of two diastereo isomers by ¹⁹F-NMR (ratio 3:2). The isomers were separated by column chromatography (SiO₂, hexane-CH₂Cl₂, 3:2). **4**: One isomer: Colorless crystals. mp 87–88°C. MS *m/z*: 256 (M⁺). HR-MS Calcd for C₉H₈ClF₃OS (M⁺): 255.994. Found: 255.987. ¹⁹F-NMR (CDCl₃) δ : -5.73 (3F, d, *J*=7.0 Hz). ¹H-NMR (CDCl₃) δ : 2.44 (3H, s), 4.65 (1H, q, *J*=7.0 Hz), 7.37 (2H, d, *J*=8.3 Hz), 7.58 (2H, d, *J*=8.3 Hz). The other isomer: A colorless oil. MS *m/z*: 256 (M⁺). HR-MS Calcd for C₉H₈ClF₃OS (M⁺): 255.994. Found: 255.988. ¹⁹F-NMR (CDCl₃) δ : -3.95 (3F, d, *J*=7.0 Hz). ¹H-NMR (CDCl₃) δ : 2.45 (3H, s), 4.81 (1H, q, *J*=7.0 Hz), 7.37 (2H, d, *J*=8.3 Hz), 7.69 (2H, d, *J*=8.3 Hz).

2-Chloro-1,1,1-trifluoro-2-(4-methylbenzenesulfonyl)ethane (5) In an atmosphere of Ar, **3** (240 mg, 1 mmol) was added drop by drop to a solution of 60% *m*-CPBA (862 mg, 3 mmol) in CH₂Cl₂ (15 ml). After the mixture was stirred at room temperature for 1 h, it was treated with 20% NaHSO₃ and extracted with CH₂Cl₂. The CH₂Cl₂ layer was washed with saturated NaHCO₃ and brine, then dried over MgSO₄. After evaporation of the solvent, the residue was purified by column chromatography (SiO₂, hexane-CH₂Cl₂, 1:1) to give **5** (245 mg, 90%). **5**: Colorless crystals. mp 66–68°C. MS *m/z*: 272 (M⁺). HR-MS Calcd for C₉H₈ClF₃O₂S (M⁺): 271.989. Found: 271.981. ¹⁹F-NMR (CDCl₃) δ : -4.07 (3F, d, *J*=6.2 Hz). ¹H-NMR (CDCl₃) δ : 2.49 (3H, s), 5.06 (1H, q, *J*=6.2 Hz), 7.42 (2H, d, *J*=8.3 Hz), 7.88 (2H, d, *J*=8.3 Hz).

Reaction of 3 with α -Methylstyrene in the Presence of Tributyltin Hydride In an atmosphere of Ar, tributyltin hydride (0.35 ml, 1.3 mmol) was added to a boiling solution of AIBN (10 mg, 0.06 mmol), α -methylstyrene (0.65 ml, 5 mmol) and **3** (240 mg, 1 mmol) in benzene (10 ml). After the mixture was refluxed for 1 h, it was treated with cold 10% KF, then extracted with Et₂O. The Et₂O layer was washed with saturated NaHCO₃ and brine, then dried over MgSO₄. After evaporation of the solvent, the residue was purified by column chromatography (SiO₂, hexane) to give 2,2,2-trifluoroethyl 4-methylphenyl sulfide (**6**, 75 mg, 36%). **6**: A colorless oil. MS *m/z*: 206 (M⁺). HR-MS Calcd for C₉H₉F₃S (M⁺): 206.038. Found: 206.038. ¹⁹F-NMR (CDCl₃) δ : -3.35 (3F, t, *J*=9.8 Hz). ¹H-NMR (CDCl₃) δ : 2.34 (3H, s), 3.38 (2H, q, *J*=9.8 Hz), 7.14 (2H, d, *J*=9.5 Hz), 7.40 (2H, d, *J*=9.5 Hz).

Reaction of 4 with α -Methylstyrene in the Presence of Tributyltin Hydride In an atmosphere of Ar, tributyltin hydride (0.35 ml, 1.3 mmol) was added to a boiling solution of AIBN (10 mg, 0.06 mmol), **4** (256 mg, 1 mmol) and α -methylstyrene (0.65 ml, 5 mmol) in benzene (10 ml). After the mixture was refluxed for 1 h, it was treated with cold 10% KF and extracted with Et₂O. The Et₂O layer was washed with saturated NaHCO₃ and brine, then dried over MgSO₄. After evaporation of the solvent, the residue was purified by column chromatography (SiO₂, hexane-CH₂Cl₂, 3:2) to give 1,1,1-trifluoro-2-(4-methylbenzenesulfonyl)ethane (**7**, 151 mg, 68%). **7**: Colorless crystals. mp 58–59°C. MS *m/z*: 222 (M⁺). HR-MS Calcd for C₉H₈F₃OS (M⁺): 222.033. Found: 222.033. ¹⁹F-NMR (CDCl₃) δ : 1.59 (3F, dd, *J*=10.1, 10.1 Hz). ¹H-NMR (CDCl₃) δ : 2.44 (3H, s), 3.38 (1H, dq, *J*=14.3, 10.1 Hz), 3.55 (1H, dq, *J*=14.3, 10.1 Hz), 7.38 (2H, d, *J*=8.2 Hz), 7.59 (2H, d, *J*=8.2 Hz).

Reaction of 5 with α -Methylstyrene in the Presence of Tributyltin Hydride In an atmosphere of Ar, tributyltin hydride (0.35 ml, 1.3 mmol) was added dropwise to a boiling solution of AIBN (10 mg, 0.06 mmol), **5** (272 mg, 1 mmol) and α -methylstyrene (0.65 ml, 5 mmol) in benzene (10 ml). After the mixture was refluxed for 1 h, it was treated with cold 10% KF and extracted with Et₂O. The Et₂O layer was washed with saturated NaHCO₃ and brine, then dried over MgSO₄. After evaporation of the solvent under a vacuum, the residue was purified by column chromatography (SiO₂, hexane-CH₂Cl₂, 1:1) to give 1,1,1-trifluoro-2-(4-methylbenzenesulfonyl)ethane (**8**, 190 mg, 80%). **8**: Colorless crystals. mp 80–81°C. MS *m/z*: 238 (M⁺). HR-MS Calcd for C₉H₈F₃O₂S (M⁺): 238.028. Found: 238.027. ¹⁹F-NMR (CDCl₃) δ : 1.31 (3F, t, *J*=9.0 Hz). ¹H-NMR (CDCl₃) δ : 2.46 (3H, s), 3.91 (2H, q, *J*=9.0 Hz), 7.39 (2H, d, *J*=8.4 Hz), 7.84 (2H, d, *J*=8.4 Hz).

Reaction of 3 with Allyltributyltin Using 2 eq of Reagent: In an atmosphere of Ar, a solution of AIBN (8 mg, 0.05 mmol), **3** (60 mg, 0.25 mmol) and allyltributyltin (0.16 ml, 0.5 mmol) in benzene (1.5 ml) was refluxed under stirring for 9 h. The cooled mixture was treated with 10% KF and extracted with Et₂O. The Et₂O layer was washed with saturated NaHCO₃ and brine, then dried over MgSO₄. After evaporation of the solvent, the residue was purified by column chromatography (SiO₂, hexane) to give 5,5,5-trifluoro-4-(4-methylphenylthio)-1-pentene (**9**, 13 mg, 21%). **9**: A col-

orless oil. MS m/z : 246 (M^+). HR-MS Calcd for $C_{12}H_{13}F_3S$ (M^+): 246.069. Found: 246.068. ^{19}F -NMR ($CDCl_3$) δ : -7.23 (3F, d, $J=8.5$ Hz). 1H -NMR ($CDCl_3$) δ : 2.34 (3H, s), 2.38 (1H, dddt, $J=15.0, 9.8, 4.8, 1.2$ Hz), 2.64 (1H, dddt, $J=15.0, 7.0, 4.3, 1.2$ Hz), 3.30 (1H, ddq, $J=12.5, 9.8, 8.5$ Hz), 5.18—5.23 (2H, m), 5.89—6.00 (1H, ddm, $J=17.1, 10.1$ Hz), 7.12 (2H, d, $J=7.9$ Hz), 7.41 (2H, d, $J=7.9$ Hz).

Using 4 eq of the Reagent: In an atmosphere of Ar, a solution of AIBN (8 mg, 0.05 mmol), **3** (60 mg, 0.25 mmol) and allyltributyltin (0.31 ml, 1 mmol) in benzene (1.5 ml) was refluxed under stirring for 9 h. The cooled mixture was treated with 10% KF and extracted with Et_2O . The Et_2O layer was washed with saturated $NaHCO_3$ and brine, then dried over $MgSO_4$. After evaporation of the solvent, the residue was purified by column chromatography (SiO_2 , hexane) to give **9** (28 mg, 45%).

The same reactions of **4** with allyltributyltin as those of **3**, with much prolonged reaction times (72 h), did not afford any objective product (**10**). The starting material (**4**) was not recovered. This suggested that **4** was not stable in this reaction condition.

Reaction of 5 with Allyltributyltin Using 2 eq of the Reagent: In an atmosphere of Ar, a solution of AIBN (8 mg, 0.05 mmol), **5** (68 mg, 0.25 mmol) and allyltributyltin (0.16 ml, 0.5 mmol) in benzene (1.5 ml) was refluxed under stirring for 3 h. The cooled mixture was treated with 10% KF and extracted with Et_2O . The Et_2O layer was washed with saturated $NaHCO_3$ and brine, then dried over $MgSO_4$. After evaporation of the solvent under a vacuum, the residue was purified by column chromatography (SiO_2 , hexane- CH_2Cl_2 , 1:1) to give 5,5,5-trifluoro-4-(4-methylbenzenesulfonyl)-1-pentene (**11**, 62 mg, 89%). **11**: Colorless crystals. mp 42°C. MS m/z : 278 (M^+). HR-MS Calcd for $C_{13}H_{13}F_3O_2S$ (M^+): 278.059. Found: 278.059. ^{19}F -NMR ($CDCl_3$) δ : -0.84 (3F, d, $J=7.6$ Hz). 1H -NMR ($CDCl_3$) δ : 2.47 (3H, s), 2.68 (1H, dddt, $J=15.3, 7.6, 7.6, 1.2$ Hz), 2.97 (1H, ddm, $J=15.6, 5.2$ Hz), 3.69 (1H, dqd, $J=7.7, 7.6, 5.1$ Hz), 5.14—5.22 (2H, m), 5.86 (1H, ddm, $J=16.8, 10.1$ Hz), 7.38 (2H, d, $J=8.2$ Hz), 7.81 (2H, d, $J=8.2$ Hz).

Using 4 eq of the Reagent: In an atmosphere of Ar, a solution of AIBN (8 mg, 0.05 mmol), **5** (68 mg, 0.25 mmol) and allyltributyltin (0.31 ml, 1 mmol) in benzene (1.5 ml) was refluxed under stirring for 3 h. The cooled mixture was worked up as above to give **11** (63 mg, 91%).

5,5,5-Trifluoro-4-(4-methylphenylthio)-1-pentene (9) through a Cationic Reaction of 3 Using $BF_3 \cdot Et_2O$ as a Lewis Acid: In an atmosphere of Ar, $BF_3 \cdot Et_2O$ (0.38 ml, 3 mmol) was added slowly to a solution of **3** (240 mg, 1 mmol) and allyltrimethylsilane (0.27 ml, 3 mmol) in CH_2Cl_2 (5 ml) at room temperature. After the mixture was stirred for 48 h at room temperature, it was poured into ice-water and extracted with CH_2Cl_2 . The CH_2Cl_2 layer was washed with saturated $NaHCO_3$ and brine, then dried over $MgSO_4$. After evaporation of the solvent under a vacuum, the residue was purified by column chromatography (SiO_2 , hexane) to give **9** (10 mg, 4%).

The results of reactions using other Lewis acids are summarized in Table 3.

1,1,1-Trifluoro-2-(4-methylphenylthio)-2-phenylethane (14) In an atmosphere of Ar, $TiCl_4$ (0.33 ml, 3 mmol) was added slowly to a solution of **3** (240 mg, 1 mmol) and benzene (0.27 ml, 3 mmol) in CH_2Cl_2 (5 ml) at room temperature. After the mixture was stirred for 24 h at this temperature, it was poured into ice-water and extracted with CH_2Cl_2 . The CH_2Cl_2 layer was washed with saturated $NaHCO_3$ and brine, then dried over $MgSO_4$. After evaporation of the solvent under a vacuum, the residue was purified by column chromatography (SiO_2 , hexane) to give **14** (219 mg, 78%). **14**: A colorless oil. MS m/z : 282 (M^+). HR-MS Calcd for $C_{15}H_{13}F_3S$: 282.070 (M^+). Found: 282.070. ^{19}F -NMR ($CDCl_3$) δ : -4.54 (3F, d, $J=8.6$ Hz). 1H -NMR ($CDCl_3$) δ : 2.31 (3H, s), 4.45 (1H, q, $J=8.6$ Hz), 7.06—7.33 (9H, m).

1,1,1-Trifluoro-2-(2- and 4-methylphenyl)-2-(4-methylphenylthio)ethanes (15 and 16) In an atmosphere of Ar, $TiCl_4$ (0.33 ml, 3 mmol) was added slowly to a solution of **3** (240 mg, 1 mmol) and toluene (0.32 ml, 3 mmol) in CH_2Cl_2 (5 ml) at room temperature. After the mixture was stirred for 12 h at this temperature, it was poured into ice-water and extracted with CH_2Cl_2 . The CH_2Cl_2 layer was washed with saturated $NaHCO_3$ and brine, then dried over $MgSO_4$. After evaporation of the solvent, the residue was

separated by column chromatography (SiO_2 , hexane) to give 1,1,1-trifluoro-2-(2-methylphenyl)-2-(4-methylphenylthio)ethane (**15**, 46 mg, 16%) and 1,1,1-trifluoro-2-(4-methylphenyl)-2-(4-methylphenylthio)ethane (**16**, 242 mg, 82%). **15**: A colorless oil. MS m/z : 296 (M^+). HR-MS Calcd for $C_{16}H_{15}F_3S$: 296.084 (M^+). Found: 296.084. ^{19}F -NMR ($CDCl_3$) δ : -4.71 (3F, d, $J=8.6$ Hz). 1H -NMR ($CDCl_3$) δ : 2.32 (3H, s), 2.34 (3H, s), 4.42 (1H, q, $J=8.6$ Hz), 7.08 (2H, d, $J=8.2$ Hz), 7.15 (2H, d, $J=8.2$ Hz), 7.22 (2H, d, $J=8.2$ Hz), 7.33 (2H, d, $J=8.2$ Hz). **16**: A colorless oil. MS m/z : 296 (M^+). HR-MS Calcd for $C_{16}H_{15}F_3S$: 296.085 (M^+). Found: 296.085. ^{19}F -NMR ($CDCl_3$) δ : -3.93 (3F, d, $J=8.6$ Hz). 1H -NMR ($CDCl_3$) δ : 2.33 (6H, s), 4.75 (1H, q, $J=8.6$ Hz), 7.09 (2H, d, $J=8.2$ Hz), 7.16—7.42 (4H, m), 7.33 (2H, d, $J=8.2$ Hz).

1,1,1-Trifluoro-2-(4-methylphenylthio)-2-(1-naphthyl)ethane (17) In an atmosphere of Ar, $TiCl_4$ (0.33 ml, 3 mmol) was added slowly to a solution of **3** (240 mg, 1 mmol) and naphthalene (0.38 g, 3 mmol) in CH_2Cl_2 (5 ml) at room temperature. After the mixture was stirred for 10 h, it was worked up as above to give 1,1,1-trifluoro-2-(4-methylphenylthio)-2-(1-naphthyl)ethane (**17**, 298 mg, 90%). **17**: A colorless oil. MS m/z : 332 (M^+). HR-MS Calcd for $C_{19}H_{15}F_3S$: 332.085 (M^+). Found: 332.085. ^{19}F -NMR ($CDCl_3$) δ : -3.38 (3F, d, $J=7.3$ Hz). 1H -NMR ($CDCl_3$) δ : 2.33 (3H, s), 5.39 (1H, br), 7.06—8.01 (11H, m).

1,1,1-Trifluoro-2-(2- and 4-hydroxyphenyl)-2-(4-methylphenylthio)ethanes (18 and 19) In an atmosphere of Ar, $TiCl_4$ (0.33 ml, 3 mmol) was added slowly to a solution of **3** (240 mg, 1 mmol) and phenol (0.26 ml, 3 mmol) in CH_2Cl_2 (5 ml). After the mixture was stirred for 3 h, it was worked up as above, then separated by column chromatography (SiO_2 , hexane to hexane- CH_2Cl_2 , 7:3) to give 1,1,1-trifluoro-2-(2-hydroxyphenyl)-2-(4-methylphenylthio)ethane (**18**, 44 mg, 15%) and 1,1,1-trifluoro-2-(4-hydroxyphenyl)-2-(4-methylphenylthio)ethane (**19**, 72 mg, 24%). **18**: A colorless oil. MS m/z : 298 (M^+). HR-MS Calcd for $C_{15}H_{13}F_3OS$: 298.064 (M^+). Found: 298.064. ^{19}F -NMR ($CDCl_3$) δ : -4.22 (3F, d, $J=8.6$ Hz). 1H -NMR ($CDCl_3$) δ : 2.45 (3H, s), 5.10 (1H, q, $J=8.6$ Hz), 5.19 (1H, s), 6.78—7.35 (4H, m), 7.08 (2H, d, $J=8.2$ Hz), 7.36 (2H, d, $J=8.2$ Hz). **19**: Colorless crystals. mp 98—100°C. MS m/z : 298 (M^+). HR-MS Calcd for $C_{15}H_{13}F_3OS$: 298.063 (M^+). Found: 298.063. ^{19}F -NMR ($CDCl_3$) δ : -5.23 (3F, d, $J=8.5$ Hz). 1H -NMR ($CDCl_3$) δ : 2.32 (3H, s), 4.40 (1H, q, $J=8.5$ Hz), 4.81 (1H, s), 6.79 (2H, d, $J=8.5$ Hz), 7.08 (2H, d, $J=7.9$ Hz), 7.21 (2H, d, $J=8.5$ Hz), 7.30 (2H, d, $J=7.9$ Hz).

References and Notes

- 1) A part of this work was reported at the 119th annual meeting of the Pharmaceutical Society of Japan, March 1999, Tokushima, Japan.
- 2) "Organofluorine Compounds in Medicinal Chemistry and Biomedical Applications," ed. by Filler R., Kobayashi Y., Yagupolskii L. M., Elsevier, Amsterdam, 1993.
- 3) a) Takagi T., Takesue A., Koyama M., Ando A., Miki T., Kumadaki I., *J. Org. Chem.*, **57**, 3921—3923 (1992); b) Takagi T., Takesue A., Isowaki A., Koyama M., Ando A., Kumadaki I., *Chem. Pharm. Bull.*, **43**, 1071—1075 (1995); c) Takagi T., Takahashi J., Nakatsuka H., Koyama M., Ando A., Kumadaki I., *ibid.*, **44**, 280—283 (1996); d) Takagi T., Okikawa N., Johnoshita S., Koyama M., Ando A., Kumadaki I., *Synlett*, **1996**, 82—84; e) Takagi T., Nakamoto M., Sato K., Koyama M., Ando A., Kumadaki I., *Tetrahedron*, **52**, 12667—12676 (1996); f) Takagi T., Kanai K., Omote M., Ando A., Kumadaki I., *J. Fluorine Chem.*, **89**, 233—234 (1998).
- 4) Tsai Y.-M., Chang F.-C., Huang J., Shiu C.-L., *Tetrahedron Lett.*, **30**, 2121—2124 (1989).
- 5) Giardina A., Giovannini R., Petrini M., *Tetrahedron Lett.*, **38**, 1995—1998 (1997).
- 6) a) Böhme H., *Chem. Ber.*, **74**, 248—256 (1941); b) Böhme H., Fischer H., Frank R., *Justus Liebigs Ann. Chem.*, **563**, 54—72 (1949).
- 7) Uneyama K., Momota M., Hayashida K., Itoh T., *J. Org. Chem.*, **55**, 5364—5368 (1990).

Polyphenols from *Eriobotrya japonica* and Their Cytotoxicity against Human Oral Tumor Cell Lines

Hideyuki ITO,^a Eri KOBAYASHI,^a Yoshie TAKAMATSU,^a Shu-Hua LI,^a Tsutomu HATANO,^a Hiroshi SAKAGAMI,^b Kaoru KUSAMA,^c Kazue SATOH,^d Daigo SUGITA,^e Susumu SHIMURA,^e Yoshio ITOH,^e and Takashi YOSHIDA^{*,a}

Faculty of Pharmaceutical Sciences, Okayama University,^a Tsushima, Okayama 700–8530, Japan, and Department of Dental Pharmacology,^b Department of Oral Pathology,^c Meikai University School of Dentistry, Sakado, Saitama 350–0283, Japan, and Analysis Center, School of Pharmaceutical Sciences, Showa University,^d Shinagawa-ku, Tokyo 142–8555, Japan, and Central Research Institute of Lotte Co. Ltd.,^e Urawa, Saitama 336–0027, Japan.

Received December 8, 1999; accepted January 29, 2000

Three new flavonoid glycosides, together with 15 known flavonoids, have been isolated from the leaves of *Eriobotrya japonica*, and characterized as (2S)- and (2R)-naringenin 8-C- α -L-rhamnopyranosyl-(1 \rightarrow 2)- β -D-glucopyranosides, and cinchonain Id 7-O- β -D-glucopyranoside, respectively, based on spectral analyses including two dimensional (2D) NMR techniques. Higher proanthocyanidin fraction in the water-soluble portion of the extract was characterized as a procyanidin oligomer mixture mainly composed of undecameric procyanidin. These polyphenols have also been assessed for cytotoxic activity against two human oral tumor (human squamous cell carcinoma and human salivary gland tumor) cell lines. Selective cytotoxicity of the procyanidin oligomer between tumor and normal gingival fibroblast cells, and its possible mechanism, were also described.

Key words *Eriobotrya japonica*; Rosaceae; cinchonain Id 7-O- β -D-glucopyranoside; naringenin 8-C- α -L-rhamnopyranosyl-(1 \rightarrow 2)- β -D-glucopyranoside; undecameric procyanidin; human oral tumor cell line

Eriobotrya japonica Lindl. (Rosaceae) is a well-known medicinal plant in Japan and China. Its astringent leaves have been used a long time to treat chronic bronchitis, coughs, phlegm, high fever and gastroenteric disorders. A decoction of the leaves has been known to be a cooling beverage preventing sunstroke and thirst, and has also been applied locally to wounds, ulcers and cancers.¹⁾ The occurrence of triterpenoids with anti-inflammatory²⁾ and antiviral³⁾ effects, megastigmane glycoside⁴⁾ and a small amount of amygdalin²⁾ in the leaves has been reported. Although many of the rosaceous plants are known to be rich in flavonoids and tannins, only several polyphenolic constituents of *E. japonica* have been reported.⁵⁾ In addition, the anti-tumorigenic effect has not been extensively examined for any ingredients with a defined structure.

This paper describes the isolation and characterization of 18 polyphenolic compounds from the leaves of this plant, three of which are new flavonoid glycosides. Furthermore, a higher oligomeric proanthocyanidin fraction in the water-soluble portion of the extract was characterized to be composed mainly of procyanidin undecamer with 4 β \rightarrow 8 interflavanil linkages. In order to clarify which constituents of this plant contribute to its anti-tumorigenic effect, we also investigated here the cytotoxic effect of these polyphenols against human oral tumor cell lines [human squamous cell carcinoma (HSC-2), human salivary gland tumor (HSG)], in comparison with the effect on human normal gingival fibroblasts (HGF), and found that the procyanidin oligomer among the isolated polyphenols exhibited potent selective cytotoxicity to tumor cell lines. Apoptosis-inducing activity of the oligomer against tumor cell lines, as revealed by agarose gel electrophoresis which detects DNA fragments,⁶⁾ and immunocytochemical staining with M30 monoclonal antibody, which reacts with the degradation product of cytokeratin 18 by activated caspases,⁷⁾ is also demonstrated.

Results and Discussion

A 70% aqueous acetone homogenate of the leaves of *E. japonica* was extracted successively with ether, AcOEt and 1-butanol. Repeated chromatographies of the AcOEt and 1-butanol extracts over polystyrene and polyvinyl gels gave 19 polyphenols, including three new compounds (**1**, **2**, **3**).

Known polyphenols were identified as chlorogenic acid,⁸⁾ 3-O-caffeoylquinic acid, 4-O-caffeoylquinic acid, 4-O-*p*-coumaroylquinic acid, quercetin,⁹⁾ isoquercitrin,¹⁰⁾ quercetin 3-O-sophoroside,¹¹⁾ kaempferol 3-O-sophoroside,¹¹⁾ kaempferol 3-O- α -rhamnopyranosyl-(1 \rightarrow 2)- β -D-glucopyranoside,¹²⁾ (–)-epicatechin (**5**), procyanidin B-2 (**6**),¹³⁾ procyanidin C-1 (**7**),¹⁴⁾ 1-O-feruloyl- β -D-glucopyranose,¹⁵⁾ and 4-O- β -glucopyranosyl-*cis-p*-coumaric acid.¹⁶⁾ From the water-soluble fraction remaining after 1-butanol extraction, cinchonain Ia (**4**)^{17,18)} and procyanidin oligomer (**8**) were obtained.

Structures of Flavonoid Glycosides Compound **1** was isolated as a pale yellow amorphous powder. The molecular formula of **1** was determined to be C₂₇H₃₂O₁₄ based on high-resolution electrospray ionization mass spectrum (HR ESI-MS) [*m/z* 581.1815 (M+H)⁺ (Calcd for C₂₇H₃₂O₁₄+H, 581.1870)]. The UV spectrum showed an absorption maximum at 290 nm with a shoulder at 325 nm, characteristic of a flavanone skeleton.¹⁹⁾ The ¹H-NMR spectrum (acetone-*d*₆+D₂O) of **1** showed mutually coupled methine and methylene proton signals [δ 5.40 (dd, *J*=2, 14 Hz), δ 3.36 (dd, *J*=14, 17 Hz), δ 2.59 (dd, *J*=2, 17 Hz)], and AA'BB'-type signals [δ 7.45 (2H, d, *J*=8.5 Hz), δ 6.90 (2H, d, *J*=8.5 Hz)] and a 1H-singlet at δ 5.96 in the aromatic proton region. These spectral features, together with a hydrogen-bonded hydroxyl proton signal at δ 12.34 (s), which disappeared upon the addition of D₂O, indicated the presence of a naringenin skeleton with a C₆- or C₈-substituted A-ring in the molecule of **1**. The spectrum also exhibited signals ascribable to a sugar moiety in the aliphatic proton region. Although the presence

* To whom correspondence should be addressed. e-mail: yoshida@pheasant.pharm.okayama-u.ac.jp

of rhamnose residue was suggested by an anomeric proton signal [δ 5.29 (brs)] and a methyl signal [δ 0.76 (d, $J=6$ Hz)], full assignment of the other signals was difficult due to partial overlapping and/or broadening. Measurement of the spectrum in methanol- d_4 gave, however, well-resolved signals for all of the sugar protons, and their full assignment was made with the aid of ^1H - ^1H shift correlation spectroscopy (COSY) (see Experimental). The presence of rhamnose and glucose residues in **1** was thus revealed by coupling patterns characteristic of the respective sugars. The ^{13}C resonances of the glucose moiety, which were assigned by heteronuclear multiple quantum coherence (HMQC) spectrum (in methanol- d_4), were δ 74.4 (C-1), 78.2 (C-2), 81.1 (C-3), 71.4 (C-4), 82.2 (C-5) and 62.4 (C-6). These data, along with the appearance of a glucose H-1 signal at a higher field (δ 4.85) than that expected for *O*-glucoside, were indicative of a *C*-glucopyranosyl moiety. The *C*-glucosyl and *O*-rhamnopyranosyl structure was supported by acid hydrolysis of **1**, which liberated only rhamnose. The ^1H -detected heteronuclear multiple bond connectivity (HMBC) spectrum ($^2,3J_{\text{CH}}=6$ Hz) in acetone- d_6 + D_2O revealed that the anomeric proton signal at δ 5.29 (rhamnose H-1'') exhibited three-bond coupling with the glucose C-2'' signal (δ 77.3), indicating the presence of a rhamnopyranosyl (1 \rightarrow 2) glucopyranosyl moiety as the disaccharide sugar chain. The HMBC spectrum also showed two and three bond correlations of the anomeric proton signal (δ 4.83) of the glucose core with C-7 (δ 166.0), C-8 (δ 104.9) and C-9 (δ 161.3) of the aglycone, establishing that the glucose residue is attached to C-8 of the aglycone through a C-C bond. The absolute configuration at C-2 of the aglycone was assigned an (*S*)-orientation, based on a negative Cotton effect at 290 nm²⁰⁾ in the CD spectrum of **1**. The coupling constants of H-1'' (δ 4.83, $J=10$ Hz) and H-1''' (δ 5.29, brs) were consistent with β - and α -glycosidic linkages for glucopyranosyl and rhamnopyranosyl residues, respectively. Based on these data, taking into consideration the D- and L-series for almost all of glucose and rhamnose in higher plants, compound **1** was determined to be (2*S*)-naringenin 8-*C*- α -L-rhamnopyranosyl-(1 \rightarrow 2)- β -D-glucopyranoside.

Compound **2**, a pale yellow amorphous powder, exhibited a pseudomolecular ion peak at m/z 581.1858 ($\text{M}+\text{H}$)⁺ (Calcd for $\text{C}_{27}\text{H}_{32}\text{O}_{14}+\text{H}$, 581.1870) in an HR ESI-MS spectrum, establishing its molecular formula as $\text{C}_{27}\text{H}_{32}\text{O}_{14}$, the same as that of **1**. The spectral data (UV, MS, ^1H -NMR) of **2** were almost superimposable on those of compound **1**, except for downfield shifts for H-2 ($\Delta\delta$ 0.20 ppm) and one of the C-3 methylene proton signals ($\Delta\delta$ 0.18 ppm) as compared with the corresponding signals of **1** in the NMR spectra. A sign of the Cotton effect at 291 nm ($\Delta\epsilon$ +5.1) in the CD spectrum of **2**, which is associated with the absolute configuration at C-2 of flavanols, was opposite to that of **1**. Compound **2** was thus assigned to be a C-2 epimeric isomer of **1** [(2*R*)-naringenin 8-*C*- α -rhamnopyranosyl-(1 \rightarrow 2)- β -glucopyranoside], although it lacks further evidence because an insufficient amount was available. It is not a rare case that (2*R*)- and (2*S*)-isomers of flavanone glycosides coexist in a plant, as exemplified by previous reports for those in the *Zizyphi fructus*²¹⁾ and in *licorice*.²²⁾

The structure of compound **3**, a pale yellow amorphous powder, was determined as follows. The molecular formula was established to be $\text{C}_{30}\text{H}_{30}\text{O}_{14}$ based on HR ESI-MS that

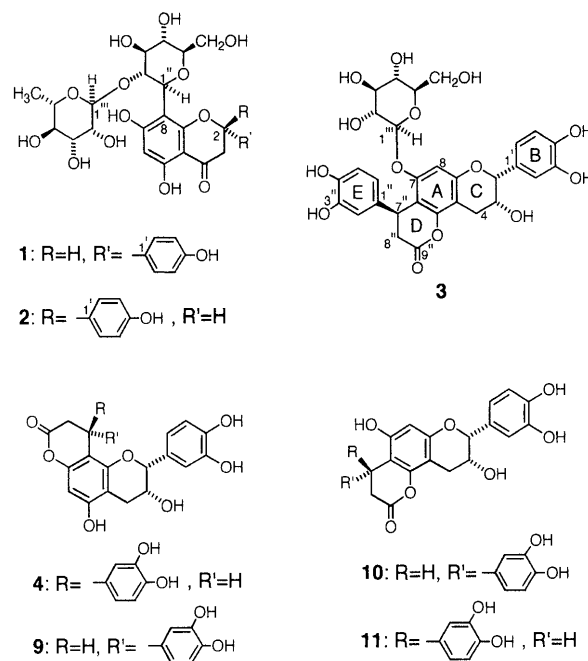


Chart 1

showed an ($\text{M}+\text{NH}_4$)⁺ ion peak at m/z 632.1990 (Calcd for $\text{C}_{30}\text{H}_{30}\text{O}_{14}+\text{NH}_4$, 632.1979). Its ^1H -NMR spectrum revealed the signals of an ABX system [δ 7.07 (d, $J=2$ Hz), δ 6.84 (dd, $J=2, 8$ Hz), δ 6.79 (d, $J=8$ Hz), B-ring], a 1H-aromatic singlet (δ 6.56, A-ring), two methine signals [δ 4.95 (br s), δ 4.28 (m)] and a methylene signal [δ 3.02 (br dd, $J=3, 17$ Hz), δ 2.83 (dd, $J=3, 17$ Hz), C-ring], suggesting the presence of an epicatechin moiety with a monosubstituted A-ring. In addition to those signals, mutually coupled methine [δ 4.72 (dd, $J=2, 7$ Hz)] and methylene [δ 3.02 (dd, $J=7, 16$ Hz), δ 2.88 (dd, $J=2, 16$ Hz), D-ring] proton signals, and ABX-type proton signals [δ 6.72 (d, $J=2.5$ Hz), δ 6.70 (d, $J=8.5$ Hz), δ 6.51 (dd, $J=2.5, 8.5$ Hz), E-ring] were observed. These data were similar to those of cinchonain-type flavanols. A sequentially coupled seven-spin system characteristic of glucopyranose residue was also observed in the ^1H -NMR spectrum. Compound **3** was thus assumed to be a glucoside of either of cinchonains Ia (**4**), Ib (**9**), Ic (**10**) or Id (**11**)^{17,18)} The HMBC spectrum of **3** exhibited three-bond correlations of one of the H-4 signals (δ 3.02) with oxygen-bearing carbon resonances at δ 155.9 (C-9) and δ 151.5 (C-5), which in turn were associated with the A-ring proton (H-8, δ 6.56) and H-7'' (δ 4.72), respectively, through two- and three-bond couplings. Both of these proton signals (H-8, H-7'') were also correlated with an oxygen-bearing carbon resonance at δ 154.3 (C-7), which showed three-bond coupling with an anomeric proton (H-1'') signal at δ 4.94 (Fig. 1). It was thus concluded that the location of the glucose residue is at O-7, and the aglycone should be either cinchonains Ic (**10**) or Id (**11**)^{17,18)} These diastereomers, **10** and **11**, were reported to be distinguished from each other by the CD spectrum.^{17,18)} The CD spectrum of **3** showed a negative Cotton effect at 286 nm ($\Delta\epsilon$ -2.2) and a positive one at 246 nm ($\Delta\epsilon$ +5.5) similar to those of **11**, establishing a (7''*S*)-configuration. Glucose was determined to be D-series by a positive reaction of acid hydrolysate from **3** to D-glucose oxidase.²³⁾ The β -glucosidic linkage was indicated by a large coupling constant ($J=7$ Hz)

of the H-1^m signal. Consequently, the structure of **7** was determined to be cinchonain Id 7-*O*- β -D-glucopyranoside. Although cinchonains were previously isolated from *Cinchona succirubra* (Rubiaceae),¹⁷⁾ *Phyllocladus trichomonoides* (Podocarpaceae)^{24,25)} and *Apocynum venetum* (Apocynaceae),²⁶⁾ compound **3** is the first example of a chinchonain glycoside.

Compound **8** was shown to be procyanidin by the formation of cyanidin (TLC, HPLC) upon heating with *n*-BuOH-HCl.²⁷⁾ Its polymeric nature was apparent from a very broad peak both on normal- and reversed-phase HPLC. Acid-catalysed cleavage of **8** in the presence of excess phloroglucinol was attempted in order to establish the identity of the constituent units and the nature of the interflavonoid linkage in the oligomer.²⁸⁾ HPLC of the reaction mixture revealed formations of epicatechin (**5**) and epicatechin-(4 β →2)-phloroglucinol (**12**) as major products, along with small amounts of **6** and **7**. The phloroglucinol addition product (**12**) was produced by the reaction between nucleophilic phloroglucinol and C-4 carbocation generated by cleavage of the interflavonoid bond in an acidic medium, while **5** was produced from the terminal unit of **8** (Chart 2). These products were identified by HPLC comparison with authentic samples obtained by similar reactions of **6** or **7**. The formation of **6** and **7** from **8** provided conclusive evidence that **8** was a procyanidin oligomer in which epicatechin units link with each other predominantly through 4 β →8 interflavanyl linkages. Although it was difficult to estimate quantitatively

the products in the reaction, an average degree of polymerization was ascertained by the ¹³C-NMR spectrum. The ¹³C-NMR spectrum of **8**, which showed broad and unresolved signals reflecting a large molecular weight, was closely similar to that reported for epicatechin-(4 β →8)-epicatechin oligomers.^{29,30)} It is reported that a ratio of peak areas of the C-3 or C-4 signal of a terminal unit to that of extension units is diagnostic for estimating the polymerization degree.²⁹⁾ The peak ratio of the C-3 resonances due to terminal and extension units at δ 66.8 and 72.7 ppm, respectively, in the ¹³C-NMR spectrum of **8** was estimated as *ca.* 1 : 10, suggesting that **8** is an undecameric procyanidin. This was in agreement with the molecular weight estimated from gel permeation chromatography (GPC)³¹⁾ of an acetyl derivative of this higher oligomeric mixture, which showed that number average molecular weight (M_n) of the acetate was 5400 [weight average molecular weight (M_w): 14800], corresponding to an undecamer. The predominant (4 β →8) interflavanyl linkage in the oligomer was supported by a strong positive couplet Cotton effect centered at 211 nm.³²⁾ The procyanidin oligomer fraction was thus assigned to involve an undecamer (on the average) composed of an epicatechin-(4 β →8)-epicatechin unit.

Cytotoxic Activity of Polyphenols We recently found that epigallocatechin gallate (EGCG), a main polyphenol of green tea, and some ellagitannin monomers and oligomers from medicinal plants, exhibit potent cytotoxic activity against human oral tumor cell lines (HSG, HSC-2), and those anti-tumorigenic substances show negligible or weak toxicity to normal cells (HGF).³³⁾ In a survey of possible anti-tumor ingredients in *E. japonica*, polyphenolics isolated in the present study, *i.e.* procyanidins B-2 (**6**), C-1 (**7**) and oligomer (**8**), flavan 3-ols related with EGCG and flavonoids, were then assessed for cytotoxic activity against those tumor cell lines.

As shown in Table 1, the cytotoxic activity of procyanidins and related polyphenols against HSC-2 cells was increased as molecular weight increased: epicatechin (**5**) (CC_{50} > 1.72 mM) < procyanidin B-2 (**6**) (CC_{50} = 0.39 mM) < procyani-

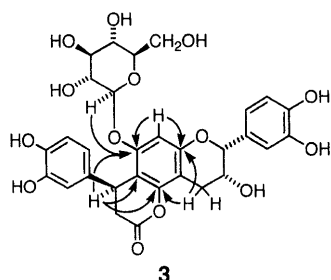


Fig. 1. Selective HMBC Correlations of **3**

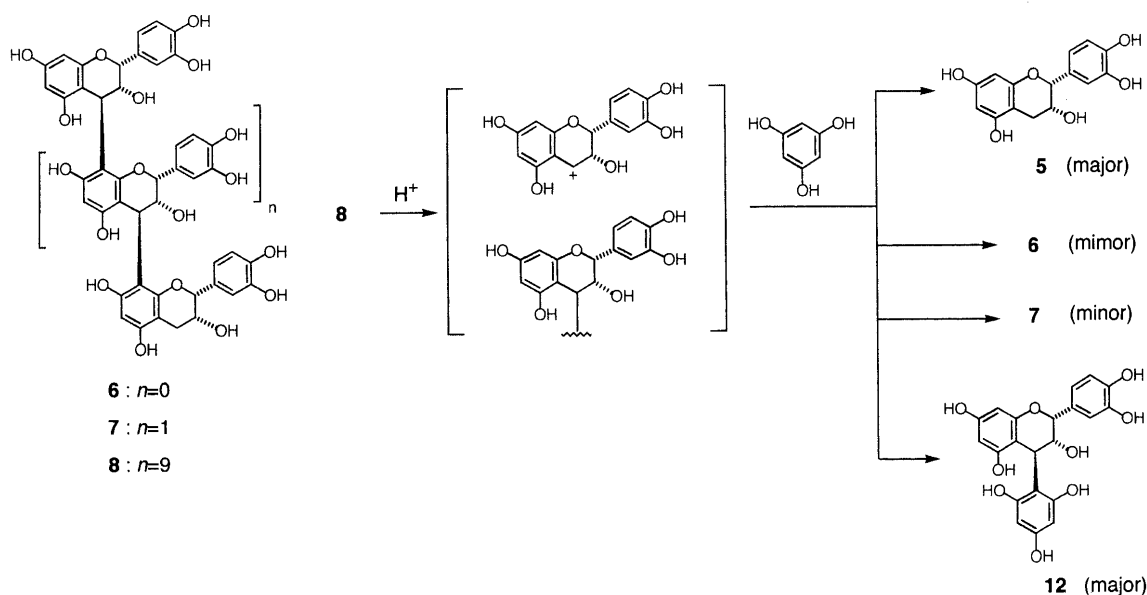


Chart 2

Table 1. Cytotoxicity (CC_{50}) of Polyphenols from *E. japonica*

	MW	CC ₅₀ (μg/ml)(mM)		
		HSC-2	HSG	HGF
Procyanidins and related flavan 3-ols				
Catechin	290	>500 (>1.72)	>500 (>1.72)	>500 (>1.72)
(–)-Epicatechin (5)	290	>500 (>1.72)	>500 (>1.72)	>2000 (>6.90)
Procyanidin B-2 (6)	578	225 (0.39)	415 (0.72)	1850 (3.20)
Procyanidin C-1 (7)	866	205 (0.24)	395 (0.46)	>2000 (>2.31)
Procyanidin oligomer (8)	3170	189 (0.060)	353 (0.11)	>2000 (>0.63)
(–)-Epigallocatechin gallate	458	206 (0.45)	216 (0.47)	870 (1.90)
Flavonoids				
Quercitrin	448	337 (0.75)	>500 (>1.12)	>500 (>1.12)
Quercetin 3- <i>O</i> -sophoroside	626	>500 (>0.80)	>500 (>0.80)	>500 (>0.80)
Kaempferol 3- <i>O</i> -sophoroside	610	>500 (>0.82)	>500 (>0.82)	>500 (>0.82)
Naringenin-8- <i>C</i> -rhamnoglucoside (1)	580	>500 (>0.86)	>500 (>0.86)	>500 (>0.86)
Others				
Gallic acid	170	77 (0.45)	80 (0.47)	90 (0.53)
Ellagic acid	334	>500 (>1.50)	>500 (>1.50)	>500 (>1.50)

Relative viable cell number (A_{540}) was determined by MTT method. The A_{540} of control HSC-2, HSG and HGF cells was 1.17, 0.59 and 0.29, respectively. Each value represents mean from triplicate assays. S.D.<10%.

din C-1 (**7**) (CC_{50} =0.24 mM)<procyanidin oligomer (**8**) (CC_{50} =0.060 mM). The cytotoxic activity of **8** in a molar basis exceeded that of gallic acid (CC_{50} =0.45 mM), ellagic acid (CC_{50} >1.5 mM) or EGCG (CC_{50} =0.45 mM) (Table 1). The cytotoxic activity of quercitrin, quercetin 3-*O*-sophoroside, kaempferol 3-*O*-sophoroside and naringenin-8-*C*-rhamnoglucoside was much less (CC_{50} >0.75 mM). As compared with the HSC-2 cell line, the human salivary gland tumor cell line HSG was slightly resistant to all of these polyphenols, whereas normal human gingival fibroblast HGF was very resistant, suggesting that these polyphenols display selective cytotoxic activity against cancer cell lines relative to normal cells.

Possible Mechanism of Cytotoxicity We have recently established that the prooxidant action of polyphenols can be detected by ESR spectroscopy, using sodium ascorbate as a radical generator.³³⁾ Figure 2A shows that the radical intensity of sodium ascorbate was slightly reduced by a lower concentration (<3 μM) of **8**, but enhanced by higher concentrations (>10 μM). This suggests that the cytotoxic activity of procyanidin oligomer observed at higher concentrations is due to their prooxidant action. This was confirmed by radical generation by **8**, under an alkaline condition (Fig. 2B). It was, however, unexpected that catalase, which decomposes extracellular H_2O_2 , did not significantly affect the cytotoxic activity of the procyanidin oligomer (B/A ratio=1.0–1.4, see Table 2), whereas the cytotoxic activity of EGCG (B/A=1.4–1.8) and gallic acid (B/A=18–29) was significantly reduced. (Table 2) Procyanidin oligomer (**8**) also induced two apoptosis-associated characteristics: DNA fragmentation (as demonstrated by agarose gel electrophoresis) (Fig. 3A) and degradation of cytokeratin 18 by activated caspase(s) (as demonstrated by cytoplasmic staining with an M30 monoclonal antibody) (Fig. 3B).

EGCG, as well as tea extracts,³⁴⁾ which are known as anti-tumor agents,^{35–38)} has been reported to induce apoptosis in various human tumor cell lines, and to inhibit neovascularization in the tumor.³⁹⁾ In the present study, procyanidin oligomer **8** showed more potent cytotoxic activity against oral tumor cell lines than EGCG. However, procyanidin

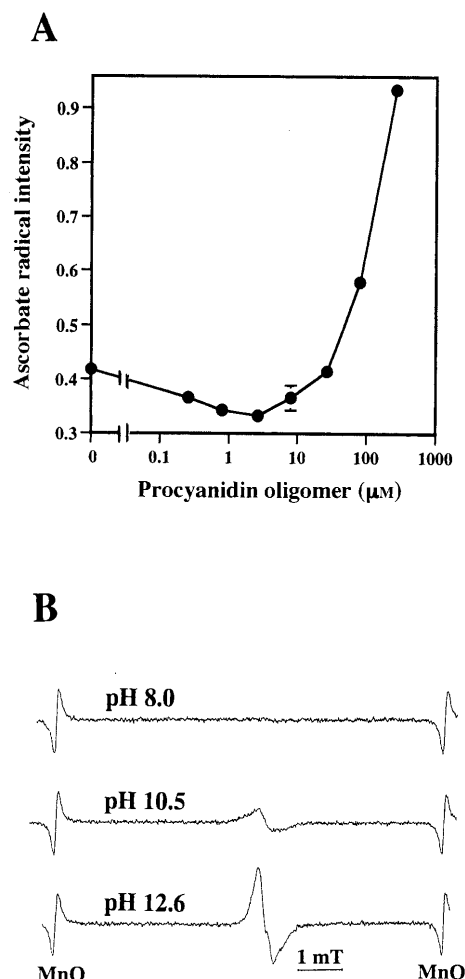


Fig. 2. Effect of Procyanidin Oligomer (**8**) on Ascorbate Radical Intensity (A) and Radical Generation by **8** (B)

(A): Sodium ascorbate (3 mM) was mixed with an equal volume of various concentrations of procyanidin oligomer in 50% DMSO, 0.08 M Tris-HCl, pH 8.0, and the radical intensity of sodium ascorbate was measured 1 min thereafter. The gain was 5×100 . Each value represents the mean from triplicate assays. S.D.<5%. (B): Procyanidin oligomer (3 mg/ml in DMSO) was mixed with an equal volume of 0.2 M Tris-HCl (pH 8.0), 0.2 M $\text{NaHCO}_3/\text{Na}_2\text{CO}_3$, pH 10.5, or 0.2 M KOH (pH 12.6), and the mixture was applied to ESR spectroscopy. The gain was 6.3×100 .

Table 2. Failure of Catalase to Inhibit the Cytotoxic Activity of Procyanidin Oligomer

Compounds	CC ₅₀ (mM)								
	HSC-2			HSG			HGF		
	(A)	(B) +Cat	B/A	(A)	(B) +Cat	B/A	(A)	(B) +Cat	B/A
Procyanidin oligomer (8)	0.046	0.065	1.4	0.10	0.10	1.0	>0.13	>0.13	1.0
EGCG	0.47	0.79	1.7	0.37	0.53	1.4	0.87	1.60	1.8
Gallic acid	0.56	9.78	17.5	0.48	13.9	29.0	0.69	>16.0	>23.2

Cells were incubated for 24 h with various concentrations of the indicated test compounds without (A) or with (B) 3000 U/ml catalase, and the relative viable cell number (A_{540}) was determined by MTT method. The A_{540} of control HSC-2, HSG and HGF cells was 1.20, 0.57 and 0.17, respectively. Each value represents mean of triplicate assays. S.D. < 10%. The ability of catalase to inhibit the cytotoxic activity of each compound was determined by the ratio of B to A.

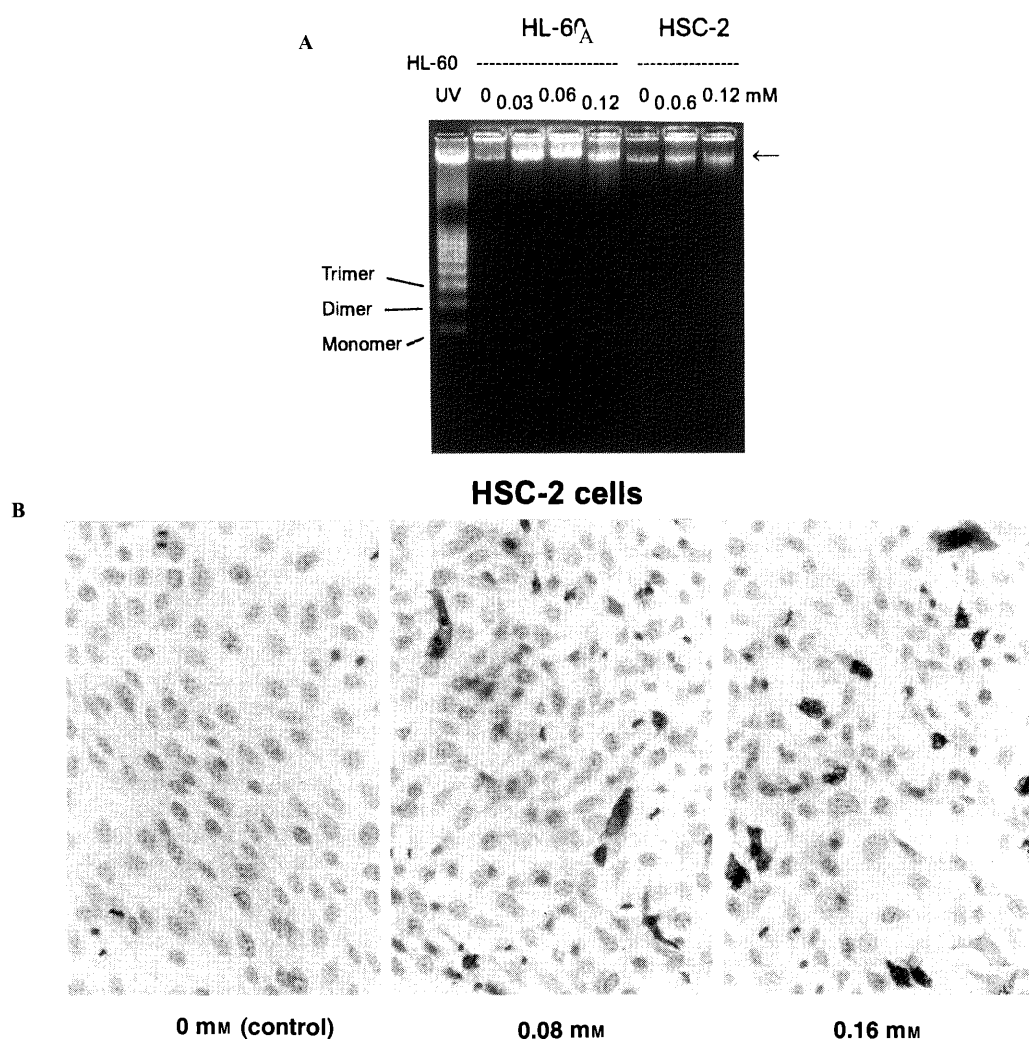


Fig. 3. Induction of DNA Fragmentation by Procyanidin Oligomer (**8**) in HSC-2 Cells (A) and Activation of Caspase by **8** (B)

(A): Near confluent HSC-2 cells and HL-60 cells (1×10^6 /ml) were treated for 6 h with the indicated concentrations of **8**. The cells were lysed, treated with RNase A and proteinase K, and DNA was isolated and applied to 1.8% agarose gel electrophoresis. Lane 1 is the DNA from UV-induced apoptotic HL-60 cells. (B): Near confluent HSC-2 cells were treated for 6 h without (control) or with 0.08 or 0.16 mM procyanidin oligomer (**8**). The cells were fixed in 95% ethanol and 5% acetic acid, then treated with M30 monoclonal antibody. Original magnification, $\times 33$. Note the cytoplasmic staining of the cytokeratin 18 degradation products in the cells treated with procyanidin oligomer.

oligomer (Fig. 2A), but not EGCG, enhanced the radical intensity of sodium ascorbate. These data suggest that these two compounds have different sites of action.

Although further details regarding the effect of procyanidin oligomer against these tumor cells remain to be investigated, the present results suggest that the extract of *E. japonica* would be beneficial in the chemoprevention of oral cancer.

Experimental

Optical rotations were recorded on a JASCO DIP-1000 polarimeter. ^1H - and ^{13}C -NMR spectra were measured in acetone- d_6 + D_2O on Varian VXR-500 (500 MHz for ^1H -NMR and 125.7 and 50 MHz for ^{13}C -NMR) instruments. Chemical shifts are given in δ (ppm) values relative to that of the solvent acetone- d_6 (δ_{H} 2.04; δ_{C} 29.8) and methanol- d_4 (δ_{C} 49.0) on a tetramethylsilane scale. ESI-MS were carried out using a Micromass Auto Spec OA-Tof mass spectrometer (solvent: 50% MeOH + 0.1% AcONH₄, flow rate: 20 $\mu\text{l}/\text{min}$). CD spectra were measured on a JASCO J-720W spectrometer. Normal-phase HPLC was conducted on a YMC-Pack SIL A-003 (YMC Co.,

Ltd.) column (4.6 mm i.d. × 250 mm) developed with *n*-hexane–MeOH–tetrahydrofuran (THF)–formic acid (55:33:11:1) containing oxalic acid (450 mg/l) (flow rate, 1.5 ml/min; detection 280 nm) at room temperature. Reversed-phase HPLC was performed on a YMC-Pack ODS-A A-302 (YMC Co., Ltd.) column (4.6 × 150 mm) developed with 10 mM H_2PO_4 –10 mM KH_2PO_4 –EtOH–AcOEt (42.5:42.5:10:5) (flow rate, 1 ml/min; detection 280 nm) at 40 °C. Detection was made with a Shimadzu SPD-6A spectrophotometric detector at 280 nm. Column chromatography was performed with Diaion HP-20 and MCI gel CHP-20P (75–150 μm) (Mitsubishi), and Toyopearl HW-40 (coarse grade) (Tosoh). Solvents were evaporated under reduced pressure below 40 °C.

Plant Materials The fresh leaves of *E. japonica* cultivated in the herbal garden of our Faculty were collected in April, 1996. A voucher specimen is deposited in the Herbarium, Faculty of Pharmaceutical Sciences, Okayama University.

Extraction and Isolation The fresh leaves (1.0 kg) of *E. japonica* were homogenized in 70% acetone (10 l), and the concentrated solution (1 l) was extracted with ether (1 × 5), AcOEt (1 × 6) and 1-butanol saturated with water (1 × 4), successively. A part (2.8 g) of the AcOEt extract (4.0 g) was chromatographed over Diaion HP-20 (3.3 cm i.d. × 40 cm) with H_2O → aqueous MeOH (10% → 30% → 50% MeOH) → MeOH → 70% acetone– H_2O . The 10% MeOH (109 mg) and 30% MeOH (230 mg) eluates were separately purified by rechromatography over MCI-gel CHP-20P (1.1 cm i.d. × 40 cm) with aqueous MeOH to give commonly chlorogenic acid (25 mg in total), 3-*O*-caffeoylquinic acid (2 mg), (–)-epicatechin (5) (14 mg) and procyanidin B-2 (6) (15 mg). The eluate from 50% MeOH (1.3 g) was subjected to column chromatography over Toyopearl HW-40 (coarse grade, 2.2 cm i.d. × 60 cm) with aqueous MeOH yielding procyanidin C-1 (7) (15 mg) and isoquercitrin (4 mg). The MeOH eluate (727 mg) was similarly submitted to column chromatography over Toyopearl HW-40 (coarse grade, 2.2 cm i.d. × 60 cm) with aqueous MeOH to give quercetin (18 mg). The 1-butanol extract (65.8 g) was chromatographed over Diaion HP-20 (2.2 cm i.d. × 60 cm) with H_2O containing increasing amounts of MeOH in a step-wise gradient mode. The 50% MeOH eluate (4.4 g) was similarly purified by a combination of column chromatographies over Toyopearl HW-40 (coarse grade) and MCI-CHP-20P to afford 4-*O*-caffeoylquinic acid (15 mg), 4-*O*-*p*-coumaroylquinic acid (11 mg), quercetin 3-*O*-sophoroside (14 mg), kaempferol 3-*O*-sophoroside (28 mg), kaempferol 3-*O*- α -rhamnopyranosyl-(1→2)- β -glucopyranoside (10 mg), 1-*O*-feruloyl β -glucopyranose (10 mg), 4-*O*- β -glucopyranosyl-*cis-p*-coumaric acid (1 mg), (2*S*)-naringenin 8-*C*- α -rhamnopyranosyl-(1→2)- β -glucopyranoside (1) (40 mg), (2*R*)-naringenin 8-*C*- α -rhamnopyranosyl-(1→2)- β -glucopyranoside (2) (3 mg) and cinchonain Id 7-*O*- β -glucopyranoside (3) (6 mg). The aqueous extract (48.6 g) was subjected to column chromatography over Diaion HP-20 (5.0 cm i.d. × 47 cm) and developed with H_2O → 10% MeOH → 20% → 30% → 40% → 60% → MeOH → 70% acetone– H_2O . A part (2.0 g) of the 60% MeOH eluate (5.0 g) was rechromatographed over Toyopearl HW-40 (coarse grade, 2.2 cm i.d. × 34 cm) with 40% MeOH → 50% → 60% → 70% → MeOH acetone– H_2O (7:1:2 → 7:2:1) → 70% aqueous acetone. The 60% MeOH eluate (23 mg) was further purified by a combination of column chromatographies over Toyopearl HW-40 (coarse grade) and MCI-CHP-20P to yield cinchonain Ia (4) (1 mg). The eluate from 70% aqueous acetone gave a procyanidin oligomer (8) (662 mg). The known compounds were identified by direct comparison with authentic specimens or by comparisons of their physicochemical data with those reported in the literature.

(2*S*)-Naringenin 8-*C*- α -Rhamnopyranosyl-(1→2)- β -glucopyranoside (1): A pale yellow amorphous powder, $[\alpha]_D^{25} +25.3^\circ$ ($c=1.0$, MeOH). ESI-MS m/z : 598 ($\text{M}+\text{NH}_4^+$), 581 ($\text{M}+\text{H}^+$). HR ESI-MS m/z 581.1815 ($\text{M}+\text{H}^+$), Calcd for $\text{C}_{27}\text{H}_{32}\text{O}_{14}+\text{H}$, 581.1870. UV λ_{max} (MeOH) nm (log ϵ): 214 (4.39), 225 (sh 4.36), 290 (4.12), 325 (sh 3.64). CD (MeOH) $\Delta\epsilon$ (nm): +10.5 (218), +1.5 (253), –9.0 (290), +2.3 (329). ^1H -NMR (methanol- d_4) δ : 7.42 (2H, d, $J=8.5$ Hz, H-2', 6'), 6.90 (2H, d, $J=8.5$ Hz, H-3', 5'), 6.02 (1H, s, H-6), 5.34 (1H, dd, $J=2, 14$ Hz, H-2), 5.27 [1H, br s, rhamnose (rha) H-1''], 4.85 [1H, d, $J=9$ Hz, glucose (glc) H-1'], 4.07 (1H, t, $J=9$ Hz, glc H-2'), 3.94 (1H, br s, rha H-2''), 3.82 (1H, br d, glc H-6'), 3.74 (1H, dd, $J=5, 12$ Hz, glc H-6'), 3.68 (1H, dd, $J=3, 9$ Hz, rha H-3''), 3.54 (1H, t, $J=9$ Hz, glc H-3'), 3.48 (1H, t, $J=9$ Hz, glc H-4'), 3.34 (1H, m, glc H-5'), 3.32 (1H, dd, $J=14, 17$ Hz, H-3), 3.25 (1H, t, $J=9$ Hz, rha H-4''), 2.79 (1H, dd, $J=6, 9$ Hz, rha H-5''), 2.64 (1H, dd, $J=2, 17$ Hz, H-3), 0.85 (3H, d, $J=6$ Hz, rha H-6''). ^{13}C -NMR (acetone- d_6 + D_2O) δ : 7.45 (2H, d, $J=8.5$ Hz, H-2', 6'), 6.90 (2H, d, $J=8.5$ Hz, H-3', 5'), 5.96 (1H, s, H-6), 5.40 (1H, dd, $J=2, 14$ Hz, H-2), 5.29 [1H, br s, rha H-1''], 4.83 (1H, d, $J=10$ Hz, glc H-1'), 3.36 (1H, dd, $J=14, 17$ Hz, H-3), 2.59 (1H, dd, $J=2, 17$ Hz, H-3), 0.76 (3H, d,

$J=6$ Hz, rha H-6''). ^{13}C -NMR (acetone- d_6 + D_2O) δ : 198.1 (C-4), 166.0 (C-7), 164.6 (C-5), 161.3 (C-9), 158.6 (C-4'), 130.5 (C-1'), 129.1 (2C) (C-2', 6'), 116.2 (2C) (C-3', 5'), 104.9 (C-8), 103.2 (C-10), 101.2 (rha C-1''), 98.0 (C-6), 81.4 (glc C-5'), 80.3 (C-2), 80.1 (glc C-3'), 77.3 (glc C-2'), 74.2 (glc C-1'), 73.1 (rha C-4''), 72.0 (rha C-2''), 71.6 (rha C-3''), 70.3 (glc C-4'), 69.0 (rha C-5''), 61.1 (glc C-6''), 43.6 (C-3), 17.9 (rha C-6'').

Acid Hydrolysis of 1 A solution of 1 (1 mg) in 2.5% H_2SO_4 (0.5 ml) was heated in a boiling-water bath for 2 h. After cooling, the reaction mixture was extracted with AcOEt. The aqueous layer was neutralized with Amberlite IR-120 (OH form), and evaporated to dryness. The residue after trimethylsilylation was analyzed by GLC (2% OV-17, column temperature: 170 °C), in which the retention time of the sugar unit was identical with that of the standard L-rhamnose.

(2*R*)-Naringenin 8-*C*- α -Rhamnopyranosyl-(1→2)- β -glucopyranoside (2): A pale yellow amorphous powder, $[\alpha]_D^{25} +5.3^\circ$ ($c=1.0$, MeOH). ESI-MS m/z : 598 ($\text{M}+\text{NH}_4^+$), 581 ($\text{M}+\text{H}^+$). HR ESI-MS m/z 581.1858 ($\text{M}+\text{H}^+$), Calcd for $\text{C}_{27}\text{H}_{32}\text{O}_{14}+\text{H}$, 581.1870. UV λ_{max} (MeOH) nm (log ϵ): 218 (4.43), 290 (4.20), 328 (sh 3.63). CD (MeOH) $\Delta\epsilon$ (nm): –4.45 (219), –0.6 (254), +5.1 (291), –1.3 (327). ^1H -NMR (acetone- d_6 + D_2O) δ : 7.39 (2H, d, $J=8.5$ Hz, H-2', 6'), 6.87 (2H, d, $J=8.5$ Hz, H-3', 5'), 5.96 (1H, s, H-6), 5.62 (1H, dd, $J=2, 14$ Hz, H-2), 5.27 (1H, br s, rha H-1''), 4.83 (1H, d, $J=8$ Hz, glc H-1'), 3.10–3.95 (H-3, glc H-2'–H-6' and rha H-2'–H-4''), 2.77 (2H, m, H-3, rha H-5''), 0.82 (3H, d, $J=6$ Hz, rha H-6'').

Cinchonain Id 7-*O*- β -Glucopyranoside (3): A pale yellow amorphous powder, $[\alpha]_D^{25} -37.5^\circ$ ($c=1.0$, MeOH). ESI-MS m/z : 632 ($\text{M}+\text{NH}_4^+$), 615 ($\text{M}+\text{H}^+$). HR ESI-MS m/z 632.1990 ($\text{M}+\text{NH}_4^+$), Calcd for $\text{C}_{30}\text{H}_{36}\text{O}_{14}+\text{NH}_4$, 632.1979. UV λ_{max} (MeOH) nm (log ϵ): 284 (3.97), 328 (3.38). CD (MeOH) $\Delta\epsilon$ (nm): +11.4 (210), –11.2 (228), +5.5 (246), –2.2 (286). ^1H -NMR (acetone- d_6 + D_2O) δ : 7.07 (1H, d, $J=2$ Hz, H-2'), 6.84 (1H, dd, $J=2, 8$ Hz, H-6'), 6.79 (1H, d, $J=8$ Hz, H-5'), 6.72 (1H, d, $J=2.5$ Hz, H-2'), 6.70 (1H, d, $J=8.5$ Hz, H-5'), 6.56 (1H, s, H-8), 6.51 (1H, dd, $J=2.5, 8.5$ Hz, H-6'), 4.95 (1H, s, H-2), 4.94 (1H, d, $J=7$ Hz, glc H-1''), 4.72 (1H, br dd, $J=2, 7$ Hz, H-7''), 4.28 (1H, m, H-3), 3.81 (1H, dd, $J=2.5, 12$ Hz, glc H-6''), 3.64 (1H, dd, $J=5, 12$ Hz, glc H-6''), 3.37–3.53 (4H, m, glc H-2'–5''), 3.02 (1H, br dd, $J=3, 17$ Hz, H-4), 3.02 (1H, dd, $J=7, 16$ Hz, H-8''), 2.88 (1H, dd, $J=2, 16$ Hz, H-8''), 2.83 (1H, dd, $J=3, 17$ Hz, H-4). ^{13}C -NMR (126 MHz, in acetone- d_6 + D_2O) δ : 168.6 (C-9''), 155.9 (C-9), 154.3 (C-7), 151.5 (C-5), 145.8 (C-3''), 145.4 (2C) (C-3', 4'), 144.7 (C-4''), 134.6 (C-1''), 131.4 (C-1'), 119.2 (C-6'), 118.5 (C-6''), 115.9 (C-5''), 115.4 (C-5'), 115.2 (2C) (C-2', 2''), 108.9 (C-6), 103.6 (C-10), 102.6 (glc C-1''), 100.1 (C-8), 79.7 (C-2), 77.5 (glc C-3'', 5''), 74.9 (glc C-2''), 70.7 (glc C-4''), 65.9 (C-3), 62.1 (glc C-6''), 37.3 (C-8''), 34.1 (C-7''), 29.0 (C-4).

Acid Hydrolysis of 3 A solution of 3 (0.5 mg) in 1% H_2SO_4 (0.5 ml) was heated in a boiling-water bath for 2 h. After cooling, the reaction mixture was subjected to a Bond Elut C_{18} cartridge column with H_2O and MeOH. Addition of the H_2O eluate to a solution of Glucose CII-test Wako (Wako Pure Chemicals Industries, Ltd.) produced a reddish color, indicating that a sugar unit of 3 was D-glucose.²³⁾

Procyanidin Oligomer (8): CD (MeOH) $[\theta]$ (nm): -4.7×10^5 (204), $+4.7 \times 10^5$ (225). ^{13}C -NMR (50 MHz, in methanol- d_4 , 45 °C): δ 154.9–157.1 (C-5, 7, 8a), 145.1–145.8 (C-3', 4'), 132.6 (C-1'), 119.2 (C-6'), 116.1 (C-5'), 115.3 (C-2'), 107.7 (C-8), 102.4 (C-4a), 97.8 (C-6), 79.8 (external C-2), 77.1 (C-2), 72.7 (C-3), 66.8 (terminal C-3), 37.6 (C-4), 30.0 (terminal C-4).

Degradation of 8 with Phloroglucinol A mixture of procyanidin polymer fraction (5 mg) and phloroglucinol (5 mg) in 1% HCl–EtOH (1 ml) was left standing overnight at room temperature. The reaction mixture was analyzed by reversed-phase HPLC to show the peaks due to (–)-epicatechin (5) and (–)-epicatechin-(4 β →2)-phloroglucinol (12) as the main products. Their identity was confirmed by HPLC comparison with authentic samples obtained by similar treatment of 6 and 7. Small peaks due to 6 and 7 were also detected in the HPLC.

GPC Analysis The fraction of the procyanidin oligomer was acetylated with acetic anhydride and pyridine. After the reaction mixture was poured into water, the acetate deposited was collected and washed with water. The acetate was then analyzed by GPC [column, TSK gel G4000H_{XL} (7.8 mm i.d. × 300 mm) (Tosoh); solvent, THF; flow rate, 0.8 ml/min; column temperature, 40 °C]. Molecular weight was calibrated by the standard peracetates of (–)-epicatechin (5), procyanidins B-2 (6) (procyanidin dimer), C-1 (7) (procyanidin trimer), and cinnamtannin A₂ (procyanidin tetramer). An average molecular weight as the acetate (M_n : 5400, M_w : 14800) of the procyanidin oligomer was defined by the equation ($\log \text{MW} = -0.67 \times t_R + 10.89$).

Assay for Cytotoxic Activity HSC-2 and HSG cell lines were main-

tained as monolayer cultures at 37 °C in Dulbecco's modified Eagle medium (DMEM) (Gibco, Grand Island, NY, U.S.A.) supplemented with 10% heat-inactivated fetal bovine serum (FBS) (JRH Biosciences, Lenexa, KS, U.S.A.) in a humidified 5% CO₂ atmosphere. HGF cells were isolated from healthy gingival biopsies from a 10-year-old female, a patient undergoing periodontal surgery, as described previously.⁴⁰⁾ Cells between the fifth and seventh passages were used.

The relative viable cell number was determined by 3-[4,5-dimethylthiazol-2-yl]-2,5-diphenyltetrazolium bromide (MTT) (Sigma Chem. Ind., St. Louis, MO, U.S.A.) method. Near confluent cells grown in a 96-microwell plate (Falcon, flat bottom, treated polystyrene, Becton Dickinson) were incubated for 24 h with or without test compounds. All tannin samples were dissolved in dimethylsulfoxide (DMSO) or 25% DMSO at 50 mg/ml. The final concentration of DMSO in the medium was below 1%. The cells were washed once with phosphate-buffered saline (PBS) and incubated for 4 h with 0.2 mg/ml MTT in DMEM medium supplemented with 10% FBS. After removing the medium, cells were lysed with 100 μ l of DMSO and the relative viable cell number was determined by measuring the absorbance at 540 nm of the cell lysate with Labsystems Multiskan[®] (Biochromatic) with a Star/DOT Matrix printer JL-10. The 50% cytotoxic concentration (CC₅₀) was determined from the dose-response curve.

Assay for Radical Intensity The radical intensity of test samples was determined at 25 °C in the indicated buffer solution using ESR spectroscopy (JEOL JES RE1X, X-band, 100 kHz modulation frequency). Instrument settings: center field, 336.0 \pm 5.0 mT; microwave power, 8 mW; modulation amplitude, 0.1 mT; gain, 5 or 6.3 \times 100; time constant, 0.1 s; scanning time, 4 min. Radical intensity was defined as the ratio of peak heights of these radicals to that of MnO.^{41,42)}

Assay for DNA Fragmentation Cells were lysed with 20 μ l lysis buffer [50 mM Tris-HCl, pH 7.8, 10 mM EDTA, 0.5% (w/v) sodium *N*-lauroyl-sarcosinate]. The solutions were incubated sequentially with 0.5 mg/ml RNase A for 60 min at 50 °C, and 0.5 mg/ml proteinase K for 60 min at 50 °C. DNA was extracted and precipitated by 70% ethanol, then dissolved in TE buffer (10 mM Tris-HCl, pH 7.4, 1 mM EDTA, pH 8.0). DNA, equivalent to 5 \times 10⁶ cells, was applied to 1.8% agarose gel electrophoresis. The DNA fragmentation pattern was examined in photographs taken under UV illumination.⁴³⁾

Immunocytochemistry Cultured cells on chamber slides were fixed with 95% ethanol and 5% acetic acid for 10 min at 4 °C. After washing in PBS, each slide was incubated in 2% bovine serum albumin (BSA)-PBS to block a nonspecific reaction for 15 min at room temperature. An appropriately diluted M30 monoclonal antibody (Boehringer Mannheim) was applied to each slide as a primary antibody and incubated for 60 min at room temperature. After washing in PBS, the slides were incubated with biotinylated horse anti-mouse IgG (H and L chains) antibody (1 : 200, Vector) for 30 min at room temperature. The slides were subsequently incubated with streptavidin-peroxidase and colored as described above. To block endogenous peroxidase activity, a 3,3'-diaminobenzidine tetrahydrochloride (DAB) solution containing 0.05% NaN₃ was used.

Acknowledgements The authors thank the SC-NMR Laboratory of Okayama University for NMR experiments using their Varian VXR-500 instrument.

References and Notes

- Perry L. M., "Medicinal Plants of East and Southeast Asia," MIT press, Cambridge, 1980, pp. 342—343.
- Shimizu M., Fukumura H., Tsuji H., Tanaami S., Hayashi T., Morita N., *Chem. Pharm. Bull.*, **34**, 2614—1617 (1986).
- De Tommasi N., De Simone F., Pizza C., Mahmood N., Orsi N., Stein M. L., *J. Nat. Prod.*, **55**, 1067—1073 (1992).
- De Tommasi N., Aquino R., De Simone F., Pizza C., *J. Nat. Prod.*, **55**, 1025—1032 (1992).
- Jung H. A., Park J. C., Chung H. Y., Kim J., Choi J. S., *Arch. Pharm. Res.*, **22**, 213—218 (1999).
- Gavrieli Y., Sherman Y., Ben-Sasson S. A., *J. Cell Biol.*, **119**, 493—501 (1992).
- Caulin C., Salvesen G. S., Oshima R. G., *J. Cell Biol.*, **138**, 1379—1394 (1997).
- Merfort I., *Phytochemistry*, **31**, 2111—2113 (1992).
- Markham K. R., Geiger H., Jaggy H., *Phytochemistry*, **31**, 1009—1011 (1992).
- Strack D., Heilemann J., Wray V., Dirks H., *Phytochemistry*, **28**, 2071—2078 (1989).
- Markham K. R., Ternal B., Stanley R., Geiger H., Mabry T. J., *Tetrahedron*, **34**, 1389—1397 (1978).
- Yasukawa K., Takido M., *Phytochemistry*, **26**, 1224—1226 (1987).
- Thompson R. S., Jacques D., Haslam E., Tanner R. J. N., *J. Chem. Soc. Perkin Trans. I*, **1972**, 1387—1399.
- Hor M., Heinrich M., Rimpler H., *Phytochemistry*, **42**, 109—119 (1996).
- Shih C. Y., Dumbroff E. B., Thompson J. E., *Plant Physiol.*, **89**, 1053—1059 (1988).
- Cui C. B., Tezuka Y., Kikuchi T., Nakano H., Tamaoki T., Park J.-H., *Chem. Pharm. Bull.*, **38**, 3218—3225 (1990).
- Nonaka G., Nishioka I., *Chem. Pharm. Bull.*, **30**, 4268—4276 (1982).
- Chen H.-F., Tanaka T., Nonaka G., Fujioka T., Mihashi K., *Phytochemistry*, **33**, 183—187 (1993).
- Mabry T. J., Markham K. R., Thomas M. B., "The Systematic Identification of Flavonoids," Springer-Verlag, New York, 1970, p. 215.
- Gaffield W., *Tetrahedron*, **26**, 4093—4108 (1970).
- Okamura N., Yagi A., Nishioka I., *Chem. Pharm. Bull.*, **29**, 3507—3514 (1981).
- Hatano T., Takagi M., Ito H., Yoshida T., *Phytochemistry*, **47**, 287—293 (1998).
- Miwa I., Okuda J., Maeda K., Okuda G., *Clin. Chim. Acta*, **37**, 538—540 (1972).
- Foo L. Y., *Phytochemistry*, **26**, 2825—2830 (1987).
- Foo L. Y., *Phytochemistry*, **28**, 2477—2481 (1989).
- Kadota S., Takamori Y., Nyein K. N., Kikuchi T., Tanaka K., Ekimoto H., *Chem. Pharm. Bull.*, **38**, 2687—2697 (1990).
- Bate-Smith E. C., *Phytochemistry*, **14**, 1107—1113 (1975).
- Foo L. Y., *Phytochemistry*, **28**, 3185—3190 (1989).
- Czochanska Z., Foo L. Y., Newman R. H., Porter L. J., *J. Chem. Soc. Perkin Trans. I*, **1980**, 2278—2286.
- Foo L. Y., Lu Y., *Food Chemistry*, **64**, 511—518 (1999).
- Williams V. M., Porter L. J., Hemingway R. W., *Phytochemistry*, **22**, 569—572 (1983).
- Barrett M. W., Klyne W., Scopes P. M., Fletcher A. C., Porter L. J., Haslam E., *J. Chem. Soc. Perkin Trans. I*, **1979**, 2375—2377.
- Sakagami H., Jiang Y., Kusama K., Atsumi T., Ueha T., Toguchi M., Iwakura I., Satoh K., Ito H., Hatano T., Yoshida T., *Phytomedicine*, in press (2000).
- Zhao Y., Cao J., Ma H., Liu J., *Cancer Lett.*, **121**, 163—167 (1997).
- Fujiki H., Suganuma M., Okabe S., Sueoka N., Komori A., Sueoka E., Kozu T., Tada Y., Suga K., Imai K., Nakachi K., *Mutat. Res.*, **402**, 307—310 (1998).
- Yoshizawa S., Horiuchi H., Fujiki H., Yoshida T., Okuda T., Sugimura T., *Phytotherapy Res.*, **1**, 44—47 (1987).
- Achiwa Y., Hibasami H., Katsuzaki H., Imai H., Komiya T., *Biosci. Biotech. Biochem.*, **61**, 1099—1101 (1997).
- Hibasami H., Komiya T., Achiwa Y., Ohnishi K., Kojima T., Nakanishi K., Akashi K., Hara Y., *Oncol. Rep.*, **5**, 527—529 (1998).
- Cao Y., Cao R., *Nature (London)*, **398**, 381 (1999).
- Fujisawa S., Kashiwagi Y., Atsumi T., Iwakura I., Ueha T., Hibino Y., Yokoe I., *J. Dent.*, **27**, 291—295 (1999).
- Sakagami H., Satoh K., Ida Y., Hosaka M., Arakawa H., Maeda M., *Free Radic. Biol. Med.*, **25**, 1013—1020 (1998).
- Sakagami H., Satoh K., Fukuchi K., Gomi K., Takeda M., *Free Radic. Biol. Med.*, **23**, 260—270 (1997).
- Fujinaga S., Sakagami H., Kuribayashi N., Takayama H., Amano Y., Sakagami T., Takeda M., *Showa Univ. J. Med. Sci.*, **6**, 135—144 (1994).

Synthesis and Antifungal Activities of R-102557 and Related Dioxane-Triazole Derivatives

Sadao OIDA*,^a Yawara TAJIMA,^a Toshiyuki KONOSU*,^a Yoshie NAKAMURA,^a Atsushi SOMADA,^a Teruo TANAKA,^a Shinobu HABUKI,^a Tamako HARASAKI,^b Yasuki KAMAI,^b Takashi FUKUOKA,^b Satoshi OHYA,^b and Hiroshi YASUDA^b

Medicinal Chemistry Research Laboratories^a and Biological Research Laboratories,^b Sankyo Co., Ltd., 2–58, Hiromachi-1-chome, Shinagawa-ku, Tokyo 140–8710, Japan. Received December 17, 1999; accepted February 18, 2000

Novel triazole compounds with a dioxane ring were synthesized. Condensation of the diol precursor 10 with various aromatic aldehydes 11–13 under acidic conditions afforded a series of dioxane-triazole compounds 14–16. The antifungal activities of the compounds 14–16 were evaluated *in vivo* in mice infection models against *Candida* and *Aspergillus* species. High activities were seen for the derivatives with one or two double bond(s) and an aromatic ring substituted with an electron-withdrawing group in the side chain. Among the derivatives, R-102557 (16R: Ar=4-(2,2,3,3-tetrafluoropropoxy)phenyl) showed excellent *in vivo* activities against *Candida*, *Aspergillus* and *Cryptococcus* species. It also showed high tolerance in a preliminary toxicity study in rats.

Key words antifungal; triazole; R-102557; structure–activity relationship; synthesis; lanosterol 14-demethylase

There have been increasing demands for antifungal agents that are effective against systemic mycosis.¹⁾ We are surrounded by fungi, and it is thanks to our immune system that our bodies are not invaded by fungi. But once our immune system becomes deficient or suppressed, as it does in AIDS patients and in those that have received cancer chemotherapy or organ transplants, then we become highly susceptible to such fungal infection. In many cases it is not the AIDS or cancer itself but the mycosis that is lethal to these patients.

Attention has been paid to triazole derivatives²⁾ because of their generally broad antifungal spectrum and low toxicity. Triazole derivatives displace lanosterol from lanosterol 14-demethylase (14DM), a cytochrome P450-dependent enzyme, and block the biosynthesis of an essential component of the fungal cell membrane, ergosterol.³⁾ Fluconazole⁴⁾ (**1**) has relatively low antifungal activity *in vitro*, but it is water-soluble, and has excellent pharmacokinetic properties. It is effective against candidiasis after both oral administration and injection. However, its activity against *Aspergillus* seems limited. Itraconazole⁵⁾ (**2**) has an excellent and broader antifungal spectrum. Newer triazole agents such as voriconazole⁶⁾ (**3**), Sch56592⁷⁾ (**4**) and ER-30346⁸⁾ (BMS-207147) (**5**), are active against *Aspergillus* and currently under clinical trials.

In our continuing program⁹⁾ aimed at finding a new triazole antifungal agent, we designed a series of dioxane-triazole compounds depicted by the general formula I (Chart 1). We presumed that the left-half portion of the molecule, shown in the box, is essential to the high antifungal activity. It is a common substructure seen in many other triazole antifungals. The 1,3-dioxane ring was introduced in the expectation that: 1) Since acetal moieties will make a molecule more hydrophilic and water-soluble than simple hydrocarbon moieties, the compound could become more available orally and would be more easily delivered to the target fungal enzyme; 2) since many other triazole antifungal agents have heteroatoms at the corresponding part of the molecule, complementary structure of the target enzyme would be implied; 3) a 2,5-substituted-1,3-dioxane ring would not create a chiral center and would generate *cis* and *trans* isomers only; and 4)

a variety of aldehydes should be available as the side chain precursor. The sulfur atom was incorporated in the 3-position because the molecule could readily be prepared from the known epoxide **8**.^{9a,b,e,10)} The methyl group at the 3-position mimics the 13 β -methyl group of lanosterol.^{9e,f)} The two fluorine atoms in the benzene ring in the left half of the molecule aim at strengthening the antifungal activity.^{4b,10c)}

In this paper, we will present our recent findings on synthesis and antifungal activities of the compounds I.

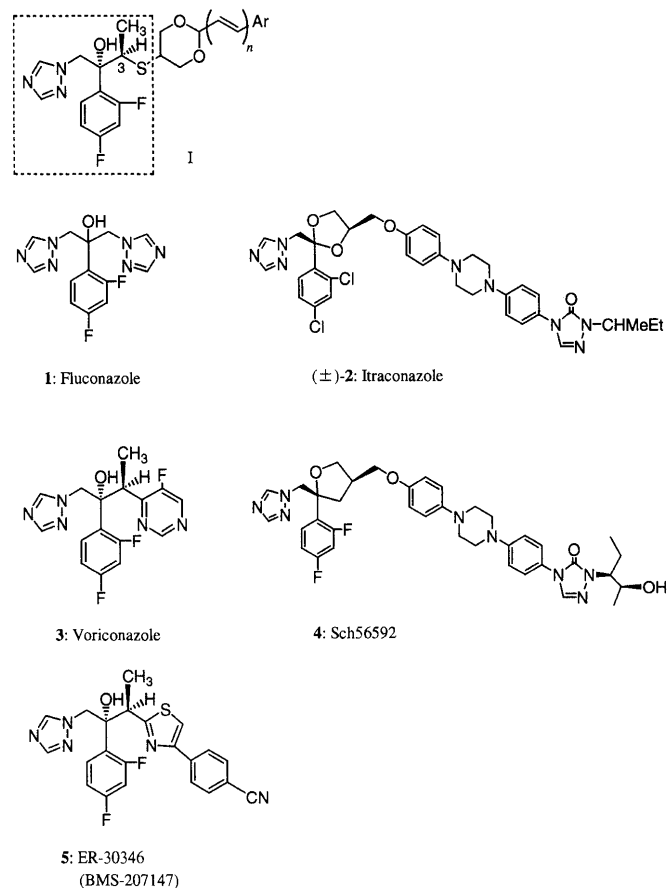


Chart 1

* To whom correspondence should be addressed.

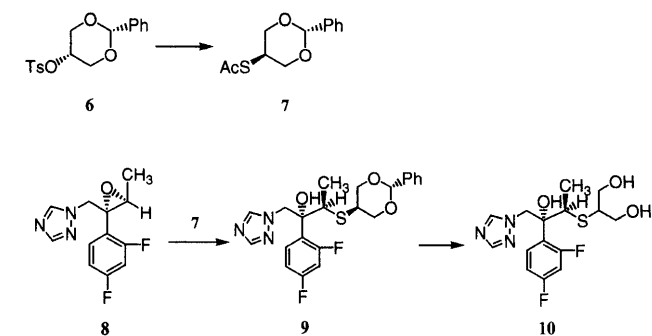
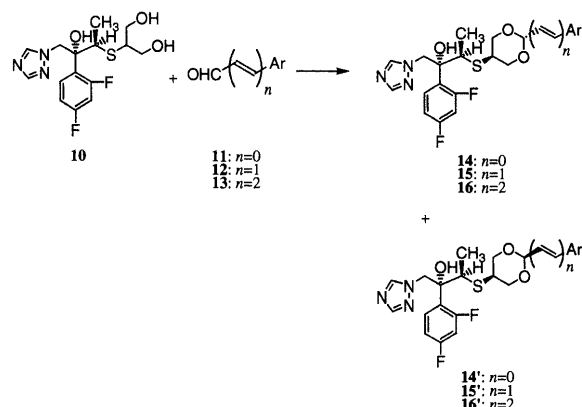


Chart 2



Ar	Ar	Ar
A:	K:	U:
B:	L:	V:
C:	M:	W:
D:	N:	X:
E:	O:	Y:
F:	P:	Z:
G:	Q:	AA:
H:	R:	AB:
I:	S:	AC:
J:	T:	AD:

Chart 3

Chemistry In order to prepare a variety of derivatives **I** in an efficient manner, the diol **10** was planned as a pivotal precursor. Preparation of the diol **10** was accomplished as follows (Chart 2). The known tosylate **6**¹¹ was heated with potassium thioacetate in *N,N*-dimethylformamide (DMF) to give the thioester **7** in 43% yield. Then, the optically active known epoxide **8**^{9a,b,e,10} was treated with the thioester **7** in the presence of sodium methoxide to afford the thioether **9** in 91% yield. The benzylidene protecting group was removed by acid treatment to furnish **10** in 88% yield.

The diol **10** was coupled with a variety of aldehydes **11**, **12**, and **13** (Chart 3). The reaction was driven by stirring a solution of a mixture of diol **10** and each aldehyde **11**–**13** in dichloromethane in the presence of *p*-toluenesulfonic acid and molecular sieves 4A. The *trans* dioxane isomers **14**, **15**, and **16** were predominantly produced, and easily separated

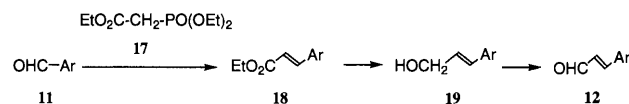
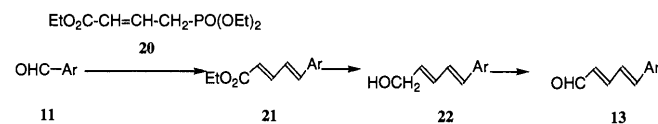


Chart 4



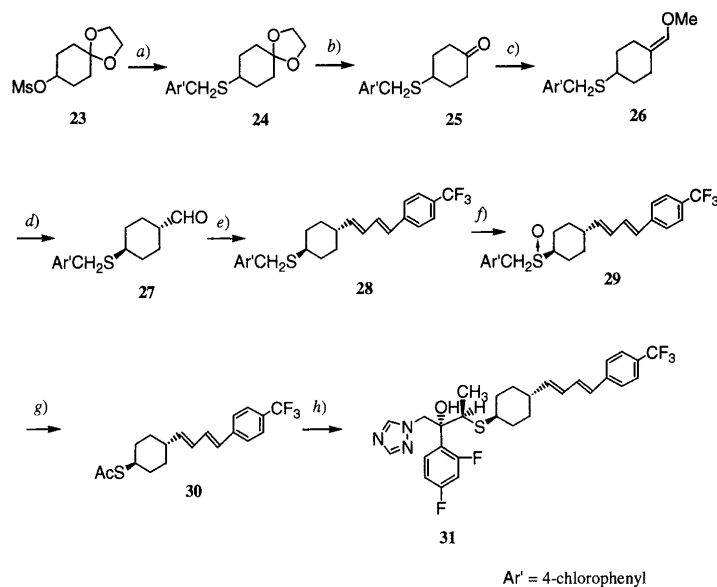
from the *cis* isomers **14'**, **15'**, and **16'** by column chromatography. The stereochemistry was elucidated by ¹H-NMR spectrum. The *trans* isomers **14**, **15**, and **16**, showed the characteristic signal for the methine proton at the 5-position of the 1,3-dioxane ring with a large coupling constant (triplet of triplets, $J=ca. 11, 5$ Hz). An analogous signal pattern was observed for the above-mentioned *trans* thioether **9**. In contrast, the *cis* isomers **14'**, **15'**, and **16'** showed small coupling constants (triplet-like, $J=ca. 2$ Hz). These data indicate that the methine protons in the isomers **14**, **15**, and **16** are axial and those in the isomers **14'**, **15'**, and **16'** are equatorial. Therefore, the sulfur atoms in the isomers **14**, **15**, and **16** are equatorial and *trans* to the olefinic substituents, whereas those in the isomers **14'**, **15'**, and **16'** are axial and *cis* to the olefinic substituents.

Most of the 3-arylacroleins **12** used in the above reactions were prepared from the corresponding aryl aldehydes **11** stereoselectively by the homologation sequence shown in Chart 4. Thus, Horner–Wadsworth–Emmons reaction with phosphonoacetate **17** gave the esters **18**; diisobutylaluminum hydride (DIBAL) reduction gave the allylic alcohols **19**; and further oxidation gave **12**. Most of the 5-aryl-2,4-pentadienals **13** were prepared from **11** in a similar manner using the phosphonocrotonate **20** via **21** and **22**. The 3-arylacroleins **12D** and **12E** were prepared in one step from the corresponding aryl aldehydes **11D** and **11E** using (triphenylphosphoranylidene)acetaldehyde following a literature procedure.¹² The aldehyde **13E** was prepared in a similar manner in one step from **11E** using (triphenylphosphoranylidene)crotonaldehyde.¹³

A cyclohexane analog **31** was prepared as shown in Chart 5 for comparing activities.

Antifungal Activity Since it is known that there is no good correlation between *in vitro* and *in vivo* activities of azole antifungal agents,¹⁴ and we have experienced this discrepancy in the antifungal evaluation of the oxazolidine derivatives,^{9f} the compounds were evaluated *in vivo* using a murine model of systemic candidiasis. The results are summarized in Table 1. In the model, a group of 10 mice were inoculated with fungi intravenously and the test compounds (16–20 mg/kg, *per dose*) were administered either orally (*p.o.*) or intraperitoneally (*i.p.*) 1, 4, and 24 h post infection. All the control (no drug) mice died within three days after infection whereas those that were given drugs survived substantially longer.

The structure–activity relationships were evaluated initially by comparing the *in vivo* activities of **9**, **14A**, **14C**, and



- a) 4-Chloro- α -toluenethiol, NaH, DMF, 50°C. b) HCl, acetone, H₂O, 50°C.
 c) [Ph₃P⁺-CH₂OMe]Cl⁻, NaH, DMSO, rt. d) HCl, acetone, H₂O, 55°C, then NaOMe, MeOH, rt.
 e) [Ph₃P⁺-CH₂-CH=CH-C₆H₄-CF₃]Cl⁻, NaH, DMSO, rt. f) mCPBA, CH₂Cl₂, 0°C.
 g) (CF₃CO)₂O, 2,6-lutidine, THF, CH₃CN, 0°C; NaHCO₃, H₂O; CH₃COCl, Et₃N, CH₂Cl₂, 0°C.
 h) **8**, NaOMe, MeOH, DMF, 55–60°C.

Chart 5

14D, which have no olefinic carbon chain between the aryl and dioxane rings. The unsubstituted phenyl compound **9** exhibited a fair activity. Introducing an electron-withdrawing group such as a fluorine atom or a nitro group to the phenyl ring resulted in slight improvement in the survival rates.

We then fixed the aryl ring Ar to 2,4-difluorophenyl, and varied the length of the olefinic carbon chain between the dioxane and aryl rings (compounds **14C**, **15C**, and **16C**). The compound **15C**, with one olefinic double bond, showed a better *in vivo* activity against *Candida albicans* than the shortest compound **14C**, and it was slightly active than the longer homolog **16C**.

Accordingly, a number of the derivatives **15**, which have one double bond, were prepared and tested. Compounds with an electron-donating substituent at the phenyl ring (e.g. the compound **15L**) showed modest activity whereas those with an electron-withdrawing substituent such as a chlorine atom or a trifluoromethyl group (e.g. the compounds **15B**, **15F**, and **15G**) showed good activity.

The 4-position seems to be the most suitable position in the phenyl ring for modification. As we can see by comparing **15A** and **15K**, introduction of a trifluoromethyl group at the 2-position, in addition to the fluorine atom at the 4-position, brought about only a small improvement in activity. The 3-trifluoromethyl derivatives **15G**, **15H** and **15J** showed much higher activities than **15K**, and the 4-trifluoromethyl derivatives **15F** and **15I** exhibited the highest activities.

The trifluoromethoxy derivatives **15N** and **15O** also showed high activities.

The *cis* (in terms of the stereochemistry on the 1,3-dioxane ring) isomers showed lower activities than the *trans* counterpart, as we can see by comparing **15B** and **15'B**, **15F** and **15'F**, and **15Q** and **15'Q**.

The activities of the pyridyl (**15W**, **15X**, **15Y**, and **15Z**) and thienyl (**15AA**) analogs were lower than those of the phenyl

analogs. However, the naphthyl ring analog **15AC** exhibited excellent activity, comparable to that of the substituted phenyl compounds.

We then prepared the homologs **16**, which have two double bonds. The relationship between the Ar groups and the antifungal activities paralleled that of the derivatives **15**. Among the compounds, **16B**, **16F**, **16N**, **16R**, **16U** and **16V** showed high *in vivo* potency.

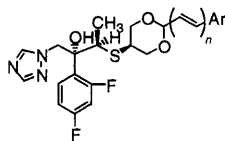
The cyclohexane ring analog **31** showed only fair activity, implying the importance of the 1,3-dioxane ring for antifungal activity.

Some of the compounds were evaluated further by a murine model of systemic aspergillosis. The results are summarized in Table 2. In this model, a group of 10 mice were inoculated with either *Aspergillus fumigatus* or *Aspergillus flavus* intravenously, and the test compounds (20 mg/kg, *per dose*) were administered orally 1, 4, 24, 31, 48 and 55 h post infection.

Among the compounds tested, **15F**, **15R**, **15V**, **15AC**, **15AD**, **16R**, and **16V** protected all mice for 14 d from both *Aspergillus fumigatus* and *Aspergillus flavus*.

In a preliminary toxicity study in rats (F344 strain, male, 5 weeks old, given drugs of 100 mg/kg/dose orally once daily for 14 d, each group consisting of five rats), all cases given **15F** (a derivative with one double bond) died in the second week of the administration, but all rats given **16F**, **16R** and **16V** (derivatives with two double bonds) survived without any apparent toxic symptoms. Among **16F**, **16R** and **16V**, the compound **16R** showed the lowest influence on adrenal glands and thyroid glands.

Finally, the compound **16R** was tested in a murine infection model of *Cryptococcus neoformans* (Table 3). In the model, a group of 10 mice were inoculated with *C. neoformans* intravenously and the test compounds were administered orally once daily for 5 d. The results are summarized in

Table 1. Comparative Antifungal Efficacies of Various Dioxane-Triazole Compounds against Systemic Infection with *Candida albicans*^{a)}

Compd. ^{b)}	Ar	n	Stereo-chemistry	Dose ^{c)} (mg/kg)	Route	% Survival rate on day				
						3	9	14	21	30
9		0	<i>trans</i>	20	<i>p.o.</i>	100	100	50	20	—
					<i>i.p.</i>	100	100	40	30	—
14A		0	<i>trans</i>	19	<i>p.o.</i>	100	80	40	20	—
					<i>i.p.</i>	100	100	80	70	—
14C		0	<i>trans</i>	19	<i>p.o.</i>	100	100	90	60	—
					<i>i.p.</i>	100	100	80	30	—
14D		0	<i>trans</i>	19	<i>p.o.</i>	100	100	70	20	—
					<i>i.p.</i>	100	100	80	40	—
15A		1	<i>trans</i>	20	<i>p.o.</i>	100	100	60	30	—
					<i>i.p.</i>	100	100	100	40	—
15B		1	<i>trans</i>	19	<i>p.o.</i>	100	100	100	60	—
					<i>i.p.</i>	100	100	100	70	—
15'B		1	<i>cis</i>	17	<i>p.o.</i>	100	100	70	50	—
					<i>i.p.</i>	100	100	80	50	—
15C		1	<i>trans</i>	19	<i>p.o.</i>	100	100	90	60	—
					<i>i.p.</i>	100	100	100	70	—
15D		1	<i>trans</i>	19	<i>p.o.</i>	100	100	70	60	—
					<i>i.p.</i>	100	100	100	80	—
15E		1	<i>trans</i>	20	<i>p.o.</i>	100	80	50	20	—
					<i>i.p.</i>	90	80	80	80	—
15F		1	<i>trans</i>	18	<i>p.o.</i>	100	100	100	100	—
					<i>i.p.</i>	100	100	100	100	—
15'F		1	<i>cis</i>	19	<i>p.o.</i>	100	100	100	90	—
					<i>i.p.</i>	100	100	100	100	—
15G		1	<i>trans</i>	20	<i>p.o.</i>	100	100	100	100	—
					<i>i.p.</i>	100	100	100	90	—
15H		1	<i>trans</i>	18	<i>p.o.</i>	100	100	100	80	—
					<i>i.p.</i>	100	100	100	100	—
15I		1	<i>trans</i>	20	<i>p.o.</i>	100	100	100	100	90
					<i>i.p.</i>	100	100	100	100	100
15J		1	<i>trans</i>	20	<i>p.o.</i>	100	100	100	90	70
					<i>i.p.</i>	100	100	100	100	90
15K		1	<i>trans</i>	18	<i>p.o.</i>	100	100	90	40	—
					<i>i.p.</i>	100	100	100	50	—
15L		1	<i>trans</i>	18	<i>p.o.</i>	100	100	50	20	—
					<i>i.p.</i>	100	100	60	40	—
15N		1	<i>trans</i>	18	<i>p.o.</i>	100	100	100	100	90
					<i>i.p.</i>	100	100	100	100	100
15O		1	<i>trans</i>	18	<i>p.o.</i>	100	100	100	100	100
					<i>i.p.</i>	100	100	100	100	50
15P		1	<i>trans</i>	19	<i>p.o.</i>	100	100	100	70	—
					<i>i.p.</i>	100	100	100	80	—
15Q		1	<i>trans</i>	20	<i>p.o.</i>	100	100	100	100	80
					<i>i.p.</i>	100	100	100	100	100
15'Q		1	<i>cis</i>	20	<i>p.o.</i>	100	100	100	60	—
					<i>i.p.</i>	100	100	100	70	—
15R		1	<i>trans</i>	19	<i>p.o.</i>	100	100	100	100	80
					<i>i.p.</i>	100	100	100	100	100
15S		1	<i>trans</i>	19	<i>p.o.</i>	100	100	70	50	—
					<i>i.p.</i>	100	100	100	70	—
15T		1	<i>trans</i>	18	<i>p.o.</i>	100	90	50	20	—
					<i>i.p.</i>	100	100	70	50	—
15V		1	<i>trans</i>	20	<i>p.o.</i>	100	100	100	100	—
					<i>i.p.</i>	100	100	100	100	—
15W		1	<i>trans</i>	16	<i>p.o.</i>	100	100	50	40	—
					<i>i.p.</i>	100	100	40	20	—
15X		1	<i>trans</i>	19	<i>p.o.</i>	100	100	80	50	—
					<i>i.p.</i>	100	100	100	80	—
15Y		1	<i>trans</i>	16	<i>p.o.</i>	100	100	80	50	—
					<i>i.p.</i>	100	100	100	80	—

Table 1. (Continued)

Compd. ^{b)}	Ar	n	Stereo-chemistry	Dose ^{c)} (mg/kg)	Route	% Survival rate on day				
						3	9	14	21	30
15Z		1	trans	20	p.o. i.p.	100 100	100 100	100 100	80 100	— —
15AA		1	trans	17	p.o. i.p.	100 100	100 100	80 90	60 90	— —
15AB		1	trans	20	p.o. i.p.	100 100	100 100	90 90	60 70	— —
15AC		1	trans	20	p.o. i.p.	100 100	100 100	100 100	100 100	— —
15AD		1	trans	20	p.o. i.p.	100 70	100 70	100 70	100 70	— —
16B		2	trans	20	p.o. i.p.	100 100	100 100	100 100	100 100	80 100
16C		2	trans	18	p.o. i.p.	100 100	90 100	50 100	40 80	— —
16E		2	trans	20	p.o. i.p.	100 100	100 100	100 100	70 100	50 ^{d)} 90 ^{d)}
16F		2	trans	18	p.o. i.p.	100 100	100 100	100 100	100 100	100 100
16M		2	trans	20	p.o. i.p.	100 100	100 100	60 100	50 70	— —
16N		2	trans	20	p.o. i.p.	100 100	100 100	100 100	100 100	100 100
16R		2	trans	20	p.o. i.p.	100 100	100 100	100 100	100 100	100 100
16S		2	trans	20	p.o. i.p.	100 100	100 100	80 100	60 100	— —
16U		2	trans	18	p.o. i.p.	100 100	100 100	100 100	100 100	— —
16V		2	trans	20	p.o. i.p.	100 100	100 100	100 100	100 100	100 100
16X		2	trans	20	p.o. i.p.	100 100	100 100	90 100	40 100	— —
16Z		2	trans	20	p.o. i.p.	100 100	100 100	100 100	60 90	— —
16AA		2	trans	20	p.o. i.p.	100 90	70 90	40 70	20 40	— —
31		2	trans (cyclohexane analog)	20	p.o. i.p.	70 60	70 60	70 60	30 60	— —
Itraconazole				20	p.o. i.p.	50 30	20 0	0		—
Fluconazole				20	p.o.	100	100	70	60	—
Control (no drug)				0		0				

—: No data. a) *In vivo* activity was determined in mice (each group consisted of ten male mice, ddY strain, 5 weeks old) infected systemically using an intravenous challenge of 6 to 9×10^6 cells of *Candida albicans* SANK 51486. The triazole compounds were administered orally (*p.o.*) or intraperitoneally (*i.p.*) 1, 4, 24 h post infection. 0.5% Aqueous tragacantha pulverata (for **16E** and **16V**, 0.5% aqueous carboxymethyl cellulose sodium salt) was used as a vehicle for *p.o.* administration. b) Oxalic acid salts of the triazole derivatives except for **15E**, **15V**, **15X**, **15AC**, **15AD**, **16E**, **16M**, **16R**, **16X** and **31** were prepared and tested. c) *Per* administration. d) On day 29.

Table 3. All the control mice started to die after 10 d post infection. Here again, **16R** showed an excellent protecting effect. This is a remarkable feature of compound **16R**, since currently used antifungal agents have low efficacies against *Cryptococcus*.

The *in vitro* antifungal activity of **16R**, compared with those of fluconazole and itraconazole, against various fungi is shown in Table 4.

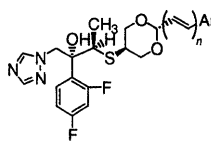
Compound **16R** has now been named R-102557, and its preclinical study is under way.

Experimental

Melting points are uncorrected. Infrared (IR) spectra were recorded either on a JASCO A-102 or Nic 5SCX spectrometer. Proton magnetic resonance ($^1\text{H-NMR}$) spectra were recorded either on a JEOL GX-270 (270 MHz), Varian EM-360L (60 MHz) or JNM GSX-400 (400 MHz) spectrometer. Mass spectra (MS) and high-resolution MS (HR-MS) were recorded on JEOL

JMS D300 spectrometer. The abbreviations used are as follows: s, singlet; d, doublet; dd, doublet of doublets; t, triplet; dt, doublet of triplets; td, triplet of doublets; tt, triplet of triplets; q, quartet; quint, quintet; m, multiplet; br, broad. Rotations were determined on a Perkin-Elmer 241 spectrometer at 25 °C. Chromatography columns were prepared with silica gel (60–110 mesh, Kanto Chemical Co., Inc.). The amount of the silica gel used is shown in parentheses. The Lobar[®] column used was LiChroprep[®] Si 60, E. Merck, 40–63 μm , Size B (310–25).

S-(trans-2-Phenyl-1,3-dioxan-5-yl) Thioacetate (7) A solution of *cis*-2-phenyl-1,3-dioxan-5-yl *p*-toluenesulfonate⁽¹¹⁾ (**6**, 29.0 g, 86.8 mmol) and sodium thioacetate (17.0 g, 149 mmol) in DMF (200 ml) was stirred at 115–120 °C for 1 h. After the mixture was cooled, it was partitioned between benzene and H_2O . The organic layer was dried and concentrated to give a brown oily residue, which was chromatographed (300 g, benzene : hexane = 2 : 1, v/v) to afford a crude product of **7** as a crystalline solid. Recrystallization from benzene–hexane gave **7** (8.99 g, 43%) as needles, mp 95–96 °C. $^1\text{H-NMR}$ (270 MHz, CDCl_3) δ : 2.37 (3H, s), 3.79 (2H, t, $J=11$ Hz), 4.03 (1H, tt, $J=11$, 5 Hz), 4.31 (2H, dd, $J=11$, 5 Hz), 5.47 (1H, s), 7.35–7.5 (5H, m). IR (CHCl_3) cm^{-1} : 1690, 1383, 1146, 1084. MS m/z :

Table 2. Comparative Antifungal Efficacies of Various Dioxane-Triazole Compounds against Systemic Infection with *Aspergillus*^{a)}

Compd. ^{b)}	Ar	n	Species	% Survival rate on day			
				3	6	9	14
15A		1	<i>A. fumigatus</i>	80	40	0	
			<i>A. flavus</i>	100	70	10	10
15B		1	<i>A. fumigatus</i>	100	100	100	100
			<i>A. flavus</i>	100	100	50	0
15C		1	<i>A. fumigatus</i>	90	70	60	50
			<i>A. flavus</i>	90	70	10	10
15D		1	<i>A. fumigatus</i>	100	100	100	70
			<i>A. flavus</i>	100	100	80	0
15E		1	<i>A. fumigatus</i>	100	80	80	80
			<i>A. flavus</i>	100	40	0	
15F		1	<i>A. fumigatus</i>	100	100	100	100
			<i>A. flavus</i>	100	100	100	100
15G		1	<i>A. fumigatus</i>	100	70	60	60
			<i>A. flavus</i>	80	40	30	0
15H		1	<i>A. fumigatus</i>	100	30	20	20
			<i>A. flavus</i>	100	100	90	20
15I		1	<i>A. fumigatus</i>	100	100	100	100
			<i>A. flavus</i>	100	100	90	30
15J		1	<i>A. fumigatus</i>	100	20	20	10
			<i>A. flavus</i>	40	20	10	0
15N		1	<i>A. fumigatus</i>	100	100	100	100
			<i>A. flavus</i>	100	90	90	70
15O		1	<i>A. fumigatus</i>	90	40	10	10
			<i>A. flavus</i>	30	0		
15P		1	<i>A. fumigatus</i>	100	100	100	100
			<i>A. flavus</i>	100	100	80	0
15Q		1	<i>A. fumigatus</i>	100	100	100	100
			<i>A. flavus</i>	100	100	100	80
15R		1	<i>A. fumigatus</i>	100	100	100	100
			<i>A. flavus</i>	100	100	100	100
15S		1	<i>A. fumigatus</i>	100	60	40	30
			<i>A. flavus</i>	100	80	0	
15T		1	<i>A. fumigatus</i>	100	80	70	50
			<i>A. flavus</i>	100	40	0	
15V		1	<i>A. fumigatus</i>	100	100	100	100
			<i>A. flavus</i>	100	100	100	100
15AC		1	<i>A. fumigatus</i>	100	100	100	100
			<i>A. flavus</i>	100	100	100	100
15AD		1	<i>A. fumigatus</i>	100	100	100	100
			<i>A. flavus</i>	100	100	100	100
16B		2	<i>A. fumigatus</i>	100	100	100	100
			<i>A. flavus</i>	100	100	100	90
16C		2	<i>A. fumigatus</i>	30	20	20	20
			<i>A. flavus</i>	90	30	0	
16E		2	<i>A. fumigatus</i>	100	100	100	100
			<i>A. flavus</i>	100	100	100	40
16F		2	<i>A. fumigatus</i>	100	100	100	100
			<i>A. flavus</i>	100	100	100	90
16N		2	<i>A. fumigatus</i>	100	100	100	100
			<i>A. flavus</i>	100	80	80	70
16R		2	<i>A. fumigatus</i>	100	100	100	100
			<i>A. flavus</i>	100	100	100	100
16U		2	<i>A. fumigatus</i>	100	100	100	100
			<i>A. flavus</i>	100	100	90	90
16V		2	<i>A. fumigatus</i>	100	100	100	100
			<i>A. flavus</i>	100	100	100	100
Itraconazole			<i>A. fumigatus</i>	100	60	50	30
			<i>A. flavus</i>	80	30	0	0
Control (no drug)			<i>A. fumigatus</i>	80	0		
			<i>A. flavus</i>	50	0		

a) *In vivo* activity was determined in mice (each group consisted of ten male mice, ddY strain, 5 weeks old) infected systemically using an intravenous challenge of either 5×10^6 conidia of *Aspergillus fumigatus* SANK 10569 or 3×10^6 conidia of *Aspergillus flavus* SANK 18497. The triazole compounds (20 mg/kg/dose) were administered orally 1, 4, 24, 31, 48 and 55 h post infection. 0.5% Aqueous tragacantha pulverata (for 16E and 16V, 0.5% aqueous carboxymethyl cellulose sodium salt) was used as a vehicle for administration. b) Oxalic acid salts of the triazole derivatives except for 15E, 15AC, 15AD and 16R were prepared and tested.

Table 3. Comparative Antifungal Efficacies of **16R**, Fluconazole and Itraconazole against Systemic Infection with *Cryptococcus neoformans*^{a)}

Compound	Dose ^{b)} (mg/kg)	% Survival rate on day			
		10	20	30	40
16R	100	100	100	100	100
	25	100	100	100	90
	6.25	100	100	100	50
	1.56	100	100	80	0
Fluconazole	100	100	100	10	0
	25	100	90	0	
	6.25	100	80	0	
Itraconazole	100	100	70	0	
Control (no drug)	0	100	40	0	

a) *In vivo* activity was determined in mice (each group consisted of ten male mice, ddY strain, 5 weeks old) infected systemically using an intravenous challenge of 1×10^6 cells of *Cryptococcus neoformans* TIMM 0362. The triazole compounds were administered orally 4, 24, 48, 72 and 96 h post infection. 0.5% Aqueous carboxymethyl cellulose sodium salt was used as a vehicle for administration. b) Per administration.

Table 4. *In Vitro* Antifungal Activities^{a)} of **16R**, Fluconazole and Itraconazole

Strain	MIC ^{b)} (μ g/ml)		
	16R	Fluconazole	Itraconazole
<i>C. albicans</i> ATCC24433	0.125	0.5	0.125
<i>C. albicans</i> SANK51486	0.016	0.25	0.031
<i>C. albicans</i> TIMM3164	0.125	>4	0.25
<i>C. albicans</i> ATCC64550	1	>4	1
<i>C. parapsilosis</i> ATCC90018	0.063	0.5	0.125
<i>C. glabrata</i> ATCC90030	1	>4	1
<i>C. krusei</i> ATCC6258	0.125	>4	0.5
<i>C. tropicalis</i> ATCC750	0.125	2	0.5
<i>C. neoformans</i> TIMM1855	0.031	>4	0.25
<i>A. fumigatus</i> ATCC26430	0.125	>4	0.25
<i>A. fumigatus</i> SANK10569	0.125	>4	0.25
<i>A. flavus</i> SANK18497	0.25	>4	0.5

a) *In vitro* antifungal activities were measured at 35 °C (30 °C for *Aspergillus* spp.) in RPMI1640 (yeast nitrogen base for *C. neoformans*) at pH 7.0. b) Minimum inhibitory concentrations (MIC) were expressed as the minimum concentration of the test compounds that inhibit the growth of the fungi by 80%.

238(M⁺), 237, 195, 162, 149, 116, 107, 73. *Anal.* Calcd for C₁₂H₁₄O₃S: C, 60.48; H, 5.92. Found: C, 60.25; H, 5.95.

(2R,3R)-2-(2,4-Difluorophenyl)-3-[(trans-2-phenyl-1,3-dioxan-5-yl)thio]-1-(1H-1,2,4-triazol-1-yl)-2-butanol (9) A 1.6N solution of sodium methoxide in MeOH (2.5 ml, 4.0 mmol) was added to a solution of (2R,3S)-2-(2,4-trifluorophenyl)-3-methyl-2-[(1H-1,2,4-triazol-1-yl)-methyl]oxirane (**8**)^{9a,b,e,10)} (1.65 g, 6.57 mmol) and the thioester **7** (2.00 g, 8.40 mmol) in DMF (20 ml) at room temperature with stirring. The whole was then heated at 65 °C for 2 h. After the mixture was cooled, it was diluted with AcOEt and washed with brine. The organic layer was dried and concentrated to give a crude oil. Chromatography (60 g, AcOEt: benzene=1:5, v/v) afforded **9** (2.53 g, 91%) as a crystalline solid, which was used for the next reaction without further purification. An analytical sample, mp 58–60 °C, was obtained by recrystallization from AcOEt–hexane. ¹H-NMR (270 MHz, CDCl₃) δ : 1.21 (3H, d, *J*=7 Hz), 3.36 (1H, q, *J*=7 Hz), 3.48 (1H, tt, *J*=11, 5 Hz), 3.75 (1H, t, *J*=11 Hz), 3.77 (1H, t, *J*=11 Hz), 4.40 (1H, ddd, *J*=11, 5, 3 Hz), 4.51 (1H, ddd, *J*=11, 5, 3 Hz), 4.84 (1H, d, *J*=14 Hz), 5.02 (1H, s), 5.05 (1H, d, *J*=14 Hz), 5.49 (1H, s), 7.7–7.8 (2H, m), 7.3–7.45 (4H, m), 7.45–7.53 (2H, m), 7.79 (2H, s). IR (CHCl₃) cm⁻¹: 3400, 1615, 1500, 1139. FAB-MS *m/z*: 448(M⁺+1). [α]_D²⁵ –88 (*c*=1.07, CHCl₃). *Anal.* Calcd for C₂₂H₂₃F₂N₃O₃S: C, 59.05; H, 5.18; N, 9.39. Found: C, 58.97; H, 5.30; N, 9.42.

(2R,3R)-2-(2,4-Difluorophenyl)-3-[[2-hydroxy-1-(hydroxymethyl)-ethyl]thio]-1-(1H-1,2,4-triazol-1-yl)-2-butanol (10) A 4M solution of HCl in 1,4-dioxane (0.35 ml, 1.4 mmol) was added to a solution of **9**

(253 mg, 0.57 mmol) in MeOH (3.5 ml) at room temperature. After the mixture was stirred at room temperature for 30 min, powdered NaHCO₃ (250 mg, 3.0 mmol) was added. The mixture was stirred at room temperature for 10 min and then filtered. The concentrated filtrate was chromatographed (5 g, MeOH–AcOEt, 1:9, v/v) to afford **10** (179 mg, 88%) as a colorless, viscous oil. ¹H-NMR (270 MHz, CDCl₃) δ : 1.20 (3H, d, *J*=7 Hz), 3.15 (1H, br), 3.25 (1H, dddd, *J*=7, 7, 6, 6 Hz), 3.48 (1H, q, *J*=7 Hz), 3.75 (1H, dd, *J*=11, 6 Hz), 3.80 (1H, dd, *J*=11, 7 Hz), 3.81 (1H, dd, *J*=11, 7 Hz), 3.95 (1H, dd, *J*=11, 6 Hz), 4.1 (1H, br), 4.84 (1H, d, *J*=14 Hz), 5.19 (1H, d, *J*=14 Hz), 5.57 (1H, br s), 6.7–6.8 (2H, m), 7.39 (1H, td, *J*=9, 7 Hz), 7.75 (1H, s), 7.91 (1H, s). IR (CHCl₃): 3400, 1618, 1500 cm⁻¹. FAB-MS *m/z*: 360 (M⁺+1). [α]_D²⁵ –61 (*c*=1.05, CHCl₃).

Aryl Aldehydes (11) The aryl aldehydes **11A**–**11L**, **11N**–**11Q**, **11S**, **11W**, and **11AA** were available at either Tokyo Kasei Kogyo Co., Ltd., Aldrich, or Fluorochem Ltd. The aldehydes **11T**¹⁵⁾ and **11AB**¹⁶⁾ are known in the literature. The preparation of the other aryl aldehydes, **11M**, **11R**, **11U**, **11V**, **11X**–**11Z**, **11AC**, and **11AD** is described below.

2-Methoxy-4-(trifluoromethyl)benzaldehyde (11M) Methyl 2-fluoro-4-(trifluoromethyl)benzoate (560 mg, 2.52 mmol) was treated with NaOMe (272 mg, 5.04 mmol) in MeOH (4.2 ml) at room temperature for 5 h. The mixture was acidified with HCl, concentrated, and diluted with AcOEt. The insoluble materials were removed by filtration. The filtrate was concentrated and the residue was chromatographed (21 g, AcOEt: hexane=1:3, v/v) to afford methyl 2-methoxy-4-(trifluoromethyl)benzoate (333 mg, 56%) as an oil. ¹H-NMR (270 MHz, CDCl₃) δ : 3.92 (3H, s), 3.96 (3H, s), 7.18 (1H, s), 7.25 (1H, d, *J*=8 Hz), 7.86 (1H, d, *J*=8 Hz).

A 1.5M solution of DIBAL in toluene (5.9 ml, 8.9 mmol) was added to a stirred solution of methyl 2-methoxy-4-(trifluoromethyl)benzoate (1.04 g, 4.45 mmol) in toluene (10 ml) at 0 °C. After the mixture was stirred at 0 °C for 1 h, a saturated solution of NH₄Cl was added, and the mixture was filtered through Celite. The precipitates were washed with toluene. The organic layer was separated and concentrated to give crude 2-methoxy-4-(trifluoromethyl)benzyl alcohol. ¹H-NMR (270 MHz, CDCl₃) δ : 2.2 (1H, br), 3.91 (3H, s), 4.73 (2H, s), 7.08 (1H, s), 7.23 (1H, d, *J*=8 Hz), 7.43 (1H, d, *J*=8 Hz), as an oil. This alcohol, without further purification, was treated with activated MnO₂ (8.6 g, 99 mmol) in CH₂Cl₂ (26 ml) at room temperature for 1.3 h. The mixture was filtered and the filtrate was concentrated to give 2-methoxy-4-(trifluoromethyl)benzaldehyde (**11M**) (756 mg, 83%) as a pale yellow solid, which was air-sensitive and unsuitable for further purification. ¹H-NMR (270 MHz, CDCl₃) δ : 3.92 (3H, s), 7.22 (1H, s), 7.29 (1H, d, *J*=8 Hz), 7.94 (1H, d, *J*=8 Hz), 10.51 (1H, s). IR (KBr) cm⁻¹: 1700.

4-(2,2,3,3-Tetrafluoropropoxy)benzaldehyde (11R) 4-Hydroxybenzaldehyde (5.3 g, 43 mmol) was added in small portions to a stirred suspension of NaH (55% mineral oil dispersion, 1.9 g, 43.5 mmol; washed with hexane) in *N,N*-dimethylacetamide (DMA) (25 ml) at 0 °C. When hydrogen gas ceased to evolve, 2,2,3,3-tetrafluoropropyl *p*-toluenesulfonate (11.14 g, 39 mmol) was added, and the whole was stirred at 120 °C for 2.3 h. After the solution was cooled, it was diluted with a mixture of benzene and hexane (*ca.* 1:1) and was washed with H₂O. The organic layer was dried and concentrated to give **11R** (8.85 g, 96%) as an air-sensitive oil, which was unsuitable for further purification. ¹H-NMR (270 MHz, CDCl₃) δ : 4.45 (2H, t, *J*=11.9 Hz), 6.06 (1H, tt, *J*=53, 5 Hz), 7.06 (2H, d, *J*=9 Hz), 7.88 (2H, d, *J*=9 Hz), 9.93 (1H, s). IR (neat) cm⁻¹: 1701.

4-(Trifluoromethylthio)benzaldehyde (11U) A 1.0M solution of DIBAL in toluene (9.8 ml, 9.8 mmol) was added to a stirred solution of 4-(trifluoromethyl)benzonitrile (1.0 g, 4.9 mmol) in toluene (10 ml) at –30 °C. The mixture was worked up by adding a 10% aqueous solution of KHSO₄. The product was extracted with toluene. The organic layer was concentrated, and the residual oil was chromatographed (10 g, AcOEt: hexane=1:5, v/v) to afford **11U** (703 mg, 69%) as a crystalline solid, whose further purification was difficult owing to its air-sensitivity. ¹H-NMR (270 MHz, CDCl₃) δ : 7.81 (2H, d, *J*=8 Hz), 7.94 (2H, d, *J*=8 Hz), 10.09 (1H, s).

4-(Trifluoromethylsulfonyl)benzaldehyde (11V) A mixture of 4-(trifluoromethylthio)benzyl alcohol (500 mg, 2.4 mmol) and *m*-chloroperbenzoic acid (mCPBA, 70–75%, 1.48 g) in CHCl₃ (5 ml) was stirred at room temperature for 16 h and then at 70 °C for 5 h. After the mixture was cooled, it was washed with an aqueous solution of Na₂SO₃. Solvents were removed *in vacuo* to afford crude 4-(trifluoromethylsulfonyl)benzyl alcohol (507 mg, 88%) as a crystalline mass, mp 40–42 °C. ¹H-NMR (270 MHz, CDCl₃) δ : 2.5 (1H, br), 4.89 (1H, d, *J*=8 Hz), 7.68 (2H, d, *J*=8 Hz), 8.01 (2H, d, *J*=8 Hz). IR (KBr) cm⁻¹: 3397 (br), 1597, 1370, 1217, 1205, 1187, 1141, 1072, 1052. MS *m/z*: 240 (M⁺), 171, 107, 89, 77. *Anal.* Calcd for C₈H₇F₃O₃S: C, 40.00; H, 2.94. Found: C, 40.25; H, 3.15.

In a manner similar to that described above for the preparation of the alde-

hyde **11M**, 4-(trifluoromethylsulfonyl)benzyl alcohol (19.82 g, 82.5 mmol) was oxidized with activated MnO_2 (200 g, 2.3 mol) in CH_2Cl_2 (200 ml) to afford **11V** (14.1 g, 72%) as a crystalline solid, whose further purification was difficult owing to its air-sensitivity. $^1\text{H-NMR}$ (270 MHz, CDCl_3) δ : 8.18 (2H, d, $J=8.3$ Hz), 8.25 (2H, d, $J=8$ Hz), 10.20 (1H, s). MS (EI) m/z : 238 (M^+), 185, 169, 105, 77. IR (CHCl_3) cm^{-1} : 1700, 1373, 1218, 1141, 1074.

6-Chloropyridine-3-carbaldehyde (11X) Ethyl chloroformate (758 mg, 7.0 mmol) was added to a stirred solution of 6-chloro-3-nicotinic acid (1.0 g, 6.4 mmol) and Et_3N (642 mg, 6.3 mmol) in tetrahydrofuran (THF) (12 ml) at -15°C . After the mixture was stirred for 15 min, a solution of NaBH_4 (648 mg, 17 mmol) in H_2O (6 ml) was added. The whole was stirred at -15°C for 20 min, and then diluted with AcOEt (80 ml). The mixture was washed with brine and dried. Evaporation of the solvent and chromatographic purification (10 g, AcOEt :hexane=3:2) of the residue afforded (6-chloro-3-pyridyl)methanol (785 mg, 86%) as needles, mp $63\text{--}65^\circ\text{C}$. $^1\text{H-NMR}$ (270 MHz, CDCl_3) δ : 2.09 (1H, brt, $J=6$ Hz), 4.80 (2H, brd, $J=6$ Hz), 7.29 (1H, dd, $J=8$, 5 Hz), 7.89 (1H, dd, $J=8$, 2 Hz), 8.33 (1H, dd, $J=5$, 2 Hz). IR (KBr) cm^{-1} : 3266 (br), 1411, 1044. MS m/z : 143 (M^+), 108. *Anal.* Calcd for $\text{C}_6\text{H}_5\text{ClNO}$: C, 50.20; H, 4.21; N, 9.76. Found: C, 50.39; H, 4.35; N, 9.71.

A solution of dimethyl sulfoxide (DMSO) (1.02 g, 12.9 mmol) in CH_2Cl_2 (1 ml) was added to a solution of oxalyl chloride (1.37 g, 10.8 mmol) in CH_2Cl_2 (15 ml) at -78°C . After the mixture was stirred at -78°C for 10 min, a solution of (6-chloro-3-pyridyl)methanol (773 mg, 5.4 mmol) and Et_3N (2.18 g, 21.5 mmol) in CH_2Cl_2 (10 ml) was added. The mixture was allowed to warm to -15°C over 20 min, and then treated with a saturated aqueous solution of NH_4Cl (25 ml). The product was extracted with AcOEt , and the organic layer was dried and concentrated to afford an oily residue, which was chromatographed (10 g, AcOEt :hexane=1:4, v/v) to afford **11X** (700 mg, 92%) as needles, mp $72\text{--}73^\circ\text{C}$, whose further purification was difficult owing to its air-sensitivity. $^1\text{H-NMR}$ (270 MHz, CDCl_3) δ : 7.43 (1H, dd, $J=8$, 5 Hz), 8.24 (1H, dd, $J=8$, 2 Hz), 8.62 (1H, dd, $J=5$, 2 Hz), 10.64 (1H, s). IR (KBr) cm^{-1} : 1697, 1581, 1263. MS m/z : 141 (M^+), 112, 105.

2-Chloropyridine-3-carbaldehyde (11Y) In a manner similar to that described above for the preparation of the aldehyde **11X**, 2-chloro-3-nicotinic acid (1.0 g, 6.4 mmol) was reduced (ethyl chloroformate, NaBH_4) and then oxidized (DMSO, oxalyl chloride, Et_3N) to afford, after chromatography, **11Y** (664 mg, 74%) as a crude, crystalline solid, mp $37\text{--}41^\circ\text{C}$, whose further purification was difficult owing to its air-sensitivity. $^1\text{H-NMR}$ (270 MHz, CDCl_3) δ : 7.43 (1H, dd, $J=7$, 5 Hz), 8.24 (1H, dd, $J=7$, 2 Hz), 8.62 (1H, dd, $J=5$, 2 Hz), 10.46 (1H, s). IR (CHCl_3) cm^{-1} : 1700, 1575, 1375. MS m/z : 141 (M^+), 112, 105.

6-(2,2,3,3-Tetrafluoropropoxy)-3-pyridinecarbaldehyde (11Z) 2,2,3,3-Tetrafluoropropanol was added slowly to a suspension of NaH (55% mineral oil dispersion, 840 mg, 19.3 mmol; washed with hexane) in DMF (40 ml) at 0°C . When hydrogen gas ceased to evolve, a solution of ethyl 6-chloro-3-niconinate (3.40 g, 18.3 mmol) in DMF (15 ml) was added over a period of 30 min. After the mixture was stirred at 0°C for 30 min, it was poured into ice water and the product was extracted with benzene. The extract was dried and the solvents were evaporated to give an oily residue, which was chromatographed (50 g, benzene:hexane=2:3) to afford ethyl 6-(2,2,3,3-tetrafluoropropoxy)-3-nicotinate (4.42 g, 86%) as an oil. $^1\text{H-NMR}$ (270 MHz, CDCl_3) δ : 1.40 (3H, t, $J=7$ Hz), 4.39 (2H, q, $J=7$ Hz), 4.81 (2H, brt, $J=13$ Hz), 6.00 (1H, tt, $J=53$, 5 Hz), 6.87 (1H, d, $J=9$ Hz), 8.24 (1H, dd, $J=9$, 2.5 Hz), 8.83 (1H, d, $J=2.5$ Hz). IR (CHCl_3) cm^{-1} : 1717, 1604, 1280, 1119. MS m/z : 281 (M^+), 236, 180, 152, 151, 123, 122, 93.

In a manner similar to that described above for the preparation of the aldehyde **11M**, ethyl 6-(2,2,3,3-tetrafluoropropoxy)-3-nicotinate (2.2 g, 7.8 mmol) was reduced (DIBAL) and then oxidized (activated MnO_2) to afford **11Z** (1.76 g, 96%) as an air-sensitive oil. $^1\text{H-NMR}$ (270 MHz, CDCl_3) δ : 4.86 (2H, brt, $J=13$ Hz), 6.01 (1H, tt, $J=53$, 4 Hz), 6.97 (1H, d, $J=9$ Hz), 8.15 (1H, dd, $J=9$, 2.3 Hz), 8.65 (1H, d, $J=2.3$ Hz), 10.00 (1H, s). IR (CHCl_3) cm^{-1} : 1701, 1605, 1574, 1489, 1364, 1118. MS m/z : 237 (M^+), 186, 166, 136, 107, 106, 78.

6-Bromo-2-naphthaldehyde (11AC) A solution of methyl 6-bromo-2-naphthoate (2.50 g, 9.4 mmol) in THF (10 ml) was added to a stirred suspension of LiAlH_4 (537 mg, 14.1 mmol) in THF (15 ml) at $5\text{--}10^\circ\text{C}$. After the mixture was stirred at $5\text{--}10^\circ\text{C}$ for 1 h, the reaction was worked up by adding a solution of NaOH (46 mg, 1.15 mmol) in H_2O (1.6 ml). The insoluble materials were removed by filtration and the filtrate was concentrated to afford crude product of (6-bromo-2-naphthyl)methanol (2.0 g, gross yield=90%) as a powder, which was used for the next reaction without further purification.

In a manner similar to that described for the preparation of the aldehyde **11M**, the crude product of (6-bromo-2-naphthyl)methanol (1.0 g) obtained above was oxidized with activated MnO_2 (2.73 g, 31.4 mmol) to afford **11AC** (900 mg, 91%) as an oil. $^1\text{H-NMR}$ (270 MHz, CDCl_3) δ : 7.67 (1H, dd, $J=9$, 2 Hz), 7.83—7.89 (2H, m), 7.98 (1H, dd, $J=9$, 1.5 Hz), 8.08 (1H, d, $J=2$ Hz), 8.32 (1H, s), 10.15 (1H, s). MS m/z : 236, 234 (M^+), 207, 205, 189, 155, 126.

6-(2,2,3,3-Tetrahydropropoxy)-2-naphthaldehyde (11AD) Methyl 6-hydroxy-2-naphthoate (200 mg, 0.99 mmol) was added slowly to a stirred suspension of NaH (60% mineral oil dispersion, 39.6 mg, 0.99 mmol; washed with hexane) in DMA (2 ml) at 0°C . When hydrogen gas ceased to evolve, a solution of 2,2,3,3-tetrafluoropropyl *p*-toluenesulfonate (311 mg, 1.09 mmol) in DMA (1 ml) was added at the same temperature. The whole was stirred at 100°C for 2 h. After the solution was cooled, it was poured into ice water and the product was extracted with AcOEt . The organic layer was dried and concentrated to give an oily residue, which was chromatographed (5 g, AcOEt :hexane=1:9, v/v) briefly to afford methyl 6-(2,2,3,3-tetrafluoropropoxy)-2-naphthoate (302 mg, gross yield=96%) as a crude crystalline solid, which was used for the next reaction without further purification. $^1\text{H-NMR}$ (270 MHz, CDCl_3) δ : 3.95 (3H, s), 4.46 (2H, brt, $J=11.9$ Hz), 6.14 (1H, tt, $J=53$, 5 Hz), 7.10 (1H, d, $J=2.4$ Hz), 7.17 (1H, brd, $J=8.8$ Hz), 7.69 (1H, d, $J=8.8$ Hz), 7.80 (1H, d, $J=8.8$ Hz), 8.02 (1H, d, $J=8.8$ Hz), 8.49 (1H, s).

In a manner similar to that described for the preparation of the aldehyde **11M**, the crude product of methyl 6-(2,2,3,3-tetrafluoropropoxy)-2-naphthoate (300 mg) was reduced (DIBAL) and then oxidized (MnO_2) to afford **11AD** (210 g, 75%) as a colorless, air-sensitive solid. $^1\text{H-NMR}$ (270 MHz, CDCl_3) δ : 4.52 (2H, brt, $J=12$ Hz), 6.12 (1H, tt, $J=53$, 5 Hz), 7.22 (1H, d, $J=2.5$ Hz), 7.28 (1H, brd, $J=8$ Hz), 7.84 (1H, d, $J=8$ Hz), 7.96 (2H, d, $J=8$ Hz), 8.29 (1H, s).

(E)-3-Aryl-2-propenals (12) The aldehydes **12A—12C**, **12F—12L**, **12N—12T** and **12V—12AD** were prepared from the corresponding aryl aldehydes **11A—11C**, **11F—11L**, **11N—11T** and **11V—11AD** via a homologation sequence using triethyl phosphonoacetate (**17**). As a typical example the preparation of **12F** is described below. The aldehyde **12E** was prepared from **11E** according to the literature¹²⁾ using (triphenylphosphoranylidene)acetaldehyde. The aldehyde **12D** was prepared from **11D** in a similar manner as follows.

(E)-p-Nitrocinnamaldehyde (12D) A mixture of *p*-nitrobenzaldehyde (**11D**) (302 mg, 2.0 mmol), (triphenylphosphoranylidene)acetaldehyde (608 mg, 2.0 mmol) and toluene (5 ml) was refluxed for 100 min. The cooled mixture was concentrated *in vacuo* to give a brown mass, which was chromatographed on silica gel (20 g, AcOEt :hexane=1:9, v/v) to afford a crude product of **12D**. Recrystallization from benzene–hexane afforded a pure material of **12D** (237 mg, 67%) as yellow needles, mp $105\text{--}110^\circ\text{C}$. $^1\text{H-NMR}$ (270 MHz, CDCl_3) δ : 6.80 (1H, dd, $J=17$, 7 Hz), 7.53 (1H, d, $J=17$ Hz), 7.74 (2H, d, $J=9$ Hz), 8.30 (2H, d, $J=9$ Hz), 7.98 (1H, d, $J=7$ Hz). IR (KBr) cm^{-1} : 1682, 1518, 1346, 1124. MS m/z : 177 (M^+), 160, 130, 103, 102, 77. *Anal.* Calcd for $\text{C}_9\text{H}_7\text{NO}_2$: C, 61.02; H, 3.98; N, 7.91. Found: C, 61.06; H, 4.04; N, 7.71.

(E)-p-(Trifluoromethyl)cinnamaldehyde (12F) Triethyl phosphonoacetate (**17**) (4.63 g, 20.7 mmol) was added dropwise to a stirred suspension of NaH (55% mineral oil dispersion, 903 mg, 20.7 mmol; washed with hexane) in 1,2-dimethoxyethane (DME) (60 ml) at 0°C . After the mixture was stirred at 0°C for 15 min, 4-(trifluoromethyl)benzaldehyde (**11F**) (2.0 g, 11.5 mmol) was added. After the mixture had been stirred for 15 min, it was diluted with AcOEt and washed with H_2O . The organic layer was dried and concentrated to give an oily residue, which was chromatographed on silica gel (50 g, AcOEt :hexane=1:24, v/v) to afford ethyl (*E*)-*p*-(trifluoromethyl)cinnamate (**18F**) (2.75 g, 98%) as a crystalline mass, mp $31\text{--}32.5^\circ\text{C}$. $^1\text{H-NMR}$ (270 MHz, CDCl_3) δ : 1.35 (3H, t, $J=7$ Hz), 4.28 (1H, q, $J=7$ Hz), 6.51 (1H, d, $J=16$ Hz), 7.66 (4H, s), 7.69 (1H, d, $J=16$ Hz). IR (KBr) cm^{-1} : 1709, 1336, 1112. MS m/z : 244 (M^+), 216, 199, 171. *Anal.* Calcd for $\text{C}_{12}\text{H}_{11}\text{F}_3\text{O}_2$: C, 59.02; H, 4.54. Found: C, 59.22; H, 4.66.

A 1.5 M solution of DIBAL in toluene (16.4 ml, 24.6 mmol) was added to a stirred solution of **18F** (3.00 g, 12.3 mmol) in toluene (15 ml) at 0°C . After the mixture was stirred at 0°C for 20 min, iced water was added carefully in small portions with stirring. The mixture was diluted with AcOEt and filtered through Celite. The organic layer was separated and concentrated to give a solid residue, which was recrystallized from benzene–hexane to give (*E*)-*p*-(trifluoromethyl)cinnamyl alcohol (**19F**) (2.36 g, 96%) as colorless needles, mp $53\text{--}55^\circ\text{C}$. $^1\text{H-NMR}$ (270 MHz, CDCl_3) δ : 1.57 (1H, br), 4.36 (2H, brt, $J=5$ Hz), 6.44 (1H, dt, $J=16$, 5 Hz), 6.66 (1H, d, $J=16$ Hz), 7.47 (2H, d, $J=8$ Hz), 7.56 (2H, d, $J=8$ Hz). IR (KBr) cm^{-1} : 1332, 1127, 1067.

MS m/z : 202 (M^+), 160. *Anal.* Calcd for $C_{10}H_9F_3O$: C, 59.41; H, 4.49. Found: C, 59.19; H, 4.54.

A mixture of **19F** (2.15 g, 10.6 mmol) and activated MnO_2 (14 g, 161 mmol) in CH_2Cl_2 (30 ml) was stirred at room temperature for 2 h. The mixture was filtered, and the filtrate was concentrated to give a crystalline residue, which was recrystallized from benzene–hexane to give (*E*)-*p*-(trifluoromethyl)cinnamaldehyde (**12F**) (1.92 g, 90%) as colorless needles, mp 60–61 °C. 1H -NMR (270 MHz, $CDCl_3$) δ : 6.78 (1H, dd, $J=16$, 7 Hz), 7.53 (1H, d, $J=16$ Hz), 7.69 (4H, s), 9.76 (1H, d, $J=7$ Hz). IR (KBr) cm^{-1} : 1680, 1630, 1321, 1173, 1123, 1066. MS m/z : 200 (M^+), 199, 171, 151, 145, 131, 103, 102. *Anal.* Calcd for $C_{10}H_7F_3O$: C, 60.01; H, 3.52. Found: C, 59.85; H, 3.55.

(2E,4E)-5-Aryl-2,4-pentadienals (13) The aldehydes **13B**, **13C**, **13F**, **13M**, **13N**, **13R**, **13S**, **13U**, **13V**, **13X**, **13Z** and **13AA** were prepared from the corresponding aryl aldehydes **11B**, **11C**, **11F**, **11M**, **11N**, **11R**, **11S**, **11U**, **11V**, **11X**, **11Z** and **13AA** via a homologation sequence using triethyl phosphonocrotonate (**20**). As a typical example, the preparation of **13F** is described below. The aldehyde **13E** was prepared from **11E** using (triphenylphosphoranyliden)crotonaldehyde as follows.

4-[(1E,3E)-5-Oxo-1,3-pentadienyl]benzonitrile (13E) A mixture of 4-formylbenzonitrile (**11E**) (13.1 g, 99 mmol), (triphenylphosphoranyliden)crotonaldehyde¹³⁾ (40 g, 120 mmol) and CH_2Cl_2 (200 ml) was stirred overnight. The mixture was concentrated *in vacuo* and the residual solid was chromatographed on silica gel (250 g) to remove polar byproducts. Elution with AcOEt afforded a crude product, which contained geometrical isomers, as judged by TLC. Then the mixture was dissolved in toluene (150 ml) and the solution was irradiated and refluxed for 12 h with a 300W tungsten lamp (visible light). The mixture was cooled and concentrated *in vacuo* to leave a solid residue, which was chromatographed on silica gel (1.2 kg). The fractions eluted with AcOEt–toluene (1 : 9, v/v) was concentrated and the crystals emerged were collected by filtration to give **13E** (3.46 g, 19%) as light brown needles, mp 147–150 °C. 1H -NMR (400 MHz, $CDCl_3$) δ : 6.36 (1H, dd, $J=15.3$, 7.8 Hz), 7.00 (1H, d, $J=15.6$ Hz), 7.09 (1H, dd, $J=15.6$, 10.3 Hz), 7.27 (1H, dd, $J=15.3$, 10.3 Hz), 7.59 (2H, d, $J=8.4$ Hz), 7.67 (2H, d, $J=8.4$ Hz), 9.67 (1H, d, $J=7.8$ Hz). IR (KBr) cm^{-1} : 2226, 1683, 1670, 1626. MS m/z : 183 (M^+), 154, 140, 127, 115. *Anal.* Calcd for $C_{12}H_9NO$: C, 78.67; H, 4.95; N, 7.65. Found: C, 78.56; H, 5.05; N, 7.62.

(2E,4E)-5-[4-(Trifluoromethyl)phenyl]-2,4-pentadienal (13F) Triethyl phosphonocrotonate (**20**) (25.9 g, 103 mmol) was added dropwise to a stirred suspension of NaH (55% mineral oil dispersion, 4.51 g, 103 mmol; washed with hexane) in DME (70 ml) at 0 °C. After the mixture was stirred at 0 °C for 15 min, 4-(trifluoromethyl)benzaldehyde (**11F**) (10.0 g, 57.4 mmol) was added slowly. After the mixture had been stirred for 10 min, it was poured into ice water and the product was extracted with AcOEt. The organic layer was dried and concentrated to give an oily residue, which was chromatographed (150 g, AcOEt:hexane=3 : 47, v/v) to afford **21F** (11.2 g, 72%) as an oil. 1H -NMR (270 MHz, $CDCl_3$) δ : 1.32 (3H, t, $J=7$ Hz), 4.24 (2H, q, $J=7$ Hz), 6.05 (1H, d, $J=15$ Hz), 6.85–7.0 (2H, m), 7.44 (1H, ddd, $J=15$, 8, 2.6 Hz), 7.55 (2H, d, $J=9$ Hz), 7.61 (2H, d, $J=9$ Hz). IR ($CHCl_3$) cm^{-1} : 1707, 1631, 1326, 1171, 1133, 1068. MS m/z : 270 (M^+), 225, 197, 177, 128.

A 1.5 M solution of DIBAL in toluene (27.7 ml, 41.6 mmol) was added to a stirred solution of **21F** (5.31 g, 19.6 mmol) in toluene (50 ml) at 0 °C. After the mixture was stirred at 0 °C for 45 min, ice water were added in small portions with stirring. The mixture was diluted with AcOEt and filtered through Celite. The organic layer was separated and concentrated to give a solid residue, which was chromatographed (100 g, AcOEt:hexane=1 : 4, v/v) and recrystallized from benzene–hexane to give **22F** (2.47 g, 55%) as colorless needles, mp 72–75 °C. 1H -NMR (270 MHz, $CDCl_3$) δ : 1.47 (1H, t, $J=6$ Hz), 4.28 (1H, t, $J=6$ Hz), 6.04 (1H, dt, $J=15$ Hz, $J=6$ Hz), 6.45 (1H, dd, $J=15$, 11 Hz), 6.57 (1H, d, $J=16$ Hz), 6.87 (1H, dd, $J=16$, 11 Hz), 7.47 (2H, d, $J=9$ Hz), 7.56 (2H, d, $J=9$ Hz). IR (KBr) cm^{-1} : 1327, 1120, 1070. MS m/z : 228 (M^+), 172, 159. *Anal.* Calcd for $C_{11}H_{11}F_3O$: C, 63.16; H, 4.86. Found: C, 62.90; H, 4.69.

A mixture of **22F** (1.19 g, 5.21 mmol) and activated MnO_2 (14.28 g, 164.2 mmol) in CH_2Cl_2 (10 ml) was stirred at room temperature for 0.5 h. The mixture was filtered, and the filtrate was concentrated to give **13F** (1.09 g, 92%) as an oil. 1H -NMR (270 MHz, $CDCl_3$) δ : 6.33 (1H, dd, $J=15$, 7 Hz), 7.0–7.35 (3H, m), 7.60 (2H, d, $J=9$ Hz), 7.64 (2H, d, $J=9$ Hz), 9.65 (1H, d, $J=7$ Hz). IR (neat) cm^{-1} : 1674, 1622, 1323, 1067. MS m/z : 226 (M^+), 177, 129.

(2R,3R)-2-(2,4-Difluorophenyl)-3-[(trans-2-substituted-1,3-dioxan-5-yl)thio]-1-(1H-1,2,4-triazol-1-yl)-2-butanols (14–16) and Their cis Isomers (14'–16') These compounds were prepared by acetalization reac-

tion between the alcohol **10** and the corresponding aldehydes **11**, **12** and **13**. The *trans* isomers **14–16** were predominantly produced and easily separated from the *cis* isomers **14'–16'** by silica gel column chromatography. The *trans/cis* ratio was between 5 : 1 and 10 : 1. As a typical example the preparation of **15F** and **15'F** is described below. The spectral data are listed in Table 5.

(2R,3R)-2-(2,4-Difluorophenyl)-1-(1H-1,2,4-triazol-1-yl)-3-[(trans-2-[(E)-2-[4-(trifluoromethyl)phenyl]vinyl]-1,3-dioxan-5-yl)thio]-2-butanol (15F) Molecular sieves 4A (pellet, 57.6 g) was added to a stirred solution of the alcohol **10** (5.90 g, 16.4 mmol), aldehyde **12F** (4.93 g, 24.6 mmol), and *p*-toluenesulfonic acid hydrate (4.69 g, 24.6 mmol) in CH_2Cl_2 (200 ml) at room temperature. After the mixture was stirred at room temperature for 4 h, it was treated with a diluted aqueous solution of $NaHCO_3$. The mixture was filtered, and the organic layer was dried and concentrated to give an oily residue, which was purified by column chromatography (250 g). Elution with AcOEt–hexane (1 : 24, v/v) gave the recovered aldehyde **12F** (2.19 g). Elution with AcOEt–hexane (1 : 1, v/v) afforded **15F** (5.93 g, 67%) as colorless crystals, mp 73–75 °C. Further elution with AcOEt–hexane (4 : 1, v/v) afforded the *cis* isomer **15'F** (753 mg, 8%) as a colorless oil.

8-(4-Chlorobenzylthio)-1,4-dioxaspiro[4.5]decane (24) 4-Chloro- α -toluenethiol (430 mg, 2.7 mmol) was added to a stirred suspension of NaH (55% mineral oil dispersion, 106 mg, 2.4 mmol; washed with hexane) in DMF (4 ml) at 0 °C. After the mixture was stirred at 0 °C for 5 min, 1,4-dioxaspiro[4.5]decan-8-yl methanesulfonate¹⁷⁾ (**23**, 512 mg, 2.2 mmol) was added. The whole was heated at 50 °C for 1 h. After the mixture was cooled, it was diluted with AcOEt and washed with brine. The organic layer was dried over $MgSO_4$ and the solvents were removed *in vacuo* to leave an oily residue, which was purified by column chromatography (30 g). Elution with AcOEt–hexane (1 : 24, v/v) afforded **24** (438 mg, 68%) as an oil. 1H -NMR (270 MHz, $CDCl_3$) δ : 1.4–2.0 (8H, m), 2.61 (1H, tt, $J=6$, 4 Hz), 3.70 (2H, s), 3.93 (4H, brs), 7.30 (4H, brs). IR ($CHCl_3$) cm^{-1} : 1496, 1371, 1208, 1123, 1110, 1033, 925. MS m/z : 298 (M^+), 173, 125, 99.

4-(4-Chlorobenzylthio)cyclohexanone (25) A 2 M solution of HCl (12.5 ml, 25 mmol) was added to a solution of **24** (11.0 g, 37 mmol) in a mixture of acetone (101 ml) and H_2O (25 ml), and the whole was stirred at 50 °C for 2 h. The cooled mixture was diluted with benzene and washed with brine. The organic layer was dried over $MgSO_4$. Solvents were removed *in vacuo* to leave **25** (9.4 g, 100%) as an oil, which was used for the next reaction without further purification. 1H -NMR (270 MHz, $CDCl_3$) δ : 1.89 (2H, dddd, $J=12$, 9, 8, 6 Hz), 2.1–2.2 (2H, m), 2.29 (2H, ddd, $J=14$, 9, 5 Hz), 2.54 (1H, dt, $J=14$, 6 Hz), 2.97 (1H, tt, $J=8$, 4 Hz), 3.75 (2H, s), 7.29 (4H, brs).

1-(4-Chlorobenzylthio)-4-(methoxymethylene)cyclohexane (26) A suspension of sodium hydride (55% mineral oil dispersion, 146 mg, 3.34 mmol; washed with hexane) in degassed DMSO (18 ml) was heated at 55 °C for 2 h to obtain an almost clear solution of dimethyl sodium. (Methoxymethyl)triphenylphosphonium chloride (1.26 g, 3.67 mmol) was then added to the mixture at room temperature to obtain an orange-red solution. Then a solution of **25** (426 mg, 1.67 mmol) in DMSO (5 ml) was added at room temperature. The reaction was quenched by addition of H_2O . The product was extracted with toluene. The organic layer was dried over $MgSO_4$ and concentrated to afford an oily residue, which was chromatographed on silica gel (20 g). Elution with CH_2Cl_2 –hexane (1 : 4, v/v) afforded **26** (370 mg, 78%) as an oil. 1H -NMR (270 MHz, $CDCl_3$) δ : 1.2–1.5 (2H, m), 1.7–2.0 (3H, m), 2.0–2.2 (1H, m), 2.5–2.8 (2H, m), 3.53 (3H, s), 3.71 (2H, s), 5.77 (1H, s), 7.27 (4H, s). IR ($CHCl_3$) cm^{-1} : 1689, 1491, 1123, 1094. MS m/z : 282 (M^+), 157, 124.

trans-4-(4-Chlorobenzylthio)cyclohexanecarbaldehyde (27) A mixture of **26** (955 mg, 3.4 mmol), 5 M HCl solution (1 ml, 5 mmol), acetone (20 ml), and H_2O (5 ml) was heated at 55 °C for 2 h. Then the mixture was concentrated *in vacuo* at room temperature. The residue was taken up in AcOEt, and the extract was washed with brine and dried over Na_2SO_4 . Evaporation of the solvent afforded an oily residue, which was chromatographed on silica gel (15 g). Elution with CH_2Cl_2 –hexane (1 : 3, v/v) afforded a *ca.* 1 : 1 mixture of **27** and its *cis* isomer (865 mg, 95%). The isomeric ratio was determined by 1H -NMR in $CDCl_3$; the benzylic protons of **27** appeared at δ 3.73 as a singlet whereas those of the *cis* isomer appeared at δ 3.67.

The above obtained mixture (865 mg) was treated, at room temperature for 2 h, with a solution of sodium methoxide prepared by dissolving sodium metal (23 mg, 1.0 mmol) in MeOH (15 ml). Acetic acid (0.2 ml) was then added and the mixture was concentrated *in vacuo*. The residue was taken up in AcOEt, and the extract was washed with brine and dried over $MgSO_4$. Evaporation of the solvents afforded a solid residue, which was a *ca.* 4 : 1 mixture of **27** and its *cis* isomer, as indicated by 1H -NMR. The residue was

Table 5. (2*R*,3*R*)-2-(2,4-Difluorophenyl)-3-[(2-substituted-1,3-dioxan-5-yl)thio]-1-(1*H*-1,2,4-triazol-1-yl)-2-butanols (**14**—**16**) and the *cis* Isomers (**15'****B**, **15'****F**, **15'****Q**)

Compd.	Yield (%)	mp (°C) (Solvent ^a) [Oxalic acid salt: mp (°C)]	IR cm ⁻¹ (State) Optical rotation ^b	¹ H-NMR (270 MHz, CDCl ₃) ^c	Formula	MS <i>m/z</i> Analysis % Calcd (Found)		
						C	H	N
14A	54	Oil [140—142]	1500, 1140, 1080 (CHCl ₃) [α] _D -79.2 (c=1.45, CHCl ₃)	1.20 (3H, d, 7), 3.35 (1H, q, 7), 3.44 (1H, tt, 11, 5), 3.73 (1H, t, 11), 3.75 (1H, t, 11), 4.39 (1H, ddd, 11, 5, 2), 4.50 (1H, ddd, 11, 5, 2), 4.85 (1H, d, 14), 5.02 (1H, s), 5.05 (1H, d, 14), 5.45 (1H, s), 6.65—6.8 (2H, m), 7.0—7.1 (3H, m), 7.37 (1H, td, 9, 7), 7.47 (2H, dd, 9, 6), 7.78 (2H, s)	C ₂₂ H ₂₂ F ₃ N ₃ O ₃ S	466 (M ⁺ + 1), 342, 224		
14C^d	56	Oil [159—159]	1500, 1140 (CHCl ₃) [α] _D -75.2 (c=1.01, CHCl ₃)	1.20 (3H, d, 7), 3.34 (1H, q, 7), 3.5—4.0 (3H, m), 4.2—4.6 (2H, m), 4.78 (1H, d, 14), 5.01 (1H, d, 1.5), 5.07 (1H, d, 14), 5.70 (1H, s), 6.5—7.8 (6H, m), 7.79 (2H, s)	C ₂₂ H ₂₁ F ₄ N ₃ O ₃ S	483 (M ⁺), 224		
14D	27	Oil [149—152]	1520, 1350 (CHCl ₃) [α] _D -74.2 (c=1.02, CHCl ₃)	1.20 (3H, d, 7), 3.15—4.0 (4H, m), 4.1—4.6 (2H, m), 4.77 (1H, d, 14), 5.00 (1H, d, 1.5), 5.02 (1H, d, 14), 5.48 (1H, s), 6.5—7.0 (2H, m), 7.2—7.6 (1H, m), 7.76 (2H, d, 8), 7.80 (2H, s), 8.26 (2H, d, 8)	C ₂₂ H ₂₂ F ₂ N ₄ O ₃ S	492 (M ⁺), 224		
15A	62	Oil [132—136]	1500, 1140 (CHCl ₃) [α] _D -72.2 (c=1.00, CHCl ₃)	1.19 (3H, d, 7), 3.34 (1H, q, 7), 3.42 (1H, tt, 11, 5), 3.65 (1H, t, 11), 3.67 (1H, t, 11), 4.32 (1H, ddd, 11, 5, 2), 4.44 (1H, ddd, 11, 5, 2), 4.82 (1H, d, 14), 5.01 (1H, s), 5.04 (1H, d, 14), 5.11 (1H, d, 4), 6.09 (1H, dd, 16, 4), 6.65—6.8 (2H, m), 6.77 (1H, d, 16), 7.02 (1H, t, 9), 7.3—7.4 (3H, m), 7.79 (2H, s)	C ₂₄ H ₂₄ F ₃ N ₃ O ₃ S	491 (M ⁺), 224		
15B	67	Oil [88—91]	1500, 1140 (CHCl ₃) [α] _D -68.2 (c=1.22, CHCl ₃)	1.19 (3H, d, 7), 3.34 (1H, q, 7), 3.41 (1H, tt, 11, 5), 3.64 (1H, t, 11), 3.66 (1H, t, 11), 4.32 (1H, ddd, 11, 5, 2), 4.44 (1H, ddd, 11, 5, 2), 4.82 (1H, d, 14), 5.01 (1H, s), 5.04 (1H, d, 14), 5.11 (1H, d, 5), 6.15 (1H, dd, 16, 5), 6.65—6.8 (2H, m), 6.76 (1H, d, 16), 7.2—7.4 (5H, m), 7.78 (2H, s)	C ₂₄ H ₂₄ ClF ₂ N ₃ O ₃ S	507 (M ⁺), 284, 224		
15'B	8	Oil [94—98]	1500, 1270, 1140 (CHCl ₃) [α] _D -79.8 (c=1.30, CHCl ₃)	1.21 (3H, d, 7), 3.11 (1H, t-like, 2), 3.50 (1H, q, 7), 4.2—4.4 (4H, m), 4.88 (1H, d, 15), 4.93 (1H, s), 5.16 (1H, d, 15), 5.23 (1H, d, 5), 6.21 (1H, dd, 17, 5), 6.65—6.8 (2H, m), 6.76 (1H, d, 17), 7.2—7.4 (5H, m), 7.77 (1H, s), 7.80 (1H, s)	C ₂₄ H ₂₄ ClF ₂ N ₃ O ₃ S	507 (M ⁺), 284, 224		
15C^d	56	Oil [143—145]	1500, 1140 (CHCl ₃) [α] _D -68.2 (c=1.02, CHCl ₃)	1.20 (3H, d, 7), 3.1—3.9 (4H, m), 4.1—4.6 (2H, m), 4.79 (2H, d, 14), 5.01 (1H, d, 1.5), 5.06 (1H, d, 14), 5.12 (1H, d, 4.5), 6.19 (1H, dd, 16, 4.5), 6.5—7.0 (5H, m), 6.92 (1H, d, 16), 7.1—7.6 (1H, m), 7.80 (2H, s)	C ₂₄ H ₂₃ F ₄ N ₃ O ₃ S	509 (M ⁺), 284, 224		
15D	40	Oil [157—160]	1500, 1270, 1140 (CHCl ₃) [α] _D -64.1 (c=2.43, CHCl ₃)	1.19 (3H, d, 7), 3.35 (1H, q, 7), 3.42 (1H, tt, 11, 5), 3.66 (1H, t, 11), 3.68 (1H, t, 11), 4.34 (1H, ddd, 11, 5, 2), 4.46 (1H, ddd, 11, 5, 2), 4.83 (1H, d, 14), 5.04 (1H, d, 14), 5.04 (1H, s), 5.16 (1H, d, 4), 6.32 (1H, dd, 16, 4), 6.65—6.8 (2H, m), 6.87 (1H, d, 16), 7.36 (1H, td, 9, 8), 7.53 (2H, d, 9), 7.79 (1H, s), 7.80 (1H, s), 8.19 (2H, d, 9)	C ₂₄ H ₂₄ F ₂ N ₄ O ₃ S	518 (M ⁺), 284, 224		
15E	66	164—165 (A—H)	2230, 1499, 1141 (CHCl ₃) [α] _D -77.9 (c=0.52, CHCl ₃)	1.20 (3H, d, 7), 3.34 (1H, q, 7), 3.41 (1H, tt, 11, 5), 3.65 (1H, t, 11), 3.67 (1H, t, 11), 4.33 (1H, ddd, 11, 5, 2), 4.46 (1H, ddd, 11, 5, 2), 4.83 (1H, d, 14), 5.03 (1H, s), 5.04 (1H, d, 14), 5.14 (1H, d, 4), 6.28 (1H, dd, 16, 4), 6.7—6.8 (2H, m), 6.82 (1H, d, 16), 7.3—7.45 (1H, m), 7.49 (2H, d, 8), 7.62 (2H, d, 8), 7.79 (2H, s)	C ₂₅ H ₂₄ F ₂ N ₄ O ₃ S	498 (M ⁺), 284, 224 60.23 4.85 11.24 (60.34 5.05 11.03)		
15F	67	73—75 (A—H)	1617, 1500, 1326, 1136 (KBr) [α] _D -73.8 (c=1.00, CHCl ₃)	1.20 (3H, d, 7), 3.34 (1H, q, 7), 3.43 (1H, tt, 11, 5), 3.65 (1H, t, 11), 3.67 (1H, t, 11), 4.33 (1H, ddd, 11, 5, 2), 4.46 (1H, ddd, 11, 5, 2), 4.83 (1H, d, 14), 5.03 (1H, s), 5.04 (1H, d, 14), 5.14 (1H, d, 4), 6.26 (1H, dd, 16, 4), 6.7—6.8 (2H, m), 6.84 (1H, d, 16), 7.36 (1H, td, 9, 7), 7.50 (2H, d, 8), 7.58 (2H, d, 8), 7.79 (2H, s)	C ₂₅ H ₂₄ F ₅ N ₄ O ₃ S	541 (M ⁺), 521, 224 55.45 4.47 7.76 (55.70 4.57 7.37)		
15'F	8	Oil [112—114]	1618, 1499, 1326, 1140, 1131 (CHCl ₃) [α] _D -83.1 (c=1.03, CHCl ₃)	1.22 (3H, d, 7), 3.14 (1H, t-like), 3.50 (1H, q, 7), 4.2—4.4 (4H, m), 4.88 (1H, d, 15), 4.94 (1H, s), 5.16 (1H, d, 15), 5.27 (1H, d, 5), 6.33 (1H, dd, 17, 5), 6.6—6.8 (2H, m), 6.84 (1H, d, 17), 7.37 (1H, td, 9, 7), 7.50 (2H, d, 8), 7.58 (2H, d, 8), 7.78 (1H, s), 7.81 (1H, s)	C ₂₅ H ₂₄ F ₅ N ₄ O ₃ S	541 (M ⁺), 521, 224		
15G	57	Oil [63—69]	1499, 1334, 1135 (CHCl ₃) [α] _D -73.9 (c=0.59, CHCl ₃)	1.20 (3H, d, 7), 3.34 (1H, q, 7), 3.43 (1H, tt, 11, 5), 3.65 (1H, t, 11), 3.68 (1H, t, 11), 4.33 (1H, ddd, 11, 5, 2), 4.45 (1H, ddd, 11, 5, 2), 4.84 (1H, d, 14), 5.03 (1H, s), 5.04 (1H, d, 14), 5.14 (1H, d, 4), 6.24 (1H, dd, 16, 4), 6.7—6.8 (2H, m), 6.84 (1H, d, 16), 7.73—7.76 (4H, s), 7.65 (1H, s), 7.79 (2H, s)	C ₂₅ H ₂₄ F ₅ N ₃ O ₃ S	541 (M ⁺), 318, 284, 224		
15H	60	Oil [56—71]	1499, 1468, 1334, 1142 (CHCl ₃) [α] _D -73.4 (c=1.06, CHCl ₃)	1.20 (3H, d, 7), 3.35 (1H, q, 7), 3.43 (1H, tt, 11, 5), 3.66 (1H, t, 11), 3.68 (1H, t, 11), 4.33 (1H, ddd, 11, 5, 2), 4.45 (1H, ddd, 11, 5, 2), 4.84 (1H, d, 14), 5.03 (1H, s), 5.04 (1H, d, 14), 5.15 (1H, d, 4), 6.31 (1H, dd, 16, 4), 6.7—6.8 (2H, m), 6.98 (1H, d, 16), 7.21 (1H, t), 7.36 (1H, q, 8), 7.52 (1H, t, 8), 7.67 (1H, t), 7.79 (2H, s)	C ₂₅ H ₂₃ F ₆ N ₃ O ₃ S	559 (M ⁺), 540, 336, 224		
15I	66	Oil [149—152]	1499, 1332, 1137 (CHCl ₃) [α] _D -72.1 (c=0.63, CHCl ₃)	1.20 (3H, d, 7), 3.34 (1H, q, 7), 3.41 (1H, tt, 11, 5), 3.65 (1H, t, 11), 3.68 (1H, t, 11), 4.34 (1H, m), 4.46 (1H, m), 4.83 (1H, d, 14), 5.04 (1H, d, 14), 5.04 (1H, s), 5.15 (1H, d, 4), 6.36 (1H, dd, 16, 4), 6.7—6.8 (2H, m), 6.97 (1H, d, 16), 7.3—7.45 (3H, m), 7.58 (1H, t, 8), 7.79 (2H, s)	C ₂₅ H ₂₃ F ₆ N ₃ O ₃ S	559 (M ⁺), 540, 336, 224		

Table 5. (Continued)

Compd.	Yield (%)	mp (°C) (Solvent ^a) [Oxalic acid salt: mp (°C)]	IR cm ⁻¹ (State) Optical rotation ^b	¹ H-NMR (270 MHz, CDCl ₃) ^c	Formula	MS <i>m/z</i> Analysis % Calcd (Found)		
						C	H	N
15J	66	Oil [105—113]	1500, 1334, 1135 (CHCl ₃) [α] _D -72.7 (c=0.55, CHCl ₃)	1.20 (3H, d, 7), 3.34 (1H, q, 7), 3.42 (1H, tt, 11, 5), 3.65 (1H, t, 11), 3.67 (1H, t, 11), 4.33 (1H, ddd, 11, 5, 2), 4.46 (1H, ddd, 11, 5, 2), 4.84 (1H, d, 14), 5.03 (1H, s), 5.04 (1H, d, 14), 5.14 (1H, d, 4), 6.34 (1H, dd, 16, 4), 6.7—6.8 (2H, m), 6.96 (1H, d, 16), 7.16 (1H, t, 9), 7.36 (1H, q, 8), 7.52 (1H, m), 7.74 (1H, dd, 6, 2), 7.79 (2H, s)	C ₂₅ H ₂₃ F ₆ N ₃ O ₅ S	559 (M ⁺), 540, 336, 224		
15K	43	Oil [124—130]	1499, 1479, 1134, 1142 (CHCl ₃) [α] _D -73.7 (c=1.00, CHCl ₃)	1.20 (3H, d, 7), 3.34 (1H, q, 7), 3.41 (1H, tt, 11, 5), 3.65 (1H, t, 11), 3.67 (1H, t, 11), 4.33 (1H, ddd, 11, 5, 2), 4.45 (1H, ddd, 11, 5, 2), 4.83 (1H, d, 14), 5.03 (1H, s), 5.04 (1H, d, 14), 5.13 (1H, d, 4), 6.10 (1H, dd, 16, 4), 6.7—6.8 (2H, m), 7.11 (1H, d, 16), 7.22 (1H, td, 8, 3), 7.3—7.4 (2H, m), 7.63 (1H, dd, 9, 5), 7.79 (2H, s)	C ₂₅ H ₂₃ F ₆ N ₃ O ₅ S	559 (M ⁺), 540, 336, 224		
15L	44	Oil [70—72]	1510, 1240, 1140, 965 (CHCl ₃) [α] _D -75.9 (c=1.45, CHCl ₃)	1.19 (3H, d, 7), 3.34 (1H, q, 7), 3.41 (1H, tt, 11, 5), 3.64 (1H, t, 11), 3.66 (1H, t, 11), 3.81 (3H, s), 4.32 (1H, ddd, 11, 5, 2), 4.43 (1H, ddd, 11, 5, 2), 4.83 (1H, d, 14), 5.01 (1H, s), 5.04 (1H, d, 14), 5.10 (1H, d, 4), 6.04 (1H, dd, 16, 4), 6.65—6.8 (2H, m), 6.74 (1H, d, 16), 6.86 (2H, d, 9), 7.3—7.4 (1H, m), 7.34 (2H, d, 9), 7.79 (1H, s), 7.80 (1H, s)	C ₂₅ H ₂₇ F ₂ N ₃ O ₄ S	503 (M ⁺), 265, 224, 219		
15N	43	Amorphous [68—71]	1500, 1255, 1140, 965 (CHCl ₃) [α] _D -77.1 (c=0.52, CHCl ₃)	1.20 (3H, d, 7), 3.34 (1H, q, 7), 3.42 (1H, tt, 11, 5), 3.65 (1H, t, 11), 3.67 (1H, t, 11), 4.32 (1H, ddd, 11, 5, 2), 4.45 (1H, ddd, 11, 5, 2), 4.83 (1H, d, 14), 5.01 (1H, s), 5.03 (1H, d, 14), 5.12 (1H, d, 4), 6.15 (1H, dd, 16, 4), 6.7—6.8 (2H, m), 6.79 (1H, d, 16), 7.17 (2H, d, 9), 7.3—7.45 (1H, m), 7.42 (2H, d, 9), 7.79 (2H, s)	C ₂₅ H ₂₄ F ₆ N ₃ O ₄ S	557 (M ⁺), 538, 334, 224		
15O	53	Amorphous [72—77]	1500, 1257, 1217, 1140 (CHCl ₃) [α] _D -73.2 (c=0.62, CHCl ₃)	1.20 (3H, d, 7), 3.34 (1H, q, 7), 3.42 (1H, tt, 11, 5), 3.65 (1H, t, 11), 3.67 (1H, t, 11), 4.33 (1H, ddd, 11, 5, 2), 4.45 (1H, ddd, 11, 5, 2), 4.83 (1H, d, 14), 5.01 (1H, s), 5.04 (1H, d, 14), 5.13 (1H, d, 4), 6.20 (1H, dd, 16, 4), 6.7—6.8 (2H, m), 6.79 (1H, d, 16), 7.13 (1H, d, 7), 7.2—7.4 (3H, m), 7.79 (2H, s)	C ₂₅ H ₂₄ F ₆ N ₃ O ₄ S	557 (M ⁺), 538, 334, 224		
15P	64	Oil [71—76]	1509, 1499, 1382, 1132 (CHCl ₃) [α] _D -68.4 (c=0.57, CHCl ₃)	1.19 (3H, d, 7), 3.34 (1H, q, 7), 3.42 (1H, tt, 11, 5), 3.65 (1H, t, 11), 3.67 (1H, t, 11), 4.32 (1H, ddd, 11, 5, 2), 4.45 (1H, ddd, 11, 5, 2), 4.83 (1H, d, 14), 5.02 (1H, s), 5.04 (1H, d, 14), 5.12 (1H, d, 4), 6.13 (1H, dd, 16, 4), 6.51 (1H, t, 74), 6.7—6.8 (2H, m), 6.78 (1H, d, 16), 7.08 (2H, d, 9), 7.3—7.4 (1H, m), 7.40 (2H, d, 9), 7.79 (2H, s)	C ₂₅ H ₂₅ F ₄ N ₃ O ₄ S	539 (M ⁺), 520, 284, 265, 224		
15Q	60	Oil [71—78]	1507, 1500, 1278, 1184, 1133 (CHCl ₃) [α] _D -71.7 (c=0.66, CHCl ₃)	1.19 (3H, d, 7), 3.34 (1H, q, 7), 3.42 (1H, tt, 11, 5), 3.65 (1H, t, 11), 3.67 (1H, t, 11), 4.33 (1H, ddd, 11, 5, 2), 4.45 (1H, ddd, 11, 5, 2), 4.83 (1H, d, 14), 5.02 (1H, s), 5.04 (1H, d, 14), 5.12 (1H, d, 4), 5.91 (1H, tt, 53, 3), 6.15 (1H, dd, 16, 4), 6.7—6.8 (2H, m), 6.79 (1H, d, 16), 7.17 (2H, d, 9), 7.3—7.45 (1H, m), 7.41 (2H, d, 9), 7.79 (2H, s)	C ₂₆ H ₂₅ F ₆ N ₃ O ₄ S	589 (M ⁺), 570, 538, 366, 224		
15'Q	7	Oil [99—101]	1508, 1500, 1278, 1184, 1130 (CHCl ₃) [α] _D -74.6 (c=0.89, CHCl ₃)	1.22 (3H, d, 7), 3.12 (1H, t-like, 2), 3.51 (1H, q, 7), 4.2—4.4 (4H, m), 4.89 (1H, d, 15), 4.93 (1H, s), 5.17 (1H, d, 15), 5.25 (1H, d, 5), 5.90 (1H, tt, 53, 3), 6.22 (1H, dd, 17, 5), 6.65—6.8 (2H, m), 6.79 (1H, d, 17), 7.17 (2H, d, 9), 7.37 (1H, td, 9, 7), 7.42 (2H, d, 9), 7.78 (1H, s), 7.81 (1H, s)	C ₂₆ H ₂₅ F ₆ N ₃ O ₄ S	589 (M ⁺), 570, 538, 342, 224		
15R	63	Oil [72—79]	1511, 1499, 1277, 1140, 1133 (CHCl ₃) [α] _D -73.1 (c=0.55, CHCl ₃)	1.19 (3H, d, 7), 3.34 (1H, q, 7), 3.41 (1H, tt, 11, 5), 3.64 (1H, t, 11), 3.67 (1H, t, 11), 4.33 (1H, m), 4.35 (2H, t, 12), 4.44 (1H, ddd, 11, 5, 2), 4.83 (1H, d, 14), 5.01 (1H, s), 5.04 (1H, d, 14), 5.11 (1H, d, 4), 6.06 (1H, tt, 53, 5), 6.08 (1H, dd, 16, 4), 6.65—6.8 (2H, m), 6.75 (1H, d, 16), 6.88 (2H, d, 9), 7.3—7.45 (1H, m), 7.33 (2H, d, 9), 7.79 (2H, s)	C ₂₇ H ₂₇ F ₆ N ₃ O ₄ S	603 (M ⁺), 319, 265, 224		
15S	37	Oil [79—81]	1517, 1497, 1275, 1136, 965 (CHCl ₃) [α] _D -62.9 (c=0.75, CHCl ₃)	1.19 (3H, d, 7), 2.48 (3H, s), 3.33 (1H, q, 7), 3.41 (1H, tt, 11, 5), 3.64 (1H, t, 11), 3.67 (1H, t, 11), 4.32 (1H, ddd, 11, 5, 2), 4.44 (1H, ddd, 11, 5, 2), 4.83 (1H, d, 14), 5.01 (1H, s), 5.04 (1H, d, 14), 5.11 (1H, d, 4), 6.13 (1H, dd, 16, 4), 6.65—6.8 (2H, m), 6.74 (1H, d, 16), 7.19 (2H, d, 9), 7.3—7.4 (1H, m), 7.32 (2H, d, 9), 7.79 (2H, s)	C ₂₅ H ₂₇ F ₂ N ₃ O ₅ S ₂	519 (M ⁺), 284, 265, 234, 224		
15T ^e	58	Oil [87—92]	1500, 1140 (CHCl ₃) [α] _D -62.2 (c=0.95, CHCl ₃)	1.20 (3H, d, 7), 3.00 (3H, s), 3.33 (1H, q, 7), 3.5—4.0 (3H, m), 4.2—4.8 (2H, m), 4.80 (1H, d, 14), 5.08 (1H, d, 14), 5.15 (1H, d, 4), 6.30 (1H, dd, 17, 4), 6.55—7.0 (2H, m), 6.90 (1H, d, 17), 7.2—7.6 (1H, m), 7.58 (2H, d, 9), 7.80 (2H, s), 7.94 (2H, d, 8)	C ₂₅ H ₂₇ F ₂ N ₃ O ₅ S ₂	551 (M ⁺), 284, 265, 224		
15V	65	Amorphous [86—88]	1594, 1500, 1368, 1218, 1141 (KBr) [α] _D -62.7 (c=1.01, CHCl ₃)	1.20 (3H, d, 7), 3.34 (1H, q, 7), 3.44 (1H, tt, 11, 5), 3.65 (1H, t, 11), 3.68 (1H, t, 11), 4.34 (1H, ddd, 11, 5, 2), 4.47 (1H, ddd, 11, 5, 2), 4.83 (1H, d, 14), 5.03 (1H, s), 5.03 (1H, d, 14), 5.16 (1H, d, 4), 6.38 (1H, dd, 16, 4), 6.65—6.8 (2H, m), 6.89 (1H, d, 16), 7.36 (1H, td, 9, 7), 7.66 (2H, d, 9), 7.80 (2H, s), 8.00 (2H, d, 9)	C ₂₅ H ₂₄ F ₅ N ₃ O ₅ S ₂	606 (M ⁺ + 1, FAB) 49.58 4.00 6.94 (49.51 3.94 6.69)		

Table 5. (Continued)

Compd.	Yield (%)	mp (°C) (Solvent ^a) [Oxalic acid salt: mp (°C)]	IR cm ⁻¹ (State) Optical rotation ^b	¹ H-NMR (270 MHz, CDCl ₃) ^c	Formula	MS <i>m/z</i> Analysis % Calcd (Found)		
						C	H	N
15W	52	Oil [ca. 80]	1500, 1140 (CHCl ₃) [α] _D -62.2 (c=0.90, CHCl ₃)	1.20 (3H, d, 7), 3.34 (1H, q, 7), 3.43 (1H, tt, 11, 5), 3.65 (1H, t, 11), 3.68 (1H, t, 11), 4.33 (1H, ddd, 11, 5, 2), 4.46 (1H, ddd, 11, 5, 2), 4.83 (1H, d, 14), 5.04 (1H, s), 5.04 (1H, d, 14), 5.14 (1H, d, 4), 6.25 (1H, dd, 17, 4), 6.7—6.8 (2H, m), 6.81 (1H, d, 17), 7.29 (1H, dd, 8, 5), 7.3—7.45 (1H, m), 7.73 (dt, 8, 1), 7.80 (2H, s), 8.51 (dd, 5, 1), 8.62 (1H, d, 1)	C ₂₃ H ₂₄ F ₂ N ₄ O ₃ S	474 (M ⁺), 284, 265, 224		
15X	63	73—76 (A-H)	1500, 1460, 1275, 1140, 1100 (CHCl ₃) [α] _D -75.6 (c=0.52, CHCl ₃)	1.19 (3H, d, 7), 3.33 (1H, q, 7), 3.43 (1H, tt, 11, 5), 3.64 (1H, t, 11), 3.67 (1H, t, 11), 4.32 (1H, ddd, 11, 5, 2), 4.46 (1H, ddd, 11, 5, 2), 4.83 (1H, d, 14), 5.03 (1H, d, 14), 5.04 (1H, s), 5.13 (1H, d, 4), 6.23 (1H, dd, 17, 4), 6.7—6.8 (2H, m), 6.78 (1H, d, 17), 7.30 (1H, d, 8), 7.35 (1H, td, 9, 7), 7.70 (1H, dd, 8, 2), 7.79 (2H, s), 8.38 (1H, d, 2)	C ₂₃ H ₂₃ ClF ₂ N ₄ O ₃ S	508 (M ⁺), 285, 265, 224		
15Y ^d	73	Oil	1500, 1400, 1140, 965 (CHCl ₃) [α] _D -69.7 (c=0.69, CHCl ₃)	1.20 (3H, d, 7), 3.34 (1H, q, 7), 3.43 (1H, tt, 11, 5), 3.66 (1H, t, 11), 3.68 (1H, t, 11), 4.33 (1H, ddd, 11, 5, 2), 4.46 (1H, ddd, 11, 5, 2), 4.83 (1H, d, 14), 5.04 (1H, d, 14), 5.04 (1H, s), 5.17 (1H, d, 5), 6.23 (1H, dd, 17, 5), 6.7—6.8 (2H, m), 7.13 (1H, d, 17), 7.24 (1H, dd, 8, 5), 7.36 (1H, td, 9, 7), 7.79 (2H, s), 7.85 (1H, dd, 8, 2), 8.31 (1H, dd, 5, 2)	C ₂₃ H ₂₃ ClF ₂ N ₄ O ₃ S	508 (M ⁺), 342, 285, 224		
15Z	39	Oil [101—109]	1602, 1490, 1278, 1139, 1128 (CHCl ₃) [α] _D -61.4 (c=0.74, CHCl ₃)	1.19 (3H, d, 7), 3.33 (1H, q, 7), 3.42 (1H, tt, 11, 5), 3.64 (1H, t, 11), 3.67 (1H, t, 11), 4.33 (1H, ddd, 11, 5, 2), 4.45 (1H, ddd, 11, 5, 2), 4.74 (2H, tt, 13, 1), 4.82 (1H, d, 14), 5.01 (1H, s), 5.03 (1H, d, 14), 5.12 (1H, d, 5), 6.01 (1H, tt, 53, 5), 6.11 (1H, dd, 16, 5), 6.65—6.85 (4H, m), 7.36 (1H, td, 9, 7), 7.73 (1H, dd, 9, 2), 7.79 (2H, s), 8.13 (1H, d, 2)	C ₂₆ H ₂₆ F ₆ N ₄ O ₄ S	604 (M ⁺), 489, 381, 320, 224		
15AA	50	Oil [53—57]	1500, 1275, 1140, 960 (CHCl ₃) [α] _D -75.7 (c=0.56, CHCl ₃)	1.19 (3H, d, 7), 3.33 (1H, q, 7), 3.40 (1H, tt, 11, 5), 3.62 (1H, t, 11), 3.64 (1H, t, 11), 4.30 (1H, ddd, 11, 5, 2), 4.42 (1H, ddd, 11, 5, 2), 4.82 (1H, d, 14), 5.01 (1H, d, 5), 5.04 (1H, d, 14), 5.05 (1H, s), 5.89 (1H, dd, 16, 5), 6.65—6.85 (3H, m), 6.78 (2H, s), 7.36 (1H, m), 7.87 (2H, s)	C ₂₂ H ₂₂ ClF ₂ N ₃ O ₃ S ₂	513 (M ⁺), 284, 224		
15AB	22	Oil [78—79.5]	1618, 1499, 1141, 966 (CHCl ₃) [α] _D -70.7 (c=0.88, CHCl ₃)	1.20 (3H, d, 7), 3.35 (1H, q, 7), 3.44 (1H, tt, 11, 5), 3.68 (1H, t, 11), 3.70 (1H, t, 11), 4.34 (1H, ddd, 11, 5, 2), 4.46 (1H, ddd, 11, 5, 2), 4.84 (1H, d, 14), 5.01 (1H, s), 5.05 (1H, d, 14), 5.18 (1H, d, 5), 6.30 (1H, dd, 16, 5), 6.65—6.80 (2H, m), 6.98 (1H, d, 16), 7.37 (1H, td, 9, 7), 7.4—7.5 (2H, m), 7.60 (1H, dd, 10, 1), 7.7—7.9 (4H, m), 7.79 (2H, s)	C ₂₈ H ₂₇ F ₂ N ₃ O ₃ S	525 (M ⁺ + 1, FAB)		
15AC	44	167—168 (A-H)	1617, 1596, 1499, 1135 (KBr) [α] _D -40.6 (c=0.50, MeOH)	1.20 (3H, d, 7), 3.35 (1H, q, 7), 3.4—3.5 (1H, m), 3.67 (1H, t, 11), 3.69 (1H, t, 7), 4.35 (1H, dd, 11, 5, 2), 4.46 (1H, dd, 11, 5, 2), 4.85 (1H, d, 14), 5.02 (1H, s), 5.05 (1H, d, 14), 5.17 (1H, d, 4), 6.30 (1H, dd, 16, 4), 6.7—6.8 (2H, m), 6.94 (1H, d, 16), 7.3—7.4 (1H, m), 7.5—7.8 (7H, m), 7.96 (1H, s)	C ₂₈ H ₂₆ BrF ₂ N ₃ O ₃ S	601 (M ⁺), 523, 448, 378, 318, 262, 224 55.82 4.35 6.97 (55.65 4.31 6.90)		
15AD	45	115—117 (A-H)	1617, 1620, 1500, 1274, 1135 (KBr) [α] _D -65.9 (c=1.00, CHCl ₃)	1.20 (3H, d, 7), 3.35 (1H, q, 7), 3.4—3.5 (1H, m), 3.67 (1H, t, 11), 3.69 (1H, t, 7), 4.35 (1H, dd, 11, 5, 2), 4.4—4.5 (1H, m), 4.47 (2H, t, 11), 4.84 (1H, d, 14), 5.02 (1H, s), 5.05 (1H, d, 14), 5.17 (1H, d, 5), 6.11 (1H, tt, 53, 5), 6.27 (1H, dd, 16, 5), 6.7—6.8 (2H, m), 6.94 (1H, d, 16), 7.1—7.2 (2H, m), 7.3—7.4 (1H, m), 7.6—7.9 (6H, m)	C ₃₁ H ₂₉ F ₆ N ₃ O ₄ S	653 (M ⁺), 613, 589, 511, 402, 369, 342, 284 56.96 4.47 6.43 (56.75 4.25 6.68)		
16B	65	Amorphous [112—114]	1499, 1275, 1140, 1050, 966 (KBr) [α] _D -76.8 (c=1.02, CHCl ₃)	1.19 (3H, d, 7), 3.33 (1H, q, 7), 3.39 (1H, tt, 11, 5), 3.62 (1H, t, 11), 3.64 (1H, t, 11), 4.30 (1H, ddd, 11, 5, 2), 4.41 (1H, ddd, 11, 5, 2), 4.82 (1H, d, 14), 5.00 (1H, s), 5.03 (1H, d, 14), 5.05 (1H, d, 5), 5.79 (1H, dd, 16, 5), 6.57 (1H, dd, 16, 10), 5.57 (1H, d, 15), 6.65—6.80 (3H, m), 7.2—7.4 (5H, m), 7.79 (2H, s)	C ₂₆ H ₂₆ ClF ₂ N ₃ O ₃ S	533 (M ⁺), 284, 252, 224 58.48 4.91 7.87 (58.15 5.07 7.67)		
16C	61	Amorphous [88—91]	1614, 1500, 1276, 1139 (CHCl ₃) [α] _D -79.1 (c=1.04, CHCl ₃)	1.18 (3H, d, 7), 3.33 (1H, q, 7), 3.39 (1H, tt, 11, 5), 3.62 (1H, t, 11), 3.64 (1H, t, 11), 3.90 (3H, s), 4.30 (1H, ddd, 11, 5, 2), 4.42 (1H, ddd, 11, 5, 2), 4.82 (1H, d, 14), 5.00 (1H, s), 5.03 (1H, d, 14), 5.05 (1H, d, 5), 5.80 (1H, dd, 16, 5), 6.62 (1H, dd, 15, 10), 6.65—6.80 (2H, m), 6.85 (1H, dd, 16, 10), 6.96 (1H, d, 16), 7.06 (1H, s), 7.18 (1H, d, 8), 7.36 (1H, q, 8), 7.54 (1H, d, 8), 7.79 (2H, s)	C ₂₆ H ₂₅ F ₄ N ₃ O ₃ S	536 (M ⁺ + 1, FAB)		
16E	81	147—149 (A-H)	2225, 1617, 1603, 1500, 1140 (KBr) [α] _D -73.4 (c=1.30, CHCl ₃)	1.19 (3H, d, 7), 3.33 (1H, q, 7), 3.40 (1H, tt, 11, 5), 3.62 (1H, t, 11), 3.64 (1H, t, 11), 4.31 (1H, ddd, 11, 5, 2), 4.43 (1H, ddd, 11, 5, 2), 4.83 (1H, d, 14), 5.00 (1H, s), 5.03 (1H, d, 14), 5.06 (1H, d, 4), 5.87 (1H, dd, 15, 4), 6.59 (1H, dd, 15, 10), 6.61 (1H, 15), 6.7—6.8 (2H, m), 6.87 (1H, 15, 10), 7.35 (1H, td, 8, 7), 7.48 (2H, d, 8), 7.60 (2H, 8), 7.79 (2H, s)	C ₂₇ H ₂₆ F ₂ N ₄ O ₃ S	525 (M ⁺ + 1, FAB) 61.82 5.00 10.68 (62.00 5.01 10.56)		
16F	64	Oil [62—64]	1651, 1456, 1325, 1128, 1068 (CHCl ₃) [α] _D -69.8 (c=1.00, CHCl ₃)	1.19 (3H, d, 7), 3.33 (1H, q, 7), 3.40 (1H, tt, 11, 5), 3.62 (1H, t, 11), 3.64 (1H, t, 11), 4.30 (1H, ddd, 11, 5, 2), 4.42 (1H, ddd, 11, 5, 2), 4.82 (1H, d, 14), 5.00 (1H, s), 5.03 (1H, d, 14), 5.06 (1H, d, 5), 5.84 (1H, dd, 15, 5), 6.60 (1H, dd, 15, 11), 6.7—6.8 (2H, m), 6.73 (1H, d, 16), 6.85 (1H, dd, 16, 11), 7.3—7.45 (1H, m), 7.49 (2H, d, 9), 7.56 (2H, d, 9), 7.78 (2H, s)	C ₂₇ H ₂₆ F ₃ N ₃ O ₃ S	567 (M ⁺), 547, 284, 224		

Table 5. (Continued)

Compd.	Yield (%)	mp (°C) (Solvent ^a) [Oxalic acid salt: mp (°C)]	IR cm ⁻¹ (State) Optical rotation ^b	¹ H-NMR (270 MHz, CDCl ₃) ^c	Formula	MS <i>m/z</i> Analysis % Calcd (Found)		
						C	H	N
16M	61	Amorphous	1501, 1418, 1328, 1241, 1140 (KBr) [α] _D -65.1 (<i>c</i> =1.06, CHCl ₃)	1.18 (3H, d, 7), 3.33 (1H, q, 7), 3.39 (1H, tt, 11, 5), 3.62 (1H, t, 11), 3.64 (1H, t, 11), 3.90 (3H, s), 4.30 (1H, ddd, 11, 5, 2), 4.41 (1H, ddd, 11, 5, 2), 4.83 (1H, d, 14), 5.00 (1H, s), 5.03 (1H, d, 14), 5.05 (1H, d, 5), 5.79 (1H, dd, 15, 5), 6.58 (1H, dd, 15, 9), 6.7—6.9 (6H, m), 7.2—7.6 (2H, m), 7.79 (2H, s)	C ₂₈ H ₂₈ F ₃ N ₃ O ₄ S	597 (M ⁺), 284, 224		
16N	66	Amorphous [75—79]	1507, 1500, 1262, 1141 (CHCl ₃) [α] _D -73.3 (<i>c</i> =0.70, CHCl ₃)	1.18 (3H, d, 7), 3.33 (1H, q, 7), 3.40 (1H, tt, 11, 5), 3.62 (1H, t, 11), 3.64 (1H, t, 11), 4.30 (1H, ddd, 11, 5, 2), 4.42 (1H, ddd, 11, 5, 2), 4.83 (1H, d, 14), 5.01 (1H, s), 5.03 (1H, d, 14), 5.05 (1H, d, 4), 5.80 (1H, dd, 16, 4), 6.58 (1H, dd, 16, 10), 6.60 (1H, d, 16), 6.7—6.9 (3H, m), 7.17 (2H, d, 9), 7.36 (1H, m), 7.42 (2H, d, 9), 7.79 (2H, s)	C ₂₇ H ₂₆ F ₃ N ₃ O ₄ S	583 (M ⁺), 564, 360, 342, 284, 224		
16R	66	73—76 (E-H)	1605, 1510, 1277, 1254, 1140 (KBr) [α] _D -68.1 (<i>c</i> =1.22, CHCl ₃)	1.18 (3H, d, 7), 3.33 (1H, q, 7), 3.39 (1H, tt, 11, 5), 3.62 (1H, t, 11), 3.64 (1H, t, 11), 4.30 (1H, ddd, 11, 5, 2), 4.35 (1H, t, 12), 4.41 (1H, ddd, 11, 5, 2), 4.82 (1H, d, 14), 4.99 (1H, s), 5.03 (1H, d, 14), 5.04 (1H, d, 5), 5.75 (1H, dd, 16, 5), 6.06 (1H, tt, 53, 5), 6.56 (1H, dd, 16, 10), 6.57 (1H, d, 15), 6.68 (1H, dd, 15, 10), 6.7—6.9 (2H, m), 6.88 (2H, d, 9), 7.3—7.4 (1H, m), 7.37 (2H, d, 9), 7.79 (2H, s)	C ₂₉ H ₂₉ F ₆ N ₃ O ₄ S	629 (M ⁺), 345, 285, 259, 224 55.32 4.64 6.67 (55.26 4.64 6.73)		
16S	40	Amorphous [78—80]	1618, 1595, 1499, 1277, 1141 (KBr) [α] _D -68.1 (<i>c</i> =1.44, CHCl ₃)	1.18 (3H, d, 7), 2.48 (3H, s), 3.33 (1H, q, 7), 3.38 (1H, tt, 11, 5), 3.61 (1H, t, 11), 3.63 (1H, t, 11), 4.30 (1H, ddd, 11, 5, 2), 4.41 (1H, ddd, 11, 5, 2), 4.82 (1H, d, 14), 5.00 (1H, s), 5.02 (1H, d, 14), 5.04 (1H, d, 5), 5.75 (1H, dd, 16, 5), 6.56 (1H, dd, 16, 10), 6.57 (1H, d, 15), 6.68 (1H, dd, 15, 10), 6.5—6.65 (2H, m), 6.65—6.8 (3H, m), 7.23 (2H, d, 9), 7.3—7.4 (1H, m), 7.32 (2H, d, 9), 7.78 (2H, s)	C ₂₇ H ₂₉ F ₂ N ₃ O ₅ S ₂	545 (M ⁺), 370, 284, 261, 224		
16U	56	Foam [83—85]	1621, 1680, 1621, 1501, 1117 (KBr) [α] _D -68.2 (<i>c</i> =0.72, CHCl ₃)	1.19 (3H, d, 7), 3.33 (1H, q, 7), 3.40 (1H, tt, 11, 5), 3.62 (1H, t, 11, 5), 3.62 (1H, t, 11), 3.64 (1H, t, 11), 4.31 (1H, ddd, 11, 5, 2), 4.42 (1H, ddd, 11, 5, 2), 4.83 (1H, d, 14), 5.01 (1H, d, 5), 5.03 (1H, d, 14), 5.06 (1H, d, 5), 5.83 (1H, dd, 15, 5), 6.60 (1H, dd, 15, 9), 6.62 (1H, d, 16), 6.7—6.8 (2H, m), 6.84 (1H, dd, 16, 10), 7.3—7.4 (1H, m), 7.44 (2H, d, 8), 7.60 (2H, d, 8), 7.79 (2H, s)	C ₂₇ H ₂₆ F ₅ N ₃ O ₅ S ₂	599 (M ⁺), 376, 346, 284, 224		
16V ^g	71	Amorphous	1591, 1500, 1368, 1217, 1139 (KBr) [α] _D -59.0 (<i>c</i> =1.05, CHCl ₃)	1.19 (3H, d, 7), 3.33 (1H, q, 7), 3.41 (1H, tt, 11, 5), 3.62 (1H, t, 11), 3.64 (1H, t, 11), 4.31 (1H, ddd, 11, 5, 2), 4.44 (1H, ddd, 11, 5, 2), 4.83 (1H, d, 14), 5.02 (1H, s), 5.03 (1H, d, 14), 5.08 (1H, d, 4), 5.96 (1H, dd, 16, 4), 6.63 (1H, dd, 15, 11), 6.68 (1H, d, 15), 6.7—6.8 (2H, m), 6.98 (1H, dd, 16, 11), 7.36 (1H, td, 9, 7), 7.65 (2H, d, 8), 7.787 (1H, s), 7.793 (1H, s), 7.97 (2H, d, 8)	C ₂₇ H ₂₆ F ₅ N ₃ O ₅ S ₂	632 (M ⁺ + 1, FAB) 51.34 4.15 6.65 (51.26 4.20 6.40)		
16X	69	88—90 (A-H)	1618, 1499, 1463, 1277, 1141 (KBr) [α] _D -55.2 (<i>c</i> =0.62, CHCl ₃)	1.18 (3H, d, 7), 3.33 (1H, q, 7), 3.40 (1H, tt, 11, 5), 3.62 (1H, t, 11), 3.64 (1H, t, 11), 4.30 (1H, ddd, 11, 5, 2), 4.42 (1H, ddd, 11, 5, 2), 4.82 (1H, d, 14), 5.01 (1H, s), 5.03 (1H, d, 14), 5.05 (1H, d, 4), 5.82 (1H, dd, 16, 4), 6.56 (1H, d, 15), 6.58 (1H, dd, 15, 11), 6.65—6.75 (3H, m), 7.28 (1H, d, 8), 7.39 (1H, td, 9, 7), 7.70 (1H, dd, 8, 2), 7.79 (2H, s), 8.37 (1H, d, 2)	C ₂₇ H ₂₅ ClF ₂ N ₃ O ₅ S ₂	534 (M ⁺), 499, 311, 284, 224		
16Z	63	Amorphous [64—69]	1598, 1488, 1278, 1140, 1128 (CHCl ₃) [α] _D -58.6 (<i>c</i> =0.52, CHCl ₃)	1.19 (3H, d, 7), 3.33 (1H, q, 7), 3.39 (1H, tt, 11, 5), 3.62 (1H, t, 11), 3.64 (1H, t, 11), 4.30 (1H, ddd, 11, 5, 2), 4.42 (1H, ddd, 11, 5, 2), 4.74 (2H, brt, 13), 4.82 (1H, d, 14), 5.01 (1H, s), 5.03 (1H, d, 14), 5.05 (1H, d, 5), 5.78 (1H, dd, 16, 5), 6.01 (1H, tt, 53, 5), 6.51—6.62 (2H, m), 6.65—6.78 (3H, m), 6.81 (1H, d, 9), 7.35 (1H, m), 7.74 (1H, dd, 9, 2), 7.79 (2H, s), 8.11 (1H, d, 2)	C ₂₈ H ₂₈ F ₆ N ₄ O ₄ S	630 (M ⁺), 284, 224		
16AA	69	Oil [90—110]	1500, 1275, 1140 (CHCl ₃) [α] _D -55.2 (<i>c</i> =0.56, CHCl ₃)	1.18 (3H, d, 7), 3.32 (1H, q, 7), 3.38 (1H, tt, 11, 5), 3.60 (1H, t, 11), 3.63 (1H, t, 11), 4.29 (1H, m), 4.41 (1H, m), 4.82 (1H, d, 14), 5.00 (1H, s), 5.02 (1H, d, 14), 5.03 (1H, d, 14), 5.74 (1H, dd, 14, 5), 6.4—6.55 (2H, m), 6.60 (1H, d, 15), 6.7—6.8 (4H, m), 7.36 (1H, q, 8.2), 7.79 (2H, s)	C ₂₄ H ₂₄ ClF ₂ N ₃ O ₃ S	507 (M ⁺), 284, 224		

^a) Recrystallization solvent: A, AcOEt; H, hexane; E, ether. ^b) Rotations were measured at 25 °C. ^c) Chemical shifts are given with proton numbers, absorption patterns and coupling constants in Hz in parenthesis. ^d) The ¹H-NMR spectra of **14C** and **15C** were taken using a 60 MHz spectrometer in CDCl₃. ^e) The ¹H-NMR spectrum of **15T** was taken using a 60 MHz spectrometer in CDCl₃ containing D₂O. ^f) The [α]_D value shows the optical rotation of the oxalic acid salt of **15Y**. The melting point of the oxalic acid salt was difficult to measure because of the hygroscopicity. ^g) The ¹H-NMR spectrum of **16V** was taken using a 400 MHz spectrometer in CDCl₃.

recrystallized twice from cold Et₂O-hexane to afford pure isomer **27** (220 mg, 24% from **26**) as colorless plates, mp 44—46 °C. ¹H-NMR (270 MHz, CDCl₃) δ: 1.2—1.5 (4H, m), 1.95—2.15 (2H, m), 2.15—2.35 (1H, m), 2.35—2.55 (1H, m), 3.73 (2H, s), 7.27 (5H, s), 9.61 (1H, s). IR (KBr) cm⁻¹: 1732, 1493, 1448, 1092. MS *m/z*: 268 (M⁺), 125, 110. Anal. Calcd for C₁₄H₁₇ClOS: C, 62.56; H, 6.38. Found: C, 62.44; H, 6.31.

trans-1-(4-Chlorobenzylthio)-4-[(1E,3E)-4-[4-(trifluoromethyl)phenyl]-1,3-butadienyl]cyclohexane (28) A suspension of sodium hydride (55% mineral oil dispersion, 50 mg, 1.14 mmol) in DMSO (7 ml) was

heated at 55 °C for 2.5 h to obtain an almost clear solution of dimethyl sodium. [(E)-(p-(Trifluoromethyl)cinnamyl)triphenylphosphonium chloride (607 mg, 1.26 mmol) was then added to the mixture at room temperature to obtain an orange solution. Then **27** (170 mg, 0.63 mmol) was added at room temperature. After the mixture was stirred at room temperature for 15 min, it was treated with H₂O. Then it was diluted with toluene and washed successively with H₂O and brine. The organic layer was dried over MgSO₄ and the solvent was removed *in vacuo* to afford an oily residue, which was chromatographed on silica gel (5 g). Elution with CH₂Cl₂-hexane (1 : 2, v/v) af-

forded a mixture of geometrical isomers of olefins (303 mg) as a yellow solid, which was recrystallized from hexane to afford a pure *E,E*-isomer **28** (86 mg, 31%) as pale yellow needles, mp 142–144 °C. ¹H-NMR (270 MHz, CDCl₃) δ: 1.1–1.3 (2H, m), 1.3–1.5 (2H, m), 1.7–2.0 (2H, m), 2.46 (1H, tt, *J*=12, 4 Hz), 3.74 (2H, s), 5.81 (1H, dd, *J*=15, 7 Hz), 6.20 (1H, dd, *J*=15, 10 Hz), 6.47 (1H, d, *J*=16 Hz), 6.81 (1H, dd, *J*=16, 10 Hz), 7.29 (4H, s), 7.46 (2H, d, *J*=8 Hz), 7.55 (2H, d, *J*=8 Hz). IR (KBr) cm⁻¹: 1612, 1490, 1326, 1127, 1068. MS *m/z*: 436 (M⁺), 311, 277, 235, 159, 125. Anal. Calcd for C₂₄H₂₄ClF₃S: C, 65.97; H, 5.54. Found: C, 65.68; H, 5.45.

trans-1-(4-Chlorobenzylsulfinyl)-4-[(1*E*,3*E*)-4-[4-(trifluoromethyl)phenyl]-1,3-butadienyl]cyclohexane (29) mCPBA (80% purity, 104 mg, 0.48 mmol) was added to a solution of **28** (211 mg, 0.48 mmol) in CH₂Cl₂ (20 ml) at 0 °C. After the mixture was stirred for 5 min, it was treated with an aqueous solution of Na₂SO₃ and the product was extracted with AcOEt. The organic layer was washed with an aqueous solution of NaHCO₃ and brine, successively. The extract was dried over MgSO₄, and the solvents were removed to afford a solid residue, which was recrystallized from AcOEt–hexane to afford **29** (168 mg, 77%) as a colorless, crystalline powder, mp 212–214 °C. ¹H-NMR (270 MHz, CDCl₃) δ: 1.1–1.3 (2H, m), 1.5–1.8 (2H, m), 1.9–2.3 (5H, m), 2.42 (1H, tt, *J*=12, 4 Hz), 3.87 (1H, d, *J*=13 Hz), 3.97 (1H, d, *J*=13 Hz), 5.80 (1H, dd, *J*=15, 7 Hz), 6.22 (1H, dd, *J*=15, 10 Hz), 6.48 (1H, d, *J*=16 Hz), 6.80 (1H, dd, *J*=16, 10 Hz), 7.25 (2H, d, *J*=8 Hz), 7.36 (2H, d, *J*=8 Hz), 7.45 (2H, d, *J*=8 Hz), 7.55 (2H, d, *J*=8 Hz). IR (KBr) cm⁻¹: 1612, 1492, 1325, 1168, 1128, 1069. MS *m/z*: 452 (M⁺), 327, 278, 277, 159, 125. Anal. Calcd for C₂₄H₂₄ClF₃OS: C, 63.64; H, 5.34. Found: C, 63.61; H, 5.38.

S-[trans-4-[(1*E*,3*E*)-4-[4-(Trifluoromethyl)phenyl]-1,3-butadienyl]cyclohexyl] Thioacetate (30) Trifluoroacetic anhydride (165 mg, 0.79 mmol) was added to a mixture of **29** (178 mg, 0.39 mmol), 2,6-lutidine (168 mg, 1.6 mmol), THF (8 ml) and CH₃CN (3 ml) at 0 °C. After the mixture was stirred at room temperature for 3 min, it was treated with an aqueous solution of NaHCO₃. The product was extracted with AcOEt. The extract was dried over MgSO₄ and solvents were removed *in vacuo* to leave an oily residue of crude thiol. This residue was treated with triethylamine (119 mg, 1.17 mmol) and acetyl chloride (62 mg, 0.79 mmol) in CH₂Cl₂ (10 ml) at 0 °C. After the mixture was stirred at room temperature for 1 h, it was diluted with AcOEt and washed with an aqueous solution of NaHCO₃ and brine, successively. The organic layer was dried over MgSO₄ and the solvents were removed *in vacuo* to leave an oily residue, which was purified by column chromatography (5 g). Elution with CH₂Cl₂–hexane (1 : 1, v/v) gave a crude product, which was purified further with a Lobar[®] column using AcOEt–hexane (1 : 19, v/v) as an eluent to afford **30** (98 mg, 70%) as a crystalline powder, mp 113–115 °C. ¹H-NMR (270 MHz, CDCl₃) δ: 1.2–1.5 (4H, m), 1.7–1.9 (2H, m), 2.0–2.2 (3H, m), 2.31 (3H, s), 3.37 (1H, tt, *J*=12, 4 Hz), 5.82 (1H, dd, *J*=15, 7 Hz), 6.20 (1H, dd, *J*=15, 10 Hz), 6.47 (1H, d, *J*=16, 7 Hz), 6.81 (1H, dd, *J*=16, 10 Hz), 7.45 (2H, d, *J*=8 Hz), 7.54 (2H, d, *J*=8 Hz). IR (KBr) cm⁻¹: 1688, 1326, 1117, 1068. HR-MS *m/z*: 354.1252 (Calcd for C₁₉H₂₁F₃OS: 354.1265). MS *m/z*: 354 (M⁺), 311, 277, 236, 159, 43.

(2*R*,3*R*)-2-(2,4-Difluorophenyl)-1-(1*H*-1,2,4-triazol-1-yl)-3-[[trans-4-[(1*E*,3*E*)-4-[4-(trifluoromethyl)phenyl]-1,3-butadienyl]cyclohexyl]thio]-2-butanol (31) A solution of sodium methoxide (0.4 M in MeOH, 0.2 ml, 0.08 mmol) was added to a mixture of **30** (96 mg, 0.27 mmol), **8** (70 mg, 0.28 mmol) and DMF (5 ml), and the mixture was heated at 55–60 °C for 2 h. After the mixture was cooled, it was diluted with toluene and washed with H₂O and brine, successively. The organic layer was dried over MgSO₄, and the solvents were removed *in vacuo* to afford an oily residue, which was chromatographed on silica gel (5 g). Elution with AcOEt–CH₂Cl₂ (1 : 5, v/v) afforded **31** (90 mg, 59%) as a crystalline powder, mp 74–76 °C. ¹H-NMR (270 MHz, CDCl₃) δ: 1.1–1.6 (4H, m), 1.17 (3H, d, *J*=7 Hz), 1.8–2.0 (2H, m), 2.0–2.2 (3H, m), 2.69 (1H, tt, *J*=12, 3 Hz), 3.35 (1H, q, *J*=7 Hz), 4.64 (1H, s), 4.83 (1H, d, *J*=15 Hz), 5.10 (1H, d, *J*=15 Hz), 5.83 (1H, dd, *J*=15, 7 Hz), 6.22 (1H, dd, *J*=15, 10 Hz), 6.48 (1H, d, *J*=15 Hz), 6.74 (2H, t-like, *J*=8 Hz), 6.81 (1H, dd, *J*=15, 10 Hz), 7.2–7.5 (1H, m), 7.45 (2H, d, *J*=8 Hz), 7.54 (2H, d, *J*=8 Hz), 7.76 (1H, s), 7.84 (1H, s). IR (CHCl₃) cm⁻¹: 1615, 1500, 1325, 1125, 1068. HR-MS *m/z*: 563.2036 (Calcd for C₂₉H₃₀F₅N₃OS: 563.2030). MS (EI) *m/z*: 563 (M⁺), 544, 340, 310, 277, 224 (100%). [α]_D²⁵ –82.8 (c=0.90, CHCl₃).

Acknowledgements We acknowledge the contribution of Mr. Makoto Mori of our laboratories in active discussions and in the preparation of various intermediates.

References and Notes

- Graybill J. R., *Clin. Infect. Dis.*, **22** (Suppl 2), S166–178 (1996); Georgopapadakou N. H., Walsh T. J., *Antimicrob. Agents Chemother.*, **40**, 279–291 (1996); Turner W. W., Rodriguez M. J., *Curr. Pharm. Des.*, **2**, 209–224 (1996).
- Sheehan D. J., Hitchcock C. A., Sibley C. M., *Clin. Microbiol. Rev.*, **12**, 40–79 (1999).
- Vanden Bossche H., "Current Topics in Medical Mycology," Vol. 1, ed. by McGuinnis M. R., Springer-Verlag, Berlin, 1985, pp. 313–351; Aoyama Y., Yoshida Y., Sato R., *J. Biol. Chem.*, **259**, 1661–1666 (1984); Trzaskos J. M., Bowen W. D., Shafiee A., Fischer R. T., Gaylor J. L., *ibid.*, **259**, 13402–13412 (1984).
- a) Richardson K., Brammer K. W., Marriott M. S., Troke P. F., *Antimicrob. Agents Chemother.*, **27**, 832–835 (1985); b) Richardson K., Cooper K., Marriott M. S., Tarbit M. H., Troke P. F., Whittle P. J., *Ann. N. Y. Acad. Sci.*, **544**, 6–11 (1988).
- Van Cutsem J., Van Gerven F., Janssen P. A. J., "Recent Trends in the Discovery, Development, and Evaluation of Antifungal Agents," ed. by Fromtling R. A., J. R. Prous Publisher, Barcelona, 1987, pp. 177–192.
- Dickinson R. P., Bell A. S., Hitchcock C. A., Nayayanaswami S., Ray S. J., Richardson K., Troke P. F., *Bioorg. Med. Chem. Lett.*, **6**, 2031–2036 (1996).
- Fromtling R. A., *Drugs Future*, **21**, 160–166 (1996); Saksena A. K., Girijavallabhan V. M., Wang H., Liu Y.-T., Pike R. E., Ganguly A. K., *Tetrahedron Lett.*, **37**, 5657–5660 (1996).
- Hata K., Kimura J., Miki H., Toyosawa T., Moriyama M., Katsu K., *Antimicrob. Agents Chemother.*, **40**, 2237–2242 (1996); *idem*, *ibid.*, **40**, 2243–2247 (1996); Kaku Y., Tsuruoka A., Kakinuma H., Tsukada I., Yanagisawa M., Naito T., *Chem. Pharm. Bull.*, **46**, 1125–1129 (1998).
- A part of the present study was presented by the authors at the 19th Symposium on Medicinal Chemistry/the 8th Annual Meeting of Division of Medicinal Chemistry, the Pharmaceutical Society of Japan, Nov. 11–13, 1999, Tokyo. For previous studies see: a) Konosu T., Tajima Y., Miyaoka T., Oida S., *Tetrahedron Lett.*, **32**, 7545–7548 (1991); b) Konosu T., Miyaoka T., Tajima Y., Oida S., *Chem. Pharm. Bull.*, **40**, 562–564 (1992); c) Tanaka T., Takeda N., Konosu T., Yasuda H., Oida S., *ibid.*, **40**, 661–665 (1992); d) Konosu T., Tajima Y., Takeda N., Miyaoka T., Kasahara M., Yasuda H., Oida S., *ibid.*, **39**, 2581–2589 (1991); e) Konosu T., Miyaoka T., Tajima Y., Oida S., *ibid.*, **39**, 2241–2246 (1991); f) Konosu T., Tajima Y., Takeda N., Miyaoka T., Kasahara M., Yasuda H., Oida S., *ibid.*, **38**, 2476–2486 (1990).
- a) Saji I., Tamoto K., Tanaka Y., Miyauchi H., Fujimoto K., Ohashi N., *Bull. Chem. Soc. Jpn.*, **67**, 1427–1433 (1994); b) Tasaka A., Tanuma N., Matsushita Y., Teranishi K., Hayashi R., Okonogi K., Itoh K., *Chem. Pharm. Bull.*, **41**, 1035–1042 (1993); c) Tasaka A., Tsuchimori N., Kitazaki T., Hiroe K., Hayashi R., Okonogi K., Itoh K., *ibid.*, **43**, 441–449 (1995).
- Van Lohuizen O. E., Verkade P. E., *Recl. Trav. Chim. Pays Bas*, **78**, 460–472 (1959).
- Andrews B. M., Gray G. W., Bradshaw M. J., *Mol. Cryst. Liq. Cryst.*, **123**, 257–269 (1985); Trippett S., Walker D. M., *J. Chem. Soc.*, **1961**, 1266–1272.
- Berenguer M. J., Castelles J., Fernández J., Galard R. M., *Tetrahedron Lett.*, **1971**, 493–494; Berenguer M. J., Castelles J., Galard R. M., Moreno-Mañas M., *ibid.*, **1971**, 495–496.
- Boyle F. T., Ryley J. F., Wilson R. G., "Recent Trends in the Discovery, Development, and Evaluation of Antifungal Agents," ed. by Fromtling R. A., J. R. Prous Publisher, Barcelona, 1987, pp. S1: 31–41.
- Ulman A., Urankar E., *J. Org. Chem.*, **54**, 4691–4692 (1989).
- Williams J. W., *Org. Syn. Coll. Vol.*, **3**, pp. 626–630 (1955).
- Cheng C.-Y., Wu S.-C., Hsin L.-W., Tam S. W., *J. Med. Chem.*, **35**, 2243–2247 (1992).

Intermediate State during the Crystal Transition in Aspartame, Studied with Thermal Analysis, Solid-State NMR, and Molecular Dynamics Simulation

Kazuyoshi EBISAWA,^a Nobuya NAGASHIMA,^a Ken-ichi FUKUHARA,^a Satoshi KUMON,^a Shin-ichi KISHIMOTO,^a Ei-ichiro SUZUKI,^{*,a} Shigetaka YONEDA,^b and Hideaki UMEYAMA^c

Central Research Laboratories, Ajinomoto Co., Inc.,^a 1–1 Suzuki-cho, Kawasaki-ku, Kawasaki, Kanagawa 210–8681, Japan, School of Science, Kitasato University,^b 1–15–1 Kitasato, Sagami-hara, Kanagawa 228–8555, Japan, and School of Pharmaceutical Sciences, Kitasato University,^c 5–9–1 Shirokane, Minato-ku, Tokyo 108–8641, Japan.

Received December 21, 1999; accepted February 1, 2000

Aspartame (L- α -aspartyl-L-phenylalanine methyl ester) is a dipeptide sweetener about 200 times as sweet as sugar. It exists in crystal forms such as IA, IB, IIA, and IIB, which differ in crystal structure and in the degree of hydration. Among these, IIA is the most stable crystal form, and its crystal structure has been well determined (Hatada *et al.*, *J. Am. Chem. Soc.*, 107, 4279–4282 (1985)). To elucidate the structural factors of thermal stability in the IIA form of aspartame and to examine the physical process in the crystal transformation between the IIA and IIB forms, we performed a thermal analysis and solid-state NMR measurements. We found that a *quasi-stable* intermediate state exists in the transformation, and it has the same crystal lattice as the usual IIA form, despite the dehydration from 1/2 mol to 1/3 mol per 1 mol of aspartame. The results of the energy component analysis and the molecular dynamics simulation suggest that the entropic effect promotes the generation of the intermediate state, which is presumably caused by the evaporation of the water of crystallization and the increase of molecular motion in aspartame. Thus, the thermal stability of the IIA form is attributable to a structural property, *i.e.*, the crystal lattice itself is retained during the above dehydration. Moreover, the molecular dynamics simulations suggest that the aspartame molecules have two kinds of conformational flexibility in the intermediate state.

Key words aspartame; crystal transformation; thermal analysis; solid-state NMR; molecular dynamics simulation

Aspartame (L- α -aspartyl-L-phenylalanine methyl ester) is a low-calorie sweetener possessing about 200 times the sweetness of sugar, and has a sweetening quality similar to that of sugar.¹⁾ It can be digested, absorbed and metabolized in the human body in the same way as the natural peptides.²⁾ Aspartame is used in various foods and beverages and is also reported to be effective as part of a diet for diabetics using calorie control.^{3,4)} Thus, for industrial and pharmaceutical purposes, aspartame has been extensively studied; *e.g.*, the structure–taste relationships,^{5–7)} the model of the receptor site,^{8–10)} its conformation in aqueous solution,^{11,12)} and its interaction with cyclodextrin in the solid state.¹³⁾

The X-ray crystal structure of aspartame was reported by Hatada *et al.*¹⁴⁾ in 1985, and an interesting arrangement of molecules was revealed; the space group is $P4_1$, so there are four aspartame molecules with the same conformation in one unit cell, with a fourfold screw along the *c*-axis, while the water molecules are located almost at the center of the hydrophilic channel that consists of the NH_3^+ and COO^- groups of aspartame and form an infinite column along the *c*-axis. Since the four symmetry-related positions of the water molecules are too close to exist simultaneously in each position, they occupy the two sites side by side out of the four crystallographic sites. Thus, the occupancy rate of water molecule at each site is 50%.

We call the crystal form of the above structure the IIA form of aspartame, according to the classification by Sugiyama *et al.*; they first recognized the difference among the crystal forms of aspartame and defined the crystal forms as IA, IB, IIA, and IIB based on the results of powder X-ray diffraction (XRD) studies.^{15,16)} IA is the high-hydrated crystal form and converts to IB by drying. IIA is less hydrated

than are IA and IB. IIB is the anhydrous form which is obtained at high temperatures; its crystal structure has not been determined. The degree of hydration in the IIA form is 0.5 mol per 1 mol of aspartame,¹⁴⁾ and the crystal transformation proceeds along with the dehydration.^{15,16)}

The thermal stability of each crystal form has been well studied in our laboratories, and is one of the properties important to the manufacturing process. We found that the IIA form is very stable at a wide temperature range, while the IIB form easily converts to the IIA form by water adsorption, *e.g.*, at 34 °C in 78% relative humidity, in which the equilibrium moisture content of the sample is 3% (w/w)^{15,16)} and corresponds to the degree of hydration in the IIA form. However, the factors of thermal stability in the IIA form have not been identified in terms of structure, nor have the details of the structural changes produced by the crystal transformation of the IIA form.

Therefore, to elucidate the thermal stability factors and the physical process of the crystal transformation in the IIA form, thermogravimetry and differential thermal analyses (TG/DTA), powder XRD and solid-state NMR measurements were carried out in the present study. The details of the crystal transition from the IIA form to an intermediate state will be discussed together with the structural feature of the intermediate state and its relationship with the thermal stability of the IIA form.

Moreover, energy calculations and molecular dynamics (MD) simulations for the IIA form and the intermediate state were performed to elucidate the stabilization mechanism and the structural properties of the intermediate state.

* To whom correspondence should be addressed. e-mail: eiichiro_suzuki@ajinomoto.com

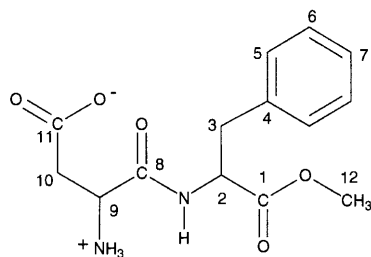


Fig. 1. The Molecular Structure of Aspartame

The carbon numbering is based on the numbering system of the IUPAC. ^{13}C -NMR signal assignments in the IIA form were shown in Table 1 and Fig. 7a.

Experimental

Materials and Crystallization The aspartame sample was the product of Ajinomoto Co., Inc. The IIA form sample was obtained by heating the IB form at 80 °C in 70% relative humidity. The IB form was obtained by drying the IA form *in vacuo*. The IA form was crystallized from the aqueous solution without stirring. The molecular structure and atom-numbering scheme are shown in Fig. 1.

Powder XRD Measurement The powder XRD patterns were obtained using an X-ray diffractometer (PW1700, Phillips) with $\text{CuK}\alpha$ radiation (40 kV, 30 mA). The sample was maintained in a constant temperature environment with a variable temperature unit, and scanned in the 2θ range from 3° to 30° with a scanning speed of 0.05°/s. The isothermal powder XRD was performed at each temperature from 30 °C to 70 °C at 5 °C increments. The crystal form identification was performed before and after the NMR measurement. Since no diffraction peak of CaCl_2 , which partially filled the NMR rotor (*vide infra*), was observed at a lower angle ($2\theta < 14$ degree), it did not disturb the crystal form identification.

TG/DTA Measurement The TG/DTA curves were obtained using a TG/DTA220 system (SEIKO Electronics). The measurement was performed on the IIA form sample (ca. 5 mg) in an open aluminum pan from room temperature (r.t.) to 90 °C at a heating rate of 0.5 °C/min. The initial relative humidity was ca. 50% at r.t.

^{13}C -Cross-Polarization Magic-Angle Spinning (CPMAS)-NMR Spectroscopy The 100.6 MHz high-resolution solid-state ^{13}C -NMR spectra of the IIA form were recorded on a DSX-400WB NMR spectrometer (Bruker) by means of CPMAS at eleven temperatures from r.t. (24 °C) to 80 °C. The IIA form sample (ca. 150 mg) was contained in a cylindrical rotor and spun at 6 kHz, sandwiched by anhydrous CaCl_2 upper and lower layers. This device was not indispensable for the dehydration at a low temperature range (r.t.–40 °C), but it was used to ensure the smooth dehydration at a higher temperature range in a closed system. The free induction decay was recorded with 4 K data points and a spectral width of 35211 Hz. The data were zero-filled to 8 K prior to Fourier transformation. The durations of the 90° pulse, contact time, and repetition time were 4.2 μs , 1.0 ms and 5 s, respectively. The ^{13}C chemical shifts were calibrated by using the carboxyl peak of glycine (176.03 ppm) and converted to the value from tetramethylsilane. The actual temperature within the spinning sample was calibrated using samarium acetate tetrahydrate.¹⁷⁾ Since it was found to be almost the same as the indicated temperature on the spectrometer, e.g., the actual temperature was 39.3 °C when the indication was 40 °C, the indicated temperatures are used in the Results and Discussion sections.

Carbon $T_{1\rho}$ Measurement To examine the conformational flexibility in the Phe moiety in aspartame, the measurements of ^{13}C spin-lattice relaxation time in the rotating frame ($T_{1\rho}$) were carried out at r.t. and 45 °C using a standard cross-polarization $T_{1\rho}$ pulse sequence. The ^{13}C spin locking periods of 2, 10, 30, 60, 80, 100, 120 ms were used in each measurement.

Deuterium NMR Measurement The 46.07 MHz static deuterium NMR spectra of the IIA form were measured on a DSX-300 NMR spectrometer (Bruker) using a standard quadrupolar echo pulse sequence at r.t. (24 °C) and 45 °C. To prepare the D_2O type IIA form, the sample (H_2O type) was placed in cold D_2O (4 °C) for a few minutes, and then filtered, and transformed to the IIA form by heating. (Since the protons in NH_3^+ group form the hydrogen bonds with COO^- groups in the crystal, the deuteration rate in NH_3^+ group is considered to be lower than that in the water molecules; the deuteration rate in water molecules itself was found to be rather low judging from the signal sensitivity in D-NMR.) The durations of the 90° pulse, and the τ value of the refocusing period were 3.0 and 30 μs , respectively. Recycle delays of 1.0 and 3.0 s were used at each temperature for checking the ef-

fect of T_1 relaxation on the signal intensity. Since the integrated areas of D-NMR signal in the different recycle delays were constant at the same temperature, the area ratio at r.t. (24 °C) and 45 °C was determined using the spectra in the recycle delay of 1.0 s.

Computer and Programs A personal computer IRIS Indigo2 (Silicon Graphics Inc.) was used for the graphical display, the energy minimization and MD simulation of the crystal structure. The energy component analysis and the conformational flexibility analysis for the IIA form and the intermediate state were performed with the Cerius2 program (Molecular Simulation Inc.), and the calculation of the time-averaged structure in the IIA form was performed with the APRICOT program.^{18,19)} The lattice parameters were fixed at the experimental values in all energy minimizations and MD simulations.

X-Ray Structure of the IIA Form and the Model Structures of the Initial IIA Form and the Intermediate State The X-ray crystal structure of the IIA form¹⁴⁾ was taken from the Cambridge data base (reference code DAWGOX). Since the coordinates of hydrogen atoms in the water molecule were not contained in DAWGOX, their coordinates were generated with the standard orientation and all hydrogen atoms were structurally optimized using the Cerius2 program so as to exclude the van der Waals short contact. The coordinates for one unit cell were made by the $P4_1$ symmetry operation for the X-ray structure data, and then the two sets of water coordinates were removed so that the occupied site and the unoccupied site were located alternately, because the occupancy rate of water molecules is 50% (as described above). When two water molecules were located side by side, the van der Waals contact between them was extensive, so such an initial position was found to be unstable and not actual, as Hatada *et al.* pointed out.¹⁴⁾ Since the degree of hydration is 1/2 mol per 1 mol of aspartame in the IIA form and 1/3 mol in the intermediate state (*vide infra*), hereafter we designate the former as IIA(1/2 H_2O) and the latter as IIA(1/3 H_2O).

In the calculation with the Cerius2 program, the model structure for IIA(1/2 H_2O) was made by stacking up three unit cells in the direction of the *c*-axis as shown in Fig. 2. The model structure for IIA(1/3 H_2O) was generated by removing each water molecule (marked by arrow in Fig. 2b) from the first and second layers in the above IIA(1/2 H_2O) model.

In generating the intermediate model, the representative permutations of water locations along the *c*-axis are $\langle \text{v o v o o o} \rangle$, $\langle \text{v o o v o o} \rangle$ and $\langle \text{o o v v o o} \rangle$ (v; vacant, o; occupied) in three unit cells, because $\langle \text{v o v o o o} \rangle$ is the same state as $\langle \text{o v o v o o} \rangle$ or $\langle \text{o o v o v o} \rangle$ under the periodic boundary conditions. The energy minimization results showed that the IIA(1/3 H_2O) model in the water location $\langle \text{v o v o o o} \rangle$ were most stable among the three locations; ΔE was ca. 3.0 and 3.5 kJ per three units for $\langle \text{v o o v o o} \rangle$ and $\langle \text{o o v v o o} \rangle$, respectively. Thus, we selected IIA(1/3 H_2O) in the water location $\langle \text{v o v o o o} \rangle$ as a starting model of the intermediate state. The trajectory in MD simulation was thought not to be affected by the selection of the initial permutation of the water location essentially, because 1) ΔE between the states was not so large, and 2) we used the doubling temperature in starting the MD simulation. Additionally, the animation of the trajectory showed that the location of water along the *c*-axis was not always fixed to a constant permutation after the equilibrium of temperature by appearances. Since a calculational unit includes twelve aspartame molecules, one course of MD simulation was thought to be enough for the structural sampling in the aspartame dynamics. In the MD simulation with the APRICOT program, the model structure for IIA(1/2 H_2O) was made by stacking up four unit cells in the direction of the *c*-axis for the detailed investigation of the hydrogen bond length. The whole procedure of the modeling and simulation was showed in Fig. 3.

Energy Component Analysis The energy component analysis for IIA(1/2 H_2O) and IIA(1/3 H_2O) was performed for the comparison of the enthalpic energy between these two states. A system of three unit cells ($17.685 \times 17.685 \times 14.757 \text{ \AA}^3$) in periodic boundary conditions was used for each model. The Ewald method²⁰⁾ was used for the calculations of the electrostatic and van der Waals interactions, and the cutoff distance was set at 10.2 Å for the former and 17.1 Å for the latter.

The electrostatic potential (ESP) charges used for the aspartame molecule were calculated by the MNDO method without the structural optimization, after the structural optimization by the PM3 method using MOPAC 6.01. In case some atoms are chemically equivalent such as protons in NH_3^+ , the ESP charges were averaged. The total of all charges was adjusted to zero.

The energy of the initial model structure was minimized by the conjugate gradient method using the Dreiding force field²¹⁾ and 1.0 of dielectric constant, before the energy component analysis was carried out. The minimization continued until the root mean square gradient became $0.3 \text{ kcal mol}^{-1} \text{ \AA}^{-1}$.

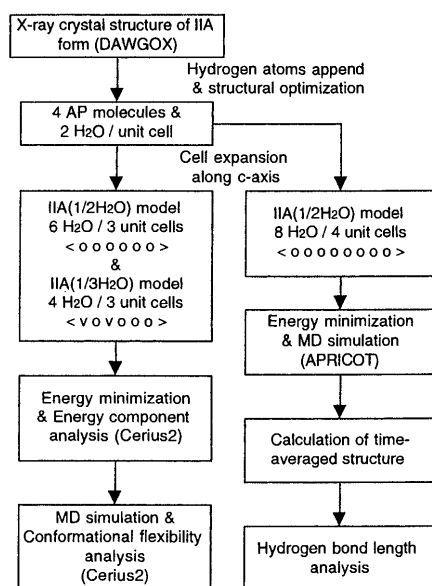


Fig. 3. The Whole Procedure of the Model Building and the MD Simulation

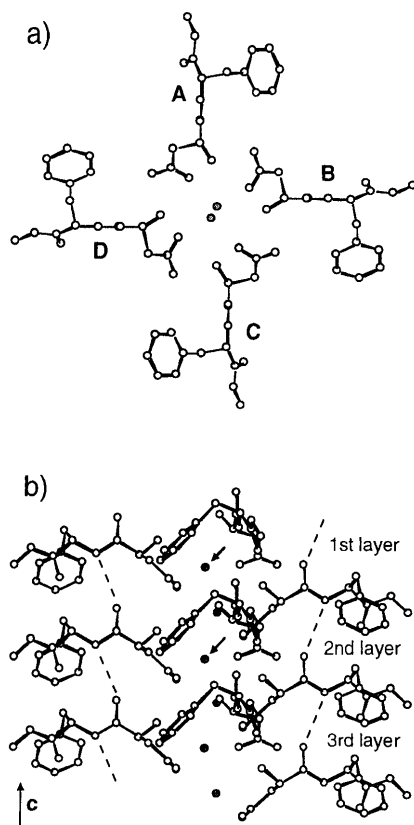


Fig. 2. The Calculational Unit with Cerius2 Program for the Model Structures of IIA(1/2H₂O) and IIA(1/3H₂O)

a) The projection along the *c*-axis, b) The side view except for the position A molecules. Two water molecules (marked by closed circles) are located in the hydrophilic channel of one unit cell, since its occupancy is 50%.¹⁴⁾ The hydrogen bonds between the peptide bond sites are shown as broken lines. The model structure for IIA(1/2 H₂O) was made by stacking up three unit cells, while that for IIA(1/3 H₂O) was generated by removing each water molecule marked by arrow. *a*=*b*=17.685 Å, and *c*=14.757 Å, which show the calculational unit size.

Conformational Flexibility Analysis After the energy minimization, the sequential MD simulation of 50 ps was performed in periodic boundary conditions using the Nose–Hoover method²²⁾ with the Cerius2 program. The final simulation temperature was set at 300 K for IIA(1/2H₂O) and at 320 K for IIA(1/3H₂O). A timestep of 1 fs was used, and the coordinates were

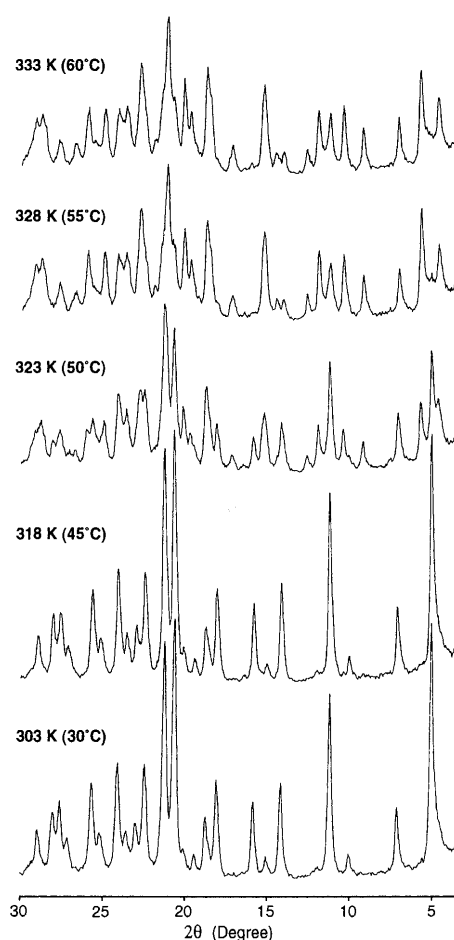


Fig. 4. Temperature Dependence of Powder XRD Pattern from 30 °C to 60 °C

The initial pattern is that of the IIA form, and the pattern at 50 °C shows that of a mixture of the IIA and IIB forms. The powder patterns at 35 °C, 40 °C, 65 °C, and 70 °C were omitted.

stored with an interval of 0.5 ps. The time-averaged dihedral angle, χ_1 (C γ –C β –C α –N), in the Phe moiety was calculated using the sampling structures in 15.0–50.0 ps.

Molecular Dynamics Simulation of IIA(1/2H₂O) For a detailed examination of the time-averaged structure in IIA(1/2H₂O), the energy minimization by the conjugate gradient method and the sequential MD simulation of 50 ps were performed with the APRICOT program. A system of four unit cells (17.685×17.685×19.676 Å³) in periodic boundary conditions was used. The AMBER version 3.0 force field²³⁾ (all atom type) for the aspartame molecule and the TIP3P potential for water²⁴⁾ were used. The cut-off distance for nonbonded interactions was set at 8.8 Å in the minimization, and all non-bonded atom pairs in the periodic boundary were calculated in the MD simulation. The dielectric constant, the atomic charges and convergence condition were the same as in the energy component analysis. A timestep of 2 fs was used in the MD simulation using the SHAKE method.²⁵⁾ The temperature of the initial random velocity was 150 K. Velocity scaling²⁶⁾ was used to increase the temperature to 300 K with a relaxation time of 0.5 ps. The coordinates were stored with an interval of 0.5 ps. The time-averaged length of the intermolecular hydrogen bond between amide nitrogen and carbonyl oxygen atoms in the peptide bond was calculated using the sampling structures in 0.5–50.0 ps (see Fig. 2).

Results

Thermal Analysis by Powder XRD and TG/DTA The powder XRD patterns remained identical to that of the IIA form during the temperature change from 30 °C to 45 °C, and the crystal transformation to the IIB form started at 50 °C and was almost complete at 60 °C, as shown in Fig. 4.

The results of the TG/DTA are shown in Fig. 5. The de-

gree of hydration, which was 1/2 mol per 1 mol of aspartame at r.t., was gradually reduced by heating and showed a plateau of 1/3 mol per 1 mol of aspartame at 40 °C–50 °C, and the transformation to the IIB form started at around 55 °C.

The same lot sample was measured after one week to check the reproducibility of the results. The TG/DTA curve obtained was almost the same. Additionally, the stability of the plateau with 1/3 mol of H₂O was checked by holding the temperature at 46 °C for about three hours. Figure 6 shows the weight change of this intermediate state. It was observed that this state was very stable at 46 °C and returns quickly to the initial state with 1/2 mol of H₂O after switching off the heating system.

The crystal form of the intermediate state is the IIA form, because the powder XRD pattern at 45 °C shows the exact IIA form. This is the reason that we designated the intermediate state as “IIA(1/3 H₂O)” in the experimental section.

Solid-State ¹³C-CPMAS-NMR Spectroscopy a) Signal Assignments in the IIA Form: The signal assignments in the

IIA form were carried out based mainly on the comparison with the complete assignments in a solution state (Table 1, Fig. 7a). Especially for the discrimination between the amide carbonyl and the methyl ester carbonyl carbons, the assignment was based on the deuterium isotope effect (–COND– / –CONH–) observed in the recrystallized sample from D₂O solution.

b) ¹³C-CPMAS-NMR Spectra in the Crystal Transformation: Figure 7 illustrates the spectral changes of the IIA form in the heating process from r.t. to 40 °C, and Fig. 8 shows the enlarged lower magnetic field regions (120–180 ppm) of the same spectra. The powder XRD pattern of the sample showed the characteristic features of the IIA form when measured immediately after the solid-state NMR measurement at 40 °C, and the NMR spectrum of the same refilled sample showed the specific pattern to the dehydration state again even at room temperature, as shown in Fig. 7e; it corresponds to the state between those shown in Figs. 7b and 7c. Therefore, these results indicate that the crystal form at 40 °C is

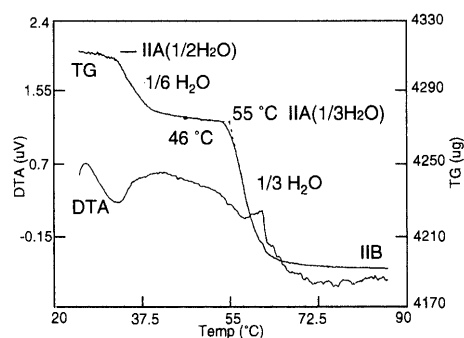


Fig. 5. The TG/DTA Curve of the Aspartame Crystal from r.t. to 90 °C. The heating rate was 0.5 °C/min.

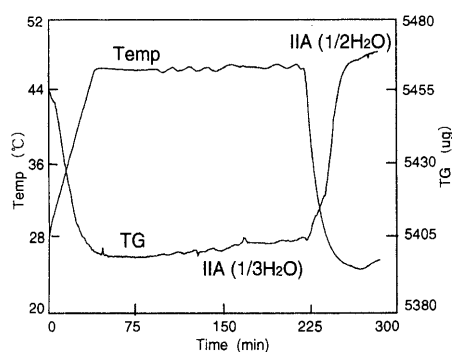


Fig. 6. The Stability Check of the Intermediate State by Thermogravimetry.

The heating rate was 0.5 °C/min to 46 °C from r.t., and the temperature was held at 46 °C for about 3 h.

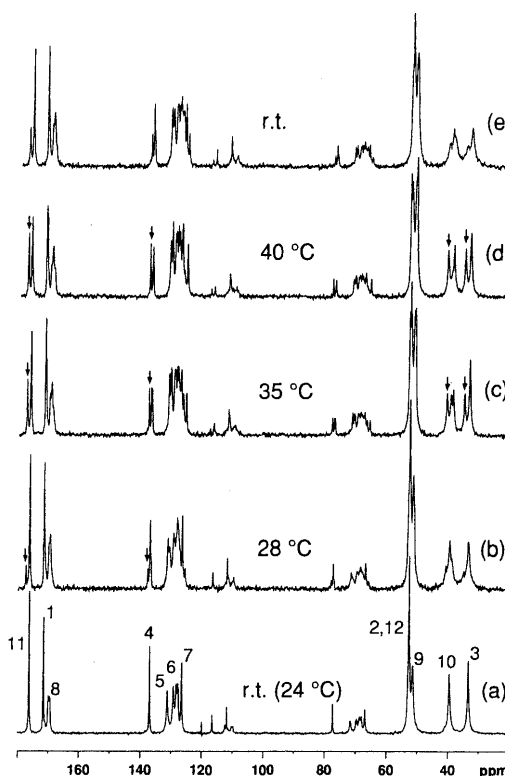


Fig. 7. ¹³C-CPMAS-NMR Spectra of the IIA Form at r.t. (a), 28 °C (b), 35 °C (c), 40 °C (d), and r.t. (e) (Refilled Sample).

The number at each signal in (a) corresponds to the carbon numbering in Fig. 1. The new signals due to the transition were marked by arrow. The chemical shift difference between the new and original signals was approximately 1.1, 1.0, and 1.8–2.0 ppm in the carboxyl carbon of the Asp moiety, in the γ-carbon of the Phe moiety and in each methylene carbon, respectively.

Table 1. Signal Assignments^{a)} of Aspartame in ¹³C-CPMAS-NMR and Solution NMR

	Carbon No.											
	1	2	3	4	5	6	7	8	9	10	11	12
IIA	171.5	52.8	33.3	137.0	131.3	128.3	126.6	170.0	51.5	39.6	176.2	52.8
					129.3	127.7		169.5				
Solution	174.0	55.4	37.3	137.3	130.1	129.8	128.2	170.8	51.5	38.2	177.0	53.9

a) Unit of ¹³C chemical shift in ppm.

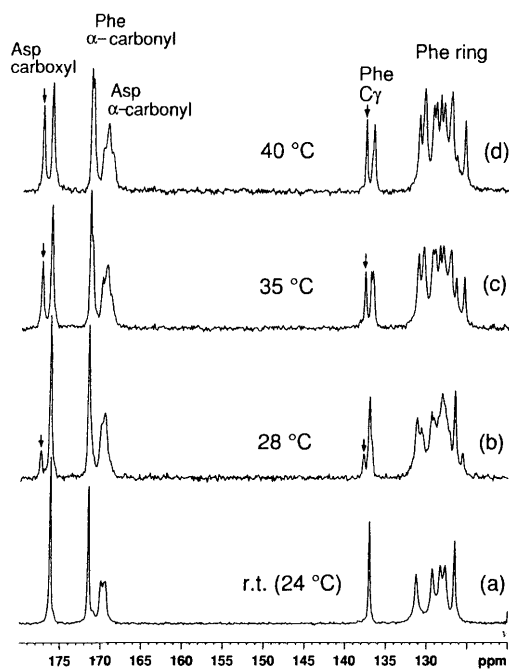


Fig. 8. The Enlarged Lower Magnetic Field Regions in Fig. 7a—d. The new signals due to the transition were marked by arrow.

still the IIA form, and that at the same time the dehydration is induced at 40 °C to a restricted extent from 1/2 H₂O toward 1/3 H₂O, which was evaluated from the TG results; *i.e.*, the IIA form has a zeolitic property in the early stage of crystal transformation. The spectrum in Fig. 7e is thought to show a slightly humidified state produced by the cooling down to r.t. As shown in Figs. 7 and 8, it was found that a new signal (marked by arrow) gradually appeared in the field nearby and lower than each original signal as the temperature rose in the carboxyl carbon of the Asp moiety, and in the γ -carbon of the Phe moiety and in each methylene carbon. The signal intensity ratio of the new and original signals eventually reached 1 : 1 at 45 °C, as shown in Fig. 9a.

Figure 9 illustrates the spectral changes from 45 °C to 80 °C. The signal pattern turned out to be almost invariable during the 40 °C—50 °C period, and this is well in agreement with the finding by TG measurement that the intermediate state is comparatively stable at this temperature range.

c) Carbon $T_{1\rho}$ Measurement: The ^{13}C spin-lattice relaxation time in the rotating frame ($T_{1\rho}$) was measured for the conformational flexibility analysis in the Phe moiety in aspartame. As the results, $T_{1\rho}$ in the γ -carbon of the Phe moiety was 208 ms at r.t., and it decreased to 135 and 172 ms at 45 °C, in a new signal (marked by arrow in Fig. 7) and in an original position signal, respectively.

Deuterium NMR Measurement Figure 10 shows the static D-NMR spectra of the D₂O type IIA form at r.t. and 45 °C. It was found that the integrated area ratio at r.t. and 45 °C is 0.5 : 0.33, and this is well in agreement with the amount ratio of water of crystallization in IIA(1/2 H₂O) and IIA(1/3 H₂O). The splitting width at the peak top was *ca.* 7.0 kHz at r.t., and it was *ca.* 15.6 kHz at 45 °C, respectively. The result of the line shape measurements indicates that the molecular motion of some water molecules in IIA(1/3 H₂O) reduced compared with the case in IIA (1/2 H₂O). In other words, the result suggests that some water molecules, which

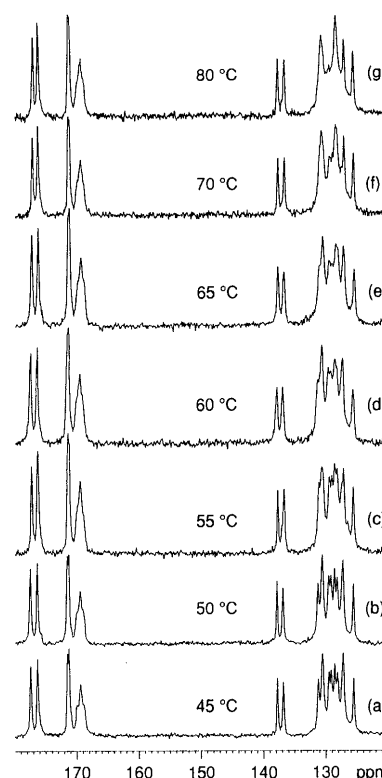


Fig. 9. ^{13}C -CPMAS-NMR Spectra at 45 °C (a), 50 °C (b), 55 °C (c), 60 °C (d), 65 °C (e), 70 °C (f), and 80 °C (g). (120—180 ppm)

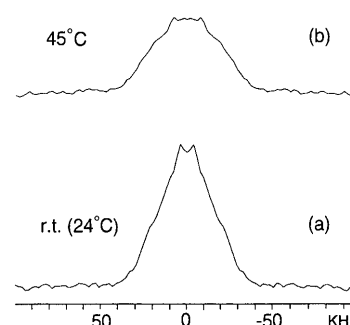


Fig. 10. D-NMR Spectra of the D₂O Type IIA Form at r.t. (a) and 45 °C (b)

remained in IIA(1/3 H₂O) after the dehydration, moved to the more stable position in the hydrophilic channel and reduced their mobility and partly helped the crystal lattice retention in IIA(1/3 H₂O).

Energy Calculations of IIA(1/2 H₂O) and IIA(1/3 H₂O)

Table 2 shows the results of the energy component analysis in the model structures of IIA(1/2 H₂O) and IIA(1/3 H₂O). We found that IIA(1/2 H₂O) is more stable than IIA(1/3 H₂O) regarding the total potential energy ($\Delta E = \text{ca. } 138 \text{ kJ}$ per three unit cells). In the detailed comparison, IIA(1/2 H₂O) turned out to be more stable (*ca.* 294 kJ) regarding the electrostatic term including H-bonds and to have a more unstable (*ca.* 140 kJ) van der Waals term than IIA(1/3 H₂O). The two states were not so different regarding the energies of bonds, angles and torsions.

MD Simulations a) Averaged Location of Water Molecules in IIA(1/2 H₂O): We found that the time-averaged location of the water molecules has 2₁ symmetry and that the in-

Table 2. Decomposition of Potential Energy^{a)} in IIA(1/2H₂O) and IIA(1/3 H₂O)

	IIA(1/2 H ₂ O)	IIA(1/3 H ₂ O)	$\Delta E^{b)}$
Total potential energy	-4270.5	-4132.3	138.2
Internal interaction			
Bonds	204.1	218.3	14.2
Angles	504.0	468.2	-35.8
Torsions	205.9	209.1	3.2
Inversions	1.1	3.9	2.8
Total	915.1	899.5	-15.6
Nonbonded interaction			
van der Waals	820.9	681.2	-139.7
Electrostatic	-5324.8	-5149.9	174.9
H-bonds	-681.7	-563.1	118.6
Total	-5185.6	-5031.8	153.8

a) Units in kJ per three unit cells. b) $\Delta E = E_{\text{IIA}(1/3\text{H}_2\text{O})} - E_{\text{IIA}(1/2\text{H}_2\text{O})}$.

Table 3. Intermolecular Hydrogen Bond Length^{a)} in IIA(1/2 H₂O)

	Position ^{b)}			
	A	B	C	D
1st layer	2.95 (0.10)	3.07 (0.17)	2.97 (0.11)	3.06 (0.16)
2nd layer	2.95 (0.12)	3.04 (0.13)	2.95 (0.13)	3.07 (0.16)
3rd layer	2.99 (0.12)	3.06 (0.15)	2.94 (0.11)	3.07 (0.17)

a) Time-averaged values for the trajectory of 50 ps MD simulation. Units in Å. The figures in parentheses denote the standard deviations. b) Position A and C sites are face-to-face about the location of the aspartame molecules around the *c*-axis, whereas the position A and B sites are side-by-side. The four positions and three layers are shown in Fig. 2.

interval of each water molecule along the *c*-axis is about 2.46 Å, which is half of the *c*-axis length (4.92 Å). The free movement of water molecule from the first crystallographic site to the second was not observed during 50 ps.

b) Averaged Structure of Aspartame Molecules: As shown in Fig. 2, the intermolecular hydrogen bonds are formed in IIA(1/2H₂O) between the peptide bond sites such as NH \cdots O=C in the direction of the *c*-axis. Table 3 shows the time-averaged length of the hydrogen bond calculated based on the MD simulation in 50 ps.

We found that there are two types of length in the time average of this hydrogen bond; they locate alternately around the hydrophilic channel, and the difference between them is about 0.1 Å, whereas the time-averaged conformation of the aspartame molecule is almost identical. It is reasonable that the fluctuation of the hydrogen bond length was smaller in positions A and C, where the hydrogen bond length is shorter.

c) Conformational Flexibility of Aspartame Molecule: Table 4 shows the comparison of the conformational flexibility in the aspartame molecule between IIA(1/2 H₂O) and IIA(1/3 H₂O), using the time-averaged values and the variances of the χ_1 dihedral angle in the Phe moiety. The mean value of the time-averaged χ_1 angles was 63.4° and 63.5° in IIA(1/2 H₂O) and IIA(1/3 H₂O), respectively, and the time-averaged conformation turned out to be about the same between the two states. However, the mean value of the variances was 33.2 in IIA(1/2 H₂O), while it was grouped into 33.4 or 52.5 in IIA(1/3 H₂O) assuming that the ratio of rigid molecules and flexible molecules was almost 1 : 1. Thus, it was found that there were at least two kinds of conforma-

Table 4. Conformational Flexibility in IIA(1/2 H₂O) and IIA(1/3 H₂O)

	Position ^{a)}							
	A	B	C	D	A	B	C	D
	IIA(1/2 H ₂ O)				IIA(1/3 H ₂ O)			
a) Time-averaged values ^{b)} of χ_1 angle in Phe moiety for the trajectory of 15–50 ps MD simulation								
1st layer	64.7	62.7	64.4	63.1	62.7	63.8	62.9	62.5
2nd layer	61.9	61.5	64.2	63.9	62.8	64.5	62.9	61.3
3rd layer	63.9	63.3	63.8	63.1	64.0	68.7	62.2	63.9
Mean	63.4 ^{c)}				63.5 ^{c)}			
b) Variances ^{d)} of χ_1 angle in Phe moiety								
1st layer	36.7	31.6	32.4	40.9	42.2	<u>22.8</u>	<u>28.7</u>	43.8
2nd layer	33.3	30.7	31.9	32.7	49.2	59.4	<u>31.9</u>	<u>36.4</u>
3rd layer	30.6	32.1	33.4	31.7	<u>41.4</u>	67.3	<u>39.1</u>	53.1
Mean	33.2 ^{e)}				33.4 ^{f)} , 52.5 ^{g)}			

a) The four positions and three layers are shown in Fig. 2. b) Units in degree. c) The mean value of the time-averaged χ_1 angle in all positions. d) Variances = $\Sigma(\chi_{1i} - \chi_{1\text{mean}})^2 / (n - 1)$, n = number of χ_{1i} . e) The mean value of χ_1 angle variances in all positions. f, g) The mean value of χ_1 angle variances underlined (smaller half) ^{f)} and those in the other (larger half) ^{g)}, respectively.

tional flexibility in IIA(1/3 H₂O).

Discussion

Thermal Stability Factors in the IIA Form of Aspartame

In our laboratories, the IIA form of aspartame has been recognized to be very stable over a wide temperature range, whereas IIB has a strong tendency to convert to IIA by water adsorption. However, the transformation mechanism between IIA and IIB forms has not been analyzed in detail. In the present study, the temperature-dependent change of the powder XRD pattern in a IIA sample and the TG/DTA curve were observed. It was revealed that the intermediate state exists at 40 °C–50 °C in the transformation between IIA and IIB, and its crystal form does not change from the initial IIA form, despite the different hydration number. In other words, the hydration number is variable in the IIA form to some extent, as in zeolites.²⁷⁾ In addition, the intermediate state was found to be stable as long as the temperature is held at 46 °C, *i.e.*, the amounts of adsorption and desorption of water are balanced, as in an equilibrium state. The results of the static D-NMR measurements at r.t. and 45 °C also proved that the hydration number ratio of the initial IIA form and the intermediate state was 0.5 : 0.33, *i.e.*, they were IIA(1/2 H₂O) and IIA(1/3 H₂O), respectively. The transition starting point was different by 5 degrees between the TG/DTA result (*ca.* 55 °C) and the powder XRD analysis (*ca.* 50 °C), and the former better explains the results of ¹³C-CPMAS-NMR. The sample was in the non-crushed crystal state in the TG/DTA and NMR measurements, and it was well-ground in the powder XRD analysis; this may have caused the difference, because the transition would easily proceed in a crushed sample, and the difference in the heating process, *i.e.*, isothermal (powder XRD) or nonisothermal (TG/DTA), may also be a factor.

Thus, the IIA form can retain the crystal lattice in dehydration to some extent by generating a stable intermediate state, and these physical properties are thought to underlie the thermal stability of the IIA form.

The Specific Features of the Crystal Transition In general, an organic crystal lattice is often destroyed by dehydration when it is stabilized by the hydrogen bonding net-

work in which the water molecules play an important part. In aspartame, this is the case with the whole transformation between the IIA and IIB forms, but not with the transition between the IIA form and the intermediate state. Thus, the crystal transformation of the IIA form is a very interesting phenomenon from the view point that the dehydration proceeds in a manner similar to that in zeolites at the initial stage, generates the intermediate state, and finally brings on the crystal lattice change as in an ordinary organic crystal.

As Endo *et al.* reported for an orthogonal bis(resorcinol)-anthracene compound,²⁸⁾ there is an exceptional case where an organic crystal has a function of zeolite. In addition, as Sugawara *et al.* described for disodium ATP,²⁹⁾ there is a special case where a single crystal state is retained during a humidity-controlled transition. In both cases, there is a common structural feature in that the framework is stabilized by aromatic stacking, and large supramolecular cavities for solvent molecules or columns consisting of water molecules are present in the structure, respectively. As described before and shown in Fig. 2, a similar feature exists in the crystal structure of the IIA form, *i.e.*, the water molecules form the infinite columns reaching the crystal surface, and aspartame molecules form the surrounding frame stabilized by the intermolecular hydrogen bonds and the ring stacking in the Phe moiety.

Therefore, the crystal lattice retention in the IIA form is attributable to such a structural feature. The transition type should be that of zeolites when the frame is rigid enough, and it should be topochemical as in the case of disodium ATP²⁹⁾ when the frame is not very rigid but is firm enough to maintain the single crystallinity for the gradual change of lattice parameters.

Transformation Analysis and Characterization of IIA(1/3 H₂O) by Solid-State NMR and Energy Component Analysis Solid-state NMR is useful for the investigation of temperature-dependent structural properties in crystalline materials.³⁰⁾ The transformation analysis of the aspartame crystal is a case in point, because it has a strong tendency to crystallize as very fine fibers, and it would be difficult to elucidate the process of the structural changes by X-ray crystallographic studies.

In the transition from IIA(1/2 H₂O) to IIA(1/3 H₂O) shown in Fig. 7a—d, the original state partly remains as it was, and “a new kind of state” (marked by arrow in the spectra) is generated concerning the carboxyl carbon of the Asp moiety, the γ -carbon of the Phe moiety and each methylene carbon, and finally the intensity ratio of the new and original signals reaches 1 : 1 in IIA(1/3 H₂O). Since the chemical shift difference between the new and original signals is 1.0 ppm or more in each case, there clearly exists a new physical state, not a chemical exchange. The partial loss of the hydrogen bonds within the crystal by the dehydration presumably generated a new carboxyl carbon signal of the Asp moiety; however, this is not enough to account for “a new chemical shift in the γ -carbon of the Phe moiety.” Since the intensity ratio in the powder XRD was almost the same between IIA(1/2 H₂O) and IIA(1/3 H₂O), and their intramolecular energies are not very different (Table 2), we do not think that a large conformational change occurs in the new state.

As shown in Table 4, the conformational flexibility analysis in the Phe moiety of IIA(1/2 H₂O) and IIA(1/3 H₂O) sug-

gested that the time-averaged and space-averaged conformation of aspartame molecules is almost the same between the two states, and that is consistent with the results observed in the powder XRD. Simultaneously, the above computational analysis revealed that IIA(1/3 H₂O) has at least two kinds of flexibility in the χ_1 dihedral angle in the Phe moiety, and IIA(1/2 H₂O) has the only rigid molecules. Moreover, the $T_{1\rho}$ measurements in the γ -carbon of the Phe moiety revealed that the conformational flexibility in the Phe moiety increased in IIA(1/3 H₂O) than in IIA(1/2 H₂O), especially in IIA(1/3 H₂O) the new γ -carbon was thought to be more flexible than the original position γ -carbon, since the $T_{1\rho}$ was 208 ms at r.t., and it was 135 and 172 ms at 45 °C, in the new signal and in the original position signal, respectively.

Therefore, it is suggested that “the new NMR signal in the γ -carbon of the Phe moiety” corresponds to the flexible γ -carbon newly generated in IIA(1/3 H₂O); in a crystal, the spatial anisotropy causes the non-linear correlation between the chemical shift and the dihedral angle, and it presumably gave different effects on the chemical shifts of the flexible molecule and the rigid molecule.

The energy component analysis for the models of IIA(1/2 H₂O) and IIA(1/3 H₂O) revealed that the potential energy in the latter was higher than in the former. This is a static result, and the degree of nonstabilization must be estimated after a dynamics simulation sampling for a strict discussion; however, it is an experimental finding that the IIA(1/3 H₂O) exists in a *quasi*-stable intermediate state. Therefore, the existence of IIA(1/3 H₂O) should be explained by the entropic stabilization in a whole system. The entropic stabilization is presumably caused by the evaporation of the water of crystallization and the increase of molecular motion in aspartame, because the conformational flexibility analysis showed the increase of flexibility in the intermediate state.

It is also important that in the solid-state NMR, the signal broadening of the Phe ring carbons started from around 55 °C and corresponded to the transition starting point from IIA(1/3 H₂O) to the IIB form. Though the signal broadening of the Asp carboxyl carbon and the Phe ring carbons increase over 60 °C, presumably the former means the increase of conformation, and the latter means the increase of flip-flop motion, it is interesting that the spectral pattern basically resembles that of IIA(1/3 H₂O) at 45 °C except for the line width. Such a resemblance in spectral pattern indicates that the large rearrangement of aspartame molecules does not occur in the crystal transformation from IIA to IIB.

MD Simulation of IIA(1/2 H₂O) It is of note that the space group of the IIA form is $P4_1$ and the occupancy rate of the water molecules is 50%.¹⁴⁾ This is crystallographically a correct expression, and it means that the molecules in the IIA form show $P4_1$ symmetry in the space-averaged and time-averaged state. However, from the microscopic point of view, the arrangement of the water molecules is not 4_1 but 2_1 , because its occupancy rate is 50% and its free movement between the crystallographic sites was not observed in the MD simulation. Accordingly, in each unit cell of the crystal, the microscopic state of aspartame molecules strictly may not be $P4_1$, reflecting the 2_1 symmetry of the water molecule arrangement. Thus, we interpret the MD simulation results observed in IIA(1/2 H₂O) and IIA(1/3 H₂O) as follows. In IIA(1/2 H₂O), the 2_1 symmetry of the water molecule

arrangement influences the microscopic state of aspartame molecules, and a slight difference (*ca.* 0.1 Å) was caused in the time-averaged length of the intermolecular hydrogen bond formed between the peptide bond sites. The further that the dehydration proceeds, the more differences are partially caused such as the conformational flexibility increase in IIA(1/3 H₂O).

Conclusion

A *quasi*-stable intermediate state was discovered in the transformation between the IIA form and the IIB form of aspartame. The crystal lattice in the IIA form is retained in the intermediate state, despite the dehydration from 1/2 mol to 1/3 mol. Such a specific feature in the crystal transition originally is thought to be due to the existence of the water columns reaching the crystal surface, the framework stabilized by the aromatic ring stacking and the intermolecular hydrogen bonds in its crystal structure. The intermediate state, IIA(1/3 H₂O), is stable during the 40 °C–50 °C period of the transformation. Since IIA(1/2 H₂O) is more stable than IIA(1/3 H₂O) regarding the total potential energy, the generation of IIA(1/3 H₂O) is considered to be promoted by the entropic effect, which is caused by the evaporation of the water of crystallization and the increase of molecular motion in aspartame. Thus, the thermal stability of the IIA form is attributable to a structural property, *i.e.*, the crystal lattice itself is retained during the dehydration to some extent. Moreover, it was suggested that a) the arrangement of water molecules has 2₁ symmetry in IIA(1/2 H₂O), and this influences the microscopic state of aspartame molecules; b) a slight difference is caused in the hydrogen bond length between the peptide bond sites; c) the aspartame molecules have two kinds of flexibility in IIA(1/3 H₂O), and d) clear differences are caused in the NMR chemical shift.

Acknowledgments We express our sincere thanks to Prof. Yuji Ohashi (Tokyo Institute of Technology) for his helpful discussion on the crystal lattice retention, and Kazuo Yamauchi (Bruker Japan Co., Ltd.) for help with the deuterium NMR measurement.

References and Notes

- 1) Mazur R. H., Schlatter J. M., Goldkamp A. H., *J. Am. Chem. Soc.*, **91**, 2684–2691 (1969).
- 2) Ranney R. E., Oppermann J. A., Muldoon E., McMahon F. G., *J. Toxicol. Environ. Health*, **2**, 441–451 (1976).
- 3) Stern S. B., Bleicher S. J., Flores A., Gombos G., Recitas D., Shu J., *J. Toxicol. Environ. Health*, **2**, 429–439 (1976).
- 4) Horwitz D. L., "Aspartame Physiology and Biochemistry," ed. by Stegink L. D., Filer L. J., Marcel Dekker Inc., 1984, pp. 633–639.
- 5) van der Heijden A., "Sweet-Taste Chemoreception," ed. by Mathlouthi M., Kanters J. A., Birch G. G., Elsevier Science Publishers Ltd., 1993, pp. 114–127.
- 6) Yamazaki T., Benedetti E., Kent D., Goodman M., *Angew. Chem. Int. Ed. Engl.*, **33**, 1437–1451 (1994).
- 7) Kim Y. J., Han S. J., Kim S. C., Kang Y. K., *Biopolymers*, **34**, 1037–1048 (1994).
- 8) Temussi P. A., Lelj F., Tancredi T., *J. Med. Chem.*, **21**, 1154–1158 (1978).
- 9) Temussi P. A., Lelj F., Tancredi T., Castiglione-Morelli M. A., Pastore A., *Int. J. Quantum Chem.*, **26**, 889–906 (1984).
- 10) Culbertson J. C., Walters D. E., "Sweeteners," ed. by Walters D. E., Orthoefer F. T., DuBois G. E., American Chemical Society: Symposium Series Vol. 450, Washington, DC, 1991, pp. 214–223.
- 11) Lelj F., Tancredi T., Temussi P. A., Toniolo C., *J. Am. Chem. Soc.*, **98**, 6669–6675 (1976).
- 12) Young K. K., *Int. J. Peptide Protein Res.*, **38**, 79–83 (1991).
- 13) Takahashi S., Suzuki E., Amino Y., Nagashima N., Nishimura Y., Tsuboi M., *Bull. Chem. Soc. Jpn.*, **59**, 93–96 (1986).
- 14) Hatada M., Jancarik J., Graves B., Kim S.-H., *J. Am. Chem. Soc.*, **107**, 4279–4282 (1985).
- 15) Sugiyama K., Ozawa T., Nagashima N., Uchida Y., *United States Patent*, 4579747 (1986).
- 16) Sugiyama K., Ozawa T., Nagashima N., Uchida Y., Japan. Patent Publication, 6-31312 (1994).
- 17) Campbell G. C., Crosby R. C., Haw J. F., *J. Magn. Reson.*, **69**, 191–195 (1986).
- 18) Yoneda S., Umeyama H., *J. Chem. Phys.*, **97**, 6730–6736 (1992).
- 19) The free energy perturbation (FEP) method is available in APRICOT, and the MD simulation carried out using APRICOT is a part of our on-going study on aspartame by the FEP method, while the Ewald method is available in Cerius2, and unavailable in APRICOT.
- 20) Karasawa N., Goddard III W. A., *J. Phys. Chem.*, **93**, 7320–7327 (1989).
- 21) Mayo S. L., Olafson B. D., Goddard III, W. A., *J. Phys. Chem.*, **94**, 8897–8909 (1990).
- 22) Hoover W., *Phys. Rev.*, **A31**, 1695–1697 (1985).
- 23) Weiner S. J., Kollman P. A., Case D. A., Singh U. C., Ghio C., Alagona G., Profeta S., Jr., Weiner P., *J. Am. Chem. Soc.*, **106**, 765–784 (1984).
- 24) Jorgensen W. L., Chandrasekhar J., Madura J. D., Impey R. W., Klein M. L., *J. Chem. Phys.*, **79**, 926–935 (1983).
- 25) van Gunsteren W. F., Berendsen H. J. C., *Mol. Phys.*, **34**, 1311–1327 (1977).
- 26) Berendsen H. J. C., Postma J. P. M., van Gunsteren W. F., DiNola A., Haak J. R., *J. Chem. Phys.*, **81**, 3684–3690 (1984).
- 27) Breck D. W., "Zeolite Molecular Sieves, Structure, Chemistry, and Use," John Wiley and Sons, New York, 1974.
- 28) Endo K., Sawaki T., Koyanagi M., Kobayashi K., Masuda H., Aoyama Y., *J. Am. Chem. Soc.*, **117**, 8341–8352 (1995).
- 29) Sugawara Y., Kamiya N., Iwasaki H., Ito T., Satow Y., *J. Am. Chem. Soc.*, **113**, 5440–5445 (1991).
- 30) Alcobe X., Estop E., Harris A. E. A. & K. D. M., Rodriguez-Carvajal J., Rius J., *Journal of Solid State Chemistry*, **110**, 20–27 (1994).

Stereocontrolled Synthesis of Piperidine-Condensed Tricyclic Carbapenems (5-Azatrinem) and Their Antibacterial Activities

Makoto MORI,* Atsushi SOMADA, and Sadao OIDA

Medicinal Chemistry Research Laboratories, Sankyo Co., Ltd., 2–58, Hiromachi 1-chome Shinagawa-ku, Tokyo 140–8710, Japan. Received January 17, 2000; accepted February 21, 2000

Stereocontrolled synthesis of tricyclic carbapenem (5-azatrinem) derivatives 4, in which a piperidine ring is condensed to the carbapenem skeleton, was achieved. The pivotal tricyclic intermediate 2, allyl (8*S*,9*R*,10*S*)-5-(*tert*-butoxycarbonyl)-10-[(*R*)-1-(*tert*-butyldimethylsilyloxy)ethyl]-11-oxo-1,5-diazatricyclo[7.2.0.0^{3,8}]undec-2-ene-2-carboxylate, was synthesized starting from an acetoxyazetidinone chiron 6 in a practical manner based on a C–C bond formation reaction between 6 and piperidinone-ester 5, palladium-catalyzed de(allyloxy)carbonylation of 7b and Wittig-type cyclization via an oxalimide 9. Selective deprotection of the *N*-Boc group of 2 was found to proceed smoothly by treatment with trimethylsilyl trifluoromethanesulfonate and 2,6-lutidine to give the amino compound 3, whose functionalization on the nitrogen atom to derivatives 10 followed by deprotection led to various 5-azatrinem acids 4. These compounds showed potent *in vitro* activities against gram-positive and gram-negative bacteria.

Key words carbapenem; trinem; antibacterial activity; synthesis; azatrinem; intramolecular Wittig-type reaction

Since the discovery of thienamycin in 1976 by the Merck research group,¹⁾ a huge number of carbapenem derivatives have been synthesized with the development of new synthetic methodologies for seeking potent antibacterial agents.²⁾ With the growing concern over the emergence of antibiotic-resistant bacteria, some structurally unique carbapenem analogs have been explored to overcome this serious problem. For this goal, tricyclic carbapenems (referred to as trinems), such as Sanfetrinem, which has a fused cyclohexane ring possessing a 4*α*-methoxy substituent (Fig. 1, X=OCH₃), were reported by the Glaxo Wellcome research group.³⁾ In a further study of the trinem series,⁴⁾ some thia- or oxa-analogs containing a sulfur or an oxygen atom in the cyclohexane ring, that is 4-, 6- and 7-thia-trinem, or 5- and 7-oxo-analogs have also been synthesized and their antibacterial activities have been reported.⁵⁾ However, there have been no reports on the corresponding aza-analog.⁶⁾ We were particularly interested in 5-azatrinem, because there were only a few reports on 5-substituted trinem derivatives⁷⁾ and introduction of a nitrogen atom at the 5-position is convenient for modifying the molecule at this position. Therefore our principal aim in this project was to develop an efficient synthetic route to 5-azatrinem and to evaluate these compounds as possible antibacterial agents.

Here we report a stereocontrolled synthesis of a piperidine-condensed tricyclic key intermediate 2 which is suitable via 3 for modification on the nitrogen atom, its subsequent derivatization to a variety of 5-azatrinem 4 and their *in vitro* antibacterial activities.

Synthesis Analysis of our target structure led us to prepare a 3-azacyclohexanone derivative 1, which has the same configuration at the C-8 position as trinem, utilizing a stereocontrolled decarboxylation reaction of a β -ketoester 7b ac-

cording to a literature procedure.⁸⁾ A coupling reaction of the commercially available acetoxyazetidinone 6 with the sodium salt of allyl β -ketoester 5, which was provided by the transesterification reaction of the corresponding ethyl ester with sodium allyloxide in allyl alcohol, in tetrahydrofuran (THF) gave a 3:2 mixture of two diastereoisomers 7a in quantitative yield. After protecting the NH group of 7a by treatment with *tert*-butyldimethylsilyl triflate (TBSOTf) and 2,6-lutidine in dichloromethane (CH₂Cl₂), the product 7b was subjected to the stereocontrolled decarboxylation reaction in the presence of triethylamine (Et₃N), formic acid and a catalytic amount of tetrakis(triphenylphosphine)palladium(0) in ethyl acetate (EtOAc).⁹⁾ The reaction occurred readily at 0 °C to afford the ketone 8a with desired stereochemistry¹⁰⁾ in 77% yield from 7a. The ketone 8a was not stable enough, probably due to its basicity, to store for weeks in a refrigerator even in a crystalline form. Therefore, the *N*-benzyl group was exchanged to the *N*-*tert*-butoxycarbonyl (*N*-Boc) group as follows. Hydrogenolysis of 8a using 10% Pd-charcoal under a hydrogen atmosphere in EtOAc in the presence of di-*tert*-butyl dicarbonate (Boc₂O) gave a quantitative yield of 8b. The ketone 8b was stable in cold storage, but it was found to be sensitive to silica gel, on which chromatography brought about partial epimerization at the α -position of the ketone group. This epimerization was also observed in the next reaction to deprotect the *N*-TBS group of 8b. The results of *N*-desilylation of 8b with tetrabutylammo-

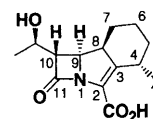


Fig. 1. General Structure of Trinem Template

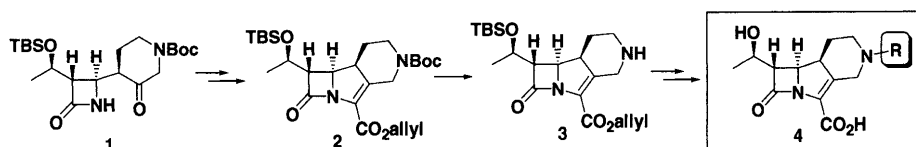


Chart 1

* To whom correspondence should be addressed. e-mail: morimk@shina.sankyo.co.jp

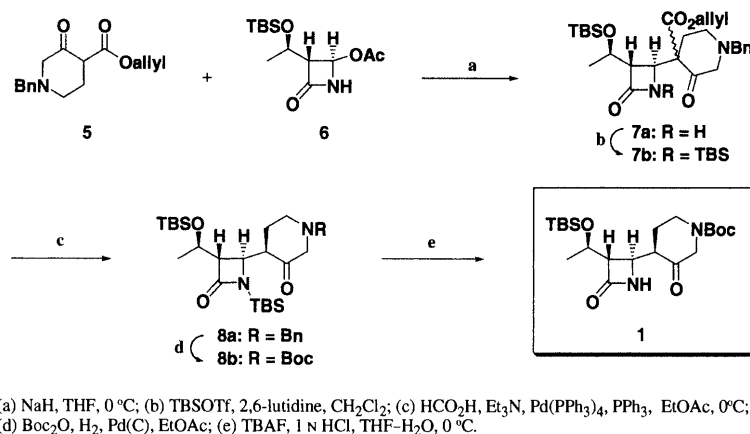


Chart 2

Table 1. The Product Ratio in Deprotecting Reaction of the *N*-TBS Group of **8b**

Run	Reagents (eq)	Solvent	Temp./°C	Time/h	Ratio (1 : 1') ^{a)}
1	TBAF(1.0)	THF	0	0.1	Decomposition
2	TBAF(1.0)-AcOH(1.0)	THF	0	1	1 : 1
3	TBAF(1.0)-AcOH(2.0)	THF	0	1	2.2 : 1
4	TBAF(1.0)-HCO ₂ H(2.0)	THF	r.t.	1	3.2 : 1
5	TBAF(1.0)-HCO ₂ H(5.0)	THF	r.t.	1	3.7 : 1
6	TBAF(1.0)-HF(2.0)	THF-H ₂ O (10 : 1)	0	1	4.3 : 1
7	TBAF(1.0)-HCl(1.0)	THF-H ₂ O (10 : 1)	0	2.5	10 : 1

^{a)} The ratio was determined by ¹H-NMR spectrum of the crude product.

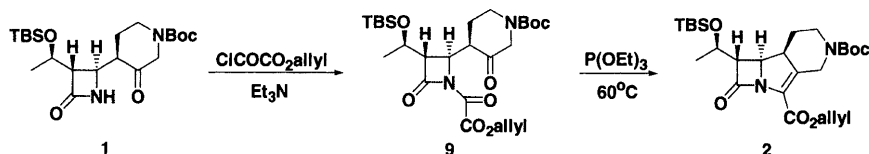


Chart 3

mium fluoride (TBAF) in the presence of various acids are summarized in Table 1. Treatment of **8b** with TBAF (1 eq) in the presence of AcOH (1 eq) in THF (run 2) gave a 1 : 1 mixture of **1** and its epimer **1'**. Use of excess acid retarded the epimerization. Hydrogen fluoride gave better results than organic acids. The best result was obtained by using a combination of TBAF (1 eq) and HCl (1 eq) to give a 10 : 1 ratio of **1** : **1'** (run 7).

The ketone **1** also isomerized during silica gel chromatography. Fortunately, the crude product crystallized without chromatography and it could be purified by recrystallization from hexane to afford the pure ketone **1** in 66% yield in two steps from **8a**, which was found to be stable during storage at room temperature. The ketone **1** could be transformed to the piperidine-condensed tricyclic compound **2** in a conventional manner *via* an intramolecular Wittig-type reaction¹¹⁾ as follows. Treatment of **1** with allyloxyoxalyl chloride in the presence of Et₃N in CH₂Cl₂ afforded the oxalimide **9**, which was then heated with excess triethyl phosphite in toluene at 60 °C for 3 h. The ylide formation and subsequent cyclization occurred simultaneously at this temperature and the pure crys-

tals of **2** were obtained in 67% yield by recrystallization of the crude product. The stereochemistry at the C8 position of **2** was confirmed by nuclear Overhauser effect (NOE) experiment. The NOEs were observed between 8-H and 9-H, and 7-H and 10-H, respectively.

With the precursor **2** of 5-azatrinem derivatives in hand, we investigated the selective deprotection of its *N*-Boc group to provide the NH compound **3**. The 5-azatrinem skeleton could not survive under the usual acidic conditions to deprotect the *N*-Boc group. Recently, TBSOTf/2,6-lutidine or trimethylsilyl triflate (TMSOTf)/2,6-lutidine has been reported as an efficient reagent for chemoselective removal of the *N*-Boc group.¹²⁾ We applied this procedure to our sensitive compound. Treatment of **2** with 1.2 eq of TMSOTf in the presence of 2,6-lutidine (1.2–1.5 eq) in CH₂Cl₂ at 0 °C to room temperature for 10–15 min and subsequent aqueous workup afforded a free piperidine derivative **3** in quantitative yield. This amine was not stable. So, it was immediately transformed to a variety of *N*-modified precursors **10** for azatrinems such as amides, amines, ureas, thiourea, and amidines by reaction with various electrophiles as shown in

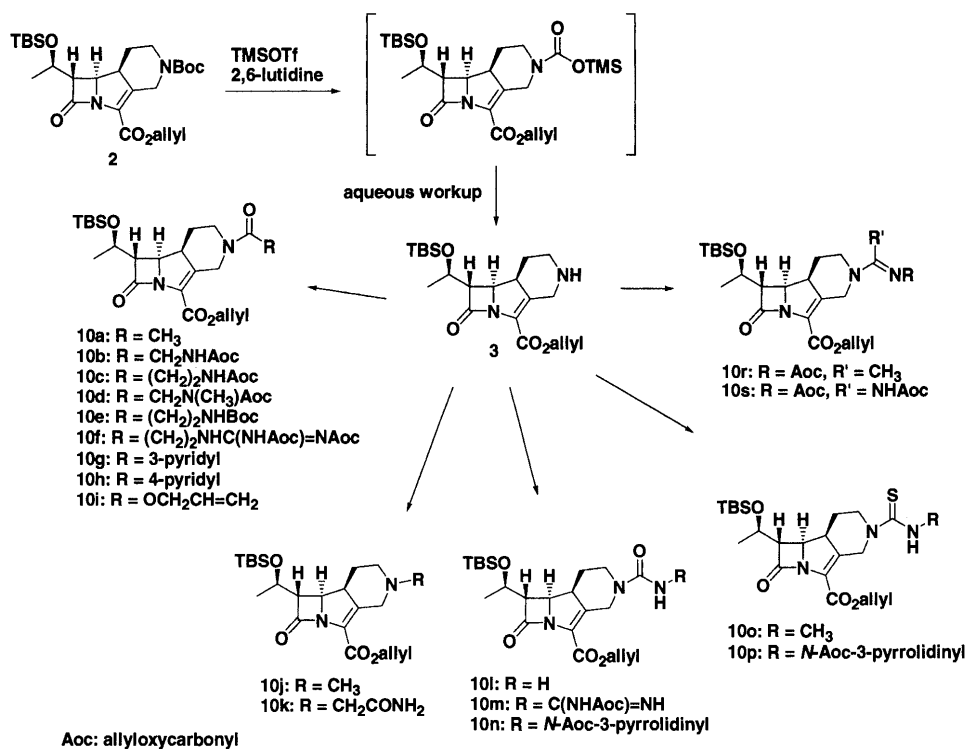


Chart 4

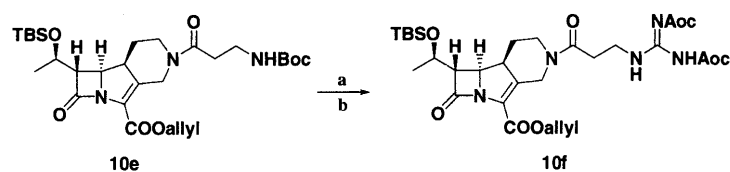
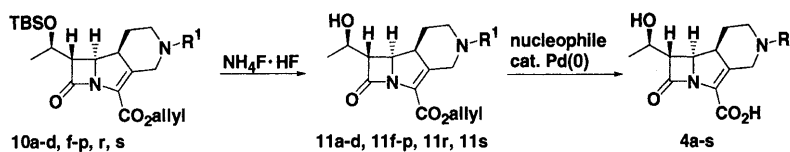
(a) TMSOTf, 2,6-lutidine, CH₂Cl₂, 0°C-r.t.; (b) *N,N'*-bis(Aoc)amidinopyrazole, THF, r.t.

Chart 5



	R ¹ (for 10 and 11)		R (for 4)
a	COCH ₃	a	COCH ₃
b	COCH ₂ NHAoc	b	COCH ₂ NH ₂
c	CO(CH ₂) ₂ NHAoc	c	CO(CH ₂) ₂ NH ₂
d	COCH ₂ N(CH ₃)Aoc	d	COCH ₂ NH(CH ₃)
e	CO(CH ₂) ₂ NHBoc	e	COCH ₂ N(CH ₃)CH=NH
f	CO(CH ₂) ₂ NHC(NHAoc)=NAoc	f	CO(CH ₂) ₂ NHC(NH ₂)=NH
g	CO-4-pyridyl	g	CO-4-pyridyl
h	CO-3-pyridyl	h	CO-3-pyridyl
i	Aoc	i	H
j	CH ₃	j	CH ₃
k	CH ₂ CONH ₂	k	CH ₂ CONH ₂
l	CONH ₂	l	CONH ₂
m	CONHC(NHAoc)=NH	m	CONHC(NH ₂)=NH
n	CO-N-Aoc-3-pyrrolidinyl	n	CO-NH-3-pyrrolidinyl
o	CSNHCH ₃	o	CSNHCH ₃
p	CS-N-Aoc-3-pyrrolidinyl	p	CS-NH-3-pyrrolidinyl
r	C(CH ₃)=NAoc	q	CH=NH
s	C(NAoc)=NAoc	r	C(CH ₃)=NH
		s	C(NH)=NH

Chart 6

Chart 4.

The amide-type precursors **10a—e, g, h** were synthesized by treatment of **3** with the corresponding acid chloride or acylimidazolidine. A precursor **10i** for unsubstituted 5-azatrinem **4i** (R=H) was obtained by reaction of **3** with allyl chloroformate. 3-Guanidinopropionyl derivative **10f** was prepared from **10e** as follows (Chart 5). The *N*-Boc group of **10e** was removed by use of the above mentioned TM-SOTf/2,6-lutidine combination and subsequent treatment with *N,N'*-bis(allyloxycarbonyl)amidinopyrazole¹³⁾ afforded **10f**. *N*-Alkylation of **3** with alkyl iodide in the presence of triethylamine or potassium carbonate afforded the tertiary amines **10j, k**. The ureas **10l, n** were synthesized by treatment of **3** with trimethylsilyl isocyanate and 3-isocyanato-*N*-Aoc-pyrrolidine, respectively. On the other hand, **10m** was prepared by reaction of the piperidine **3** with triphosgene, followed by treatment with *N*-Aoc-guanidine, in the presence of 4-dimethylaminopyridine (DMAP). The thioureas **10o, p** were synthesized by treatment of **3** with isothiocyanates, which were prepared by reaction of 1,1'-thiocarbonyldiimidazole and primary amines. The amidine precursor **10r** and guanidine precursor **10s** were synthesized by treatment of **3** with *N*-(allyloxycarbonyl)acetamide hydrochloride and *N,N'*-bis(allyloxycarbonyl)amidinopyrazole, respectively.

The 5-azatrinem precursors **10** thus obtained could be transformed to the fully deprotected acids **4** in 2 steps. Firstly, the TBS protecting group of **10** was removed by treatment with NH_4F HF in a 1:1 mixture of *N,N'*-dimethylformamide (DMF) and *N*-methylpyrrolidinone¹⁴⁾ to give the alcohols **11** in moderate yields. Then, the allyl ester group and/or *N*-allyloxycarbonyl group(s) in the side chain of **11** were deprotected by Pd(0) catalyzed deallylation reaction¹⁵⁾ in the presence of a suitable allyl scavenger such as dione, potassium 2-ethylhexanoate or *n*-butyltin hydride to give the piperidine-condensed tricyclic carbapenems **4** (Chart 6). Amidines **4e** and **4q** were prepared by formimidoylation of the amines **4d** and **4i**, respectively, with excess benzyl formimidate hydrochloride in a buffered aqueous acetonitrile in the presence of *N,N'*-diisopropylethylamine.

Biological Properties The *in vitro* antibacterial activities (minimal inhibitory concentrations (MICs)) of these 5-azatrinem (**4a—s**) are shown in Table 2. Among amide-type derivatives **4a—h**, 5-acetyl derivative **4a** has reasonable antibacterial potency, although its activity was generally weaker than Sanfetrinem. The pyridylcarbonyl compounds **4g, h** showed decreased activity. Introduction of the amino, amidino or guanidino function on the acyl side chain as shown such as glycine and β -alanine analogs **4b—f** improved potency against both gram-positive and -negative bacteria. But they have weak activity against *Proteus vulgaris*, *Morganella morganii* and methicillin-resistant-*Staphylococcus aureus* (MRSA). The simple amines **4i** and **4j**, whose nitrogen atom in the piperidine ring is basic, showed less antibacterial activity than glycine and β -alanine analogs **4b—f**. The *tert*-amine derivative **4k** with the methyl group modified by the carbamoyl group recovered some antibacterial activities in contrast to **4j**, probably due to the hydrophilic property of the carbamoyl group and increased stability of the compound coming from the decreased basicity by attaching the electron-withdrawing group. In a series of urea and thiourea compounds **4l—p**, the simple urea **4l** and the guani-

Table 2. Antibacterial Activity (MIC, $\mu\text{g}/\text{ml}$)^{a)} of Azatrinem **4a—s** and Sanfetrinem (GV104326)

	Sanfetrinem	4a	4b	4c	4d	4e	4f	4g	4h	4i	4j	4k	4l	4m	4n	4o	4p	4q	4r	4s
<i>Staphylococcus aureus</i> 209P	0.02	0.1	0.05	0.1	0.05	0.1	0.02	0.4	1.5	0.05	0.1	0.02	0.1	0.02	0.2	0.2	0.1	<0.01	<0.01	<0.01
<i>S. aureus</i> 56R	0.05	0.2	0.1	0.2	0.2	0.4	0.1	0.8	1.5	0.2	0.4	0.1	0.2	0.02	0.8	0.4	0.4	0.02	0.05	0.02
<i>S. aureus</i> 535 (MRSA)	12.5	25	100	100	>100	>100	25	25	100	50	50	100	25	12.5	>100	50	100	12.5	12.5	6.2
<i>Enterococcus faecalis</i> 681	0.8	3.1	1.5	1.5	1.5	3.1	1.5	6.2	25	25	50	6.2	1.5	1.5	6.2	6.2	6.2	0.8	1.5	0.4
<i>Escherichia coli</i> NIHJ	0.2	0.1	0.1	0.2	0.2	0.8	0.2	0.8	3.1	3.1	3.1	0.4	0.05	0.1	0.8	0.4	3.1	0.1	0.2	0.1
<i>E. coli</i> 609	1.5	0.8	12.5	1.5	12.5	3.1	0.8	6.2	25	25	25	6.2	1.5	0.8	12.5	3.1	50	0.8	0.8	3.1
<i>Salmonella enteritidis</i>	0.2	0.2	0.2	0.4	0.8	1.5	0.2	1.5	6.2	6.2	12.5	0.8	0.4	0.4	1.5	0.4	6.2	0.4	0.4	0.2
<i>Klebsiella pneumoniae</i> 806	0.4	0.2	0.2	0.4	0.2	0.8	0.2	0.8	3.1	3.1	6.2	0.8	0.1	0.2	1.5	0.4	6.2	0.2	0.4	0.2
<i>K. pneumoniae</i> 846	1.5	0.2	0.1	0.2	0.2	0.4	0.2	6.2	25	3.1	6.2	0.8	0.2	0.4	0.8	12.5	100	0.1	0.2	0.1
<i>Enterobacter cloacae</i> 903	6.2	3.1	25	12.5	25	12.5	3.1	25	100	50	50	6.2	3.1	1.5	12.5	12.5	50	3.1	6.2	3.1
<i>Serratia marcescens</i> 1184	0.8	0.2	0.2	0.4	0.4	0.8	0.4	1.5	6.2	6.2	12.5	1.5	0.1	0.2	1.5	0.8	25	0.4	0.4	0.2
<i>Proteus vulgaris</i> 1420	0.4	12.5	>100	100	>100	>100	25	25	50	>100	>100	100	25	12.5	100	12.5	>100	50	100	50
<i>Morganella morganii</i> 1510	0.8	12.5	>100	100	>100	>100	25	50	100	>100	>100	50	12.5	12.5	100	12.5	>100	50	50	50
<i>Pseudomonas aeruginosa</i> 1001	100	>100	6.2	12.5	6.2	25	12.5	>100	>100	25	100	>100	>100	50	>100	>100	>100	3.1	6.2	3.1

a) MIC was determined by the agar dilution method with an inoculum of 10^7 cfu/ml.

dinocarbonyl derivative **4m** exhibited potent and broad-spectrum activity comparable to Sanfetrinem. None of these azatrinems showed any interesting antibacterial activity against *Pseudomonas aeruginosa*. The amidine and guanidine derivatives **4q**—**s** showed a good potency against gram-positive and -negative bacteria. In particular, the formamidine **4p** and guanidine **4s** expressed high activity with a well-balanced spectrum including activity against *P. aeruginosa*. This antipseudomonal activity supports the hypothesis that a positively charged functional group facilitates the penetration of β -lactams into *Pseudomonas* spp.⁴⁾ In order to estimate the biological stability of the 5-azatrinem, urinary recovery of the formimidoyl compound **4q** was determined by subcutaneous administration to mice. Forty-seven percent of the 5-formimidoyl-5-azatrinem **4q** was recovered in urine.

Conclusion

The convenient 5-azatrinem precursor **2** was synthesized starting from an acetoxazetidinone **6** in a practical manner based on stereocontrolled palladium-catalyzed de(allyloxy)-carbonylation and Wittig-type cyclization *via* an oxalimide **9**. Selective deprotection of the *N*-Boc group of **2** by treatment with TMSOTf and 2,6-lutidine to give the amino compound **3**, whose functionalization on the nitrogen atom to derivatives **10** followed by deprotection led to various 5-azatrinem analogs **4**. In the course of our study for seeking 5-azatrinem derivatives that show potent antibacterial activities, we found 5-amidino-type compounds that possessed potent *in vitro* activities against gram-positive and -negative bacteria.

Experimental

Melting points are uncorrected. ¹H-NMR spectra were recorded on a JEOL JNM-EX-270 (270 MHz) or a JEOL JNM-GX-270 (270 MHz) spectrometer and ¹³C-NMR spectra were recorded on a JEOL JNM-GSX-400 (100 MHz) spectrometer. Chemical shifts are shown in ppm downfield from internal tetramethylsilane in CDCl₃ or sodium 2,2-dimethyl-2-silapentane-5-sulfonate in D₂O. The abbreviations used in the ¹H-NMR data are as follows: s, singlet; d, doublet; t, triplet; q, quartet; dd, doublet of doublets; dq, doublet of quartets; br, broad; m, multiplet. Infrared (IR) spectra were recorded on a JASCO A-102, FT/IR-8300 or FT/IR-8900 spectrometer. Optical rotations were measured on a Perkin-Elmer 141 spectrometer at 25 °C. Mass spectra (MS) were obtained on a JEOL JMS-D300 or JMS-AX505H spectrometer. Chromatography columns were prepared with Silica gel 60 (230—400 mesh, E. Merck) or Cosmosil 75C₁₈-PREP (Nacalai Tesque). High pressure liquid chromatography (HPLC) was performed on an LC-908 (Japan Analytical Industry Co., Ltd.) with joined two GPC columns in succession (a JAIGEL-1H (20 mm i.d.×600 mm) and a JAIGEL-2H (20 mm i.d.×600 mm)).

***N*-(Allyloxycarbonyl)amino Acids** *N*-(allyloxycarbonyl)amino acids were prepared from the corresponding amino acids following the literature procedure.^{15d)} The preparation of 3-(allyloxycarbonylamino)propionic acid is described below as a typical example. To a solution of 3-aminopropionic acid (5.0 g, 5.6×10⁻² mol) in a mixture of H₂O—THF (2 : 1, 90 ml) were added a solution of allyl chloroformate (5.9 ml, 5.6×10⁻² mol) in THF (30 ml) and 2 N NaOH (56 ml) at room temperature. After being stirred for 1 h, the mixture was concentrated under reduced pressure to ca. 30 ml and then acidified to ca. pH 2 by addition of 2 N HCl. The product was extracted with EtOAc. The extract was dried and concentrated under reduced pressure to give 3-(allyloxycarbonylamino)propionic acid (9.68 g) as a colorless oil in quantitative yield. ¹H-NMR (CDCl₃) δ : 2.61 (2H, brt, *J*=6 Hz), 3.47 (2H, br q, *J*=6 Hz), 4.56 (2H, d, *J*=5 Hz), 5.22 (1H, d, *J*=10 Hz), 5.31 (1H, d, *J*=17 Hz), 5.35 and 6.39 (1H, brs×2), 5.91 (1H, ddt, *J*=17, 19, 5 Hz), 10.81 (1H, m).

N-Allyloxycarbonylsarcosine was prepared in a similar manner in 93% yield as a colorless oil. ¹H-NMR (CDCl₃) δ : 3.01 (3H, s), 4.00—4.15 (2H, m), 4.55—4.65 (2H, m), 5.15—5.40 (2H, m), 5.80—6.05 (1H, m), 8.40 (1H, brs). These products were used for the next reaction without further purification.

Allyl 1-Benzyl-3-oxo-4-piperidinecarboxylate (5**)** A solution of ethyl

1-benzyl-3-oxo-4-piperidinecarboxylate (22.0 g, 8.42×10⁻² mol) in allyl alcohol (50 ml) was added to a solution of sodium allyloxide, prepared by dissolving sodium stick (2.1 g, 9.1×10⁻² mol) in allyl alcohol (200 ml), with stirring at 0 °C, and the mixture was heated under reflux for 10 h. After being cooled, the reaction mixture was slowly poured into ice-cold 1 N HCl (200 ml), and then neutralized by addition of a saturated aqueous solution of NaHCO₃. The product was extracted with EtOAc, and the extract was washed with brine, dried over anhydrous magnesium sulfate, and concentrated under reduced pressure. The residue was subjected to column chromatography on silica gel (400 g) using a mixture of hexane and EtOAc (5 : 1) as eluent to give **5** (14.2 g, 62%) as a pale yellow oil. ¹H-NMR (CDCl₃) δ : 2.36 (2H, t, *J*=5.8 Hz), 2.59 (2H, t, *J*=5.8 Hz), 3.11 (2H, s), 3.61 (2H, s), 4.67 (2H, brt, *J*=5.4 Hz), 5.24 (1H, dd, *J*=10.5, 1.2 Hz), 5.33 (1H, dd, *J*=17.2, 1.6 Hz), 5.93 (1H, ddt, *J*=17.2, 10.5, 5.4 Hz), 7.32 (1H, s). IR (neat): 1736, 1665, 1626 cm⁻¹.

(3*S*,4*R*)-4-[4-(Allyloxycarbonyl)-1-benzyl-3-oxopiperidin-4-yl]-3-[(*R*)-1-(*tert*-butyldimethylsilyloxy)ethyl]-2-azetidinone (7a**)** To a suspension of sodium hydride (55% mineral oil dispersion, 3.60 g, 82.5 mmol, washed with hexane) in THF (75 ml) was added a solution of **5** (20.5 g, 75.0 mmol) in THF (75 ml) at 0 °C and the mixture was stirred at room temperature for 30 min. After the mixture was cooled at 0 °C, a solution of (3*R*,4*R*)-4-acetoxy-3-[(*R*)-1-(*tert*-butyldimethylsilyloxy)ethyl]-2-azetidinone (**6**, 21.55 g, 74.98 mmol) in THF (150 ml) was added. After being stirred at 0 °C for 30 min, the mixture was partitioned between a diluted aqueous solution of ammonium chloride (100 ml) and EtOAc (50 ml). The organic layer was separated, washed with brine, dried over anhydrous magnesium sulfate, and concentrated under reduced pressure. The residue was subjected to column chromatography on silica gel (400 g) using a mixture of hexane and EtOAc (3 : 1) as eluent, to give **7a** (37.0 g, 99%) as a colorless oil which was shown by ¹H-NMR spectrum to be a 3 : 2 mixture of two diastereoisomers.

Major Isomer: *R*_f 0.36 (hexane : EtOAc = 2 : 1). ¹H-NMR (CDCl₃) δ : 0.05 (3H, s), 0.06 (3H, s), 0.86 (9H, s), 1.19 (3H, d, *J*=6.2 Hz), 1.6—1.8 (1H, m), 2.5—2.8 (3H, m), 3.02 (1H, d, *J*=16.3 Hz), 3.20 (1H, m), 3.23 (1H, d, *J*=16.3 Hz), 3.51 (1H, d, *J*=13.1 Hz), 3.59 (1H, d, *J*=13.1 Hz), 3.87 (1H, d, *J*=2.2 Hz), 4.1—4.2 (1H, m), 4.59 (1H, dd, *J*=13.0, 6.0 Hz), 4.69 (1H, dd, *J*=13.0, 6.0 Hz), 5.23 (1H, d, *J*=10.5 Hz), 5.25 (1H, dd, *J*=17.0 Hz), 5.81 (1H, ddt, *J*=17.0, 10.5, 6.0 Hz), 5.95 (1H, brs), 7.2—7.4 (5H, m). IR (CHCl₃): 3421, 1764, 1719 cm⁻¹. MS (FAB) *m/z*: 501 (M+H)⁺.

Minor Isomer: *R*_f 0.25 (hexane : EtOAc = 2 : 1). ¹H-NMR (CDCl₃) δ : 0.06 (6H, s), 0.87 (9H, s), 1.00 (3H, d, *J*=6.5 Hz), 1.9—2.1 (1H, m), 2.5—2.7 (2H, m), 2.8—2.9 (1H, m), 2.94 (1H, d, *J*=16.8 Hz), 3.03 (1H, brt, *J*=2.4 Hz), 3.27 (1H, br d, *J*=16.8 Hz), 3.51 (1H, d, *J*=13.2 Hz), 4.23 (1H, dq, *J*=6.5, 2.6 Hz), 4.36 (1H, d, *J*=2.2 Hz), 4.5—4.8 (2H, m), 5.26 (1H, dd, *J*=10.5, 1.2 Hz), 5.30 (1H, dd, *J*=17.2, 1.2 Hz), 5.67 (1H, brs), 5.84 (1H, ddt, *J*=17.2, 10.5, 5.9 Hz), 7.2—7.4 (5H, m). IR (CHCl₃): 3166, 3098, 1765, 1726 cm⁻¹. MS (FAB) *m/z*: 501 (M+H)⁺.

(3*R*,4*S*)-4-[(*R*)-1-Benzyl-3-oxopiperidin-4-yl]-1-(*tert*-butyldimethylsilyl)-3-[(*R*)-1-(*tert*-butyldimethylsilyloxy)ethyl]-2-azetidinone (8a**)** To a solution of **7a** (37.0 g, 7.39×10⁻² mol) and 2,6-lutidine (18.9 ml, 8.25×10⁻² mol) in CH₂Cl₂ (250 ml) was added TBSOTf (9.7 ml, 8.3×10⁻² mol) at 0 °C. After being stirred for 10 min, water and a mixture of EtOAc and hexane (4 : 1, 750 ml) were added to the reaction mixture. The organic layer was separated, washed with a saturated aqueous solution of NaHCO₃, a saturated aqueous solution of NH₄Cl and brine, successively, and dried. After evaporation of the solvent, the crude product was subjected to chromatography on silica gel (400 g) using a mixture of hexane and EtOAc (4 : 1) as eluent, to give the *N*-TBS-protected product **7b** as a colorless oil (47 g). A solution of **7b** in EtOAc (250 ml) was added to a mixture of tetrakis(triphenylphosphine)palladium (867 mg, 7.50×10⁻⁴ mol), triphenylphosphine (984 mg, 3.75×10⁻³ mol), Et₃N (36.7 ml, 2.63×10⁻¹ mol) and formic acid (8.49 ml, 2.25×10⁻¹ mol) in EtOAc (300 ml) at 0 °C. The mixture was stirred at the same temperature for 2.5 h, diluted with hexane (200 ml), and washed with a saturated aqueous solution of NH₄Cl (200 ml×3), water (200 ml), and brine (200 ml×2), dried, and concentrated under reduced pressure. The residue was subjected to flash chromatography on silica gel (1.2 kg) using a mixture of ethyl acetate and hexane (1 : 5 to 1 : 1) as eluent to give the product **8a** (30.1 g, 77%) as pale yellow crystals, mp 96—99 °C. ¹H-NMR (CDCl₃) δ : 0.06 (3H, s), 0.07 (3H, s), 0.08 (3H, s), 0.29 (3H, s), 0.85 (9H, s), 0.95 (9H, s), 1.25 (3H, d, *J*=6.0 Hz), 1.8—2.1 (2H, m), 2.4—2.6 (2H, m), 2.72 (1H, d, *J*=14.8 Hz), 2.94 (1H, dd, *J*=7.9, 2.7 Hz), 3.06 (1H, br d, *J*=11 Hz), 3.28 (1H, dd, *J*=14.8, 1.5 Hz), 3.54 (1H, d, *J*=13.2 Hz), 3.63 (1H, d, *J*=13.2 Hz), 4.07 (1H, dq, *J*=7.9, 6.0 Hz), 4.23 (1H, m), 7.2—7.4 (5H, m). ¹³C-NMR (CDCl₃) δ : -5.1, -4.8, -4.6, -4.4, 17.9, 19.0, 22.9, 24.5, 25.8 (3C), 26.4 (3C), 49.8, 51.6, 51.9, 61.9, 62.4,

64.5, 67.8, 127.4, 128.4 (2C), 128.8 (2C), 137.2, 173.3, 205.1. IR (KBr): 2953, 2930, 2886, 2858, 1733, 1718 cm^{-1} .

(3*R*,4*S*)-4-[(*R*)-1-(*tert*-Butoxycarbonyl)-3-oxopiperidin-4-yl]-3-[(*R*)-1-(*tert*-butyldimethylsilyloxy)ethyl]-2-azetidinone (1) A solution of **8a** (30.0 g, 5.65×10^{-2} mol) and di-*tert*-butyldicarbonate (13.0 g, 5.96×10^{-2} mol) in EtOAc (300 ml) was stirred with 10% Pd-C (10 g) under a hydrogen atmosphere at room temperature for 4 h. After removal of the catalyst by filtration, the filtrate was concentrated under reduced pressure. The residue was dissolved in THF (150 ml), and a mixture of 1 N HCl (55 ml) and 1 M TBAF THF solution (57 ml) was added at 0°C. After being stirred at 0°C for 1.5 h, the mixture was quenched by addition of phosphate buffer (200 ml) and extracted with EtOAc (400 ml). The extract was washed with a saturated aqueous solution of NaHCO_3 , a saturated aqueous solution of NH_4Cl , and then brine. The organic layer was dried and concentrated under reduced pressure to give a pale yellow oil, which was purified by recrystallization from hexane to give **1** (15.8 g, 66%) as colorless crystals, mp 139–142°C. $^1\text{H-NMR}$ (CDCl_3) δ : 0.07 (3H, s), 0.08 (3H, s), 0.87 (9H, s), 1.24 (3H, d, $J=6.2$ Hz), 1.47 (9H, s), 1.75–1.95 (1H, m), 2.10–2.25 (1H, m), 2.60–2.70 (1H, m), 2.93 (1H, dd, $J=4.9, 2.5$ Hz), 3.50–3.70 (1H, m), 3.80–3.95 (1H, m), 3.97 (1H, d, $J=17.8$ Hz), 4.09 (1H, d, $J=17.8$ Hz), 4.15–4.30 (2H, m), 5.67 (1H, brs). $^{13}\text{C-NMR}$ (CDCl_3) δ : -5.0, -4.2, 18.0, 22.6, 23.1, 25.8 (3C), 28.3 (3C), 41.7, 48.5, 49.7, 54.3, 60.9, 65.8, 80.9, 154.4, 168.4, 206.0. IR (KBr): 3265, 2956, 2931, 2887, 2858, 1762, 1721, 1682 cm^{-1} . $[\alpha]_D^{25} + 34^\circ$ ($c=0.74$, CHCl_3). Anal. Calcd for $\text{C}_{21}\text{H}_{38}\text{N}_2\text{O}_5\text{Si}$: C, 59.12; H, 8.98; N, 6.57. Found: C, 58.92; H, 9.01; N, 6.53. MS (FAB) m/z : 427 ($\text{M}+\text{H}^+$). **1'** (Epimer of **1**): $^1\text{H-NMR}$ (CDCl_3) δ : 0.06 (3H, s), 0.07 (3H, s), 0.88 (9H, s), 1.23 (3H, d, $J=6.2$ Hz), 1.47 (9H, s), 1.55–1.80 (1H, m), 2.10–2.25 (1H, m), 2.45 (1H, ddd, $J=12.9, 9.6, 5.7$ Hz), 2.76 (1H, m), 3.30–3.50 (1H, m), 3.62 (1H, dd, $J=9.6, 2.0$ Hz), 3.80–4.05 (1H, m), 3.90 (1H, brd, $J=18$ Hz), 4.15 (1H, d, $J=17.8$ Hz), 4.10–4.25 (1H, m), 6.19 (1H, brs).

Allyl (8*S*,9*R*,10*S*)-5-(*tert*-Butoxycarbonyl)-10-[(*R*)-1-(*tert*-butyldimethylsilyloxy)ethyl]-11-oxo-1,5-diazatricyclo[7.2.0.0^{3,8}]undec-2-ene-2-carboxylate (2) To a solution of **1** (3.75 g, 8.79×10^{-3} mol) in CH_2Cl_2 (37 ml) were added Et_3N (1.84 ml, 1.32×10^{-2} mol) and allyloxyoxalyl chloride (1.96 g, 1.32×10^{-2} mol), successively, at -78°C. After being stirred at 0°C for 10 min, the mixture was quenched with phosphate buffer and extracted with EtOAc (400 ml). The extract was washed with water, a saturated aqueous solution of NaHCO_3 , a saturated aqueous solution of NH_4Cl and brine, successively. The organic layer was dried and concentrated under reduced pressure to give **9** as an oil. $^1\text{H-NMR}$ (CDCl_3) δ : 0.04 (3H, s), 0.08 (3H, s), 0.85 (9H, s), 1.23 (3H, d, $J=6$ Hz), 1.47 (9H, s), 1.70–1.90 (1H, m), 2.05–2.20 (1H, m), 3.10 (1H, dt, $J=13, 5$ Hz), 3.22 (1H, t, $J=4$ Hz), 3.30–3.50 (1H, m), 3.90–4.10 (1H, m), 3.92 (1H, d, $J=18$ Hz), 4.16 (1H, d, $J=18$ Hz), 4.31 (1H, qd, $J=6, 4$ Hz), 4.51 (1H, t, $J=4$ Hz), 4.80 (2H, d, $J=6$ Hz), 5.32 (1H, d, $J=11$ Hz), 5.41 (1H, dd, $J=17, 1$ Hz), 5.97 (1H, ddt, $J=17, 10, 6$ Hz). IR (CHCl_3): 1810, 1754, 1727, 1695 cm^{-1} . This crude oil was dissolved in toluene (4 ml) and triethyl phosphite (12 ml) was added, and the whole was heated at 60°C for 3 h. After removal of excess triethyl phosphite and solvent under reduced pressure, the residue was subjected to column chromatography on silica gel (100 g) using a mixture of hexane and EtOAc (4:1) as eluent. The eluate was concentrated under reduced pressure to give a pale yellow oil, which was crystallized from hexane to give **2** (3.03 g, 67%) as colorless crystals, mp 86–89°C. $^1\text{H-NMR}$ (CDCl_3) δ : 0.08 (6H, s), 0.88 (9H, s), 1.22 (3H, d, $J=6.1$ Hz), 1.46 (9H, s), 1.50–1.70 (1H, m), 1.75–1.90 (1H, m), 2.86 (1H, brt, $J=12.0$ Hz), 2.99 (1H, td, $J=12.0, 5.0$ Hz), 3.22 (1H, dd, $J=5.2, 3.6$ Hz), 3.51 (1H, br d, $J=14.8$ Hz), 4.15–4.20 (1H, m), 4.24 (1H, dd, $J=6.5, 3.6$ Hz), 4.20–4.40 (1H, m), 4.70 (1H, brdd, $J=13.4, 5.4$ Hz), 4.81 (1H, brdd, $J=13.4, 5.4$ Hz), 5.26 (1H, dd, $J=10.5, 1.2$ Hz), 5.43 (1H, dd, $J=17.2, 1.5$ Hz), 5.62 (1H, d, $J=14.8$ Hz), 5.97 (1H, ddt, $J=17.2, 10.5, 5.4$ Hz). $^{13}\text{C-NMR}$ (CDCl_3) δ : -4.9, -4.2, 18.0, 22.4, 25.7 (3C), 28.4 (3C), 28.8, 42.9, 43.0, 46.0, 54.7, 61.8, 65.7, 66.1, 76.7, 80.4, 118.5, 125.8, 131.5, 140.3, 154.5, 160.6, 176.8. IR (KBr): 2977, 2951, 2930, 2858, 1777, 1715, 1699, 1649 cm^{-1} . $[\alpha]_D^{25} + 104^\circ$ ($c=0.85$, CHCl_3). Anal. Calcd for $\text{C}_{26}\text{H}_{42}\text{N}_2\text{O}_8\text{Si}$: C, 61.63; H, 8.36; N, 5.53. Found: C, 61.69; H, 8.56; N, 5.56. MS (FAB) m/z : 507 ($\text{M}+\text{H}^+$).

Allyl (8*S*,9*R*,10*S*)-10-[(*R*)-1-(*tert*-Butyldimethylsilyloxy)ethyl]-11-oxo-1,5-diazatricyclo[7.2.0.0^{3,8}]undec-2-ene-2-carboxylate (3) To a solution of **2** (600 mg, 1.18×10^{-3} mol) and 2,6-lutidine (206 μl , 1.77×10^{-3} mol) in CH_2Cl_2 (6 ml) was added TMSOTf (284 μl , 1.47×10^{-3} mol) at 0°C. After being stirred at the same temperature for 15 min, a saturated aqueous solution of NaHCO_3 was added and the mixture was extracted with EtOAc. The extract was washed with brine, dried and concentrated under reduced pressure to give **3** (440 mg, 91%) as a pale yellow oil, which was immediately used for the next reaction without further purification due to its instability.

$^1\text{H-NMR}$ (CDCl_3) δ : 0.08 (6H, s), 0.88 (9H, s), 1.24 (3H, d, $J=6.2$ Hz), 1.57 (1H, qd, $J=12, 4$ Hz), 1.50–1.80 (1H, m), 1.85–1.95 (1H, m), 2.79 (1H, ddd, $J=14, 12, 2$ Hz), 2.97 (1H, brtd, $J=12, 5$ Hz), 3.18 (1H, dd, $J=6.4, 3.5$ Hz), 3.24 (1H, brd, $J=14$ Hz), 3.36 (1H, d, $J=14.2$ Hz), 4.17 (1H, dd, $J=10.4, 3.5$ Hz), 4.15–4.20 (1H, m), 4.68 (1H, dd, $J=13.5, 5.4$ Hz), 4.78 (1H, dd, $J=13.5, 5.4$ Hz), 5.25 (1H, d, $J=10.6$ Hz), 5.42 (1H, brd, $J=17.0$ Hz), 5.93 (1H, ddt, $J=17.0, 10.6, 5.4$ Hz).

Allyl (8*S*,9*R*,10*S*)-5-Acetyl-10-[(*R*)-1-(*tert*-butyldimethylsilyloxy)ethyl]-11-oxo-1,5-diazatricyclo[7.2.0.0^{3,8}]undec-2-ene-2-carboxylate (10a) To a solution of the above-mentioned crude product **3** (217 mg, 5.34×10^{-4} mol) and Et_3N (117 μl , 0.84×10^{-4} mol) in CH_2Cl_2 (2.5 ml) was added acetyl chloride (57 μl , 8.0×10^{-4} mol) at 0°C. After being stirred for 15 min, the mixture was diluted with EtOAc and washed with a saturated aqueous solution of NH_4Cl , a saturated aqueous solution of NaHCO_3 , and then brine. The organic layer was dried and concentrated under reduced pressure. The residue was subjected to HPLC using CHCl_3 as eluent to afford **10a** (208 mg, 87%) as colorless crystals, mp 49–54°C. $^1\text{H-NMR}$ (CDCl_3) δ : 0.08 (6H, s), 0.88 (9H, s), 1.21 (3H, d, $J=6.2$ Hz), 1.45–1.70 (1H, m), 1.80–2.00 (1H, m), 2.11, 2.16 (3H, s $\times 2$), 2.67, 3.24 (1H, m $\times 2$), 3.00–3.15 (1H, m), 3.22 (1H, dd, $J=5.8, 3.6$ Hz), 3.40, 3.75 (1H, d $\times 2$, $J=15.2$ Hz), 3.96, 4.85 (1H, brd $\times 2$, $J=13$ Hz), 4.15–4.30 (1H, m), 4.27 (1H, dd, $J=10.8, 3.6$ Hz), 4.65–4.85 (2H, m), 5.28 (1H, d, $J=10.5$ Hz), 5.45 (1H, brd, $J=17$ Hz), 5.50, 6.09 (1H, brd $\times 2$, $J=15$ Hz), 5.90–6.05 (1H, m). IR (KBr): 1782, 1718, 1649 cm^{-1} . Anal. Calcd for $\text{C}_{23}\text{H}_{36}\text{N}_2\text{O}_5\text{Si}$: C, 61.58; H, 8.09; N, 6.24. Found: C, 61.49; H, 8.24; N, 6.13. MS (FAB) m/z : 449 ($\text{M}+\text{H}^+$).

Allyl (8*S*,9*R*,10*S*)-5-[2-(Allyloxycarbonylamino)acetyl]-10-[(*R*)-1-(*tert*-butyldimethylsilyloxy)ethyl]-11-oxo-1,5-diazatricyclo[7.2.0.0^{3,8}]undec-2-ene-2-carboxylate (10b) A solution of **3**, freshly prepared from **2** (250 mg, 4.93×10^{-4} mol) in a manner similar to that described above, in CH_2Cl_2 (0.5 ml) was added to a mixture of 1,1'-carbonyldiimidazole (CDI, 101 mg, 6.20×10^{-4} mol) and *N*-(allyloxycarbonyl)glycine^{13d} (98.2 mg, 6.17×10^{-4} mol) in CH_2Cl_2 (3 ml) at 0°C. After being stirred at the same temperature for 15 min, the mixture was diluted with EtOAc and washed with a saturated aqueous solution of NH_4Cl , a saturated aqueous solution of NaHCO_3 , and then brine. The organic layer was dried and concentrated under reduced pressure. The crude product was subjected to column chromatography on silica gel (8 g) using a mixture of EtOAc and hexane (1:1) as eluent to give **10b** (138 mg, 51%) as a colorless viscous oil. $^1\text{H-NMR}$ (CDCl_3) δ : 0.08 (6H, s), 0.88 (9H, s), 1.21 (3H, d, $J=6.0$ Hz), 1.45–1.70 (1H, m), 1.80–2.00 (1H, m), 2.70–3.30 (2H, m), 3.21 (1H, dd, $J=5.7, 3.7$ Hz), 3.46, 3.73 (1H, brd $\times 2$, $J=15.0$ Hz), 3.87, 4.80 (1H, brd $\times 2$, $J=13$ Hz), 3.90–4.20 (2H, m), 4.21 (1H, m), 4.28 (1H, dd, $J=11.0, 3.7$ Hz), 4.59 (2H, brd, $J=5.3$ Hz), 4.70–4.90 (2H, m), 5.15–5.50 (4H, m), 5.47, 6.10 (1H, brd $\times 2$, $J=15$ Hz), 5.62, 5.78 (1H, m $\times 2$), 5.75–6.15 (2H, m). IR (KBr): 3343, 1782, 1724, 1657 cm^{-1} . MS (FAB) m/z : 548 ($\text{M}+\text{H}^+$).

Allyl (8*S*,9*R*,10*S*)-5-[3-(Allyloxycarbonylamino)propionyl]-10-[(*R*)-1-(*tert*-butyldimethylsilyloxy)ethyl]-11-oxo-1,5-diazatricyclo[7.2.0.0^{3,8}]undec-2-ene-2-carboxylate (10c) A solution of **3**, freshly prepared from **2** (370 mg, 7.30×10^{-4} mol) in a manner similar to that described above, in CH_2Cl_2 (2 ml) was added to a mixture of CDI (178 mg, 1.10×10^{-3} mol) and 3-(allyloxycarbonylamino)propionic acid (190 mg, 1.10×10^{-3} mol) in CH_2Cl_2 (1.5 ml) at 0°C. After being stirred at the same temperature for 20 min, the mixture was diluted with EtOAc and washed with a saturated aqueous solution of NH_4Cl , a saturated aqueous solution of NaHCO_3 , and then brine. The organic layer was dried and concentrated under reduced pressure. The residue was subjected to column chromatography on silica gel (12 g) using a mixture of EtOAc and hexane (1:1) as eluent to give **10c** (227 mg, 55%) as a colorless viscous oil. $^1\text{H-NMR}$ (CDCl_3) δ : 0.08 (6H, s), 0.88 (9H, s), 1.21 (3H, d, $J=6.1$ Hz), 1.45–1.70 (1H, m), 1.75–2.00 (1H, m), 2.40–3.25 (5H, m), 3.38, 3.70 (1H, brd $\times 2$, $J=14$ Hz), 3.40–3.55 (2H, m), 3.97, 4.82 (1H, brd, $J=14$ Hz), 4.15–4.30 (2H, m), 4.54 (2H, brd, $J=5.4$ Hz), 4.65–4.85 (2H, m), 5.15–5.65 (5H, m), 5.48, 6.11 (1H, brd $\times 2$, $J=14$ Hz), 5.80–6.05 (2H, m). IR (KBr): 3338, 1782, 1721, 1648 cm^{-1} . MS (FAB) m/z : 562 ($\text{M}+\text{H}^+$).

Allyl (8*S*,9*R*,11*S*)-5-[2-(*N*-Allyloxycarbonyl-*N*-methylamino)acetyl]-10-[(*R*)-1-(*tert*-butyldimethylsilyloxy)ethyl]-11-oxo-1,5-diazatricyclo[7.2.0.0^{3,8}]undec-2-ene-2-carboxylate (10d) A solution of **3**, freshly prepared from **2** (2.04 g, 4.02×10^{-3} mol) in a manner similar to that described above, in DMF (8 ml) was added to a mixture of CDI (899 mg, 5.54×10^{-3} mol) and *N*-allyloxycarbonylsarcosine (870 mg, 5.02×10^{-3} mol) in DMF (17 ml) at 0°C. After being stirred at room temperature for 6 h, the mixture was diluted with EtOAc and washed with a saturated aqueous solution of NH_4Cl , a saturated aqueous solution of NaHCO_3 , and then brine. The

organic layer was dried and concentrated under reduced pressure. The residue was subjected to column chromatography on silica gel (80 g) using a mixture of EtOAc and hexane (3 : 2) as eluent to give **10d** (1.60 g, 71%) as a pale yellow viscous oil. ¹H-NMR (CDCl₃) δ: 0.08 (6H, s), 0.89 (9H, s), 1.22 (3H, d, *J*=6.2 Hz), 1.50–1.70 (1H, m), 1.80–1.95 (1H, m), 2.65–3.30 (1H, m), 2.99, 3.00 (3H, s×2), 3.08 (1H, m), 3.22 (1H, m), 3.48, 3.72 (1H, br d×2, *J*=14 Hz), 3.80–4.90 (8H, m), 4.26 (1H, dd, *J*=10.6, 3.4 Hz), 5.10–6.10 (7H, m). IR (KBr): 3338, 1782, 1721, 1648 cm⁻¹. MS (FAB) *m/z*: 562 (M+H)⁺.

Allyl (8S,9R,10S)-5-[3-(*tert*-Butoxycarbonylamino)propionyl]-10-[(*R*)-1-(*tert*-butyldimethylsilyloxy)ethyl]-11-oxo-1,5-diazatricyclo[7.2.0.0^{3,8}]-undec-2-ene-2-carboxylate (10e**)** A solution of **3**, freshly prepared from **2** (600 mg, 1.18×10⁻³ mol) in a manner similar to that described above, in DMF (4 ml) was added to a mixture of CDI (288 mg, 1.78×10⁻³ mol) and 3-(*tert*-butoxycarbonylamino)propionic acid¹⁶ (336 mg, 1.78×10⁻³ mol) in DMF (2 ml) at 0 °C. After being stirred at the same temperature for 3 h, the mixture was diluted with EtOAc and washed with a saturated aqueous solution of NH₄Cl, a saturated aqueous solution of NaHCO₃, and then brine. The organic layer was dried and concentrated under reduced pressure. The residue was subjected to column chromatography on silica gel (15 g) using a mixture of EtOAc and hexane (1 : 1) as eluent to give **10e** (591 mg, 86%) as a colorless viscous oil. ¹H-NMR (CDCl₃) δ: 0.08 (6H, s), 0.88 (9H, s), 1.22 (3H, d, *J*=6.3 Hz), 1.43 (9H, s), 1.45–1.70 (1H, m), 1.75–2.00 (1H, m), 2.40–3.25 (5H, m), 3.30–3.50 (2H, m), 3.38, 3.70 (1H, br d×2, *J*=14 Hz), 3.97, 4.82 (1H, br d×2, *J*=14 Hz), 4.15–4.30 (2H, m), 4.65–4.90 (2H, m), 5.20–5.55 (3H, m), 5.48 and 6.11 (1H, br d, *J*=14 Hz), 5.85–6.05 (1H, m). IR (KBr): 3361, 1783, 1714, 1647 cm⁻¹. MS (FAB) *m/z*: 578 (M+H)⁺.

***N,N'*-Bis(allyloxycarbonyl)amidinopyrazole** This reagent was prepared following the literature procedure for the preparation of *N,N'*-bis(*tert*-butoxycarbonyl)amidinopyrazole.¹³ To a suspension of amidinopyrazole hydrochloride (6.00 g, 40.9 mmol) in DMF–THF (1 : 1, 60 ml) were added allyl chloroformate (4.55 ml, 43 mmol) and Et₃N (11.8 ml, 85 mmol) at 0 °C. After being stirred at room temperature for 3 h, the mixture was diluted with EtOAc (100 ml) and washed with water, a saturated aqueous solution of NH₄Cl and brine, successively. The organic layer was dried and concentrated under reduced pressure. The crude product was subjected to column chromatography on silica gel (200 g) using a mixture of EtOAc and hexane (1 : 1) as eluent to give *N*-(allyloxycarbonyl)amidinopyrazole (7.02 g, 90%) as a colorless oil. ¹H-NMR (CDCl₃) δ: 4.69 (2H, d, *J*=6 Hz), 5.27 (1H, d, *J*=10 Hz), 5.38 (1H, d, *J*=17 Hz), 6.03 (1H, ddt, *J*=17, 10, 6 Hz), 6.43 (1H, m), 7.71 (1H, br s), 7.60–7.90 (1H, m), 8.47 (1H, d, *J*=3 Hz), 9.07 (1H, m). To a solution of this oil (4.60 g, 27.7 mmol) in THF (100 ml) was added sodium hydride (55% mineral oil dispersion, 2.55 g, 58.4 mmol, washed with hexane) at 0 °C. After being stirred at room temperature for 30 min, a solution of diallyl dicarbonate (5.6 g, 30 mmol) in THF (10 ml) was added at 0 °C and the mixture was stirred at room temperature for 1.5 h. The reaction mixture was quenched with a saturated aqueous NH₄Cl solution and extracted with EtOAc. The extract was washed with brine, dried and concentrated under reduced pressure. The residue was subjected to column chromatography on silica gel (350 g) using a mixture of EtOAc and hexane (2 : 1) as eluent to give *N,N'*-bis(allyloxycarbonyl)amidinopyrazole (5.4 g, 70%) as a colorless oil. ¹H-NMR (CDCl₃) δ: 4.65–4.75 (4H, m), 5.20–5.50 (4H, m), 5.85–6.15 (2H, m), 6.47 (1H, dd, *J*=3, 1 Hz), 7.67 (1H, m), 8.32 (1H, d, *J*=3 Hz), 9.31 (1H, br s).

Allyl (8S,9R,10S)-5-[3-[[*N,N'*-Bis(allyloxycarbonyl)amido]amino]propionyl]-10-[(*R*)-1-(*tert*-butyldimethylsilyloxy)ethyl]-11-oxo-1,5-diazatricyclo[7.2.0.0^{3,8}]-undec-2-ene-2-carboxylate (10f**)** To a solution of **10e** (485 mg, 8.39×10⁻⁴ mol) and 2,6-lutidine (294 μl, 2.52×10⁻³ mol) in CH₂Cl₂ (6 ml) was added TMSOTf (352 μl, 1.82×10⁻³ mol) at 0 °C. After being stirred at room temperature for 15 min, the mixture was quenched with a saturated aqueous solution of NaHCO₃, and extracted with EtOAc. The extract was washed with brine, dried and concentrated under reduced pressure. The residue was dissolved in THF (3 ml), and a solution of *N,N'*-bis(allyloxycarbonyl)amidinopyrazole (234 mg, 8.40×10⁻⁴ mol) in THF (2 ml) was added at room temperature. After being stirred at the same temperature for 15 h, the mixture was diluted with EtOAc and washed with a saturated aqueous solution of NH₄Cl and brine. The organic layer was dried and concentrated under reduced pressure. The crude product was subjected to HPLC using CHCl₃ as eluent to give **10f** (203 mg, 35%) as a pale yellow viscous oil. ¹H-NMR (CDCl₃) δ: 0.08 (6H, s), 0.88 (9H, s), 1.21 (3H, d, *J*=6.3 Hz), 1.45–1.65 (1H, m), 1.75–2.00 (1H, m), 2.50–3.25 (3H, m), 3.07 (1H, m), 3.21 (1H, dd, *J*=5.8, 3.6 Hz), 3.41, 3.69 (1H, br d×2, *J*=14 Hz), 3.70–3.85 (2H, m), 3.98, 4.89 (1H, br d×2, *J*=14 Hz), 4.15–4.25 (1H, m), 4.27 (1H, dd, *J*=10.6, 3.6 Hz), 4.60 (2H, d, *J*=5.8 Hz), 4.65

(2H, d, *J*=5.8 Hz), 4.65–4.80 (2H, m), 5.20–5.50 (6H, m), 5.46, 6.08 (1H, br d×2, *J*=14 Hz), 5.80–6.10 (3H, m), 8.88, 9.00 (1H, br t×2, *J*=6 Hz), 11.65, 11.69 (1H, br s×2). IR (KBr): 3342, 1784, 1733, 1641, 1562 cm⁻¹. MS (FAB) *m/z*: 688 (M+H)⁺.

Allyl (8S,9R,11S)-10-[(*R*)-1-(*tert*-Butyldimethylsilyloxy)ethyl]-11-oxo-5-(3-pyridylcarbonyl)-1,5-diazatricyclo[7.2.0.0^{3,8}]-undec-2-ene-2-carboxylate (10g**)** To a solution of **3**, freshly prepared from **2** (260 mg, 5.13×10⁻⁴ mol) in a manner similar to that described above, in CH₂Cl₂ (3 ml) was added Et₃N (179 μl, 1.28×10⁻³ mol) and nicotinoyl chloride hydrochloride (114 mg, 6.40×10⁻⁴ mol) at 0 °C. After being stirred at the same temperature for 30 min, the mixture was poured into phosphate buffer (pH 7.4, 10 ml) and extracted with EtOAc. The extract was washed with brine, dried and concentrated under reduced pressure to give an oily residue, which was purified by column chromatography on silica gel (8 g) using a mixture of EtOAc and methanol (1 : 0 to 9 : 1) as eluent to afford **10g** (207 mg, 79%) as a pale yellow viscous oil. ¹H-NMR (CDCl₃) δ: 0.08 (6H, s), 0.88 (9H, s), 1.23 (3H, d, *J*=6.2 Hz), 1.60–1.80 (1H, m), 1.80–2.00 (1H, m), 2.80–3.30 (1H, m), 3.13 (1H, td, *J*=11.0, 5.0 Hz), 3.27 (1H, dd, *J*=5.4, 3.8 Hz), 3.50–4.10 (1H, m), 4.23 (1H, m), 4.28 (1H, dd, *J*=10.8, 3.8 Hz), 4.30–6.20 (7H, m), 7.36 and 7.38 (1H, d×2, *J*=8.0 Hz), 7.76, 7.77 (1H, dd×2, *J*=8.0, 2.0 Hz), 8.67, 8.68 (1H, s×2), 8.69, 8.70 (1H, d×2, *J*=2.0 Hz). IR (KBr): 1782, 1724, 1640 cm⁻¹. MS (FAB) *m/z*: 512 (M+H)⁺.

Allyl (8S,9R,10S)-10-[(*R*)-1-(*tert*-Butyldimethylsilyloxy)ethyl]-11-oxo-5-(4-pyridylcarbonyl)-1,5-diazatricyclo[7.2.0.0^{3,8}]-undec-2-ene-2-carboxylate (10h**)** A solution of **3**, freshly prepared from **2** (501 mg, 9.89×10⁻⁴ mol) in a manner similar to that described above, in DMF (0.5 ml) was added to a mixture of CDI (192 mg, 1.18×10⁻³ mol) and isonicotinic acid (152 mg, 1.24×10⁻³ mol) in DMF (4 ml) at 0 °C. After being stirred at the same temperature for 35 min, the mixture was diluted with EtOAc and washed with a saturated aqueous solution of NH₄Cl, a saturated aqueous solution of NaHCO₃, and then brine. The organic layer was dried and concentrated under reduced pressure. The crude product was subjected to column chromatography on silica gel (15 g) using a mixture of EtOAc and methanol (1 : 0 to 9 : 1) as eluent to give **10h** (350 mg, 69%) as a colorless viscous oil. ¹H-NMR (CDCl₃) δ: 0.08 (6H, s), 0.88 (9H, s), 1.23 (3H, d, *J*=6.2 Hz), 1.50–2.10 (2H, m), 2.80–3.20 (1H, m), 3.13 (1H, td, *J*=12.0, 5.0 Hz), 3.27 (1H, m), 3.40–4.00 (1H, m), 4.23 (1H, m), 4.28 (1H, dd, *J*=10.8, 3.6 Hz), 4.30–6.30 (7H, m), 7.28 (2H, d, *J*=5.8 Hz), 8.70 (2H, d, *J*=5.8 Hz). IR (KBr): 1783, 1721, 1642 cm⁻¹. MS (FAB) *m/z*: 512 (M+H)⁺.

Allyl (8S,9R,10S)-5-Allyloxycarbonyl-10-[(*R*)-1-(hydroxy)ethyl]-11-oxo-1,5-diazatricyclo[7.2.0.0^{3,8}]-undec-2-ene-2-carboxylate (10i**)** To a solution of **2** (250 mg, 4.93×10⁻⁴ mol) and 2,6-lutidine (86 μl, 7.4×10⁻⁴ mol) in CH₂Cl₂ (2.5 ml) was added TMSOTf (118 μl, 6.11×10⁻⁴ mol) at 0 °C. After being stirred at room temperature for 15 min, the mixture was cooled at 0 °C, and a saturated aqueous solution of NaHCO₃ (25 μl) was added. Stirring was continued for 15 min, then, Et₃N (86 μl, 6.2×10⁻⁴ mol) and allyl chloroformate (65 μl, 6.2×10⁻⁴ mol) were added at 0 °C, and the whole was stirred for 10 min. The mixture was diluted with EtOAc, washed with a saturated aqueous solution of NH₄Cl, a saturated aqueous solution of NaHCO₃, and then brine. The organic layer was dried and concentrated under reduced pressure. The residue was subjected to column chromatography on silica gel (8 g) using a mixture of EtOAc and hexane (1 : 1) as eluent to give **10i** (198.9 mg, 82%) as a colorless oil. ¹H-NMR (CDCl₃) δ: 0.08 (6H, s), 0.88 (9H, s), 1.22 (3H, d, *J*=6.3 Hz), 1.60 (1H, dq, *J*=13.0, 4.0 Hz), 1.80–1.90 (1H, m), 2.85–3.10 (2H, m), 3.22 (1H, dd, *J*=6.1, 3.7 Hz), 3.58 (1H, br d, *J*=15.0 Hz), 4.15–4.30 (1H, m), 4.25 (1H, d, *J*=11.0, 3.7 Hz), 4.30–4.50 (1H, m), 4.60 (2H, d, *J*=5.5 Hz), 4.65–4.85 (2H, m), 5.20–5.50 (4H, m), 5.72 (1H, d, *J*=15 Hz), 5.85–6.05 (2H, m). IR (CHCl₃): 1780, 1699, 1650 cm⁻¹. MS (FAB) *m/z*: 491 (M+H)⁺.

Allyl (8S,9R,10S)-10-[(*R*)-1-(*tert*-Butyldimethylsilyloxy)ethyl]-5-methyl-11-oxo-1,5-diazatricyclo[7.2.0.0^{3,8}]-undec-2-ene-2-carboxylate (10j**)** To a solution of **3**, freshly prepared from **2** (300 mg, 5.92×10⁻⁴ mol) in a manner similar to that described above, in DMF (2 ml) were added Et₃N (420 μl, 3.0×10⁻³ mol) and a solution of iodomethane (170 mg, 1.20×10⁻³ mol) in DMF (0.5 ml) at 0 °C. After being stirred at the same temperature for 1 h, the mixture was diluted with EtOAc and washed with a saturated aqueous solution of NaHCO₃ and brine. The organic layer was dried and concentrated under reduced pressure. The crude product was subjected to column chromatography on silica gel (25 g) using a mixture of EtOAc and methanol (95 : 5) as eluent to give **10j** (97.8 mg, 39%) as a pale yellow viscous oil. ¹H-NMR (CDCl₃) δ: 0.07 (6H, s), 0.88 (9H, s), 1.23 (3H, d, *J*=6.3 Hz), 1.75–1.85 (2H, m), 2.15–2.35 (1H, m), 2.37 (3H, s), 2.71 (1H, d, *J*=12.3 Hz), 2.75–2.90 (1H, m), 2.99 (1H, br d, *J*=12 Hz), 3.24 (1H, dd, *J*=6.3, 3.6 Hz), 4.10–4.25 (1H, m), 4.21 (1H, dd, *J*=8.3, 3.6 Hz), 4.39 (1H, d, *J*=12.3 Hz),

4.60—4.85 (2H, m), 5.25 (1H, dd, $J=10.3$, 1.2 Hz), 5.42 (1H, dd, $J=17.3$, 1.7 Hz), 5.93 (1H, ddt, $J=17.3$, 10.7, 5.3 Hz). IR (KBr): 1783, 1720, 1648 cm^{-1} . MS (FAB) m/z : 421 (M+H)⁺.

Allyl (8S,9R,10S)-10-[(R)-1-(*tert*-Butyldimethylsilyloxy)ethyl]-5-(carbamoyl)methyl-11-oxo-1,5-diazatricyclo[7.2.0.0^{3,8}]undec-2-ene-2-carboxylate (10k) To a solution of **3**, freshly prepared from **2** (506 mg, 1.00×10^{-3} mol) in a manner similar to that described above, in DMF (5 ml) were added K_2CO_3 (138 mg, 1.00×10^{-3} mol) and 2-iodoacetamide (925 mg, 5.00×10^{-3} mol) at room temperature. After being stirred at the same temperature for 1 h, the mixture was diluted with EtOAc and washed with a saturated aqueous solution of NH_4Cl and brine. The organic layer was dried and concentrated under reduced pressure. The residue was subjected to column chromatography on silica gel (20 g) using a mixture of EtOAc and methanol (1:0 to 10:1) as eluent to give **10k** (416 mg, 90%) as a colorless viscous oil. ¹H-NMR (CDCl_3) δ : 0.08 (6H, s), 0.88 (9H, s), 1.24 (3H, d, $J=6.2$ Hz), 1.60—1.90 (2H, m), 2.50 (1H, td, $J=11.6$, 2.7 Hz), 2.80—3.00 (1H, dd, $J=8.3$, 3.6 Hz), 2.92 (1H, d, $J=12.1$ Hz), 3.04 (1H, br d, $J=12$ Hz), 3.10 (2H, s), 3.23 (1H, dd, $J=6.2$, 3.5 Hz), 4.10—4.30 (2H, m), 4.45 (1H, d, $J=12.1$ Hz), 4.60—4.90 (2H, m), 5.26 (1H, dd, $J=10.5$, 1.2 Hz), 5.42 (1H, dd, $J=17.2$, 1.4 Hz), 5.70 (1H, br s), 5.95 (1H, ddt, $J=17.2$, 10.5, 5.4 Hz), 6.89 (1H, br s). IR (KBr): 3454, 3283, 1780, 1716, 1667 cm^{-1} . MS (FAB) m/z : 464 (M+H)⁺.

Allyl (8S,9R,10S)-10-[(R)-1-(*tert*-Butyldimethylsilyloxy)ethyl]-5-(carbamoyl)-11-oxo-1,5-diazatricyclo[7.2.0.0^{3,8}]undec-2-ene-2-carboxylate (10l) To a solution of **3**, freshly prepared from **2** (250 mg, 4.93×10^{-4} mol) in a manner similar to that described above, in CH_2Cl_2 (3 ml) was added trimethylsilyl isocyanate (117 μl , 8.64×10^{-4} mol) at 0°C. After being stirred at the same temperature for 1 h, the mixture was diluted with EtOAc and washed with a saturated aqueous solution of NH_4Cl . The organic layer was dried and concentrated under reduced pressure. The crude product was subjected to column chromatography on silica gel (8 g) using a mixture of EtOAc and methanol (1:0 to 95:5) as eluent and then HPLC using CHCl_3 as eluent to give **10l** (135.5 mg, 61%) as a colorless viscous oil. ¹H-NMR (CDCl_3) δ : 0.08 (6H, s), 0.88 (9H, s), 1.21 (3H, d, $J=6.4$ Hz), 1.61 (1H, qd, $J=12$, 4 Hz), 1.75—1.90 (1H, m), 2.85 (1H, ddd, $J=14$, 12, 2 Hz), 3.08 (1H, td, $J=11.5$, 5.5 Hz), 3.22 (1H, dd, $J=5.9$, 3.8 Hz), 3.67 (1H, br d, $J=15$ Hz), 4.21 (1H, m), 4.27 (1H, dd, $J=10.7$, 3.8 Hz), 4.52 (1H, br d, $J=14$ Hz), 4.60—4.90 (2H, m), 4.92 (2H, br s), 5.10 (1H, br d, $J=15$ Hz), 5.29 (1H, dd, $J=10.5$, 1.3 Hz), 5.45 (1H, br d, $J=17.2$ Hz), 5.96 (1H, ddt, $J=17.2$, 10.5, 5.3 Hz). IR (KBr): 3453, 3347, 3215, 1772, 1718, 1651, 1602 cm^{-1} . MS (FAB) m/z : 450 (M+H)⁺.

N-(Allyloxycarbonyl)guanidine To a solution of guanidine hydrochloride (2.00 g, 20.9 mmol) in a mixture of H_2O and THF (3:1, 40 ml) were added 2N NaOH (21 ml) and a solution of allyl chloroformate (2.53 g, 21.0 mmol) in THF (10 ml) at room temperature. After being stirred for 1 h, the mixture was concentrated under reduced pressure to ca. 40 ml. The resultant precipitates that emerged were sparingly soluble in water and removed by filtration. The filtrate was further concentrated under reduced pressure to ca. 5 ml. The resultant solids which were water-soluble were collected by filtration and washed with cold water to give *N*-(allyloxycarbonyl)guanidine (682 mg, 23%) as colorless crystals, mp 137—139°C. ¹H-NMR ($\text{DMSO}-d_6$) δ : 4.39 (2H, br d, $J=5$ Hz), 5.11 (1H, br d, $J=10$ Hz), 5.22 (1H, br d, $J=17$ Hz), 5.90 (1H, ddt, $J=17$, 10, 5 Hz), 6.50—7.50 (4H, m). IR (KBr): 3444, 3401, 3333, 3045, 1650, 1627, 1592, 1527 cm^{-1} . MS (EI) m/z : 143 (M)⁺.

Allyl (8S,9R,10S)-5-[[N^o-(Allyloxycarbonyl)guanidino]carbonyl]-10-[(R)-1-(*tert*-butyldimethylsilyloxy)ethyl]-11-oxo-1,5-diazatricyclo[7.2.0.0^{3,8}]undec-2-ene-2-carboxylate (10m) A solution of **3**, freshly prepared from **2** (450 mg, 8.88×10^{-4} mol) in a manner similar to that described above, and *N,N'*-diisopropylethylamine (160 μl , 9.19×10^{-4} mol) in CH_2Cl_2 (5 ml) were added to a solution of triphosgene (90.0 mg, 3.03×10^{-4} mol) in CH_2Cl_2 (1 ml) at 0°C. After being stirred at the same temperature for 30 min, DMAP (108 mg, 8.84×10^{-4} mol) and (allyloxycarbonyl)guanidine (160 mg, 1.12×10^{-3} mol) were added and the mixture was stirred at 0°C for 2 h. The mixture was diluted with EtOAc and washed with a saturated aqueous solution of NaHCO_3 and brine. The organic layer was dried and concentrated under reduced pressure. The crude product was subjected to column chromatography on silica gel (15 g) using a mixture of EtOAc and hexane (2:3) as eluent to give **10m** (187 mg, 31%) as a pale yellow viscous oil. ¹H-NMR (CDCl_3) δ : 0.07 (6H, s), 0.88 (9H, s), 1.22 (3H, d, $J=6.1$ Hz), 1.40—1.70 (1H, m), 1.75—1.90 (1H, m), 2.75—3.10 (2H, m), 3.21 (1H, dd, $J=6.1$, 3.7 Hz), 3.52 (1H, br d, $J=15$ Hz), 4.15—4.25 (1H, m), 4.23 (1H, dd, $J=10.7$, 3.7 Hz), 4.50—4.80 (2H, m), 4.65 (2H, d, $J=5.8$ Hz), 4.76 (2H, d, $J=5.4$ Hz), 5.25—5.35 (3H, m), 5.36 (1H, br d, $J=17.2$ Hz), 5.47 (1H, dd,

$J=17.2$, 1.2 Hz), 5.80—6.20 (3H, m), 7.70—8.10 (1H, m). IR (KBr): 3408, 1783, 1729, 1651 cm^{-1} . MS (FAB) m/z : 576 (M+H)⁺.

3-Amino-1-(allyloxycarbonyl)pyrrolidine Hydrogen Chloride To a solution of 3-(*tert*-butoxycarbonylamino)pyrrolidine (1.86 g, 10.0 mmol) in CH_2Cl_2 (20 ml) was added Et_3N (1.46 ml, 10.5 mmol) and allyl chloroformate (1.11 ml, 10.5 mmol) at 0°C. After being stirred at the same temperature for 1 h, a saturated aqueous solution of NH_4Cl was added and extracted with EtOAc. The extract was washed with brine, dried and concentrated under reduced pressure. The residue was dissolved in EtOAc (10 ml) and treated with 4N HCl in EtOAc (5 ml) at room temperature. A pale yellow oil that emerged was separated by decantation and dried under reduced pressure. 3-Amino-1-(allyloxycarbonyl)pyrrolidine hydrogen chloride (2.08 g, ca. 100%) thus obtained as a pale yellow oil was used for the next reaction without further purification. ¹H-NMR (CDCl_3) δ : 2.20—2.40 (2H, m), 3.40—4.15 (5H, m), 4.58 (2H, m), 5.10 (1H, d, $J=10.2$ Hz), 5.31 (1H, d, $J=17.1$ Hz), 5.91 (1H, m), 8.55 (3H, br s).

Allyl (8S,9R,10S)-5-[[1-(Allyloxycarbonyl)pyrrolidin-3-yl]carbonyl]-10-[(R)-1-(*tert*-butyldimethylsilyloxy)ethyl]-11-oxo-1,5-diazatricyclo[7.2.0.0^{3,8}]undec-2-ene-2-carboxylate (10n) To a solution of **3**, freshly prepared from **2** (100 mg, 1.97×10^{-4} mol) in a manner similar to that described above, in CH_2Cl_2 (1 ml) was added a solution of 3-isocyanato-1-(allyloxycarbonyl)pyrrolidine, which was prepared from 3-amino-1-(allyloxycarbonyl)pyrrolidine hydrogen chloride (42 mg, 2.0×10^{-4} mol) and triphosgene (20 mg, 6.7×10^{-5} mol) in the presence of ethyldiisopropylamine (90 μl , 5.0×10^{-4} mol) in CH_2Cl_2 (2 ml), at room temperature. After being stirred at the same temperature for 30 min, a saturated aqueous solution of NaHCO_3 was added and the mixture was extracted with EtOAc. The extract was washed with a saturated aqueous solution of NH_4Cl and brine, dried and concentrated under reduced pressure. After removal of solvent under reduced pressure, the residue was subjected to column chromatography on silica gel (10 g) using EtOAc as eluent to give **10n** (90.4 mg, 76%) as a colorless viscous oil. ¹H-NMR (CDCl_3) δ : 0.07 (6H, s), 0.88 (9H, s), 1.21 (3H, d, $J=6.2$ Hz), 1.55—1.95 (3H, m), 2.00—2.20 (1H, m), 2.86 (1H, br t, $J=13$ Hz), 3.00—3.40 (2H, m), 3.19 (1H, dd, $J=5.8$, 3.5 Hz), 3.50—3.75 (3H, m), 3.61 (1H, d, $J=15.4$ Hz), 4.10—4.40 (3H, m), 4.45—4.65 (3H, m), 4.65—5.10 (3H, m), 5.15—5.50 (4H, m), 5.70—6.05 (3H, m). IR (KBr): 3370, 1782, 1704 1649 cm^{-1} . MS (FAB) m/z : 603 (M+H)⁺.

Allyl (8S,9R,10S)-10-[(R)-1-(*tert*-Butyldimethylsilyloxy)ethyl]-5-(*N*-methylthiocarbamoyl)-11-oxo-1,5-diazatricyclo[7.2.0.0^{3,8}]undec-2-ene-2-carboxylate (10o) To a solution of **3**, freshly prepared from **2** (255 mg, 5.03×10^{-4} mol) in a manner similar to that described above, in CH_2Cl_2 (2 ml) was added methyl isothiocyanate (73 mg, 1.0×10^{-3} mol) at room temperature. After being stirred at the same temperature for 1 h. The mixture was concentrated under reduced pressure. The residue was subjected to column chromatography on silica gel (10 g) using a mixture of EtOAc and hexane (2:1) as eluent to give **10o** (196 mg, 81%) as a colorless viscous oil. ¹H-NMR (CDCl_3) δ : 0.07 (6H, s), 0.88 (9H, s), 1.20 (3H, d, $J=6.2$ Hz), 1.72 (1H, qd, $J=12$, 4 Hz), 1.80—1.90 (1H, m), 3.12 (3H, d, $J=5.3$ Hz), 3.10—3.30 (2H, m), 3.24 (1H, dd, $J=5.7$, 3.7 Hz), 3.75 (1H, d, $J=15.0$ Hz), 4.20 (1H, m), 4.30 (1H, dd, $J=10.7$, 3.7 Hz), 4.70—4.90 (2H, m), 5.27 (1H, br d, $J=15$ Hz), 5.30 (1H, d, $J=10.7$ Hz), 5.46 (1H, dd, $J=17.2$, 1.3 Hz), 5.58 (1H, br d, $J=12$ Hz), 5.95 (1H, ddt, $J=17.2$, 10.7, 5.4 Hz), 6.85—7.00 (1H, m). IR (KBr): 3362, 1781, 1718, 1648 cm^{-1} . MS (FAB) m/z : 480 (M+H)⁺.

1-(Allyloxycarbonyl)pyrrolidin-3-yl Isothiocyanate To a solution 3-amino-1-(allyloxycarbonyl)pyrrolidine (870 mg, 5.1 mmol), which was provided by neutralization of 3-amino-1-(allyloxycarbonyl)pyrrolidine hydrogen chloride by treatment with an aqueous solution of NaHCO_3 , in CH_2Cl_2 (8 ml) was added 1,1'-thiocarbonyldiimidazole (1.00 g, 5.61 mmol) at −78°C. After being stirred at 0°C for 3 h, phosphate buffer (pH 7, 20 ml) was added and the mixture was extracted with EtOAc. The extract was washed with brine, dried and concentrated under reduced pressure. The residue was subjected to column chromatography on silica gel (30 g) using a mixture of EtOAc and hexane (1:1) as eluent to give 1-(allyloxycarbonyl)pyrrolidin-3-yl isothiocyanate (896 mg, 83%) as a pale yellow oil. ¹H-NMR (CDCl_3) δ : 2.19 (2H, m), 3.50—3.75 (4H, m), 4.31 (1H, m), 4.62 (2H, d, $J=5.5$ Hz), 5.23 (1H, d, $J=10.3$ Hz), 5.32 (1H, d, $J=17.2$ Hz), 5.95 (1H, m). IR (CH_2Cl_2): 2090, 1700 cm^{-1} . MS (EI) m/z : 212 (M)⁺.

Allyl (8S,9R,10S)-5-[[N-(Allyloxycarbonyl)pyrrolidin-3-yl]thiocarbamoyl]-10-[(R)-1-(*tert*-butyldimethylsilyloxy)ethyl]-11-oxo-1,5-diazatricyclo[7.2.0.0^{3,8}]undec-2-ene-2-carboxylate (10p) To a solution of **3**, freshly prepared from **2** (300 mg, 5.92×10^{-4} mol) in a manner similar to that described above, in CH_2Cl_2 (2 ml) was added *N*-(allyloxycarbonyl)pyrrolidin-3-yl isothiocyanate (188 mg, 8.88×10^{-4} mol) at room temperature. After being stirred for 1 h, the mixture was concentrated under reduced pres-

sure. The residue was subjected to column chromatography on silica gel (10 g) using a mixture of EtOAc and hexane (1 : 1) as eluent and then HPLC using CHCl_3 as eluent to give **10p** (280 mg, 77%) as a colorless viscous oil. $^1\text{H-NMR}$ (CDCl_3) δ : 0.07 (6H, s), 0.88 (9H, s), 1.20 (3H, d, $J=6.1$ Hz), 1.72 (1H, qd, $J=12$, 4 Hz), 1.80—2.35 (3H, m), 3.10—3.65 (5H, m), 3.24 (1H, dd, $J=5.7$, 3.7 Hz), 3.70—3.85 (1H, m), 3.74 (1H, d, $J=14.8$ Hz), 4.20 (1H, m), 4.30 (1H, m), 4.50—5.05 (5H, m), 5.15—5.55 (5H, m), 5.60 (1H, br d, $J=14$ Hz), 5.85—6.05 (2H, m), 7.09 (1H, m). IR (KBr): 3336, 1783, 1701, 1648, 1539 cm^{-1} . MS (FAB) m/z : 619 ($\text{M}+\text{H}$) $^+$.

***N*-(Allyloxycarbonyl)acetamide hydrochloride** To a solution of acetamide hydrochloride (10.4 g, 1.10×10^{-2} mol) in a mixture of 1 *N* NaOH (220 ml) and THF (100 ml) was added allyl chloroformate (11.6 ml, 1.10×10^{-2} mol) dropwise at 0°C. After being stirred for 2 h at room temperature, the mixture was saturated with NaCl and extracted with EtOAc. The extract was washed with brine, dried and concentrated under reduced pressure. The residue was subjected to column chromatography on silica gel (125 g) using a mixture of EtOAc and MeOH (4 : 1) as eluent to give *N*-(allyloxycarbonyl)acetamide (11.4 g, 73%) as a colorless oil. $^1\text{H-NMR}$ (CDCl_3) δ : 2.12 (3H, s), 4.60 (2H, d, $J=5$ Hz), 5.22 (1H, d, $J=10$ Hz), 5.35 (1H, d, $J=17$ Hz), 5.96 (1H, ddt, $J=17$, 10, 5 Hz), 6.22 (1H, m), 9.25 (1H, m). IR (KBr): 3367, 1777, 1578 cm^{-1} . MS (EI) m/z : 142 (M) $^+$. To a solution of this oil (5.0 g, 35 mmol) in EtOAc (40 ml) was added 4 *N* HCl in EtOAc (20 ml) at 0°C. The solid that emerged was collected by filtration, and washed with EtOAc to afford *N*-(allyloxycarbonyl)acetamide hydrochloride (5.54 g, 89%) as a colorless viscous oil. $^1\text{H-NMR}$ (D_2O) δ : 2.44 (3H, s), 4.83 (2H, d, $J=6$ Hz), 5.39 (2H, d, $J=11$ Hz), 5.46 (2H, d, $J=17$ Hz), 6.04 (1H, ddt, $J=17$, 11, 6 Hz). IR (KBr): 3325, 1754, 1742, 1560, 1550, 1255 cm^{-1} .

Allyl (8*S*,9*R*,10*S*)-5-[*N*-(Allyloxycarbonyl)acetimidoyl]-10-[(*R*)-1-(*tert*-butyldimethylsilyloxy)ethyl]-11-oxo-1,5-diazatricyclo[7.2.0.0 3,8]undec-2-ene-2-carboxylate (10r) To a solution of **3**, freshly prepared from **2** (1.00 g, 1.97×10^{-3} mol) in a manner similar to that described above, in CH_2Cl_2 (10 ml) was added *N*-(allyloxycarbonyl)acetamide hydrochloride (530 mg, 2.97×10^{-3} mol) at 0°C. After being stirred at room temperature for 21 h, the mixture was diluted with EtOAc and washed with a saturated aqueous solution of NaHCO_3 and brine. The organic layer was dried and concentrated under reduced pressure. The crude product was subjected to column chromatography on silica gel (40 g) using a mixture of EtOAc and hexane (2 : 3) as eluent to give **10r** (121 mg, 12%) as a colorless viscous oil. $^1\text{H-NMR}$ (CDCl_3) δ : 0.08 (6H, s), 0.88 (9H, s), 1.21 (3H, d, $J=6.2$ Hz), 1.50—1.80 (1H, m), 1.75—1.95 (1H, m), 2.29 (3H, s), 2.65—3.05 (1H, m), 3.10 (1H, td, $J=12.2$, 6.3 Hz), 3.24 (1H, dd, $J=5.8$, 3.6 Hz), 3.69 (1H, d, $J=14.6$ Hz), 4.22 (1H, m), 4.28 (1H, dd, $J=10.8$, 3.6 Hz), 4.61 (2H, d, $J=5.8$ Hz), 4.65—4.80 (2H, m), 4.80—5.20 (1H, m), 5.22 (1H, dd, $J=10.2$, 1.0 Hz), 5.27 (1H, dd, $J=11.2$, 1.0 Hz), 5.33 (1H, dd, $J=17.3$, 1.6 Hz), 5.44 (1H, dd, $J=17.3$, 1.7 Hz), 5.45—5.80 (1H, m), 5.85—6.10 (2H, m). IR (KBr): 1784, 1716, 1681, 1648, 1567 cm^{-1} . MS (FAB) m/z : 532 ($\text{M}+\text{H}$) $^+$.

Allyl (8*S*,9*R*,10*S*)-5-[*N,N'*-Bis(allyloxycarbonyl)amidino]-10-[(*R*)-1-(*tert*-butyldimethylsilyloxy)ethyl]-11-oxo-1,5-diazatricyclo[7.2.0.0 3,8]undec-2-ene-2-carboxylate (10s) To a solution of **3**, freshly prepared from **2** (600 mg, 1.18×10^{-3} mol) in a manner similar to that described above, in THF (2 ml) was added a solution of *N,N'*-bis(allyloxycarbonyl)amidinopyrazole (334 mg, 1.20×10^{-3} mol) in THF (1 ml) at room temperature. After being stirred at the same temperature for 1 h, the mixture was diluted with EtOAc and washed with a saturated aqueous solution of NH_4Cl and brine. The organic layer was dried and concentrated under reduced pressure. The crude product was subjected to column chromatography on silica gel (20 g) using a mixture of EtOAc and hexane (1 : 2) as eluent and then HPLC using CHCl_3 as eluent to give **10s** (440 mg, 60%) as a colorless viscous oil. $^1\text{H-NMR}$ (CDCl_3) δ : 0.07 (6H, s), 0.88 (9H, s), 1.21 (3H, d, $J=6.2$ Hz), 1.75—2.00 (2H, m), 3.05—3.20 (2H, m), 3.26 (1H, dd, $J=6.0$, 3.7 Hz), 3.87 (1H, br d, $J=15.3$ Hz), 4.21 (1H, m), 4.27 (1H, dd, $J=10.9$, 3.7 Hz), 4.50—4.80 (7H, m), 5.20—5.60 (7H, m), 5.85—6.10 (3H, m), 10.5 (1H, br s). IR (KBr): 3274, 1785, 1757, 1726, 1640, 1610 cm^{-1} . MS (FAB) m/z : 617 ($\text{M}+\text{H}$) $^+$.

Allyl (8*S*,9*R*,10*S*)-5-Acetyl-10-[(*R*)-1-hydroxyethyl]-11-oxo-1,5-diazatricyclo[7.2.0.0 3,8]undec-2-ene-2-carboxylate (11a) A mixture of **10a** (192 mg, 4.28×10^{-4} mol), ammonium hydrogen fluoride ($\text{NH}_4\text{F} \cdot \text{HF}$, 74 mg, 1.3×10^{-3} mol), DMF (1 ml) and *N*-methylpyrrolidinone (NMP, 1 ml) was stirred at room temperature for 64 h. An aqueous solution of NaHCO_3 was added and the mixture was saturated with NaCl and extracted with EtOAc. The extract was dried and concentrated under reduced pressure. The residue was subjected to column chromatography on silica gel (8 g) using a mixture of EtOAc and methanol (1 : 0 to 9 : 1) as eluent and then HPLC using CHCl_3 as eluent to give **11a** (41.0 mg, 29%) as a colorless viscous oil. $^1\text{H-NMR}$ (CDCl_3) δ : 1.31 (3H, d, $J=6.3$ Hz), 1.45—1.70 (1H, m), 1.85—2.20 (2H,

m), 2.11, 2.16 (3H, s \times 2), 2.60—3.30 (2H, m), 3.27 (1H, dd, $J=6.4$, 3.6 Hz), 3.40, 3.77 (1H, d \times 2, $J=15.2$ Hz), 3.97, 4.85 (1H, br d \times 2, $J=14$ Hz), 4.15—4.35 (1H, m), 4.33 (1H, dd, $J=10.7$, 3.6 Hz), 4.65—4.90 (2H, m), 5.30 (1H, d, $J=10.5$ Hz), 5.45 (1H, br d, $J=16$ Hz), 5.50, 6.08 (1H, br d \times 2, $J=14$ Hz), 5.90—6.05 (1H, m). IR (KBr): 3379, 1780, 1719, 1645, 1627 cm^{-1} . MS (FAB) m/z : 335 ($\text{M}+\text{H}$) $^+$.

Allyl (8*S*,9*R*,10*S*)-5-[2-(Allyloxycarbonylamino)acetyl]-10-[(*R*)-1-hydroxyethyl]-11-oxo-1,5-diazatricyclo[7.2.0.0 3,8]undec-2-ene-2-carboxylate (11b) A mixture of **10b** (200 mg, 3.65×10^{-4} mol), ammonium hydrogen fluoride ($\text{NH}_4\text{F} \cdot \text{HF}$, 31.4 mg, 5.50×10^{-4} mol), DMF (1 ml) and NMP (1 ml) was stirred at room temperature for 7 d. The mixture was quenched with an aqueous solution of NaHCO_3 , saturated with NaCl and extracted with EtOAc. The extract was dried and concentrated under reduced pressure. The residue was subjected to column chromatography on silica gel (8 g) using a mixture of EtOAc and methanol (97 : 3 to 90 : 10) as eluent to give **11b** (97.7 mg, 62%) as a colorless viscous oil. $^1\text{H-NMR}$ (CDCl_3) δ : 1.31 (3H, d, $J=6.4$ Hz), 1.45—1.70 (1H, m), 1.82 (1H, d, $J=4.8$ Hz), 1.80—2.10 (1H, m), 2.70—3.30 (2H, m), 3.26 (1H, dd, $J=6.3$, 3.5 Hz), 3.47, 3.75 (1H, d \times 2, $J=15.0$ Hz), 3.88, 4.83 (1H, br d \times 2, $J=13$ Hz), 3.90—4.20 (2H, m), 4.25 (1H, m), 4.33 (1H, dd, $J=10.7$, 3.5 Hz), 4.59 (2H, br d, $J=5.3$ Hz), 4.70—4.90 (2H, m), 5.20—5.50 (4H, m), 5.38, 6.10 (1H, d \times 2, $J=15$ Hz), 5.61, 5.77 (1H, m \times 2), 5.85—6.10 (2H, m). IR (KBr): 3402, 1777, 1720, 1651 cm^{-1} . MS (FAB) m/z : 434 ($\text{M}+\text{H}$) $^+$.

Allyl (8*S*,9*R*,10*S*)-5-[3-(Allyloxycarbonylamino)propionyl]-10-[(*R*)-1-hydroxyethyl]-11-oxo-1,5-diazatricyclo[7.2.0.0 3,8]undec-2-ene-2-carboxylate (11c) A mixture of **10c** (200 mg, 3.56×10^{-4} mol), $\text{NH}_4\text{F} \cdot \text{HF}$ (63 mg, 1.1×10^{-3} mol), DMF (1 ml) and NMP (1 ml) was stirred at room temperature for 72 h. An aqueous solution of NaHCO_3 was added and the mixture was saturated with NaCl and extracted with EtOAc. The extract was dried and concentrated under reduced pressure. The residue was subjected to column chromatography on silica gel (8 g) using a mixture of EtOAc and methanol (95 : 5) as eluent and then HPLC using CHCl_3 as eluent to give **11c** (79.0 mg, 50%) as a colorless viscous oil. $^1\text{H-NMR}$ (CDCl_3) δ : 1.31 (3H, d, $J=6.3$ Hz), 1.45—1.70 (1H, m), 1.75—2.00 (1H, m), 2.10—2.30 (1H, m), 2.40—3.30 (4H, m), 3.27 (1H, dd, $J=6.2$, 3.5 Hz), 3.41, 3.71 (1H, br d \times 2, $J=14.6$ Hz), 3.40—3.55 (2H, m), 3.97, 4.82 (1H, br d \times 2, $J=14$ Hz), 4.20—4.30 (1H, m), 4.32 (1H, dd, $J=10.7$, 3.5 Hz), 4.55 (2H, br d, $J=5.4$ Hz), 4.65—4.85 (2H, m), 5.15—5.65 (5H, m), 5.48, 6.10 (1H, br d \times 2, $J=14$ Hz), 5.80—6.05 (2H, m). IR (KBr): 3393, 1779, 1717, 1636 cm^{-1} . MS (FAB) m/z : 448 ($\text{M}+\text{H}$) $^+$.

Allyl (8*S*,9*R*,10*S*)-5-[2-[(*N*-Allyloxycarbonyl-*N*-methyl)amino]acetyl]-10-[(*R*)-1-hydroxyethyl]-11-oxo-1,5-diazatricyclo[7.2.0.0 3,8]undec-2-ene-2-carboxylate (11d) A mixture of **10d** (563 mg, 1.00×10^{-3} mol), $\text{NH}_4\text{F} \cdot \text{HF}$ (167 mg, 2.92×10^{-3} mol), DMF (3 ml) and NMP (3 ml) was stirred at room temperature for 72 h. An aqueous solution of NaHCO_3 was added and the mixture was saturated with NaCl and extracted with EtOAc. The extract was dried and concentrated under reduced pressure. The residue was subjected to column chromatography on silica gel (18 g) using a mixture of EtOAc and methanol (95 : 5) as eluent and then HPLC using CHCl_3 as eluent to give **11d** (262 mg, 59%) as a colorless viscous oil. $^1\text{H-NMR}$ (CDCl_3) δ : 1.32 (3H, d, $J=6.4$ Hz), 1.50—1.70 (1H, m), 1.71 (1H, d, $J=4.8$ Hz), 1.85—2.00 (1H, m), 2.65—3.30 (1H, m), 2.98, 3.00 (3H, s \times 2), 3.12 (1H, m), 3.27 (1H, m), 3.50, 3.74 (1H, br d \times 2, $J=15$ Hz), 3.85—4.90 (8H, m), 4.26 (1H, dd, $J=10.5$, 3.4 Hz), 5.10—6.10 (7H, m). IR (KBr): 3434, 1780, 1706, 1660, 1651 cm^{-1} . MS (FAB) m/z : 448 ($\text{M}+\text{H}$) $^+$.

Allyl (8*S*,9*R*,10*S*)-5-[3-[[*N,N'*-Bis(allyloxycarbonyl)amidino]amino]propionyl]-10-[(*R*)-1-hydroxyethyl]-11-oxo-1,5-diazatricyclo[7.2.0.0 3,8]undec-2-ene-2-carboxylate (11f) A mixture of **10f** (182 mg, 2.56×10^{-4} mol), $\text{NH}_4\text{F} \cdot \text{HF}$ (45 mg, 7.9×10^{-4} mol), DMF (1 ml) and NMP (1 ml) was stirred at room temperature for 70 h. An aqueous solution of NaHCO_3 was added to the mixture and extracted with a mixture of EtOAc and CH_2Cl_2 (10 : 1). The extract was dried and concentrated under reduced pressure. The residue was subjected to HPLC using CHCl_3 as eluent to give **11f** (98.0 mg, 54%) as a colorless viscous oil. $^1\text{H-NMR}$ (CDCl_3) δ : 1.31 (3H, d, $J=6.2$ Hz), 1.45—1.65 (1H, m), 1.76 (1H, br d, $J=3.9$ Hz), 1.85—2.00 (1H, m), 2.55—3.25 (4H, m), 3.26 (1H, dd, $J=6.3$, 3.6 Hz), 3.43, 3.71 (1H, br d \times 2, $J=14.6$ Hz), 3.65—3.90 (2H, m), 4.01, 4.90 (1H, br d \times 2, $J=14$ Hz), 4.20—4.35 (1H, m), 4.32 (1H, dd, $J=10.7$, 3.6 Hz), 4.60 (2H, d, $J=5.8$ Hz), 4.66 (2H, d, $J=5.8$ Hz), 4.65—4.85 (2H, m), 5.20—5.50 (6H, m), 5.48, 6.09 (1H, br d \times 2, $J=14$ Hz), 5.80—6.10 (3H, m), 8.87, 8.99 (1H, br t \times 2, $J=6$ Hz), 11.64, 11.69 (1H, br s \times 2). IR (KBr): 3342, 1781, 1733, 1641, 1565 cm^{-1} . MS (FAB) m/z : 574 ($\text{M}+\text{H}$) $^+$.

Allyl (8*S*,9*R*,10*S*)-5-[(*R*)-1-Hydroxyethyl]-11-oxo-5-(3-pyridylcarbonyl)-1,5-diazatricyclo[7.2.0.0 3,8]undec-2-ene-2-carboxylate (11g) A mix-

ture of **10g** (200 mg, 5.13×10^{-4} mol), ammonium hydrogen fluoride ($\text{NH}_4\text{F} \cdot \text{HF}$, 45 mg, 7.9×10^{-4} mol), DMF (1 ml) and NMP (1 ml) was stirred at room temperature for 7 d. An aqueous solution of NaHCO_3 was added and the mixture was saturated with NaCl and extracted with EtOAc. The extract was dried and concentrated under reduced pressure. The residue was subjected to column chromatography on silica gel (6 g) using a mixture of EtOAc and methanol (1 : 0 to 8 : 2) as eluent to give **11g** (85 mg, 54%) as a colorless viscous oil. $^1\text{H-NMR}$ (CDCl_3) δ : 1.32 (3H, d, $J=6.2$ Hz), 1.50–1.80 (1H, m), 1.90–2.40 (2H, m), 2.80–3.30 (1H, m), 3.19 (1H, td, $J=11.0$, 5.0 Hz), 3.31 (1H, dd, $J=5.9$, 3.7 Hz), 3.40–4.00 (1H, m), 4.26 (1H, m), 4.34 (1H, dd, $J=10.8$, 3.7 Hz), 4.40–6.30 (7H, m), 7.37, 7.39 (1H, d \times 2, $J=8.0$ Hz), 7.76, 7.77 (1H, dd \times 2, $J=8.0$, 2.0 Hz), 8.66, 8.67 (1H, s \times 2), 8.69, 8.70 (1H, d \times 2, $J=2.0$ Hz). IR (KBr): 3422, 1779, 1720, 1634 cm^{-1} . MS (FAB) m/z : 398 ($\text{M}+\text{H}$) $^+$.

Allyl (8S,9R,10S)-10-[(R)-1-Hydroxyethyl]-11-oxo-5-(4-pyridylcarboxyl)-1,5-diazatricyclo[7.2.0.0 3,8]undec-2-ene-2-carboxylate (11h) A mixture of **10h** (350 mg, 6.84×10^{-4} mol), $\text{NH}_4\text{F} \cdot \text{HF}$ (195 mg, 3.42×10^{-3} mol), DMF (2 ml) and NMP (2 ml) was stirred at room temperature for 24 h. An aqueous solution of NaHCO_3 was added and the mixture was saturated with NaCl and extracted with EtOAc. The extract was dried and concentrated under reduced pressure. The residue was subjected to column chromatography on silica gel (9 g) using a mixture of EtOAc and methanol (9 : 1) as eluent to give **11h** (48 mg, 18%) as a colorless viscous oil. $^1\text{H-NMR}$ (CDCl_3) δ : 1.33 (3H, d, $J=6.4$ Hz), 1.50–2.20 (3H, m), 2.80–3.20 (1H, m), 3.18 (1H, td, $J=11.5$, 5.0 Hz), 3.30 (1H, m), 3.40–4.00 (1H, m), 4.25 (1H, m), 4.33 (1H, dd, $J=10.7$, 3.5 Hz), 4.30–6.40 (7H, m), 7.28 (2H, d, $J=5.8$ Hz), 8.70 (2H, d, $J=5.8$ Hz).

Allyl (8S,9R,10S)-5-Allyloxycarbonyl-10-[(R)-1-hydroxyethyl]-11-oxo-1,5-diazatricyclo[7.2.0.0 3,8]undec-2-ene-2-carboxylate (11i) A mixture of **10i** (220 mg, 4.48×10^{-4} mol), ammonium hydrogen fluoride ($\text{NH}_4\text{F} \cdot \text{HF}$, 76.7 mg, 1.34×10^{-3} mol), DMF (1 ml) and NMP (1 ml) was stirred at room temperature for 3 d. The mixture was quenched with an aqueous solution of NaHCO_3 , saturated with NaCl and extracted with EtOAc. The extract was dried and concentrated under reduced pressure. The residue was subjected to column chromatography on silica gel (8 g) using a mixture of ethyl acetate and hexane (2 : 1 to 1 : 0) as eluent to give **11i** (94.0 mg, 56%) as a colorless viscous oil. $^1\text{H-NMR}$ (CDCl_3) δ : 1.32 (3H, d, $J=6.4$ Hz), 1.60 (1H, dq, $J=12.3$, 4.1 Hz), 1.85–2.00 (1H, m), 1.90 (1H, d, $J=4.7$ Hz), 2.85–3.15 (2H, m), 3.27 (1H, dd, $J=6.3$, 3.5 Hz), 3.60 (1H, brd, $J=14.8$ Hz), 4.20–4.30 (1H, m), 4.30 (1H, dd, $J=10.7$, 3.5 Hz), 4.30–4.45 (1H, m), 4.60 (2H, d, $J=5.6$ Hz), 4.65–4.85 (2H, m), 5.20–5.50 (4H, m), 5.73 (1H, d, $J=14.8$ Hz), 5.85–6.05 (2H, m). IR (KBr): 3610, 1782, 1718, 1698, 165 cm^{-1} . MS (FAB) m/z : 377 ($\text{M}+\text{H}$) $^+$.

Allyl (8S,9R,10S)-10-[(R)-1-Hydroxyethyl]-5-methyl-11-oxo-1,5-diazatricyclo[7.2.0.0 3,8]undec-2-ene-2-carboxylate (11j) A mixture of **10j** (110 mg, 2.62×10^{-4} mol), $\text{NH}_4\text{F} \cdot \text{HF}$ (45 mg, 7.85×10^{-4} mol), DMF (0.5 ml) and NMP (0.5 ml) was stirred at room temperature for 47 h. An aqueous solution of NaHCO_3 was added and the mixture was saturated with NaCl and extracted with EtOAc. The extract was dried and concentrated under reduced pressure. The residue was subjected to column chromatography on silica gel (9 g) using a mixture of EtOAc and methanol (4 : 1) as eluent and then HPLC using CHCl_3 as eluent to give **11j** (31.0 mg, 39%) as a pale yellow viscous oil. $^1\text{H-NMR}$ (CDCl_3) δ : 1.32 (3H, d, $J=6.1$ Hz), 1.65–1.90 (2H, m), 1.83 (1H, d, $J=3.4$ Hz), 2.15–2.35 (1H, m), 2.37 (3H, s), 2.72 (1H, d, $J=12.2$ Hz), 2.80–2.95 (1H, m), 3.00 (1H, brd, $J=12$ Hz), 3.29 (1H, dd, $J=6.3$, 3.6 Hz), 4.20–4.30 (1H, m), 4.26 (1H, dd, $J=10.5$, 3.6 Hz), 4.40 (1H, d, $J=12.2$ Hz), 4.60–4.90 (2H, m), 5.26 (1H, dd, $J=10.6$, 1.2 Hz), 5.42 (1H, dd, $J=17.2$, 1.3 Hz), 5.97 (1H, ddt, $J=17.2$, 10.6, 5.4 Hz).

Allyl (8S,9R,10S)-10-[(R)-1-Hydroxyethyl]-5-(carbamoyl)methyl-11-oxo-1,5-diazatricyclo[7.2.0.0 3,8]undec-2-ene-2-carboxylate (11k) A mixture of **10k** (215 mg, 4.64×10^{-4} mol), $\text{NH}_4\text{F} \cdot \text{HF}$ (106 mg, 1.85×10^{-3} mol), DMF (1 ml) and NMP (1 ml) was stirred at room temperature for 46 h. An aqueous solution of NaHCO_3 was added and the mixture was saturated with NaCl and extracted with EtOAc. The extract was dried and concentrated under reduced pressure. The residue was subjected to HPLC using CHCl_3 as eluent to give **11k** (39.0 mg, 24%) as a pale yellow viscous oil. $^1\text{H-NMR}$ (CDCl_3) δ : 1.33 (3H, d, $J=6.4$ Hz), 1.60–2.00 (3H, m), 2.51 (1H, td, $J=11.9$, 2.4 Hz), 2.80–3.00 (1H, dd, $J=8.3$, 3.6 Hz), 2.94 (1H, d, $J=12.0$ Hz), 3.05 (1H, brd, $J=12$ Hz), 3.11 (2H, s), 3.28 (1H, dd, $J=6.4$, 3.5 Hz), 4.20–4.30 (1H, m), 4.28 (1H, dd, $J=10.6$, 3.5 Hz), 4.46 (1H, d, $J=12.0$ Hz), 4.60–4.90 (2H, m), 5.28 (1H, dd, $J=10.5$, 1.1 Hz), 5.42 (1H, dd, $J=16.2$, 1.2 Hz), 5.50 (1H, brs), 5.96 (1H, ddt, $J=16.2$, 10.5, 5.6 Hz), 6.88 (1H, brs). IR (neat): 3435, 3342, 1775, 1718, 1674 cm^{-1} . MS (FAB)

m/z : 350 ($\text{M}+\text{H}$) $^+$.

Allyl (8S,9R,10S)-5-Carbamoyl-10-[(R)-1-hydroxyethyl]-11-oxo-1,5-diazatricyclo[7.2.0.0 3,8]undec-2-ene-2-carboxylate (11l) A mixture of **10l** (115 mg, 2.56×10^{-4} mol), $\text{NH}_4\text{F} \cdot \text{HF}$ (44 mg, 7.7×10^{-4} mol), DMF (1 ml) and NMP (1 ml) was stirred at room temperature for 96 h. An aqueous solution of NaHCO_3 was added and the mixture was saturated with NaCl and extracted with EtOAc. The extract was dried and concentrated under reduced pressure. The residue was subjected to column chromatography on silica gel (9 g) using a mixture of EtOAc and methanol (9 : 1) as eluent and then HPLC using CHCl_3 as eluent to give **11l** (44.3 mg, 52%) as a colorless viscous oil. $^1\text{H-NMR}$ (CDCl_3) δ : 1.31 (3H, d, $J=6.2$ Hz), 1.66 (1H, qd, $J=12$, 4 Hz), 1.80–1.95 (1H, m), 2.12 (1H brs), 2.86 (1H, ddd, $J=14$, 12, 2 Hz), 3.13 (1H, td, $J=11.2$, 5.4 Hz), 3.27 (1H, dd, $J=6.4$, 3.5 Hz), 3.69 (1H, brd, $J=15$ Hz), 4.15–4.30 (1H, m), 4.33 (1H, dd, $J=10.6$, 3.5 Hz), 4.52 (1H, brd, $J=14$ Hz), 4.60–4.90 (2H, m), 4.92 (2H, brs), 5.12 (1H, brd, $J=15$ Hz), 5.30 (1H, brd, $J=11$ Hz), 5.45 (1H, brd, $J=17.2$ Hz), 5.96 (1H, ddt, $J=17.2$, 11.0, 5.5 Hz). IR (KBr): 3367, 1775, 1719, 1651, 1596 cm^{-1} . MS (FAB) m/z : 336 ($\text{M}+\text{H}$) $^+$.

Allyl (8S,9R,10S)-5-[[N $^{\omega}$ -(Allyloxycarbonyl)guanidino]carbonyl]-10-[(R)-1-hydroxyethyl]-11-oxo-1,5-diazatricyclo[7.2.0.0 3,8]undec-2-ene-2-carboxylate (11m) A mixture of **10m** (195 mg, 2.56×10^{-4} mol), $\text{NH}_4\text{F} \cdot \text{HF}$ (58 mg, 1.0×10^{-3} mol), DMF (1 ml) and NMP (1 ml) was stirred at room temperature for 43 h. An aqueous solution of NaHCO_3 was added and the mixture was saturated with NaCl and extracted with EtOAc. The extract was dried and concentrated under reduced pressure. The residue was subjected to column chromatography on silica gel (9 g) using a mixture of EtOAc and hexane (4 : 1) as eluent and then HPLC using CHCl_3 as eluent to give **11m** (48.0 mg, 41%) as a pale yellow viscous oil. $^1\text{H-NMR}$ (CDCl_3) δ : 1.31 (3H, d, $J=6.0$ Hz), 1.40–1.70 (2H, m), 1.80–1.95 (1H, m), 2.70–3.15 (2H, m), 3.26 (1H, dd, $J=6.0$, 3.8 Hz), 3.53 (1H, brd, $J=14$ Hz), 4.20–4.30 (1H, m), 4.27 (1H, dd, $J=10.4$, 3.8 Hz), 4.50–4.80 (4H, m), 4.67 (2H, d, $J=5.5$ Hz), 5.25–5.35 (3H, m), 5.36 (1H, d, $J=17.2$ Hz), 5.47 (1H, dd, $J=17.2$, 1.2 Hz), 5.80–6.20 (3H, m), 7.70–8.10 (1H, m).

Allyl (8S,9R,10S)-5-[[1-(Allyloxycarbonyl)pyrrolidin-3-yl]carbamoyl]-10-[(R)-1-hydroxyethyl]-11-oxo-1,5-diazatricyclo[7.2.0.0 3,8]undec-2-ene-2-carboxylate (11n) A mixture of **10n** (235 mg, 3.90×10^{-4} mol), $\text{NH}_4\text{F} \cdot \text{HF}$ (68 mg, 1.2×10^{-3} mol), DMF (1.2 ml) and NMP (1.2 ml) was stirred at room temperature for 48 h. An aqueous solution of NaHCO_3 was added and the mixture was saturated with NaCl and extracted with EtOAc. The extract was dried and concentrated under reduced pressure. The residue was subjected to column chromatography on silica gel (9 g) using a mixture of EtOAc and methanol (1 : 0 to 9 : 1) as eluent and then HPLC using CHCl_3 as eluent to give **11n** (45.2 mg, 24%) as a pale yellow viscous oil. $^1\text{H-NMR}$ (CDCl_3) δ : 1.31 (3H, d, $J=6.4$ Hz), 1.50–1.95 (3H, m), 2.00–2.35 (2H, m), 2.86 (1H, brt, $J=13$ Hz), 3.00–3.35 (2H, m), 3.24 (1H, dd, $J=6.5$, 3.4 Hz), 3.40–3.80 (3H, m), 3.63 (1H, d, $J=15.4$ Hz), 4.10–4.35 (3H, m), 4.45–4.65 (3H, m), 4.65–5.10 (3H, m), 5.15–5.50 (4H, m), 5.70–6.05 (3H, m). IR (KBr): 3382, 1777, 1699 1647 cm^{-1} . MS (FAB) m/z : 459 ($\text{M}+\text{H}$) $^+$.

Allyl (8S,9R,10S)-10-[(R)-1-Hydroxyethyl]-5-(N-methylthiocarbamoyl)-11-oxo-1,5-diazatricyclo[7.2.0.0 3,8]undec-2-ene-2-carboxylate (11o) A mixture of **10o** (196 mg, 4.05×10^{-4} mol), $\text{NH}_4\text{F} \cdot \text{HF}$ (88 mg, 1.5×10^{-3} mol), DMF (1 ml) and NMP (1 ml) was stirred at room temperature for 30 h. An aqueous solution of NaHCO_3 was added and the mixture was saturated with NaCl and extracted with EtOAc. The extract was dried and concentrated under reduced pressure. The residue was subjected to column chromatography on silica gel (9 g) using a mixture of EtOAc and methanol (1 : 0 to 95 : 5) as eluent and then HPLC using CHCl_3 as eluent to give **11o** (59.8 mg, 40%) as a colorless viscous oil. $^1\text{H-NMR}$ (CDCl_3) δ : 1.30 (3H, d, $J=6.0$ Hz), 1.64 (1H, brs), 1.65–1.80 (1H, m), 1.85–1.95 (1H, m), 3.12 (3H, d, $J=4.3$ Hz), 3.10–3.30 (2H, m), 3.29 (1H, dd, $J=6.2$, 3.7 Hz), 3.78 (1H, d, $J=15.2$ Hz), 4.24 (1H, m), 4.36 (1H, dd, $J=10.6$, 3.7 Hz), 4.70–4.90 (2H, m), 5.29 (1H, dd, $J=15.2$, 1.9 Hz), 5.32 (1H, brd, $J=10$ Hz), 5.46 (1H, dd, $J=15.2$, 1.2 Hz), 5.58 (1H, brd, $J=12$ Hz), 5.97 (1H, ddt, $J=15.2$, 10.1, 5.6 Hz), 6.85–7.00 (1H, m). IR (KBr): 3369, 1776, 1717, 1646 cm^{-1} . MS (FAB) m/z : 366 ($\text{M}+\text{H}$) $^+$.

Allyl (8S,9R,10S)-5-[[1-(Allyloxycarbonyl)pyrrolidin-3-yl]thiocarbamoyl]-10-[(R)-1-hydroxyethyl]-11-oxo-1,5-diazatricyclo[7.2.0.0 3,8]undec-2-ene-2-carboxylate (11p) A mixture of **10p** (250 mg, 4.05×10^{-4} mol), $\text{NH}_4\text{F} \cdot \text{HF}$ (89 mg, 1.6×10^{-3} mol), DMF (1.25 ml) and NMP (1.25 ml) was stirred at room temperature for 48 h. An aqueous solution of NaHCO_3 was added and the mixture was saturated with NaCl and extracted with EtOAc. The extract was dried and concentrated under reduced pressure. The residue was subjected to column chromatography on silica gel (3 g)

using a mixture of EtOAc and methanol (9:1) as eluent and then HPLC using CHCl_3 as eluent to give **11p** (137.5 mg, 67%) as a colorless viscous oil. $^1\text{H-NMR}$ (CDCl_3) δ : 1.30 (3H, d, $J=6.4$ Hz), 1.65–2.35 (4H, m), 1.84 (1H, br d, $J=4$ Hz), 1.72 (1H, qd, $J=12$, 4 Hz), 3.10–3.65 (5H, m), 3.28 (1H, dd, $J=6.3$, 3.6 Hz), 3.70–3.85 (1H, m), 3.76 (1H, d, $J=14.7$ Hz), 4.23 (1H, m), 4.36 (1H, dd, $J=10.5$, 3.6 Hz), 4.50–5.05 (5H, m), 5.15–5.55 (5H, m), 5.60 (1H, br d, $J=13$ Hz), 5.85–6.05 (2H, m), 7.09 (1H, m). IR (KBr): 3338, 1781, 1697, 1648, 1539 cm^{-1} . MS (FAB) m/z : 505 ($\text{M}+\text{H}$) $^+$.

Allyl (8S,9R,10S)-5-[N-(Allyloxycarbonyl)acetimidoyl]-10-[(R)-1-hydroxyethyl]-11-oxo-1,5-diazatricyclo[7.2.0.0 3,8]undec-2-ene-2-carboxylate (11r) A mixture of **10r** (87.0 mg, 1.56×10^{-4} mol), NH_4F HF (27 mg, 4.68×10^{-4} mol), DMF (0.4 ml) and NMP (0.4 ml) was stirred at room temperature for 24 h. An aqueous solution of NaHCO_3 was added and the mixture was saturated with NaCl and extracted with EtOAc. The extract was dried and concentrated under reduced pressure. The residue was subjected to column chromatography on silica gel (5 g) using a mixture of EtOAc and methanol (95:5) as eluent and then HPLC using CHCl_3 as eluent to give **11r** (16.0 mg, 27%) as a colorless viscous oil. $^1\text{H-NMR}$ (CDCl_3) δ : 1.31 (3H, d, $J=6.4$ Hz), 1.55–1.80 (2H, m), 1.85–2.00 (1H, m), 2.29 (3H, s), 2.70–3.00 (1H, m), 3.15 (1H, brtd, $J=12$, 5 Hz), 3.27 (1H, dd, $J=6.3$, 3.6 Hz), 3.71 (1H, d, $J=14.9$ Hz), 4.15–4.35 (1H, m), 4.33 (1H, dd, $J=10.7$, 3.6 Hz), 4.50–5.10 (3H, m), 4.61 (2H, d, $J=5.9$ Hz), 5.22 (1H, dd, $J=10.5$, 1.2 Hz), 5.29 (1H, dd, $J=10.5$, 1.2 Hz), 5.34 (1H, dd, $J=17.3$, 1.3 Hz), 5.44 (1H, dd, $J=17.2$, 1.3 Hz), 5.50–6.05 (3H, m).

Allyl (8S,9R,10S)-5-[N,N'-(bis(allyloxycarbonyl)amidino)-10-[(R)-1-hydroxyethyl]-11-oxo-1,5-diazatricyclo[7.2.0.0 3,8]undec-2-ene-2-carboxylate (11s) A mixture of **10s** (410 mg, 6.65×10^{-4} mol), NH_4F HF (114 mg, 2.00×10^{-3} mol), DMF (2 ml) and NMP (2 ml) was stirred at room temperature for 70 h. An aqueous solution of NaHCO_3 was added and the mixture was saturated with NaCl and extracted with EtOAc. The extract was dried and concentrated under reduced pressure. The residue was subjected to column chromatography on silica gel (9 g) using a mixture of EtOAc, hexane and methanol (3:1:0 to 15:5:2) as eluent and then HPLC using CHCl_3 as eluent to give **11s** (205 mg, 61%) as a colorless viscous oil. $^1\text{H-NMR}$ (CDCl_3) δ : 1.30 (3H, d, $J=6.4$ Hz), 1.70–2.00 (2H, m), 1.98 (1H, d, $J=4.8$ Hz), 3.10–3.25 (2H, m), 3.31 (1H, dd, $J=6.2$, 3.7 Hz), 3.89 (1H, d, $J=15.3$ Hz), 4.20–4.30 (1H, m), 4.32 (1H, dd, $J=10.7$, 3.7 Hz), 4.40–4.85 (7H, m), 5.20–5.80 (7H, m), 5.85–6.10 (3H, m), 10.5 (1H, brs). IR (KBr): 3285, 1757, 1723, 1640, 1606 cm^{-1} . MS (FAB) m/z : 503 ($\text{M}+\text{H}$) $^+$.

Potassium (8S,9R,10S)-5-Acetyl-10-[(R)-1-hydroxyethyl]-11-oxo-1,5-diazatricyclo[7.2.0.0 3,8]undec-2-ene-2-carboxylate (4a) To a suspension of **11a** (37.0 mg, 1.13×10^{-4} mol), $\text{Pd}(\text{PPh}_3)_4$ (2.5 mg) and PPh_3 (2.8 mg) in EtOAc (1 ml) was added 0.5 M EtOAc solution of potassium 2-ethylhexanoate (0.22 ml) at room temperature and stirred for 10 min. Pale yellow precipitates that emerged were collected by filtration and washed with EtOAc. The crude solid thus obtained was purified by column chromatography on Cosmosil 75C $_{18}$ -PREP (10 ml) using water as eluent. Combined eluates were concentrated to ca. 10 ml under reduced pressure and then lyophilized to give **4a** (29.5 mg, 80%) as a colorless powder. $^1\text{H-NMR}$ (D_2O) δ : 1.27 (3H, d, $J=6.5$ Hz), 1.45–1.70 (1H, m), 1.90–2.05 (1H, m), 2.14, 2.20 (3H, s \times 2), 2.87, 3.32 (1H, m \times 2), 3.15–3.30 (1H, m), 3.44 (1H, dd, $J=5.7$, 3.4 Hz), 3.45, 3.87 (1H, d \times 2, $J=13.9$ Hz), 4.07, 4.55 (1H, br d \times 2, $J=14$ Hz), 4.20–4.30 (1H, m), 4.28 (1H, dd, $J=10.4$, 3.4 Hz), 5.46, 5.83 (1H, br d \times 2, $J=14$ Hz). IR (KBr): 3378, 1758, 1604 cm^{-1} . MS (FAB) m/z : 333 ($\text{M}+\text{H}$) $^+$.

(8S,9R,10S)-5-Aminoacetyl-10-[(R)-1-hydroxyethyl]-11-oxo-1,5-diazatricyclo[7.2.0.0 3,8]undec-2-ene-2-carboxylic Acid (4b) To a mixture of **11b** (45.0 mg, 1.04×10^{-4} mol), $\text{Pd}(\text{PPh}_3)_4$ (3 mg) and PPh_3 (3 mg) in a mixture of EtOAc and THF (1:1, 1.5 ml) was added dimedone (58 mg, 4.2×10^{-4} mol) at room temperature. After being stirred for 45 min, the precipitates that emerged were collected by filtration and washed with a mixture of THF and EtOAc. The crude solid thus obtained was subjected to column chromatography on Cosmosil 75C $_{18}$ -PREP (20 ml) using water as eluent. Combined eluates were concentrated to ca. 10 ml under reduced pressure and then lyophilized to give **4b** (8.2 mg, 26%) as a colorless powder. $^1\text{H-NMR}$ (D_2O) δ : 1.27 (3H, d, $J=5.9$ Hz), 1.40–1.70 (1H, m), 1.90–2.10 (1H, m), 2.85–3.35 (2H, m), 3.35–3.45 (1H, m), 3.53, 3.87 (1H, d \times 2, $J=14.0$ Hz), 4.00–4.35 (4H, m), 4.03, 4.55 (1H, br d \times 2, $J=13$ Hz), 5.25, 5.85 (1H, d \times 2, $J=14.0$ Hz). IR (KBr): 3420, 1757, 1655, 1592 cm^{-1} . MS (FAB) m/z : 310 ($\text{M}+\text{H}$) $^+$.

(8S,9R,10S)-5-(3-Aminopropionyl)-10-[(R)-1-hydroxyethyl]-11-oxo-1,5-diazatricyclo[7.2.0.0 3,8]undec-2-ene-2-carboxylic Acid (4c) To a mixture of **11c** (70.0 mg, 1.56×10^{-4} mol) and bis(triphenylphosphine)palladium dichloride ($\text{Pd}(\text{PPh}_3)_2\text{Cl}_2$, 5.4 mg) in CH_2Cl_2 (1.5 ml) was added *n*-Bu $_3\text{SnH}$

(168 μl , 6.24×10^{-4} mol) at 0 $^\circ\text{C}$. After being stirred at room temperature for 15 min, hexane (5 ml) was added to the reaction mixture. Pale yellow precipitates that emerged were collected by filtration and washed with EtOAc. The crude solid thus obtained was purified by column chromatography on Cosmosil 75C $_{18}$ -PREP (10 ml) using water as eluent. Combined eluates were concentrated to ca. 10 ml under reduced pressure and then lyophilized to give **4c** (31 mg, 61%) as a colorless powder. $^1\text{H-NMR}$ (D_2O) δ : 1.27 (3H, d, $J=6.3$ Hz), 1.45–1.70 (1H, m), 1.90–2.05 (1H, m), 2.75–2.95 (2H, m), 3.00–3.15 (1H, m), 3.15–3.40 (3H, m), 3.42 (1H, dd, $J=5.8$, 3.3 Hz), 3.46, 3.85 (1H, d \times 2, $J=14.2$ Hz), 4.03, 4.58 (1H, br d \times 2, $J=14$ Hz), 4.20–4.30 (1H, m), 4.28 (1H, dd, $J=10.4$, 3.3 Hz), 5.43, 5.88 (1H, d \times 2, $J=14.2$ Hz). IR (KBr): 3378, 3235, 1763, 1624 cm^{-1} . MS (FAB) m/z : 324 ($\text{M}+\text{H}$) $^+$.

(8S,9R,10S)-10-[(R)-1-Hydroxyethyl]-5-[2-(*N*-methylamino)acetyl]-11-oxo-1,5-diazatricyclo[7.2.0.0 3,8]undec-2-ene-2-carboxylic Acid (4d) To a mixture of **11d** (70.0 mg, 1.56×10^{-4} mol) and $\text{Pd}(\text{PPh}_3)_2\text{Cl}_2$ (5.4 mg) in CH_2Cl_2 (1.5 ml) was added *n*-Bu $_3\text{SnH}$ (168 μl , 6.24×10^{-4} mol) at 0 $^\circ\text{C}$. After being stirred at room temperature for 15 min, hexane was added to the reaction mixture. Pale yellow precipitates that emerged were collected by filtration and washed with EtOAc. The crude solid thus obtained was purified by column chromatography on Cosmosil 75C $_{18}$ -PREP (10 ml) using water as eluent. Combined eluates were concentrated to ca. 10 ml under reduced pressure and then lyophilized to give **4d** (31 mg, 61%) as a colorless powder. $^1\text{H-NMR}$ (D_2O) δ : 1.30 (3H, d, $J=6.3$ Hz), 1.50–1.70 (1H, m), 1.95–2.10 (1H, m), 2.80, 2.81 (3H, s \times 2), 2.95–3.40 (1H, m), 3.30 (1H, brtd, $J=11$, 5 Hz), 3.46 (1H, dd, $J=5.6$, 3.3 Hz), 3.56, 3.91 (1H, br d \times 2, $J=14$ Hz), 4.10, 4.58 (1H, br d \times 2, $J=14$ Hz), 4.10–4.40 (4H, m), 5.26, 5.88 (1H, br d \times 2, $J=14$ Hz). IR (KBr): 3380, 1760, 1653, 1597 cm^{-1} . MS (FAB) m/z : 364 ($\text{M}+\text{H}$) $^+$.

(8S,9R,11S)-10-[(R)-1-Hydroxyethyl]-5-iminomethyl-1,5-diazatricyclo[7.2.0.0 3,8]undec-2-ene-2-carboxylic Acid (4e) To a mixture of **4d** (39 mg, 1.2×10^{-4} mol), CH_3CN (1.3 ml) and phosphate buffer (pH 7.4, 1.3 ml) were added benzyl formimidate hydrochloride (439 mg, 2.55×10^{-3} mol) and *N,N*-diisopropylethylamine (270 μl , 1.55×10^{-3} mol) at 0 $^\circ\text{C}$. After being stirred for 1 h, water (5 ml) was added to the reaction mixture. The aqueous solution was washed with diethyl ether, and was concentrated under reduced pressure. The residue was purified by column chromatography on Cosmosil 75C $_{18}$ -PREP (12 ml) using water as eluent and then high pressure liquid chromatography on Cosmosil 5C $_{18}$ -AR (20 mm i.d. \times 250 mm, Nacalai Tesque) using water as eluent. Combined eluates were concentrated to ca. 10 ml under reduced pressure and then lyophilized to give **4e** (5.3 mg, 13%) as a colorless powder. $^1\text{H-NMR}$ (D_2O) δ : 1.29 (3H, d, $J=6.4$ Hz), 1.50–1.70 (1H, m), 1.95–2.10 (1H, m), 2.95–3.40 (2H, m), 3.09, 3.27 (3H, s \times 2), 3.45 (1H, dd, $J=5.5$, 3.2 Hz), 3.56, 3.90, 3.92 (1H, br d \times 3, $J=14$ Hz), 4.20–4.35 (2H, m), 4.40–4.95 (3H, m), 5.29, 5.32, 5.86 (1H, br d \times 3, $J=14$ Hz), 7.86, 7.89, 8.01 (1H, s \times 3). IR (KBr): 3370, 1756, 1712, 1652, 1592 cm^{-1} .

(8S,9R,10S)-5-(3-Guanidinopropionyl)-10-[(R)-1-hydroxyethyl]-11-oxo-1,5-diazatricyclo[7.2.0.0 3,8]undec-2-ene-2-carboxylic Acid (4f) To a mixture of **11f** (70.0 mg, 1.22×10^{-4} mol) and $\text{Pd}(\text{PPh}_3)_2\text{Cl}_2$ (2 mg) in CH_2Cl_2 (4 ml) was added *n*-Bu $_3\text{SnH}$ (200 μl , 7.44×10^{-4} mol) at 0 $^\circ\text{C}$. After being stirred at room temperature for 15 min, hexane (8 ml) was added. Pale yellow precipitates that emerged were collected by filtration and washed with EtOAc. The crude solid thus obtained was purified by column chromatography on Cosmosil 75C $_{18}$ -PREP (10 ml) using water as eluent. Combined eluates were concentrated to ca. 10 ml under reduced pressure and then lyophilized to give **4f** (31 mg, 61%) as a colorless powder. $^1\text{H-NMR}$ (D_2O) δ : 1.27 (3H, d, $J=6.4$ Hz), 1.40–1.65 (1H, m), 1.90–2.05 (1H, m), 2.60–3.15 (3H, m), 3.15–3.35 (1H, m), 3.33, 3.86 (1H, d \times 2, $J=14.0$ Hz), 3.42 (1H, dd, $J=5.9$, 3.2 Hz), 3.40–3.60 (2H, m), 4.10, 4.61 (1H, br d \times 2, $J=13$ Hz), 4.20–4.30 (1H, m), 4.29 (1H, dd, $J=10.5$, 3.2 Hz), 5.49, 5.91 (1H, d \times 2, $J=14.0$ Hz). IR (KBr): 3378, 3235, 1763, 1624 cm^{-1} . MS (FAB) m/z : 366 ($\text{M}+\text{H}$) $^+$.

Potassium (8S,9R,10S)-10-[(R)-1-Hydroxyethyl]-11-oxo-5-(3-pyridylcarbonyl)-1,5-diazatricyclo[7.2.0.0 3,8]undec-2-ene-2-carboxylate (4g) To a suspension of **11g** (45.0 mg, 1.13×10^{-4} mol), $\text{Pd}(\text{PPh}_3)_4$ (1.3 mg) and PPh_3 (1.5 mg) in EtOAc (0.5 ml) was added 0.5 M EtOAc solution of potassium 2-ethylhexanoate (0.24 ml) at room temperature and stirred for 30 min. Pale yellow precipitates that emerged were collected by filtration and washed with EtOAc. The crude solid thus obtained was purified by column chromatography on Cosmosil 75C $_{18}$ -PREP (20 ml) using water as eluent. Combined eluates were concentrated to ca. 10 ml under reduced pressure and then lyophilized to give **4g** (29.2 mg, 65%) as a colorless powder. $^1\text{H-NMR}$ (D_2O) δ : 1.27, 1.29 (3H, d \times 2, $J=6.6$ Hz), 1.6–1.8 (1H, m), 1.9–2.2 (1H,

m), 3.14, 3.36 (1H, m×2), 3.2—3.4 (1H, m), 3.4—3.5 (1H, m), 3.70, 3.96 (1H, d×2, $J=14.0$ Hz), 3.85, 4.30 (1H, m×2), 4.20—4.40 (2H, m), 5.23, 6.01 (1H, d×2, $J=14.0$ Hz), 7.50—7.60 (1H, m), 7.80—8.00 (1H, m), 8.50—8.70 (2H, m). IR (KBr): 3385, 1758, 1606 cm^{-1} .

Potassium (8S,9R,10S)-10-[(R)-1-Hydroxyethyl]-11-oxo-5-(4-pyridyl-carbonyl)-1,5-diazatricyclo[7.2.0.0^{3,8}]undec-2-ene-2-carboxylate (4h) To a suspension of **11h** (48 mg, 1.2×10^{-4} mol), $\text{Pd}(\text{PPh}_3)_4$ (1.5 mg) and PPh_3 (1.7 mg) in EtOAc (0.5 ml) was added 0.5 M EtOAc solution of potassium 2-ethylhexanoate (0.27 ml) at room temperature and stirred for 20 min. Pale yellow precipitates that emerged were collected by filtration and washed with EtOAc. The crude solid thus obtained was purified by column chromatography on Cosmosil 75C₁₈-PREP (20 ml) using water as eluent. Combined eluates were concentrated to ca. 10 ml under reduced pressure and then lyophilized to give **4h** (29.2 mg, 65%) as a colorless powder. ¹H-NMR (D_2O) δ : 1.27, 1.28 (3H, d×2, $J=6.7$ Hz), 1.5—1.8 (1H, m), 1.8—2.2 (1H, m), 3.13, 3.33 (1H, m×2), 3.2—3.4 (1H, m), 3.4—3.6 (1H, m), 3.69, 3.97 (1H, d×2, $J=14.0$ Hz), 3.74, 4.61 (1H, m×2), 4.20—4.40 (2H, m), 5.13, 6.00 (1H, d×2, $J=14.0$ Hz), 7.40—7.60 (2H, m), 8.66 (2H, d, $J=5.6$ Hz). IR (KBr): 3372, 1759, 1600 cm^{-1} . MS (FAB) m/z : 396 (M+H)⁺.

(8S,9R,10S)-10-[(R)-1-Hydroxyethyl]-11-oxo-1,5-diazatricyclo[7.2.0.0^{3,8}]undec-2-ene-2-carboxylic Acid (4i) To a mixture of **11i** (85.0 mg, 2.26×10^{-4} mol) and $\text{Pd}(\text{PPh}_3)_2\text{Cl}_2$ (7.7 mg) in CH_2Cl_2 (2 ml) was added *n*-Bu₃SnH (0.24 ml, 8.9×10^{-4} mol) at room temperature. After being stirred for 15 min, hexane was added to the reaction mixture. Pale yellow precipitates that emerged were collected by filtration and washed with hexane. The crude solid thus obtained was subjected to column chromatography on Cosmosil 75C₁₈-PREP (10 ml) using water as eluent. Combined eluates were concentrated to ca. 10 ml under reduced pressure and then lyophilized to give **4i** (21.4 mg, 38%) as a colorless powder. ¹H-NMR (D_2O) δ : 1.27 (3H, d, $J=5.9$ Hz), 1.83 (1H, qd, $J=13.1$, 3.7 Hz), 2.05—2.20 (1H, m), 3.20—3.35 (2H, m), 3.50—3.55 (1H, m), 3.52 (1H, dd, $J=5.2$, 3.4 Hz), 3.62 (1H, br d, $J=13.0$ Hz), 3.80 (1H, d, $J=13.3$ Hz), 4.26 (1H, m), 4.35 (1H, dd, $J=10.3$, 3.4 Hz), 4.86 (1H, d, $J=13.3$ Hz). IR (KBr): 3393, 1766, 1601 cm^{-1} . MS (FAB) m/z : 253 (M+H)⁺.

(8S,9R,10S)-10-[(R)-1-Hydroxyethyl]-5-methyl-11-oxo-1,5-diazatricyclo[7.2.0.0^{3,8}]undec-2-ene-2-carboxylic Acid (4j) To a mixture of **11j** (30.0 mg, 9.79×10^{-5} mol) and $\text{Pd}(\text{PPh}_3)_2\text{Cl}_2$ (4 mg) in CH_2Cl_2 (0.3 ml) was added *n*-Bu₃SnH (80 μl , 2.97×10^{-4} mol) at room temperature. After being stirred for 30 min, water (5 ml) was added to the reaction mixture. The mixture was washed with EtOAc and the aqueous layer was concentrated to ca. 1 ml under reduced pressure. The aqueous solution thus obtained was subjected to column chromatography on Cosmosil 75C₁₈-PREP (5 ml) using water as eluent. Combined eluates were concentrated to ca. 5 ml under reduced pressure and then lyophilized to give **4j** (16.6 mg, 64%) as a colorless powder. ¹H-NMR (D_2O) δ : 1.30 (3H, d, $J=6.4$ Hz), 1.85—2.05 (1H, m), 2.10—2.25 (1H, m), 2.96 (3H, s), 3.20—3.40 (2H, m), 3.56 (1H, dd, $J=5.6$, 3.5 Hz), 3.68 (1H, br d, $J=12$ Hz), 3.82 (1H, br d, $J=13$ Hz), 4.20—4.35 (1H, m), 4.39 (1H, dd, $J=10.5$, 3.5 Hz), 4.94 (1H, br d, $J=13$ Hz). IR (KBr): 3381, 1764, 1603 cm^{-1} . MS (FAB) m/z : 267 (M+H)⁺.

(8S,9R,11S)-10-[(R)-1-Hydroxyethyl]-5-(carbamoyl)methyl-11-oxo-1,5-diazatricyclo[7.2.0.0^{3,8}]undec-2-ene-2-carboxylic Acid (4k) To a mixture of **11k** (30 mg, 8.6×10^{-5} mol) and $\text{Pd}(\text{PPh}_3)_2\text{Cl}_2$ (0.7 mg) in CH_2Cl_2 (1.5 ml) was added *n*-Bu₃SnH (50 μl , 1.7×10^{-4} mol) at room temperature. After being stirred for 10 min, water (10 ml) and methanol (0.5 ml) were added to the reaction mixture. The mixture was washed with EtOAc and the aqueous phase was concentrated to ca. 1 ml under reduced pressure, and was subjected to column chromatography on Cosmosil 75C₁₈-PREP (5 ml) using water as eluent. Combined eluates were concentrated to ca. 5 ml under reduced pressure and then lyophilized to give **4k** (17.5 mg, 66%) as a colorless powder. ¹H-NMR (D_2O) δ : 1.27 (3H, d, $J=6.4$ Hz), 1.90—2.25 (2H, m), 3.20—3.50 (2H, m), 3.55 (1H, dd, $J=5.6$, 3.5 Hz), 3.65—3.75 (1H, m), 3.92 (1H, br d, $J=13$ Hz), 4.05 (2H, s), 4.28 (1H, m), 4.37 (1H, dd, $J=10.4$, 3.5 Hz), 4.94 (1H, br d, $J=13$ Hz). IR (KBr): 3388, 1765, 1694, 1603 cm^{-1} . MS (FAB) m/z : 310 (M+H)⁺.

Potassium (8S,9R,10S)-5-Carbamoyl-10-[(R)-1-hydroxyethyl]-11-oxo-1,5-diazatricyclo[7.2.0.0^{3,8}]undec-2-ene-2-carboxylate (4l) To a solution of **11l** (28.5 mg, 8.50×10^{-5} mol), $\text{Pd}(\text{PPh}_3)_4$ (1.5 mg) and PPh_3 (1.7 mg) in a mixture of THF, CH_2Cl_2 and methanol (10:10:1, 2 ml) was added 0.5 M EtOAc solution of potassium 2-ethylhexanoate (170 μl) at room temperature and stirred for 15 min. Pale yellow precipitates that emerged were collected by filtration and washed with EtOAc. The crude solid thus obtained was purified by column chromatography on Cosmosil 75C₁₈-PREP (10 ml) using water as eluent. Combined eluates were concentrated to ca. 10 ml under reduced pressure and then lyophilized to give **4l** (29.2 mg, 65%) as a colorless

powder. ¹H-NMR (D_2O) δ : 1.28 (3H, d, $J=6.5$ Hz), 1.55 (1H, qd, $J=12.5$, 4.0 Hz), 1.85—2.00 (1H, m), 3.05 (1H, ddd, $J=14$, 12, 2 Hz), 3.24 (1H, br t, $J=11$, 5 Hz), 3.44 (1H, dd, $J=5.8$, 3.3 Hz), 3.73 (1H, d, $J=15.0$ Hz), 4.18 (1H, br d, $J=14$ Hz), 4.20—4.30 (1H, m), 4.29 (1H, dd, $J=10.4$, 3.3 Hz), 5.13 (1H, d, $J=15.0$ Hz). IR (KBr): 3357, 1775, 1657, 1595 cm^{-1} . MS (FAB) m/z : 334 (M+H)⁺.

(8S,9R,10S)-5-[(Guanidino)carbonyl]-10-[(R)-1-hydroxyethyl]-11-oxo-1,5-diazatricyclo[7.2.0.0^{3,8}]undec-2-ene-2-carboxylic Acid (4m) To a mixture of **11m** (47.0 mg, 1.02×10^{-4} mol) and $\text{Pd}(\text{PPh}_3)_2\text{Cl}_2$ (4 mg) in CH_2Cl_2 (0.5 ml) was added *n*-Bu₃SnH (260 μl , 9.66×10^{-4} mol) at room temperature. After being stirred for 45 min, water (5 ml) was added to the reaction mixture. The mixture was washed with EtOAc and the aqueous phase was concentrated to ca. 1 ml under reduced pressure. The aqueous solution thus obtained was subjected to column chromatography on Cosmosil 75C₁₈-PREP (5 ml) using a mixture of water and CH_3CN (98:2) as eluent. Combined eluates were concentrated to ca. 10 ml under reduced pressure and then lyophilized to give **4m** (6.1 mg, 18%) as a colorless powder. ¹H-NMR (D_2O) δ : 1.29 (3H, d, $J=6.4$ Hz), 1.64 (1H, qd, $J=12.5$, 4.1 Hz), 1.95—2.05 (1H, m), 3.19 (1H, br t, $J=13$ Hz), 3.35—3.40 (1H, m), 3.46 (1H, dd, $J=5.8$, 3.3 Hz), 3.83 (1H, br d, $J=15$ Hz), 4.20—4.40 (2H, m), 4.34 (1H, dd, $J=10.3$, 3.3 Hz), 5.10—5.50 (1H, m). IR (KBr): 3354, 1762, 1698, 1593 cm^{-1} .

(8S,9R,10S)-10-[(R)-1-Hydroxyethyl]-11-oxo-5-[(pyrrolidin-3-yl)carbamoyl]-1,5-diazatricyclo[7.2.0.0^{3,8}]undec-2-ene-2-carboxylic Acid (4n) To a mixture of **11n** (38.0 mg, 1.02×10^{-4} mol) and $\text{Pd}(\text{PPh}_3)_2\text{Cl}_2$ (1 mg) in CH_2Cl_2 (1 ml) was added *n*-Bu₃SnH (84 μl , 3.1×10^{-4} mol) at room temperature. After being stirred for 30 min, water (5 ml) was added to the reaction mixture. The mixture was washed with EtOAc and the aqueous phase was concentrated to ca. 1 ml under reduced pressure. The aqueous solution thus obtained was subjected to column chromatography on Cosmosil 75C₁₈-PREP (5 ml) using a mixture of water and CH_3CN (1:0 to 99:1) as eluent. Combined eluates were concentrated to ca. 10 ml under reduced pressure and then lyophilized to give **4n** (12.6 mg, 44%) as a colorless powder. ¹H-NMR (D_2O) δ : 1.27 (3H, d, $J=6.4$ Hz), 1.40—1.55 (1H, m), 1.85—2.15 (2H, m), 2.20—2.40 (1H, m), 3.00—3.15 (1H, m), 3.20—3.45 (4H, m), 3.50—3.60 (2H, m), 3.74, 3.74 (1H, d×2, $J=15.1$ Hz), 4.15—4.50 (4H, m), 4.92, 4.99 (1H, br d×2, $J=15$ Hz). IR (KBr): 3367, 2967, 1760, 1626, 1600, 1541 cm^{-1} . MS (FAB) m/z : 365 (M+H)⁺.

Potassium (8S,9R,10S)-10-[(R)-1-Hydroxyethyl]-5-(N-methylthiocarbamoyl)-11-oxo-1,5-diazatricyclo[7.2.0.0^{3,8}]undec-2-ene-2-carboxylate (4o) To a mixture of **11o** (48.0 mg, 1.31×10^{-4} mol), $\text{Pd}(\text{PPh}_3)_4$ (1 mg) and PPh_3 (5 mg) in EtOAc (1 ml) was added 0.5 M EtOAc solution of potassium 2-ethylhexanoate (500 μl) at room temperature. After being stirred for 90 min, EtOAc (2 ml) was added and the mixture was extracted with water (3 ml×3 times). Combined aqueous layers were concentrated under reduced pressure and subjected to column chromatography on Cosmosil 75C₁₈-PREP (10 ml) using water as eluent. Combined eluates were concentrated to ca. 10 ml under reduced pressure and then lyophilized to give **4o** (28.6 mg, 60%) as a colorless powder. ¹H-NMR (D_2O) δ : 1.26 (3H, d, $J=6.2$ Hz), 1.58 (1H, qd, $J=12.5$, 4.0 Hz), 1.90—2.00 (1H, m), 3.03 (3H, s), 3.25—3.40 (2H, m), 3.42 (1H, dd, $J=5.8$, 3.2 Hz), 3.88 (1H, d, $J=14.8$ Hz), 4.23 (1H, m), 4.30 (1H, dd, $J=10.3$, 3.2 Hz), 5.05 (1H, br d, $J=14.0$ Hz), 5.23 (1H, dd, $J=14.8$, 1.8 Hz). IR (KBr): 3250, 1754, 1699 cm^{-1} . MS (FAB) m/z : 364 (M+H)⁺.

(8S,9R,10S)-10-[(R)-1-Hydroxyethyl]-11-oxo-5-[(pyrrolidin-3-yl)thiocarbamoyl]-1,5-diazatricyclo[7.2.0.0^{3,8}]undec-2-ene-2-carboxylic Acid (4p) To a mixture of **11p** (100 mg, 1.98×10^{-4} mol) and $\text{Pd}(\text{PPh}_3)_2\text{Cl}_2$ (2.8 mg) in CH_2Cl_2 (2 ml) was added *n*-Bu₃SnH (213 μl , 7.92×10^{-4} mol) at room temperature. After being stirred for 30 min, water (5 ml) was added to the reaction mixture. The mixture was washed with hexane and the aqueous phase was concentrated to ca. 1 ml under reduced pressure. The aqueous solution thus obtained was subjected to column chromatography on Cosmosil 75C₁₈-PREP (10 ml) using a mixture of water and CH_3CN (1:0 to 9:1) as eluent. Combined eluates were concentrated to ca. 10 ml under reduced pressure and then lyophilized to give **4p** (24 mg, 32%) as a colorless powder. ¹H-NMR (D_2O) δ : 1.26 (3H, d, $J=6.4$ Hz), 1.50—1.70 (1H, m), 1.90—2.00 (1H, m), 2.00—2.25 (1H, m), 2.30—2.50 (1H, m), 3.05—3.75 (7H, m), 3.92, 3.93 (1H, d×2, $J=14.8$ Hz), 4.15—4.35 (2H, m), 4.95—5.20 (2H, m), 5.24, 5.27 (1H, br d×2, $J=15$ Hz). IR (KBr): 3413, 3239, 1761, 1589 cm^{-1} . MS (FAB) m/z : 381 (M+H)⁺.

(8S,9R,10S)-10-[(R)-1-Hydroxyethyl]-5-iminomethyl-11-oxo-1,5-diazatricyclo[7.2.0.0^{3,8}]undec-2-ene-2-carboxylic Acid (4q) To a mixture of **4i** (62.0 mg, 2.46×10^{-4} mol), CH_3CN (0.9 ml) and phosphate buffer (pH 7.4, 0.9 ml) were added benzyl formimidate hydrochloride (204 mg,

1.19×10^{-3} mol) and *N,N*-diisopropylethylamine (210 μ l, 1.21×10^{-3} mol) at 0°C. After being stirred for 30 min, water (5 ml) was added to the reaction mixture. The aqueous solution was washed with diethyl ether, and was concentrated under reduced pressure. The residue was purified by column chromatography on Cosmosil 75C₁₈-PREP (10 ml) using water as eluent followed by HPLC on Cosmosil 5C₁₈-AR (20 mm i.d. \times 250 mm, Nacalai Tesque) using water as eluent. Combined eluates were concentrated to ca. 10 ml under reduced pressure and then lyophilized to give **4q** (17.6 mg, 27%) as a colorless powder. ¹H-NMR (D₂O) δ : 1.30 (3H, d, $J=6.5$ Hz), 1.65—1.90 (1H, m), 2.05—2.20 (1H, m), 3.25—3.45 (2H, m), 3.50 (1H, dd, $J=5.6, 3.5$ Hz), 3.70, 3.95 (1H, d \times 2, $J=14.0$ Hz), 4.00, 4.15 (1H, m \times 2), 4.20—4.35 (1H, m), 4.37 (1H, dd, $J=10.5, 3.4$ Hz), 5.26, 5.43 (1H, d \times 2, $J=14.4$ Hz), 7.85, 7.90 (1H, s \times 2). IR (KBr): 3367, 1777, 1578 cm⁻¹. MS (FAB) m/z : 280 (M+H)⁺.

(8S,9R,10S)-10-[(R)-1-Hydroxyethyl]-5-acetimido-1,5-diazatri-cyclo[7.2.0.0^{3,8}]undec-2-ene-2-carboxylic Acid (4r) To a mixture of **11f** (27 mg, 6.5×10^{-5} mol) and Pd(PPh₃)₂Cl₂ (2.4 mg) in CH₂Cl₂ (0.3 ml) was added *n*-Bu₃SnH (90 μ l, 3.3×10^{-4} mol) at room temperature. After being stirred for 30 min, water (5 ml) was added. The mixture was washed with EtOAc and the aqueous phase was concentrated to ca. 1 ml under reduced pressure. The aqueous solution thus obtained was subjected to column chromatography on Cosmosil 75C₁₈-PREP (5 ml) using water as eluent. Combined eluates were concentrated to ca. 10 ml under reduced pressure and then lyophilized to give **4r** (8.4 mg, 45%) as a colorless powder. ¹H-NMR (D₂O) δ : 1.30 (3H, d, $J=6.4$ Hz), 1.65—1.85 (1H, m), 2.05—2.20 (1H, m), 2.35, 2.42 (3H, s \times 2), 3.30—3.60 (2H, m), 3.47 (1H, dd, $J=5.6, 3.5$ Hz), 3.96, 4.03 (1H, d \times 2, $J=14.3$ Hz), 4.10—4.35 (2H, m), 4.37 (1H, dd, $J=10.3, 3.5$ Hz), 5.34, 5.56 (1H, d \times 2, $J=14.3, 1.5$ Hz). IR (KBr): 3335, 1760, 1673, 1609 cm⁻¹. MS (FAB) m/z : 294 (M+H)⁺.

(8S,9R,10S)-5-Amidino-10-[(R)-1-hydroxyethyl]-11-oxo-1,5-diazatri-cyclo[7.2.0.0^{3,8}]undec-2-ene-2-carboxylic Acid 2/3 Hydrate (4s) To a mixture of **11s** (176 mg, 3.50×10^{-4} mol) and Pd(PPh₃)₂Cl₂ (5 mg) in CH₂Cl₂ (7 ml) was added *n*-Bu₃SnH (565 μ l, 2.10×10^{-3} mol) at room temperature. After being stirred for 15 min, hexane was added to the reaction mixture. Pale yellow precipitates that emerged were collected by filtration and washed with hexane. The crude solid thus obtained was subjected to column chromatography on Cosmosil 75C₁₈-PREP (20 ml) using water as eluent. Crystalline precipitates were emerged during concentration of the combined eluates under reduced pressure. The precipitates were collected by filtration and washed with cold water to give **4s** (31 mg, 29%) as colorless crystals, mp 208°C (dec.). ¹H-NMR (D₂O) δ : 1.27 (3H, d, $J=6.3$ Hz), 1.64 (1H, qd, $J=12.6, 4.0$ Hz), 1.95—2.05 (1H, m), 3.25—3.35 (1H, m), 3.35—3.45 (1H, m), 3.44 (1H, dd, $J=6.3, 3.4$ Hz), 3.85 (1H, d, $J=14.6$ Hz), 4.00—4.10 (1H, m), 4.25 (1H, quintet, $J=6.3$ Hz), 4.32 (1H, dd, $J=10.2, 3.4$ Hz), 5.07 (1H, dd, $J=14.6, 1.9$ Hz). IR (KBr): 3483, 3371, 3204, 1732, 1684, 1654, 1604 cm⁻¹. Anal. Calcd for C₁₃H₁₈N₄O₄ \cdot 3/2H₂O: C, 48.59; H, 6.59; N, 17.44. Found: C, 48.36; H, 6.78; N, 17.39. MS (FAB) m/z : 295 (M+H)⁺.

Measurement of Antibacterial Activity MICs were measured on Nutrient agar (Eiken Chemical Ltd.) by the twofold dilution method. The inoculum size of the bacteria was one-loopful of 107 cfu/ml.

Determination of Urinary Recovery Urine was collected at 8 and 24 h after administration. Excretion as the parent 5-formimidoyl-5-azatrinem **4q** was determined by bioassay using *Bacillus subtilis* ACTT6633. Urinary recovery (%; 0—24 h) was calculated based on the excretion and the initial dose.

References and Notes

- 1) a) Kahan J. S., Kahan F. M., Goegelman R., Currie S. A., Jackson M., Stapley E. O., Miller T. W., Hendlin D., Mochales S., Hernandez S., Woodruff H. B., 16th. Intersci. Conf. Antimicrob. Agents Chemother., Chicago (1976), Abstract No. 227; b) Albers-Schonberg G., Arison B. H., Hensens O. D., Hirshfield J., Hoogsteen K., Kaczka E. A., Rhodes R. E., Kahan J. S., Kahan F. M., Ratcliffe R. W., Walton E., Ruswinkle L. J., Morin R. B., Christensen B. G., *J. Am. Chem. Soc.*, **100**, 6491—6499 (1978).
- 2) For a review see: a) Kawamoto I., *Drugs Fut.*, **23**, 181—189 (1998); b) Berks A. H., *Tetrahedron*, **52**, 331—375 (1996).
- 3) a) Di Modugno E., Erbetti L., Ferrari L., Galassi G., Hammond S. H., Xerri L., *Antimicrob. Agents Chemother.*, **38**, 2362—2368 (1994); b) Gaviraghi G., *Eur. J. Med. Chem.*, **30** (suppl.), 467s—478s (1995).
- 4) For a recent review on trinemins see: Biondi S., "Anti-Infectives: Recent Advances in Chemistry and Structure-Activity Relationships," ed. by Bentley P. H., O'Hanlon P. J., The Royal Society of Chemistry, Cambridge, Special Publication No. 198, 1977, pp. 86—100.
- 5) a) Biondi S., Piga E., Rossi T., Vigelli G., *Bioorg. Med. Chem. Lett.*, **7**, 2061—2066 (1997); b) Schmidt G., Schrock W., Endermann R., *ibid.*, **3**, 2193—2198 (1993); c) Andreotti D., Rossi T., Marchioro C., *ibid.*, **6**, 2589—2594 (1996).
- 6) 6-Azatrinem derivatives were claimed in a patent from Takeda Chemical Industries Ltd.: Sendai M., Miwa T., Eur. Pat. Appl. EP422596, 9 Oct (1990) [*Chem. Abstr.*, **115**, 279692p (1991)].
- 7) a) Hanessian S., Rozema M. J., Reddy G. B., Braganza J. F., *Bioorg. Med. Chem. Lett.*, **5**, 2535—2540 (1995); b) Hanessian S., Griffin A. M., Rozema M. J., *ibid.*, **7**, 1857—1862 (1997).
- 8) Hanessian S., Rozema M. J., *J. Am. Chem. Soc.*, **118**, 9884—9891 (1996).
- 9) Decarboxylation of the NH unprotected compound **7a** under these reaction conditions afforded a 3 : 7 diastereomeric mixture of the decarboxylated products with predominant formation of the undesired diastereoisomer. For a similar stereochemical aspect of the decarboxylation reaction, see reference 8.
- 10) ¹H-NMR spectrum of the crude product **8a** showed that the reaction proceeded in a highly stereoselective manner (ca. 90% d.e.). The pure product was obtained by separation using flash chromatography.
- 11) Yoshida A., Tajima Y., Takeda N., Oida S., *Tetrahedron Lett.*, **25**, 2793—2796 (1984).
- 12) Sakaitani M., Ohfuné Y., *J. Org. Chem.*, **55**, 870—876 (1990).
- 13) *N,N'*-bis(allyloxycarbonyl)amidinopyrazole was prepared in a way similar to the one for the preparation of *N,N'*-bis(*tert*-butoxycarbonyl)amidinopyrazole which was reported in a) Darke B., Patek M., Lebl M., *Synthesis*, **1994**, 579—582 and b) Bernatowicz M. S., Wu Y., Matsueda G. R., *Tetrahedron Lett.*, **34**, 3389—3392 (1993).
- 14) Seki M., Kondo K., Kuroda T., Yamanaka T., Iwasaki T., *Synlett*, **1995**, 609—611.
- 15) a) Jeffrey P. D., McCombie S. W., *J. Org. Chem.*, **47**, 587—590 (1982); b) Guibe F., Dangles O., Balavoine G., *Tetrahedron Lett.*, **27**, 2365—2368 (1986); c) Hayakawa Y., Kato H., Uchiyama M., Kajino H., Noyori R., *J. Org. Chem.*, **51**, 2400—2402 (1986); d) Dangles O., Guibe F., Balavoine G., *ibid.*, **52**, 4984—4993 (1987).
- 16) Fujino M., Hatanaka C., *Chem. Pharm. Bull.*, **15**, 2015—2016 (1967).

Synthesis and α -Adrenergic Binding Ligand Affinities of 2-Iminoimidazolidine Derivatives

Jean Chang-FONG,^a Khalid BENAMOUR,^a Barbara SZYMOSKI,^a François THOMASSON,^b
Jean-Marc MORAND,^a and Max CUSSAC^{*,a}

Laboratoire de Chimie Thérapeutique^a and Service Commun de RMN,^b Groupe de Pharmacochimie Moléculaire, UMR 5063-CNRS, Faculté de Pharmacie, Université J. Fourier, 38706 La Tronche cedex, France.

Received June 4, 1999; accepted January 6, 2000

In order to obtain possible veinotonic drugs acting through α_2 receptor activation, we prepared clonidine analogues in which the 2-imino-imidazolidine was attached to various aliphatic or aromatic heterocycles. Among them, the two benzopyranic derivatives 16 and 22 exhibited interesting affinities (19 and 95 nM respectively on [³H]rauwolscine binding, compared to 35 nM for clonidine). Their affinity for α_1 receptors was found to be much lower: 7570 and 5030 nM for 16 and 22 respectively, suggesting 16 to be 400 times more selective for α_2 than for α_1 -adrenoceptors.

Key words adrenergic α_2 -ligand; veinotonic agent; imidazolidine derivative

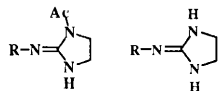
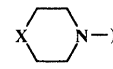
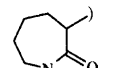
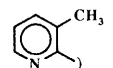
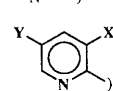
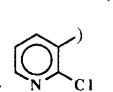
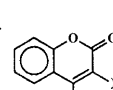
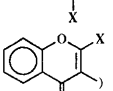
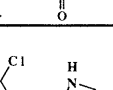
Venous pathology may result from deficiency of the venous wall contractility. The increase in venous system pressure is due to three main factors: increase of Ca²⁺ concentration in the smooth muscle cells, decrease of endothelial nitric oxide production and decrease of α -adrenergic receptors (α -AR) of the venous system.¹⁾ Our research efforts to find potentially veinotonic molecules were oriented towards α -adrenergic compounds, namely α_2 -selective agonists, devoid of any vasoconstrictor side-effect due to α_1 -AR activation, α_2 -AR being relatively more abundant in veins than in arteries.^{1–3)} Furthermore, low lipophilicity was needed to avoid hematoencephalic resorption and thus to limit the molecules' central effects. It is also well known that imidazolidine compounds enhance spontaneous mechanical activity in rat portal vein^{4,5)} and antagonize the relaxant effects of the K-channel openers.^{4–7)}

Most α_2 -adrenergic agonists belong to the classes of aralkylimidazoline and aryliminoimidazolidine derivatives, best represented by clonidine and moxonidine. With the structure–activity relationships of these aryliminoimidazolidine derivatives in mind,^{8–11)} we kept intact the 2-iminoimidazolidine fragment of the pharmacophore to preserve a good α_2 -AR binding and we only modified the aromatic moiety. Among the various structures of the R moiety linked to the imino group (Chart 1) the choice was made between aliphatic moiety and aromatic moiety which could be ortho substituted. We had a special interest in benzopyranic structures because coumarin and flavonoids are usually used as phlebotonic as well as vascular protecting agents.^{12–14)}

Chemistry The final compounds were obtained by condensation of various amines with imidazoline or imidazolidine (Chart 2) bearing adequate leaving groups in position 2 either pre-existent, as methylthio, or formed *in situ* as chloro. Starting from 2-imidazolidinethione, the hydriodide salt of 2-methylmercaptoimidazoline was prepared by the action of iodomethane¹⁵⁾ and was heated with a moderate excess of a primary amine with or without solvent until the evolution of mercaptan was complete^{16,17)} (method 1). Starting from *N*-acetylimidazolidin-2-one,¹⁸⁾ the 2-chloro derivative formed *in situ* with POCl₃^{17,19)} was condensed with the primary amine and the acetyl protecting group was finally hydrolyzed

(method 2). The initial primary amines were commercially available (series A, B) or prepared according to published procedures (series C).^{20–27)}

The structures of all compounds were confirmed by IR, ¹H-NMR, ¹³C-NMR and all final imidazolidine compounds were also confirmed by elemental analyses.

2-Iminoimidazolidine Derivatives:					
					
Series	R =	Compounds		Condensation Method	
A		X = O	1		1
		X = NCH ₃	2		
		X = CH ₃	3		
		X = (CH ₂) ₂	4		
			5		
B			6		2
		X = Y = Cl	7	8	
		X = OBz, Y = H	9	10	
			11	12	
		X = H	13	14	
C		X = CH ₃	15	16	
		X = H	17	18	
		X = CH ₃	19	20	
		X = Ph	21	22	

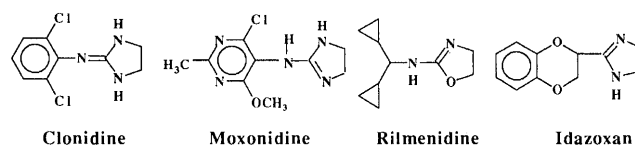


Chart 1. Top: R-Substituted Iminoimidazolidine Compounds and *N*-Protected Derivatives Bottom: Reference Compounds

* To whom correspondence should be addressed.

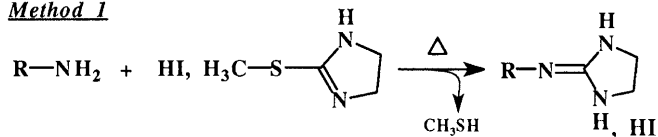
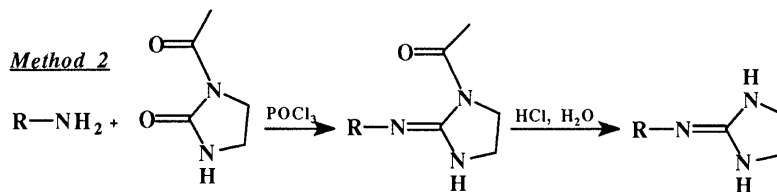
Method 1**Method 2**

Chart 2. Condensation Methods

Table 1. α_2 -Adrenoceptor IC_{50} Data by Displacement of [^3H]Clonidine with A, B Series

Compounds	IC_{50} (nM)
5	>10000
8	5000
10	3000
12	1200
Clonidine	13
Yohimbine	350

Results and Discussion

Pharmacological tests were performed with a limited number of compounds to lead our syntheses rapidly towards products bearing the required activity.

The *N*-acetylated intermediates have not been tested because this substitution of the imidazolidine moiety reduces the positive charge on the heterocycle and strongly decreases the affinity for the α_2 -AR that is tightly related to the formation of an ionic interaction between the *N*-cationic atom of the ligand and the highly conserved aspartate residue found in the helix 3 of the adrenoceptors and other G-protein coupled receptors that bind biogenic amines.²⁸⁾ α_2 -AR affinities of the first few synthesized compounds (series A, B) were estimated. The poor results of their binding abilities in comparison with clonidine and yohimbine (Table 1), a reminder that only very few products devoid of aromatic character, such as rilmenidine, have α_2 -adrenergic activity,²⁹⁾ prompted us to prepare 2-(benzopyranylimino)imidazolines. To evaluate the α_2 -AR affinities of these compounds (series C) we used [^3H]rauwolscine, a potent radiolabelled α_2 -agonist and [^3H]RX8210002, a potent radiolabelled α_2 -antagonist known to be more selective towards α_{2A} -AR. To estimate their α_2 -AR selectivities we carried out evaluation of their α_1 -AR affinities using [^3H]prazosine, a specific potent radiolabelled α_1 -agonist (Table 2). Compound **16** exhibited the most potent affinity with an IC_{50} value of 19 nM, on [^3H]rauwolscine displacement, compared to 5.7 and 35 nM for yohimbine and clonidine respectively. The binding affinity of compound **22** was lower: IC_{50} =95 nM. On [^3H]RX8210002 displacement, the affinities of **16** and **22** (IC_{50} =148 and 956 nM respectively) were lower than that of clonidine and yohimbine (IC_{50} =41 and 78 nM respectively).

These two compounds showed good α_2 -AR specificity: their α_1 -AR affinities (IC_{50} =7570 and 5030 nM for **16** and **22**

Table 2. Specific Inhibition (IC_{50} , nM) Obtained by Various Compounds Tested with Corresponding Ligand-Receptors

Compounds	Receptors		
	α_2 ([^3H]rauwolscine)	α_2 ([^3H]RX821002)	α_1 ([^3H]prazosine)
14	650	860	—
16	19	148	7570
18	410	1260	—
20	1390	4620	—
22	95	956	5030
Clonidine	35	41	610
Idazoxan	—	6	2000
Prazosine	—	—	0.3
Yohimbine	5.7	78	—

Table 3. Calculated log P Values of 2-Iminoimidazolidine Derivatives and Analogs

Compounds	CLOGP Value	Method Error	Ghose Method
1	1.33	60	-0.38
2	1.78	60	-0.24
3	3.73	60	0.69
4	4.29	60	1.08
5	1.55	60	-0.06
6	1.13	0	1.63
8	1.84	0	2.57
Clonidine	1.81	0	2.81
Idazoxan	1.65	0	0.85
10	3.06	31	2.69
12	0.71	0	1.35
14	1.71	0	0.93
16	1.67	0	1.09
18	0.85	0	0.44
20	0.81	0	0.00
22	2.95	0	1.43
Moxonidine	0.92	20	2.22
Rilmenidine	3.63	60	1.90

respectively) were low which suggests compounds **16** and **22** are respectively 50–400 times and 5–50 times more selective for α_2 -AR than for α_1 -AR. Similarly clonidine was approximately 15 times more selective for α_2 -AR than for α_1 -AR. Compound **16** is roughly as selective for α_2 -AR as idazoxan which showed an α_2 selectivity of 333.

Calculated log P (CLOGP) values of the titled compounds

and analogs (Table 3) showed some differences for moxonidine, rilmenidine and compounds **1**–**5** and **10** (probably accounted for by errors in the CLOGP method in relation with the absence of fragments in the method). Other dissimilar values might be related to the differences in the underlying principles of the two methods used for calculations. Titled compounds showed a slightly lower lipophilicity than clonidine and rilmenidine; their weakly lipophilic features can help to limit the molecules' central effects. However their possible peripheral effects should be estimated after *in vivo* experiments because some closely related compounds as moxonidine and idazoxan which have low log P values still affect central nerve system.

These preliminary results show that compound **16** exhibits good affinity for α_2 -AR, comparable to that of clonidine. Moreover its α_2 -AR selectivity is improved compared with that of clonidine and similar to that of idazoxan, which suggests that compound **16** is a potential veinotonic agent.

Experimental

Chemistry. General Procedures Melting points were determined with a Büchi 510 capillary apparatus and are uncorrected. The IR spectra were recorded on a Unicam SP1100 IR spectrophotometer using potassium bromide plates for liquid products and potassium bromide tablets for solid products; the frequencies are expressed in cm^{-1} . ^1H - and ^{13}C -NMR spectra were recorded on a Bruker AC 200 spectrometer in CDCl_3 or dimethyl sulfoxide ($\text{DMSO}-d_6$) solution. Chemical shifts are given in δ (ppm) unit relative to internal reference Me_4Si (s: singlet, d: doublet, t: triplet, q: quintet, m: multiplet, br: broad). Elemental analyses (C, H, N, Cl, I, O) were carried out in the Service Central d'Analyses, Centre National de la Recherche Scientifique, 69390 Vernaison, France, and were within $\pm 0.4\%$ of theoretical values unless otherwise noted. Reaction progress and purity of products were checked by carrying out TLC using Silica Gel Merck 60F₂₅₄; the spots were visualised by UV and iodine vapour. The log P values were calculated by two methods: CLOGP method of Leo which is basically a fragment method that accounts for steric, electronic and hydrogen bonding interactions³⁰ and Ghose and Crippen's method which uses atom-type descriptors selected by regression procedure.³¹

Synthesis of Benzopyranyl Amines 3-Aminocoumarin was prepared from salicylaldehyde and acetylglutamine according to Chakravarty *et al.*^{20,21} 3-Amino-4-methylcoumarin was prepared from hippuric acid via the 2-phenyloxazoline-5-one according to Tripathy and Mukerjee.²² 3-Aminochromone and 2-methyl-3-aminochromone were prepared by cyclization of 2'-hydroxy-2-nitroacetophenone by AcOCHO and Ac_2O respectively followed by reduction of the 3-nitro moiety according to Becket and Ellis²³ and Tanaka *et al.*²⁴ The 2'-hydroxy-2-nitroacetophenone was obtained by nitration of 4-hydroxycoumarin followed by saponification according to Huebner and Link.²⁵ 3-Amino-4-methylcoumarin was obtained by nitrosation followed by reduction of the flavanone according to Oyamada and Fukawa²⁶ and to Shimizu and Nakazawa.²⁷

Synthesis of 2-Iminoimidazolidine Compounds (Method 1) 2-(4-Morpholinyl)iminoimidazolidine (**1**): A solution of 2-methylmercapto-4,5-dihydroimidazole hydriodide (6.1 g, 25 mmol) and *N*-aminomorpholine (5.1 g, 50 mmol) in ethanol (30 ml) was refluxed for 8 h. After cooling, the solution was evaporated to give a residue which was dissolved in water (10 ml). A precipitate was obtained by alkalization with 30% aqueous NaOH (30 ml). The precipitate was filtered and purified by crystallization from CHCl_3 . Yield 3.0 g (71%); mp 214°C (Lit. 216°C).³² ^1H -NMR ($\text{DMSO}-d_6$) δ : 2.34 (4H, s), 3.18 (4H, s), 3.58 (4H, s), 5.85 (2H, brs). ^{13}C -NMR ($\text{DMSO}-d_6$) δ : 41.9 (t), 56.4 (t), 66.0 (t), 162.1 (s). *Anal.* Calcd for $\text{C}_8\text{H}_{14}\text{N}_4\text{O}$: C, 49.39; H, 8.29; N, 32.92; O, 9.40. Found: C, 49.22; H, 8.41; N, 32.61; O, 9.67.

2-[(1-(4-Methylpiperazinyl)]iminoimidazolidine Hydriodide (**2**): A solution of 2-methylmercapto-4,5-dihydroimidazole hydriodide (2.4 g, 10 mmol) and 1-amino-4-methylpiperazine (2.3 g, 20 mmol) in ethanol (20 ml) was refluxed for 8 h. After cooling, the solution was evaporated to give a residue which was washed with ether. Yield 2.9 g (67%); mp 165°C . ^1H -NMR ($\text{DMSO}-d_6$) δ : 2.17 (3H, s), 2.42 (4H, m), 2.76 (4H, t, $J=4.5$ Hz), 3.59 (4H, s), 8.11 (2H, brs). ^{13}C -NMR ($\text{DMSO}-d_6$) δ : 41.5 (q), 42.3 (t), 53.7 (t), 54.3 (t), 159.2 (s). *Anal.* Calcd for $\text{C}_8\text{H}_{18}\text{N}_5$: C, 30.88; H, 5.83; N, 22.51; I,

40.78. Found: C, 30.65; H, 5.99; N, 22.64; I, 40.74.

2-(1-Piperidinyl)iminoimidazolidine (**3**): Similarly to **1**, **3** was prepared from 2-methylmercapto-4,5-dihydroimidazole hydriodide (6.1 g, 25 mmol) and *N*-aminopiperidine (5.0 g, 50 mmol), and purified by crystallization from CH_2Cl_2 . Yield 3.2 g (76%); mp 176°C (Lit. 174°C).³² ^1H -NMR ($\text{DMSO}-d_6$) δ : 1.35 (2H, d, $J=5.0$ Hz), 1.56 (4H, t, $J=5.0$ Hz), 2.45 (4H, m), 3.40 (4H, s), 6.01 (2H, brs). ^{13}C -NMR ($\text{DMSO}-d_6$) δ : 23.6 (t), 25.5 (t), 42.3 (t), 57.1 (t), 161.7 (s). *Anal.* Calcd for $\text{C}_8\text{H}_{16}\text{N}_4$: C, 57.11; H, 9.59; N, 33.30. Found: C, 57.34; H, 9.60; N, 33.07.

2-[(1-Perhydroazepinyl)]iminoimidazolidine Hydriodide (**4**): Similarly to **2**, **4** was prepared from 2-methylmercapto-4,5-dihydroimidazole hydriodide (6.1 g, 25 mmol) and 1-aminoperhydroazepine (5.1 g, 50 mmol). Yield 6.3 g (81%); mp 138°C . ^1H -NMR ($\text{DMSO}-d_6$) δ : 1.57 (8H, brs), 2.87 (s, 4H), 3.59 (4H, s), 7.80 (2H, brs). ^{13}C -NMR ($\text{DMSO}-d_6$) δ : 25.4 (t), 26.0 (t), 42.4 (t), 159.3 (s). *Anal.* Calcd for $\text{C}_9\text{H}_{19}\text{N}_4$: C, 34.85; H, 6.17; N, 18.06; I, 40.91. Found: C, 34.87; H, 6.23; N, 17.86; I, 40.92.

2-[3-(2-Oxoperhydroazepinyl)]iminoimidazolidine Hydriodide (**5**): A solution of 2-methylmercapto-4,5-dihydroimidazole hydriodide (6.1 g, 25 mmol) and 3-amino-2-oxoperhydroazepine (3.2 g, 25 mmol) in ethanol (20 ml) was refluxed for 2 h. After cooling, the solution was evaporated to give an oily residue which was washed with ether and acetone and evaporated to dryness. Yield 2.1 g (68%); mp 225°C . ^1H -NMR ($\text{DMSO}-d_6$) δ : 1.22 (H, m), 1.51 (H, m), 1.75 (2H, brs), 1.80 (2H, brs), 3.11 (4H, m), 3.60 (4H, s), 4.31 (H, d, $J=10.0$ Hz), 7.99 (H, t, $J=6.0$ Hz), 8.02 (2H, brs). ^{13}C -NMR ($\text{DMSO}-d_6$) δ : 26.7 (t), 28.4 (t), 31.0 (t), 40.4 (t), 32.5 (t), 54.2 (d), 158.2 (s), 172.5 (s). *Anal.* Calcd for $\text{C}_9\text{H}_{17}\text{N}_4\text{O}$: C, 33.35; H, 5.29; N, 17.28; O, 4.94; I, 39.15. Found: C, 33.34; H, 5.41; N, 17.10; O, 5.34; I, 38.81.

2-[2-(3-Methylpyridinyl)]iminoimidazolidine Hydriodide (**6**): A mixture of 2-methylmercapto-4,5-dihydroimidazole hydriodide (4.0 g, 16 mmol) and 2-amino-3-picoline (5.2 g, 48 mmol) was heated under nitrogen atmosphere at 195 – 200°C for 5 h. After cooling, the residue was repeatedly washed with acetone and dried. Yield 3.6 g (74%); mp 248 – 252°C (dec.). ^1H -NMR ($\text{DMSO}-d_6$) δ : 2.28 (3H, s), 3.74 (4H, s), 7.14 (H, dd, $J=7.5$, 4.5 Hz), 7.73 (H, dd, $J=7.5$, 2.5 Hz), 8.18 (H, dd, $J=4.5$, 2.5 Hz). ^{13}C -NMR ($\text{DMSO}-d_6$) δ : 16.6 (q), 42.6 (t), 119.9 (d), 121.5 (s), 140.1 (d), 144.4 (d), 148.9 (s), 156.2 (s). *Anal.* Calcd for $\text{C}_9\text{H}_{13}\text{N}_4$: C, 35.54; H, 4.31; N, 18.42; I, 41.73. Found: C, 35.65; H, 4.10; N, 18.19; I, 41.95.

Synthesis of 2-Iminoimidazolidine Compounds (Method 2). a) Condensations of the Amines with POCl_3 1-Acetyl-2-[2-(3,5-dichloropyridinyl)]iminoimidazolidine (**7**): A solution of 1-acetylimidazolidin-2-one (3.8 g, 30 mmol) and 2-amino-3,5-dichloropyridine (3.9 g, 30 mmol) in POCl_3 (30 ml) was refluxed for 3 h. POCl_3 was evaporated, and the residue was dissolved in ice-cooled water, and the aqueous solution was alkalinized by 30% aqueous NaOH until pH 8. The crude product was extracted by CHCl_3 (3×20 ml), the collected extracts were dried over Na_2SO_4 and concentrated under reduced pressure. Recrystallization from cyclohexane gave product **7**. Yield 4.2 g (51%); mp 141°C . ^1H -NMR ($\text{DMSO}-d_6$) δ : 2.31 (3H, s), 3.40 (2H, t, $J=8.0$ Hz), 3.80 (2H, t, $J=8.0$ Hz), 7.60 (H, d, $J=2.5$ Hz), 7.67 (H, brs), 8.05 (H, d, $J=2.5$ Hz).

1-Acetyl-2-[2-(3-benzoyloxypropyl)]iminoimidazolidine (**9**): This compound was prepared from 1-acetylimidazolidin-2-one (3.8 g, 30 mmol) and 2-amino-3-benzoyloxypropylamine (6.0 g, 30 mmol) and was recrystallized from isopropanol. Yield 2.2 g (24%); mp 184°C . ^1H -NMR ($\text{DMSO}-d_6$) δ : 7.84 (brs, H, NH), 7.60 (dd, H, H_6 , $J=5.0$, 1.5 Hz), 7.40 (m, 5H, 5Ar-H), 7.10 (dd, H, H_4 , $J=8.0$, 1.5 Hz), 6.60 (dd, H, H_5 , $J=8.0$, 5.0 Hz), 5.21 (s, 2H, CH_2), 3.60 (t, 2H, CH_2 , C_{12} , $J=8.0$ Hz), 3.20 (t, 2H, CH_2 , C_{13} , $J=8.0$ Hz), 2.38 (s, 3H, CH_3).

1-Acetyl-2-[3-(2-chloropyridinyl)]iminoimidazolidine (**11**): This compound was prepared from 1-acetylimidazolidin-2-one (3.8 g, 30 mmol) and 3-amino-2-chloropyridine (3.8 g, 30 mmol) and was recrystallized from ethyl acetate. Yield 5.3 g (74%); mp 181°C . ^1H -NMR ($\text{DMSO}-d_6$) δ : 2.53 (3H, s), 3.30 (2H, t, $J=8.0$ Hz), 3.83 (2H, t, $J=8.0$ Hz), 7.06 (H, brs), 7.28 (H, dd, $J=8.0$, 4.5 Hz), 7.39 (H, dd, $J=8.0$, 2.0 Hz), 7.97 (H, dd, $J=4.5$, 2.0 Hz).

1-Acetyl-2-(2-oxo-2H-benzopyran-3-yl)iminoimidazolidine (**13**): This compound was prepared from 1-acetylimidazolidin-2-one (1.3 g, 10 mmol), 3-aminocoumarin (1.6 g, 10 mmol) and POCl_3 (10 ml) and was recrystallized from ethanol. Yield 0.8 g (30%); mp 250°C (dec.). ^1H -NMR ($\text{DMSO}-d_6$) δ : 2.18 (3H, s), 3.85 (4H, m), 7.34 (3H, m), 7.62 (H, dd, $J=7.5$, 1.5 Hz), 8.61 (H, s), 9.61 (H, brs).

1-Acetyl-2-(4-methyl-2-oxo-2H-benzopyran-3-yl)iminoimidazolidine (**15**): This compound was prepared from 1-acetylimidazolidin-2-one (1.3 g, 10 mmol), 3-amino-4-methylcoumarin (1.8 g, 10 mmol) and POCl_3 (10 ml). The product was chromatographed with $\text{CHCl}_3/\text{MeOH}$, 9:1 as eluent. Yield 1.4 g (50%); mp 174°C (dec.). ^1H -NMR (CDCl_3) δ : 2.23 (3H, s), 2.35 (3H,

s), 3.53 (2H, t, $J=8.5$ Hz), 4.13 (2H, t, $J=8.5$ Hz), 7.27 (H, m), 7.33 (H, m), 7.42 (H, m), 7.57 (H, dd, $J=7.5$, 2.0 Hz), 8.61 (H, s).

1-Acetyl-2-(4-oxo-4H-benzopyran-3-yl)iminoimidazolidine (17): In the first step, the 3-aminochromone was converted by action with gaseous HCl in ethanol into its hydrochloride salt: mp 200 °C. The mixture of 3-aminochromone hydrochloride (2.0 g, 10 mmol) and 1-acetylimidazolidin-2-one (1.3 g, 10 mmol) was dissolved in POCl_3 (10 ml) at 50 °C and stirred for 20 h. The product was chromatographed with $\text{CHCl}_3/\text{MeOH}$, 9:1 as eluent. Yield 1.4 g (53%): mp 257 °C (dec.). $^1\text{H-NMR}$ (CDCl_3) δ : 2.25 (3H, s), 3.95 (4H, s), 7.37 (H, ddd, $J=8.0$, 7.0, 1.0 Hz), 7.47 (H, dd, $J=8.5$, 1.0 Hz), 7.65 (H, ddd, $J=8.5$, 7.0, 1.5 Hz), 8.29 (H, dd, $J=8.0$, 1.5 Hz), 9.38 (H, s), 10.42 (H, brs).

1-Acetyl-2-(2-methyl-4-oxo-4H-benzopyran-3-yl)iminoimidazolidine (19): Similarly to 17, 19 was prepared from the 3-amino-2-methylchromone that was first converted into its hydrochloride salt: mp 230 °C and then condensed with 1-acetylimidazolidin-2-one dissolved in POCl_3 . Yield 1.5 g (65%): mp 248 °C (dec.). $^1\text{H-NMR}$ (CDCl_3) δ : 2.46 (3H, s), 2.65 (3H, s), 3.43 (2H, dt, $J=8.0$, 1.5 Hz), 3.94 (2H, t, $J=8.0$ Hz), 5.36 (H, brs), 7.32 (H, dd, $J=8.0$, 7.0 Hz), 7.38 (H, d, $J=8.5$ Hz), 7.58 (H, ddd, $J=9.5$, 7.0, 1.5 Hz), 8.15 (H, dd, $J=8.0$, 1.5 Hz).

1-Acetyl-2-(4-oxo-2-phenyl-4H-benzopyran-3-yl)iminoimidazolidine (21): This compound was prepared from 1-acetylimidazolidin-2-one (1.3 g, 10 mmol), 3-aminoflavone (2.4 g, 10 mmol), and POCl_3 (10 ml) at 50 °C for 20 h. The product was chromatographed with $\text{CHCl}_3/\text{MeOH}$, 9:1 as eluent. Yield 0.8 g (22%): mp 175 °C. $^1\text{H-NMR}$ ($\text{DMSO}-d_6$) δ : 2.47 (3H, s), 3.26 (2H, t, $J=8.0$ Hz), 3.84 (2H, t, $J=8.0$ Hz), 6.99 (H, brs), 7.45 (H, ddd, $J=8.0$, 7.5, 1.5 Hz), 7.51 (3H, m), 7.69 (H, dd, $J=8.5$, 1.5 Hz), 7.78 (H, ddd, $J=8.5$, 7.5, 1.5 Hz), 8.02 (2H, ddd, $J=8.0$, 2.5, 1.5 Hz), 8.09 (H, dd, $J=8.0$, 1.5 Hz).

b) N-Desacetylation 2-[2-(3,5-Dichloropyridinyl)]iminoimidazolidine (8): The acetylated compound 7 was refluxed in water until full dissolution. After cooling, the precipitate obtained by basification with 30% aqueous NaOH was washed with acetone and dried. Yield 2.0 g (58%): mp 184 °C. $^1\text{H-NMR}$ ($\text{DMSO}-d_6$) δ : 3.47 (4H, s), 7.75 (H, d, $J=2.5$ Hz), 7.78 (2H, s), 8.00 (H, d, $J=2.5$ Hz). $^{13}\text{C-NMR}$ ($\text{DMSO}-d_6$) δ : 41.3 (t), 118.6 (s), 123.0 (s), 136.1 (d), 142.6 (d), 157.4 (s), 161.2 (s). *Anal.* Calcd for $\text{C}_8\text{H}_8\text{Cl}_2\text{N}_4$: C, 41.96; H, 3.49; N, 24.25; Cl, 30.69. Found: C, 41.62; H, 3.42; N, 20.00; Cl, 30.98.

2-[2-(3-Benzyloxy-pyridinyl)]iminoimidazolidine (10): Similarly to 8, the acetylated compound 9 was hydrolyzed to give 10. Yield 1.0 g (24%): mp 142 °C. $^1\text{H-NMR}$ ($\text{DMSO}-d_6$) δ : 3.42 (4H, s), 5.04 (2H, s), 6.60 (H, dd, $J=8.0$, 5.0 Hz), 7.07 (H, dd, $J=8.0$, 1.5 Hz), 7.35 (5H, m), 7.66 (H, dd, $J=5.0$, 1.5 Hz), 7.78 (2H, brs). $^{13}\text{C-NMR}$ ($\text{DMSO}-d_6$) δ : 41.3 (t), 69.5 (t), 114.1 (d), 119.0 (d), 127.7 (d), 127.9 (d), 128.3 (d), 137.4 (d), 137.5 (s), 146.7 (s), 154.2 (s), 160.8 (s). *Anal.* Calcd for $\text{C}_{15}\text{H}_{16}\text{N}_4\text{O}$: C, 67.14; H, 6.01; N, 20.88; O, 5.97. Found: C, 66.75; H, 6.20; N, 20.69; O, 6.36.

2-[2-(2-Chloropyridinyl)]iminoimidazolidine (12): Similarly to 8, the acetylated compound 11 was hydrolyzed to give 12. Yield 3.5 g (81%): mp 178 °C. $^1\text{H-NMR}$ ($\text{DMSO}-d_6$) δ : 3.34 (4H, s), 6.37 (2H, brs), 7.15 (H, dd, $J=8.0$, 4.5 Hz), 7.31 (H, dd, $J=4.5$, 2.0 Hz), 7.79 (H, dd, $J=8.0$, 2.0 Hz). $^{13}\text{C-NMR}$ ($\text{DMSO}-d_6$) δ : 41.7 (t), 123.1 (d), 131.1 (d), 139.6 (d), 144.8 (s), 145.0 (s), 158.4 (s). *Anal.* Calcd for $\text{C}_8\text{H}_9\text{ClN}_4$: C, 48.86; H, 4.61; N, 28.49; Cl, 18.03. Found: C, 49.05; H, 4.67; N, 28.34; Cl, 17.93.

2-(2-Oxo-2H-benzopyran-3-yl)iminoimidazolidine Hydrochloride (14): 13 (1.8 g, 7 mmol) was dissolved in 1 N HCl (10 ml) and water (20 ml) at 50 °C. The cooled solution was alkalinized by dilute aqueous NaOH. The crude product was filtered, dried, and converted into its hydrochloride salt with gaseous HCl in ethanol. Yield 0.7 g (46%): mp 246 °C (dec.). $^1\text{H-NMR}$ ($\text{DMSO}-d_6$) δ : 3.67 (4H, s), 7.39 (H, ddd, $J=8.5$, 7.5, 1.0 Hz), 7.44 (H, dd, $J=7.0$, 1.0 Hz), 7.62 (H, ddd, $J=8.5$, 7.0, 1.5 Hz), 7.75 (H, dd, $J=7.5$, 1.5 Hz), 8.11 (H, s), 9.22 (2H, brs). $^{13}\text{C-NMR}$ ($\text{DMSO}-d_6$) δ : 42.7 (t), 116.0 (d), 118.7 (s), 122.5 (s), 124.8 (d), 128.5 (d), 131.5 (d), 135.1 (d), 151.7 (s), 157.7 (s), 158.1 (s). *Anal.* Calcd for $\text{C}_{12}\text{H}_{12}\text{ClN}_3\text{O}_2$: C, 54.24; H, 4.55; N, 15.82; O, 12.04; Cl, 13.34. Found: C, 53.88; H, 4.65; N, 15.65; O, 12.44; Cl, 13.40.

2-(4-Methyl-2-oxo-2H-benzopyran-3-yl)iminoimidazolidine (16): 15 (1.4 g, 5 mmol) was dissolved in 1 N HCl (20 ml) at 50 °C. The cooled solution was alkalinized by dilute aqueous NaOH. The crude product was filtered, dried, and recrystallized from a mixture of ethanol and dry ether. Yield 0.5 g (42%): mp 265–270 °C (dec.). $^1\text{H-NMR}$ ($\text{DMSO}-d_6$) δ : 2.18 (3H, s), 3.30 (4H, s), 7.29 (3H, m), 7.50 (H, dd), 9.14 (2H, brs). $^{13}\text{C-NMR}$ ($\text{DMSO}-d_6$) δ : 12.8 (q), 41.7 (t), 115.4 (d), 122.0 (s), 123.7 (d), 127.6 (d), 131.8 (s), 132.1 (d), 134.4 (s), 149.7 (s), 158.2 (s). *Anal.* Calcd for $\text{C}_{13}\text{H}_{13}\text{N}_3\text{O}_2$: C, 64.18; H, 5.39; N, 17.27; O, 13.15. Found: C, 64.26; H, 5.37; N, 17.13; O,

13.24.

2-(4-Oxo-4H-benzopyran-3-yl)iminoimidazolidine Hydrochloride (18): A solution of 17 (1.0 g, 5 mmol) in conc. HCl (10 ml) and water (10 ml) was refluxed for 1 h. After cooling the solution was basified with dilute aqueous NaOH to give a precipitate which was filtered, dried, and converted into its hydrochloride salt by gaseous HCl in ethanol. Yield 0.7 g (78%): mp 271 °C (dec.). $^1\text{H-NMR}$ ($\text{DMSO}-d_6$) δ : 3.64 (4H, s), 7.55 (H, ddd, $J=8.0$, 7.0, 1.0 Hz), 7.74 (H, dd, $J=8.5$, 1.0 Hz), 7.88 (H, ddd, $J=8.5$, 7.0, 1.5 Hz), 8.11 (H, dd, $J=8.0$, 1.5 Hz), 8.48 (2H, brs), 8.68 (H, s). $^{13}\text{C-NMR}$ ($\text{DMSO}-d_6$) δ : 42.6 (t), 118.6 (d), 120.9 (s), 123.6 (s), 125.2 (d), 125.8 (d), 134.6 (d), 155.6 (s), 156.1 (d), 159.5 (s), 173.4 (s). *Anal.* Calcd for $\text{C}_{12}\text{H}_{12}\text{ClN}_3\text{O}_2$: C, 54.24; H, 4.55; N, 15.82; O, 12.04; Cl, 13.34. Found: C, 54.09; H, 4.61; N, 15.73; O, 12.40; Cl, 13.17.

2-(2-Methyl-4-oxo-4H-benzopyran-3-yl)iminoimidazolidine Hydrochloride (20): Starting with 19 (1.4 g, 5 mmol), conc. HCl (25 ml) and water (25 ml), this compound was prepared similarly to 18. Yield 0.9 g (65%): mp 222–224 °C (dec.). $^1\text{H-NMR}$ ($\text{DMSO}-d_6$) δ : 2.28 (3H, s), 3.28 (4H, s), 5.95 (2H, brs), 7.35 (H, ddd, $J=8.0$, 7.0, 1.0 Hz), 7.51 (H, dd, $J=8.5$, 1.0 Hz), 7.66 (H, ddd, $J=8.5$, 7.0, 1.5 Hz), 8.00 (H, dd, $J=8.0$, 1.5 Hz). $^{13}\text{C-NMR}$ ($\text{DMSO}-d_6$) δ : 16.8 (q), 41.8 (t), 117.6 (d), 123.2 (s), 123.8 (d), 125.3 (d), 131.6 (s), 132.3 (d), 154.6 (s), 156.1 (s), 159.8 (s), 173.4 (s). *Anal.* Calcd for $\text{C}_{13}\text{H}_{14}\text{ClN}_3\text{O}_2$: C, 55.82; H, 5.05; N, 15.02; O, 11.44; Cl, 12.68. Found: C, 55.62; H, 5.04; N, 14.75; O, 11.57; Cl, 13.01.

2-(4-Oxo-2-phenyl-4H-benzopyran-3-yl)iminoimidazolidine Hydrochloride (22): Starting with 21 (2.2 g, 6 mmol), conc. HCl (20 ml) and water (20 ml), this compound was prepared similarly to 18. Yield 0.8 g (45%): mp 286 °C (dec.). $^1\text{H-NMR}$ ($\text{DMSO}-d_6$) δ : 3.55 (4H, s), 7.58 (4H, m), 7.78 (H, d, $J=8.5$ Hz), 7.87 (3H, m), 8.12 (H, d, $J=8.0$ Hz), 8.49 (2H, brs). $^{13}\text{C-NMR}$ ($\text{DMSO}-d_6$) δ : 42.6 (t), 117.5 (s), 118.6 (d), 122.9 (s), 125.3 (d), 125.9 (d), 128.6 (d), 128.7 (d), 130.4 (s), 131.6 (d), 134.8 (d), 155.4 (s), 159.3 (s), 163.1 (s), 174.3 (s). *Anal.* Calcd for $\text{C}_{18}\text{H}_{16}\text{ClN}_3\text{O}_2$: C, 63.25; H, 4.72; N, 12.30; O, 9.36; Cl, 10.37. Found: C, 63.11; H, 4.82; N, 12.31; O, 9.33; Cl, 10.43.

Binding Studies. Competition with [^3H]Clonidine According to Moret et al.³³ Rat forebrain membranes were incubated in triplicate at 25 °C for 30 min, at the final concentration of 5.6 mg/ml of tissue, with [^3H]clonidine (5 nM) (Amersham), with tested compounds at various concentrations with buffer (50 mM Tris-HCl) alone at pH 7.5 (total binding), or with buffer containing clonidine (1 μM) (nonspecific binding) in a total volume of 2 ml. Membranes were filtered on Whatman GF/C fiberglass filter paper and washed with ice-cold buffer. Bound activity was then determined by liquid scintillation spectrometry. Specific binding was defined as the difference between total binding and nonspecific binding. The IC_{50} values were determined after appropriate displacement results by the log-probit linear regression analysis. Clonidine and yohimbine were used as reference molecules.

Competition with [^3H]Rauwolsine According to Diop et al.³⁴ Binding studies were performed in triplicate with rat crude cerebrocortical membranes incubated at 25 °C for 30 min with [^3H]rauwolsine (1 nM) (Dupont NEN) with 10^{-7} , 10^{-6} and 10^{-5} M concentrations of tested compounds, either with buffer (Tris-HCl, pH=7.5) alone (total binding), or with buffer containing 100 μM (–) noradrenaline (Sigma)(nonspecific binding) in a total volume of 300 μl . Membranes were filtered and washed with ice-cold incubation buffer using a cell harvester (Brandel). Bound radioactivity was determined by counting with a Beckman LS 6000 liquid scintillation counter. IC_{50} values of tested compounds with corresponding ligand-receptors were calculated through linear regression analysis. These were mean values from 3 independent determinations.

Competition with [^3H]RX821002 According to Uhlen and Wikberg³⁵ These assays were performed as previously reported, using [^3H]RX821002 (2 nM) (Dupont NEN), (–) adrenaline (10 μM) (Sigma) as nonspecific ligand, and yohimbine as the reference molecule. Results are given as IC_{50} values as before.

Competition with [^3H]Prazosine According to Greengrass and Bremner³⁶ These assays were performed as previously reported, using [^3H]prazosine (0.25 nM) (Dupont NEN) and prazosine (0.5 M) (Sigma) as nonspecific ligand, and a 60 min/25 °C incubation. Results are given as IC_{50} values as before.

Acknowledgments The authors thank Pierre-Emmanuel Colle, Ahcene Boumendjel and Jacques-Antoine Duret for their helpful assistance.

References

- McGrath J. C., Brown C. M., Wilson V. G., *Med. Res. Rev.*, **9**, 506–507 (1989).

- 2) Flavahan N. A., Rimele T. J., Cooke J. P., Vanhoutte P. M., *J. Pharmacol. Exp. Ther.*, **230**, 699—705 (1984).
- 3) Daly C., Mc Grath J., Wilson V., *Brit. J. Pharmacol.*, **94**, 1085—1090 (1988).
- 4) Noack T., Edwards G., Deitmer P., Greengrass P., Morita T., Andersson P. O., Criddle D., Wyllie M. G., Weston A. H., *Brit. J. Pharmacol.*, **106**, 17—24 (1992).
- 5) Schwietert R., Wilhem D., Wilffert B., van Zwieten P. A., *Eur. J. Pharmacol.*, **211**, 87—95 (1992).
- 6) McPherson G. A., Angus J. A., *Brit. J. Pharmacol.*, **97**, 941—949 (1989).
- 7) Ibbotson T., Edwards G., Weston A. H., *Brit. J. Pharmacol.*, **110**, 1556—1564 (1993).
- 8) Rouot B., Leclerc G., Wermuth C. G., *Eur. J. Med. Chem.*, **5**, 545—551 (1973).
- 9) Rouot B., Leclerc G., Wermuth C. G., Miesch F., Schwartz J., *J. Med. Chem.*, **19**, 1049—1054 (1976).
- 10) Timmermans P. B. M. W. M., Van Zwieten P. A., *J. Med. Chem.*, **20**, 1636—1644 (1977).
- 11) Timmermans P. B. M. W. M., Hoefke W., Stähle H., Van Zwieten P. A., *Progr. Pharmacol.*, **3**, 1—104 (1980).
- 12) Reuter H. D., "Les Phytomédicaments Vaso-actifs, in Phytothérapie, aromatothérapie," Vol. 9 ed. by Editions Techniques, Encycl. Méd. Nat., Paris, 1991, D-5, 24 p.
- 13) Vin F., Varices, "Cardiologie-Angéiologie," ed. by Editions Techniques, Encycl. Méd. Chir., Paris, 1992, **11720A**¹⁰, p. 14.
- 14) Bruneton J., Flavonoïdes, "Pharmacognosie, Phytochimie, Plantes Médicinales," 2nd ed., ed. by Tech. Doc., Paris, **1997**, pp. 265—300.
- 15) Aspinall S. R., Bianco E. J., *J. Am. Chem. Soc.*, **73**, 602—603 (1951).
- 16) Najer H., Guidicelli R., Sette J., *Bull. Soc. Chim. France*, **1961**, 2114—2116.
- 17) Chapleo C. B., Butter R. C. M., England D. C., Myers P. L., Roach A. G., Smith C. F. C., Stillings M. R., Tulloch I. F., *J. Med. Chem.*, **32**, 1627—1630 (1989).
- 18) Roberts J. G., *J. Chem. Soc.*, **1964**, 176—178.
- 19) Nathanson J. A., Kaugars G., *J. Med. Chem.*, **32**, 1795—1799 (1989).
- 20) Chakravarty D., Dutta S. P., Mitra A. K., *Current Sci.*, **34**, 177—179 (1965).
- 21) Chakravarty D., Das R., *J. Indian Chem. Soc.*, **48**, 371—374 (1971).
- 22) Tripathy P. K., Mukerjee A. K., *Heterocycles*, **26**, 1517—1520 (1987).
- 23) Becket G. J. P., Ellis G. P., *Tetrahedron Lett.*, **1976**, 719—720.
- 24) Tanaka M., Murakami Y., Morita H., Takagi K., *Chem. Pharm. Bull.*, **33**, 2129—2132 (1985).
- 25) Huebner C. F., Link K. P., *J. Am. Chem. Soc.*, **67**, 99—102 (1945).
- 26) Oyamada T., Fukawa T., *J. Chem. Soc. Jpn.*, **64**, 1163—1166 (1943).
- 27) Shimizu M., Nakazawa S., *J. Chem. Soc. Jpn.*, **73**, 522—523 (1953).
- 28) Strader C., Fong T., Tota M., Underwood D., Dixon R., *Annu. Rev. Biochem.*, **63**, 101—134 (1994).
- 29) Guicheney P., Dausse J.-P., Meyer P., *J. Pharmacol. (Paris)*, **12**, 255—262 (1981).
- 30) Leo A., *Chem. Rev.*, **93**, 1281—1306 (1993).
- 31) Ghose A., Crippen G., *J. Comp. Chem.*, **7**, 565—577 (1986).
- 32) Laboratoire Lafon., Belg. Pat. 812,749 (Cl. C 07 d) (15 Jul 1974) 8 p.
- 33) Moret C., Charveron M., Finberg J. P. M., Couzinier J. P., Briley M., *Neuropharmacol.*, **24**, 1211—1219 (1985).
- 34) Diop L., Dausse J. P., Meyer P., *J. Neurochem.*, **41**, 710—715 (1983).
- 35) Uhlen S., Wikberg J. E., *Pharmacol. Toxicol.*, **69**, 341—350 (1991).
- 36) Greengrass P., Bremner R., *Eur. J. Pharmacol.*, **55**, 323—326 (1979).

Studies on Bioadhesive Granules I: Granules Formulated with *Prosopis africana* (Prosopis) Gum

Anthony A. ATTAMA,* Michael U. ADIKWU, and Ngozi D. OKOLI

Division of Physical Pharmaceutics, Faculty of Pharmaceutical Sciences, University of Nigeria Nsukka, Nigeria.

Received August 5, 1999; accepted November 2, 1999

Prosopis gum (PG) extracted from *Prosopis africana* was investigated for bioadhesive delivery of theophylline (TPL). Bioadhesive granules containing TPL were formulated and the bioadhesive properties evaluated using adhesion of the granules onto a porcine intestinal mucus surface. The bioadhesion of the gum dispersion was also evaluated using coated glass beads and the strength of the films formulated from the gums was also determined. The release properties of the TPL-containing granules were assessed by diffusion of TPL from the granules through porcine intestinal wall into a sink solution. Sodium carboxymethylcellulose (SCMC) was used as the standard bioadhesive polymer. Results indicated that PG is highly bioadhesive compared to SCMC. The result of the release studies also showed that PG could be used to deliver TPL in a bioadhesive dosage form.

Key words bioadhesion; granules; prosopis gum, sodium carboxymethylcellulose.

Most biological tissues contain mucosal epithelia covered by mucus.¹⁾ This makes it possible for bioadhesive polymers to interact with such tissues producing the phenomenon of bioadhesion. Glycoproteins present in mucus are believed to be responsible for interaction between mucus and biopolymers.²⁾ However, many factors play a role in bioadhesion.^{3–5)} Many *in vitro* methods are used to evaluate bioadhesion,^{6,7)} but *in vivo* evaluation remains the most informative.⁸⁾ Indeed, the method employed for evaluation of the bioadhesive properties of a polymer is generally formulation-specific and many biopolymers have been evaluated for bioadhesive delivery of drugs,⁹⁾ however applicability depends on the target area and the physicochemical properties of the candidate polymer. In this study, prosopis gum (PG) obtained from the tropical plant, *Prosopis africana* (Fam. Mimosaceae) was used for bioadhesive-prolonged delivery of theophylline (TPL), an antiasthmatic drug whose physicochemical properties favour such a delivery system.¹⁰⁾ *Prosopis africana* has been the subject of interest of many workers and has been assessed in many dosage forms.^{11–15)} Gums are made up of highly branched polysaccharides with chain structure formed when monosaccharides condense with the elimination of water molecule(s). PG is a natural polysaccharide consisting chiefly of glucose, fructose, galactose and xylose as the monosaccharide units, as determined by thin layer chromatography and complete acid hydrolysis analysis.¹⁶⁾

Materials and Methods

Materials Sodium carboxymethylcellulose (SCMC) (Aqualon); sodium chloride and hydrochloric acid (Merck); TPL (BDH); and acetone and ethanol (M and B) were used without further purification. All other reagent solvents were of analytical grade and were used as supplied. Distilled water was obtained from a glass still while PG was obtained from a batch processed in our laboratory.

Preparation of PG PG was extracted from the seeds of *Prosopis africana* using the method described in an earlier study.¹⁶⁾

Evaluation of the Bioadhesive Strength of the Polymers Use of Coated Glass Beads Increasing concentrations of PG and SCMC were used to coat glass beads with an average diameter of 3 mm and average weight 56 mg. The beads were coated to an average weight of 65 mg, by successive dipping in the polymer solution, air-drying and storage in a desiccator until use. Concentrations of polymers used for the study were 1.0, 2.0, 2.5, 5.0 and 10.0% w/v. The apparatus designed and used in this study is shown in Fig. 1, and consists of a separating funnel clamped to a retort stand with a rubber tube attached at the end of the funnel. A metal support was used to

position a plastic support at an angle of 30°. Freshly excised hog jejunum (1.7×15.0 cm) was pinned on the plastic support, and a beaker was placed directly under the plastic support to collect the detached beads. Before coating the glass beads, they were thoroughly cleaned with distilled water and then with acetone to maximize the roughness factor.¹⁷⁾ Twenty coated beads were placed on the exposed mucus surface of the tissue (Fig. 1). Mucus-polymer interaction and polymer hydration was allowed to take place over a period of 15 min. Simulated intestinal fluid (SIF) without pepsin (250 ml) at pH 7.2, contained in the separating funnel, was allowed to flow over the beads at a rate of 30 ml per min. The number of undetached beads was noted and used as a measure of bioadhesion. The experiment was repeated five times and the average value recorded.

Use of the Tensiometer Preparation of Mucin: The mucin solution used for the study was prepared as described elsewhere.¹⁸⁾

Bioadhesion Experiment: This was performed using a tensiometer (A. Kruss, model No. Nr 3124, Germany) adapted to measure bioadhesive strength. The same polymer concentrations used in the coated bead experiment were used. A 2 ml volume of the prepared mucin solution was poured into a watch glass, which was placed on the platform of the zeroed tensiometer. The plate on which the aqueous polymer dispersion was coated to 2 mm thickness was dried for 5 h in a desiccator and then hung on the lever arm of the tensiometer and the platform gradually moved to establish contact with the coated plate. A 15 min contact time between the polymer coat and the mucin was allowed to ensure proper interaction. The glass plate was raised by means of a screw until it just detached from the surface of the mucin. The force required to remove the glass plate from the surface of the mucin was read off from the microform balance in degrees and conversion of this to tension was done using Eq. 1.¹⁹⁾ In each case, an average of three determinations was taken.

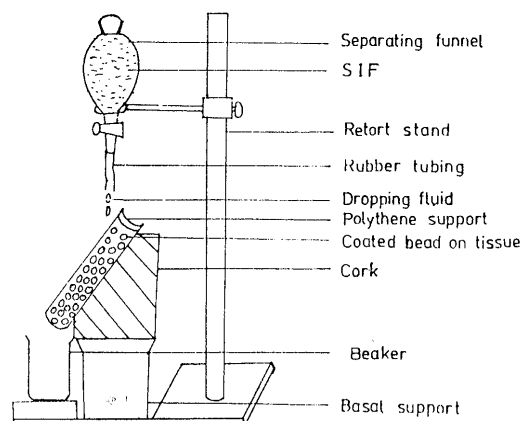


Fig. 1. Apparatus for Bioadhesion of Coated Glass Beads on the Tissue (Hog Jejunum)

* To whom correspondence should be addressed.

$$T = \frac{Mg}{2L} F \quad (1)$$

Where T is the tension equivalent to bioadhesive strength, M is the mass required to return the lever pointer to its original position, L is the perimeter of the plate, F is a constant dependent on the perimeter,¹⁹⁾ and g is the acceleration due to gravity.

Preparation of the Films Films of equal thickness and diameter were prepared by casting a 10% w/v aqueous dispersion of PG and SCMC individually in petri dishes of 15 cm internal diameter. The casts were dried at 40 °C for 10 h in an oven (Model 854, Memmert, Germany) and thereafter stored in a desiccator until required for use.

Evaluation of the Films The prepared films were microscopically and macroscopically examined for some physical parameters such as homogeneity, cracking tendency, *etc.* Average thicknesses of the films were also recorded.

Evaluation of the Mechanical Properties of the Films Films sectioned squarely (10 cm²) were padded with equal area of cellophane and held with a cyanoacrylate adhesive. One end of the film was attached to a clamped strong inelastic hook and to the other end was attached increasing weights. The load at which the film broke was noted for each film. An average of five determinations for each film was taken as the film strength.

Preparation of Granules Different batches of granules were prepared to contain 1:1, 2:1, 3:1 and 4:1 ratios of either PG or SCMC and TPL. The granules were prepared by wet granulation, as in tablet production. The dried granules were sized and those falling within a size range of 1–2 mm were used for the bioadhesion study. Granules without TPL were similarly prepared.

Bioadhesion Test on the Granules The apparatus designed for the coated bead experiment above was used. In this instance however, a 1 g quantity of the granules was uniformly spread on the everted tissue. At the end of the SIF flow the undetached granules were recovered, dried and weighed. A similar experiment was run with the bland granules. The bioadhesion percent was evaluated by the equation below:

$$\% \text{ bioadhesion} = \frac{W_g^1 - W_g^0}{W_0} \times \frac{100}{1} \quad (2)$$

where W_g^0 is the recovered weight of granules without TPL, W_g^1 is the recovered weight of the granules with TPL, W_0 is the weight of the granules used for the bioadhesion test.

$$\% \text{ bioadhesion} = (W_g^0 - W_g^1) \times 100 \quad (3)$$

A 1 g quantity of granules was used throughout the experiment, hence Eq. 2 reduces to Eq. 3.

Absolute Drug Content Measurement A 1 g quantity of each batch of the granules was placed in a 100 ml volumetric flask. The flask was made up to volume with a decinormal solution of HCl, and allowed to hydrate for 24 h at 28 °C. The solution was thereafter analysed spectrophotometrically at 272 nm using a spectrophotometer (SP 450, UV Vis, Pye Unicam). The drug concentration was calculated with reference to Beer's law plot for TPL.

Release Studies A 1 g quantity of each granule batch was introduced into a cut portion of jejunum (10 cm in length), which was tied at one end. A period of 15 min was allowed for bioadhesion to take place. A 10 ml quantity of SIF was introduced into the jejunum tube and the second end tied firmly. This set-up was introduced into a dissolution apparatus (DTD, Erweka, Germany) containing 500 ml of the dissolution medium (SIF) maintained at 37 ± 1 °C. At predetermined time intervals, samples of the dissolution medium were withdrawn and analyzed for TPL spectrophotometrically at 282 nm. An average of two absorbance readings at each time interval were recorded. The absorbance readings were thereafter converted to concentrations with reference to Beer's law plot.

Results and Discussion

Table 1 shows the results of the bioadhesion test using coated glass beads. The results indicated that PG is more bioadhesive than SCMC at equivalent concentration. PG coated glass beads had maximum resistance to washing at a lower concentration (2.5% w/v) than SCMC (10%). This invariably leads to the conclusion that based on the bioadhesion of coated glass beads, PG is more bioadhesive than

Table 1. Bioadhesion of Coated Glass Beads on the Mucus Surface

Concentration (% w/v)	Percentage of glass beads undetached (%)	
	PG (mean ± S.D.)	SCMC (mean ± S.D.)
1.0	1.8 ± 0.21	0.7 ± 0.12
2.0	74.2 ± 0.11	0.8 ± 0.31
2.5	100.0	14.8 ± 0.19
5.0	100.0	79.9 ± 0.21
10.0	100.0	91.5 ± 0.51

Table 2. Tensiometric Test of Polymers

Concentration (% w/v)	Bioadhesive strength (mN m ⁻¹)	
	PG (mean ± S.D.)	SCMC (mean ± S.D.)
1.0	19.24 ± 0.11	1.29 ± 0.19
2.0	22.81 ± 0.71	4.44 ± 0.11
2.5	38.51 ± 0.31	7.25 ± 0.12
5.0	40.78 ± 0.25	16.22 ± 0.41
10.0	41.81 ± 0.29	19.41 ± 0.21

SCMC. The differing values of resistance to washing of the coated glass beads may be due to differences in the strength of the gel network of the gum dispersions.¹³⁾ There may be a greater interaction of the PG molecules in the gel and glycoprotein in the mucus, producing an interpolymer complex with greater bond strength than that produced by SCMC and mucus gel. The results of tensiometric determination of the bioadhesive interaction confirmed those of the bioadhesion assay using coated glass beads (Table 2). PG dispersions produced higher bioadhesive force than SCMC dispersions, possibly due to the reasons indicated above. It may also be due to the fact that PG gels were thicker and more adhesive than SCMC gels and thus adhered faster to the glass plate. The coat thickness of 2 mm was thus achieved faster with PG. Coating of the plate was very difficult with SCMC gels because of lower adhesive properties. This made the interaction with the mucus very weak and thus weaker bond strengths were developed, compared to PG gels.

Results of the macroscopic studies on the films indicated that the formed films were hard, brittle and opaque. Microscopic examination showed that all the films were homogeneous and had no marked difference in their porosities ($p > 0.05$). These properties may not be directly related to the bioadhesive properties of the polymers. However, they may give insight to how films deposited on glass beads or coated plates may behave prior to the bioadhesive experiments. Cracked films may lead to adhesive bond failure. Very hard films may prevent sorption of fluid which leads to swelling and bioadhesive interaction. Thus, bioadhesion may be delayed and the dosage form coated with polymer may pass through the gastrointestinal tract (GIT) without any gastro-adhesive process occurring. This could result in a significant fraction of the drug being wasted.²⁰⁾ The strength of the films however indicated that the films cannot withstand the shock of handling and transportation. The polymers had low values: PG (103.2 ± 2.3 N) and SCMC (83.8 ± 5.2 N). These indicate that the films of tablets coated with these polymers may crack and the objective of using these polymers to deliver a bioadhesive tablet formulation may not be achieved. This re-

Table 3. Bioadhesion Ability of the Granules

Polymer/Drug Ratio	Percentage of granules undetached (%)	
	PG (mean \pm S.D.)	SCMC (mean \pm S.D.)
1 : 1	85.1 \pm 0.2	58.7 \pm 0.7
2 : 1	81.9 \pm 0.4	55.9 \pm 0.4
3 : 1	81.7 \pm 0.6	54.9 \pm 0.2
4 : 1	79.2 \pm 0.1	41.8 \pm 0.8

sult is in agreement with earlier studies.²¹⁾ The results of bioadhesion test and on formulated granules indicated that granules formulated with PG were more bioadhesive than those formulated with SCMC. They had a higher percentage of bioadhesion (Table 3). This result conforms to result of the bioadhesion of the coated glass bead on the everted jejunum. However, there was a decrease in the percentage bioadhesion with increase in the proportion of TPL in the granule batches. This may be due to a dilution effect on the part of the gum. Similar effects were reported by other research.²²⁾ These results show that TPL can be successfully delivered to jejunum, since bioadhesion, absorption and a possible prolonged effect on absorption could be achieved. It is possible for the bioadhesive granules to be encapsulated using capsule shells designed to withstand the acid environment of the stomach so that the shells could reach the ileum intact. Also, the formulated granules could be coated with pH sensitive polymers that are favoured by alkaline pH.²³⁾ Thus, the polymer hydrates after passing the stomach to allow the bioadhesive process to take place. This process is similar to the disintegration of the capsule shell above to liberate the bioadhesive formulation. Drugs that are sensitive to acidic pH, enzymatic attack in the stomach or those that cause unbearable gastric irritation or erosion are good candidates for this method of bioadhesive drug delivery. The physicochemical properties of the granulated drug must favour these conditions. The results of the release study corresponding to the diffusion of TPL through the jejunal membrane into the sink solution are shown in Figs. 2 and 3, and indicated a higher diffusion rate in granules containing a lower quantity of PG or SCMC. An increase in the quantity of gum retarded the diffusion of drug out of the granules. This is in accordance with the release of drugs from polymer matrices. Higher concentrations of polymers are known to retard drug release.²⁴⁾ This is because the gel barrier created by the polymer on swelling leads to entrapment of the drug molecules and an increase in tortuosity of the entire system. Similar results were obtained for both PG and SCMC, however, there was higher diffusion of TPL from granules prepared with PG than those prepared with SCMC. This may be due to a higher incidence of drug binding in SCMC than PG. Drug binding has been shown to retard drug release. It may also be due to the high swelling rate of PG.¹²⁾

Conclusion

This study showed that TPL could be delivered in a bioadhesive dosage form formulated with PG, a natural polymer. This gum (PG) was found to be more bioadhesive than SCMC and could be harnessed in the formulation of bioadhesive dosage forms of some specialised drugs.

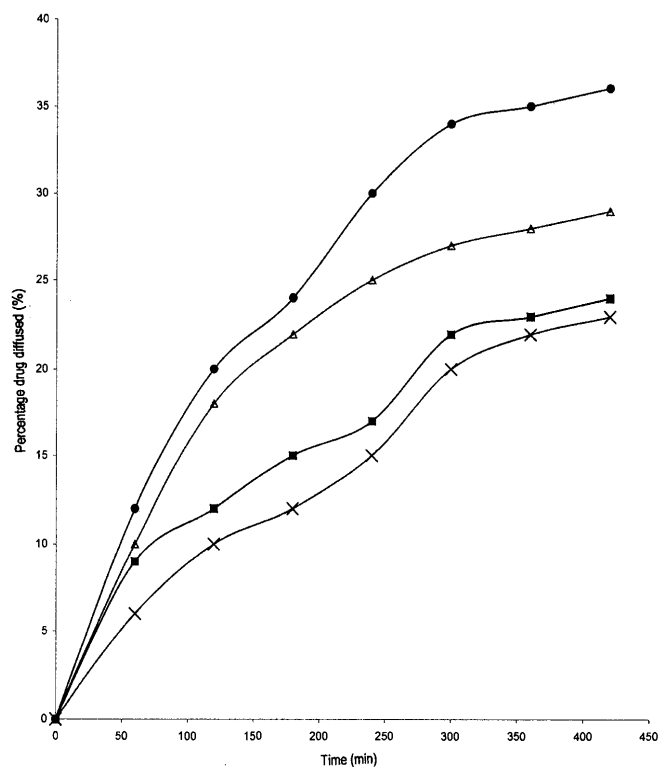


Fig. 2. Percent Theophylline Diffused from PG Granule Matrix as a Function of Time Using Hog Jejunum as Diffusion Barrier

●, 1 : 1 (PG : TPL); △, 2 : 1 (PG : TPL); ■, 3 : 1 (PG : TPL); X, 4 : 1 (PG : TPL).

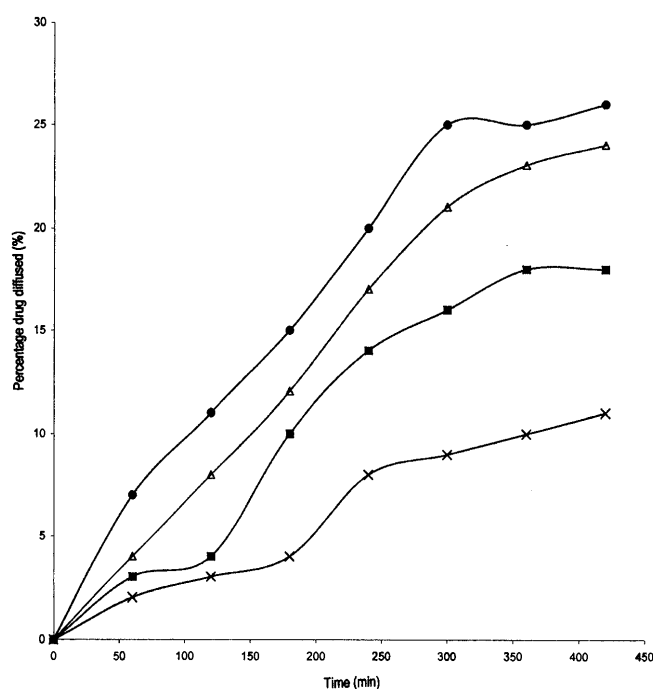


Fig. 3. Percent Theophylline Diffused from SCMC Granule Matrix as a Function of Time Using Hog Jejunum as Diffusion Barrier.

●, 1 : 1 (SCMC : TPL); △, 2 : 1 (SCMC : TPL); ■, 3 : 1 (SCMC : TPL); X, 4 : 1 (SCMC : TPL).

References

- 1) Labat-Robot J., Decaene C., *Path. Biol.*, **27**, 241 (1979).
- 2) Ment E. W., *Ann N. Y. Acad. Sci.*, **283**, 6 (1977).
- 3) Derjaguin B. V., Smilga V. R., "Adhesion: Fundamentals and Practices," Vol. 4, McLaren, London, 1967, p. 20.
- 4) Huntsberger T. R., "Treaties on Adhesion and Adhesives," ed. by Patrick R. L., Vol. 2, Marcel Dekker, New York, 1967, p. 120.

- 5) Kinloch A. J., *J. Mar. Sci.*, **15**, 2141 (1981).
- 6) Baskin T. M., Barisav O. V., Karoev A. K., Zhuliona E. B., *Biopolymer*, **24**, 2051 (1985).
- 7) Castillo E. J., Koenig J. L., Anderson J. M., Jentoft N., *Biomaterials*, **7**, 9 (1986).
- 8) Peppas N. A., Ponchel G., Duchene D., *J. Control. Rel.*, **5**, 143 (1987).
- 9) Smart J. D., Kellaway D., Worthington H. E. C., *J. Pharm. Pharmacol.*, **36**, 295 (1985).
- 10) Katzung B. G. (ed.) "Basic and Clinical Pharmacology," 5th ed., Prentice-Hall, U.S.A., 1992, p. 36.
- 11) Attama A. A., Adikwu M. U., Esimone C. O., *Chem. Pharm. Bull.*, Submitted, (1999).
- 12) Chukwu K., Chukwu A., *Acta Pharm.*, **46**, 207 (1996).
- 13) Attama A. A., Adikwu M. U., *Boll. Chim. Farm.*, In Print (1999).
- 14) Attama A. A., Adikwu M. U., *Boll. Chim. Farm.*, **137**, 97 (1998).
- 15) Adikwu M. U., Udeala O. K., Ohiri F. C., *S.T.P. Pharma. Sci.*, **2**, 221 (1992).
- 16) Adikwu M. U., Ph. D. Thesis, University of Nigeria Nsukka, 1994.
- 17) Bikermann J. J., "Surface Chemistry: Theory and Application," 2nd ed., Academic Press, New York, 1958, pp. 195—199.
- 18) Niibuchi J., Aramaki Y., Tsuchiya S., *Int. J. Pharm.*, **30**, 181 (1986).
- 19) Harkins W. D., Jordan H. F., *J. Am. Chem. Soc.*, **52**, 1751 (1930).
- 20) Tur K. M., Ch'ng H. S., Baie S., *Int. J. Pharm.*, **148**, 63 (1997).
- 21) Attama A. A., M. Pharm. Thesis, University of Nigeria Nsukka, 1997.
- 22) Taylan B., Capan Y., Guven O., Kes S., Hincal A. A., *J. Control. Rel.*, **38**, 11 (1996).
- 23) Ishibashi T., Hatano H., Kobayashi M., Mizobe M., Yoshino H., *Int. J. Pharm.*, **168**, 31 (1998).
- 24) Vazquez M.-J., Caslderrey M., Duro R., Gomez-Amoza J.-L., Martinez-Pacheco R., Souto C., Concheiro A., *Eur. J. Pharm. Sci.*, **4**, 39 (1996).

Two New Quinones from *Iris bungei*

Atta-ur-RAHMAN,^a M. Iqbal CHOUDHARY,^{*a} M. Nur-e-ALAM,^{a,1)} Purev Ö. NDOGNII,^b
T. BADARCHIIN,^b and G. PUREVSUREN^b

HEJ Research Institute of Chemistry, University of Karachi,^a Karachi-75270, Pakistan and Department of Chemistry, Mongolian State University,^b City of Hovd Mongolia. Received August 30, 1999; accepted October 20, 1999

Two new benzoquinone derivatives, bungeiquinone (1) and dihydrobungeiquinone (2), and two known derivatives, 3-hydroxyirisquinone (3) and 3-hydroxydihydroirisquinone (4), were isolated from the roots of *Iris bungei*. The structures of the new compounds were established on the basis of spectroscopic methods.

Key words *Iris bungei*; bungeiquinone; dihydrobungeiquinone; benzoquinone

Iris species (Family Iridaceae) have been used in Mongolian traditional medicine for the treatment of various diseases, especially in the treatment of cancer and as antiinflammatory and antibacterial agents. A number of benzoquinone derivatives (irisquinone-type) have been isolated from various species of family Iridaceae.^{2–6)} The previously isolated irisquinone²⁾ and dihydroirisquinone have been used in cancer chemotherapy.^{3,5)} The plant *Iris bungei* has, however, not yet been investigated and this paper describes the structure elucidation of two new irisquinone derivatives isolated from the roots of this plant.

The high resolution electron impact (HR-EI) MS of bungeiquinone (**1**) showed the $[M]^+$ at m/z 404.2909 in agreement with the molecular formula $C_{25}H_{40}O_4$ (Calcd 404.2916). The mass spectrum showed the base peak at m/z 182.0629 ($C_9H_{10}O_4$). The mass fragmentation pattern of **1** was similar to some other benzoquinone derivatives.⁵⁾ The peak at m/z 182.06 resulted from the cleavage of the C-1'/C-2' bond and indicating the presence of an *O*-ethyl group attached at the benzoquinone ring. A significant ion at m/z 378.2871 $[M-C_2H_4]^+$ corresponded to the loss of an ethyl group from M^+ .

The IR spectrum of **1** exhibited strong absorptions at 3446 (OH), 2892 (CH), 1662, 1641 (C=O) and 1610 (C=C) cm^{-1} . The ¹H-NMR spectrum of **1** showed signals for two methyls, three olefinic protons and thirty methylene protons. Of the two 3H triplets, the one resonating at δ 1.48 was due to the methyl of *O*-ethyl group (t , $J=7.0$ Hz) and the other triplet resonating at δ 0.86 (t , $J=7.0$ Hz) was due to the methyl of the C-3 side chain. A 1H singlet at δ 5.79 was assigned to the olefinic H-6.⁶⁾ A broad signal at δ 7.19, which disappears upon addition of D₂O, was due to the OH proton. The side chain olefinic protons resonated at δ 5.33 (2H, m , $W_{1/2}=5.0$ Hz), which indicated a (*Z*)-configuration for the (C=C). The (*Z*)-configuration was also proved by the lack of an IR absorption in the region 980–960 cm^{-1} . The methylene protons of the *O*-ethyl group resonated as a quartet at δ 4.02 ($J=7.0$ Hz). The C-1' methylene proton next to the benzoquinone ring resonated as a triplet at δ 2.42 ($J=7.5$ Hz). A 4H multiplet centered at δ 1.98 was assigned to the C-9' and C-12' methylene protons of the C-3 side chain. The other methylene protons resonated in the region δ 1.19–1.31 as overlapping broad signals. The olefinic protons centered at δ 5.33 (H-10'/H-11') displayed couplings with CH₂-9' and CH₂-12' resonating at δ 1.98 in the correlation spectroscopy (COSY)-45° spectrum.

The ¹³C-NMR spectrum of **1** showed resonances for all 25 carbons in the molecule. The distortionless enhancement by polarization transfer (DEPT) spectra revealed the presence of two methyl, fifteen methylene, three methine and five quaternary carbons. Two downfield signals at δ 183.0 (C-4) and 181.8 (C-1) indicated the presence of two ketonic carbonyl carbons, while the signals at δ 160.4 (C-5), 151.4 (C-2), 129.9 (C-10'/C-11'), 119.2 (C-3) and 102.4 (C-6) indicated the presence of three double bonds in the molecule along with the substitution of hydroxy and *O*-ethyl functionalities. The ¹³C-NMR spectra of **1** showed a typical signal pattern for a *cis*- ω -7 mono-enyl group.⁷⁾ This indicated that the compound **1** must have the same side chain as found in the known compound **3**.⁵⁾ In the heteronuclear multiple quantum coherence (HMQC) spectrum, the protons resonating at δ 5.79 (H-6), 5.33 (CH₂-10'/CH₂-11'), 4.02 (CH₂ of *O*-ethyl), 2.42 (CH₂-1'), 1.98 (CH₂-9'/CH₂-12'), 1.48 (CH₃ of *O*-ethyl) and 0.87 (CH₃-17') were found to be coupled with the carbons resonating at δ 102.4, 129.9, 65.8, 28.0, 27.2, 13.7 and 14.1, respectively. In the heteronuclear multiple-bond correlation spectroscopy (HMBC) spectrum of **1** (Fig. 1), H-6 (δ 5.79) was found to be coupled with C-4 (δ 183.0), C-1 (δ 181.8), C-5 (δ 160.4) and C-2 (δ 151.4). The coupling of protons at 4.02 (CH₂ of *O*-ethyl) with C-5 (δ 160.4) and C-2'' methyl (δ 14.1) suggested that the *O*-ethyl group should be substituted at C-5. CH₂-1' (δ 2.42) showed couplings with C-4 (δ 183.0), C-2 (δ 151.1) and C-3 (δ 119.2) which indicated that the hydrocarbon chain is connected at C-3 of the benzoquinone skeleton. On the basis of these findings, structure **1** (5-ethoxy-3-[(*Z*)-heptadecenyl]-2-hydroxy-2,5-cyclohexadiene-1,4-dione) was deduced for the compound. It is interesting to note that the ethoxy group is not a common substituent in this class of compounds.

The ¹H-NMR spectrum of dihydrobungeiquinone (**2**), $C_{25}H_{42}O_4$, resembled that of **1**, the major differences being the absence of signals at δ 5.33 and 1.98 which indicated the absence of the double bond in the side chain. The downfield

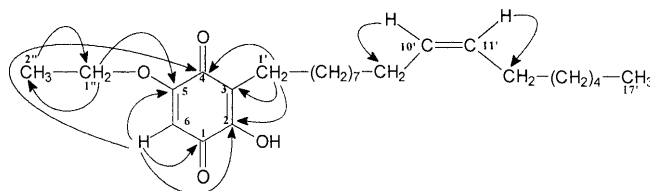
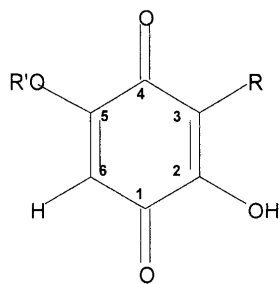


Fig. 1. Important HMBC Interactions in Compound **1**

* To whom correspondence should be addressed.



1 R = (CH₂)₉-CH=CH-(CH₂)₅-CH₃, R' = CH₂-CH₃

2 R = (CH₂)₁₆-CH₃, R' = CH₂-CH₃

3 R = (CH₂)₉-CH=CH-(CH₂)₅-CH₃, R' = CH₃

4 R = (CH₂)₁₆-CH₃, R' = CH₃

olefinic signal at δ 129.9 (C-10'/C-11' in **1**) was also absent in the ¹³C-NMR spectrum of **2**. MS, ¹H- and ¹³C-NMR of **2** further confirmed that the compound **2** is the C-10'/C-11' saturated analogue of compound **1**.

Compounds **3** and **4** have previously been reported from other natural sources and this is the first report of their isolation from this plant. Their structures were identified by comparison of the spectral data with the literature values.^{5,6)}

Experimental

The IR spectra were recorded on a JASCO A-302 spectrophotometer. The UV spectra were measured on a Hitachi U-3200 spectrophotometer. The low resolution (LR)-EI and HR-EI MS were recorded on JMS HX 110 mass spectrometer with the data system DA 5000. The ¹H-NMR spectra were recorded on Bruker AM 400 and AMX 500 NMR spectrometers using UNIX data system at 400 and 500 MHz, respectively, while ¹³C-NMR spectra were recorded at 100 and 125 MHz on the same instruments, respectively.

Plant Material The roots of *Iris bungei* Maxim. were collected in September 1997 from Choir Somone (Dornogov area) of Mongolia. A herbarium specimen of this plant (# N659) was deposited at the Botanical Institute of the Mongolian Academy of Sciences, Ulaanbaatar, Mongolia.

Extraction and Isolation The dried plant (100 g) was extracted with methanol at room temperature for two weeks and the resulting extract was

concentrated to a gum. This gum (8 g) was loaded on to a silica gel (150 g) column and eluted with CHCl₃. Two orange yellow fractions were obtained (0.5 g) which were further purified on TLC plates impregnated with 10% AgNO₃ (solvent system 100% CHCl₃) leading to the isolation of compounds **1–4**.

Bungeiquinone (1): 7 mg, Gum, IR $\nu_{\text{max}}^{\text{CHCl}_3}$ cm⁻¹: 3446 (OH), 2892 (CH), 1662, 1641 (C=O), 1610 (C=C); UV λ_{max} (MeOH): 288.2 nm (log ϵ 4.41). EI-MS: m/z : 404.1 (88), 374.0 (43), 183.0 (65), 182.0 (100), 181.0 (92); ¹H-NMR (CDCl₃) δ : 7.19 (s, -OH), 5.79 (s, H-5), 5.33 (m, H-10'/H-11'), 4.02 (q, $J_{1',2'}=7.0$ Hz, H-1''), 2.42 (t, $J_{1',2'}=7.5$ Hz, H-1'), 1.98 (m, H-9'/12'), 1.48 (t, $J_{2',1'}=7.0$ Hz, H-2''), 1.35–1.19 (for other CH₂), 0.86 (t, $J_{17',16'}=7.0$ Hz, H-17'); ¹³C-NMR (CDCl₃) δ : 181.8 (1), 151.4 (2), 119.2 (3), 183.0 (4), 160.4 (5), 102.4 (6), 65.8 (1''), 13.8 (2''), 28.01 (1'), 129.9 (10'/11'), 27.2 (9'/12'), 22.6 (16'), 28.9–31.9 (others CH₂), 14.1 (17').

Dihydrobungeiquinone (2): 7.5 mg, Gum, IR $\nu_{\text{max}}^{\text{CHCl}_3}$ cm⁻¹: 3431 (OH), 2884 (CH), 1661, 1639 (C=O), 1608 (C=C); UV λ_{max} (MeOH): 288.8 nm (log ϵ 4.35). EI-MS: m/z : 406.1 (60), 376.0 (100), 183.0 (64), 182.0 (65), 181.0 (44); ¹H-NMR (CDCl₃) δ : 7.19 (s, -OH), 5.78 (s, H-5), 4.01 (q, $J_{1',2'}=7.0$ Hz, H-1''), 2.41 (t, $J_{1',2'}=7.5$ Hz, H-1'), 1.48 (t, $J_{2',1'}=7.0$ Hz, H-2''), 1.35–1.19 (for other CH₂), 0.86 (t, $J_{17',16'}=7.0$ Hz, H-17'); ¹³C-NMR δ : 181.8 (1), 151.4 (2), 119.2 (3), 183.0 (4), 160.4 (5), 102.4 (6), 65.8 (1''), 13.8 (2''), 28.01 (1'), 22.6 (16'), 28.9–31.9 (others CH₂), 14.1 (17').

Acknowledgments One of us (M. Nur-e-Alam) gratefully acknowledge the financial support of BIRDEM (Bangladesh Institute of Research & Rehabilitation on Diabetic, Endocrine and Metabolic Disorders), Dhaka and also ANRAP (Asian Network of Research on Antidiabetic Plants). The plant was identified by Dr. U. Ligaa of the Botanical Institute, Academy of Sciences, Ulaanbaatar, Mongolia.

References and Notes

- 1) On leave from Research Division, BIRDEM, 122 Kazi Nazrul Islam Avenue, Dhaka-1000, Bangladesh.
- 2) Seki K., Kaneko R., *Chem. Ind. (London)*, **1975**, 349.
- 3) Wu S. J., Zhang L., Yang X., Li D., *Huaxue Xuebao*, **39**, 767 (1981).
- 4) Wu S. J., Yang Q. Z., *Hua Hsueh Pao*, **38**, 156 (1980).
- 5) Seki K., Haga K., Kaneko R., *Phytochemistry*, **38**, 965 (1995).
- 6) Marner F. J., Horper W., *Helv. Chem. Acta*, **75**, 1557 (1992); Nakanishi K., Solomon P. H., *Infrared Absorption Spectroscopy*, Holden-Day, San Francisco, 1977.
- 7) Gunstone F. D., Pollard M. R., Scrimgeour C. M., Vedanayagam H. S., *Chem. Phys. Lipids*, **18**, 115 (1977).

Synthesis and Evaluation of Some Hydroxyproline-Derived Peptidomimetics as Isoprenyltransferase Inhibitors

Celeste E. O'CONNELL, Cheryl A. ROWELL, Karen ACKERMANN, Ana Maria GARCIA, Michael D. LEWIS, and James J. KOWALCZYK*

Eisai Research Institute, 4 Corporate Drive, Andover, MA 01810, U.S.A.

Received September 20, 1999; accepted December 17, 1999

CA₁A₂X peptidomimetics containing a modified proline at position A₂ were prepared and evaluated for their ability to inhibit farnesyltransferase (FTase) and geranylgeranyltransferase I (GGTase I) in enzymatic and cell-based assays. These compounds inhibited farnesylation of H-ras *in vitro* in the high nanomolar to low micromolar IC₅₀ range.

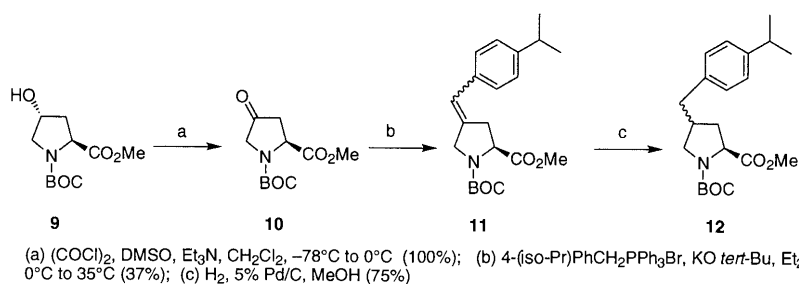
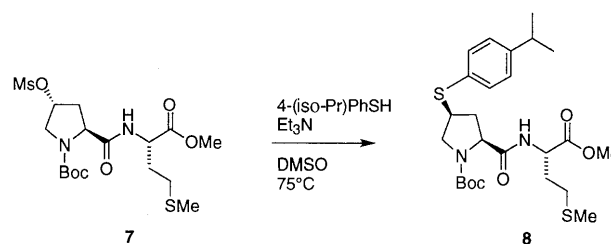
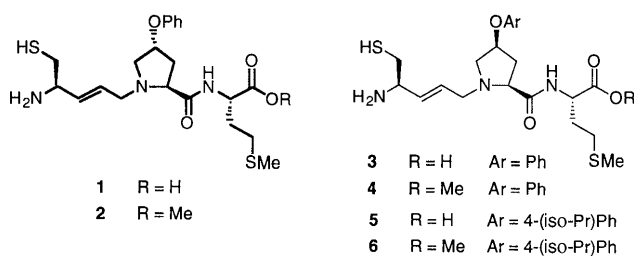
Key words farnesyltransferase inhibitor; CAAX; peptidomimetic; hydroxyproline; H-ras

During the course of an ongoing project to prepare farnesyltransferase (FTase) inhibitors as potential drug candidates in an anti-cancer program targeting tumors with ras mutations,¹⁾ we found CAAX peptidomimetics, such as 1–6, to have very good *in vitro* potency against FTase (Fig. 1).²⁾ *Trans*-isomers, such as 1, were less active against the enzyme than *cis*-isomers (*e.g.*, 3). Furthermore, one such compound (6) showed interesting specificity for inhibition of geranylgeranyltransferase I (GGTase I) vs. FTase in a whole cell assay.

In order to expand the structure–activity relationship of this class of inhibitor, we examined the effects of changes at the 4-position of the hydroxyproline in compounds of type 3 (and the corresponding esters, 4) by preparing a number of analogs in which the ether oxygen was replaced by a sulfur atom or an alkyl chain or removed completely, while keeping the remainder of the peptidomimetic scaffold intact. In particular, we wished to examine how replacement of oxygen with carbon or sulfur might affect the lipophilicity or stability of such compounds.

Chemistry Thioether compounds³⁾ were prepared by

S_N2 displacement of mesylate 7 with 4-isopropylthiophenol to give 8. The yield of this reaction was low (15%), but 7 could be recovered (81%) and recycled. Attempts to prepare 8 using standard Mitsunobu conditions (as used in the preparation of compounds 1–6) failed to give any of the desired product. Arylalkyl derivatives with a one-carbon linker connecting the aromatic group to the proline were prepared as shown in Chart 2. *N*-Boc-*trans*-4-hydroxy-L-proline methyl ester (9) was oxidized to ketone 10 under Swern conditions. The ketone was converted under Wittig conditions^{3a)} to a mixture of olefins (11). Hydrogenation of 11 gave 12 as a 2.5:1 mixture of diastereomers. These isomers were not readily separable neither at this stage nor at subsequent stages in the synthetic sequence. The major isomer was assumed to be the *cis*-isomer (hydrogenation from the less hindered face) based on a literature precedent⁴⁾ and ¹H-NMR analysis. This mixture was carried forward, and, as the final compounds did not display any improved qualities over analogs 3–6 (see Discussion), the individual isomers were never separated. Arylalkyl derivatives with a two-carbon linker were prepared as shown in Chart 3. *N*-Boc-*trans*-4-hy-



* To whom correspondence should be addressed. e-mail: Jim_Kowalczyk@eri.eisai.com

droxy-L-proline methyl ester (**9**) was converted to the *cis*-iodide⁵ (**13**) under Mitsunobu-type conditions. The iodide was treated with AIBN/*n*-Bu₃SnH in the presence of *p*-isopropylstyrene to give **14** as a mixture of *cis*- and *trans*-isomers (as determined by ¹H-NMR).⁶ Once again, this pair of compounds was evaluated as a mixture since the isomers were not readily separable by silica gel chromatography or reverse phase HPLC.

Aryl-substituted derivatives with no linker were prepared as shown in Chart 4. Ketone **10** was converted into enol triflate **15** in moderate yield.⁷ This triflate was cross-coupled with various arylboronic acids under palladium catalysis

(Suzuki coupling⁸) to give **16** in good yield.^{7,8} We found it more convenient to use Stille's catalyst⁹ in place of the more air-sensitive Pd(PPh₃)₄ in these cross-coupling reactions. Hydrogenation of each alkene gave a single isomer (¹H-NMR), assumed to be the *cis*-isomer by a literature precedent for related hydrogenations.^{3a}

For each target series, the remainder of the synthesis² was completed by carrying out the necessary steps as shown in Charts 5 and 6.

Discussion

Screening results for the compounds described above are summarized in Table 1. The values for compounds **1**–**6** are presented for comparison. The *in vitro* assays¹⁰ used recombinant FTase or GGTase, and measured the intrinsic activity and selectivity of the carboxylic acid forms of the analogs for inhibition of protein prenylation. The whole-cell assays used activated H-ras transfected NIH3T3 fibroblasts¹⁰ and measured protein processing (H-ras or Rap 1A) in the presence of the methyl ester form of the inhibitors.

As can be seen in Table 1, every modification described herein led to compounds less active than compounds **3**–**6**.

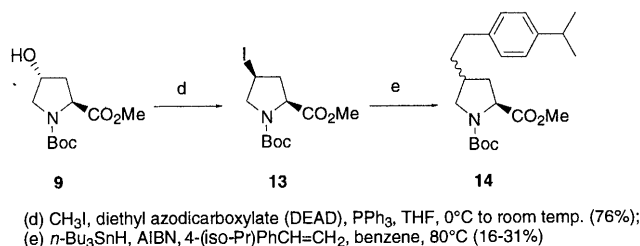


Chart 3

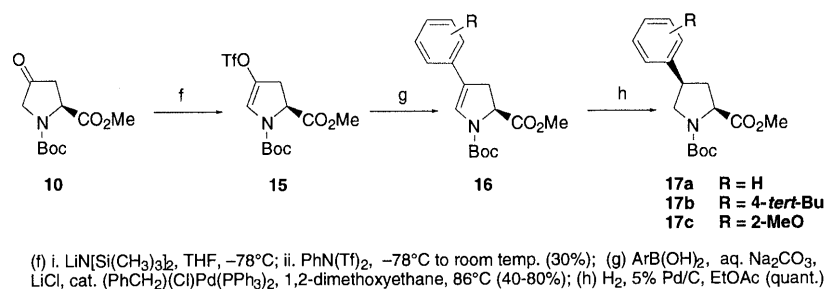


Chart 4

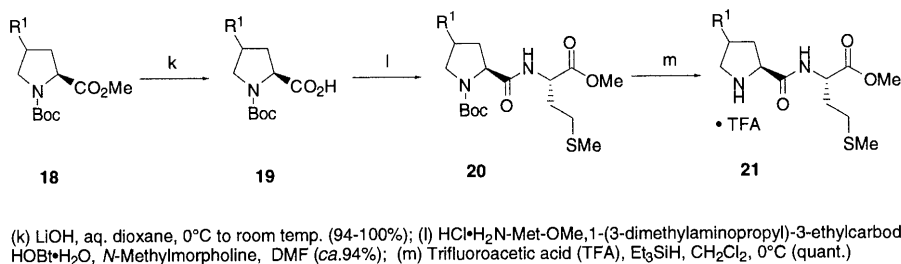


Chart 5

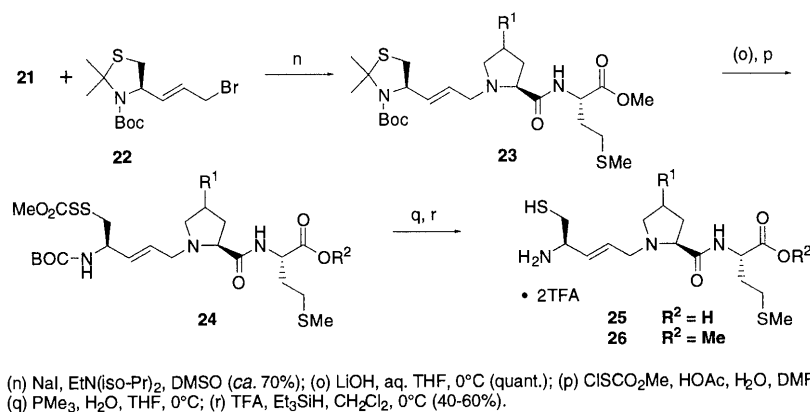


Chart 6

Table 1. Biological Evaluation of 4-Substituted L-Proline CAAX Mimetics (**25**, **26**)

R ¹ isomer	R ¹	Compd. R ² =H	FTase <i>in vitro</i> ^{a)} IC ₅₀ (μM)	GGTase I <i>in vitro</i> ^{b)} IC ₅₀ (μM)	Compd. R ² =Me	FTase whole cells ^{c)} IC ₅₀ (μM)	GGTase I whole cells ^{d)} IC ₅₀ (μM)
<i>Trans</i>	PhO-	1	4.0	8.0	2	>50	>50
<i>Cis</i>	PhO-	3	0.057	0.053	4	5.3	21.9
<i>Cis</i>	4-(iso-Pr)PhO-	5	0.082	0.21	6	3.0	0.39
<i>Cis</i>	4-(iso-Pr)PhS-	25a	0.16	0.34	26a	>25	3.1
<i>Cis</i>	Ph-	25b	0.79	1.8	26b	4.1	>30
<i>Cis</i>	4-(<i>tert</i> -Bu)Ph-	25c	1.0	0.27	26c	>10	~10
<i>Cis</i>	2-(MeO)Ph-	25d	0.19	0.19	26d	3.8	>30
<i>Cis/trans</i> 2.5:1	4-(iso-Pr)- PhCH ₂	25e	8.3	16.3	26e	>25	13.3
<i>Cis/trans</i> 1:1.7	4-(iso-Pr)- PhCH ₂ CH ₂ -	25f	1.8	2.8	26f	>10	>10

a) Farnesylation of H-ras protein. b) Geranylgeranylation of H-ras-CAIL protein. c) Farnesylation of H-ras protein in NIH3T3 cells transformed with activated H-ras. d) Geranylgeranylation of Rap-1A protein in NIH3T3 cells transformed with activated H-ras.

Thus, replacement of the ether oxygen with sulfur or carbon neither improved *in vitro* activity, nor improved activity in whole cells. In general, the carboxylic acids (**25**) were more active against FTase than GGTase I *in vitro*, with the exception of compound **25c** which was somewhat more potent against GGTase I than FTase *in vitro* (Table 1), and the corresponding methyl ester (**26c**) showed the same trend in whole cells. Interestingly, compounds **26a** and **26e** were slightly more potent in their inhibition of Rap 1A processing (GGTase I) than in their inhibition of H-ras processing in whole cells, although their corresponding carboxylic acids (**25a**, **25e**) were slightly more potent in their inhibition of FTase *in vitro*. We currently have no explanation for this curious phenomenon.

In summary, we have prepared a series of CA₁A₂X peptidomimetic isoprenyltransferase inhibitors based on hydroxyproline at the A₂ position, and although none of the compounds prepared in this study offered significant improvement over the most potent that we reported previously (**3**—**6**),²⁾ nonetheless several were relatively potent inhibitors of FTase or GGTase I *in vitro*. We found no evidence that replacing or removing the ether oxygen in compounds such as **3**—**6** improved the stability or lipophilicity. However, this class of compounds expands the field of isoprenyltransferase inhibitors and may be useful in future development of anti-cancer drugs.

Acknowledgements We thank Dr. C. Eric Schwartz for helpful discussions.

References and Notes

- 1) a) Barbacid M., *Ann. Rev. Biochem.*, **56**, 779—827 (1987); b) Khosravi-Far R., Der C. J., *Cancer Metastasis Rev.*, **13**, 67—89 (1994); c) Sebti S. M., Hamilton A. D., *Drug Discovery Today*, **3**, 26—33 (1998).
- 2) O'Connell C. E., Ackermann K., Rowell C. A., Garcia A. M., Lewis M. D., Schwartz C. E., *Bioorg. Med. Chem. Lett.*, **9**, 2095—2100 (1999).
- 3) 4-(Arylthio)hydroxyproline derivatives have been prepared by the reaction of 4-hydroxyproline derivatives with *N*-(arylthio)succinimides and by displacement of a *trans*-tosylate with the sodium salt of thio-phenol or an alkyl mercaptan: a) Krapcho J., Turk C., Cushman D. W., Powell J. R., DeForrest J. M., Spitzmiller E. R., Karanewsky D. S., Duggan M., Rovnyak G., Schwartz J., Sesha N., Godfrey J. D., Ryono D. E., Neubeck R., Atwal K. S., Petrillo, Jr., E. W., *J. Med. Chem.*, **31**, 1148—1160 (1998); b) Smith E. M., Swiss G. F., Neustadt B. R., Gold E. H., Sommer J. A., Brown A. D., Chiu P. J. S., Moran R., Sybertz E. J., Baum T., *ibid.*, **31**, 875—885 (1988).
- 4) a) *N*-CBZ-4-Benzylidene-(2*S*)-proline has been hydrogenated using H₂ and Pd/C to give exclusively *cis*-4-benzyl-(2*S*)-proline: ref. 3a; b) Likewise, *N*-Boc-4-benzylidene-(2*S*)-proline ethyl ester has been hydrogenated using H₂ and PtO₂ to give the *cis*-isomer: Ezquerro J., Pedregal C., Yruretagoyena B., Almudena R., *J. Org. Chem.*, **60**, 2925—2930 (1995); c) Ezquerro J., Pedregal C., Rubio A., Escribano A., Sánchez-Ferrando F., *Tetrahedron*, **49**, 8665—8678 (1993); d) *cis*-*N*-Boc-4-alkyl-(2*S*)-proline *tert*-butyl esters have been prepared by hydrogenation and reduction of alkylidene pyroglutamates: Moody C. M., Young D. W., *J. Chem. Soc., Perkin Trans. 1*, **1997**, 3519—3530.
- 5) Dormoy J.-R., *Synthesis*, **1982**, 753.
- 6) a) The reaction of the *trans*-iodide with styrene under *n*-Bu₃SnH/AIBN conditions has been reported to yield the *trans* product (no yield was given): Klein S. I., Dener J. M., Molino B. F., Gardner C. J., D'Alisa R., Dunwiddie C. T., Kasiewski C., Leadley R. J., *Bioorg. Med. Chem. Lett.*, **6**, 2225—2230 (1996); b) The chemical shift and splitting pattern of the C2 methine proton was used for identification of *cis*- and *trans*-isomers, but the ¹H-NMR spectrum of **14** is further complicated by the presence of Boc rotamers at room temperature. For the synthesis and characterization of *trans*-*N*-Boc-(4*R*)-(3-phenylpropyl)proline, see example 2, p. 51, in: Llinas-Brunet M., Bailey M. D., Halmos T., Poupert M.-A., Tsantrizos Y., Wernic D., PCT Int. Appl. WO 9907734 A2 19990218, 1999.
- 7) Similar enol triflates have been prepared and used in Suzuki couplings: a) Baldwin J. E., Bamford S. J., Fryer A. M., Wood M. E., *Tetrahedron Lett.*, **36**, 4869—4872 (1995); b) Baldwin J. E., Fryer A. M., Pritchard G. J., Spyvee M. R., Whitehead R. C., Wood M. E., *ibid.*, **39**, 707—710 (1998); c) Baldwin J. E., Fryer A. M., Pritchard G. J., Spyvee M. R., Whitehead R. C., Wood M. E., *Tetrahedron*, **54**, 7465—7484 (1998).
- 8) a) Shieh W.-C., Carlson J. A., *J. Org. Chem.*, **57**, 379—381 (1992); b) Oh-e T., Miyaura N., Suzuki A., *ibid.*, **58**, 2201—2208 (1993); c) Suzuki A., Miyaura N., *Chem. Rev.*, **95**, 2457—2483 (1995).
- 9) a) Labadie J. W., Stille J. K., *J. Am. Chem. Soc.*, **105**, 6129 (1983); b) Stille J. K., *Angew. Chem. Int. Ed. Engl.*, **25**, 508—524 (1986).
- 10) a) Garcia A. M., Rowell C., Ackermann K., Kowalczyk J. J., Lewis M. D., *J. Biol. Chem.*, **268**, 18415 (1993). b) At concentrations >10—30 μM most of the methyl esters exhibited some toxicity towards whole cells.

Δ^9 -Tetrahydrocannabinol Content in Cannabis Plants of Greek Origin

Maria STEFANIDOU,* Sotiris ATHANASELIS, Giorgos ALEVISOPOULOS, John PAPOUTSIS, and Antonis KOUTSELINIS

Department of Forensic Medicine and Toxicology, University of Athens, Medical School, 75, Mikras Asias str., Goudi, Athens 115.27, Greece. Received September 30, 1999; accepted December 28, 1999

The Δ^9 -tetrahydrocannabinol (Δ^9 -THC) content was identified and determined quantitatively using a Gas Chromatography Detector (Gas Chromatography - Electron Ion Detector) instrument in samples of illicit herbal cannabis. Law enforcement authorities sent the samples to the Department of Forensic Medicine and Toxicology, University of Athens, for toxicological analysis. The concentrations of Δ^9 -THC in these samples ranged from 0.08% to 4.41%. Such concentrations suggest that Greece might be at high risk, as an area for the illicit cultivation of "pedigree" cannabis plants. The forensic aspects of cannabis classification are discussed.

Key words cannabis, Δ^9 -tetrahydrocannabinol, Gas Chromatography Detector, forensic analysis, Greece

Marihuana continues to be the most readily available drug of abuse in Greece and the number and size of marihuana seizures have also increased. The major portion of cannabis seized is of Albanian origin, since Albania has become a major supplier of cannabis to Greece and Italy.¹⁾ The fibre-type plants are legally cultivated in some regions of the Mediterranean area, including Greece, under specific permission.^{2,3)} However, significant illegal cannabis cultures do exist in various areas of Greece.

The aim of this study was the determination of Δ^9 -tetrahydrocannabinol (Δ^9 -THC) content in forensic cannabis samples seized last year by customs and police authorities in two areas of Greece (Ipiros and Lakonia).

Experimental

Thirty illicit herbal cannabis samples, seized last year from two different districts of Greece (the first located in the North-Ipiros and the second one in the South-Lakonia), were sent to the Department of Forensic Medicine and Toxicology of the University of Athens, for forensic chemical analysis. The samples were fresh upon receipt and dried until analysed.

The upper part of the main stem of each flowering cannabis plant was chosen and dried in the dark and then was stored for less than three months⁴⁾ in a paper box at room temperature. After removing seeds and stems, the dried leaves were ground to a powder.

Each sample consisted of 20 mg of the ground powder and was extracted overnight⁵⁾ with 1 ml of hexane, to ensure complete extraction of all the cannabinoids from the samples. The complete extraction was confirmed by the analysis of a second extract of the residue of each sample, which showed no detectable amounts of cannabinoids. Tetracosane was added to each sample as an internal standard, at a final concentration of 100 μ g/ml. After centrifugation, 500 μ l of the supernatant of each sample was evaporated and the dry residue was diluted with 500 μ l of ethyl acetate, 1 μ l of which was analysed by Gas Chromatography Detector (GCD). GCD is an advanced GC system introduced by Hewlett Packard in 1994 and consists of a chromatograph, an electron ionisation detector (EID) for m/z up to 420 and a data system. The EID generates retention time, abundance and the mass spectral data, so one can obtain results comparable with those obtained with a GC-MS instrument.

The conditions of the analysis were as follows: column: Hewlett - Packard HP-5 crosslinked 5% phenylmethylsilicone capillary column (30 m in length, 0.25-mm i.d., film thickness 0.25- μ m); column temperature and initial temperature, 100 °C; initial time, 0 min; rate 15 °C/min, final temperature 300 °C, final time 8.00 min; injection port temperature, 280 °C; interface temperature, 300 °C. The helium flow rate was 1 ml/min. Δ^9 -THC content of the analysed samples was measured against a standard solution containing 100 μ g/ml of Δ^9 -THC.

Results

The Δ^9 -THC content of cannabis samples was identified

and determined quantitatively using GCD. The retention times of Δ^9 -THC and tetracosane were determined to be 12.30 min and 11.44 min respectively. The total ion chromatogram of a cannabis sample is presented in Fig. 1.

The quantitation of Δ^9 -THC was performed by using the areas of its major ions: (m/z 299, 314, 231). The percentage of the Δ^9 -THC content of the analysed cannabis samples is presented in Table 1.

Discussion

Cannabis (*Cannabis sativa* L.) and its preparations remain by far the most popular and heavily used substances on the illicit market.^{6–10)}

As it is known, cannabis has been broadly classified into fibre-type or drug-type.^{5,11–14)} According to the European Union, the fibre-type plant does not exceed 0.3% of THC, while the drug-type plant usually contains up to 5% of THC, though higher percentages (up to 10%) have been reported.¹⁵⁾ It is widely accepted that only the presence of Δ^9 -THC in substantial quantities (>0.3%) qualifies a sample of cannabis as a drug, since cannabidiol or cannabinol may be absent even from fresh samples.¹⁶⁾

There are wide variations in the relative amounts of

Table 1. The Percentage of Δ^9 -THC in Cannabis Samples from Lakonia and Ipiros

Cannabis samples	% Δ^9 -THC	
	Lakonia	Ipiros
1	0.75	1.31
2	1.57	1.20
3	2.73	0.24
4	0.69	1.97
5	1.58	3.56
6	0.41	1.34
7	2.53	0.55
8	0.09	4.41
9	3.83	3.40
10	0.08	3.74
11	3.28	1.42
12	0.18	0.73
13	1.16	2.35
14	3.47	1.22
15	0.09	—
16	0.38	—

* To whom correspondence should be addressed. e-mail: sathan@cc.uoa.gr.

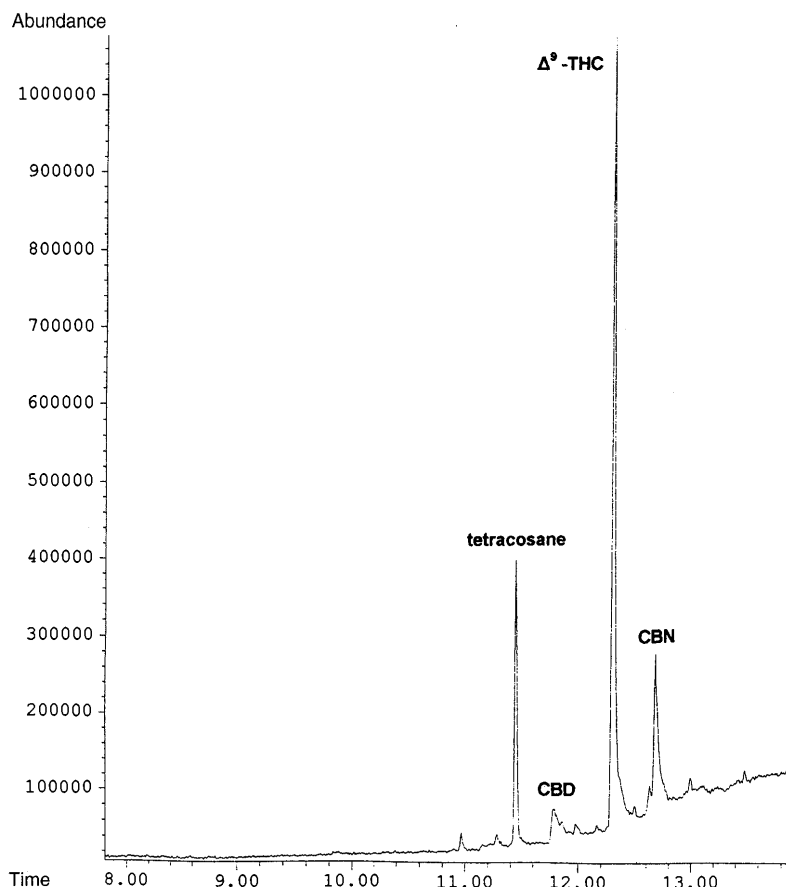


Fig. 1. Total Ionic Chromatogram of a Cannabis Sample, Extracted with Ethyl Acetate, which Contained Tetracosane as Internal Standard

cannabinoids in cannabis plants, depending on many factors. The predominant factors are the genetic characteristics of the seedstock,^{17,18)} the environment in which the plant is grown,^{19,20)} the maturity, sex, the part of the plant harvested, the time elapsed between harvesting and chemical analysis, and the conditions of storage of the plant.²¹⁾ Nevertheless, the generation plays a substantial role in the cannabinoid content, *e.g.* plants by the third generation have shown a significant increase in cannabinoid content and by the fifth generation all plants have become Δ^9 -THC rich.²⁰⁾ Since Δ^9 -THC concentration of the plant gradually decreases over time as a result of oxidation to CBN,^{22–24)} it has been suggested that the formula Δ^9 -THC+CBN could approximate the total Δ^9 -THC content, regardless the degradative process. The quantitative determination of CBN in our samples showed insignificant amounts of this degradative product, less than 0.7%.

According to the literature,³⁾ the typical THC level of the three illicit cannabis products is 0.5–5% for herbal cannabis, 2–10% for the resin and 10–30% for the hashish oil.

It should be noted that these values are only a guide to levels likely to be encountered by the forensic analyst. Many samples of herbal, resin or liquid cannabis will have a THC content outside these limits.³⁾ Hybrid plants have a higher THC content than the traditional varieties and there are some reports, in the literature, that quantities of Δ^9 -THC up to 17% have been determined.¹⁾

According to the present work the Δ^9 -THC content varies from 0.24–4.41% in Ipiros samples and from 0.08–3.83% in Lakonia samples. The results suggest that the illicitly cul-

tivated cannabis in Greece is of “good quality”, with no major variations in cannabinoid content, at least in the two tested areas. The term “good quality” refers to the potency of the cannabis plants, which reflects the contained amount of Δ^9 -THC.^{5,10)} These relatively high concentrations of active substances in cannabis plants may be due to the warm climate, the sun, the fertile soil of Greece, and possibly the quality of the seeds. This evidence suggests that Greece might be a high-risk area for the illicit cultivation of some new “pedigree” cannabis plants with high amounts of cannabinoid content.

References

- 1) United Nations, Report of the International Narcotics Control Board for 1997, United Nations, New York (1998).
- 2) United Nations, Special issue on cannabis. *Bulletin on Narcotics*, XXXVII, 4, 1–94 (1985).
- 3) United Nations, International Drug Control Programme “Recommended methods for the detection and assay of heroin, cannabinoids, cocaine, amphetamine, methamphetamine and ring-substituted amphetamine derivatives in biological specimens,” Manual for use by National Laboratories, United Nations, New York, 31–46 (1995).
- 4) Pitts J. E., O’Neil P. J., Leggo K. P., *J. Pharm. Pharmacol.*, **42**, 817–820 (1990).
- 5) Giroud C., Rivier L., *TIAFT Bulletin*, **26**, 2, 30–34 (1996).
- 6) United Nations, “Rapid testing methods of drugs of abuse. Manual for use by National Law Enforcement and Narcotics Laboratory Personnel,” United Nations, New York (1994).
- 7) Mechoulam R., “Marijuana,” Vol. 2, Academic Press, New York, (1973), p. 158.
- 8) Nahas G. “Symposium on Marijuana,” Reims, France, 22–23 July, *Bulletin on Narcotics*, **30**, 3, 23–32 (1978).
- 9) Baker P. B., Gough T. A., Taylor B. J., *Bulletin on Narcotics*, XXXII: 2, 31–40 (1980).

- 10) Jaffe J. H., "The Pharmacological Basis of Therapeutics," ed. by Goodman and Gilman's, Eighth Edition, Pergamon Press, 1990, pp. 522—573.
- 11) Debruyne D., Moulin M., Bigot M. C., Camsonne R., *Bulletin on Narcotics*, **XXXIII**, 2, 49—58 (1981).
- 12) Avico U., Pacifici R., Zuccaro P., *Bulletin on Narcotics*, **XXXVII**, 4, 61—66 (1985).
- 13) de Meijer EPM., van der Kamp H. J., van Eeuwijk F. A., *Euphytical*, **62**, 187—200 (1992).
- 14) Stefanidou M., Loutsidis C., Stiakakis I., Bolino G., Koutselinis A., *Jura Medica*, 1/2: 149—159 (1993).
- 15) Reglement (CEE). "Reglement No 1164/89 de la commission du 28 avril 1989, relatif aux modalites concernant l' aide pour le lin textile et le chanvre," 1989.
- 16) Debruyne D., Albessard F., Bigot M. C., Moulin M., *Bulletin on Narcotics*, **XLVI**, 2, 109—121 (1994).
- 17) Fetterman P. S., Keith E. S., Waller C. W., Guerrero O., Doorenbos N. J., Quimby M. W., *J. Pharm. Sci.*, **60**, 8, 1246—1249 (1971).
- 18) Masoud, A. N., Doorenbos, N. J., *J. Pharm. Sci.*, **62**, 313—315 (1973).
- 19) Taylor B. J., Neal J. D., Gough T. A., *Bulletin on Narcotics*, **XXXVII**, 4, 75—81 (1985).
- 20) Pitts J. E., Neal J. D., Gough T. A., *J. Pharm. Pharmacol.*, **44**, 947—951 (1992).
- 21) Baker P. B., Fowler R., Bagon K. R., Gough T. A., *J. Anal. Toxicol.*, **4**, 145—152 (1980).
- 22) Levine J., *J. Amer. Chem. Soc.*, **66**, 1868 (1944).
- 23) Pars H. G., Razdan R. K., *Ann. N. Y. Acad. Sci.*, **191**, 15—22 (1971).
- 24) El Kheir Y. M., Mohamed M. I., Hakim H. A., *Fitoterapia*, **57**, 4, 235—237 (1986).

Studies of the Constituents of *Gardenia* Species. II.¹⁾ Terpenoids from *Gardeniae Fructus*

Koichi MACHIDA, Kazumi OYAMA, Mutsumi ISHII, Rie KAKUDA, Yasunori YAOITA and Masao KIKUCHI*

Tohoku Pharmaceutical University, 4-4-1 Komatsushima, Aoba-ku, Sendai, Miyagi 981-8558, Japan.

Received November 18, 1999; accepted January 22, 2000

Four new terpenoids, gardenate A (1), 2-hydroxyethyl gardenamide A (2), (1R,7R,8S,10R)-7,8,11-trihydroxyguai-4-en-3-one 8-O- β -D-glucopyranoside (3) and Jasminoside F (4), were isolated from *Gardeniae Fructus*. Their structures were established on the basis of spectral analysis.

Key words *Gardeniae Fructus*; Rubiaceae; iridoid; guaiane-type sesquiterpene; safranal-type monoterpene

In a previous paper,¹⁾ we reported the isolation and structural elucidation of nine new monoterpenoids, gardenamide A, 6 α -butoxygeniposide, 6 β -butoxygeniposide, 6''-O-*p*-cis-coumaroylgenipin gentiobioside, and jasminosides A–E, from *Gardeniae Fructus*. In the course of further studies on the constituents of this plant, four new terpenoids have been isolated. This paper deals with the structural elucidation and identification of these compounds. The isolation procedure is described in detail in the experimental section.

Compound **1**, named gardenate A, was obtained as an amorphous powder, $[\alpha]_D -206.8^\circ$ (MeOH). Its molecular formula $C_{12}H_{18}O_6$ (obs. m/z 258.1076) was determined from the high resolution electron impact mass spectrum (HR-EI-MS). The 1H - and ^{13}C -NMR spectra of **1** revealed the presence of a tri-substituted double bond [δ_H : 5.83 (1H, brdd, $J=2.7, 1.5$ Hz); δ_C : 144.5, 129.8], two oxymethylene [δ_H : 4.03 (2H, brs), 3.82 (1H, dd, $J=11.0, 3.9$ Hz), 3.69 (1H, dd, $J=11.0, 6.8$ Hz); δ_C : 63.7, 60.9], two carbomethoxy [δ_H : 3.69, 3.63 (each 3H, s); δ_C : 176.1, 175.1, 52.1, 52.0], three methine [δ_H : 3.49 (1H, ddd, $J=8.1, 2.2, 1.0$ Hz), 2.83 (1H, ddt, $J=11.7, 10.2, 8.1$ Hz), 2.71 (1H, ddd, $J=11.7, 7.6, 1.0$ Hz); δ_C : 53.9, 51.2, 43.1] and methylene [δ_H : 2.46 (1H, dddt, $J=15.6, 8.1, 2.7, 1.0$ Hz), 2.31 (1H, dddt, $J=15.6, 10.2, 4.2, 2.2$ Hz); δ_C : 36.4] groups. These data suggested that **1** was an iridoid derivative. Detailed analysis of the 1H - and ^{13}C -NMR spectra of **1** were undertaken with the aid of 1H - 1H shift correlation spectroscopy (COSY) and 1H -detected multiple-bond correlation (HMBC) experiments and the planar structure of **1** was established to be as shown in Fig. 1. The stereochemistry of **1** was clarified by nuclear Overhauser effect spectroscopy (NOESY) and circular dichroism (CD) spectra. Nuclear Overhauser effect (NOE) was observed between 5-H and 9-H, suggesting these protons are on the same face. The absolute configurations at C-5 and C-9 of **1** were determined by application of the β,γ -unsaturated ketone Octant rule.²⁾ The CD spectrum of **1** showed a negative Cotton effect at 222.0 nm ($\Delta\epsilon -12.3$), suggesting that both C-5 and C-9 have *S*-configuration. From the above data, the structure of **1** was established to be as shown in Chart 1.³⁾

Compound **2** was obtained as an amorphous powder, $[\alpha]_D +325.0^\circ$ (MeOH). Its molecular formula $C_{13}H_{17}NO_5$ (obs. m/z 267.1109) was determined from the HR-EI-MS. Its 1H - and ^{13}C -NMR spectral patterns were similar to those of gardenamide A,¹⁾ except for the presence of an ethylene moiety (δ_C 61.0, 51.3) in **2**. Furthermore, the ^{13}C -NMR chemical shift at C-3 (δ 140.5) in **2** was shifted downfield by

+8.4 ppm compared with that of gardenamide A, suggesting that the 2-hydroxyethyl group is located at the 2-nitrogen. This finding was supported by the HMBC correlations from 1'-H₂ to C-1 and 3-H to C-1'. Furthermore, an NOE interaction was observed between 5-H and 9-H. From the above data, the structure of **2** was deduced to be 2-hydroxyethyl gardenamide A.

Compound **3** was obtained as an amorphous powder, $[\alpha]_D -18.5^\circ$ (MeOH). The FAB-MS exhibited an ion at m/z 457 ($M+Na$)⁺. The 1H -NMR spectral pattern closely resembled that of 8-epi-torilolone 8-O- β -D-glucopyranoside obtained by alkaline hydrolysis of 11-O-acetyl-8-epi-torilolone 8-O- β -D-glucopyranoside, which was isolated from *Torillia japonica* Fruit.⁴⁾ The ^{13}C -NMR spectrum of **3**, however, lacked a signal for the quaternary carbon at C-7 in 8-epi-torilolone 8-O- β -D-glucopyranoside and instead showed a signal characteristic of an oxygenated quaternary carbon at δ 80.3 in **3**. Furthermore, the location of an additional hydroxyl group at C-7 in **3** was suggested by downfield shifts of the signals due to C-6 [δ 33.0 (+3.7 ppm)], C-8 [δ 89.1 (+7.7 ppm)] and C-11 [δ 78.1 (+5.5 ppm)] on comparison of the ^{13}C -NMR spectrum of **3** and 8-epi-torilolone 8-O- β -D-glucopyranoside. Detailed analyses of the 1H - and ^{13}C -NMR spectra of **3** were undertaken with the aid of 1H - 1H COSY and HMBC experiments (Fig. 1). From these data, **3** was suggested to be a guaiane-type sesquiterpenoid, having a hydroxyl group at C-7. The stereochemistry of **3** was clarified from the NOESY experiment. NOEs were observed between 10-H/1-H and 8-H, suggesting that they were all on the same face (β) of the molecule. The isopropanol group at C-7 was determined to be on the same side as 8-H from the observed NOE interactions between 8-H/12-CH₃ (δ 1.39), one of the methylene protons at C-6 (δ 2.26)/8-H and 12-CH₃, and one of the methylene protons at C-6 (δ 2.99)/13-CH₃ (δ 1.36) and 15-CH₃ (δ 1.72). The absolute configuration at C-1 of **3** was determined as *R* from the CD curve and the sign of the optical rotation. The CD spectrum of **3** showed a positive Cotton effect at 312.0 nm ($\Delta\epsilon +0.32$) and a negative Cotton effect at 241.0 nm ($\Delta\epsilon -3.2$), which is a very similar CD curve to that of (1R)-4-guaien-3-one type sesquiterpenoids.⁵⁾ Furthermore, the optical rotation ($[\alpha]_D -18.5^\circ$) of **3** exhibited the same sign when compared with (1R)-4-guaien-3-one type sesquiterpenoids.^{4,6)} Therefore, **3** was determined to be (1R,7R,8S,10R)-7,8,11-trihydroxyguai-4-en-3-one 8-O- β -D-glucopyranoside.

Compound **4**, named jasminoside F, was purified as its

* To whom correspondence should be addressed. e-mail: mkikuchi@tohoku-pharm.ac.jp

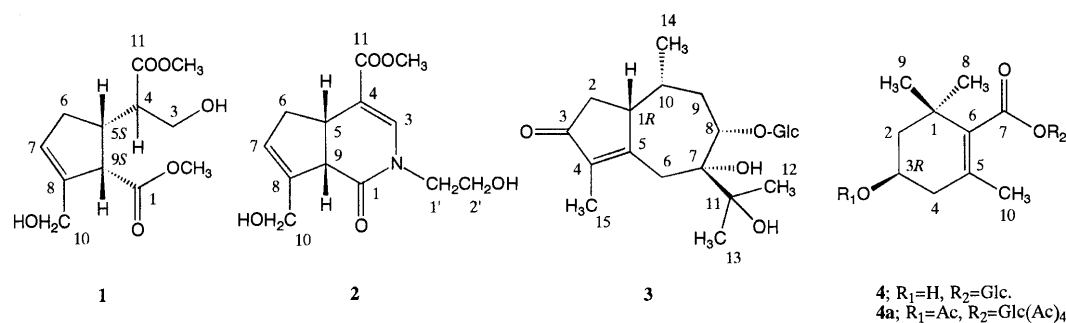


Chart 1

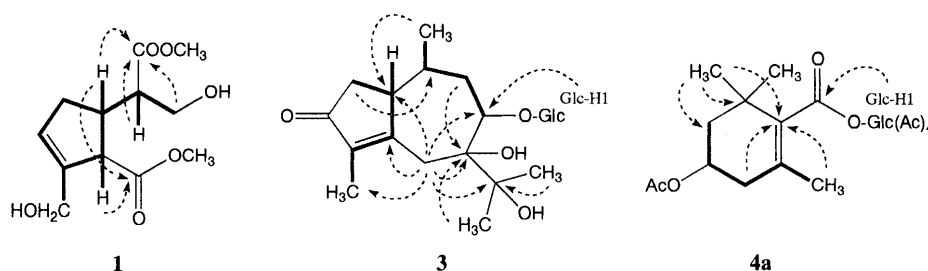
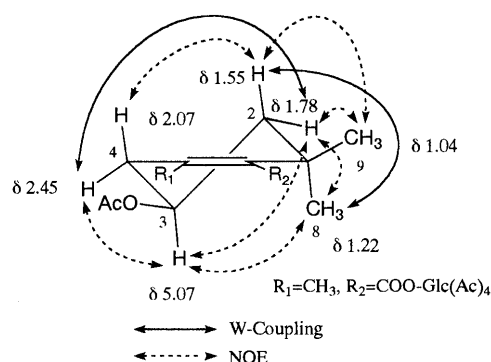


Fig. 1. The Main HMBC Correlations

Heavy lines indicate partial structures inferred from ^1H - ^1H COSY.

Fig. 2. NOE Correlations and W-Couplings of **4a**

pentaacetate (**4a**), $[\alpha]_D -24.1^\circ$ (MeOH). The ^1H - and ^{13}C -NMR spectral data of **4a** indicated structural similarity with picrocinic acid [4-(β -D-glucopyranosyloxy)-2,6,6-trimethyl-1-cyclohexene-1-carboxylic acid] isolated from the fruit of *Gardenia jasminoides* ELLIS forma *grandiflora* (LOUR.) MAKINO.⁷⁾ However, the anomeric carbon signal in **4a** was shifted upfield of ca. 10 ppm (δ 91.5) in comparison with that of an etheral bonded one. From this finding, including the number of acetyl groups of **4a**, the glucosyl group is on the ester moiety at C-7, and not on the hydroxyl moiety at C-3. The location of the glucosyl group on the ester moiety at C-7 was further supported from the HMBC spectrum; that is, the anomeric proton (Glc-H₁) showed an HMBC correlation with the ester carbonyl carbon (δ 167.8). From the above data, including the other HMBC correlations of **4a** (Fig. 1), the planar structure of **4** was established to be as shown in Fig. 1. The relative configuration of C-3 was determined from the ^1H - ^1H COSY and NOESY experiments. As shown in Fig. 2, the ^1H - ^1H COSY and NOESY spectra indicated 3-H to be quasi-axial with respect to the half-chair form of the cyclohexene. Furthermore, an NOE was observed between one of the quasi-axial methyl protons (δ 1.22) at C-1 and 3-

H, showing that they were on the same face of the molecule. The absolute configuration of **4a** was determined from the CD spectrum. The CD spectrum of **4a** showed a negative Cotton effect at 237.4 nm ($\Delta\epsilon -2.1$), suggesting that the methylene proton (δ 2.07) at C-4 and the methyl protons (δ 1.22) at C-1 are β and α -quasi-axial, respectively.⁸⁾ Therefore, the absolute configuration at C-3 of **4a** was deduced as *R*. This was further confirmed by comparison of the sign of the optical rotation of similar monoterpenoids.⁹⁾ From this evidence, the full structure of **4** was established as shown in Chart 1.

Experimental

Optical rotations were determined with a JASCO DIP-360 digital polarimeter. UV Spectra were recorded with a Beckman DU-64 spectrometer. The CD spectra were obtained with a JASCO J-700 spectropolarimeter. ^1H - and ^{13}C -NMR spectra were recorded with JEOL JNM-EX 270 (270 and 67.8 MHz, respectively) and JEOL JNM-GSX 400 (400 and 100 MHz, respectively) spectrometers. Chemical shifts are given in the δ (ppm) scale with tetramethylsilane as an internal standard (s, singlet; d, doublet; t, triplet; dd, double doublet; q, quartet; ddd, double double doublet; dddd, double double double doublet; m, multiplet; br, broad). MS were recorded on a JEOL JMS-DX 303 mass spectrometer (FAB-MS were obtained with glycerol as the matrix). Column chromatography was carried out on Kieselgel 60 (Merck; 70–230 mesh), Sephadex LH-20 (Pharmacia Fine Chemicals) and Cosmosil 75C₁₈-OPN (Nacalai Tesque). A preparative HPLC system (pump, CCPD; detector, UV-8010) using Cosmosil 5C₁₈-AR (Nacalai Tesque, 10 mm i.d. \times 25 cm) and TSK-gel Silica-60 (Tosoh, 7.8 mm i.d. \times 30 cm) columns was used. TLC was carried out with precoated Kieselgel 60 plates (Merck) and detection was achieved by spraying with 5% H_2SO_4 followed by heating.

Isolation Procedure Dried fruit of *Gardenia jasminoides* ELLIS forma *grandiflora* (LOUR.) MAKINO (1.0 kg) collected in Guangxi prefecture (广西), China were extracted with MeOH under reflux for 5.0 h. The MeOH extract was concentrated under reduced pressure and the residue was suspended in water (400 ml). The suspension was successively extracted with CHCl_3 , Et_2O , EtOAc and *n*-BuOH. The CHCl_3 -soluble fraction was concentrated under reduced pressure to produce a residue (29.8 g). The residue was chromatographed on a silica-gel column using *n*-hexane–EtOAc (4:1–1:1) and eluate was separated into twelve fractions (frs. 1–12). Fraction 11 was rechromatographed on a C18 open column using MeOH– H_2O (2:1) and the

eluate was separated into twelve fractions (frs. 11-1—11-12). Fractions 11-2 and 11-3 were subjected to prep. HPLC [Cosmosil 5C18-AR column, MeOH-H₂O (1:1), flow rate: 1.5 ml/min, 220 nm] to give four peaks (peaks 1—4), respectively. Peak 1 was purified by prep. HPLC [Cosmosil 5C18-AR column, MeOH-H₂O (1:2), flow rate: 1.4 ml/min; 220 nm. TSK-gel Silica-60 column, *n*-hexane-acetone (3:2), flow rate: 1.5 ml/min; 205 nm] to give **1** (6.0 mg). Peak 2 was purified by prep. HPLC [Cosmosil 5C18-AR column, MeOH-H₂O (1:2), flow rate: 1.5 ml/min; 220 nm] to give **2** (3.0 mg). The *n*-BuOH-soluble fraction was concentrated under reduced pressure to produce a residue (51.0 g). The residue was chromatographed on a silica-gel column using CHCl₃-MeOH-H₂O (30:10:1) and the eluate was separated into thirteen fractions (frs. 1—13). Fraction 3 was rechromatographed on a Sephadex LH-20 column using 50% MeOH and the eluate was separated into seventeen fractions (frs. 3-1—3-17). Fraction 3-2 was subjected to prep. HPLC [Cosmosil 5C18-AR column, MeOH-H₂O (1:1), flow rate: 1.2 ml/min, 242 nm] to give **3** (10.0 mg). Fraction 6 was rechromatographed on a Sephadex LH-20 column using 50% MeOH and the eluate was separated into seven fractions (frs. 6-1—6-7). Fraction 6-3 was subjected to prep. HPLC [Cosmosil 5C18-AR column, MeOH-H₂O (1:2), flow rate: 1.2 ml/min; 234 nm] to give crude **4**, which was acetylated with Ac₂O in pyridine. After the usual work-up, the crude product was purified by prep. HPLC [Cosmosil 5C18-AR column, MeOH-H₂O (3:1), flow rate: 1.5 ml/min; 230 nm] to give **4a** (4.0 mg).

Gardenate A (1) An amorphous powder, $[\alpha]_D^{26} -206.8^\circ$ ($c=0.46$, MeOH). EI-MS m/z : 258 M⁺. HR-MS m/z : 258.1076 (M⁺) (Calcd for C₁₂H₁₈O₆: 258.1104). ¹H-NMR (400 MHz, CD₃OD) δ : 5.83 (1H, brdd, $J=2.7, 1.5$ Hz, 7-H), 4.03 (2H, brs, 10-H₂), 3.82 (1H, dd, $J=11.0, 3.9$ Hz, 3-H_B), 3.69 (1H, dd, $J=11.0, 6.8$ Hz, 3-H_A), 3.69 (3H, s, 11-COOCH₃), 3.63 (3H, s, 1-COOCH₃), 3.49 (1H, ddd, $J=8.1, 2.2, 1.0$ Hz, 9-H), 2.83 (1H, ddt, $J=11.7, 10.2, 8.1$ Hz, 5-H), 2.71 (1H, ddd, $J=11.7, 6.8, 3.9$ Hz, 4-H), 2.46 (1H, dddd, $J=15.6, 8.1, 2.7, 1.0$ Hz, 6-H_B), 2.31 (1H, dddd, $J=15.6, 10.2, 4.2, 2.2$ Hz, 6-H_A). ¹³C-NMR (100 MHz, CD₃OD) δ : 175.1 (C-1), 63.7 (C-3), 51.2 (C-4), 43.1 (C-5), 36.4 (C-6), 129.8 (C-7), 144.5 (C-8), 53.9 (C-9), 60.9 (C-10), 176.1 (C-11), 52.1, 52.0 (COOCH₃). CD ($c=3.59 \times 10^{-4}$ M, MeOH) $\Delta\epsilon$ (nm): -12.3 (222.0).

2-Hydroxyethyl Gardenamide A (2) An amorphous powder, $[\alpha]_D^{26} +325.0^\circ$ ($c=0.16$, MeOH). EI-MS m/z : 267 M⁺. HR-MS m/z : 267.1109 (M⁺) (Calcd for C₁₃H₁₇NO₅: 267.1107). ¹H-NMR (400 MHz, CD₃OD) δ : 7.39 (1H, s, 3-H), 5.83 (1H, brdd, $J=2.9, 1.5$ Hz, 7-H), 4.37 (2H, brs, 10-H₂), 3.74 (3H, s, 11-COOCH₃), 3.67 (5H, m, 9-H, 1',2'-H₂), 3.52 (1H, ddd, $J=8.5, 8.5, 8.3$ Hz, 5-H), 2.84 (1H, dddd, $J=14.6, 8.3, 2.9, 1.5$ Hz, 6-H_B), 2.22 (1H, ddt, $J=14.6, 8.5, 2.2$ Hz, 6-H_A). ¹³C-NMR (100 MHz, CD₃OD) δ : 171.6 (C-1), 140.5 (C-3), 111.0 (C-4), 38.9 (C-5), 40.8 (C-6), 128.2 (C-7), 143.9 (C-8), 50.2 (C-9), 61.8 (C-10), 168.9 (C-11), 52.0 (COOCH₃), 51.3 (C-1'), 61.0 (C-2').

(1R,7R,8S,10R)-7,8,11-Trihydroxyguai-4-en-3-one 8-O-β-D-Glucopyranoside (3) An amorphous powder, $[\alpha]_D^{26} -18.5^\circ$ ($c=0.27$, MeOH). FAB-MS m/z : 457 [M+Na]⁺. UV λ_{max}^{MeOH} nm (log ϵ): 242.0 (4.07). ¹H-NMR (270 MHz, CD₃OD) δ : 4.52 (1H, d, $J=7.9$ Hz, Glc-H₁), 4.05 (1H, dd, $J=10.7, 2.8$ Hz, 8-H), 3.84 (1H, dd, $J=11.7, 2.2$ Hz, Glc-H_{6B}), 3.64 (1H, dd, $J=11.7, 5.3$ Hz, Glc-H_{6A}), 3.13 (1H, dd, $J=9.0, 7.9$ Hz, Glc-H₂), 2.99 (1H, d, $J=13.0$ Hz, 6-H_B), 2.90 (1H, m, 1-H), 2.34 (1H, dd, $J=17.4, 6.0$ Hz, 2-H_B), 2.26 (1H, d, $J=13.0$ Hz, 6-H_B), 2.16 (1H, q, $J=7.6$ Hz, 10-H), 2.07 (1H, dd,

$J=17.4, 3.9$ Hz, 2-H_A), 1.88 (1H, dd, $J=13.9, 2.8$ Hz, 9-H_B), 1.72 (3H, d, $J=2.2$ Hz, 15-CH₃), 1.64 (1H, dd, $J=13.9, 10.7$ Hz, 9-H_A), 1.39 (3H, s, 12-CH₃), 1.36 (3H, s, 13-CH₃), 1.03 (3H, d, $J=7.6$ Hz, 14-CH₃). ¹³C-NMR (67.8 MHz, CD₃OD) δ : 48.0 (C-1), 38.5 (C-2), 211.9 (C-3), 141.6 (C-4), 175.7 (C-5), 33.0 (C-6), 80.3 (C-7), 89.1 (C-8), 34.9 (C-9), 31.1 (C-10), 78.1 (C-11), 26.7 (C-12), 26.2 (C-13), 20.7 (C-14), 9.0 (C-15), 105.9 (Glc-C₁), 75.2 (Glc-C₂), 78.2 (Glc-C₃), 71.6 (Glc-C₄), 78.3 (Glc-C₅), 62.8 (Glc-C₆). CD ($c=1.3 \times 10^{-4}$ M, MeOH) $\Delta\epsilon$ (nm): +0.32 (312.0), -3.2 (241.0).

Jasminoside F Pentaacetate (4a) An amorphous powder, $[\alpha]_D^{26} -24.1^\circ$ ($c=0.29$, MeOH). FAB-MS m/z : 579 [M+Na]⁺. ¹H-NMR (400 MHz, CDCl₃) δ : 5.84 (1H, d, $J=8.3$ Hz, Glc-H₁), 5.18 (1H, dd, $J=10.0, 9.3$ Hz, Glc-H₄), 5.14 (1H, dd, $J=9.3, 8.3$ Hz, Glc-H₂), 5.26 (1H, t, $J=9.3$ Hz, Glc-H₃), 5.07 (1H, m, 3-H), 4.29 (1H, dd, $J=12.2, 4.9$ Hz, Glc-H_{6B}), 4.13 (1H, dd, $J=12.2, 2.4$ Hz, Glc-H_{6A}), 3.86 (1H, ddd, $J=10.0, 4.9, 2.4$ Hz, Glc-H₅), 2.45 (1H, dd, $J=17.4, 6.0$ Hz, 4-H_B), 2.07 (1H, m, 4-H_A), 1.99, 2.01, 2.04, 2.05, 2.06 (each 3H, s, COCH₃), 1.78 (1H, dd, $J=12.3, 2.3$ Hz, 2-H_B), 1.68 (3H, s, 10-CH₃), 1.55 (1H, m, 2-H_B), 1.22 (3H, s, 8-CH₃), 1.04 (3H, s, 9-CH₃). ¹³C-NMR (100 MHz, CDCl₃) δ : 35.4 (C-1), 42.8 (C-2), 67.5 (C-3), 37.0 (C-4), 133.26 (C-5), 133.35 (C-6), 167.8 (C-7), 28.4 (C-8), 28.6 (C-9), 21.3 (C-10), 91.5 (Glc-C₁), 70.1 (Glc-C₂), 72.7 (Glc-C₃), 68.1 (Glc-C₄), 73.0 (Glc-C₅), 61.6 (Glc-C₆), 170.6, 170.5, 170.1, 169.4, 169.0 (COCH₃), 20.75, 20.65, 20.58, 20.5 (COCH₃). CD ($c=3.17 \times 10^{-4}$ M, MeOH) $\Delta\epsilon$ (nm): -2.1 (237.4).

Acknowledgements The authors are grateful to Mrs. S. Sato and T. Matsuki of our university for NMR analyses and MS measurements.

References and Notes

- Machida K., Onodera R., Furuta K., Kikuchi M., *Chem. Pharm. Bull.*, **46**, 1295—1300 (1998).
- Snatzke G., Schaffner K., *Helv. Chim. Acta*, **51**, 986—999 (1968).
- The stereochemistry at C-4 could not be established.
- Kitajima J., Suzuki N., Tanaka Y., *Chem. Pharm. Bull.*, **46**, 1743—1747 (1998).
- "Shin Jikken Kagaku Koza 13, Yuki Kozo (II)," ed. by Nippon Kagaku Kai, Maruzen, Tokyo, 1977, pp. 833—834; Buchi G., Kauffman J. M., Loewenthal J. E., *J. Am. Chem. Soc.*, **88**, 3403—3408 (1966).
- Chikamatsu H., Maeda M., Nakazaki M., *Tetrahedron*, **25**, 4751—4765 (1969); Matsuo A., Nakayama M., Sato S., Nakamoto T., Uto S., Hayashi S., *Experientia*, **30**, 321—322 (1974); Bohlmann F., Borthakur N., *Phytochemistry*, **21**, 1160—1162 (1982); Bohlmann F., Zdero C., King R. M., Robinson H., *Phytochemistry*, **22**, 1201—1206 (1983); Mishi M., Luengo D. H., Mabry T. J., *Phytochemistry*, **26**, 199—200 (1987); Jakupovic J., Pathak V. P., Grenz M., Banerjee S., Wolfrum C., Baruah R. N., Bohlmann F., *Phytochemistry*, **26**, 1049—1052 (1987).
- Takeda Y., Nishimura H., Kadota O., Inouye H., *Chem. Pharm. Bull.*, **24**, 2644—2646 (1976).
- "Shin Jikken Kagaku Koza 13, Yuki Kozo (II)," ed. by Nippon Kagaku Kai, Maruzen, Tokyo, 1977, pp. 821—830; Burgstahler A. W., Barkhurst R. C., *J. Am. Chem. Soc.*, **92**, 7601—7603 (1970).
- Miyase T., Ueno A., Takizawa N., Kobayashi H., Oguchi H., *Chem. Pharm. Bull.*, **36**, 2475—2488 (1988).

Sterol Constituents from Two Edible Mushrooms, *Lentinula edodes* and *Tricholoma matsutake*¹⁾

Naoko OHNUMA, Keiko AMEMIYA, Rie KAKUDA, Yasunori YAOITA, Koichi MACHIDA and Masao KIKUCHI*

Tohoku Pharmaceutical University, 4-1-1 Komatsushima Aoba-ku, Sendai, Miyagi 981-8558, Japan.

Received November 19, 1999; accepted January 29, 2000

Two new sterols, (22E)-23-methylergosta-5,7,22-trien-3 β -ol (1) and 5 α ,6 α -epoxy-(22E)-ergosta-8,14,22-triene-3 β ,7 α -diol (2), have been isolated from two edible mushrooms, *Lentinula edodes* and *Tricholoma matsutake*, respectively, together with twelve known ones (3–14). The structures of the new compounds were elucidated on the basis of their spectral data.

Key words sterol; *Lentinula edodes*; *Tricholoma matsutake*; mushroom

Recently we reported the isolation and structural elucidation of sterols^{1,2)} and sesquiterpenoids³⁾ from twelve mushrooms. In a continuation of our investigation of the chemical constituents of mushrooms, we describe here the isolation and structural elucidation of two new sterols, (22E)-23-methylergosta-5,7,22-trien-3 β -ol (1) and 5 α ,6 α -epoxy-(22E)-ergosta-8,14,22-triene-3 β ,7 α -diol (2), as well as twelve known ones, (22E)-ergosta-7,22-dien-3 β -ol (3),^{2c,4)} 5 α ,8 α -epidioxy-(22E)-ergosta-6,22-dien-3 β -ol (4),^{2a,5)} 5 α ,6 α -epoxy-(22E)-ergosta-8(14),22-diene-3 β ,7 α -diol (5),^{2a,6)} 5 α ,6 α :8 α ,9 α -diepoxy-(22E)-ergost-22-ene-3 β ,7 α -diol (6),^{2e)} 3 β ,5 α -dihydroxy-(22E)-ergosta-7,22-dien-6-one (7),^{2a,7)} 3 β ,5 α ,9 α -trihydroxy-(22E)-ergosta-7,22-dien-6-one (8),^{2a,8)} 3 β ,5 α ,9 α -trihydroxyergost-7-en-6-one (9),^{2b)} 3 β ,5 α ,9 α ,14 α -tetrahydroxy-(22E)-ergosta-7,22-dien-6-one (10),^{2b)} (22E)-ergosta-7,22-diene-3 β ,5 α ,6 β -triol (11),^{2a,9)} ergost-7-ene-3 β ,5 α ,6 β -triol (12),^{2b,10)} (22E)-ergosta-7,22-diene-3 β ,5 α ,6 α ,9 α -tetrol (13)^{2b)} and (22E)-ergosta-7,22-diene-3 β ,5 α ,6 β ,9 α -tetrol (14)^{2a,8)} from two edible mushrooms, *Lentinula* (*L.*) *edodes* (BERK.) SING. (Shiitake in Japanese, Pleurotaceae, compounds 1 and 3) and *Tricholoma* (*T.*) *matsutake* (S. ITO et IMAI) SING. (Matsutake in Japanese, Tricholomataceae, compounds 2, 4–14). This is the first time that compound 3 and compounds 4–14 have been isolated from *L. edodes* and *T. matsutake*, respectively.

Compound 1 was isolated as an amorphous powder, $[\alpha]_D -78.9^\circ$. The molecular formula was determined to be C₂₉H₄₆O by high-resolution (HR)-MS. The IR spectrum showed the presence of a hydroxyl group (3468 cm⁻¹). The UV absorption maxima at 270, 280 and 291 nm implied the presence of a $\Delta^{5,7}$ -diene system in a sterol skeleton.¹¹⁾ The electron ionization (EI)-MS gave fragment ion peaks at m/z 392 (M⁺–H₂O) and 253 (M⁺–H₂O–side chain), indicating that 1 has a hydroxyl group and a mono-unsaturated C₁₀-side chain. The ¹H- (*vide* Experimental) and ¹³C-NMR spectra (*vide* Experimental), obtained with the aid of ¹H–¹H shift correlation spectroscopy (¹H–¹H COSY) and ¹H-detected heteronuclear multiple quantum coherence (HMQC) spectra, showed signals due to two tertiary methyl groups [δ_H : 0.65 (3H, H₃-18), 0.95 (3H, H₃-19); δ_C : 12.2 (C-18), 16.3 (C-19)], four secondary methyl groups [δ_H : 0.79 (3H, H₃-26), 0.84 (3H, H₃-27), 0.94 (3H, H₃-28), 0.96 (3H, H₃-21); δ_C : 16.9 (C-28), 20.1 (C-27), 20.8 (C-21), 21.7 (C-26)], three secondary methyl-bearing methine groups [δ_H : 1.52 (1H, H-25),

1.64 (1H, H-24), 2.36 (1H, H-20); δ_C : 30.8 (C-25), 34.8 (C-20), 50.2 (C-24)], an olefinic methyl group [δ_H : 1.51 (3H, H₃-29); δ_C : 13.2 (C-29)], a side chain-bearing methine group [δ_H : 1.29 (1H, H-17); δ_C : 56.6 (C-17)], an oxymethine group [δ_H : 3.64 (1H, H-3); δ_C : 70.5 (C-3)] and three trisubstituted double bonds [δ_H : 4.91 (1H, H-22), 5.38 (1H, H-7), 5.57 (1H, H-6); δ_C : 116.3 (C-7), 119.6 (C-6), 131.5 (C-22), 135.5 (C-23), 139.8 (C-5), 141.4 (C-8)]. Inspection of the spectral data revealed that 1 was identical to ergosterol¹²⁾ except for the structure of the side chain part. Detailed analysis of the ¹H–¹H COSY spectrum of 1 implied connectivities of H-17–H-20, H-20–H₃-21, H-20–H-22, H-24–H-25, H-24–H₃-28, H-25–H₃-26 and H-25–H₃-27. The ¹H-detected heteronuclear multiple bond connectivity (HMBC) correlations of H₃-21 to C-17, C-20 and C-22 revealed that an H₃-21 methyl group was attached to C-20. The presence of H₃-26 and H₃-27 methyl groups at C-25 were indicated by HMBC correlations of H₃-26 and H₃-27 to C-24 and C-25. An H₃-28 methyl group was attached at C-24 judging from HMBC correlations of H₃-28 to C-23, C-24 and C-25. The ¹H–¹³C long-range correlations of H₃-29 to C-22, C-23 and C-24 revealed that an H₃-29 methyl group was attached to C-23. These spectral data indicated the presence of a 23,24-dimethyl- Δ^{22} -sterol side chain in 1. The stereochemistry at C-22 and C-24 was determined to be *E* and *R*, respectively, by comparison with the ¹H-NMR data reported for (22E)-23-methylergosta-5,22-dien-3 β -ol.^{13f)} Based on this evidence, the structure of 1 was determined to be (22E)-23-methylergosta-5,7,22-trien-3 β -ol. Although a sterol with the (22E,24R)-23,24-dimethyl- Δ^{22} -side chain has been detected in marine organisms,¹³⁾ the isolation of a sterol with this side chain from terrestrial sources is rare.^{2e,14)}

Compound 2 was isolated as an amorphous powder, $[\alpha]_D -61.9^\circ$. The molecular formula was determined to be C₂₈H₄₂O₃ by HR-MS. The IR spectrum showed the presence of a hydroxyl group (3176 cm⁻¹). The ¹H- and ¹³C-NMR spectra, obtained with the aid of ¹H–¹H COSY and HMQC spectra, showed signals due to two tertiary methyl groups [δ_H : 0.83 (3H, H₃-19), 0.84 (3H, H₃-18); δ_C : 15.6 (C-18), 23.1 (C-19)], four secondary methyl groups [δ_H : 0.91 (3H, H₃-26), 0.92 (3H, H₃-27), 1.00 (3H, H₃-28), 1.13 (3H, H₃-21); δ_C : 18.0 (C-28), 19.9 (C-26), 20.2 (C-27), 21.3 (C-21)], a side chain-bearing methine group [δ_H : 1.63 (1H, H-17); δ_C : 56.6 (C-17)], a methylene group attached to double bond

* To whom correspondence should be addressed. e-mail: mkikuchi@tohoku-pharm.ac.jp

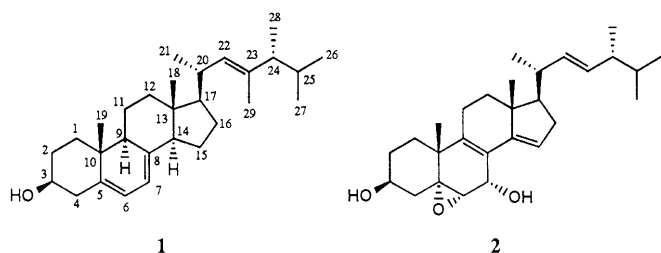


Chart 1

$[\delta_{\text{H}}: 2.18 (1\text{H}, \text{H}_A-16), 2.45 (1\text{H}, \text{H}_B-16); \delta_{\text{C}}: 37.6 (\text{C}-16)]$, a trisubstituted epoxide $[\delta_{\text{H}}: 3.02 (1\text{H}, \text{H}-6); \delta_{\text{C}}: 62.5 (\text{C}-6), 65.2 (\text{C}-5)]$, two oxymethine groups $[\delta_{\text{H}}: 3.82 (1\text{H}, \text{H}-3), 4.34 (1\text{H}, \text{H}-7); \delta_{\text{C}}: 67.7 (\text{C}-7), 68.3 (\text{C}-3)]$, a disubstituted double bond $[\delta_{\text{H}}: 5.28 (1\text{H}, \text{H}-22), 5.33 (1\text{H}, \text{H}-23); \delta_{\text{C}}: 132.5 (\text{C}-23), 136.0 (\text{C}-22)]$, a trisubstituted double bond $[\delta_{\text{H}}: 6.50 (1\text{H}, \text{H}-15); \delta_{\text{C}}: 123.9 (\text{C}-15), 146.9 (\text{C}-14)]$ and a fully substituted double bond $[\delta_{\text{C}}: 123.0 (\text{C}-8), 139.1 (\text{C}-9)]$. These spectral data were similar to those of $5\alpha,6\alpha$ -epoxy-(22*E*)-ergosta-8,22-diene-3 β ,7 α -diol^{2a,6,15)} except for the presence of the trisubstituted double bond. The position of this double bond was determined as follows. The ^1H - ^1H COSY spectrum of **1** showed correlation peaks revealing the sequences from H-15 to H-17 via H₂-16. In the HMBC spectrum, ^1H - ^{13}C long-range correlations were observed from H-15 to C-16 and C-17; H₂-16 to C-14; and the H₃-18 methyl group to C-14 and C-17. These spectral data indicated that the trisubstituted double bond is Δ^{14} . The UV spectrum of **2** showed an absorption maximum at 247 nm. This also supported the above conclusion. Thus, the structure of **2** was determined to be $5\alpha,6\alpha$ -epoxy-(22*E*)-ergosta-8,14,22-triene-3 β ,7 α -diol. The $5\alpha,6\alpha$ -epoxy-3 β ,7 α -dihydroxy- $\Delta^{8,14}$ moiety is unprecedented in the natural sterols previously known.

Experimental

General Procedures Optical rotations were determined using a JASCO DIP-360 digital polarimeter. IR spectra were recorded with a Perkin-Elmer FT-IR 1725X IR spectrophotometer and UV spectra on a Beckman DU-64 spectrophotometer. ^1H - and ^{13}C -NMR spectra were recorded with a JEOL JNM-LA 600 (600 and 150 MHz, respectively) spectrometer. Chemical shifts are given on a δ (ppm) scale with tetramethylsilane as an internal standard (s, singlet; d, doublet; dd, double doublet; ddd, double double doublet; br, broad; m, multiplet). The EI- and HR-MS were recorded on a JEOL JMS-DX 303 mass spectrometer. Column chromatography was carried out on Kieselgel 60 (Merck; 230–400 mesh). Preparative HPLC was carried out on a Tosoh HPLC system (pump, CCPD; detector, RI-8010) using a TSK gel ODS-120T (7.8 mm i.d. \times 30 cm) column (Tosoh).

Material *L. edodes* (from Sendai, Japan) and *T. matsutake* (from Korea) were purchased in a food market in Sendai, Japan.

Extraction and Isolation *L. edodes*: The fresh fruit bodies of *L. edodes* (4.7 kg) were extracted three times with Et₂O at room temperature for 2 weeks. The Et₂O extract (7.1 g) was chromatographed on a silica-gel column using *n*-hexane–EtOAc (7:3–1:7), EtOAc and MeOH, to afford 25 fractions (frs. 1–25). Fraction 4 was purified by preparative HPLC [mobile phase, MeOH; flow rate, 1.0 ml/min; column temperature, 40 °C] to give **1** (0.4 mg) and **3** (0.5 mg).

T. matsutake: The fresh fruit bodies of *T. matsutake* (4.7 kg) were extracted four times with Et₂O at room temperature for 2 weeks. The Et₂O extract (8.7 g) was chromatographed on a silica-gel column using *n*-hexane–EtOAc (7:3–1:7), EtOAc and MeOH, to afford 31 fractions (frs. 1–31). Fraction 7 was purified by preparative HPLC [mobile phase, MeOH–H₂O (9:1); flow rate, 1.0 ml/min; column temperature, 40 °C] to give **4** (0.2 mg). Fraction 15 was purified by preparative HPLC [mobile phase, MeOH–H₂O (9:1); flow rate, 1.0 ml/min; column temperature, 40 °C] to give **2** (1.0 mg), **5** (1.1 mg) and **7** (1.0 mg). Fraction 17 was purified

by preparative HPLC [mobile phase, MeOH–H₂O (9:1); flow rate, 1.0 ml/min; column temperature, 40 °C] to give **8** (2.3 mg), **9** (0.3 mg) and **10** (0.5 mg). Fraction 27 was purified by preparative HPLC [mobile phase, MeOH–H₂O (9:1); flow rate, 1.0 ml/min; column temperature, 40 °C] to give **6** (0.3 mg), **11** (3.1 mg), **12** (0.3 mg) and **13** (0.3 mg). Fraction 29 was purified by preparative HPLC [mobile phase, MeOH–H₂O (9:1); flow rate, 1.0 ml/min; column temperature, 40 °C] to give **14** (5.0 mg).

All known compounds (**3**–**14**) were identified by comparison of their chromatographic behavior and ^1H -NMR data with those of authentic samples.

(22*E*)-23-Methylergosta-5,7,22-trien-3 β -ol (**1**): Amorphous powder. $[\alpha]_{\text{D}}^{27} -78.9^\circ$ ($c=0.04$, CHCl₃). IR $\nu_{\text{max}}^{\text{CHCl}_3}$ cm⁻¹: 3468. UV $\lambda_{\text{max}}^{\text{MeOH}}$ nm (log ϵ): 270 (3.7), 280 (3.7), 291 (3.4). HR-MS m/z : 410.3535 (M^+ , Calcd for C₂₉H₄₆O: 410.3549). EI-MS m/z : 410 (M^+), 392 ($\text{M}^+ - \text{H}_2\text{O}$), 253 ($\text{M}^+ - \text{H}_2\text{O} - \text{side chain}$). ^1H -NMR (600 MHz, CDCl₃) δ : 0.65 (3H, s, H₃-18), 0.79 (3H, d, $J=6.6$ Hz, H₃-26), 0.84 (3H, d, $J=6.6$ Hz, H₃-27), 0.94 (3H, d, $J=7.0$ Hz, H₃-28), 0.95 (3H, s, H₃-19), 0.96 (3H, d, $J=6.6$ Hz, H₃-21), 1.29 (1H, m, H-17), 1.51 (3H, d, $J=1.1$ Hz, H₃-29), 1.52 (1H, m, H-25), 1.64 (1H, m, H-24), 2.29 (1H, dd, $J=14.3, 12.5$ Hz, H-4 β), 2.36 (1H, m, H-20), 2.47 (1H, ddd, $J=14.3, 4.4, 2.2$ Hz, H-4 α), 3.64 (1H, m, H-3), 4.91 (1H, br d, $J=9.5$ Hz, H-22), 5.38 (1H, m, H-7), 5.57 (1H, m, H-6). ^{13}C -NMR (150 MHz, CDCl₃) δ : 12.2 (C-18), 13.2 (C-29), 16.3 (C-19), 16.9 (C-28), 20.1 (C-27), 20.8 (C-21), 21.1 (C-11), 21.7 (C-26), 23.0 (C-15), 27.7 (C-16), 30.8 (C-25), 32.0 (C-2), 34.8 (C-20), 37.0 (C-10), 38.4 (C-1), 39.1 (C-12), 40.8 (C-4), 42.8 (C-13), 46.3 (C-9), 50.2 (C-24), 54.5 (C-14), 56.6 (C-17), 70.5 (C-3), 116.3 (C-7), 119.6 (C-6), 131.5 (C-22), 135.5 (C-23), 139.8 (C-5), 141.4 (C-8).

$5\alpha,6\alpha$ -Epoxy-(22*E*)-ergosta-8,14,22-triene-3 β ,7 α -diol (**2**): Amorphous powder. $[\alpha]_{\text{D}}^{33} -61.9^\circ$ ($c=0.1$, CHCl₃). IR $\nu_{\text{max}}^{\text{CHCl}_3}$ cm⁻¹: 3176. UV $\lambda_{\text{max}}^{\text{MeOH}}$ nm (log ϵ): 247 (3.9). HR-MS m/z : 426.3152 (M^+ , Calcd for C₂₈H₄₂O₃: 426.3134). ^1H -NMR (600 MHz, C₆D₆) δ : 0.83 (3H, s, H₃-19), 0.84 (3H, s, H₃-18), 0.91 (3H, d, $J=7.0$ Hz, H₃-26), 0.92 (3H, d, $J=7.0$ Hz, H₃-27), 1.00 (3H, d, $J=6.6$ Hz, H₃-28), 1.13 (3H, d, $J=6.6$ Hz, H₃-21), 1.63 (1H, m, H-17), 1.87 (1H, dd, $J=12.8, 11.4$ Hz, H-4 β), 2.18 (1H, dd, $J=16.9, 11.4$ Hz, H_A-16), 2.31 (1H, m, H-20), 2.45 (1H, ddd, $J=16.9, 7.3, 3.3$ Hz, H_B-16), 3.02 (1H, d, $J=2.6$ Hz, H-6), 3.82 (1H, m, H-3), 4.34 (1H, dd, $J=11.2, 2.6$ Hz, H-7), 5.28 (1H, dd, $J=15.4, 8.1$ Hz, H-22), 5.33 (1H, dd, $J=15.4, 7.3$ Hz, H-23), 6.50 (1H, dd, $J=3.3, 1.8$ Hz, H-15). ^{13}C -NMR (150 MHz, C₆D₆) δ : 15.6 (C-18), 18.0 (C-28), 19.9 (C-26), 20.2 (C-27), 21.3 (C-21), 23.1 (C-19), 23.5 (C-11), 30.8 (C-2), 31.3 (C-1), 33.4 (C-25), 35.7 (C-12), 37.6 (C-16), 38.9 (C-10), 39.3 (C-20), 39.5 (C-4), 43.3 (C-24), 45.6 (C-13), 56.6 (C-17), 62.5 (C-6), 65.2 (C-5), 67.7 (C-7), 68.3 (C-3), 123.0 (C-8), 123.9 (C-15), 132.5 (C-23), 136.0 (C-22), 139.1 (C-9), 146.9 (C-14).

Acknowledgments We are grateful to Mr. S. Sato and Mr. T. Matsuki of this university for measurement of the mass and NMR spectra.

References and Notes

- Part VIII in a series of studies on the constituents of mushrooms; Part VII: Ueno T., Kakuda R., Yaoita Y., Machida K., Kikuchi M., *J. Tohoku Pharmaceutical University*, "accepted".
- a) Ishizuka T., Yaoita Y., Kikuchi M., *Chem. Pharm. Bull.*, **45**, 1756–1760 (1997); b) Yaoita Y., Amemiya K., Ohnuma H., Furumura K., Masaki A., Matsuki T., Kikuchi M., *ibid.*, **46**, 944–950 (1998); c) Ishizuka T., Yaoita Y., Kikuchi M., *Natural Medicines*, **52**, 276–278 (1998); d) *Idem*, *Tohoku Yakka Daigaku Kenkyu Nempo*, **45**, 135–138 (1998); e) Yaoita Y., Endo M., Tani Y., Machida K., Amemiya K., Furumura K., Kikuchi M., *Chem. Pharm. Bull.*, **47**, 847–851 (1999).
- Yaoita Y., Machida K., Kikuchi M., *Chem. Pharm. Bull.*, **47**, 894–896 (1999).
- Arthur H. R., Halsall T. G., Smith R. D., *J. Chem. Soc.*, **1958**, 2603–2605.
- Wieland P., Prelog V., *Helv. Chim. Acta*, **30**, 1028–1030 (1947).
- Petzoldt K., Kieslich K., *Justus Liebigs Ann. Chem.*, **724**, 194–198 (1969).
- Aiello A., Fattorusso E., Magno S., Menna M., *Steroids*, **56**, 337–340 (1991).
- Valisollalao J., Luu B., Ourisson G., *Tetrahedron*, **39**, 2779–2785 (1983).
- Alt G. H., Barton D. H. R., *J. Chem. Soc.*, **1954**, 1356–1361.
- Iorizzi M., Minale L., Riccio R., Lee J., Yasumoto T., *J. Nat. Prod.*, **51**, 1098–1103 (1988).
- Dorfman L., *Chem. Rev.*, **53**, 47–144 (1953).
- Shirane N., Takenaka H., Ueda K., Hashimoto Y., Katoh K., Ishii H., *Phytochemistry*, **41**, 1301–1308 (1996).

- 13) a) Shimizu Y., Alam M., Kobayashi A., *J. Am. Chem. Soc.*, **98**, 1059—1060 (1976); b) Bohlin L., Sjostrand U., Djerassi C., Sullivan B. W., *J. Chem. Soc., Perkin Trans. 1*, **1981**, 1023—1028; c) Kokke W. C. M. C., Fenical W., Djerassi C., *Phytochemistry*, **20**, 127—134 (1981); d) Withers N. W., Kokke W. C. M. C., Fenical W., Djerassi C., *Proc. Natl. Acad. Sci. U.S.A.*, **79**, 3764—3768 (1982); e) Kokke W. C. M. C., Bohlin L., Fenical W., Djerassi C., *Phytochemistry*, **21**, 881—887 (1982); f) Kobayashi J., Ishibashi M., Nakamura H., Ohizumi Y., Hirata Y., *J. Chem. Soc., Perkin Trans. 1*, **1989**, 101—103; g) John L. M. D., Tino W. F., McLean S., Reynolds W. F., *J. Nat. Prod.*, **56**, 144—146 (1993); h) He H., Kulanthaivel P., Baker B. J., Kalter K., Darges J., Cofield D., Wolff L., Adams L., *Tetrahedron*, **51**, 51—58 (1995); i) Rodriguez A. D., Rivera J., Boulanger A., *Tetrahedron Lett.*, **39**, 7645—7648 (1998); j) Rama Rao M., Venkatesham U., Venkata Rami Reddy M., Venkateswarlu Y., *J. Nat. Prod.*, **62**, 785—786 (1999).
- 14) Akihisa T., Kokke W. C. M. C., Hayashi Y., Kimura Y., Yokota T., Tamura T., *Chem. Pharm. Bull.*, **41**, 624—626 (1993).
- 15) The ^1H - and ^{13}C -NMR spectra of authentic sample of 5 α ,6 α -epoxy-(22*E*)-ergosta-8,22-diene-3 β ,7 α -diol isolated from *Grifola frondosa* were measured in C_6D_6 .

New Megastigmane and Tetraketide from the Leaves of *Euscaphis japonica*

Yoshio TAKEDA,*^a Yoshihiro OKADA,^a Toshiya MASUDA,^a Eiji HIRATA,^b Takakazu SHINZATO,^c Anki TAKUSHI,^d Qian YU,^e and Hideaki OTSUKA^e

Faculty of Integrated Arts and Sciences, The University of Tokushima,^a 1–1 Minamijosanjima-cho, Tokushima 770–8502, Japan, Faculty of Agriculture, University of the Ryukyus,^b 1 Senbaru, Nishihara-cho, Nakagami-gun, Okinawa 903–0213, Japan, University Forest, Faculty of Agriculture, University of the Ryukyus,^c 685 Yona, Kunigami-gun, Okinawa 905–1427, Japan, 134 Furugen, Yomitan-son,^d Nakagami-gun, Okinawa 904–0300, Japan, and Institute of Pharmaceutical Sciences, Hiroshima University Faculty of Medicine,^e 1–2–3 Kasumi, Minami-ku, Hiroshima 734–8551, Japan.
Received November 29, 1999; accepted January 19, 2000

New megastigmane (1) and tetraketide (2) were isolated from the leaves of *Euscaphis japonica* and the structures were elucidated by means of spectroscopic and chemical evidence.

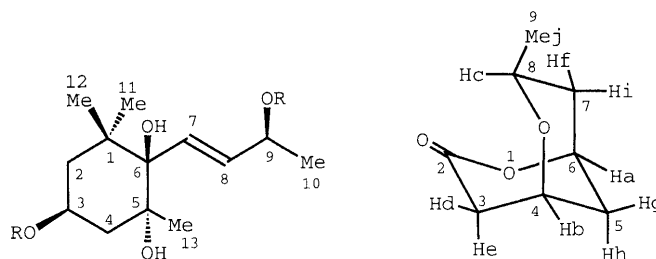
Key words *Euscaphis japonica*; Staphyleaceae; megastigmane; bicyclic tetraketide

Euscaphis (*E.*) *japonica* KANITZ. (Staphyleaceae) is a tree which is grown in southwestern parts of Japan and in central China.¹⁾ From the capsule of the plant, flavonol glycosides and anthocyanin,²⁾ and compounds³⁾ which are positive to Ehrlich's reagent have already been isolated and characterized. In the course of the studies on the constituents of the plants grown in a subtropical climate, we have investigated the constituents of the leaves of *E. japonica* harvested in Okinawa Prefecture, Japan and earlier reported the isolation and structure elucidation of euscapholide and its glucoside.⁴⁾ Further studies on the constituents resulted in the isolation of two new compounds, one is a megastigmane and the other a tetraketide. This report deals with the isolation and structural elucidation of the new compounds.

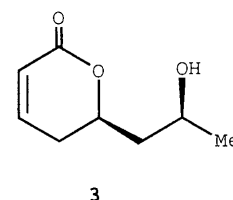
The *n*-BuOH soluble portion of the MeOH extract of the leaves of *E. japonica* upon repeated column chromatographies over highly porous synthetic resin, Diaion HP-20 and silica gel, and HPLC, afforded two new compounds 1 and 2.

Compound 1 was obtained as an amorphous powder, $[\alpha]_D^{26} -25.7^\circ$ (MeOH) and the molecular formula was determined as C₁₃H₂₄O₄ based on its negative ion high resolution (HR)-FAB-MS. The ¹H-NMR spectrum displayed a secondary methyl signal at δ 1.27 (H_a), three tertiary methyl signals at δ 0.87 (H_b), 1.10 (H_c) and 1.22 (H_d), two methylene signals at δ 1.45 (H_e), 1.64 (H_f) (each 1H) and 1.76 (H_g) (2H), two secondary carbinyl proton signals at δ 4.06 (H_h) and 4.34 (H_i), and signals due to *trans*-double bond at δ 5.79 (H_j) and 6.07 (H_k). The ¹³C-NMR spectrum (Table 1), in addition to the signals due to the above functional groups, showed signals due to a quaternary carbon atom at δ 40.6 and two quaternary carbon atoms with an oxygen atom at δ 77.7 and 78.8. In the ¹H–¹H correlation spectroscopy (COSY) spectrum, the cross peaks were followed starting from H_a to H_i→H_j→H_k, successively, establishing the structure of side chain portion (C-7—C-10). Starting from H_e and H_f, the cross peaks were followed to H_h and H_g, successively. Two singlet methyl groups (H_b and H_d) constitute the *gem*-dimethyl system, since the cross peaks due to long-range coupling were observed between these signals. The cross peaks between H_f and H_d were also observed. Thus, the structure around C-1—C-4 was elucidated. A quaternary carbon atom with a hydroxyl group was assigned to C-6 since carbon signals as-

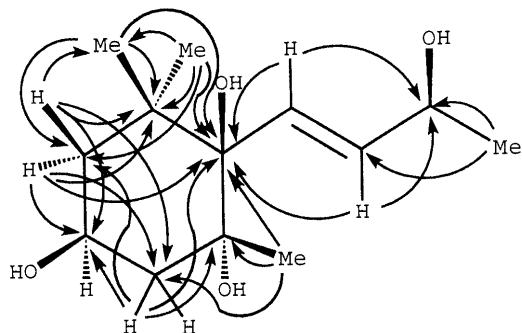
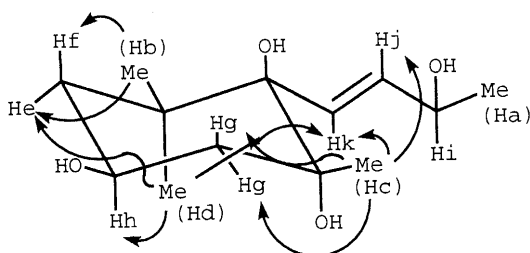
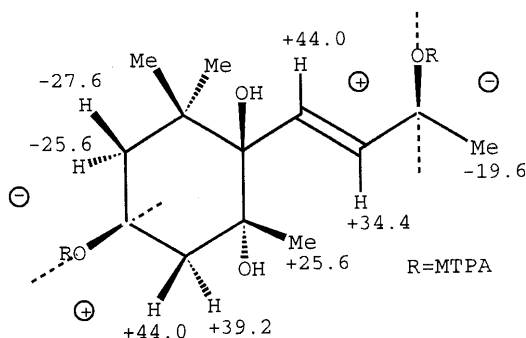
signed to C-1 and C-6 resonated in almost the same region as those of closely related compounds, dendranthemside A⁵⁾ (δ 40.5 and 78.3, respectively). Considering the elemental composition and the above functional groups, compound 1 is monocyclic so that the remaining tertiary methyl group and a quaternary carbon atom with hydroxyl group could be assigned to C-13 and C-5. Thus, compound 1 was presumed to have a structure with megastigm-7-ene carbon skeleton to which four hydroxyl groups are introduced on C-3, 5, 6 and 9, and the presumption was supported by the results of the heteronuclear multiple bond correlation spectroscopy (HMBC) spectrum which are shown in Fig. 1. The planar structure thus elucidated is the same as that of the aglycone part of kiwiionoside.⁶⁾ The relative stereochemistry of the secondary hydroxyl group on C-3 was determined to take an equatorial orientation as judged from the coupling pattern of H₂-2 (axial-H, t, *J*=12.2 Hz, H_f; equatorial-H, ddd, *J*=12.2, 4.0, 2.0 Hz, H_e). The relative stereochemistry was further examined by phase-sensitive nuclear Overhauser enhancement



1 R=H
1a R=(R)-MTPA
1b R=(S)-MTPA



* To whom correspondence should be addressed. e-mail: takeda@ias.tokushima-u.ac.jp

Fig. 1. HMBC Correlations ($J=8$ Hz, $^1\text{H} \rightarrow ^{13}\text{C}$) for Compound **1**Fig. 2. NOE Correlations for Compound **1**Fig. 3. $\Delta\delta$ Values in Hz ($\delta_S - \delta_R$, 400 MHz)

and exchange spectroscopy (NOESY) and differential nuclear Overhauser enhancement (NOE) experiments. The results shown in Fig. 2 clearly demonstrated that both the methyl group at C-5 and the side chain take equatorial orientations. To determine the absolute stereochemistry, compound **1** was subjected to a modified Mosher's method.⁷⁾ Namely, compound **1** was treated with (*R*)- and (*S*)- α -methoxy- α -trifluoromethylphenyl acetic acid (MTPA) in the presence of dicyclohexyl carbodiimide (DCC) and 4-dimethylaminopyridine (DMAP) to give the 3,9-di-(*R*)-MTPA ester (**1a**) and the 3,9-di-(*S*)-MTPA ester (**1b**), respectively. As shown in Fig. 3, the signals due to protons at C-4, 7, 8 and 13 in **1a** resonated at a higher field as compared to those in **1b**, while the signals due to protons on C-2 and C-10 resonated at a lower field. Consequently, the absolute configurations at C-3 and C-9 have been elucidated as 3*S* and 9*S*, respectively, and the structure of compound **1** was determined to be as shown.

Compound **2** was obtained as colorless needles, mp 86–87 °C, $[\alpha]_D^{26} -13.9^\circ$ (MeOH) and the molecular formula was determined as $\text{C}_8\text{H}_{12}\text{O}_3$ based on its high resolution electron impact MS (HR-EI-MS). Its IR spectrum showed the pres-

Table 1. ^{13}C -NMR Data for Compounds **1** and **2**^{a)}

Carbon	1 ^{b)}	2 ^{c)}
1	40.6	—
2	46.3	169.7
3	65.1	36.4
4	45.5	65.8
5	77.7	29.5
6	78.8	73.0
7	130.9	38.4
8	135.9	61.9
9	69.4	21.3
10	24.0	—
11	27.5	—
12	26.1	—
13	27.1	—

a) The assignments were based on noise decoupling, distortionless enhancement by polarization transfer (DEPT), ^1H - ^{13}C COSY and HMBC spectra. b) Taken in CD_3OD . c) Taken in CDCl_3 .

ence of a δ -lactone (ν_{max} 1720 cm^{-1}). The ^1H -NMR spectrum showed a clearly resolved spectrum when measured in CDCl_3 and C_6D_6 (1 : 1): it showed signals due to a secondary methyl group (δ 0.99) (H_j), three methylene groups [δ 2.32 (H_e) and 2.60 (H_d), 1.33 (H_g) and 1.48 (H_h), and 1.08 (H_f) and 1.12 (H_i)], one (H_d , H_e) of which located vicinal at a carbonyl group and three methine protons [δ 3.68 (H_c), 3.89 (H_b) and 4.40 (H_a)] geminal at an oxygen atom. The ^{13}C -NMR spectrum (Table 1) showed the presence of a lactonic carbon atom at δ 169.7 in addition to the signals arising from the above functional groups. These facts together with the elemental composition demonstrated that compound **2** has a bicyclic ring system. The planar structure was deduced as shown by interpretation of the ^1H - ^1H COSY spectrum. Thus, the cross peaks, $\text{H}_j \rightarrow \text{H}_c \rightarrow \text{H}_i$ (H_f) $\rightarrow \text{H}_a \rightarrow \text{H}_h$ (H_g) $\rightarrow \text{H}_b \rightarrow \text{H}_e$ (H_d) were followed successively. Several long-range couplings via a W-letter interaction were observed between H_b and H_a , H_d and H_g , and H_f and H_h . In addition, H_i was observed as a doublet of double doublets ($J=12.0$, 11.6, 2.0 Hz) indicating that H_i takes an axial orientation and the methyl group (H_j) an equatorial orientation. The observed long-range coupling via W-letter interaction clearly supported the proposed bicyclic structure, so that the relative stereostructure of compound **2** was elucidated as shown. The absolute stereochemistry was established as shown by the chemical correlation of euscapholide (**3**)^{4,8)} with known absolute stereochemistry. Euscapholide (**3**) was treated with sodium hydride in CH_2Cl_2 ⁹⁾ to give compound **2**.

Experimental

^1H - (400 MHz) and ^{13}C -NMR (100 MHz) spectra were recorded on a JEOL JNM EX-400 or α -400 spectrometer, using tetramethylsilane as internal standard. Two dimensional spectra and NOE were measured by the usual pulse sequences with which the spectrometer was equipped; mass spectra were obtained on a JEOL JMS SX-102 spectrometer. FAB-MS were recorded using PEG-400, PEG-600 or *m*-nitrobenzyl alcohol as a matrix. IR spectra were taken on Shimadzu IR-400 or Perkin-Elmer 1720 infrared FT spectrophotometer. Specific optical rotations were determined using a JASCO DIP-360 digital polarimeter. For compound purification, the following were used: the highly porous synthetic resin, Diaion HP-20 (Mitsubishi Chemical Co., Ltd., Tokyo), silica gel 60 (Merck, 230–400 mesh), packed column for HPLC (Cosmosil 10 C18, 20 \times 250 mm) and silica gel 60 F₂₅₄ TLC plates (Merck, 0.25 and 0.5 mm in thickness).

Plant Material The leaves of *E. japonica* KANITZ. were collected in August, 1994, at Kunigami-son, Okinawa Prefecture, Japan. A specimen was authenticated by one of the authors (A.T.) and a voucher herbarium speci-

men (EJ-Okinawa 9407) is deposited in the Herbarium of the Institute of Pharmaceutical Sciences, Hiroshima University Faculty of Medicine.

Extraction and Isolation Dried leaves (2.9 kg) of *E. japonica* were extracted with MeOH (45 l) at room temperature for 3 weeks. Concentration of MeOH extract *in vacuo* gave a residue which was dissolved in 90% MeOH (2.1 l). After washing with *n*-hexane (1 l), the 90% MeOH solution was concentrated *in vacuo*. The residue was suspended in H₂O (1 l) and the suspension was extracted successively with EtOAc (1 l) and *n*-BuOH (1 l). The *n*-BuOH extract was concentrated *in vacuo* to give a residue (77 g) which was chromatographed on Diaion HP-20 (i.d. = 78 mm, L = 536 mm) with stepwise increase of MeOH content in H₂O [0 (4 l), 10 (5 l), 30 (6 l), 40 (6.5 l), 50 (6.5 l), 70 (6.5 l) and 100 (6 l)]; fractions of 500 ml were collected.

Fractions 14–17 were combined and concentrated *in vacuo* to give a residue (10.7 g) which was separated by silica gel (400 g) column chromatography with CHCl₃–MeOH as eluent with an increasing amount of MeOH. The fractions which contained a spot (*R*_f 0.41) on TLC (solvent: CHCl₃–MeOH–H₂O, 15 : 6 : 1) were combined and the solvent was removed *in vacuo* to give a residue (180.4 mg) which was further purified by preparative HPLC (MeOH–H₂O, 1 : 4, 6 ml/min, detection 210 nm) to give compound **1** (*t*_R 37 min) (106.7 mg) as an amorphous powder.

Fractions 18–23 were combined and concentrated *in vacuo* to give a residue (12.2 g) which was subjected to silica gel (400 g) column chromatography with CHCl₃–MeOH as eluent with an increasing amount of MeOH content. The fraction which contained a spot (*R*_f 0.44) on TLC (solvent: CHCl₃–Me₂CO, 4 : 1) was purified by repeated silica gel chromatography (solvent: Et₂O, CHCl₃–MeOH) to give compound **2** (335 mg) as colorless needles.

Compound 1 An amorphous powder, [α]_D²⁵ –25.7° (*c* = 1.52, MeOH). IR (dry film): 3691 (br, OH) cm^{–1}. ¹H-NMR (CD₃OD) δ : 0.87 (3H, s, H-12), 1.10 (3H, s, H-13), 1.22 (3H, s, H-11), 1.27 (3H, d, *J* = 6.4 Hz, H-10), 1.45 (1H, ddd, *J* = 2.0, 4.0, 12.2 Hz, H-2_{eq}), 1.64 (1H, t, *J* = 12.2 Hz, H-2_{ax}), 1.76 (2H, m, H-4), 4.06 (1H, m, H-3), 4.34 (1H, qd, *J* = 6.4, 1.2 Hz, H-9), 5.79 (1H, dd, *J* = 6.4, 16.0 Hz, H-8), 6.07 (1H, dd, *J* = 1.2, 16.0 Hz, H-7). ¹³C-NMR: given in Table 1. Negative HR-FAB-MS *m/z*: 243.1584 [M–H][–] (Calcd for C₁₃H₂₃O₄: 243.1596).

Compound 2 Colorless needles, mp 86–87 °C, [α]_D²⁶ –13.9° (*c* = 2.18, MeOH). IR (CHCl₃): 1720 (lactone) cm^{–1}. ¹H-NMR (C₆D₆–CDCl₃, 1 : 1) δ : 0.99 (3H, d, *J* = 5.6 Hz, H-8), 1.12 (1H, ddd, *J* = 2.0, 11.6, 12.0 Hz, H-7_{ax}), 1.33 (1H, br dt, *J* = 13.6, 2.0 Hz, H-5_{eq}), 1.48 (1H, ddt, *J* = 13.6, 4.0, 2.0 Hz, H-5_{ax}), 1.68 (1H, br d, *J* = 13.6 Hz, H-7_{eq}), 2.32 (1H, dd, *J* = 5.2, 18.8 Hz, H-3_{ax}), 2.60 (1H, br d, *J* = 18.8 Hz, H-3_{eq}), 3.68 (1H, ddq, *J* = 11.2, 2.4, 5.6 Hz, H-8), 3.89 (1H, br s, *W*/2 = 10 Hz, H-4), 4.40 (1H, br s, *W*/2 = 9 Hz, H-6). ¹³C-NMR given in Table 1. HR-EI-MS *m/z*: 156.0801 [M]⁺ (Calcd for C₈H₁₂O₃: 156.0786).

(R)-MTPA Ester (1a) of Compound 1 Compound **1** (15.3 mg) was dissolved in CH₂Cl₂ (10 ml). (*R*)-MTPA (purchased from Merck) (65.7 mg), DCC (57.0 mg) and DMAP (19.1 mg) were added to the solution and the solution was stirred at room temperature for 10 min. After dilution with EtOAc, the solution was washed with 5% HCl, saturated NaHCO₃ aqueous solution and saturated NaCl aqueous solution, successively, dried (MgSO₄) and evaporated *in vacuo*. The residue was purified by silica gel (5 g) column chromatography (CHCl₃) and then preparative TLC (solvent: CHCl₃–

Me₂CO, 19 : 1) to give the di-(*R*)-MTPA ester (**1a**) (9.4 mg) as an amorphous powder. IR (CHCl₃): 1715 cm^{–1}. ¹H-NMR (CDCl₃) δ : 0.80 (3H, s, H-12), 1.09 (3H, s, H-13), 1.25 (3H, s, H-11), 1.46 (3H, d, *J* = 6.4 Hz, H-10), 1.68 (1H, ddd, *J* = 12.2, 4.0, 2.2 Hz, H-2_{eq}), 1.81 (1H, t, *J* = 12.2 Hz, H-2_{ax}), 1.86 (1H, ddd, *J* = 12.7, 4.9, 2.0 Hz, H-4_{eq}), 1.91 (1H, t, *J* = 12.7 Hz, H-4_{ax}), 3.56, 3.57 (each 3H, s, 2×OMe), 5.47 (1H, dddd, *J* = 12.7, 12.2, 4.9, 4.0 Hz, H-3), 5.69 (1H, quintet, *J* = 6.4 Hz, H-9), 5.70 (1H, dd, *J* = 14.7, 6.4 Hz, H-8), 6.18 (1H, d, *J* = 14.7 Hz, H-7), 7.39 (6H, m), 7.53 (4H, m). HR-FAB-MS *m/z*: 699.2322 [M+Na]⁺ (Calcd for C₃₃H₃₈F₆NaO₈: 699.2369).

(S)-MTPA Ester (1b) of Compound 1 Compound **1** (15.5 mg) was treated as above to give the di-(*S*)-MTPA ester (**1b**) (14.4 mg) as an amorphous powder. IR (CHCl₃): 1715 cm^{–1}. ¹H-NMR (CDCl₃) δ : 0.81 (3H, s, H-12), 1.15 (3H, s, H-13), 1.28 (3H, s, H-11), 1.41 (1H, d, *J* = 6.4 Hz, H-10), 1.62 (1H, ddd, *J* = 12.2, 4.4, 2.2 Hz, H-2_{eq}), 1.74 (1H, t, *J* = 12.2 Hz, H-2_{ax}), 1.96 (1H, ddd, *J* = 12.7, 4.9, 2.0 Hz, H-4_{eq}), 2.02 (1H, t, *J* = 12.7 Hz, H-4_{ax}), 3.54, 3.56 (each 3H, s, 2×OMe), 5.49 (1H, dddd, *J* = 12.7, 12.2, 4.9, 4.4 Hz, H-3), 5.66 (1H, dd, *J* = 15.6, 7.1 Hz, H-9), 5.79 (1H, dd, *J* = 6.8, 15.6 Hz, H-8), 6.29 (1H, d, *J* = 15.6 Hz, H-7), 7.41 (6H, m), 7.53 (4H, m). HR-FAB-MS *m/z*: 699.2413 [M+Na]⁺ (Calcd for C₃₃H₃₈F₆NaO₈: 699.2369).

Conversion of Euscapholide (3) to Compound 2 Euscapholide (**3**) (85.5 mg) was dissolved in CH₂Cl₂ (5 ml) and 60% NaH in oil (400 mg) was added to the solution after washing with *n*-hexane. After standing for 10 min at room temperature, the reaction was quenched with EtOAc (35 ml) and the precipitates were removed by filtration. The filtrate was concentrated *in vacuo* to give a residue which was purified by silica gel (10 g) column chromatography with CHCl₃ as eluant to give compound **2** (70.2 mg), mp 88–89 °C, [α]_D²⁵ –17.8° (*c* = 1.12, MeOH). HR-EI-MS *m/z*: 156.0792 [M]⁺ (Calcd for C₈H₁₂O₃: 156.0786). This compound was identified with natural **2** by mixed melting point determination and comparisons of the ¹H- and ¹³C-NMR spectra.

Acknowledgement We thank the Cooperative Center of the University of Tokushima for permitting us to access to the NMR instrument.

References and Notes

- 1) Makino T., "Makino's New Illustrated Flora of Japan," Hokuryu-kan Publishing Co., Ltd., Tokyo, 1970, p. 364.
- 2) Ishikura N., *Bot. Mag. (Tokyo)*, **84**, 1–7 (1971).
- 3) Konishi T., Ohtani Y., Kiyosawa S., *Chem. Pharm. Bull.*, **44**, 863–864 (1996).
- 4) Takeda Y., Okada Y., Masuda T., Hirata E., Takushi A., Otsuka H., *Phytochemistry*, **49**, 2565–2568 (1998).
- 5) Otsuka H., Takeda Y., Yamasaki K., Takeda Y., *Planta Med.*, **58**, 373–375 (1992).
- 6) Murai F., Tagawa M., Ohishi H., *Planta Med.*, **58**, 112–113 (1992).
- 7) Ohtani I., Kusumi T., Kashman Y., Kakisawa H., *J. Am. Chem. Soc.*, **113**, 4092–4096 (1991).
- 8) Murakami N., Wang W., Aoki M., Tsutsui Y., Higuchi K., Aoki S., Kobayashi M., *Tetrahedron Lett.*, **38**, 5533–5536 (1997).
- 9) Drewes S. E., Horn M. M., Shaw R. S., *Phytochemistry*, **40**, 321–323 (1995).

Studies on the 1,4-Oxazepine Ring Formation Reaction Using the Molecular Orbital Method

Hisao MATSUZAKI,^{*,a} Isao TAKEUCHI,^b Yoshiki HAMADA,^b and Keiichiro HATANOC

Tohoku Pharmaceutical University,^a 4-4-1 Komatsushima, Aoba-ku, Sendai 981-8558, Japan, Faculty of Pharmacy, Meijo University,^b 150 Yagotoyama Tempaku-ku, Nagoya 468-8503, Japan, and Faculty of Pharmaceutical Sciences, Nagoya City University,^c Tanabe-dori 3-1, Mizuho-ku, Nagoya 467-0027, Japan. Received December 8, 1999; accepted March 15, 2000

1,4-Oxazepine formation reactions of 1,8-naphthyridine derivatives (1–4) with peroxy acid have been studied using a semiempirical MO method (AM1) and an *ab initio* molecular orbital method (Gaussian 94). The energies of molecules involved in the reaction paths were calculated and the transition states related to experimental products were obtained. For the reactions of 1–3, the calculated energies of the transition states predicted the previously obtained products. However, the calculated values for the reaction of 4 suggested a different type of oxazepine compound, which was verified in further experiments.

Key words mechanism; transition state; oxazepine; naphthyridine; MO method

Nitrogen-containing heterocyclic compounds have extensive pharmaceutical applications. Some chemical derivatives of these polyheterocyclic compounds express anticancer activity. Therefore, it is useful to examine the mechanism of known reactions in terms of energy along the reaction path, for the purpose of synthesizing new types of compounds. In previous papers, Takeuchi *et al.* reported the oxidation reactions of naphtho [2,1-b][1,8] naphthyridine (**1**) and naphtho [1,2-b][1,8] naphthyridine (**2**), and benzo[b] [1,8] naphthyridine (1,9-diazaanthracene) (**3**) with peracetic acid (**5**) and/or *m*-chloroperbenzoic acid (*m*-CPBA) (**6**),^{1,2)} producing compounds with a seven-membered 1,4-oxazepine ring moiety. In the present paper, we studied theoretically the 1,4-oxazepine ring formation reactions of **1**–**3** and naphtho [2,3-b][1,8] naphthyridine (**4**) and/or **5** and **6**, considering two routes to produce the 1,4-oxazepine ring¹⁾ (Chart 1). For the reactions of **1**–**3**, the experiments and calculated results indicated one type of 1,4-oxazepine ring formation (P1 type). But the calculated result for the linear-type compound (**4**) suggested the formation of another type of 1,4-oxazepine ring (P2 type). To investigate the calculated result for the reaction of **4** experimentally, we performed new synthesis and

oxidation of the compound (**4**) (Chart 2).

The following calculations were performed using the semiempirical molecular orbital AM1 method³⁾ in the MOPAC 93 program package.⁴⁾ The effect of solvent was not considered. All structure parameters were optimized. We assume that the reaction of **1** with **5** (reaction 1) proceeds as follows: The C₅-atom of the 1,8-naphthyridine skeleton in **1** has the maximum LUMO amplitude (0.4522). Then we can predict that the peracetate ion is added to the C₅-atom of **1**.⁵⁾ When the O₁-atom of the peracetate ion approaches the C₅-atom of **1**, the minimum energy state (C₅–O₁ distance = 3.04 Å and heat of formation [HF] = 14.11 kcal/mol) is achieved. Then a new C–O bond is formed through the transition state (TS) (C₅–O₁ = 2.159 Å and HF = 23.76 kcal/mol). After attracting the H⁺ ion without energy barriers, the intermediate state (Eq) (C₅–O₁ = 1.474 Å and HF = 35.50 kcal/mol) is achieved (Chart 1).

In the ring expansion process, we can assume two reaction paths (Chart 1).¹⁾ In path 1, the product P1 will be formed through TS1 (O₁–O₂ = 1.866 Å, HF = 79.71 kcal/mol), Eq1' (O₁–O₂ = 3.977 Å, HF = 57.09 kcal/mol), and TS1' (O₁–O₂ = 3.716 Å, HF = 61.87 kcal/mol). The O₂-atom in TS1 or TS1' has a large minus charge, but the LUMO density of the C₅-atom is very small (0.043) in TS1 and large (0.33) in TS1'. Therefore we may think that the C₅–O₂ bond cannot be formed directly *via* TS1 but can be *via* TS1'. We performed the intrinsic reaction coordinate calculation and confirmed that Eq1' is actually produced from Eq *via* TS1 and P1 is produced from Eq1' *via* TS1'. In path 2, the product P2 is formed through TS2 (O₁–O₂ = 1.871 Å, HF = 83.24 kcal/mol). Since the calculated value of TS1 energy is 3.53 kcal/mol lower than that of TS2, path 1 is preferred and product P1 is expected. The calculated structure of P1 coincides with the experimental product, the structure

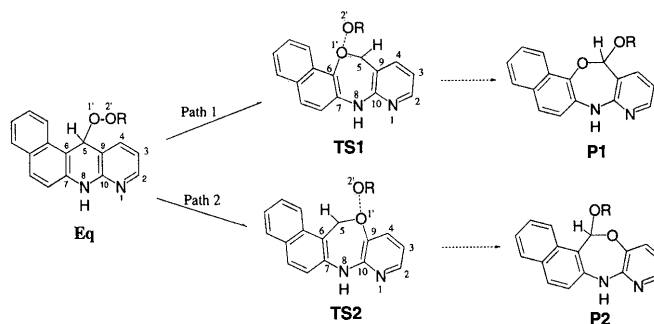


Chart 1. Reaction Paths for the Ring Expansion Process for Reactions 1 (R = COCH₃) and 3 (R = COC₆H₄Cl)

Table 1. Calculated Energies (kcal/mol) for the Ring Expansion Process and the Corresponding Experimental Yields (%)

Reaction	Reactant	E0 ^{a)}	TS1	TS2	ΔE	ΔE(G94) ^{b)}	Ea	Yield ^{c)}	Temp., Time
1	1 + 5	37.69	79.71	83.24	3.53	11.43	42.02	56	60–65 °C, 4 h
2	2 + 5	36.72	81.20	84.03	2.83	8.89	44.48	19	60–65 °C, 4 h
3	1 + 6	66.61	106.16	109.55	3.39	10.74	39.55	22	r.t., 2 h
4	2 + 6	65.64	107.70	110.37	2.67	8.52	42.06	1	r.t., 15 h
5	3 + 6	51.41	90.53	90.53	0.00	1.63	39.12	71	20 °C, 3 h
6	4 + 6	75.56	111.39	109.78	–1.61	–0.45	34.22	16 ^{d)}	20 °C, 10 min

Energies are expressed in terms of the heat of formation calculated using the AM1 method except for ΔE(G94). ΔE denotes the energy difference between TS1 and TS2. a) Sum of energies of the reactants. b) Energy difference between TS1 and TS2 calculated using Gaussian 94 with RHF/3-21G.⁶⁾ c) Yield denotes the sum of the experimental yields of the products with a 1,4-oxazepine ring.⁷⁾ d) Yield of product (**10**) with a 1,4-oxazepine ring of the P2 type (see Chart 1).

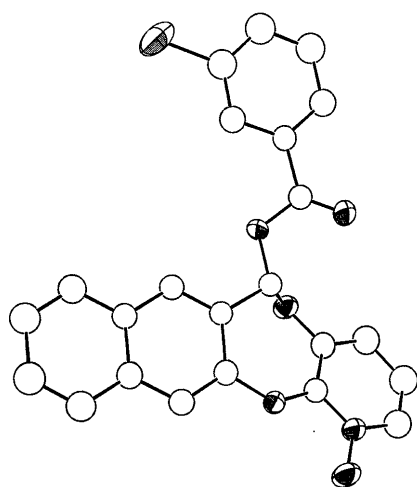
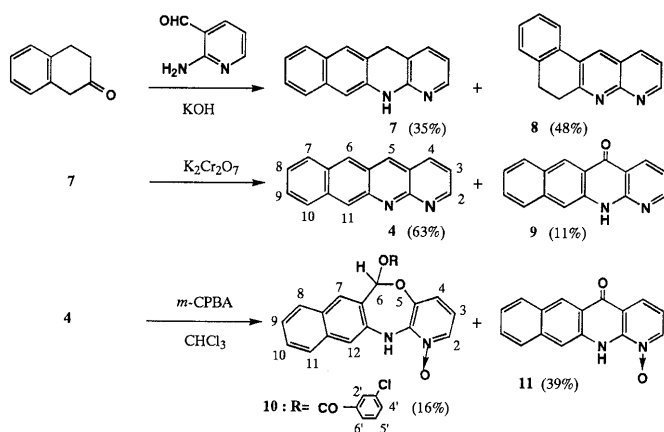


Fig. 1. A Perspective View of the Molecular Structure of **10** Determined Using X-ray Crystallography

of which was determined using X-ray crystallography.¹⁾ The root mean square error of these structures is 0.05 Å for 19 heavy atoms in the four rings when the structure of P1 is re-optimized using the restricted Hartree-Fock (RHF) method in the Gaussian 94 program package with the 3-21G basis set (RHF/3-21G).⁶⁾

We also assume that the other reactions of **1**, **2**, **3**, and **4** with **5** and/or **6** (reactions 2 to 6) proceed in the same way. We summarize the calculated energies for the ring expansion process in Table 1, together with the experimental yields of products with a 1,4-oxazepine ring.⁷⁾ To confirm the results of the AM1 method, we optimized the structures of TS1 and TS2 using RHF/3-21G. The structures of TS1 and TS2 optimized using RHF/3-21G are almost the same as those optimized using the AM1 method. The differences in these TS1 and TS2 energies obtained by RHF/3-21G are also shown in Table 1. For reactions 1 to 5, the calculated energies of TS1 are lower than those of TS2. Therefore the ring expansion process occurs through path 1 and products corresponding to P1 are produced. In experiments, P1-type products with a

1,4-oxazepine ring via TS1 were synthesized, but compounds via TS2 were not obtained.^{1,2)}

On the other hand, in the reaction of **4** with **6** (reaction 6), the calculated energy of TS1 is greater than that of TS2 (see Table 1). Therefore it is anticipated that a product with another type of oxazepine moiety via TS2 will be obtained in reaction 6 (Chart 1). To verify the calculated result for reaction 6, we performed the following experiments (Chart 2): We produced dihydro compounds (**7** and **8**) using the condensation of β -tetralone and 2-aminonicotinaldehyde and obtained the desired linear compound (**4**)⁸⁾ with oxidation of compound (**7**). Compound (**4**) was treated with *m*-CPBA at 20 °C for 10 min, producing the expected 1,4-oxazepine compound (**10**,⁹⁾ 16%) and another compound (**11**, 39%). The molecular structure of **10** was determined using X-ray crystallography. A perspective view of product (**10**) is shown in Fig. 1. The 1,4-oxazepine ring of **10** has the same structure (P2 type) as predicted from the calculated energies of TS1 and TS2 for reaction 6.

The activation energy (*E*_a) of the reaction is estimated from the difference between TS1 energy (TS2 for reaction 6) and the energy of reactants. The values of *E*_a are shown in Table 1.

References and Notes

- 1) Takeuchi I., Asai K., Hamada Y., Masuda K., Suezawa H., Hirota M., Kurono Y., Hatano H., *Heterocycles*, **43**, 2139–2152 (1996).
- 2) Takeuchi I., Naga N., Kariyama T., Hamada Y., Matsuzaki H., *Heterocycles*, **48**, 2125–2132 (1998).
- 3) Stewart J. J. P., *J. Comput. Chem.*, **10**, 209–220; 221–264 (1989).
- 4) MOPAC 93 release 2, Stewart J. J. P., Fujitsu Limited, Tokyo, Japan, 1994.
- 5) Fukui K., Yonezawa T., Shingu H., *J. Chem. Phys.*, **20**, 722–725 (1952); Fukui K., Yonezawa T., Nagata C., Shingu H., *J. Chem. Phys.*, **22**, 1433–1442 (1954).
- 6) Gaussian 94, Revision B.3, Frisch M. J., Trucks G. W., Schlegel H. B., Gill P. M. W., Johnson B. G., Robb M. A., Cheeseman J. R., Keith T., Petersson G. A., Montgomery J. A., Raghavachari K., Al-Laham M. A., Zakrzewski V. G., Ortiz J. V., Foresman J. B., Peng C. Y., Ayala P. Y., Chen W., Wong M. W., Andres J. L., Replogle E. S., Gomperts R., Martin R. L., Fox D. J., Binkley J. S., Defrees D. J., Baker J., Stewart J. P., Head-Gordon M., Gonzalez C., Pople J. A., Gaussian, Inc., Pittsburgh PA, U.S.A., 1995.
- 7) We take a sum of the yields of products with a 1,4-oxazepine ring as the experimental yield in reactions 1–3, and 5 (see refs. 1 and 2).
- 8) Selected data for **4**: mp 238–240 °C (dec.) (AcOEt). FAB-MS *m/z*: 231 (*M*⁺+1). ¹H-NMR (270 MHz, CDCl₃) δ : 7.40 (1H, dd, *J*=8.5, 3.9 Hz, H-3), 7.49 (1H, m, H-8), 7.53 (1H, m, H-9), 8.04 (1H, m, H-7), 8.13 (1H, m, H-10), 8.36 (1H, dd, *J*=8.5, 3.9 Hz, H-4), 8.68 (1H, s, H-6), 9.03 (1H, s, H-11), 9.06 (1H, s, H-5), 9.29 (1H, dd, *J*=3.9, 2.0 Hz, H-2). Anal. Calcd for C₁₆H₁₀N₂: C, 83.46; H, 4.38; N, 12.17. Found: C, 83.35; H, 4.42; N, 12.09.
- 9) Selected data for **10**: mp 203–205 °C (dec.) (AcOEt). FAB-MS *m/z*: 419 (*M*⁺+1). ¹H-NMR (270 MHz, CDCl₃) δ : 6.71 (1H, dd, *J*=8.3, 6.3 Hz, H-3), 7.27 (1H, dd, *J*=8.3, 1.0 Hz, H-4), 7.29 (1H, s, H-12), 7.32 (1H, t, *J*=8.0 Hz, H-5'), 7.34 (1H, m, H-9), 7.40 (1H, s, H-6), 7.47 (1H, m, H-10), 7.52 (1H, m, H-4'), 7.65 (1H, br, s, NH), 7.68 (1H, m, H-11), 7.78 (1H, m, H-8), 7.81 (1H, m, H-6'), 7.89 (1H, s, H-7), 7.92 (1H, d, *J*=2.4 Hz, H-2'), 7.97 (1H, dd, *J*=6.3, 1.0 Hz, H-2). Anal. Calcd for C₂₃H₁₅ClN₂O₄: C, 65.96; H, 3.61; N, 6.69. Found: C, 65.92; H, 3.80; N, 6.57.